

Optical Networks

*Series Editor:* Biswanath Mukherjee

Massimo Tornatore

Gee-Kung Chang

Georgios Ellinas *Editors*

# Fiber-Wireless Convergence in Next-Generation Communication Networks

Systems, Architectures, and  
Management



Springer

# **Optical Networks**

**Series editor**

Biswanath Mukherjee, Davis, USA

The book series in Optical Networks encompasses both optical communications and networks, including both theoretical and applied books. The series describes current advances at the cutting edge of the field and is aimed especially at industry practitioners, researchers, and doctoral students.

The series emphasizes the following major areas:

- optical network architectures;
- enabling technologies for optical communication networks;
- wavelength-division multiplexing (WDM) based networks;
- optical access and metro networks;
- long-haul optical networks;
- optical packet networks;
- optical burst-switched networks;
- fault-tolerant optical networks;
- optical network control and management; and
- emerging industry standards.

The series features the following types of books:

- Intermediate to advanced level textbooks as well as expository books that extend and unify our knowledge and understanding of particular areas;
- Handbooks and professional reference works that redefine “state-of-the-art,” emphasizing expository surveys, completely new advances, and combinations thereof;
- Encyclopedias containing articles dealing with the entire range of knowledge in the field or its specialty subtopics; and
- Research monographs that make substantial contributions to new knowledge in specialty subtopics.

These peer-reviewed titles ensure the highest quality content.

More information about this series at <http://www.springer.com/series/6976>

Massimo Tornatore · Gee-Kung Chang  
Georgios Ellinas  
Editors

# Fiber-Wireless Convergence in Next-Generation Communication Networks

Systems, Architectures, and Management

 Springer

*Editors*

Massimo Tornatore  
Department of Electronics, Information  
and Bioengineering, DEIB  
Politecnico di Milano  
Milan  
Italy

Georgios Ellinas  
Department of Electrical and Computer  
Engineering  
University of Cyprus  
Cyprus  
Cyprus

Gee-Kung Chang  
School of Electrical and Computer  
Engineering  
Georgia Institute of Technology  
Atlanta, GA  
USA

ISSN 1935-3839

Optical Networks

ISBN 978-3-319-42820-8

DOI 10.1007/978-3-319-42822-2

ISSN 1935-3847 (electronic)

ISBN 978-3-319-42822-2 (eBook)

Library of Congress Control Number: 2016954914

© Springer International Publishing Switzerland 2017

This work is subject to copyright. All rights are reserved by the Publisher, whether the whole or part of the material is concerned, specifically the rights of translation, reprinting, reuse of illustrations, recitation, broadcasting, reproduction on microfilms or in any other physical way, and transmission or information storage and retrieval, electronic adaptation, computer software, or by similar or dissimilar methodology now known or hereafter developed.

The use of general descriptive names, registered names, trademarks, service marks, etc. in this publication does not imply, even in the absence of a specific statement, that such names are exempt from the relevant protective laws and regulations and therefore free for general use.

The publisher, the authors and the editors are safe to assume that the advice and information in this book are believed to be true and accurate at the date of publication. Neither the publisher nor the authors or the editors give a warranty, express or implied, with respect to the material contained herein or for any errors or omissions that may have been made.

Printed on acid-free paper

This Springer imprint is published by Springer Nature  
The registered company is Springer International Publishing AG  
The registered company address is: Gewerbestrasse 11, 6330 Cham, Switzerland

*Gee-Kung Chang dedicates this book to his  
wife Sharon*

*Georgios Ellinas dedicates this book  
to his nephew Nicolas and his niece Carina*

*Massimo Tornatore dedicates this book  
to his father Antonio*

# Foreword

Optical fiber networks and wireless networks have recently undergone significant technological and architectural evolution through, e.g., massive deployments of 4G mobile networks and passive optical networks (PON). These sustained infrastructure upgrades have led to enormous investments for operators (billions of dollars). The next important step is near, as 5G communication networks are expected to be deployed by 2020, featuring unprecedented performance in terms of higher data rates, lower latency, and network flexibility. To achieve this, 5G will resort to solutions such as small-cell deployment (micro, femto, etc.), coordinated multi-cell processing, and centralized radio access networks that will ultimately burden the optical metro/access segment due to the massive amount of mobile traffic to be backhauled with sub-ms latency. Operators are now looking at a promising set of techniques characterized by strict cooperation between fiber-based and wireless-based technologies. These techniques are generically referred to as fiber-wireless convergence, forming the main subject of this book.

This book's editors have done an excellent job in capturing the various technical facets of fiber-wireless convergence. They present, using a set of clear and cohesive edited contributions, the impact and role of fiber-wireless convergence in various areas of network engineering, covering transmission systems, network architectures, and network management and control.

The book has been co-edited by Professor Gee-Kung Chang of Georgia Tech University in Atlanta, Professor George Ellinas of University of Cyprus, and Professor Massimo Tornatore of Politecnico di Milano, Italy. The editorial team has diverse and complementary expertise on the various areas of fiber-wireless convergence, which is then reflected in the comprehensive coverage of the book that spans, e.g., from detailed description of key transmission systems such as digital radio-over-fiber (D-RoF), to the role of software-defined network (SDN) control for convergence.

The book is divided into four parts: (1) path towards convergence; (2) systems; (3) architectures; and (4) management. In Part I, the reader is introduced to fiber-wireless convergence, both from the point of view of today's market trends

and from the point of view of the 5G technical challenges that call for convergence. In Part II, transmission systems which are more directly affected by convergence are overviewed, with a description of analog and D-RoF techniques, millimeter-wave wireless, and a detailed overview of system challenges that can be addressed by SDN. Part III captures the relevant problems and challenges on network architectures, covering topics as PON-based convergence, hoteling of remotized baseband functions “BBU hoteling”, and the “No Cell” vision of future mobile networks. Finally, Part IV includes relevant management and control problems such as the new role of metropolitan central office (Next Generation Point of Presence), and impact of SDN and radio coordination on convergence.

The editors deserve praise for the excellent lineup of contributing authors, who come from leading companies, reputable universities, and research laboratories, and with strong geographical diversity. This book is highly recommended as it offers timely, comprehensive, and authoritative reference to information on fiber-wireless convergence. We expect that the reader will enjoy the book.

August 2016

Biswanath Mukherjee  
University of California  
Davis, USA

# Preface

Communication networks must continuously evolve to ensure a sustainable growth of our “Internet Society.” It has been repeatedly observed that the push for more and more advanced network services leads inevitably to an exponential growth of traffic volumes and to higher quality-of-service requirements by the users; only by resorting to novel technologies and architectural solutions network, operators can keep pace with users’ requirements. The next big innovations in the telecom industry seem to be the forecasted massive deployment of IoT devices (hence the related machine-to-machine communication paradigm), the explosion of video-content network distribution, and the development of ultra-low latency network services. To address the technical challenges associated with these services, many companies, research institutes, and standardization bodies have now started the race towards the 5th generation of mobile communications. Fifth-generation networks are expected to support unprecedented bit rates, guaranteeing strict latency and reliable performance, and offering support for connecting together a tremendous number of devices. Fifth-generation networks will use very dense, low-power, small-cell networks with a high spatial reuse and a high degree of coordination due to strong inter-cell interference. Both fiber-based and wireless-based backhaul solutions will be used to connect small cells and the core network, but so far, access and backhaul are individually designed and therefore not jointly optimized. Hence, the design of 5G networks has long dictated the necessity to merge the currently distinct fiber and wireless infrastructures into an amalgamated network capable of combining the strength of both technologies: the stability and high bandwidth of optical fibers with the flexibility and mobility of wireless networks. This process of integration of the two technologies is usually referred as fiber-wireless convergence (or fixed-wireless convergence) and comprises a large set of technical challenges and solutions.

In this book, we provide the recent developments in the field of fiber-wireless convergence, concentrating on solutions that will be used to support the backhaul, midhaul, and fronthaul of 5G networks. The text presents the trends of industry, as well as current research, in state-of-the-art architectures of converged systems and networks, and takes a vertically layered approach starting from systems,

to architectures, to management/control issues of fixed-mobile convergence. This book is different from a number of other works on 5G networks that tend to focus heavily on the wireless aspects of 5G. Instead, we decided to look at both networking and systems issues, and focus on the latest research developments in a number of areas including radio over fiber, centralized cloud radio access network, and coordinated multi-point transmission for multiple base stations. This book is meant to be an introduction for any reader interested in having a holistic approach to the technical issues in fiber-wireless convergence and to readers interested in understanding some key aspects in more depth. The aim of the editors is to present a body of work that can provide the research scientist, company engineer, and the university professor/researcher with a better understanding on fiber-wireless convergence and ensure that experienced as well as novice researchers can have a single handy source of reference on this topic.

The book is divided into four parts that can appeal to different needs of readers, who are interested in various networking domains and issues. Part I is comprised of the introduction, the market, and the technical motivations for fiber-wireless convergence. Part II presents and discusses transmission systems for wireless-signal transport over fiber (A-RoF and D-RoF), and competing technology to these systems (namely multi-band RF and millimeter-wave transmission), and a set of opportunities that software-defined networks (SDNs) enable for such transmission systems. Part III concentrates on architectural issues related to network integration of fiber and wireless technologies (including use of PONs for mobile backhauling, baseband-unit hoteling, and centralized/coordinated architectures for radio access network, as the No-More-Cell architecture). Finally, Part IV covers management/control topics related to how and which network functions should converge in specific metro offices (Next Generation Point of Presence), as well as provides a closer look to some of these functions such as radio coordination and other SDN-controlled cloud services.

**Acknowledgments** We are extremely grateful to our past advisors and mentors, colleagues, students, and friends, who have motivated, inspired, and guided us to work in the new field of fiber-wireless convergence. All of them offered us their invaluable advise, exceptional insight, and foresight. They provided us with valuable guidance throughout the years and helped us better understand and appreciate various aspects of this new technological area. We would also be remiss if we did not extend a thank you to Professor Biswanath Mukherjee for taking the time to write the Foreword for this book and for his patience and encouragement while this book was being prepared and delivered. We also wish to express our thanks to Zoe Kennedy, Mary James, and the entire publishing team at Springer Verlag, for their effort and patience in order to bring this project to fruition. Also, a special thanks goes to all the authors who contributed chapters for this book. Finally, Georgios Ellinas is greatly indebted to his family for their understanding and patience during this undertaking. Gee-Kung Chang wishes to thank his wife for her unwavering support and express profound gratitude to Ken Byers who endows an eminent scholar chair professor in advanced telecommunications research at Georgia Tech for several decades. Massimo Tornatore gratefully acknowledges his family and his

fiancée Angela, for their constant love and support. Massimo Tornatore wants to acknowledge the European Community’s COMBO project, during which he gained an invaluable amount of knowledge on the topics of this book.

Milan, Italy

Massimo Tornatore  
Associate Professor

Atlanta, USA

Gee-Kung Chang  
Professor  
Byers Eminent Scholar  
Chair Professor in Optical Networking  
Georgia Research Alliance Eminent Scholar

Cyprus, Cyprus

Georgios Ellinas  
Associate Professor

# Contents

## Part I The Path Towards Convergence

<b>1</b>	<b>Future Radio Access, Wi-Fi-LTE, LTE-Advanced: The Path to 5G</b> . . . . .	<b>3</b>
	Rajarajan Sivaraj and Prasant Mohapatra	
1.1	Introduction . . . . .	3
1.1.1	LTE Principles of Operation and Deployment. . . . .	4
1.2	Carrier Aggregation . . . . .	9
1.2.1	Definitions and Terminologies. . . . .	9
1.2.2	Types of Carrier Aggregation . . . . .	10
1.2.3	Radio Resource Management Framework for CA . . . . .	15
1.3	Transmission Diversity and Spatial Multiplexing . . . . .	18
1.3.1	Transmit Diversity—Definition and Terminologies . . . . .	18
1.3.2	MIMO and Spatial Multiplexing—Definition and Terminologies . . . . .	18
1.3.3	Coordinated Multi-point Transmission. . . . .	19
1.3.4	Types of CoMP. . . . .	22
1.3.5	Advancements: 3D Beamforming . . . . .	24
1.3.6	Applications . . . . .	25
1.4	Wi-Fi-LTE, Unlicensed LTE . . . . .	27
1.4.1	Definition and Terminologies . . . . .	27
1.4.2	CA of LTE-Licensed and LTE-U CCs . . . . .	28
1.5	Network Heterogeneity: Self-organizing HetNets . . . . .	30
1.5.1	Definition and Terminologies . . . . .	30
1.5.2	Background on Inter-cell Interference Coordination (ICIC) . . . . .	31
1.5.3	Enhanced Inter-cell Interference Coordination (EICIC) . . . . .	34

- 1.5.4 Defining the CRE Region . . . . . 35
- 1.5.5 Enhancements: eICIC with CA . . . . . 37
- 1.6 Conclusion . . . . . 38
- References. . . . . 39
- 2 Evolution and Trends of Broadband Access Technologies and Fiber-Wireless Systems . . . . . 43**  
Yiran Ma and Zhensheng Jia
- 2.1 Traffic Trend. . . . . 43
- 2.2 Technologies of Broadband Access Networks . . . . . 45
  - 2.2.1 Broadband Wireline Access Networks. . . . . 45
  - 2.2.2 Broadband Wireless Access Networks. . . . . 60
- 2.3 Fiber-Wireless Convergence and Technology Evolution. . . . . 69
  - 2.3.1 Fiber-Based Distributed Antenna Systems (DASs) . . . 69
  - 2.3.2 Ultra-High-Speed Fiber-Wireless Transmission . . . . . 70
  - 2.3.3 Fiber-Wireless for Backhaul and the Fronthaul of HetNet. . . . . 71
- 2.4 Conclusions . . . . . 74
- References. . . . . 74
- 3 The Benefits of Convergence Through Fiber-Wireless Integration and Networking . . . . . 77**  
Gee-Kung Chang and Lin Cheng
- 3.1 Introduction . . . . . 77
- 3.2 Convergence of Architectures. . . . . 80
  - 3.2.1 Centralization . . . . . 80
  - 3.2.2 Resource Sharing. . . . . 83
- 3.3 Convergence of Links. . . . . 84
  - 3.3.1 Mobile Backhaul . . . . . 84
  - 3.3.2 Mobile Midhaul and Fronthaul . . . . . 87
- 3.4 Convergence of Bands . . . . . 89
  - 3.4.1 All-Band Coverage . . . . . 89
  - 3.4.2 MMW Links . . . . . 91
- 3.5 Conclusion . . . . . 92
- References. . . . . 93
- Part II Novel Systems/Subsystems for Fi-Wi Networks**
- 4 Analog and Digitized Radio-over-Fiber . . . . . 99**  
Maurice Gagnaire
- 4.1 Existing Radio Cellular Networks. . . . . 100
- 4.2 A-RoF Versus Baseband-over-Fiber . . . . . 102
  - 4.2.1 Option 1: RF-Modulated Signals. . . . . 103
  - 4.2.2 Option 2: IF Modulated Signals . . . . . 103
  - 4.2.3 Option 3: Baseband-over-Fiber . . . . . 104
  - 4.2.4 Conclusion. . . . . 104

- 4.3 Transmission of Microwave Signals on Optical Fibers . . . . . 104
  - 4.3.1 Intensity Modulation (IM) and Direct Detection (DD) . . . . . 105
  - 4.3.2 External Modulation and Direct Detection (EM-DD) . . . . . 106
  - 4.3.3 Photo-detector-Based Heterodyning (HE) with Direct Detection (HE-DD) . . . . . 107
  - 4.3.4 Conclusion . . . . . 109
- 4.4 Analog Radio-over-Fiber (A-RoF) . . . . . 109
  - 4.4.1 A-RoF for “RF-over-Fiber” . . . . . 110
  - 4.4.2 A-RoF for “IF-over-Fiber” . . . . . 111
  - 4.4.3 A-RoF for Multi-antennas Sites by Means of Sub-carrier Multiplexing (SCM) . . . . . 112
  - 4.4.4 A-RoF for Multi-antennas Sites by Means of Wavelength-Division Multiplexing (WDM) . . . . . 114
- 4.5 Digitized Radio-over-Fiber (D-RoF) . . . . . 117
  - 4.5.1 Band-pass Sampling Theory . . . . . 118
  - 4.5.2 D-RoF for a Single-Antenna Site . . . . . 120
  - 4.5.3 D-RoF for a Multiple-Antenna Site . . . . . 122
- 4.6 Conclusion . . . . . 124
- References . . . . . 125
- 5 Overview of Standardization for D-RoF . . . . . 127**
  - Silvano Frigerio, Alberto Lometti and Vincenzo Sestito
  - 5.1 CPRI . . . . . 128
    - 5.1.1 Specification Overview . . . . . 129
    - 5.1.2 System Description . . . . . 129
    - 5.1.3 Main Requirements . . . . . 130
    - 5.1.4 Interface Description . . . . . 131
    - 5.1.5 CPRI Compression and CPRI Throughput Examples . . . . . 137
  - 5.2 OBSAI . . . . . 138
    - 5.2.1 OBSAI Specifications Status . . . . . 139
    - 5.2.2 System Architecture Overview . . . . . 139
    - 5.2.3 RP3-01 Insight . . . . . 142
    - 5.2.4 CPRI Versus OBSAI RP3-01 . . . . . 145
  - 5.3 D-RoF Transport Over Optical Networks . . . . . 146
    - 5.3.1 CPRI Over OTN . . . . . 149
    - 5.3.2 Viable Network Applications for CPRI Over WDM/OTN . . . . . 153
  - 5.4 ORI . . . . . 154
  - 5.5 Conclusions . . . . . 155
  - References . . . . . 156

<b>6</b>	<b>Wireless Delivery of over 100 Gb/s mm-Wave Signal in the W-band</b> . . . . .	157
	Jianjun Yu	
6.1	Introduction . . . . .	157
6.2	Approaches for the Realization of Large Capacity (>100 Gb/s) Fiber Wireless Integration System . . . . .	160
6.2.1	Optical PDM Combined with MIMO Reception . . . . .	161
6.2.2	Advanced Multi-level Modulation . . . . .	166
6.2.3	Optical Multi-carrier Modulation . . . . .	169
6.2.4	Electrical Multi-carrier Modulation . . . . .	173
6.2.5	Antenna Polarization Multiplexing . . . . .	175
6.2.6	Multi-band Multiplexing . . . . .	178
6.3	Problems Existing in the Large Capacity Fiber Wireless Integration System and Corresponding Solutions . . . . .	182
6.3.1	Wireless Multi-path Effects Due to Different Wireless Transmission Distances . . . . .	182
6.3.2	Advance Algorithms Based on DSP . . . . .	184
6.4	Conclusion . . . . .	184
	References . . . . .	185
<b>7</b>	<b>Systems Challenges for SDN in Fiber Wireless Networks</b> . . . . .	189
	Neda Cvijetic and Ting Wang	
7.1	Introduction . . . . .	190
7.2	System-Level Fiber Wireless Network Challenges . . . . .	192
7.2.1	Signaling Formats . . . . .	193
7.2.2	Network Densification . . . . .	194
7.2.3	Network Topology . . . . .	195
7.3	SDN-Based Control Plane . . . . .	196
7.3.1	SDN-Based Control in Fiber Wireless Networks . . . . .	198
7.4	Recent Progress in SDN for Fiber Wireless Networks . . . . .	201
7.5	Conclusions . . . . .	206
	References . . . . .	207
<b>Part III Novel Network Architectures for Fi-Wi Networks</b>		
<b>8</b>	<b>Architectural Evolution and Novel Design of Fiber-Wireless Access Networks</b> . . . . .	213
	Cheng Liu	
8.1	Introduction . . . . .	213
8.2	Overview of Existing Fiber-Wireless Access Architectures . . . . .	215
8.2.1	Macrocell and Small Cell with Fiber-Optic Backhaul . . . . .	215
8.2.2	Distributed Antenna System . . . . .	219
8.2.3	Cloud Radio Access Network (C-RAN) . . . . .	221
8.3	Novel Cloud Radio-Over-Fiber Access Architecture . . . . .	224

8.3.1	Generic Cloud-RoF Architecture and Operational Principle . . . . .	224
8.3.2	Reconfigurable Cloud-RoF Architecture with WDM Techniques . . . . .	226
8.3.3	Multi-Service Delivery Including Future-Proof Millimeter-Wave Services . . . . .	228
8.4	Summary . . . . .	232
	References. . . . .	232
<b>9</b>	<b>Advanced Architectures for PON Supporting Fi-Wi Convergence . . . . .</b>	<b>235</b>
	Georgios Ellinas, Kyriakos Vlachos, Chrysovalanto Christodoulou and Mohamed Ali	
9.1	Introduction . . . . .	236
9.2	Backhauling Wireless Traffic . . . . .	236
9.3	Passive Optical Network (PON): Standards and Technology Options. . . . .	239
9.4	Technology Options . . . . .	239
	9.4.1 TDM-PON. . . . .	239
	9.4.2 WDM-PON. . . . .	241
	9.4.3 OFDM-PON . . . . .	244
	9.4.4 Hybrid PONs. . . . .	245
9.5	PON Standards . . . . .	246
	9.5.1 GPON/EPON. . . . .	246
9.6	10G-PON . . . . .	247
9.7	10G-Epon. . . . .	247
	9.7.1 NG-PON2 . . . . .	248
	9.7.2 Evolution Scenarios. . . . .	250
9.8	Challenges in PON Design . . . . .	251
9.9	Distributed Ring-Based WDM-PON Architecture. . . . .	251
9.10	Architecture Design . . . . .	253
9.11	Allocation of Network Resources . . . . .	255
	9.11.1 Dynamic Bandwidth Allocation. . . . .	256
	9.11.2 Upstream Traffic Flows Rerouting and Sharing. . . . .	256
9.12	Wavelength Assignment/Sharing for Downstream Traffic. . . . .	257
9.13	Fault Detection and Recovery. . . . .	257
	9.13.1 Fault Detection . . . . .	259
	9.13.2 Fault Recovery . . . . .	259
9.14	Fronthauling Mobile Traffic . . . . .	260
9.15	Conclusions . . . . .	261
	References. . . . .	262

**10 BBU Hotelling in Centralized Radio Access Networks . . . . . 265**  
 Nicola Carapellese, M. Shamsabardeh, Massimo Tornatore  
 and Achille Pattavina

10.1 Introduction . . . . . 265

10.2 Mobile Network . . . . . 266

10.3 Evolving the Base Station: BBU and RRH. . . . . 267

10.4 Advantages of BBU Hotelling . . . . . 268

    10.4.1 Cost Reduction . . . . . 268

    10.4.2 Energy Savings . . . . . 269

    10.4.3 Improved Radio Performance . . . . . 269

10.5 Challenges of BBU Hotelling: Fronthaul . . . . . 270

    10.5.1 High, Constant Bitrate. . . . . 270

    10.5.2 Maximum End-to-End Latency . . . . . 271

    10.5.3 Strict QoS Requirements . . . . . 273

10.6 RAN Architectures Based on BBU Hotelling. . . . . 273

    10.6.1 Classification on BBU Placement . . . . . 274

    10.6.2 Classification on Fronthaul Transport . . . . . 276

    10.6.3 Classification on BBU Implementation . . . . . 278

10.7 An FMC Network Architecture for BBU Hotelling . . . . . 280

    10.7.1 General Network Architecture . . . . . 280

    10.7.2 BBU Placement. . . . . 281

    10.7.3 Traffic Routing . . . . . 282

10.8 The BPTR Optimization Problem. . . . . 283

10.9 A Heuristic Greedy Algorithm for BPTR. . . . . 284

    10.9.1 Notation and Input Data . . . . . 284

    10.9.2 Heuristic Subroutines. . . . . 285

    10.9.3 Heuristic Scheme. . . . . 286

10.10 A Case Study for the BPTR . . . . . 286

10.11 Conclusion and Open Issues. . . . . 289

References. . . . . 290

**11 Rethink Ring and Young: Green and Soft RAN for 5G. . . . . 293**  
 Chih-Lin I, Jinri Huang, Ran Duan, Gang Li and Chunfeng Cui

11.1 Introduction . . . . . 293

11.2 No More Cells: One Key 5G Vision . . . . . 294

11.3 Cloud RAN: The Key Enablers to NMC . . . . . 296

    11.3.1 The Concept of C-RAN. . . . . 296

    11.3.2 C-RAN Features . . . . . 298

    11.3.3 Advantages of C-RAN . . . . . 299

11.4 Challenges and Potential Solutions for C-RAN Realization . . . . . 299

    11.4.1 Challenges on Transport Networks for  
         Centralization . . . . . 299

    11.4.2 Potential Fronthaul Solutions. . . . . 300

    11.4.3 Challenges on Virtualization Implementation  
         to Realize Resource Cloudification . . . . . 302

- 11.5 Recent Progress on C-RAN from China Mobile. . . . . 304
  - 11.5.1 Field Trials on Centralization with Different FH Solutions . . . . . 304
  - 11.5.2 Exploitation of C-RAN Virtualization . . . . . 307
- 11.6 Evolving Toward 5G . . . . . 310
  - 11.6.1 C-RAN to Enable Key 5G Technologies. . . . . 310
  - 11.6.2 Rethink CPRI: CPRI Redefinition . . . . . 311
  - 11.6.3 Edge Application on C-RAN. . . . . 313
- 11.7 Conclusions . . . . . 314
- References. . . . . 315

**Part IV Novel Management Strategies for Fi-Wi Networks**

- 12 Next-Generation PoP with Functional Convergence Redistributions.** . . . . 319
 

Philippe Bertin, Tahar Mamouni and Stéphane Gosselin

  - 12.1 Introduction . . . . . 319
  - 12.2 What Services at the Network Edge? . . . . . 321
    - 12.2.1 Virtual Residential Gateway . . . . . 322
    - 12.2.2 Broadband Network Gateway . . . . . 324
    - 12.2.3 Distributed Evolved Packet Core. . . . . 326
    - 12.2.4 Highly Distributed Content Delivery Networks . . . . . 328
  - 12.3 The Path Toward Fixed and Mobile Convergence . . . . . 329
    - 12.3.1 Converged Subscriber Data and Session Management . . . . . 329
    - 12.3.2 Universal Access Gateway . . . . . 331
  - 12.4 Implementing the NG PoP . . . . . 333
    - 12.4.1 Design Principles. . . . . 333
    - 12.4.2 Dimensioning the NG PoP . . . . . 334
  - 12.5 Conclusions . . . . . 335
  - References. . . . . 336
- 13 Coordinated Multi-point (CoMP) Systems.** . . . . 337
 

Yizhuo Yang, Christina Lim and Ampalavanapillai Nirmalathas

  - 13.1 Introduction on CoMP . . . . . 337
  - 13.2 Requirements on the Backhaul Network. . . . . 339
    - 13.2.1 Latency . . . . . 340
    - 13.2.2 Synchronization . . . . . 340
    - 13.2.3 Capacity . . . . . 340
  - 13.3 Backhaul Architecture. . . . . 341
    - 13.3.1 GROW-Net Architecture . . . . . 342
    - 13.3.2 FUTON Prototype . . . . . 345
    - 13.3.3 Adaptive Photonics-Aided CoMP for MMW Small Cells . . . . . 348
    - 13.3.4 Converged Fiber–Wireless Architecture. . . . . 349

- 13.4 Fiber–Wireless Integration Schemes Enabling CoMP . . . . . 350
  - 13.4.1 BS Configuration . . . . . 350
  - 13.4.2 Performance Analysis . . . . . 352
  - 13.4.3 Implementation of CoMP . . . . . 354
  - 13.4.4 Experimental Demonstration . . . . . 355
- 13.5 Summary . . . . . 356
- References. . . . . 357
- 14 Converged Wireless Access/Optical Metro Networks  
in Support of Cloud and Mobile Cloud Services**
- Deploying SDN Principles. . . . . 359**  
 Anna Tzanakaki, Markos Anastasopoulos, Bijan Rofoee,  
 Shuping Peng, George Zervas, Reza Nejabati, Dimitra Simeonidou,  
 Giada Landi, Giacomo Bernini, Roberto Monno, Nicola Ciulli,  
 Gino Carrozzo, Kostas Katsalis, Thanasis Korakis,  
 Leandros Tassiulas, Georgios Dimosthenous, Dora Christofi,  
 Jordi Ferrer Riera, Eduard Escalona, Jacopo Pianigiani,  
 Dirk Van Den Borne and Gert Grammel
- 14.1 Introduction . . . . . 360
- 14.2 Existing Technology Solutions Supporting Cloud  
and Mobile Cloud Services. . . . . 362
  - 14.2.1 Physical Infrastructure Solutions  
Supporting Cloud Services . . . . . 362
  - 14.2.2 Infrastructure Management . . . . . 363
  - 14.2.3 Service Provisioning . . . . . 365
- 14.3 Proposed Converged Network Architecture . . . . . 366
  - 14.3.1 Vision and Architectural Approach . . . . . 366
  - 14.3.2 Physical Infrastructure Layer . . . . . 369
  - 14.3.3 Infrastructure Management . . . . . 371
  - 14.3.4 Virtual Infrastructure Control Layer. . . . . 373
  - 14.3.5 Converged Service Orchestration. . . . . 378
- 14.4 Architecture Evaluation. . . . . 379
  - 14.4.1 Network Scenario and Related Work. . . . . 379
- 14.5 Conclusions . . . . . 386
- References. . . . . 387
- Conclusion and Future Topics . . . . . 389**
- Index . . . . . 395**

# Introduction

**Abstract** Fifth-generation mobile access networks will feature unprecedented performance, not only in terms of higher data rates and lower latencies, but also in terms of the “intelligence” of the network. To achieve these targets, 5G networks will resort to solutions such as small-cell deployment (micro-, femto-, etc.), coordinated multi-cell processing (CoMP, eICIC) and centralized/cloud RAN. Such techniques will ultimately burden the optical fiber access/aggregation network needed to backhaul the mobile traffic, as this section of the network will be responsible to serve massive traffic with very strict latency. Hence, the trend toward an actual convergence of fiber and wireless technologies in access/aggregation networks, which has been emerging in the last decade, is expected to gain increased importance, as it indirectly impacts on radio access performance. This book introduces several key enabling techniques for next-generation fiber-wireless convergent communication systems in 5G and mobile backhaul networks. The book features fourteen excellent contributions, authored by well-renowned industrial practitioners and academic researchers, in three main thematic areas: system technologies (radio-over-fiber, millimeter-wave transmission, SDN-controlled optical technologies, LTE-advanced), network architectures (TWDM PON, BBU Hotelling, 5G RAN), and network management (SDN-controlled access, CoMP, Next Generation Point of Presence). The focus of various chapters goes beyond the description of state of the art, also presenting the evolutionary paths for fiber-wireless convergence toward 5G implementation.

## The overall picture

Mobile traffic growth due to the proliferation of smart mobile devices and bandwidth demanding applications is accelerating the evolution of radio access networks (RAN) from 2G, 3G, to 4G, and beyond. Looking into the future, 5G wireless technology is on the horizon. The exact definition of 5G is still under active

discussions, and many research activities are being carried out in both industry and academia. For link spectrum efficiency, the existing wireless technologies have been pushed very close to the Shannon theoretical limit by using higher-level modulation formats (e.g., 64QAM-OFDM), multiple-input and multiple-output (MIMO) techniques, and advanced channel coding schemes (e.g., low-density parity-check (LDPC) and turbo codes). However, there is a great potential in enhancing the system spectrum efficiency. For example, by coordinating adjacent cells to jointly transmit signals to cell-edge users, coordinated multi-point transmission (CoMP) [2] can significantly improve the data rate of the users who used to suffer from strong inter-cell interference, thus enhancing the system spectrum efficiency (see Chap. 13). In another dimension, people are always looking for more spectrum, mostly in higher radio frequencies, e.g., exploring the millimeter-wave band [3, 4] (see Chap. 6). Last but not the least, small-cell solutions are being increasingly implemented and are becoming the trend for future wireless communication. By reducing the cell size, limited spectral resources can be reused among cells more frequently, thus enhancing the total system capacity. There are also many discussions on merging WLAN (e.g., Wi-Fi) with cellular small cells to provide a uniform platform for 5G wireless access (see Chap. 2). The main directions of future wireless communications [1] will be overviewed in more detail in Chap. 3.

On the other hand, supporting such techniques will strain the optical fiber-based access/aggregation network that provides the backhaul for the wireless access network. Such “mobile backhaul” or “mobile transport” network will be required to serve the massive traffic amount coming from the mobile users (generated via a plethora of broadband mobile applications) with very strict latency constraints. Hence, the trend toward an actual convergence of fiber and wireless technologies in access/aggregation networks, which has been emerging in the last decade, is expected to have an increased importance, as it indirectly impacts on radio access performance.

*In this book, aligned with the directions of future 5G networks, several key enabling technologies, network architectures, and management/control approaches for fiber–wireless convergence for 5G mobile transport networks are introduced.*

More importantly, the concept of centralized radio access network (CRAN), as well as the associated concept of RAN virtualization (cloud RAN), is comprehensively reviewed in the book. CRAN is a recent solution which radically changes the classical architecture of the RAN. It separates mobile baseband units (BBU) from corresponding Remote Radio Heads (RRH) and consolidates them into common locations, also known as “hotels” (in fact, the paradigm of CRAN is often referred to as BBU hoteling or hosteling). Each BBU/RRH pair exchanges digital radio-over-fiber (D-RoF) data (see Chap. 5), also known as “fronthaul,” obtained from the baseband digitization of radio interface signals (see Chap. 4). Thanks to the sharing of backplanes, power, computational, and maintenance resources of BBUs hosted in the same hotel, a significant amount of OPEX saving can be achieved by adopting this mobile backhauling architecture (see Chap. 10). Moreover, increased coordination will allow to optimize RAN throughput (e.g.,

using the previously mentioned CoMP technique, see Chap. 14), and to even move towards more exciting and future-prone CRAN paradigms as the “No More Cells” approach (see Chap. 11). Note that, conventionally, backhaul/fronthaul networks can be based on T1 lines, microwave point-to-point links, and not only fiber links. However, since the backhaul/fronthaul capacity requirement increases drastically as the wireless access techniques evolve, optical fibers are considered as the ultimate transport media to provide sufficient bandwidth as well as future-proof capacity upgrade. In particular, passive optical networks (PONs) are a relevant candidate for mobile backhaul/fronthaul applications (see Chaps. 8 and 9).

In light of the previous discussion, it clearly emerges that the envisioned fiber-wireless-convergent backhaul network will require enhanced “intelligence” in terms of reconfigurability and coordination, among others. To enable such intelligence, research is currently focusing also on the role that software-defined networking (SDN) will play as an enabler for advanced functionalities for fiber-wireless convergence (see Chap. 7, for applications of SDN in the next-generation optical access segment, and “Conclusion and Future Topics”, for a proposal of an SDN-controlled fiber-wireless converged network supporting cloud computing services).

Finally, there is increased interest from network operators in leveraging access/aggregation infrastructure for fixed traffic to also perform backhaul/fronthaul of mobile traffic, in a related concept to *fiber-wireless convergence*, which is typically referred as *fixed-mobile convergence* (see Chap. 13) [5].

The topic of fiber-wireless convergence is currently an actively researched topic, and clearly it is impossible to cover in this book all the latest progress in the field. Nevertheless, as of today, a comparably comprehensive collection of up-to-date, relevant, and logically organized works on this topic has not been yet made available. The aim of this book in putting together this collection of chapters is to ensure that experienced as well as novice researchers can have a single handy source of reference on this topic. The following chapters do not only cover exciting long-term research proposals originating mostly from academia and research laboratories but they also contain the current vision of practitioners working in leading technology vendor and network operator companies.

The intended audience of the book consists of students in academia learning about and doing research on fiber-wireless convergent networks in support of 5G and mobile backhaul networks, industrial practitioners that are evaluating the introduction of these technologies in the design of current 4G network as well as those starting to build a 5G-prone backhaul infrastructure, and faculty members and researchers in academia wishing to teach an advanced course on next-generation network design, or conducting research in the area of fiber-wireless convergence and 5G. The objective of the book is to provide the reader with a comprehensive source of information on this interesting and timely topic that can foster novel ideas and research lines, as well as inspire new ways to go forward and find new solutions for the numerous remaining challenges.

## Book Organization

The book is organized into four parts covering different subject areas. Part I (Chaps. 1–3) overviews market and technological trends that motivate the book and discusses the benefits of convergence. An introduction to the evolution of cellular technology toward 5G is also provided for readers that need to catch up with recent trends, especially in LTE. Part II (Chaps. 4–7) focuses on enabling technologies for fiber-wireless convergence. Part III (Chaps. 8–11) deals with rising paradigms for network architectures in the fiber-wireless convergent access/metro network segments, and Part IV (Chaps. 12–14) discusses some challenges in terms of management of a fiber-wireless converged network. In the last chapter of the book, we conclude the book and overview very novel and recent areas of research which have been emerging during the preparation of the book.

Chapter 1 by Ma and Jia provides an introduction to technical trends and market status of both broadband wireline and wireless access networks, and also summarizes the current forecasts on technology evolution of fiber-wireless networks. As a useful introduction to technologies discussed throughout the rest of the book, the chapter overviews broadband wireline access networks including xDSL, coaxial cable, and hybrid fiber coax (HFC), and various PON architectures and then moves to broadband wireless access technologies such as Wi-Fi, WiMAX, and mobile cellular systems.

Chapter 2 by Sivarajan and Mohapatra presents in a comprehensive manner the foundational concepts of the design principles used in LTE-A radio access networks, such as bandwidth aggregation, transmission diversity, interference management, and MIMO spatial diversity. These concepts are instrumental to the entire book as they provide a clear technical roadmap to the 5G technologies.

Chapter 3 by Chang and Cheng introduces the concept of multi-tier radio access network (RAN) combining the strength of fiber-optic and radio access technologies. This concept, which will be complemented by the specific contributions in the rest of the book, employs adaptive microwave photonics interfaces and radio-over-fiber (RoF) techniques for future heterogeneous wireless communications. Coexistence of current and future mobile network standards such as 4G and 5G with optimized and continuous cell coverage using multi-tier RoF, regardless of the underlying network topology or protocol, is also discussed.

Chapter 4 by Gagnaire overviews the basic principles, drawbacks, and benefits of the various analog- and digital radio-over-fiber techniques currently available, by providing a detailed state-of-the-art picture of the level of advancement of these two techniques. These techniques are a key for the implementation of the signal transport in the CRAN architectures. A detailed overview of the current RoF options provides a useful insight on the transmission technologies that support the communication between RRH and BBU in CRAN.

Chapter 5 by Frigerio, Lometti, and Sestito introduces the reader to the current standardization activities related to D-RoF, namely those relative to the definition of the digital interface between radio units and base stations (CPRI, OBSAI, ORI)

and those aimed at allowing for the transport of such interfaces over a geographical network. The latest aspect is specifically important in view of the modern CRAN paradigm.

Chapter 6 by Yu summarizes several different approaches for the realization of large capacity (>100Gb/s) fiber-wireless integrated systems, including optical polarization-division-multiplexing (PDM) combined with MIMO reception, advanced multi-level and multi-carrier modulation, antenna polarization multiplexing, and multi-band multiplexing. These spectral efficient modulation and multiplexing techniques are important for providing high-speed, high-capacity, free space transmission links as an alternative to fiber based mobile backhaul and fronthaul systems to overcome difficult terrains or fiber-cut.

Chapter 7 by Cvijetic and Wang introduces the reader to system-level challenges for SDN in fiber-wireless networks, including important aspects from both the control and data plane perspectives. The requirements for and ramifications of SDN-based control in fiber-wireless networks are examined, and a survey of recent research and development advances in SDN for fiber-wireless (at both the system and network levels) is also presented.

Chapter 8 by Liu reviews several existing and emerging fiber-wireless access networks including macrocells, small cells, distributed antenna systems, and cloud RAN. A novel cloud radio-over-fiber access network is subsequently introduced as a promising fiber-wireless convergent access architecture for future 5G networks. Proof-of-concept experiments are presented to demonstrate multi-operator/multi-service infrastructure-sharing capabilities in the cloud-RoF systems.

Chapter 9 by Ellinas et al., reviews passive optical network (PON) architectures as it is generally accepted that fiber deployment to cell towers is the only future-proof solution to build mobile backhauls, which will scale to the increased capacity requirements of future NG-WBAN technologies. Further, among the optical network architectures, PONs meet the needs for such a high-capacity access architecture. Different PON technologies, including TDM-PON, WDM-PON, OFDM-PON, and hybrid TDM-WDM, OFDM-WDM co-designs are described, followed by PON technology standards (GPON/EPON, 10G-PON, 10G-EPON, NG-PON2) and evolutionary scenarios. A novel fully distributed ring-based WDM-PON architecture is subsequently introduced as a promising access architecture that not only enables the support of a converged 4G/5G mobile infrastructure but also supports distributed network control as well as management operations.

Chapter 10 by Carapellese, Shamsabardeh, Tornatore, and Pattavina focuses on the role of BBU hoteling in fiber-wireless converged architectures. A classification of the various architectural solutions for BBU hoteling is given, regarding BBU placement and implementation, and fronthaul transport. The authors introduce a novel network optimization problem, namely the BPTR (BBU Placement and Traffic Routing) problem, which addresses the questions of “how and where to place the BBUs” so as to minimize the number of hotels or the transport capacity of the network.

Chapter 11 by I, Huang, Duan, Li, and Cui follows a different, evolutionary approach for 5G systems termed “No More Cells” (NMC). NMC transfers the

traditional cell-centric network design to a user-centric design principle. It is pointed out that NMC realization could be facilitated by the CRAN architecture, which is demonstrated and verified through extensive field trials.

Chapter 12 by Bertin, Mamouni, and Gosselin discusses how to realize convergence in the framework of the Next Generation Point of Presence (NG PoP). The NG PoP is a new concept of a flexible platform in the telecom network hierarchy that combines aggregation of fixed and mobile access traffic, IP edge routing, and the ability of hosting additional network functions and services. In addition, two more essential concepts in the path towards convergence are introduced, namely the converged subscriber data and session management and the universal access gateway.

Chapter 13 by Yang, Lim, and Nirmalathas provides a brief introduction on the cooperative multiple point (CoMP) technologies and the backhaul requirements for enabling CoMP techniques in LTE-A. The CoMP backhaul architectures and CRAN configurations based on various RoF technologies are also presented.

Chapter 14 authored by several of the researchers working on the EU project CONTENT proposes a next-generation converged infrastructure to support fixed and mobile cloud computing services. The proposed infrastructure facilitates efficient and seamless interconnection of fixed and mobile end users to computational resources through a fiber-wireless convergent network. The proposed architecture is well aligned and fully compliant with current SDN paradigms.

Finally, the conclusion elaborates on the diverse contributions of the book and how these contributions are brought together toward the ultimate goal, namely the implementation of the 5G mobile access network. Further, it overviews a set of rising and recent areas of research which have been emerging during the preparation of the book, such as the impact of Internet of Things and Mobile Edge Computing on fiber-wireless convergence, as well as the new proposals of “mid-haul” solutions (also called “split function” solutions) to decrease the fronthaul traffic on CRAN. Since energy efficiency becomes a critical challenge of 5G systems, a short discussion is also included on potential solutions to this issue, including recourse a location, network planning, renewable energy, and hardware architectures.

Massimo Tornatore  
Gee-Kung Chang  
George Ellinas

## References

1. Alamouti S (2012) Networks of the future—Some challenges ahead, wireless communication and networking conference (WCNC), keynote speech
2. Lee D, Seo H, Clerckx B, Hardouin E, Mazzaresse D, Nagata S, Sayana K (2012) Coordinated multipoint transmission and reception in LTE-advanced: deployment scenarios and operational challenges. *IEEE Commun Mag* 50(2):148–155

3. Pi Z, Khan F (2011) An introduction to millimeter-wave mobile broadband systems. *IEEE Commun Mag* 49(6):101–107
4. Yu J, Chang G-K, Jia Z, Chowdhury A, Huang M-F, Chien H-C, Hsueh Y-T, Jian W, Liu C, Dong Z (2010) Cost-effective optical millimeter technologies and field demonstrations for very high throughput wireless-over-fiber access systems. *IEEE/OSA J Lightwave Technol* 28(16):2376–2397
5. Gosselin S, Pizzinat A, Grall X, Breuer D, Bogenfeld E, Krauß S, Torrijos Gijón J, Hamidian J, Fonseca N, Skubic B (2015) Fixed and mobile convergence: which role for optical networks?. *IEEE/OSA J Lightwave Technol* 7(11):1075–1083

**Part I**  
**The Path Towards Convergence**

# Chapter 1

## Future Radio Access, Wi-Fi-LTE, LTE-Advanced: The Path to 5G

Rajarajan Sivaraj and Prasant Mohapatra

**Abstract** With the proliferation of IP-based bandwidth-intensive video services and smartphones, there has been an unprecedented exponential increase in mobile broadband data. This has resulted in increasing demand for additional wireless capacity. In order to increase the wireless capacity multifold, the next-generation radio access networks (RAN) boast of a number of sophisticated technologies, such as Carrier Aggregation (CA), Evolved-Multicast/Broadcast Multimedia Services (eMBMS) using Single-Frequency Networks (SFN), enhanced Inter-Cell Interference Coordination (eICIC) in self-organized Heterogeneous Networks (HetNets), Coordinated Multi-Point (CoMP) transmission in Multiple-Input–Multiple-Output (MIMO) systems using 2D/3D Beamforming, and full-duplex communication. Some of the above technologies are standardized in 3GPP Release 10+ systems like LTE-Advanced and are seen as a roadmap to 5G RANs. This chapter provides a comprehensive overview of each of these technologies and surveys the key open issues concerning them in terms of radio resource management (RRM) to facilitate maximum wireless capacity and provide Quality-of-Service (QoS) to the users. It also explores the synergies between these technologies towards developing holistic optimization techniques for the design of 4G+ and 5G systems.

### 1.1 Introduction

Recent proliferation of mobile broadband data is accelerated by the unprecedented increase in the subscription of next-generation bandwidth-intensive multimedia services by IP-based smartphone and tablet/computer users. 3GPP LTE, the latest 4G wireless broadband standard based on OFDMA, promises higher data rates than its predecessors from the legacy 3GPP systems. This is due to the independently modulated orthogonal and flat-fading sub-carriers that constitute a frequency-selective OFDM carrier. Furthermore, the multi-user diversity feature of OFDMA enables

---

R. Sivaraj (✉) · P. Mohapatra  
Department of Computer Science, University of California, Davis, CA, USA  
e-mail: rsivaraj@ucdavis.edu

multiplexing different users with different requirements, by supporting different Modulation and Coding Scheme (MCS) rates on every sub-channel. However, the LTE operators face a significant challenge in satisfying the Quality-of-Service (QoS) demands of the multimedia services, such as HD video streaming/gaming and video broadcast, due to the limited and expensive resources of the licensed spectrum. This challenge is further compounded by the channel dynamics of the network due to factors such as user mobility, inter-cell interference, fading, and attenuation. Especially, the users close to the cell edges are significantly penalized. This is because of their poorer channel quality that they are not being allocated adequate radio resources to satisfy their QoS [1].

An effective Radio Resource Management (RRM), accounting for the dynamic channel characteristics and traffic demands of the user, is essential in meeting the QoS objectives of the services offered by the network operator, and in turn enhancing the Quality-of-Experience (QoE) of the subscriber. Hence, an efficient RRM strategy calls for continuous innovation in the state of art for network configuration, effective deployment, and utilization of the spectrum resources to improve the system performance. This chapter provides a comprehensive overview on the latest advancements in RRM techniques that serve as a roadmap to 5G telecommunication deployments. It also delineates the challenges and open issues associated with each of these techniques. The 3GPP Release 10+ standardizes some of the techniques detailed in this chapter.

LTE-A aims to meet the advanced requirements of International Mobile Telecommunications (IMT) to support high downlink data rates of up to 1 Gbps for low-speed mobile or stationary User Equipments (UE) or 100 Mbps for high-speed mobile UEs and peak uplink rates of up to 500 Mbps, for facilitating the next-generation telecommunication services. IMT requirements for LTE-A generally aimed at improving the average performance and spectral efficiency of cell-edge UEs, rather than enhancing the peak spectral efficiency of individual applications (such as VoIP) [1].

### ***1.1.1 LTE Principles of Operation and Deployment***

Each LTE mobile network operator is auctioned chunks of licensed frequency sub-bands. A licensed frequency sub-band deployed over each LTE base station, called Evolved Node B or alternatively, eNB, with scalable bandwidths ranging from 1.4 to 20 MHz (that includes 1.4, 3, 5, 10, 15, and 20 MHz), is called a Component Carrier (CC). Each CC consists of orthogonal, independently modulated and flat-fading sub-carriers (where a single distinct modulation scheme is used within the frequency domain of one sub-carrier), such that each sub-carrier has a phase shift of  $90^\circ$  with the adjacent ones [2, 3]. Each sub-carrier in LTE is 15 kHz in bandwidth. There are around 1200 sub-carriers in a 20-MHz CC. Each LTE frame consists of 10 sub-frames of 1 ms duration each. The minimum unit of radio resource allocation in the two-dimensional time–frequency domain is a Physical Resource Block (PRB) [4]. It consists of 12 OFDMA sub-carriers, pointing to a frequency sub-band

chunk, from the frequency domain and 7 symbols or a half sub-frame (0.5 ms) from the time domain. The bandwidth of a PRB is 180 kHz. Considering the compromise in bandwidth due to the guard band interval between sub-carriers needed to preserve orthogonality, mitigate inter-symbol interference, and maintain significant cyclic prefixes, the number of PRBs in a 20-MHz CC is 100. Any User Equipment (UE), admitted for service by an LTE eNB, is allocated at least two PRBs. Each UE sends channel quality feedback to the eNB, which uses this information to choose an appropriate Modulation and Coding Scheme (MCS) rate, supported by the UE, for encoding the data signals to be transmitted to the UE. The encoded data rate is a function of the MCS, where a higher MCS rate indicates a higher amount of data delivered to the UE. The recent advancements in radio access technologies are broadly based on the following principles:

**a. Bandwidth aggregation:** This technique is employed to increase the bandwidth of the radio access network by aggregating spectrum resources, deployed in the form of Component Carriers (CC). It is one of the design techniques supported in LTE-Advanced systems from 3GPP Release 10 onwards, standardized by the term Carrier Aggregation (CA) [4, 5]. More than one CC, belonging to the same or different central band frequencies, are integrated as an aggregated carrier and deployed over the LTE eNBs. At most 5 different CCs can be aggregated and deployed over an LTE eNB, resulting in a maximum possible bandwidth of 100 MHz. Hence, a LTE-A eNB supporting CA can serve more than one cell, as shown in Fig. 1.1. Theoretically, CA facilitates peak downlink rates of up to 1 Gbps for stationary/low-speed mobile UEs and around 100 Mbps for high-mobile UEs [1].

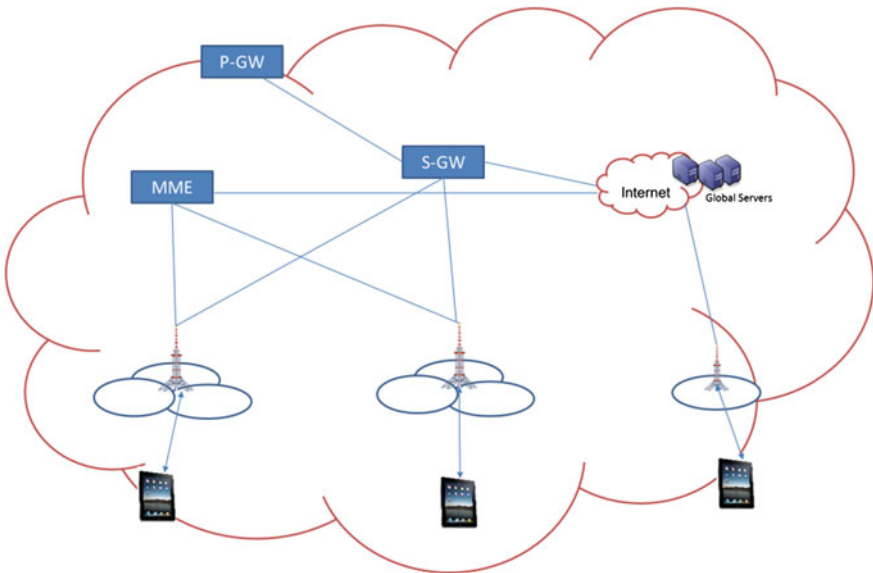
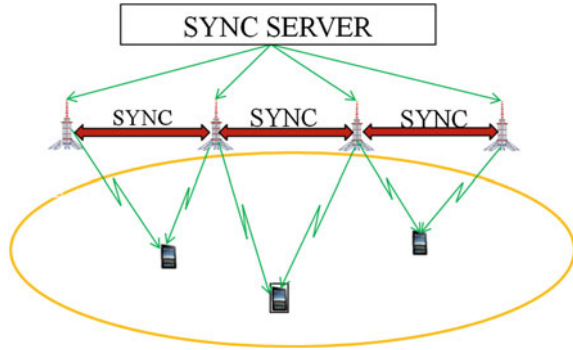


**Fig. 1.1** Carrier aggregation serving more than one cell per eNB

**Fig. 1.2** Synchronized eNBs serving UEs



**b. Transmission diversity:** In this technique, the same information signals are transmitted from more than one eNB that are synchronized to jointly schedule the UEs, as shown in Fig. 1.2. The CCs deployed across the synchronized eNBs belong to the same central band frequency, forming a Single-Frequency Network (SFN) [6–9]. The eNBs coordinate with each other to schedule a common set of UEs on the same PRBs across the eNBs using the same MCS rates, based on the radio channel characteristics from each synchronized eNB. This results in constructive interference at the UE and causes diversity gains, due to a decrease in the number of interfering eNBs and (consequently) an increase in the number of signal-transmitting sources. This principle is used in Evolved-Multicast Broadcast Multimedia Services (eMBMS) feature of LTE [6], standardized in 3GPP Release 8, and in Coordinated Multi-Point transmission feature (CoMP), supported by LTE-Advanced [1]. While the former leverages the diversity gains to improve multicast performance, the latter enhances the performance of cell-edge UEs that otherwise have a higher cell-outage probability.

**c. Network Heterogeneity:** This design principle aims at enhancing the performance of LTE macrocell networks through small-cell deployments, as shown in Fig. 1.3. Small-cell eNBs are cheaper, lower power eNBs that are densely deployed within the coverage region of one or more LTE macro-eNBs [10, 11]. A dedicated set of radio resources are deployed in the form of CCs over the small-cell eNBs. This increases the network capacity, especially when the macro-cell eNBs face a shortage of residual resources in case of high data demand. Small-cell deployments also provide extended network coverage to macro-cell UEs, especially to the ones at the cell edges of the macro. LTE-Advanced small cells typically use CCs belonging to the same central band frequencies as the ones in the macrocell eNBs, resulting in higher frequency reuse. However, the deployment can lead to high co-channel interference, if resource sharing is not carefully planned. The UEs in the network have a larger degree of freedom in their cell association, as each of them could associate with either one of the small cells or an interfering macro.

**d. Spatial diversity and multiplexing:** Spatial diversity employs at the eNB multiple transmit antennae with identical design that are physically separated from each other, usually by at least a half-wavelength. In conventional single-stream

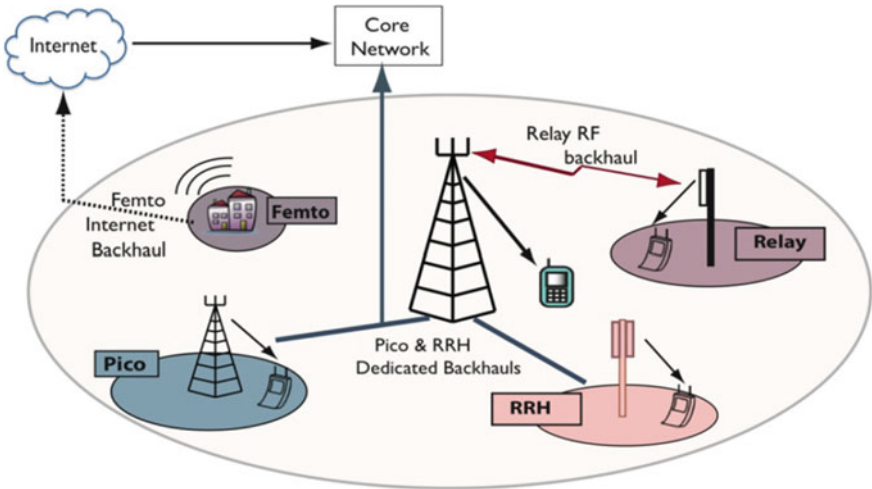


Fig. 1.3 Coexistence of heterogeneous transmission devices (macrocell, small cells)

beamforming, the same signal is transmitted from each transmit antenna in the array with appropriate weights, based on phase and channel gain, so as to maximize the throughput. Antenna arrays mitigate the destructive multi-path interference among the reflections of the transmitted signal by leveraging the different transmission and fading characteristics of each antenna with respect to the receiver, and combining them at the receiver. This improves the downlink channel quality at the UE. Spatial diversity is one of the operating principles used in Multiple-Input–Multiple-Output (MIMO) systems, shown in Fig. 1.4, where the downlink capacity is further enhanced by using multiple receiver antennae at the UE. In order to maximize the throughput of the UE equipped with multiple receiver antennae, a multi-stream transmission using spatial multiplexing is considered [12]. For a given sub-channel, a channel matrix is constructed for each eNB–UE pair from the channel quality value between each transmit–receive antenna pair. Multi-stream beamforming uses

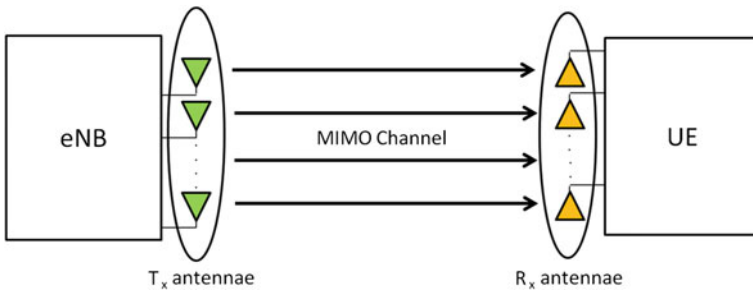


Fig. 1.4 Communication over a multi-antenna MIMO channel

this matrix to independently encode multiple data streams using a precoding vector and transmitting the information signals from each of the antennae in the array. This spatial multiplexing of different downlink data streams onto the MIMO channel exploits the additional degree-of-freedom gain, considering the varying channel characteristics between each transmit–receive antennae pair at the eNB and UE, respectively. Multiuser MIMO-OFDMA with 2D/3D-beamforming features is a recent sophistication, actively considered and tested in LTE-Advanced and 5G deployments.

The above principles are on the basis of LTE and will partake in shaping the 5G technology and, in turn, influence the backhaul infrastructure from the perspective of Fi-Wi convergence. This chapter discusses some of the open issues in each of the aforementioned radio access techniques from the perspectives of PHY and MAC layers. In the rest of this introductory section, we quickly introduce the main open issues at PHY and MAC layer that will be elaborated in the rest of the chapter.

**PHY Layer:** The challenges in the PHY layer are typically concerned with improving the channel quality of the users, e.g., increasing the Signal-to-Interference-plus-Noise Ratio (SINR) of the individual UEs. The factors that affect SINR include assignment of CCs to the UEs as the central band frequency of the CC impacts the path loss yielded to the UE, appropriate cell association based on its link quality with the UE, appropriate choice of precoding/beamforming vectors to manage the signal strength and inter-cell interference for the UEs multiplexed onto the MIMO channel, the number of eNBs synchronized in an SFN which impacts the diversity gain of the UEs served by the SFN, etc. The channel quality of the UEs helps in determining appropriate MCS rates chosen by the eNBs in serving the UEs and subsequently, the net system capacity. The crucial component in the net system performance is the channel quality of the cell-edge UEs. (e.g., in applications like eMBMS, the performance of a multicast/broadcast group is limited by the UEs, especially at the cell edges, who have minimum throughput).

**MAC Layer:** The issues in the MAC layer are centered on the allocation of frequency–time PRBs and scheduling them to the UEs. The key utility metrics in the MAC layer are throughput, fairness, and effective spectrum utilization. Throughput deals with achieving a higher net system capacity as a result of allocating PRBs and choosing appropriate MCS rates to serve the UEs, whereas fairness deals with allocating a fair share of PRBs to every UE in the network, accounting for its radio channel characteristics and traffic dynamics. Scheduling schemes like Proportional Fairness (PF) [13] balance the trade-off between throughput and fairness, where the related system utility function is seen as a logarithmic function of the throughput rates. Scheduling frequency–time PRBs to the UEs in the network impacts the Quality-of-Service (QoS) of the applications served by the eNBs and helps in evaluating related performance metrics, such as call/session admissibility.

Effective spectrum utilization is a measure of the fraction of the net deployed frequency–time PRBs that is scheduled to the UEs with appropriate MCS values. A higher value of this metric indicates that the licensed spectrum resources (in the

form of PRBs) are being effectively deployed by allocating them appropriately to the UEs. Proportional Fair (PF) schedulers are also used to enhance the effective spectrum utilization of the eNB, as the sum of the logarithmic rates of the UEs would be higher if the eNB schedules a larger number of UEs with the best-possible MCS rates. The linear additive factor in the sum log rate helps in serving higher number of UEs and the log factor in the metric helps in ensuring fairness to each of them.

## 1.2 Carrier Aggregation

### 1.2.1 Definitions and Terminologies

3GPP LTE-Advanced (LTE-A) attempts to serve the next-generation telecommunication services, such as real-time high-definition video streaming, mobile HDTV, and high-quality video conferencing. LTE-A facilitates higher data rates in response to the requirements proposed by IMT-Advanced for providing higher QoS to mobile applications. LTE-A provides peak uplink and downlink data rates of 500 Mbps and 1 Gbps, respectively, for low-speed UEs and around 100 Mbps for fast-moving users [14, 15]. The bandwidths of LTE-A systems in both uplink and downlink can go up to 100 MHz, achieved by the aggregation of individual CCs through Carrier Aggregation (CA). Each CC corresponds to a cell or a coverage region and serves the UEs present in the region, which are associated with the cell. So, an LTE eNB supporting CA can serve more than one cell. An LTE-A Release 10+ UE can be scheduled on more than one CC, unlike an LTE Release 8/9 UE that can be scheduled on at most one CC. However, LTE-A UEs, supporting CA, are backward-compatible with LTE UEs, supporting operation on only one CC at the eNBs.

When an LTE-A UE attaches to an eNB and establishes or re-establishes a radio resource control connection with the eNB, only one cell corresponding to a CC is configured for the UE. This is termed as the primary cell. The CC corresponding to the primary cell is termed as primary CC. Then, depending on the serving traffic load on the primary CC and the Quality-of-Service (QoS) requirements of the UE, additional serving cells can be configured on the UE, termed as secondary cells [14]. The CCs corresponding to the secondary cells are called secondary CCs. Hence, an LTE-A UE can be associated with more than one cell. For every LTE-A UE, the primary cell is configured mandatorily, and the other configured secondary cells are based on the QoS requirements of the traffic profiles subscribed by the UE. The primary CCs across the LTE-A UEs need not be the same as in the aggregated carrier; they are UE-specific and can be different for different UEs served by the eNB. While both the primary and secondary CCs are involved in scheduling their PRBs to the UEs, the additional responsibility of the primary CC is to maintain the Radio Resource Control (RRC) connection of the corresponding UEs, which

includes state information about location registration, connection establishment/re-establishment, termination, and handover. An LTE-A UE has only one RRC connection with the network. It establishes/re-establishes the RRC connection (using the random access procedure which registers the UE in the network) on the primary cell and uses additional RRC signaling to add, remove, or re-configure secondary cells. Hence, the primary CC for every UE cannot be changed dynamically as long as the UE is associated with an eNB, unlike the secondary CCs which can be dynamically configured and managed [5, 14, 15].

The PHY layer channel quality measurements taken by each UE are used to assist configuring, assigning, and managing CCs for the UE. The UE sends these channel quality values to the eNB using the uplink control channel on its primary CC. Although multiple cells are configured or assigned for an LTE-A UE, the UE is assigned a single-cell radio network temporary identifier, corresponding to the cell ID of the primary cell. This is used to uniquely identify the RRC connection of the UE for transmitting scheduling information on the downlink control channel corresponding to either the primary CC or the secondary CCs. The primary CC for a UE is selected through either a channel-aware or a traffic load-balancing technique. Typically, the former assigns the CC which yields the highest Reference Signal Received Power (RSRP, a measure of the received signal strength, discussed in Sect. 1.4.1) or conversely the lowest path loss to the UE, as the primary cell. Load-balancing can be used to designate the primary and secondary CCs. The CC with the highest number of residual PRBs, after serving the current traffic load, is selected as the primary CC for the UE. This is done to make sure that adequate PRBs are available to be allocated to the UE to satisfy its traffic demands. Additionally, this also helps in preventing resource exhaustion.

## 1.2.2 Types of Carrier Aggregation

The types of CA [16, 17] are as follows

a. **Intra-band contiguous CA** manages the aggregation of CCs in adjacent frequencies of contiguous bandwidths from the same frequency band [5]. It is the easiest to implement as the CCs are adjacent to each other. The aggregated carrier is considered as a single enlarged wideband channel from the RF standpoint and hence, the UE requires only one transceiver. Even with the aggregated increase in bandwidth, the power consumption and cost requirements are considerably less stringent allowing for greater flexibility in RF design due to the already-existent multi-carrier nature of OFDM-enabled eNBs. However, it is difficult for the operator to obtain a contiguous large chunk of aggregated bandwidth, say up to 100 MHz, during the auctioning process due to competitive bidders, limited availability, and expensive deployment of licensed spectrum resources.

b. **Intra-band non-contiguous CA** manages the aggregation of CCs from non-adjacent, non-contiguous sub-band frequencies belonging to the same frequency band [5]. This design is more complicated than intra-band contiguous CA,

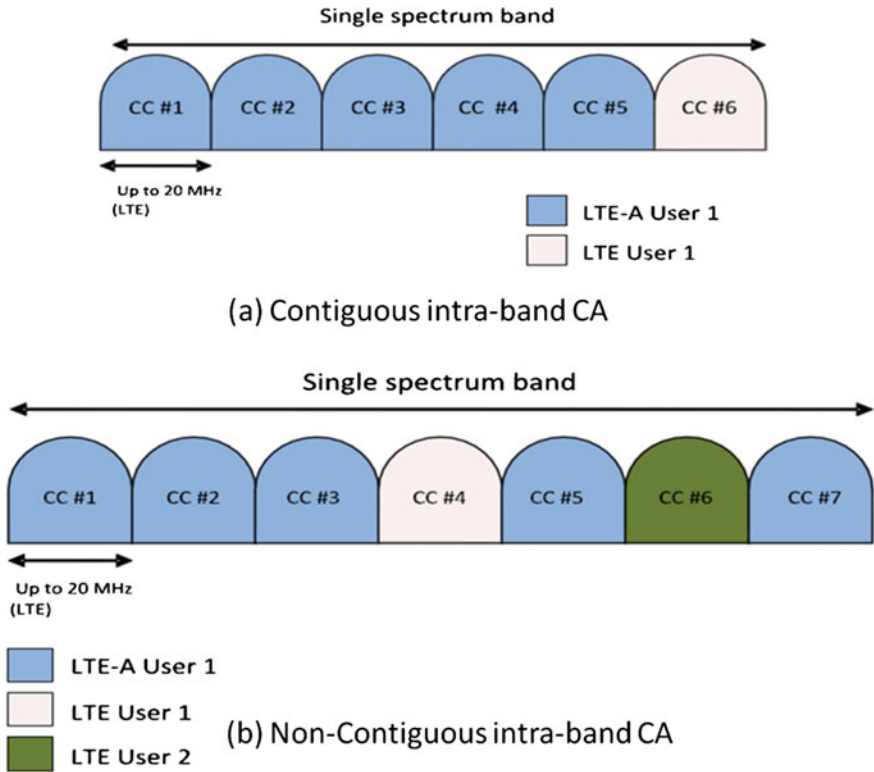


Fig. 1.5 Intra-band carrier aggregation

as the multi-carrier signals from non-adjacent sub-bands can no longer be treated as a single distinct signal, thus requiring two or more transceivers. This adds complexity to the RF design in terms of power consumption and cost. However, this addresses the challenge in allocating large chunks of aggregated bandwidth due to the non-contiguity nature in the auctioning and deployment of non-adjacent CCs to every bidding mobile operator.

Moreover, the radio channel characteristics yielded by the CCs from the intra-band non-contiguous CA to any UE are not drastically different from each other, except for the random slow and fast-fading attenuations and Doppler shifts, as the CCs correspond to the same frequency band. An illustration of intra-band contiguous and non-contiguous CA is shown in Fig. 1.5.

c. **Inter-band non-contiguous CA** manages the aggregation of non-adjacent CCs belonging to different frequency bands [5]. The fragmented frequency sub-band chunks that are aggregated as CCs at the eNB are of varying bandwidths. As network operators may not win adjacent spectrum slots, they also aggregate bandwidths that may be not contiguous. Moreover, since each CC corresponds to a different central band frequency, the transmission characteristics such as path loss,

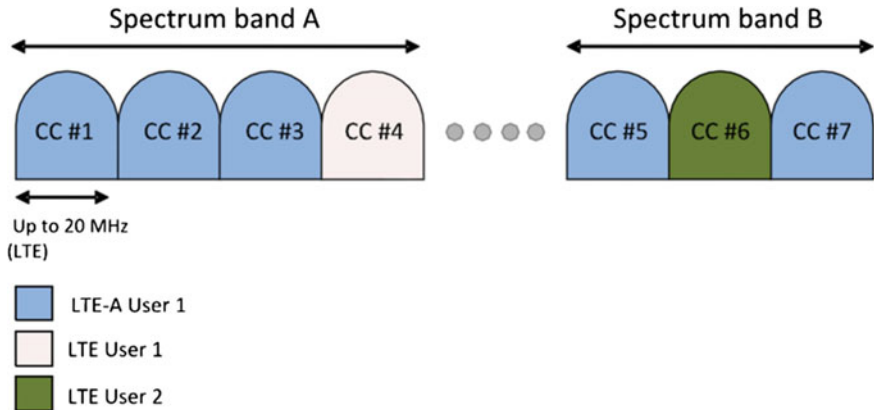


Fig. 1.6 Inter-band carrier aggregation

Doppler shifts, fading and attenuation, pertaining to each CC, are different from one another. This results in different received signal values from each CC, measured by the corresponding RSRP values, as shown in Sect. 1.4.1. Figure 1.6 shows aggregation of CCs from different frequency bands. Hence, the different combinations of one or more CCs yield varying multiplexing gains for any UE, while being assigned to it. The UE requires the use of multiple transceivers to transmit/receive signals to/from the different aggregated CCs, thereby introducing additional complexity to the RF design in power and cost, as in the case of intra-band non-contiguous CA.

Carrier Aggregation is possible in both uplink and downlink directions. While there are a good number of similarities between uplink [4, 18] and downlink CA, in the following we highlight the significant differences between these two forms of CA.

**Uplink CA:** The performance of uplink CA is limited by the transmission power at the UEs. This limits the UEs from having high data rates yielded by the large bandwidths facilitated by CA. When LTE-A UEs transmit bandwidth-intensive multiple applications like HD videos in the uplink, they require being allocated larger PRBs and using higher modulation rates, in order to satisfy QoS and to make maximum usage of the allocated bandwidths, respectively. Both of these requirements increase the Peak-to-Average Power Ratio (PAPR) [19] at the UEs and hence, result in a higher consumption of battery life at the UEs. The expected transmission power (in dB) for UE  $u$  as a result of transmitting to eNB  $m$  on CC  $c$ , given by  $P'_{u,m,c}$ , is given in [4].

In order to reduce uplink power consumption, LTE uses Single-Carrier FDMA (SC-FDMA) [20] in the uplink, where the entire CC is available for the UE as a single channel, but the symbol time is of a much shorter duration, when compared to OFDMA. SC-FDMA requires allocation of contiguous PRBs across the deployed CC to each UE and this reduces the PAPR of the UE in the uplink. Moreover, the

peak modulation rates availed by using SC-FDMA in the uplink are comparatively smaller than the ones obtained by using OFDMA in the downlink. Usage of higher MCS rates requires lower PRBs to be allocated to any UE for satisfying its QoS. But using higher rates increases the PAPR. On the other hand, using lower MCS rates requires using larger PRBs to be allocated to the UE. But, even larger PRBs increase the PAPR, as shown in [4]. However, a linear increase in PRBs only results in a logarithmic increase in the UE's transmission power. So, SC-FDMA manages this trade-off by using lower peak modulation rates and contiguous chunk of PRBs, for which a collective feedback is sent less frequently.

**Downlink CA:** The eNBs are not so limited by power in their downlink as the UEs, in the uplink. So, LTE uses OFDMA in the downlink that supports higher peak MCS rates, thereby resulting in an increased PAPR. In the downlink, OFDMA also supports allocation of non-contiguous independently modulated PRBs to the UEs so as to maximize the gains resulting from frequency diversity. While most of the issues pertaining to RRM and cell-edge user performance [4] are applicable to downlink CA, the exclusive aspects of downlink CA deal with Evolved-Multimedia Broadcast/Multicast Services (eMBMS) [21, 8] and MIMO features in LTE-A. For video multicast/broadcast, the eNB serves groups of UEs, who collectively subscribe to the same multimedia content called session, on a common set of PRBs using common MCS rates [6].

The performance of a multicast/broadcast session is limited by the UE with the poorest channel conditions (especially those around the cell edges), as the throughput of a session is defined as the minimum throughput achieved by any UE, who subscribes to the session. This UE with the poorest channel conditions is designated as the bottleneck UE for the session. So, the MCS rate allocated by an eNB to serve a session would be the lowest rate supported by any UE in the corresponding eMBMS group.

Especially, when both cell-center and cell-edge UEs are a part of an eMBMS group, the poorer channel conditions of the cell-edge UEs and the lower MCS rates supported by them would drastically bring down the performance of the cell-center UEs in the group that exist with much better channel conditions [22]. Now, when UEs with drastically different channel conditions are grouped together, the eNB needs to jointly account for the channel dynamics of each individual UE along with the QoS requirements of the entire session in allocating PRBs. Due to the above requirements, in video multicasting services over LTE-A systems supporting CA, a common set of one or more CCs should be assigned to serve each group using the PRBs that constitute the CC(s) [23, 24]. There should be one common primary CC to carry out RRC-related functionalities for the entire group, which is a major challenge, as each UE in the network may choose a different primary CC from the rest due to varying channel conditions, traffic and mobility patterns. Similarly, the other optional secondary CCs, if configured based on the QoS requirements for the session, must also be common for the entire group. However, the key difference here is that the choice of selection of secondary CCs, allocation of PRBs, and assignment of MCS values to the eMBMS groups for QoS need not be limited by

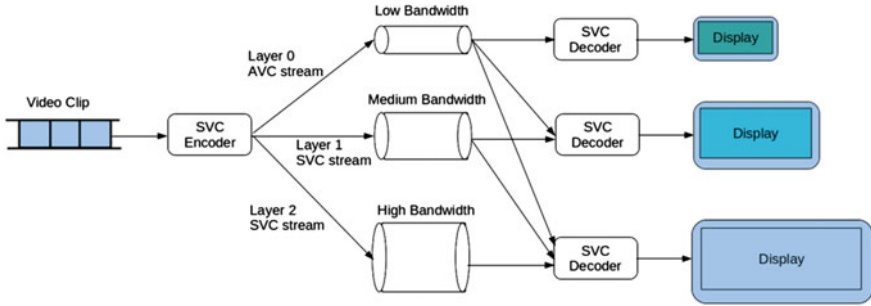


Fig. 1.7 Scalable video coding

the UE with the poorest channel conditions in each group. Let us understand this better via the following illustration (Fig. 1.7):

**Illustration:** We provide a simple illustration to discuss video multicast for downlink CA [25, 26] that downstreams a given source video into several independently encoded bit streams called layers with different resolution. The layer with the minimum resolution that can be supported by even lower underlying network bandwidths is called base layer, and the other layers are called enhancement layers. Now, to facilitate scalable video multicast over LTE-Advanced systems supporting CA, the mandatory base layer, which must be decoded by every UE in the eMBMS group, is scheduled over the primary CC, designated for the group. This selection of primary CC is, in turn, based on the channel dynamics of each UE present in the eMBMS group. As mentioned earlier, the primary CC is chosen based on either a channel-aware or a traffic load-balancing technique. Accordingly, the allocation of the primary CC should be such that it yields the required channel conditions and residual PRBs, adequate enough to provide the highest-possible data rates to the bottleneck UE for the session and/or satisfy its QoS requirements. In inter-band aggregated carrier, the primary CC for the group is usually considered as that CC corresponding to a lower central band frequency and that has a higher number of residual PRBs. A CC with a lower central band frequency yields a lower path loss value to the UEs of the group, especially crucial to those present around the cell edges. Hence, this results in the primary CC providing sufficient channel conditions required to decode the mandatory base layer of the HD video by all UEs (incl. the cell edge UEs) of the group that subscribe to the video. If the bandwidth offered by the primary CC is sufficient to serve the mandatory base layer specified by the Guaranteed Bit Rate (GBR), which is ensured by the operator to the session subscribers, then the optional enhancement layers are served to the group on the secondary CCs configured for the group [3, 22]. Now, the enhancement layers are not mandatory to be served; however, a higher number of enhancement layers served with best effort for the group subscription increases the overall session throughput, having as an upper bound the maximum bit rate (MBR) [3, 22]. So, the optional secondary CCs can schedule the enhancement layers, and the choice of

PRBs and MCS rates on the secondary CCs is not limited by the bottleneck UE of the eMBMS group subscribing to the session.

### 1.2.3 Radio Resource Management Framework for CA

The functionalities of the RRM framework for an LTE-A system supporting CA [27] are shown in Fig. 1.8. The eNB performs session admission control based on the QoS requirements and service class priorities of different UEs. A new RRM functionality, added to LTE-Advanced, is Layer-III CC Assignment and Configuration which configures and assigns a set of CCs for each UE. The other RRM functionality is Layer-II Packet Scheduling, which deals with the allocation of PRBs to the different UEs that are multiplexed on each CC assigned in the set.

**Component Carrier Assignment and Configuration:** The CC set is the collection of CCs where the UE may later-on be scheduled on its PRBs. The assignment and configuration of the CC set to the UEs is a Layer-III functionality in the LTE/LTE-A protocol stack for RRM and happens with RRC signaling to the UEs. The CC configuration functionality is important in optimizing throughput, fairness, power consumption, [4], etc. The QoS requirements, radio channel conditions, and UE capability like residual power, SNR, and antenna configuration are taken into account for assigning and configuring the CC set to the UEs.

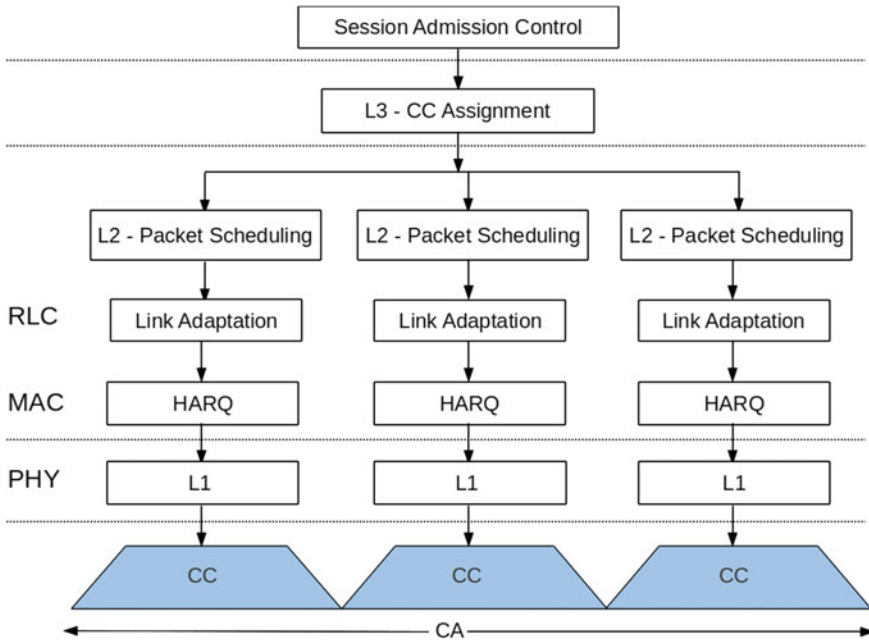


Fig. 1.8 Radio resource management framework for CA

The dedicated bearer established between the UE and the core network, corresponding to the traffic subscribed by the UE, communicates its QoS requirements in terms of the Guaranteed Bit Rate (GBR), Aggregate Maximum Bit Rate (AMBR), packet delay, loss rate tolerance, etc., indexed by the QoS class identifier [3]. Recalling the illustration above, the GBR traffic (corresponding to an SVC-encoded session's base layer), identified by a corresponding lower bound, can be assigned onto the primary CC and served for its QoS requirements to the UEs/eMBMS groups, subscribing to it. If the UEs/groups subscribe to a best-effort traffic, limited by an upper bound MBR/AMBR, then both the primary and the optional but dynamically (de-)activated secondary CCs can be invariably used to schedule the subscribed traffic (similar to serving the best-effort enhancement layers up to the MBR). The algorithms for CC assignment and configuration are open issues and are specific to eNB vendors; however, the assignment falls under the following categories:

- **Channel-blind CC Assignment:** Here, the assignment of the CCs to the UEs is agnostic of the radio channel characteristics of the UEs and is done based on balancing the traffic load served on all CCs in the set, such that each CC approximately serves equal amount of load. Some of the widely adopted techniques in a channel-blind assignment [27] include (i) Round-robin balancing, where a newly arriving UE is assigned to the CC that has the least number of UEs as the primary CC, thereby evenly distributing the load across all CCs, and (ii) Mobile hashing, where a hashing algorithm is used at the UE's end for choosing its primary CC and subsequently, establishing the RRC setup between the eNB and the UE. The output hash values are uniformly distributed among a finite set that maps on to the CC indices, thereby aiming to provide a balanced load across the CCs. The secondary CCs are similarly subsequently chosen for a UE based on its QoS specifications. Channel-blind CC assignment is mostly used for intra-band CA.
- **Channel-aware CC assignment:** The CC assignment is cognitive of the radio channel characteristics of the UEs and is widely used in inter-band CA. One of the standard techniques employed is a path loss-based CC assignment that accounts for the central band frequency of each CC in the set. Two techniques widely used in a channel-aware CC assignment include (i) throughput-based assignment [13, 28], where the UEs are sorted in decreasing order of their channel access probabilities and are assigned CCs which yield lower path loss values (usually, lower than a pre-defined threshold), and (ii) edge-prioritized CC assignment [4], which is usually done to increase the net system fairness. This sorts UEs in increasing order of their overall channel quality, with the UEs having poorer channel conditions preceding those having stronger channels. The assignment follows a similar path-based approach to UEs in the sorted order. Channel-aware CC assignment, however, needs further optimization, to evenly balance the load across the CCs.

**Downlink Packet Scheduling:** Packet scheduling is a dynamic Layer-II RRM functionality at the MAC layer of the LTE/LTE-A protocol stack and is responsible for scheduling UEs across their assigned, configured and activated CCs. It takes care of allocating the PRBs of the activated CCs, corresponding to the primary and secondary cells, to the UEs. In scheduling the PRBs to the UEs, this functionality leverages the multiuser diversity feature which supports multiplexing different UEs with different MCS values (based on the UEs' channel quality) on each independently modulated frequency sub-channel of the CC across sub-frames in the time domain. When two or more UEs are assigned onto a common CC, the individual PRBs must be scheduled to the different UEs, so as to avoid resource conflict and contention among UEs. The PRBs yield different rates to different UEs. Scheduling can be done in parallel across each individual CC in the set, including some coordination among CCs in the set to ensure optimal system performance and joint controlled signaling for UEs assigned onto multiple CCs. LTE-Advanced facilitates cross-CC scheduling which allows the eNB, supporting CA, to send scheduling grants for each UE for data transmissions corresponding to multiple CCs that are assigned to it, on the primary CC. Cross-CC scheduling allows more than one CC to jointly serve any UE, wherein the traffic subscribed by the UE can be scheduled on PRBs from more than one CC. Different types of scheduling techniques [13] include

- **Maximum Throughput Scheduling:** This scheduling technique is used to achieve the highest-possible spectral efficiency, which results in maximizing the system throughput. The operating principle is to schedule any PRB from any CC to the UE, which reports the largest possible instantaneous wideband achievable throughput on that CC. This scheduling scheme has benefits in terms of cell throughput and spectral efficiency, but comes at the cost of fairness. UEs with poorer channel conditions, especially at the cell edges, either are allocated lower number of PRBs or face resource exhaustion.
- **Blind Equal Throughput:** This heuristic attempts to yield the same throughput for all UEs, regardless of their channel quality. The operating principle is to schedule any PRB from any CC to the UE which reports the lowest past-achieved throughput on that CC. This scheduling scheme has benefits in terms of cell throughput and spectral efficiency, but comes at the cost of fairness. UEs with poorer channel conditions, especially at the cell edges, either are allocated lower number of PRBs or face resource exhaustion.
- **Proportional Fair (PF) Scheduling:** This scheduling technique handles the trade-off between the system throughput and fairness [29]. The operating principle is to schedule any PRB from any CC to the UE which reports the maximum value of the ratio of its instantaneous wideband achievable throughput to its past-achieved throughput on that CC. Different scheduling algorithms can be used across the individual CCs aggregated in the set, based on the QoS requirements of the traffic served on each CC. The RRM functionalities in the MAC layer and the PHY layer are specific to each individual CC in the set. LTE-A supports independent transport blocks, link adaptation, and HARQ on a per-CC basis and accordingly implements the scheduler for each CC.

## 1.3 Transmission Diversity and Spatial Multiplexing

### 1.3.1 *Transmit Diversity—Definition and Terminologies*

Transmission diversity involves the simultaneous transmission of the same identically modulated information-bearing data signals to a UE or an eMBMS group of UEs, originating from two or more independent eNBs operating on the same central band frequency. This requires a tighter coordination among the eNBs, thereby allowing them to synchronously transmit the same data from the synchronized eNBs on the same set of PRBs using the same MCS value. This deployment of synchronized eNBs is called Single-Frequency Network (SFN) [7, 21].

The transmit diversity feature in an SFN addresses the problem of the variable transmission channel quality between the eNBs and the UE. Consider, e.g., a single transmit antenna at each eNB in the SFN and a single receive antenna at any intended UE served by the SFN. If a link between one of the eNBs and the UE/group undergoes a deep fade as a result of poorer channel conditions that affect the transmission, it is compensated by the combined effect of the links between other eNBs and the UE that may yield better received signal strength for the UE. The transmissions of the identical signals from multiple synchronized eNBs on the same PRBs yield a higher SINR as a result of this over-the-air combining effect. This is typically useful in improving the performance of cell-edge UEs in denser eNB deployments, whose channel conditions are marred by higher inter-cell interference. On the other hand, cascading the synchronization on data transmission and resource allocation across a higher number of eNBs would be detrimental if some of them do not contribute significantly to an increase in SINR for an average individual UE. This could amount to wastage of the deployed spectrum resources at such eNBs.

### 1.3.2 *MIMO and Spatial Multiplexing—Definition and Terminologies*

The Multiple-Input and Multi-Output (MIMO) technique requires the use of multiple antennae at both the transmitter eNB and receiver UE [30]. MIMO techniques such as beamforming, spatial multiplexing, and spatial diversity play a fundamental role in LTE-Advanced. Thus, in order to maximize the net downlink throughput for a multi-antenna receiver UE, MIMO leverages multi-stream beamforming, which sends multiple streams of UE-subscribed data signals with independent and appropriate precoded weights (based on phase and gain) over the multiple antennae equipped at the transmitter. Beamforming is a signal processing technique for directional transmission of signals by the eNB toward a particular direction in the cell or cell sector served by the eNB [12]. This steering of the beam toward a particular direction helps in increasing the received signal strength of the UEs

present in that direction, thereby enhancing spatial selectivity. This is done by combining elements in a phased array such that the relative phase and gain (amplitude) of the signals are controlled at each transmitter antenna so as to enable a constructive interference of the signals at the receiver UE. Let us assume that the eNB has  $t$  transmit antennae and the UE has  $r$  receive antennae. So, there are  $t$  parallel data streams with independently coded phase and gain weights, representing a vector  $\bar{x}$  of size  $t$ . If  $\bar{y}$  is the received signal vector for the UE over the  $r$  antennae, then we have  $\bar{y} = H\bar{x} + n$ , where  $H$  is an  $r \times t$  complex channel matrix, representing the channel gain values between the eNB and the UE accounting for the multiple antennae equipped at both the eNB and the UE, respectively, and  $n$  is the noise vector of size  $r$  at the UE. In this case, one of the widely used techniques to combine the received signal vector of size  $r$  at the receiver is Minimum Mean-Square error (MMSE) estimator [31].

**MIMO-OFDMA:** A linear MIMO-OFDM system is a system where the given frequency-selective channel in any CC is divided into a set of fixed parallel flat-fading, independently modulated sub-carriers. A group of 12 sub-carriers are combined to form a sub-channel, and these sub-channels are allocated to UEs for a pair of time slots, and the unit of frequency–time resources to be allocated to every UE is called PRB, as described earlier. This concept is called OFDMA, where different UEs can be simultaneously multiplexed on to the different sub-channels of the same CC with varying MCS rates. The flexibility of using different MCS rates for different UEs across sub-channels of the same CC during the same time is called multiuser (MU) diversity [32]. MIMO-OFDMA supports using different MIMO beamforming vectors simultaneously across sub-channels for scheduling UEs [16]. Figure 1.9 shows two different UEs with different beamforming vector weights from a single eNB, scheduled across 2 PRBs. MIMO-OFDMA is based on an extended version of space division multiple access (SDMA) [12] that allows multiple transmitters to send separate signals and multiple receivers to receive separate signals simultaneously in the same band.

### 1.3.3 Coordinated Multi-point Transmission

Coordinated multipoint (CoMP) transmission and reception techniques [33] utilize MIMO transmissions from multiple eNBs to enhance the received signal quality as well as decrease the received spatial interference. It is a framework that refers to a system where several geographically distributed antenna nodes on multiple synchronized eNBs cooperate with the aim of improving the performance of the users associated with the cells of the eNBs by choice of appropriate beamforming vectors. Figure 1.10 shows how two eNBs can choose appropriate beamforming vectors to serve the two UEs in the network, so as to address inter-cell interference. CoMP leverages both transmission diversity and spatial diversity to multiplex different UEs that support different data rates. It encompasses all required system designs to achieve tight coordination for transmission and reception. It serves two main

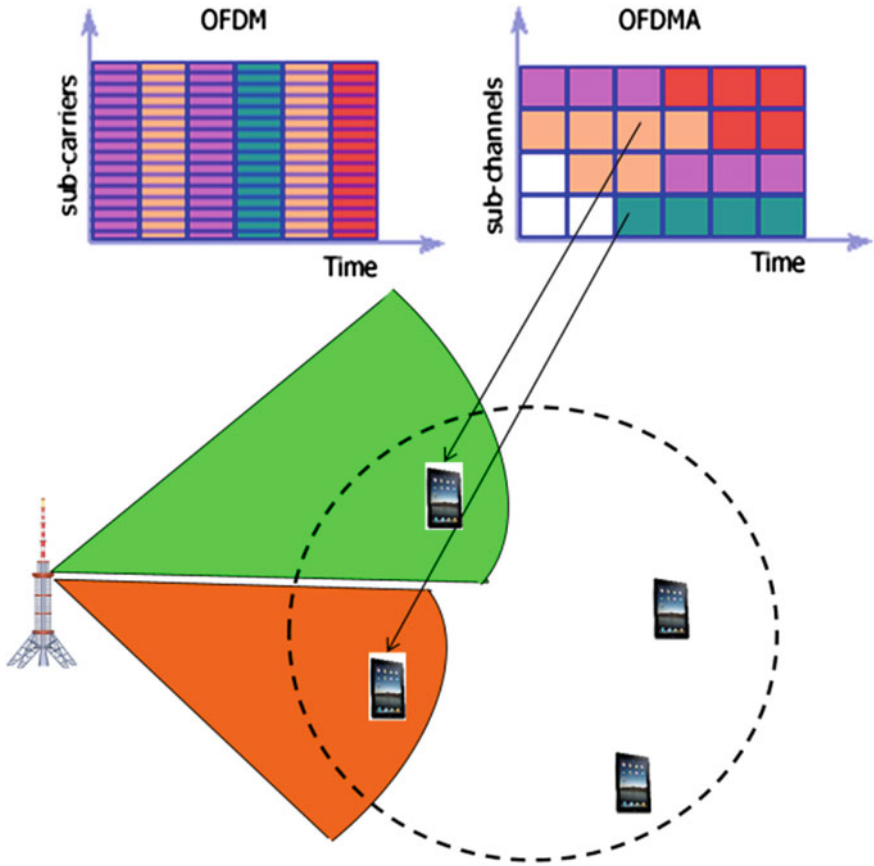


Fig. 1.9 Spatial multiplexing (MIMO OFDMA)

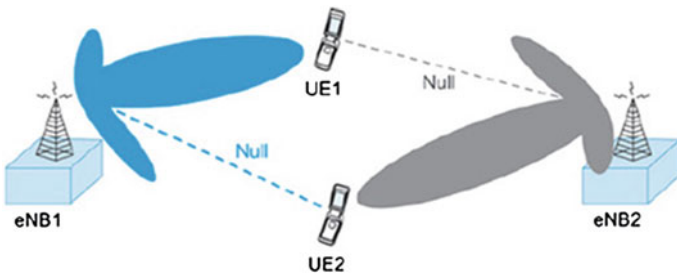


Fig. 1.10 Multi-cell beamforming

purposes: (i) increasing the received signal strength of UEs, and (ii) limiting the inter-cell interference among eNBs. Cooperation among eNBs is characterized by the need of an interconnection among the different nodes in the form of very

high-speed dedicated links like optical fiber, wired backbone connection, highly directional wireless microwave links, and RAN controller [1]. These low-latency links are essential for the success of the cooperative communication, although their design is a very challenging issue due to the large amount of data that may need to be exchanged among the nodes. LTE-Advanced uses the standardized interface  $\times 2$  for these purposes. CoMP extends the concept of MIMO to multiple cells and hence, uses multi-cell beamforming [34] techniques to maximize performance. Therefore, CoMP works on the principle of Network MIMO. Network MIMO is particularly important for users who experience channel gains on the same order of magnitude from multiple base stations.

The applicability of CoMP depends on the backhaul characteristics (latency and capacity), communication among the eNBs over the X2 interface, which condition the type of CoMP processing and the associated performance. In order to account for the various possible network topologies and backhaul characteristics, the study of CoMP in 3GPP has focused on scenarios which talk about (i) coordination between the cell sectors controlled by the same macro-eNB, (ii) coordination among cells belonging to different radio sites from a macronetwork, (iii) coordination among macro- and small cells in a HetNet, etc. The techniques associated with CoMP include (a) coordinated beamforming/scheduling and (b) joint scheduling.

**Coordinated beamforming/scheduling:** Coordinated beamforming, otherwise called multi-cell beamforming, enables multiple coordinated eNBs to share their channel state information (CSI) for multiple UEs with each other over the X2 interface. It should be noted that each of the UEs is associated with a single distinct eNB, among the coordinated set. The associated eNB serves it for its subscribed data signals. However, coordination is required to choose appropriate beamforming vector weights and transmission powers [35, 36] across the multiple eNBs to limit the inter-cell interference arising from transmissions from other eNBs in the coordinated set. This coordination among multiple eNBs for the choice of optimal transmission powers and appropriate beamforming vectors is required to improve the net system performance in terms of throughput (subject to fairness constraints), even as each eNB takes independent scheduling decisions to serve its associated UEs.

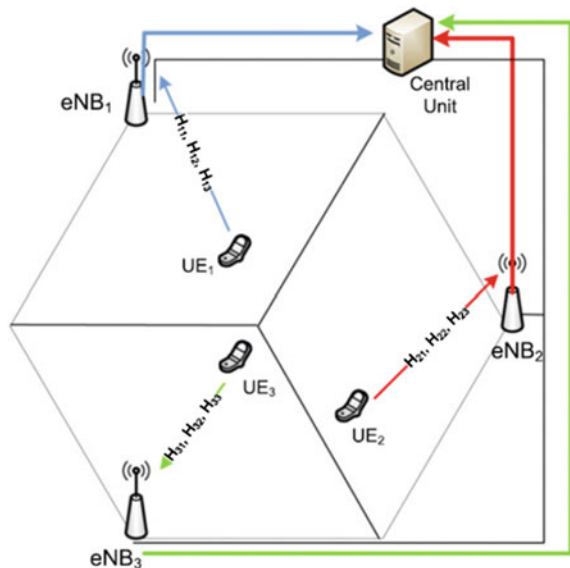
**Joint Processing:** Joint processing has two implementation techniques, which include (i) joint scheduling and (ii) dynamic cell selection [1, 33]. Joint scheduling has been discussed earlier in the context of transmission diversity. Dynamic cell selection is a joint processing scheme where the transmission to the intended UE only takes place from one eNB at a given time slot (usually, a sub-frame). This eNB must be drawn from the CoMP cooperating set serving the same UE. The most frequent switching between cell association for a given UE can happen on a sub-frame-by-sub-frame basis, thus allowing for a dynamic change in the associated eNB that is associated with the UE. The related radio resource management, packet scheduling, and common channels are tasks always performed by the single serving cell. The fact that no more than one eNB transmits at the same time implies that there is no need for the eNBs to have a tight phase synchronization. Hence,

dynamic cell selection can be implemented with relaxed RF performance requirements. Dynamic cell selection has also been used in the emerging deployments of Dynamic Single-Frequency Networks (DSFN) for multicast/broadcast transmission. In DSFN, the sets of synchronized eNBs that coordinate to serve a commonly subscribed multicast/broadcast traffic session keep changing within the given MBSFN area across time. Dynamic cell selection in DSFN helps in better multiplexing of PRBs across sessions and unicast traffic.

### 1.3.4 Types of CoMP

**Centralized CoMP:** In a centralized approach [1], a central entity as shown in Fig. 1.11 is needed in order to gather the channel information from all the UEs in the area covered by the coordinating eNBs. This entity is also in charge of performing user scheduling and signal processing operations such as precoding. Furthermore, tight time synchronization among eNBs is needed and user data should be available at all collaborating nodes. On the downlink of frequency division duplexing (FDD) systems, the UE needs to estimate the channel and derive channel coherent or non-coherent indicators (CSI/CQI) to feed back to the eNB. In time division duplexing (TDD) systems, the channel information can be obtained by using channel reciprocity. In the case of FDD operation, terminals must first estimate the channel related to the set of cooperating eNBs. The information is fed back to a single cell, known as the anchor cell, which acts as the serving cell of the UE when coordination is being employed. Once the information is gathered, each

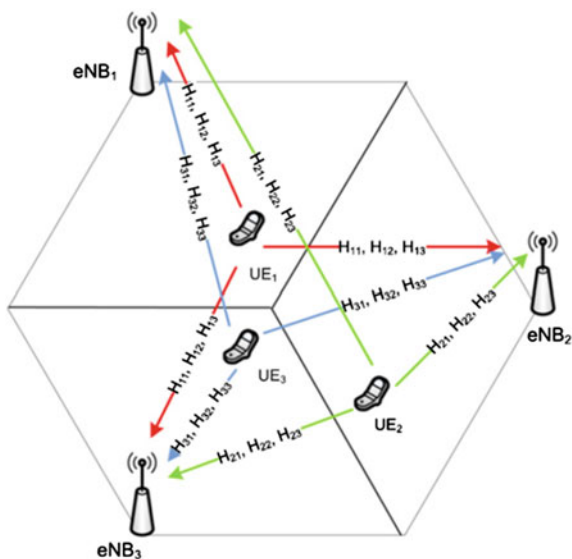
Fig. 1.11 Centralized CoMP



eNB forwards it to the central entity that is in charge of deciding the scheduling and the transmission parameters, and this new information is sent back to the eNBs. The main challenges of this architecture are related to the new associated communication links between the central entity and the eNBs. They must support very-low-latency data transmissions, and in addition, communication protocols for this information exchange must be designed. Fiber cables enable low-latency communication between eNBs.

**Distributed CoMP:** A distributed architecture [1] is another solution to perform coordination that alleviates the requirements of a centralized approach. Based on the assumption that schedulers in all eNBs are identical and channel information regarding the whole coordinating set can be available to all cooperating nodes, inter-eNB communication links are no longer necessary to perform cooperation. Thus, this architecture has the great advantage of minimizing the infrastructure and signaling protocol cost associated with these links and the central processing unit, so conventional systems need not undergo major changes. Furthermore, the radio feedback to several nodes could be achieved without additional overhead. The UE estimates the channel from all the coordinating eNBs in the very same way as in the centralized approach. The estimates are then sent back to all cooperating eNBs, and the scheduling is independently performed in each of them, as shown in Fig. 1.12. Identical schedulers are used across eNBs so as to limit the performance discrepancies among UEs, subject to coordinated scheduling. Similarly, transmission parameters are jointly selected according to a common design in the different nodes. This scheme presents some drawbacks: First, if different eNBs do not perform cooperation via a wired backhaul, the performance of the CoMP algorithms is less efficient. Furthermore, an obstacle associated with distributed transmission is the

Fig. 1.12 Distributed CoMP



handling of errors on the different feedback links. The same UE reports its channel conditions to all the eNBs in the set, but the wireless links to the different nodes might be very different and the impact of these errors on the system performance cannot be neglected.

### 1.3.5 Advancements: 3D Beamforming

Three-dimensional MIMO (3D MIMO) can be seen as an effective method to approach massive MIMO without requiring too many antennas on the transmitter or receiver [37, 38], as shown in Fig. 1.13. It introduces a vertical dimension in transmitting antennae by additionally accounting for the heights of the eNBs and the UEs. Vertical dimension is utilized in the antenna modeling, and down-tilt of the antennas becomes a significant channel parameter. For any eNB  $m$  and UE  $k$ , the respective channel coefficient matrix has three dimensions per PRB which are (i) the number of transmitting antennae on the eNB  $m$  at the corresponding CC  $c$  given by  $N_{m,c}$ , (ii) the number of receiver antennae on the UE  $k$  receiving signals corresponding to the CC  $c$  given by  $N_{k,c}$ , and (iii) the number of vertical antenna array elements  $N_a$  per transmit antenna that accounts for the height of the eNB  $m$  and UE  $k$ . The channel coefficients between eNB  $m$  and UE  $k$  over any PRB  $b$  from the bandwidth of the CC  $c$  are represented by a 3D matrix, given by the dimensions  $N_{k,c} \times (N_{m,c} \times N_a)$ . A 3D antenna requires the modeling of departure and arrival angles in the horizontal and vertical dimensions. Beamforming of linear array antenna elements merely in horizontal dimension does not give full free-space gain. This is due to the azimuth spread of the received signal as seen from the eNB.

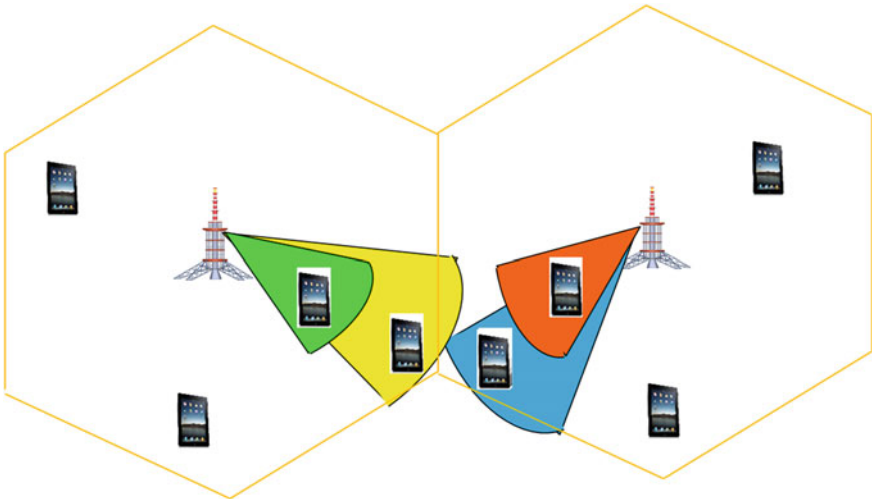


Fig. 1.13 3D beamforming

In conventional 2D MIMO scenarios, inter-cell interference is a serious problem affecting cell-edge UEs. Since the radio propagation from a transmission node to a UE is divided into the horizontal and vertical directions, the power of inter-cell interference can be reduced largely, which results in an enhancement of the SINR and hence, the net system performance.

### 1.3.6 Applications

**eMBMS Services and MBSFN:** LTE-A and evolving telecom standards are being increasingly deployed to carry commonly subscribed bandwidth-intensive broadcast sessions (such as HD video) to a larger set of subscribers. eMBMS, standardized in 3GPP Release 8, is a set of features in LTE to support over-the-air delivery of wireless content to a large audience, distributed over a wide geographical area. Applications of eMBMS are found in broadcasting live events (soccer matches, news flashes, etc.), live video at event venues (such as replays and video feeds), emergency broadcasts to the general public for safety, real-time software update over the air to a large set of mobile subscribers, etc. Multi-cell broadcast is facilitated in eMBMS by deploying an SFN and leveraging its transmit diversity feature, as shown in Fig. 1.2, where the session is subscribed by UEs, whose cell association spans across the multiple eNBs synchronized in the SFN. So, the same broadcast/multicast session is served by more than one eNB in the network managed by a mobile network operator. That is, every constituent eNB of the SFN serves the session, which is subscribed by at least one UE associated with the cell covered by the eNB (note that any UE is associated with the cell corresponding to exactly one eNB). Multi-cell eMBMS services schedule the same content over a common set of PRBs using the same MCS value across all the eNBs synchronized in the SFN. This feature of multi-cell broadcast across the SFN is called Multicast Broadcast SFN (or MBSFN). The eNBs constituting the MBSFN are collectively referred to as an MBSFN area. The diversity gain of the SFN helps in enhancing the performance of the wireless last hop of the session, which is otherwise marred by significant inter-cell interference.

**Full-duplex communication:** The basic idea here consists in using the same frequency–time radio resource for simultaneous uplink–downlink communication of independent data streams [39]. As shown in Fig. 1.14, full duplex in LTE uses the same PRBs for both uplink and downlink communication. The traditional half-duplex systems either use FDD or TDD to multiplex uplink and downlink data streams. The former consists in using separate frequency sub-bands in the deployed CC for uplink and downlink communication simultaneously, whereas the latter divides the LTE frame into independent sub-frames in the time domain, while using the entire frequency band in the CC, for uplink and downlink communication, respectively. As a result, full-duplex communication aims to double the radio system capacity, while carefully accounting for the same band self-interference due

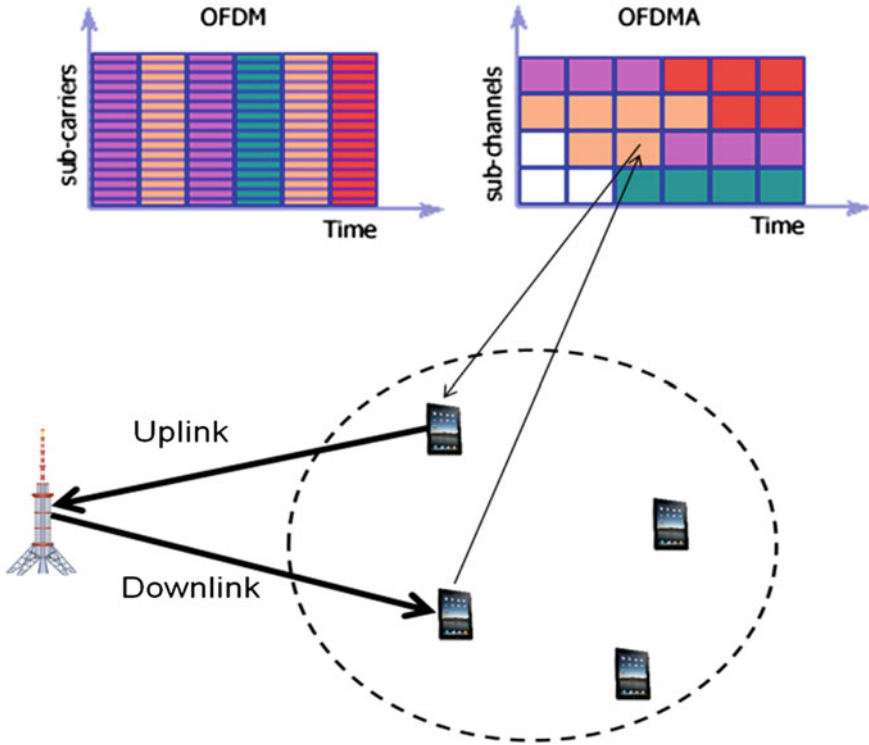


**Fig. 1.14** Full-duplex LTE (simultaneous uplink-downlink on the same PRB)

to simultaneous bidirectional communication and spatially multiplexing UEs between uplink and downlink communication.

However, there are two important challenges in achieving this objective: (i) self-interference, (ii) uplink-downlink interference [39, 40]. Uplink-downlink (UL-DL) interference [39] is the interference caused at the UEs due to their simultaneous uplink-downlink communication on the same frequency resources (PRBs) resulting in intra-cell interference for the UEs. The scenario envisioned is a set of eNBs operating on the same frequency with a random distribution of UEs, each of which is associated with a distinct eNB. Some of the UEs subscribe to downlink traffic, whereas the remaining transmit data in the uplink from to their respective associated eNBs, simultaneously. A PRB on any CC deployed over an eNB has at most two UEs scheduled on it, one for uplink and the other for downlink. Techniques such as spatial multiplexing (MU-MIMO) and beamforming are employed to limit the UL-DL interference. Optimal mitigation of UL-DL interference requires appropriate selection of distinct sets of UEs for simultaneous uplink and downlink communication with appropriate choice of multi-cell beamforming vectors, as discussed in the previous section.

## 1.4 Wi-Fi-LTE, Unlicensed LTE

### 1.4.1 Definition and Terminologies

The exponential increase in mobile broadband traffic requires deployment of more spectrum resources for LTE to support higher data rates resulting from higher bandwidths. However, there are limited remaining spectrum resources that can be additionally deployed from the licensed frequency bands for LTE, such as 700–800 MHz, 2 GHz, [3]. Moreover, spectrum resources from licensed frequency bands are expensive. This results in increasing challenges for the mobile network operators to facilitate the soaring bandwidth-intensive traffic and provide QoS to subscribers. Hence, the operators are looking beyond licensed bands to deploy additional spectrum resources for LTE from unlicensed frequency bands like 5 GHz [41]. 5-GHz bands are being traditionally used for Wi-Fi systems such as IEEE 802.11n and 802.11ac. However, there are around 500 MHz of residual spectrum resources in the 5-GHz band, apart from those being used for Wi-Fi, for deploying different radio communication technologies [42]. LTE mobile operators are exploring to deploy additional frequency bands out of these residual resources. This radio access deployment of LTE CCs with scalable bandwidths ranging from 1.4 to 20 MHz from the residual spectrum resources in the 5-GHz unlicensed band is called Unlicensed LTE (LTE-U) [42, 43].

Figure 1.15 shows the availability of 5-GHz unlicensed spectrum for the purposes of deploying frequency sub-bands as LTE CCs. However, due to the lower transmission power (23–30 dBm) imposed by regulations on transmissions in unlicensed spectrum and higher path loss resulting from the high central band frequency and sharing of the 5-GHz spectrum resources with other Wi-Fi technologies, the network coverage of an eNB that operates on U-LTE is comparatively smaller. Hence, the eNBs that operate on LTE-U are typically small cells with

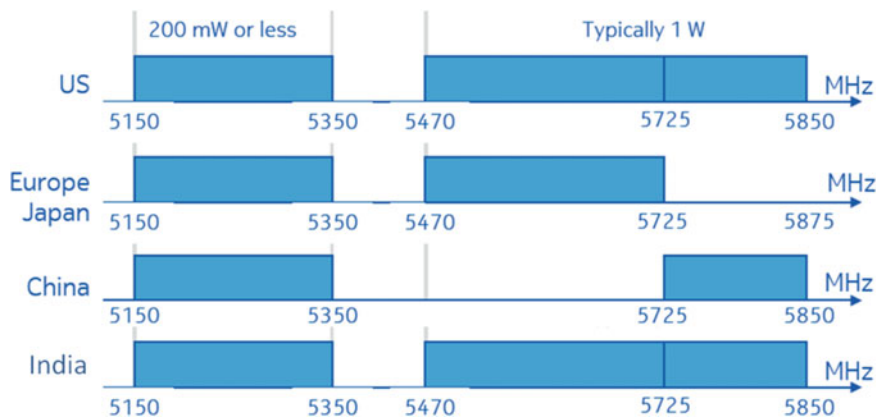


Fig. 1.15 5-GHz unlicensed spectrum availability

shorter radio coverage and comparatively lower transmission power [42]. The coexistence of Wi-Fi and LTE systems has not yielded expected performance benefits due to the lack of good coordination between the different lower layer designs of Wi-Fi and LTE technologies, such as Wi-Fi's OFDM versus LTE's OFDMA and Wi-Fi's asynchronous transmission versus LTE's synchronous transmission. The above-discussed design principles of LTE-Advanced in this chapter that are applicable for LTE-U deployment include [42, 43]:

- **Carrier aggregation**, which is used to integrate LTE-U CCs from unlicensed bands, along with LTE CCs from licensed bands. This requires distinguishing primary and secondary cells between licensed and unlicensed LTE CCs.
- **Wi-Fi-LTE interference management**, which is used to manage co-channel interference between Wi-Fi and LTE systems, deployed in unlicensed frequency bands. LTE-U uses opportunistic channel access, which takes into account the spectrum resources shared by Wi-Fi systems and other radio access technologies from the same frequency band.

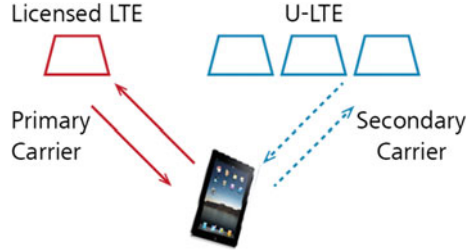
In addition to serving higher traffic volumes due to the larger available bandwidth offered by the 5-GHz unlicensed spectrum, the reasons for aggregating LTE-U include (i) high data rates and high spectral efficiency, (ii) a solution that is well integrated to the operator's existing radio network setup, avoiding multiple solutions for network management, (iii) higher data rates with better QoS, upon aggregating with LTE-licensed bands, and (iv) satisfying regulatory requirements for the LTE-U band by allowing coexistence with other technologies such as Wi-Fi, operating on the same frequency band.

#### ***1.4.2 CA of LTE-Licensed and LTE-U CCs***

Here, we discuss the strategies for integration of LTE-U CCs with LTE-licensed CCs in the form of the distinction between primary and secondary CCs, as in Sect. 1.2, and the deployment strategies for the coexistence of LTE-licensed CCs with unlicensed CCs over LTE-A eNBs [44]. This CA of LTE-U and licensed CCs is supported in 3GPP Releases 12 and 13.

**Primary and Secondary CCs:** The shorter network coverage range due to lower transmission power, higher coverage holes due to higher path loss, and opportunistic channel access over non-contiguous frequency resources due to spectrum sharing with other Wi-Fi systems render the transmission of information over common control and data channels of LTE-U CCs unreliable. Recall that, since transmission of common control information is important for radio resource control management, information signaling to maintain user-state information is a reserved functionality on the CC deployed over an LTE eNB to serve its associated UEs. So, to compensate for this unreliable nature of transmission over LTE-U, one of the recommended deployment strategies in LTE-Advanced is to aggregate a

**Fig. 1.16** CA of LTE-licensed and LTE-U CCs as primary and secondary carriers



LTE-U CC with a licensed LTE CC and designate the licensed CC as the primary CC for the UE. Since transmission over a licensed LTE CC is more reliable due to a higher transmission power, lower path loss, and orthogonal spectrum access that support higher modulation rates, the licensed CC can be designated as the primary CC for any UE. LTE-U can be used only for scheduling functionalities dealing with allocation of PRBs to UEs. Moreover, for the above distinct features between an LTE-licensed CC and an LTE-U CC, the former can be used to schedule traffic subscriptions with moderate lower bound GBR and lower latency requirements for QoS, and the latter can be used for serving best-effort traffic associated with upper bound maximum bit rate requirements. State information about UE mobility is handled by the licensed primary CC, while joint scheduling between LTE-licensed and LTE-unlicensed CCs is managed at the centralized eNB for smooth load balancing and choice of MCS values for rate adaptation. Figure 1.16 shows the CA of licensed LTE CC as the primary carrier and the LTE-U CC as the secondary CC.

**Deployment strategies:** One of the widely followed access techniques for LTE-U deployment is TDD [43]. Due to spectrum sharing with other Wi-Fi radio access technologies in unlicensed spectrum bands and opportunistic non-contiguous channel access nature of LTE-U, the support for FD-LTE results in spectrum inefficiency and ineffective spectrum utilization. By resorting to TD-LTE, the limited spectrum resources can be fully used for uplink and downlink communication, multiplexed across different sub-frames. 3GPP Release 13 supports TDD operation of LTE CC only in the downlink, whereas from 3GPP Release 14 onwards, the full bidirectional operation of the LTE CC is supported in TDD. There are two strategies for the deployment of an aggregated carrier of LTE-licensed and LTE-U CCs. One way to do it is the colocated deployment of aggregated LTE CCs from licensed and unlicensed bands over a single small-cell eNB. Since LTE-U does not support a larger coverage region, the aggregated carrier is deployed over the small-cell eNBs. This enables any UE, associated with a small-cell eNB, to be jointly scheduled on both the licensed and unlicensed CCs. Another strategy is a non-colocated deployment where a licensed CC is deployed over the LTE macrocell eNB and an unlicensed CC is deployed over the small cells, deployed within the coverage region of the macrocell. However, with this deployment, the association of UEs is split between the macrocell and the small cells such that each UE has a distinct cell association. So, a UE can be scheduled on either a licensed

CC or an unlicensed CC. The use of LTE-U is considered for indoor cells and outdoor hot spots, generally in places where there is coverage from licensed LTE bands, but where additional capacity would benefit system performance and traffic requirements. LTE-U is also deployed in corporate environments that benefit from the dedicated capacity in the unlicensed CC.

## 1.5 Network Heterogeneity: Self-organizing HetNets

### 1.5.1 Definition and Terminologies

The exponential increase in mobile broadband traffic requires making the available radio spectrum as spectrally efficient as possible. One of the promising solutions to serve the high data demand of the mobile broadband traffic is the enhancement of the LTE macrocell networks with small-cell deployments. Small cells are LTE eNBs covering a relatively shorter range but deployed with dedicated radio resource bandwidth from the same licensed frequency bands as the macrocells. Small cells are low-powered, low-cost radio access nodes that operate at a transmission power of around 23 dBm, resulting in a coverage radius of around 10 to 300 m. The collective deployment of macro- and small cells transmitting simultaneously on the same frequency channels to their respective user equipment (UE) clients is referred to as Heterogeneous Networks (HetNets) [10, 11]. Small cells are generally used to fix the coverage holes in the macrocell network and provide dedicated capacity to UEs that cannot be allocated adequate spectrum resources by the macrocell eNBs. The kind of UEs usually benefitting by deploying small cells includes (i) macrocell-edge UEs, due to their poor received signal and higher inter-cell interference causing both coverage and capacity issues, (ii) UEs in locations with high subscriber density (such as office buildings, apartment complexes, shopping malls) where the broadband traffic density is high, thereby causing capacity issues.

**Illustration:** Figure 1.17 shows a macrocell eNB and a set of small cells within the coverage of the macrocell. A couple of UEs at the cell edges of the macrocell are subscribing to high bandwidth traffic, such as video conferencing and video gaming. These UEs are seen to be having poorer channel conditions (indicated by the number of green vertical bars). Since their subscription to bandwidth-intensive traffic is further compounded by poorer channel conditions, these UEs are likely to suffer from exhaustion of resources. Hence, deployment of small cells around such UEs helps overcome this issue. Since the small cells offer stronger link stabilities and dedicated bandwidths to such UEs, the macrocell-edge UEs are served with adequate resources with better QoS.

Small cells is a general term used to refer to femtocells and picocells, whose usage is restricted to closed subscriber and open subscriber groups, respectively. The former are typically used for indoor communication up to a few tens of meters, whereas the latter cover a wider range up to a few hundred meters. Picocells are

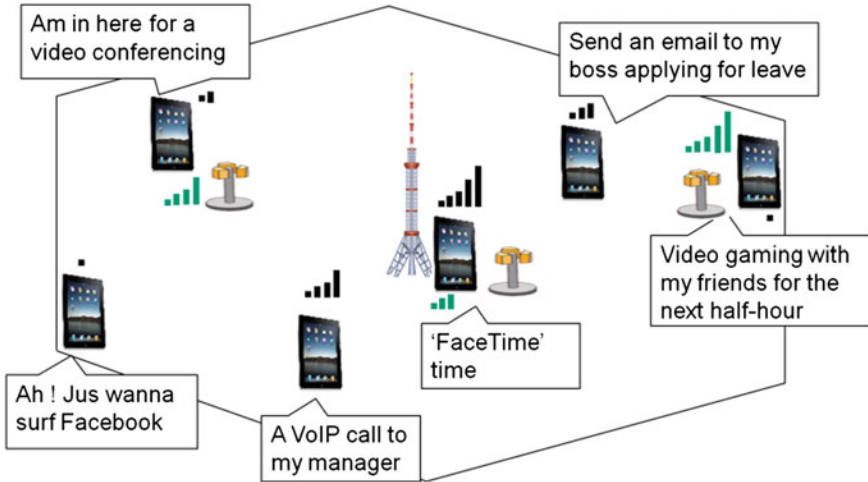


Fig. 1.17 Coverage and capacity issues addressed in HetNets

typically installed in wireless hot spot areas such as malls and near office buildings and provide access to all UEs [11]. Such heterogeneous deployments, caused by the densification of the network using small cells, are expected to dominate the broadband market in providing next-generation 4G+ and 5G telecommunication services. LTE small cells typically share the same frequency carriers with nearby macrocells; as a result, their deployment can lead to a higher co-channel interference if resource sharing is not carefully planned. This requires designing Enhanced Inter-cell Interference Coordination (eICIC) techniques for higher spectral efficiency and effective frequency reuse [45]. HetNets are standardized as part of 3GPP Release 10, and the communication among the different cells in a HetNet topology is enabled by a centralized authority such as a self-organized network (SoN) server and/or in a distributed manner via backhaul communication protocols between the macro- and the small cells, leveraging the X2 interface.

## 1.5.2 Background on Inter-cell Interference Coordination (ICIC)

### A. Macrocell ICIC

**Fractional Frequency Reuse (FFR):** FFR is an inter-cell interference mitigation mechanism for radio resource management (RRM) in cellular networks [46], as shown in Fig. 1.18. The synchronous operation of downlink and uplink transmissions across cells requires transmissions to be intelligently scheduled to manage interference. FFR partitions the licensed frequency bands of the operator into chunks of non-overlapping sub-bands and deploys them over the adjacent eNBs,

while reusing a fraction of the sub-bands commonly over all the eNBs. The reused frequency resources are meant for serving the UEs at the cell center that normally get reduced interference from adjacent eNBs and stronger links from their respective serving eNBs to which they are associated. On the other hand, the non-overlapping frequency sub-bands are used to serve UEs at the cell edges. The interference for such cell-edge UEs is mitigated due to the deployment of non-overlapping frequency resources over adjacent eNBs such that their transmissions do not interfere with each other. Hence, the interference caused by cell-center users is reduced while using more total spectrum than conventional spectrum reuse. The use of FFR in cellular networks leads to natural trade-offs between improvement in rate and coverage for cell-edge users, thereby addressing the trade-off between network throughput and spectral efficiency. In the popular 1-3 FFR scheme for macrocell networks, the spectrum is divided into four fixed-size bands, as shown in Fig. 1.18. One band is used by all the cell-interior clients (in each cell), who do not see interference due to the close proximity to their BS, while the other three bands are used (by cell-exterior clients) in an orthogonal manner among the three sectors of a cell to mitigate interference with sectors of adjacent cells. Thus, while the band used by cell-interior clients is reused in each cell, the reuse of the other three bands is subject to the spatial reuse. Recently, dynamic FFR [47] approaches have been proposed specifically for small cells, and determine the number and size of bands to be used by each small cell based on the aggregate traffic demand from its cell-interior and cell-exterior clients. This allows for better spectral utilization and does not rely on planned sectorization (unlike macrocells). However, the denser deployment of small cells within the coverage region of an interfering macro poses significant challenges in splitting the licensed frequency sub-bands among the interfering cells. Note that the FFR schemes only determine

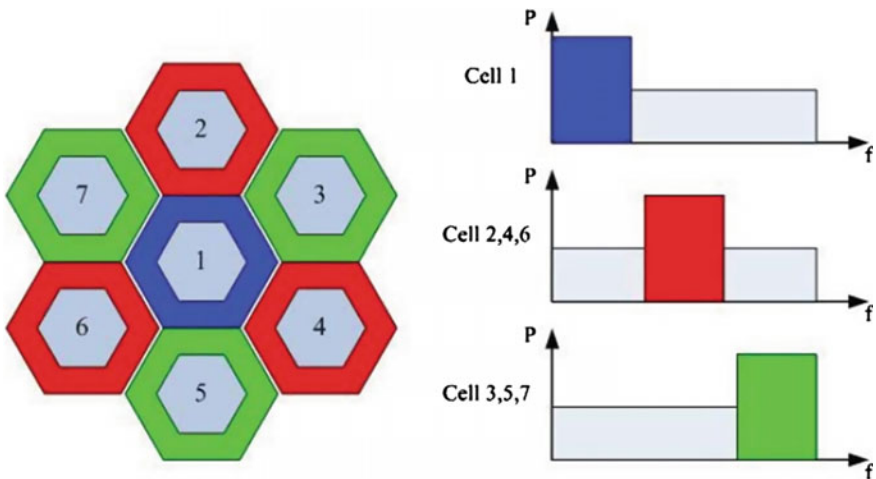


**Fig. 1.18** 1-3 fractional frequency reuse

the set of spectral resources assigned to cells—scheduling of clients within these resources is done by each cell locally (based on per-client feedback) to leverage multiuser diversity.

**Soft Frequency Reuse (SFR):** The term soft reuse is due to the fact that effective reuse of the spectrum can be accomplished by the division of powers between the frequencies used in the center and edge bands [48]. SFR makes use of the concept of zone-based reuse factors in the cell-center and cell-edge areas; however, frequency and power used in these zones are restricted. In particular, a frequency reuse factor of 1 is employed in the central region of a cell, while frequency reuse factor greater than 1 at the outer region of the cell close to the cell edge. In fact, when the mobile station is near the antenna of the base station, the received power of the wanted user signal is strong, and the interference from other cells is weak. So, at the inner part of the cell, all the sub-carriers can be used to achieve high data rate communication. For example, considering the 3-sector cell sites, the cell-edge band uses 1/3 of the available spectrum which is orthogonal to those in the neighboring cells and forms a structure of cluster size 3. The cell-center band in any sector is composed of the frequencies used in the outer zone of neighboring sectors. The benefits of the soft frequency reuse scheme include improved bit rate at cell edge, high bit rate at the cell center, decreased interference at the cell edge, so the procedures of channel estimation, synchronization, cell selection, and reselection are relatively easier.

### **B. Macrocell and small-cell ICIC**

The details of ICIC techniques between the macrocells and the small cells in a HetNet deployment are discussed in [49]. The *dedicated frequency band* allocation is the case where the same frequency band is shared by all the femtocells, and a different non-overlapping frequency band is allocated to the macrocells. This scheme is not suitable to support dense femtocells deployment, as the use of the same frequencies by the densely located femtocells would cause severe inter small cell interference. Moreover, due to the non-overlapping split of frequency bands among the small cells and the macrocells, this scheme results in inefficient spectrum utilization. In the *shared frequency band* allocation scheme, the frequencies from the same spectrum can be allocated for the femtocells and the macrocells. This scheme results in high-frequency reuse; however, it causes high interference among the small-cell and macrocell deployments. In the *static frequency reuse* scheme, the set of all cellular frequencies is divided into three equal bands and each one of the three macrocells in a macrocellular cluster uses one of these three different frequency bands. If a macrocell uses a particular frequency band, then the femtocells within that macrocell use the other two frequency bands. The *dynamic frequency reuse* scheme is similar to the static scheme; however, for each femtocell, one band is used in the center of the femtocell, while the other band is used at the edge of the femtocell. The frequency band used in the center of all femtocells of the same macrocell is the same, but the frequency bands used in the edges of the various femtocells are, in general, different, to avoid interference.

### ***1.5.3 Enhanced Inter-cell Interference Coordination (EICIC)***

The transmission power of the macrocell eNB is significantly higher than that of a small-cell eNB. The higher power macrocell eNBs are deployed for blanket coverage of urban, suburban, or rural areas, and the picocell eNBs with small RF coverage areas complement the macronetwork for filling the holes in macrocoverage and providing dedicated resources for enhancing throughput. Hence, the association of UEs to either a small or a macrocell based on the maximum transmission power would be unfair for the small cell, as it operates at lower transmission power. Lower user association to the small cells under-utilizes their licensed spectrum resources and defeats the purpose of their deployment. Moreover, users associated with the small cell are marred by interference from the adjacent macro, resulting in poorer SINR. This does not contribute to an effective reuse of the licensed frequency bands at the small cells, resulting in wastage of limited and expensive spectrum resources. Such unfairness for the small cell is compensated by the usage of an additive cell selection bias (CSB) [10] value (in dB) that is broadcast by the small cell, and the simultaneous support by adjacent macrocell(s) via blanking transmission for a certain number of time slots [10]. The additive CSB value, along with the Reference Signal Received Power (RSRP) of the UE from the small cell, can bias the decision of the UE to attach to the small cell over the macro. Moreover, such offloading of UEs to the small cell reduces the traffic load bottleneck for the macro, as a result of which, the macro can serve more incoming traffic for QoS. The geographical region comprising UEs that attach to the small cell, only upon adding the broadcast CSB value, is called the Cell-Range Expansion (CRE) region [10, 45, 50]. The UEs in the CRE region are considered to be the edge users for the small cell, and are affected by the interference from the adjacent macrocells. Therefore, an eICIC technique is required to achieve effective spectrum utilization and a better Quality-of-Service (QoS) for the small cells by facilitating higher data rates. Macro blanking is one such technique that stops the macrocell from transmitting data signals on the frequency channels for a predetermined number of time slots per LTE frame, called Almost Blank Subframes (ABS) [10, 51]. The number of ABS per LTE frame in any CC deployed over the macrocell eNB is defined as the ABS length of the CC. The reason why the blanked sub-frames are called “almost” blank is because the macro can still transmit some broadcast signals and control signals over these subframes. Since these broadcast signals only occupy a small fraction of the OFDMA PRBs, the overall interference caused by the macro to the small cells is much less during these ABS periods.

### 1.5.4 Defining the CRE Region

This section analytically profiles the CRE region of the small cell as a function of its CSB with relevant illustrations. The deployment of small cells is considered in topologies with (i) a single interfering single-carrier macro and (ii) multiple-interfering single-carrier macros. These use-cases offer insights on pertinent real-world LTE topology configurations such as FFR and SFN, respectively. FFR limits the inter-cell interference between adjacent macro-eNBs by splitting the licensed frequency band of the telecom operator into sub-bands across the adjacent eNBs. Hence, any small cell observes significant interference only from a single adjacent macrocell within whose coverage, it is deployed. However, in SFNs, since all the macrocells operate on the same frequency band, any small cell observes interference from the adjacent as well as neighboring macrocell eNBs.

#### A. Single macrocell interferer for FFR:

Consider any UE indexed  $u$  at any point in coordinate space, a macrocell  $m$ , and a small cell  $s$ . Without loss of generality, we assume that the macrocell is located at the origin  $(0, 0)$  and the small cell is located at  $(R, 0)$ . Let  $r_{s,u}$  and  $r_{m,u}$  denote the distances from the UE  $u$  to  $s$  and to  $m$ , respectively, that also accounts for the difference between the eNB and UE heights. Let  $rsrp_s(u)$  be the Reference Signal Received Power (RSRP) value at UE  $u$  with respect to  $s$ . This is given by:

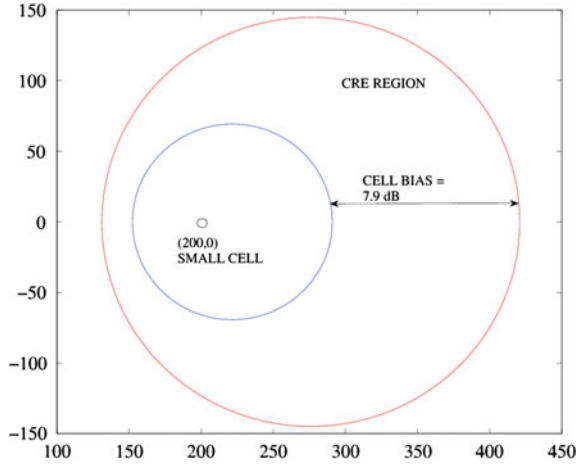
$$rsrp_s(u) \triangleq \frac{P_s \cdot \gamma \cdot e^{-|h_{s,u}|}}{r_{s,u}^{\rho_s}}$$

where  $P_s = P_s^{[T]} / f_c^{z_s}$ ,  $P_s^{[T]}$  is the transmission power at the small-cell antenna,  $P_s$  is the power transmitted from  $s$  along the frequency band  $f_c$  of any CC  $C_c$ ,  $\alpha_s$  is the frequency-dependent path loss exponent for  $s$ ,  $\gamma$  is the fraction of the transmission power available for the Cell-specific Reference Signal (CRS) [3], and  $h_{s,r}$  indicates the shadow fading of the link between the small-cell eNB  $s$  and the UE  $u$ . Usually,  $h_{s,u}$  is an independent and identically distributed Gaussian random variable, and  $\rho_s$  is the path loss exponent in terms of the distance. Similarly, the RSRP at UE indexed  $u$  w.r.t the fixed macrocell  $m$  is given by:

$$rsrp_m(u) \triangleq \frac{P_m \cdot \gamma \cdot e^{-|h_{m,u}|}}{r_{m,u}^{\rho_m}}$$

where  $P_m = P_m^{[T]} / f_c^{z_m}$  is the transmission power of the macrocell over CC  $C_c$ ; similarly,  $h_{m,u}$  is the i.i.d Gaussian shadow fading between the macrocell eNB  $m$  and UE  $u$ . Assuming equal path loss exponents for the macro- and small cells, i.e.,  $\rho_s = \rho_m = \rho$ , if a CSB value  $cb_{s,c}$  (in linear scale) is associated with small cell  $s$  on CC  $C_c$  and if the UE indexed  $u$  is inside the CRE region, the following conditions are satisfied [10, 11]: (i)  $rsrp_s(u) < rsrp_m(u)$ , and (ii)  $rsrp_s(u) \cdot cb_{s,c} > rsrp_m(u)$ .

**Fig. 1.19** CRE region with CSB 7.9 dB when macrocell to small-cell distance is 200 m

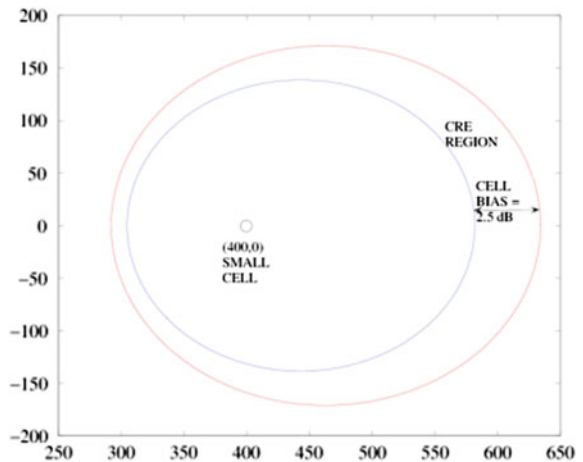


Figures 1.19 and 1.20 indicate the CRE regions of the small cell, when it is present at 200 and 400 m distance from the interfering macro. The CRE regions correspond to maximum possible CSBs that can be used in the case of a dense distribution of UEs in a HetNet scenario, such that each UE is guaranteed at least a pair of PRBs upon being served by the small cell.

**B. Multiple macrocell Interferers for SFN:**

In the presence of multiple-interfering macrocells, the small cell effective service region is the region where the RSRP of the small cell is greater than the sum of the RSRPs of the interfering macrocells. Hence, now the net CRE region is defined as the area where (a) the RSRP of the small cell is less than the sum of the RSRPs from the interfering macrocells; and (b) the product of the RSRP of the small cell and the CSB is greater than the sum of the RSRPs of the interfering macrocells.

**Fig. 1.20** CRE region with CSB 2.5 dB when macrocell to small-cell distance is 400 m



Different UEs need different sets of macrocells to blank, in order to get a better service from the small cells. In this case, at least one macrocell needs to blank, such that the UEs in the CRE region expanded by the CSB get a higher RSRP from the small cell. In the presence of multiple-interfering macrocells, we have:

$$\frac{p_s \cdot \gamma \cdot e^{-|h_{s,u}|}}{r_{s,u}^{\rho_s}} < \max_{m \in M} \frac{p_m \cdot \gamma \cdot e^{-|h_{m,u}|}}{r_{m,u}^{\rho_m}}$$

### 1.5.5 Enhancements: eICIC with CA

Inter-band CA (discussed in Sect. 1.4.1) enables the small cell to transmit and receive on multiple CCs and hence, there would be more than one CRE region, corresponding to each CC. As the CCs in an inter-band CA belong to different non-adjacent central band frequencies, they yield different radio channel conditions (such as path loss) to their UEs. These channel dynamics, along with the instantaneous traffic load on each CC, affect the assignment of CCs to UEs and thereby their QoS. Accordingly, a channel- and traffic-aware CC assignment to UEs that uses distinct CSB values across CCs is required. Hence, the corresponding CRE regions across CCs need not be identical; each CC may serve a different number of cell-edge UEs.

This results in varying user association and traffic load on each CC. Subsequently, the small cell requests the interfering macro for different ABS lengths across its aggregated CCs. Moreover, when there is resource exhaustion on one of the CCs, the small-cell eNB should decide between (i) deflection of the UE to another CC aggregated in the small cell and (ii) deflection of the UE to an appropriate CC in the macro. This subsequently requires the macro to support different ABS lengths across CCs based on the varying net QoS requirements of the UEs belonging to each distinct CRE region. This suggests that the application of one technique (CA/eICIC) may impede the performance of another (eICIC/CA), upon being agnostic of the inter-dependencies between the two. Considering two inter-band CCs  $C_c$  and  $C_c'$ , a UE present in the CRE region corresponding to  $C_c$  can be scheduled in the PRBs of any CC  $C_c'$  upon availability of sufficient residual bandwidth, if and only if the central band frequency of  $C_c$  given by  $f_c$  is higher than the central band frequency of  $C_c'$ , given by  $f_c'$ . This is because if  $f_c > f_c'$ , then transmission on  $C_c$  yields a higher path loss when compared to  $C_c'$ . So, the UEs at the CRE region corresponding to  $C_c$  need not necessarily be at the CRE region corresponding to  $C_c'$ . This shows how an efficient interference mitigation mechanism should jointly account for the inter-dependencies between the applications of CA and eICIC. Figure 1.21 shows an illustration of using eICIC along with CA with different CRE regions for the small cells corresponding to different CCs and varying ABS lengths for the interfering macrocell across the CCs.

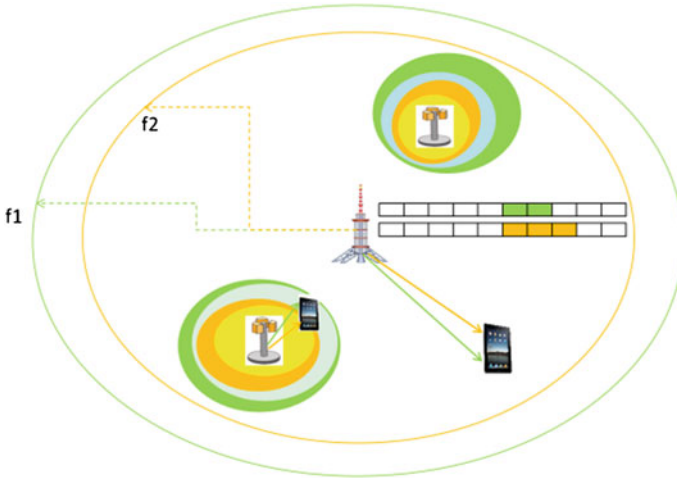


**Fig. 1.21** eICIC enhancement with CA

## 1.6 Conclusion

This chapter introduces the reader comprehensively to the foundational concepts of the design principles used in the radio access of next-generation telecommunication systems such as LTE-A. They provide a roadmap to the 5G centralized radio access technologies. The design principles are based on bandwidth aggregation, transmission diversity, interference management, MIMO spatial diversity, etc. It specifically emphasizes upon the recent advancements in 5G radio access technologies, such as the aggregation of LTE-licensed and unlicensed bands, and full-duplex communication, based on the aforementioned design principles. It highlights some of the key PHY and MAC layer issues pertinent to the design techniques. In traditional legacy 3GPP systems, the end-to-end performance was limited by the coverage and capacity bottlenecks of the wireless medium. However, the aforementioned techniques have significantly enhanced the performance of the radio access medium.

In terms of meeting 5G requirements, these radio access techniques achieve very high data rates, up to 1 Gbps downlink and 500 Mbps uplink capacity in the case of Carrier Aggregation, up to  $2\times$  speeds in the case of full-duplex communication (e.g., facilitating HD 1080p videos in the case of downlink eMBMS traffic), up to  $10\times$  speeds in the case of HetNets using small cells, and up to  $2\times/4\times/8\times$  speeds in the case of  $2\times 2$ ,  $4\times 4$ ,  $8\times 8$  MIMO enhanced with independently precoded multi-stream beamforming.

## References

1. Akyildiz IF, Estevez DMG, Reyes EC (2010) The evolution to 4G cellular systems: LTE-Advanced. Elsevier Phys Commun 3
2. Astely D, Dahlman E, Furuskar A, Jading Y, Lindstrom M, Parkvall S (2009) LTE: the evolution of mobile broadband. IEEE Commun Mag 47(4)
3. Holma H, Toskala A (2009) LTE for UMTS: OFDMA and SC-FDMA based radio access. Wiley
4. Sivaraj R, Pande A, Zeng K, Govindan K, Mohapatra P (2012) Edge-prioritized channel- and traffic-aware uplink carrier aggregation in LTE-advanced systems. In: Proceedings of 13th IEEE WoWMoM
5. Iwamura M, Etemad K, Fong M-H, Nory R, Love R (2010) Carrier aggregation framework in 3GPP LTE-advanced [WiMAX/LTE Update]. IEEE Commun Mag 48(08)
6. Lu S, Cai Y, Zhang L, Li J, Skov P, Wang C, He Z (2009) Channel-aware frequency domain packet scheduling for MBMS in LTE. In: Proceedings of IEEE VTC
7. Chen J, Chiang M, Erman JJ, Li G, Ramakrishnan KK, Sinha R (2015) Fair and optimal resource allocation for LTE multicast (eMBMS): group partitioning and dynamics. In: Proceedings of IEEE INFOCOM
8. Monserrat J, Calabuig J, Fernandez-Aguilella A, Barquero DG (2012) Joint delivery of unicast and eMBMS services in LTE networks. IEEE Trans Broadcast 58(2)
9. Nguyen ND, Knopp R, Nikaen N, Bonnet C (2013) Implementation and validation of multimedia broadcast multicast service for LTE/LTE-advanced in openairinterface platform. In: IEEE LCN workshop
10. Deb S, Monogioudis P, Miernik J, Seymour P (2013) Algorithms for enhanced inter cell interference coordination (eICIC) in LTE HetNets. IEEE/ACM Trans Netw 22(1):137–150
11. Vasudevan S, Pupala RN, Sivanesan K (2013) Dynamic eICIC—A proactive strategy for improving spectral efficiencies of heterogeneous LTE cellular networks by leveraging user mobility and traffic dynamics. IEEE Trans Wirel Commun 12(10)
12. Bjornson E, Jorswieck E (2012) Optimal resource allocation in coordinated multi-cell systems. Found Trends Comm Info Theory 9(2–3)
13. Kela P, Puttonen J, Kolehmainen N, Ristaniemi T, Henttonen T, Moisio M (2008) Dynamic packet scheduling performance in UTRA long term evolution downlink. In: Proceedings of International symposium wireless pervasive computing (ISWPC)
14. Pedersen KI, Frederiksen F, Rosa C, Nguyen H, Garcia LGU, Wang Y (2011) Carrier aggregation for LTE-advanced : functionality and performance aspects. IEEE Commun Mag 49(06)
15. Wang H, Rosa C, Pedersen KI (2011) Performance analysis of downlink inter-band carrier aggregation. In: Proceedings of IEEE ICC
16. Dahrouj H, Yu W (2010) Coordinated beamforming for the multicell multi-antenna wireless systems. IEEE Trans Wirel Comm 9(5)
17. Yuan G, Zhang X, Wang W, Yang Y (2010) Carrier aggregation for LTE-advanced mobile communication systems. IEEE Comm Mag 48(2):88–93
18. Wang H, Rosa C, Pedersen KI (2010) Performance of uplink carrier aggregation in LTE-advanced systems. In: IEEE VTC
19. Sundaresan K, Rangarajan S (2013) Energy efficient carrier aggregation algorithms for next generation cellular networks. In: Proceedings of IEEE ICNP
20. Dahlman E, Parkvall S, Skold J (2011) 4G: LTE/LTE-advanced for mobile broadband: LTE/LTE-advanced for mobile broadband. Academic Press, 1st edn
21. 3GPP, “TR 36.814 E-UTRA; Further Advancements for E-UTRA Physical Layer Aspects,” Rel. 9
22. Sivaraj R, Pande A, Mohapatra P (2013) Spectrum-aware radio resource management for scalable video multicast in LTE-advanced systems. In: Proceedings of IFIP Networking

23. Yoon J, Zhang H, Banerjee S, Rangarajan S (2012) Muvi: a multicast video delivery scheme for 4G cellular networks. In: Proceedings of ACM Mobicom
24. Suh C, Mo J (2008) Resource allocation for multicast services in multicarrier wireless communications. *IEEE Trans Wirel Comm* 7(1)
25. Li P, Zhang H, Zhao B, Rangarajan S (2009) Scalable video multicast in multi-carrier wireless data systems. In: Proceedings of IEEE ICNP
26. Sharangi S, Krishnamurthi R, Hefeeda M (2011) Energy-efficient multicasting of scalable video streams over WiMAX networks. *IEEE Trans Multimedia* 13(1)
27. Wang Y, Pedersen KI, Sorensen TB, Mogensen PE (2010) Carrier load balancing and packet scheduling for multi-carrier systems. *IEEE Commun Mag* 48(08)
28. Songsoong S, Chunyan F, Caili G (2009) A resource scheduling algorithm based on user grouping for LTE-advanced systems with carrier aggregation. In: Proceedings of symposium computer networking and multimedia technology
29. Jalali A, Padovani R, Pankaj R (2000) Data throughput of CDMA-HDR, a high efficiency-high data rate personal communication wireless system. In: Proceedings of IEEE VTC
30. Goldsmith A, Jafar S, Jindal N, Vishwanath S (2003) Capacity limits of MIMO channels. *IEEE J Sel Areas Commun* 21(5)
31. Jagannatham AK. Electronics-advanced 3G & 4G wireless mobile communications, national programme on technology enhanced learning, Government of India, <https://www.youtube.com/watch?v=zm0tKvOA3sQ>
32. Shi S, Schubert M, Boche H (2012) Weighted sum-rate optimization for multiuser mimo systems. In: Proceedings of IEEE CISS
33. Lee D, Seo H, Clerckx B, Hardouin E, Mazazares D, Nagata S, Sayana K (2012) Coordinated multipoint transmission and reception in lte-advanced: deployment scenarios and operational challenges. *IEEE Commun Mag* 50(02)
34. Venturino L, Prasad N, Wang X (2010) Coordinated linear beamforming in downlink multi-cell wireless networks. *IEEE Trans Wirel Commun* 9(4)
35. Farrokhi FR, Liu KJR, Tassiulas L (1998) Transmit beamforming and power control for cellular wireless systems. *IEEE J Sel Areas Commun* 16(8):1437–1450
36. Sivaraj R, Broustis I, Shankaranarayanan NK, Aggarwal V, Mohapatra P (2015) Mitigating macro-cell outage in LTE-advanced deployments. In: Proceedings of IEEE INFOCOM
37. Li Y, Ji X, Liang D, Li Y (2013) Dynamic beamforming for three-dimensional MIMO technique in LTE-advanced networks. *Hindawi J Antennas Propag* 2013(764507)
38. Eckhardt H, Klein S, Gruber M (2011) Vertical antenna tilt optimization for LTE base stations. In: Proceedings IEEE 73rd VTC Spring
39. Khojastepour M, Sundaresan K, Rangarajan S, Tehrani MF (2015) Scaling wireless full-duplex in multi-cell networks. In: Proceedings of IEEE INFOCOM
40. Aryafar E, Khojastepour MA, Sundaresan K, Rangarajan S, Chiang M (2012) Midu: enabling MIMO full duplex, 2. In: Proceedings of ACM Mobicom
41. The Prospect of LTE and Wi-Fi sharing Unlicensed Spectrum, <http://www.signalsresearch.com>
42. Nokia Networks White paper, Nokia LTE for Unlicensed spectrum, <http://networks.nokia.com>
43. Huawei White Paper, U-LTE: Unlicensed Spectrum Utilization of LTE, <http://huawei.com/link/en/download/hw327803>
44. Cavalcante A, Almeida E, Vieira R, Chaves F, Abinader F, Choudhury S, Tuomaala E, Doppler K (2013) Performance evaluation of LTE and Wi-Fi coexistence in unlicensed bands. *IEEE Veh Technol*
45. Lindbom L, Love R, Krishnamurthy S, Yao C, Miki N, Chandrasekhar V. Enhanced inter-cell interference coordination for heterogeneous networks in LTE-advanced: a survey. <http://arxiv.org/abs/1112.1344>
46. Sundaresan K, Arslan MY, Singh S, Rangarajan S, Krishnamurthy SV (2013) FluidNet: a flexible cloud-based radio access network for small cells. In: Proceedings of ACM MobiCom

47. Stolyar AL, Viswanathan H (2008) Self-organizing dynamic fractional frequency reuse in OFDMA systems. In: Proceedings of IEEE INFOCOM
48. Mao X, Maaref A, Teo KH (2008) Adaptive soft frequency reuse for inter-cell interference coordination in SC-FDMA based 3GPP LTE uplinks. In: Proceedings of IEEE Globecom
49. Chowdhury MZ, Jang YM, Haas ZJ. Cost-effective frequency planning for capacity enhancement of femtocellular networks, <http://arxiv.org/ftp/arxiv/papers/1412/1412.3639.pdf>
50. Deb S, Monogioudis P, Miernik J, Seymour P (2013) Algorithms for enhanced inter cell interference coordination (eICIC) in LTE HetNets. IEEE/ACM Trans Netw 22(1):137–150
51. Prez DL, Gven I, de la Roche G, Kountouris M, Quek TQS, Zhang J. Enhanced inter-cell interference coordination challenges in heterogeneous networks. <http://arxiv.org/abs/1112.1597>
52. Lee H, Sohn I, Kim D, Lee KB (2011) Generalized MMSE beamforming for downlink MIMO systems. In: Proceedings of IEEE ICC
53. 3GPP, “TR 36.808 Evolved Universal Terrestrial Radio Access (E-UTRA); Carrier Aggregation; Base Station (BS) Radio Transmission and Reception; Rel. 12.”

# Chapter 2

## Evolution and Trends of Broadband Access Technologies and Fiber-Wireless Systems

Yiran Ma and Zhensheng Jia

**Abstract** This chapter provides the introduction to technical trends and market status of both broadband wireline and wireless access networks and also summarizes the technology evolution of fiber and wireless networks. The technical introduction on broadband wireline access networks includes xDSL, coaxial cable and hybrid fiber coax (HFC), and various passive optical network (PON) architectures. The current global deployments on broadband wireline access are also presented here. As for the study on the broadband wireless access technologies, this chapter addresses the technical evolution path for dominant Wi-Fi, WiMAX, and mobile communications systems. As wireless and wireline technologies converge and the dividing lines become less clear, the common denominator will be optical fiber. In this chapter, technology synergies and recent research activities are also described for the integrated fiber-wireless access networks.

### 2.1 Traffic Trend

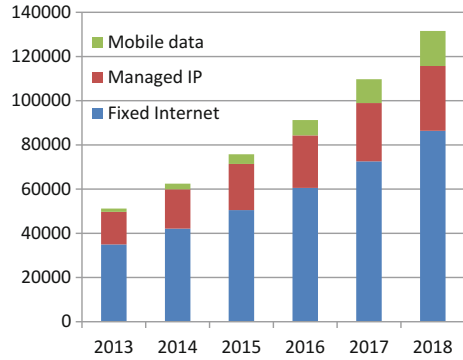
Today, the broadband access paradigm has seen phenomenal growth to almost all corners of the globe and forms an indispensable part of the daily life of billions of people. In the future, it is envisioned that this paradigm will evolve toward full broadband capability with more connections, less delay, and much higher bandwidth to satisfy the end users' demand. Internet and leased line bandwidth demand continue to grow at more than 20 % per year driven by more and more video streaming and proliferation of cloud computing, big data, social media, and mobile data delivery. In terms of video data and traffic, an enhancement of high-definition video such as 8K Ultra High Definition (UHD) will be available around 2020, and the provisional estimate of the total video communication traffic in 2020 carried

---

Y. Ma  
China Telecom Co. Ltd. Beijing Research Institute, Beijing, China

Z. Jia (✉)  
ZTE (Tx) Inc., Morristown, NJ, USA  
e-mail: sijia@cablelabs.com

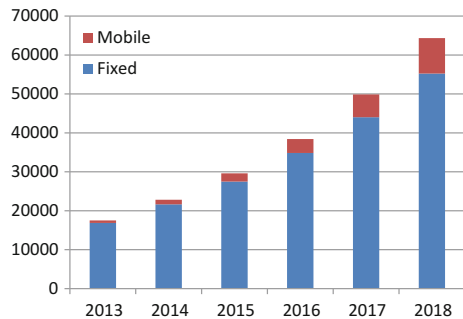
**Fig. 2.1** Global IP traffic by type (petabytes per month). *Source* Cisco VNI 2014 (adopted from [3])



over mobile and fixed systems is more than 2600 times the traffic in 2010 [1]. As for the mobile data, global mobile broadband subscriptions grew by around 35 % annually and reached 2.3 billion in Q1 2014 and are predicted to reach 7.6 billion by 2019 [2]. The growth will also be accelerated by new types of communication services, such as proximity-aware services including device-to-device (D2D) communications, which enables direct links between the wireless devices using the same spectrum and interface, and machine-to-machine communications (M2M) where the objective is to attach a large number of low-rate, low-power devices to the cellular network. Figure 2.1 shows IP traffic growth during 2013–2018 predicted by Cisco Visual Networking Index (VNI) published in 2014. Annual global IP traffic will surpass the zettabyte (1000 exabytes) threshold in 2016. By 2018, global IP traffic will reach 1.6 zettabytes per year, or 131.6 exabytes per month. Global IP traffic has increased more than fivefold in the past 5 years and will increase threefold over the next 5 years. Overall, IP traffic will grow at a compound annual growth rate (CAGR) of 21 % from 2013 to 2018, in which mobile data will increase extremely fast with a 61 % CAGR.

Figure 2.2 shows the traffic growth prediction of global consumer Internet video, which is mainly over-the-top (OTT) services. The traffic of Internet video grows even faster with 27 % CAGR for fixed Internet and 70 % for mobile Internet. The rapid growing traffic reflects a great demand for broadband with more and more

**Fig. 2.2** Global consumer Internet video by network (petabytes per month). *Source* Cisco VNI 2014 (adopted from [3])



bandwidth. It can be predicted that the broadband access data rate will be threefold in 2018 compared to 2013, and 100 Mb/s per user will be required for high-value users. Currently, Google Fiber has provided 1 Gb/s symmetric data rate for some US cities, which is a breakthrough for broadband access services.

For the future user's demand trend, more and more customers are expecting to have the same quality of experience from Internet applications anytime, anywhere, and through any means of connectivity. This expectation is now being achieved by the significant technological evolution of both broadband wireline and wireless access networks. The goal is to make full use of the synergies of the two networks by narrowing the gap between wired and wireless environments.

## **2.2 Technologies of Broadband Access Networks**

### ***2.2.1 Broadband Wireline Access Networks***

Broadband wireline access network provides promising and stable bandwidth to user premises. The medium to user premises can be coaxial cable, optical fiber, twisted pair, or hybrid of fiber and copper. Broadband services normally refer to "triple play," which is the service provisioning of broadband Internet access, television, and telephone over a single broadband connection.

In global broadband deployment, all types of wireline access networks exist simultaneously. Even in a single area, many types of wireline access networks might coexist under different conditions and for different users. PON allows user premises to connect to broadband networks via fiber with a superior bandwidth according to demand, as high as 1 Gb/s. The reach can also be up to 20 km. Consequently, PON is the most popular access network worldwide.

xDSL could take advantage of existing telephone line; hence, it is widely accepted in countries with rich copper line resources. The up-to-date xDSL technology such as VDSL and VDSL2/2+ is able to provide more than 50 Mb/s bandwidth within several hundred meters distance from user premises to the central office. Other wireline access networks based on copper include twisted pair and coaxial cable technologies, such as Ethernet, which can provide 100 Mb/s within a short range typically less than 100 m.

In some scenarios, PON and copper technologies are combined to achieve both low deployment cost and better performance. For instance, PON could connect the signal to the curb, and then, telephone line or twisted pair will carry the signal to user premises using xDSL or Ethernet.

In the following sections, these popular wireline access network technologies will be introduced in detail, including PON, xDSL, twisted pair, coaxial cable, and fiber-copper hybrid.

### 2.2.1.1 Passive Optical Network (PON)

In comparison with copper, fiber almost has infinite bandwidth. Recently, optical fiber is more and more applied in access networks instead of copper that dramatically decreases the OPEX and increases the performance of the network. The emergence of PON brings a feasible solution to the last mile for operators. PON technologies employ optical fiber as the transmission medium and all passive devices through the entire link and hence greatly reduce the maintenance cost.

The optical distribution network (ODN) is comprised of optical power splitters, fiber distribution boxes, etc. PON distributes or aggregates the signal to each optical network unit/optical network terminal (ONU/ONT) through power splitters. Figure 2.3 illustrates the basic architecture of PON technology. The key components and devices of a PON are an optical line terminal (OLT), which is normally located in the operators' central office, ONUs/ONTs at the user ends and an ODN. At the OLT, data and voice services are integrated and transmitted over 1490 nm wavelength in the downstream direction, while 1310 nm is assigned for the upstream direction. Video services occupy 1550 nm from the OLT to ONUs/ONTs. The OLT connects the PON and upper metro networks, and the ONU serves as the interface to the user. The ODN distributes the signal into multiple copies and transmits it to each ONU/ONT. The splitting ratio could be 2–64 with typical values of 8, 16, 32, and 64. In the real installation, the distance between OLT and ONU/ONT can be up to 20 km.

Different PON technologies could employ different rates, including 155 Mb/s, 622 Mb/s, 1.25 Gb/s, and 2.5 Gb/s. For instance, Ethernet PON (EPON) has a symmetric upstream and downstream data rate of 1.25 Gb/s, while Gigabit PON (GPON) has asymmetric downstream and upstream data rates of 2.5 and 1.25 Gb/s, respectively. Different PONs also apply different data encapsulations.

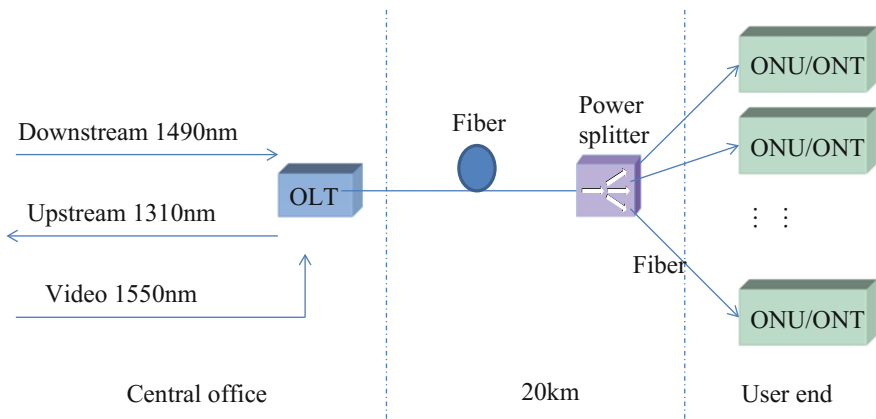


**Fig. 2.3** Architecture of PON technology

The ONU/ONT is located at the user premises. Compared with OLT, ONU/ONT always encounters an unstable environment. The functions of ONU/ONT are to provide optical interfaces with the PON, introduce the signal into the user premises, and provide possible electrical interfaces such as Ethernet and video. The ONU divides the video, data, and voice information from the OLT and transmits the information to the corresponding local interfaces. Meanwhile, the ONU processes the signal from the user premises and transmits it via an upstream channel to the OLT.

The OLT has two basic functions, which are user services control and dynamic bandwidth allocation for the ONUs. Considering that there are up to 64 ONUs using the same wavelength, there must be some multiple access methods to avoid conflict among the ONUs. The easiest way is time-division multiple access (TDMA), which allows each user to transmit and receive information during assigned time slots. Both EPON and GPON employ TDMA for upstream communication; thus, they are categorized as TDM-PONs. An efficient mechanism to allocate bandwidth is dynamic bandwidth allocation (DBA). When a time slot is empty, it will be assigned to ONUs that require more bandwidth. DBA is implemented using certain algorithms in the OLT according to users' priority, quality of service (QoS), and bandwidth demand. For downstream information, the OLT broadcasts all data to every ONU. All ONUs receive the broadcasted information from the OLT, and each ONU accepts or discards data according to the identifier (ID) in the frame head. To ensure the safety and privacy of the information, all data must be encrypted.

Fiber-to-the-home (FTTH) is the access structure that employs PON technologies and fiber from OLT all the way to the user premise. FTTH has started to be massively deployed worldwide since 2008. Especially after 2010, FTTH is the major solution for access network infrastructure installations and upgrades. The OLT is located in the central office, while the power splitter is settled in the community or inside the building. The horizontal part of the fiber (red solid line) inside the building can employ butterfly cable, and the ONU is normally set in the box outside the user premise. FTTH is the ultimate form of access network, which can provide more than 100-Mb/s bandwidth for each user. The structure of FTTH is shown in Fig. 2.4.

Nowadays, there are two types of PON technologies deployed worldwide, EPON and GPON. EPON is widely deployed in East Asia including China, Japan, and South Korea, while GPON is more accepted in Europe and USA. GPON is more and more popular recently because it can provide larger bandwidth and receives strong support from the industry.

## 1. EPON

1G EPON was proposed and standardized by IEEE802.3ah EFM working group where the main purpose of EFM is to promote Ethernet in access networks. EPON standard was published in 2004, and it defined the physical and MAC layer. EPON is the modified version of IEEE802.3, which mostly reused the contents of

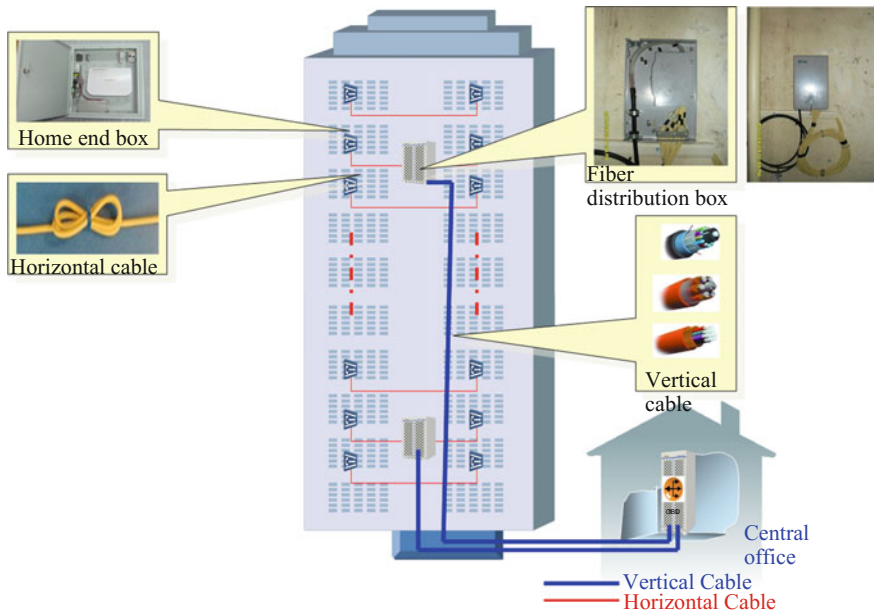


**Fig. 2.4** Structure of FTTH

IEEE802.3. EPON standard also includes Operation and Maintenance (OAM) mechanism for convenient network maintenance [4].

The signal between OLT and ONU is based on the IEEE802.3 Ethernet frame, which employs 8B/10B line coding. The data rate is symmetrical 1 Gb/s, while the line rate is 1.25 Gb/s. EPON supports 1:64 splitting ratio and a maximum of 20 km reach. The key of EPON is the multi-point control protocol (MPCP) in the MAC control layer. MPCP controls and visits point to multi-point (P2MP) topology through message, state machine, and timer. EPON provides a dedicated OAM mechanism to implement link monitoring, as well as remote loop and service layer management with expansion [5].

EPON standard sacrifices some performance to reduce the technical complexity and implementation difficulty; hence, it has shortage on bandwidth and efficiency. To further increase the competence of EPON, IEEE established 802.3av working group to study 10G EPON. 10G EPON increases the bandwidth to 10 times that of EPON, but the bandwidth efficiency has not been improved. The target of 802.3av is to define 10 Gb/s symmetric and asymmetric (upstream 1.25 Gb/s downstream 10 Gb/s) access technology. To support two types of data rates, 802.3av redefined the physical layer of 10G EPON [6]. 10G EPON is technically mature now, and operators have recently started to commercialize it.

## 2. GPON

GPON is the standard based on ITU-T G.984.x. It was first proposed by Full Service Access Network (FSAN) in 2002. Before that, FSAN had already developed Broadband PON (BPON). FSAN designed new physical and TC layers based on the BPON architecture and came up with the GPON standard. GPON employs a single fiber for upstream and downstream with 1290–1330 and 1480–1500 nm, respectively. If there is existing Cable TV (CATV) service, it will be carried on 1550 nm. The PON interface can support Class B+ and C+ optical modules. The system structure and functions of OLT and ONU are similar to EPON with additional specialties as below [7]:

- Strong full service supporting capabilities. GPON is able to carry ATM frame and GPON Encapsulation Method (GEM) frame, as well as data, voice, video, PDH/SDH, and ATM.
- The data rate of GPON can reach 2.5 Gb/s and theoretically cover 60 km distance. The maximum reach difference can be 20 km.
- Flexible bandwidth allocation with QoS guarantee.
- Supports TDM services more efficiently. TDM can be mapped to GEM frame. TC frame of GPON is also 125 us, which can support TDM directly.
- More effective encapsulation. GEM of GPON provides a flexible encapsulation protocol, which can support fixed and unfixed framing. In this way, multiple services can be mapped generally without protocol transfer. The encapsulation efficiency can be up to 94 %.
- Stronger OAM capabilities. GPON provides three types of OAM channels: embedded OAM channel, physical-layer OAM (PLOAM), and ONT Management and Control interface (OMCI).
- Complex technology with higher cost than EPON. However, as more and more operators choose GPON to deploy FTTH, the cost of GPON dramatically decreases and is currently equal to EPON.

Along with EPON and GPON's massive deployment worldwide, next-generation PON technologies have also attracted significant attention. 10G EPON and 10G GPON are the upgrade of EPON and GPON, which are developed in IEEE and ITU-T, respectively. Both 10G EPON and 10G GPON can support 1:120 splitting ratio and are able to provide more than 100-Mb/s bandwidth to each user. Currently, the devices of 10G EPON and 10G GPON are generally mature, but there are still interoperability problems. There are few 10G EPON and 10G GPON real installations because of lack of bandwidth requirements.

Either 10G EPON or 10G GPON still belongs to TDM-PON. The upstream of TDM-PON works in burst mode. When the data rate exceeds 10 Gb/s, it is very difficult to manufacture laser sources working in burst mode. While seeking for solutions of next generation of 10G PON (NGPON2), another form of multiplexing method is introduced: wavelength division multiplexing (WDM). PON technologies employing WDM include time and wavelength division multiplexed PON (TWDM-PON) and WDM-PON. TWDM-PON is widely accepted as the major

solution of NGPON2, which is a mixture of TDM-PON and WDM-PON. The wavelength channel number is 4–8, and 10G GPON is used inside each channel. There is a complex mechanism to allocate the wavelength of each user, and each user should be able to transfer among all channels. The standard series is G.989.x and G.989.1/2 (general requirements/physical layer), which have been consented, while G.989.3 (transmission convergence layer) is under development.

Different from TWDM-PON, WDM-PON employs pure wavelength multiplexing for both upstream and downstream. Each user occupies an individual wavelength, which can provide superior security and bandwidth. The data rate of each user can be 2.5 Gb/s or more. The structure is also simple, which does not require P2MP protocols but only Ethernet. The key technology of WDM-PON is colorless optical module at the user end. Fixed wavelength assignment is not acceptable in real installations. ONU has to be uniform to be installed in all users' premises. Therefore, the optical module has to be colorless. There are many ways to achieve colorless optics, such as self-seeded, tunable wavelength, and wavelength reuse. No matter the technology finally accepted, it has to be economically viable. WDM-PON has been proposed to carry wireless services such as CPRI signal between baseband unit (BBU) and remote radio unit (RRU) because of superior performance. The standardization of WDM-PON is being discussed in FSN and ITU-T SG15.

### 2.2.1.2 xDSL Technology

DSL is the abbreviation of Digital Subscriber Line. There exist many DSL technologies such as Asymmetric DSL (ADSL), Rate Automatic adapt DSL (RADSL), High-speed DSL (HDSL), and Very-high-bit-rate DSL (VDSL). For simplicity, all of these DSL technologies are called xDSL. The general system architectures of the DSL technologies are similar, but with different data rate, reach, and implementation methods.

xDSL, especially ADSL and VDSL, is widely deployed worldwide because it takes advantage of the most popular medium-copper telephone line. Users could get the benefit from the telephone services to enjoy broadband services. Tremendous amount of investment is saved in this way. Even now when fiber is more and more accepted as the main access network medium, xDSL still plays a very important role in Europe and North America.

ADSL and VDSL are candidates for today's broadband access. ADSL initially existed in two versions before discrete multi-tone (DMT) was chosen for the first ITU-T ADSL standards, G.992.1 and G.992.2 (also called G.dmt and G.lite, respectively). Therefore, all modern installations of ADSL are based on the DMT modulation scheme. At the telephone exchange, ADSL generally terminates at a digital subscriber line access multiplexer (DSLAM) where a frequency splitter separates the voice band signal for the conventional phone network. Data carried by the ADSL are typically routed to the operator's data network and eventually reach the Internet. Actual ADSL speed may reduce depending on line quality; usually, the

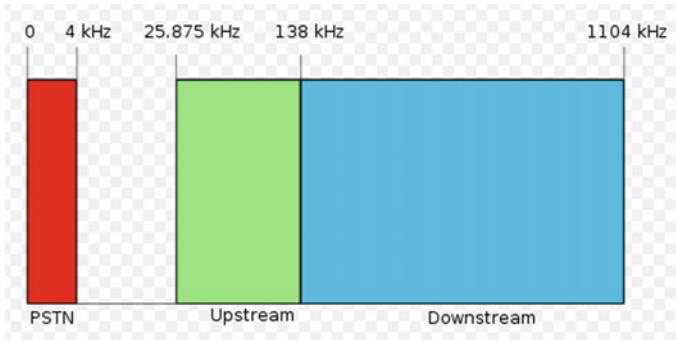


**Fig. 2.5** Upstream and downstream band of ADSL

most significant factor in line quality is the distance from the DSLAM to the customer's equipment. ADSL only supports short distances, typically less than 4 km. If more reach is required, the data rate has to be sacrificed. For example, the data rate is normally around 4 Mb/s with the distance less than 2 km.

ADSL allows a single telephone connection to be used for both broadband services and voice calls at the same time through full duplex. Full duplex is usually achieved by either frequency-division duplex (FDD), echo-canceling duplex (ECD), or time-division duplex (TDD). FDD uses two frequency bands as upstream and downstream. The upstream band is used for communication from the end user to the DSLAM. The downstream band is used for communicating from the DSLAM to the end user. With commonly deployed ADSL, the band from 26.075 to 137.825 kHz is used for upstream, while 138–1104 kHz is used for downstream, as shown in Fig. 2.5. Under the usual DMT scheme, each of these is further divided into smaller frequency channels of 4.3125 kHz.

ADSL2 is also referred as ITU-T G.992.3. It optionally extends the capability of basic ADSL in data rates to 12 Mb/s downstream and up to 3.5 Mb/s upstream (with a mandatory capability of ADSL2 transceivers of 8 Mb/s downstream and 800 kb/s upstream). ADSL2 uses the same bandwidth as ADSL but achieves higher throughput via improved modulation techniques. ADSL2+ is derived from the ADSL2 standard and also referred to as G.992.5. It extends the frequency range from 1.1 to 2.2 MHz and the subcarrier number from 256 to 512. The minimum data rate supported by ADSL2+ is downstream 16 Mb/s and upstream 800 Kb/s. The maximum downstream data rate is up to 25 Mb/s. ADSL2+ is a breakthrough of ADSL technology not only regarding the bandwidth, but also the reach, as it extends it to 6 km. ADSL2+ is a smooth migration of ADSL; hence, currently it is widely deployed in the world [8].

VDSL is the next-generation xDSL technology providing data transmission faster than ADSL, which is up to 52 Mb/s downstream and 16 Mb/s upstream. VDSL uses the frequency band from 25 kHz to 12 MHz. VDSL is capable of supporting applications such as high-definition television and cloud computing. VDSL can be deployed over existing wiring used for analog telephone service and

lower-speed ADSL connections, so it is widely accepted worldwide. VDSL is also referred to as ITU-T G.993.1. Similar to ADSL, VDSL also allows voice services and broadband to be connected at the same time through frequency-division duplex. The key technology of VDSL is DMT modulation and discrete wavelet multi-tone (DWMT). DWMT comes with better performance than DMT as it applies wavelet orthogonal transform. After wavelet transform, 99 % of the subcarriers' power concentrates on the main lobe; hence, the signal-to-noise ratio (SNR) dramatically increases.

Second-generation systems (VDSL2; ITU-T G.993.2 approved in February 2006) use frequencies of up to 30 MHz to provide data rates exceeding 100 Mbit/s simultaneously in both the upstream and downstream directions. The maximum available bit rate is achieved at a range of about 300 m; performance degrades as the distance increases. VDSL2 is the synthesizer of xDSL technology. The maximum distance of VDSL can reach up to 3 km with enhanced transmit power, echo suppression, and advanced frequency band, which is a tremendous increase compared to 1.5 km of VDSL.

VDSL2 is compatible with ADSL2+ because it defines DMT as the only modulation format and uses the same subcarrier frequency below 12 MHz. Above 12 MHz, VDSL2 applies flexible subcarrier frequency to achieve the ultimate rate of 200 Mb/s. The frequency band of VDSL2 is shown in Fig. 2.6. Therefore, VDSL2+ provides a smooth migration path from ADSL2+ to VDSL2 in order to protect the capital investment and reduce the risk of network upgrade.

Vectoring is a transmission method that employs the coordination of line signals to reduce crosstalk level and improve performance. It is based on the concept of noise cancellation, much like noise-canceling headphones. The ITU-T G.993.5 standard, "self-FEXT cancellation (vectoring) for use with VDSL2 transceivers" (2010), also known as G.vector, describes vectoring for VDSL2. The scope of Recommendation ITU-T G.993.5 is specifically limited to the self-FEXT (far-end crosstalk) cancellation in the downstream and upstream directions. The far-end cross talk (FEXT) generated by a group of near-end transceivers and interfering with the far-end transceivers of that same group is canceled. This cancellation takes place between VDSL2 transceivers, not necessarily of the same profile [9]. There are mature equipments of VDSL2 vectoring coming out at the moment; however, the real network deployment is still ahead.

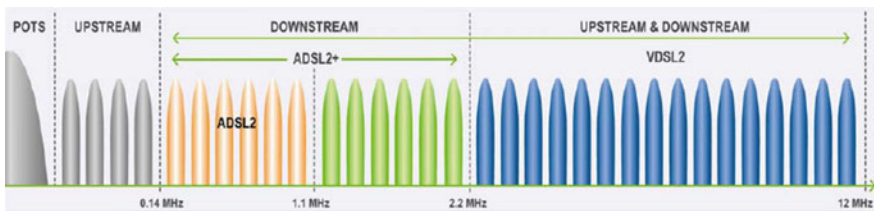


**Fig. 2.6** Upstream and downstream band of VDSL

In general, VDSL2 assembles all the advantages of different xDSL technologies. VDSL2 supports flexible and symmetric transmission rate. It has superior data rate within short reach and could cover longer distances than other xDSL technologies.

### 2.2.1.3 Twisted Pair Technology

Electrical cables are a popular wireline medium. Twisted pair is one of them in which two conductors of a single circuit are twisted together for the purposes of canceling out electromagnetic interference (EMI) from external sources, for instance, electromagnetic radiation from unshielded twisted pair (UTP) cables, and cross talk between neighboring pairs. Category 5 (cat 5) is a twisted pair cable for carrying signals, which is the most popular and widely deployed. This type of cable is used in structured cabling for computer networks such as Ethernet. The cable standard provides performance of up to 100 MHz and is suitable for 10BASE-T, 100BASE-TX (Fast Ethernet), and 1000BASE-T (Gigabit Ethernet). Cat 5 is also used to carry other signals such as telephone and video. Most cat 5 cables are unshielded, relying on the balanced line twisted pair design and differential signaling for noise rejection. To support Gigabit Ethernet, a higher performance version of cat 5, enhanced cat 5 or cat 5e has been developed. Cat 5e has new performance requirements to permit higher data rate operation [10, 11]. The cat 5e specification improves upon cat 5 by tightening some crosstalk specifications and introducing new crosstalk specifications that were not present in the original category 5 specification. The bandwidth of category 5 and 5e is the same, which is 100 MHz.

The broadband provided on twisted pair normally adopts Ethernet, which is called Ethernet over twisted pair. In 1980s, the potential of simple unshielded twisted pair by using cat 3 cable—the same simple cable used for telephone systems—has been shown. This led to the development of 10BASE-T and its successors 100BASE-TX and 1000BASE-T, supporting speeds of 10, 100, and 1000 Mbit/s, respectively. The higher-speed implementations support the lower-speed standards making it possible to mix different generations. All these standards support both full-duplex and half-duplex communication. Cat 5 is the standard cabling of newly built buildings in some countries. Therefore, to carry signals over existing cat 5 using Ethernet is an economic way to provide broadband services. Further, category 6 cable, referred to as cat 6, is also used in newly built houses nowadays that is backward compatible with the cat 5, 5e, and 3 cable standards. It provides performance of up to 250 MHz and is suitable for 10BASE-T, Fast Ethernet, Gigabit Ethernet, and 10-Gigabit Ethernet. Compared to cat 5 and cat 5e, cat 6 includes more strict specifications for crosstalk and system noise.

#### 2.2.1.4 Coaxial Cable Technology

Coaxial cable is a type of cable that has an inner conductor surrounded by a tubular insulating layer, surrounded by a tubular conducting shield. Many coaxial cables also have an insulating outer sheath or jacket. Coaxial cable is used to carry radio frequency transmission normally for broadband or cable TV (CATV).

Short coaxial cables are commonly used to connect home video equipment and computer networks, in particular Ethernet. However, twisted pair has replaced them in most applications except in the growing consumer cable modem market for broadband Internet access. Long-distance coaxial cable was used in the twentieth century to connect radio networks, television networks, and long-distance telephone networks though this has largely been superseded by later methods such as optical fiber. Shorter coaxial cables still carry CATV signals to the majority of television receivers, and this is the main application carried on coaxial cables.

In CATV systems, multiple television channels are distributed to user residences through a coaxial cable, which comes from a trunk line originating at the cable company's local distribution facility, which is called headend. The trunk line could be either coaxial cable or optical fiber. Multiple channels are transmitted through the cable by frequency-division multiplexing. At the headend, each television channel is translated to a different frequency. Therefore, television signals do not interfere with each other. At the user's residence, either the user's television or set-top box provided by the cable company translates the desired channel back to its original baseband signal. There are also upstream signals to send data from the user to the headend, for advanced features such as requesting video on demand, cable Internet access, and cable telephone service. The downstream channels occupy a band of frequencies from 50 MHz to 1 GHz, while the upstream signals occupy frequencies of 5–42 MHz.

Coaxial cables are capable of bidirectional carriage of signals as well as the transmission of large amounts of data. Cable television signals use only a portion of the bandwidth available over coaxial lines. This leaves plenty of space available for other digital services such as cable Internet and cable telephone. Broadband Internet access is achieved over coaxial cable by using cable modems to convert the network data into a type of digital signal that can be transferred over coaxial cable. One problem with some cable systems is that the older amplifiers placed along the cable routes are unidirectional. Many cable systems have upgraded or are upgrading their equipments to allow for bidirectional signals, thus allowing for broadband connections with large bandwidth. The first Ethernet standard, known as 10BASE5 (ThickNet) in the family of IEEE 802.3, specified baseband operation over 50-ohm coaxial cable, which remained the principal medium until the late 1970s. Then, 10BASE2 (ThinNet) coaxial cable replaced it in deployments in the 1980s. However, both of them were replaced in the 1990s when thinner, cheaper twisted pair technology came to dominate the market. The use of coaxial cable for Ethernet is still supported as CATV operators strive to use existing 75-ohm coaxial cable installations to carry broadband data into the home. Novel technologies are applied in the ITU-T G.hn standard to achieve higher bandwidth, which can be comparable

with fiber. The G.hn standard provides up to 1 Gb/s data rate over existing coaxial cable, power lines, and phone lines. It defines an Application Protocol Convergence (APC) layer for encapsulating standard Ethernet frames into G.hn MAC Service Data Units (MSDUs). There is also a great effort going on in IEEE 802.3 to apply EPON technology on coaxial cable which is called EPoC [12].

### 2.2.1.5 Hybrid Fiber–Copper Technology

Optical fiber has been more and more deployed because of its large bandwidth, easy maintenance, and low cost. For the last mile, it is not necessary to connect fiber to the user premise directly. If there is existing copper such as twisted pair, telephone line, or coaxial cable, it is more economical to carry the last mile service on these copper lines. Other than FTTH, fiber can be deployed midway, and then, existing copper can reach the end user.

Depending on the end point of the fiber, access networks can be divided into fiber-to-the-node (FTTN), fiber-to-the-curb (FTTC), fiber-to-the-building (FTTB), and fiber-to-the-home (FTTH). These are all called fiber-to-the-x (FTTx), which is a broadband network architecture using optical fiber to provide all or part of the access network used for last mile telecommunications. FTTN means that the fiber is terminated in a street cabinet, possibly miles away from the user premises, with the final connections being copper. FTTC is very similar to FTTN, but the street cabinet or pole is closer to the user premises, typically within the range (500 m) for high-bandwidth copper technologies such as xDSL or Ethernet. FTTB means fiber reaches the building, such as the basement in a multi-dwelling unit, with the final connection to the individual living space being made via alternative means, similar to FTTN and FTTC. These FTTx technologies employ the same architecture but with different fiber termination points; hence, the data rate provided ranges due to different copper lengths.

The fiber connecting the OLT central office and the main power splitters is called trunk fiber. The fiber from the main splitters to the fiber distribution box or multi-dwelling unit (MDU) inside the building is called feeder fiber. The last piece of fiber from the fiber distribution box or MDU to the ONU at the user premises is called drop fiber. The architecture of FTTx is shown in Fig. 2.7.

### 2.2.1.6 Global Roll-Out Strategies

Broadband has been proven to be closely related to economic growth worldwide. Lots of countries and operators have established their broadband strategies focusing on the broadband penetration and data rate increase. Therefore, fiber technologies, especially FTTH based on PON, have become the major choice, while some countries also upgrade xDSL technologies to VDSL2 or VDSL2+ which can provide as much bandwidth as FTTH and save on the previous investment. The followings are some examples [13].

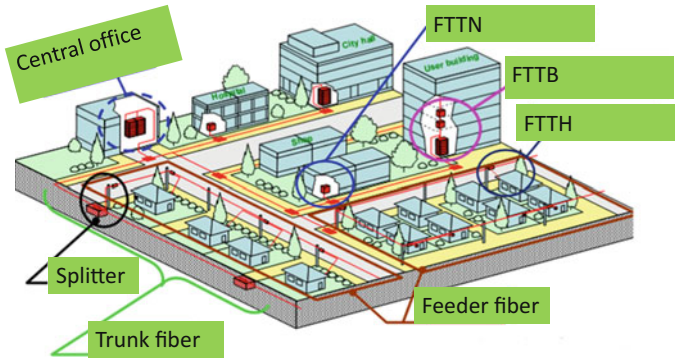


**Fig. 2.7** Architecture of FTTx

Federal Communications Commission (FCC) published an investment of 7.2 billion US dollars to develop national broadband in 2009 [14]. The main purpose of FCC's plan is to promote the penetration of broadband in the whole nation, especially for the minorities to enjoy broadband services. On March 16, 2010, FCC unveiled "Connecting America: The National Broadband Plan" to Congress. The plan is seeking to ensure that the entire broadband ecosystem is healthy. Six national broadband goals are set for the next decade, including ensuring every American has access to a robust (typically 4 Mb/s) broadband and at least 100 million homes have affordable access to 100 Mb/s broadband. As for the operators, Verizon has started FTTH deployment in 2004 to support the FIOS services. Verizon has covered more than 30 million homes using FTTH with more than 8 million ONUs really connected. Because the FTTH investment is huge, Verizon has slowed down the FTTH deployment in 2010 and has started to focus on the increase in FTTH users. GPON is the primary technology employed. However, AT&T does not put much effort on FTTH, as it relies on current copper line to deploy VDSL2+, so as to protect its previous investment. Cable TV companies such as Comcast also provide large bandwidth broadband to users through coaxial technologies.

China also published "Broadband China" strategy in 2013 with a two-stage target [15]. By the end of 2015, it aimed at 50 % of fixed broadband penetration, 4 Mb/s bandwidth in rural areas, 20 Mb/s in urban areas, 100 Mb/s in big cities, mobile broadband penetration of 32.5 %, and the whole broadband coverage exceeding 95 %. Meanwhile, Broadband China also aims at a further target of 2020, which is 70 % of fixed broadband penetration, 12 Mb/s bandwidth in rural areas, 50 Mb/s in urban areas, 1 Gb/s in big cities, mobile broadband penetration of 85 %, and the whole broadband coverage exceeding 98 %. From the operators' perspective, China Telecom and China Unicom started FTTH as early as 2009. In metropolitan areas, 100 % 20 Mb/s capability has been achieved, and in some prosperous areas, 100 Mb/s service is provided to users. In the countryside, the data rate is normally above 4 Mb/s. Both EPON and GPON are used, while there is no

10GPON deployed for FTTH yet. China Mobile uses GPON and deploys FTTH in metropolitan areas.

Japan has established “i-Japan strategy 2015,” which had four aims: easy-to-use digital technologies, breaking down the barriers that hinder the use of digital technologies, ensuring security when using digital technologies, and creating a new Japan by diffusing digital technologies and IT throughout the country [16]. The strategy also included national coverage target of 100+ Mb/s for mobile broadband and 1 Gb/s for fixed broadband by 2015. NTT started massive FTTx construction using EPON as early as 2003; by the end of 2011, the FTTH users have reached 20 million. 10G EPON has been deployed since 2010 to increase the bandwidth toward the 1 Gb/s target.

In December 2010, the UK government presented its national broadband strategy aiming to provide the best superfast broadband network in Europe by 2015, which means 2 Mb/s coverage nationwide and 90 % 24 Mb/s coverage [17]. Nine hundred and seven million US dollars have been issued to support the rural broadband program. As of 2013, 2 Mb/s broadband was available for 97 % of all, while superfast broadband reached 82 %. British Telecom (BT) started FTTx construction in 2009, among which 75 % is FTTC and 25 % is FTTH. FTTC covered 40 % of all homes by the end of 2012, and it was anticipated that FTTC/H will cover more than 2/3 by the end of 2014. GPON is used for FTTC and FTTH, and VDSL2 is used to support the last mile while using FTTC.

France’s national broadband strategy was adopted in 2011, and it aims to ensure 30 Mb/s broadband coverage by 2020 [18]. Another target is to provide superfast broadband access (100 Mb/s) to 100 % of the population through FTTH deployment. French Telecom (FT) trialed FTTH in 2006 and started deployment in 2007. By the end of 2012, 4 million homes have been connected, and it was expected that this number would increase to 9 million by the end of 2015.

Germany adopted its national broadband plan in 2009 and revised it in 2013. The revised target was to provide broadband with 50 Mb/s to 100 % of the population by 2018 [19]. Deutsche Telecom (DT) mainly deployed FTTH in Germany, Croatia, and Slovakia. DT has more than 2 million homes currently connected. In other areas, DT also relies on FTTB+VDSL2+ to provide large bandwidth broadband.

### 2.2.1.7 Penetration of Different Broadband Technologies

The Organization for Economic Co-operation and Development (OECD) publishes broadband-related information of its members every year. As China is not an OECD member but owns the most broadband users in the world, China’s broadband information is also put together in some charts with OECD information for reference.

As an example, Fig. 2.8 lists the total fixed broadband subscriptions of OECD members and China mainland by the end of 2013. China is shown to be the biggest fixed broadband market and has the most fixed broadband users totaling 189 million.

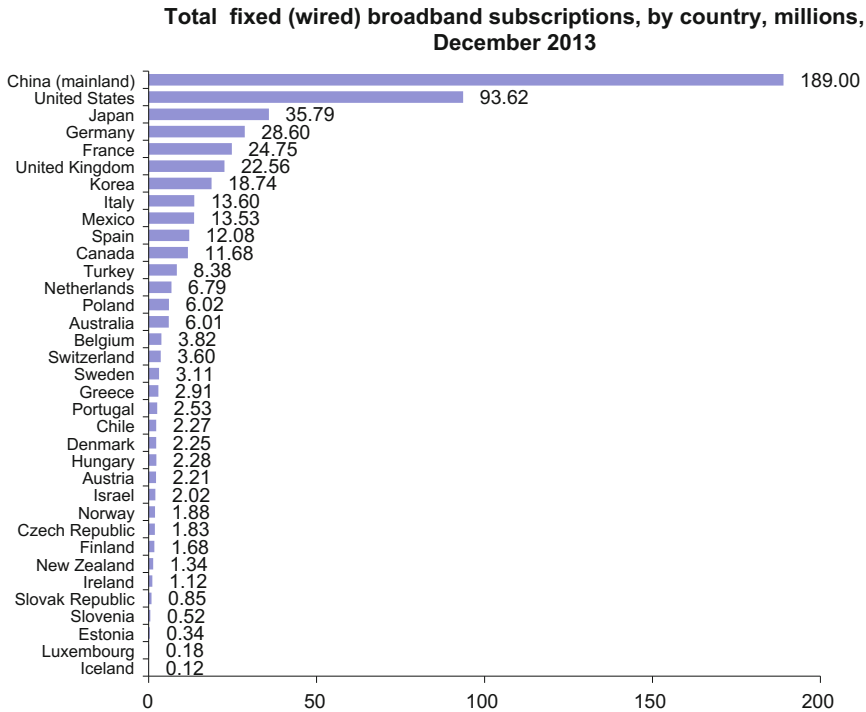


**Fig. 2.8** Fixed broadband subscriptions (in millions) in total by the end of 2013 [20]

USA is ranked second with 94 million fixed broadband users, followed by Japan and Germany. Figure 2.9 lists the total wireless broadband subscriptions of OECD members and China mainland by the end of 2013. China still has the most wireless broadband users of 500 million, while USA, Japan, Korea, and the UK are ranked as No. 2–5.

OECD also indicates the broadband penetration of different countries by technology, as shown in Fig. 2.10. The penetration rate is greatly different from the total subscriptions. China has a very low fixed broadband penetration of 12.7 % because of its imbalanced development and large population, which is a contrast to its numerous broadband users. Meanwhile, it is noted that China has a relatively high portion of FTTH and LAN access, which is owed to its recent massive FTTH deployment. European countries such as Switzerland, The Netherlands, Denmark, and France have the best penetration of fixed broadband, with Switzerland having 45 % of fixed broadband penetration and ranked as No. 1. USA's penetration is in the middle, at 29.8 %. Considering the technologies, USA behaves much differently than China. The majority of fixed broadband technology is cable (coaxial technology), which reflects a different pattern from China. The second most-used technology is xDSL, while fiber/LAN has been used by only 2.4 % of the homes. Korea and Japan have the most penetration of fiber/LAN technology; hence, the

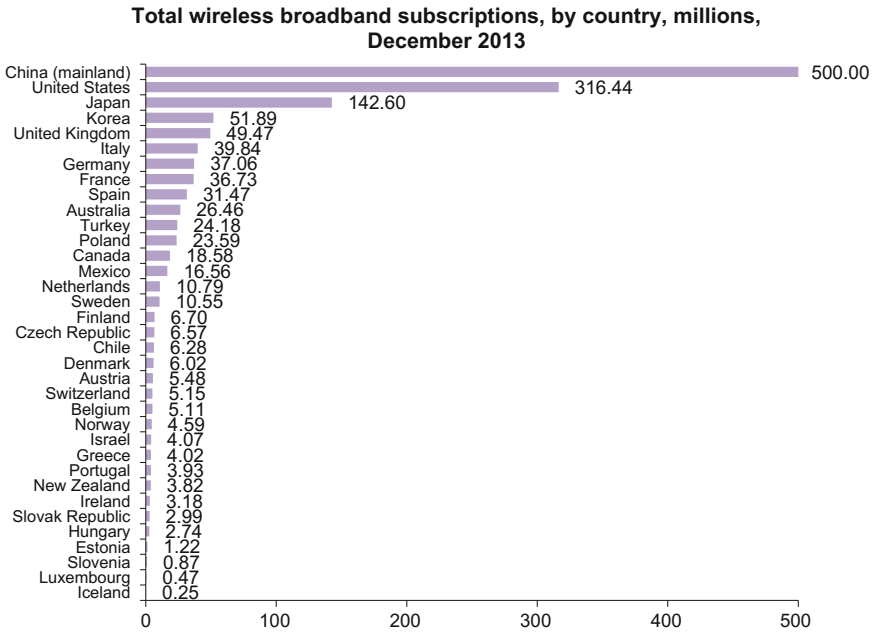


**Fig. 2.9** Wireless broadband subscriptions (in millions) in total by the end of 2013 [20]

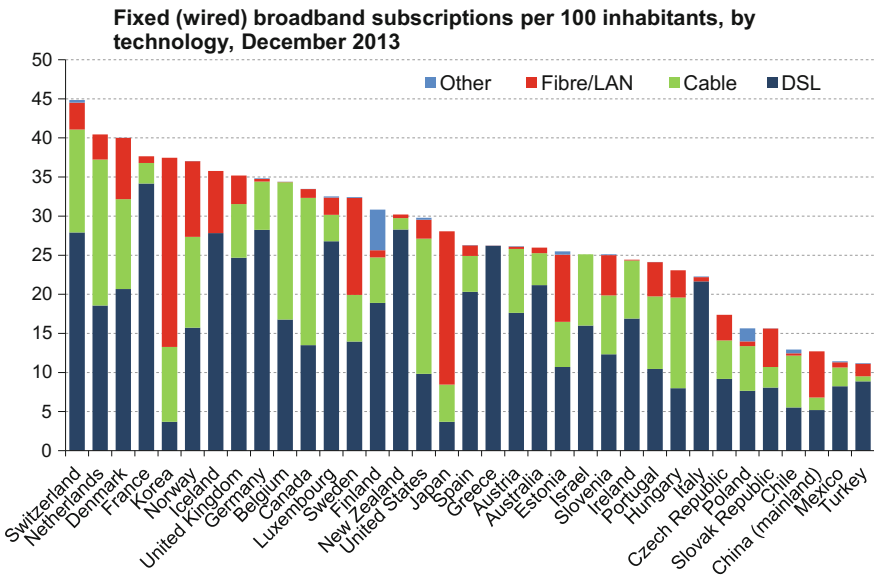


**Fig. 2.10** Fixed (wired) broadband subscriptions per 100 inhabitants, by technology, by the end of 2013 [20]

largest bandwidth was provided to the users. Overall, xDSL is still the main technology used, especially in European countries.

## **2.2.2 Broadband Wireless Access Networks**

In contrast to wired access networks, long-range wireless links can serve users over a widely distributed geographical area and can therefore be seen as a true alternative to the wired access options like fiber/PON networks. On the other hand, short-range wireless links only cover a small area such as a home or a building. Short-range wireless technologies therefore need to be augmented by wired backhaul access technologies in order to provide a complete solution for broadband access to the end user.

Many types of wireless access systems coexist and can be differentiated by spectrum, bandwidth, range, and applications. Wireless Personal Area Networks (WPANs, IEEE 802.15) allow the connectivity of personal devices within an area of about 30 feet. The current available technologies include Bluetooth, Infra Red (IR), Wireless USB, and Wireless HD, as cable replacement for peripherals. Fixed wireless access under the title “Wireless Metropolitan Area Networks” (WMANs, IEEE 802.16) become an alternative or backup to laying copper or fiber cabling. Although the 802.16-based standard has evolved to provide mobile access, due to the lack of actually developing an ecosystem with enough critical mass to justify the investment, this type of systems has not been able to gain any significant market share and will continue to see adoption in small-scale commercial and possibly military systems. As such, we will not delve into the details of this technology any further.

The two types of technologies that are most popular for providing broadband access today are the IEEE 802.11-based Wireless LAN (WLAN) standard, popularly known as Wi-Fi, and the current third, fourth, and future fifth generations of cellular technology.

### **2.2.2.1 Wi-Fi Technology Evolution and Market Status**

Wi-Fi has been the most widely adopted wireless access in the world, both in terms of devices and in terms of infrastructure. Wi-Fi chipsets have been part of the standard network interfaces in laptops and smartphones for many years now. The major growth drivers for Wi-Fi evolution for the current market include the following points:

- Integration of Wi-Fi into more consumer products: smartphones, digital cameras, e-readers, media players, gaming consoles, Blu-ray players, HDTVs;
- Increasing adoption and use of WLAN in companies, small office/home office, hospitals, etc. Enterprise market growing faster than retail market;

- Use of Wi-Fi to offload data from cellular networks;
- New applications: health/fitness, medical, smart meters, home automation.

Wi-Fi has evolved through the years to accommodate demands for faster data rates and greater bandwidth to support more feature-rich content and applications. Figure 2.11 details the evolution of the IEEE 802.11 Wi-Fi standard, demonstrating how new frequency bands, radio channels, signaling techniques, and multiple antennas have been used to dramatically increase Wi-Fi data rates. Wi-Fi is standardized by the IEEE under their 802 umbrella of standards for local area networks (LANs). Strictly speaking, “Wi-Fi certified” is the trademark name given to products that are certified to be interoperable by the Wi-Fi Alliance, which is a trade association that started in 1999 and promotes Wi-Fi and performs the certifications. As shown in Fig. 2.11, the Wi-Fi was invented in 1991 by NCR Corporation/AT&T. The first 802.11 standard was adopted in 1997. The first set of enhancements to the 802.11 standard—the 802.11a and 802.11b amendments—were ratified in September 1999. The 802.11b provided higher speeds for operation in the 2.4 GHz band by adding two higher rates—5.5 and 11 Mbit/s—to the already existing rates of 1 and 2 Mbit/s. The next speed boost for Wi-Fi systems was provided by the introduction of OFDM to the physical layer. The 802.11a standard supports rates range from 6 to 54 Mbit/s at a bandwidth of 20 MHz. Although the 802.11a standard was ratified in 1999, along with the 802.11b standard, availability of products lagged behind that of 802.11b, mainly due to the higher complexity and cost of the early implementations of OFDM chipsets [21–24].

The 802.11g standard was ratified in 2003. This version of the standard takes the OFDM PHY as specified in 802.11a and adds support for backward compatibility with legacy 802.11b systems already operating in the 2.4 GHz band. The major

- 1991: Wi-Fi was invented by NCR Corporation/AT&T with speed of 1/2Mbps.
- 1999: the Wi-Fi Alliance was formed and the first standard was released.
- 2000: first commercial use of the term Wi-Fi.

Ratified year	1997	1999	1999	2003	2009	2013	Future
IEEE Standard	802.11	802.11a	802.11b	802.11g	802.11n	802.11ac	802.11ad
Frequency Band	2.4GHz	5GHz	2.4GHz	2.4GHz	2.4GHz, 5GHz (Concurrent or selectable)	5GHz	60GHz
Max Data Rate	2Mbps	54Mbps	11Mbps	54Mbps	600Mbps	1.3Gbps	7Gbps
Technology	SISO	SISO	SISO	SISO	MIMO	MU-MIMO	MU-MIMO

**Fig. 2.11** Evolution of Wi-Fi technologies

enhancement introduced by 802.11n was the inclusion of MIMO with support for up to four spatially multiplexed streams. In addition, the bandwidth supported was doubled to 40 MHz. Over this bandwidth, with four spatial streams, 802.11n boasts a top speed of 600 Mbit/s. The highest order QAM modulation stays the same (64-QAM) as 802.11a. 802.11n has been specified for operation in both the 2.4 GHz band and the 5 GHz band.

The latest version of the WLAN standard, 802.11ac [25–27], was ratified in December 2013. The 802.11ac specification mandates operation in the 5 GHz band, where there is relatively less interference and more channels are available compared to the 2.4 GHz band. 802.11ac achieves a maximum throughput of 6.93 Gbps in 160 MHz bandwidth mode in the 5 GHz band, using eight spatial streams and 256QAM modulation. 802.11ac has also specified multi-user MIMO (MU-MIMO), which allows simultaneous transmission of MIMO streams to multiple client devices. For the initial systems which are likely to be 80 MHz, the peak speed per spatial stream is 433 Mbit/s. In addition, 802.11ac has defined a single closed-loop method for transmit beamforming, which is expected to be an optional feature of the Wi-Fi Alliance certification plan. 802.11ac has also introduced dynamic bandwidth management to optimize the use of available bandwidth. These new features of 802.11ac deliver the next leap in performance, which also includes simultaneous streaming of multiple HD video streams.

IEEE Working Group and the Wireless Gigabit Alliance (WiGig) jointly proposed IEEE 802.11ad, which is targeting short-range communication with up to 7 Gb/s speed that uses approximate 2 GHz spectrum in 60 GHz. With the huge number of existing client devices, backward compatibility with current standards using the same frequency range is vital. The goal is for all IEEE 802.11 standards to be backward compatible and for 802.11ac and 802.11ad to be compatible at the medium access control (MAC) or data-link layer. They should differ only in physical-layer (PHY) characteristics. Devices could then have three radios: 2.4 GHz for general use, 5 GHz for more robust and higher-speed applications, and 60 GHz for ultra-high-speed operation within a room—as well as support session switching among them.

IEEE 802.11ax is the successor to 802.11ac and will increase the efficiency of Wi-Fi networks. This project has the goal of providing 4× the throughput of 802.11ac used in dense deployment scenarios. 2019 is the target date for a ratified 802.11ax standard. Currently, it is in very early stage. Another newly designed protocol is IEEE 802.11ah. It utilizes sub 1 GHz license-exempt bands to provide extended range Wi-Fi networks and benefits from lower energy consumption, allowing the creation of large groups of stations or sensors that cooperate to share the signal, supporting the concept of the Internet of Things (IoT). The standard is expected to be finalized and arrive in 2016, with chips and systems based on 802.11ah already hitting the market.

From the market perspective, over 2.4 billion chipsets were expected to ship during 2014, dual-band 802.11n/802.11ac will comprise the vast majority of chipsets shipped among all the protocols as shown in Fig. 2.12 (ABI Research).

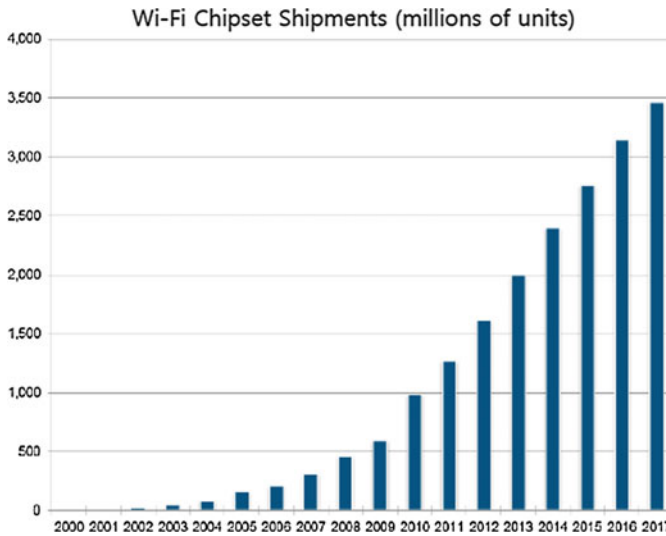


**Fig. 2.12** Wi-Fi market prediction

Nearly 18 billion more chips will ship cumulatively from 2015 to 2019 with a strong ramp of tri-band 802.11n/802.11ac/802.11ad during that period [24–27].

### 2.2.2.2 Mobile Network Technology Evolution and Market Status

Mobile networks provide connectivity over a wide geographical area and support handover mobility and cell roaming. Compared to Wi-Fi systems, mobile systems are more complex, as they are designed to support high-grade voice services, with seamless mobility, over a much greater area. Of the 6.8 billion mobile subscriptions in the world today (compared to the global population of 7 billion) [28], 2.1 billion are mobile broadband, which is three times the number of fixed broadband accounts [28].

Wireless communications have evolved from the so-called second-generation (2G) systems of the early 1990s, which first introduced digital cellular technology, through the deployment of third-generation (3G) systems with their higher-speed data networks, and the fourth-generation technology utilized today, to the much-anticipated fifth-generation technology being developed today. This evolution is illustrated in Fig. 2.13, which shows that fewer standards are being proposed for the newer generations compared to previous generations. For example, only two 4G candidates are being actively utilized today: 3GPP LTE-Advanced and IEEE 802.16 m, which is the evolution of the WiMAX standard known as Mobile WiMAX™.

The 2G systems, which are still in wide use today, are based on a technology called GSM (Global System for Mobile), which was developed only for voice

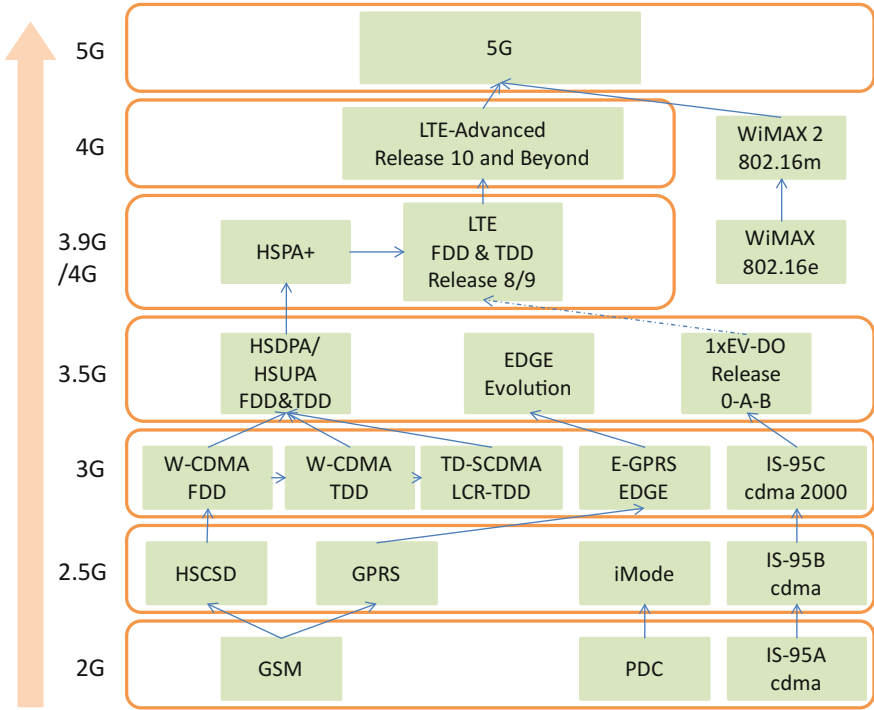


Fig. 2.13 Mobile network evolution

services. It was enhanced to support data services, first by the introduction of the GSM Packet Radio System (GPRS), and next by the addition of Enhanced Data Rates for GSM Evolution (EDGE). However, these systems were designed to depend fundamentally on the GSM air interface structure, and they were, therefore, limited in their ability to deliver true broadband speeds. The second alternative development of a new system designed to support both data and voice from the outset resulted in the third generation of cellular systems, which were based on an entirely different air interface technology. The Universal Mobile Telecommunication System (UMTS) was developed as the 3G cellular standard. UMTS is the umbrella term used for 3G systems that are based on the wideband-CDMA (WCDMA) air interface and a core network that has evolved from the GSM-based core network for circuit-switched and packet-switched services. The standardization of 3G UMTS systems was carried out under the auspices of the Third Generation Partnership Project (3GPP). This is a standards development organization (SDO) in which the partners and participation are drawn from regional standards organizations including ATIS (North America), ETSI (Europe), ARIB (Japan), TTA (Korea), TTC (Japan), and CCSA (China). Another system based on a relatively narrowband CDMA air interface, called CDMA2000,

represents a parallel technology evolution of the IS-95 standard. It was developed by a sister organization of the 3GPP called 3GPP2 [29].

There have been a number of different releases of UMTS, and the addition of High-Speed Downlink Packet Access (HSDPA) in Release 5 ushered in the informally named 3.5G. The subsequent addition of the Enhanced Dedicated Channel (E-DCH), better known as High-Speed Uplink Packet Access (HSUPA), completed 3.5G. The combination of HSDPA and HSUPA is now referred to as High-Speed Packet Access (HSPA). In the meantime, 3GPP2 developed another access technology, CDMA2000, which is conceptually very similar to WCDMA. In terms of worldwide subscribers, in early 2012, the number of CDMA2000-based 3G users represented about a fifth of the all 3G users, who were predominantly users of UMTS/HSPA. The subscribers were mainly in Asia/Pacific (Japan and Korea) and North America (subscribers of Verizon Wireless and Sprint in the USA). One of the fundamental differences between CDMA2000 and UMTS is in how it evolved to support high-speed data. The original CDMA2000 specification, called 1 RTT for 1 carrier Radio Transmission Technology, was published in 1999. A new uplink and downlink structure was developed to support high-speed data, but was designed only to carry packet-switched services. This evolution was originally called 1 eV-DO for Data Only. Later, eV-DO was modified to represent Data Optimized. However, the key difference between UMTS and CDMA2000 evolutions was that separate carriers were needed for voice and data services in CDMA2000, whereas the same carrier could support simultaneous voice and data on UMTS.

The Long-Term Evolution project was initiated in 2004. The motivation for LTE included the desire for a reduction in the cost per bit, the addition of lower cost services with better user experience, the flexible use of new and existing frequency bands, a simplified and lower cost network with open interfaces, and a reduction in terminal complexity with an allowance for reasonable power consumption. LTE arrived with the publication of the Release 8 specifications in 2008. LTE-Advanced is often abbreviated LTE-A, and the term LTE-A is now commonly used to describe Release 10 and Release 11. Small cells provide a cost-effective way for service providers to add focused capacity or coverage where needed within the nominal footprint of a macro-cell, via the use of low-power nodes. The LTE air interface is robust enough to allow the operation of such low-power small cells directly in the interference environment of a high-power macro-cell. However, in some environments, such as dense urban deployments, the footprint of the small cells may be too small for cost-effective offload of macro-cell users. As a result, the range of the small cell may need to be expanded to where the macro-cell signal may be several times stronger than that of the small cell. In order to operate the network in such a severe interference environment, a time-domain partitioning of subframes between the macro-cell and small cell, called eICIC, was introduced in the specification of Release 10.

In order to be able to keep deriving new terms to describe the technology as it evolves, the term LTE-B is now being used to describe Release 12 and beyond. The major feature added to Release 11 is the ability of multiple eNodeBs to coordinate

their transmission and reception to provide improved performance using a class of techniques called Coordinated Multi-Point, abbreviated as “CoMP.” This uses signals from multiple sources in a coordinated fashion to improve the quality of the desired signal, which can be either through the combining of useful signals in a constructive manner, or by the suppression of interfering signals in a synchronized manner. This processing usually results in the most improvement at the cell edge where interference is of most concern, because it is in this region that coordination between different eNodeBs can provide the most benefit. Like small cells, the benefit comes at the price of increased backhaul cost, because high-speed and low latency backhaul links are needed to share the information needed for coordination.

The wireless industry is quickly expanding LTE coverage in countries and cities across the world with several hundred networks in more than 100 countries. LTE-advanced, which is an evolution of LTE and a “true 4G” mobile broadband, is under development with many LTE-Advanced commercial deployments in several countries. 3GPP Release 12 (Rel-12) is the latest standard version of 3GPP to provide mobile operators with new enhancements in the three broad categories: LTE small cell and heterogeneous networks; LTE multi-antennas (e.g., MIMO and beam forming); LTE procedures for supporting diverse traffic types (further work on HSPA+ was also included).

For the current market situation, it is believed that as 3G coexists with 2G systems in integrated networks, LTE systems will coexist with 3G and 2G systems. Multi-mode devices will function across LTE/3G or even LTE/3G/2G, depending on market circumstances. However, the decline of global 2G GSM connections began in 2013, and the trending growth of 3G and 4G mobile broadband HSPA and LTE technologies continues unabated. Of the estimated 6.8 billion total wireless subscriptions as of the end of 2013, there were 1.6 billion HSPA and LTE mobile broadband subscriptions. This number is expected to grow to 5.6 billion in another 5 years. As shown in Fig. 2.14, while GSM represents 66 % of the global market in 2013, this will decline to 22 % worldwide GSM market share in 5 years. HSPA will more than double and LTE will grow eightfold.

Most industry experts saw WiMAX as a competing technology to LTE because both were designed to provide truly high-speed broadband access in a mobile

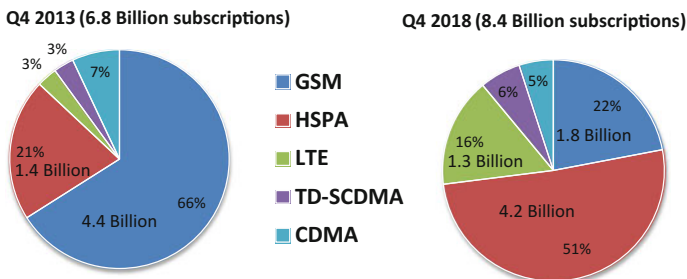


**Fig. 2.14** Global mobile technology shares 4Q 2013—Forecast 4Q 2018

setting, using a fourth-generation air interface based on OFDM. As such, WiMAX had a head start of at least a year before the Release 8 LTE specifications were ready. However, major industry players, such as Qualcomm and Ericsson, did not back the technology, and the leading operators in the USA, AT&T and Verizon, decided to deploy LTE. Only one US operator, Sprint, deployed WiMAX on a large scale, with a smattering of smaller deployments around the world.

In the future, it is believed that two significant trends will emerge: (1) Everything will be connected by wireless to enable monitoring and collection of information and control of devices. Examples of these services include remote monitoring and real-time control of a wide variety of devices, which support M2M services and the Internet of things (IoT), such as connected cars, connected homes, moving robots, and sensors; (2) wireless services will become more extensive and enhanced through richer content being delivered in real-time and with safety. Examples of such emerging services include high-resolution video streaming (4K), media-rich social networks, and augmented reality. It is also believed that besides the huge growth of total mobile traffic growth, there will be more traffic dynamics in the traffic volume depending on the time, location, application, and type of device.

Despite the advances made in the design and standard evolution of 4G mobile networks, new market trends are imposing unprecedentedly challenging requirements, which are driving the wireless industry toward next-generation mobile technologies, namely a fifth-generation system (5G). It is currently being researched and developed for deployment plans in 2020 or later with even further enhanced capabilities.

The race to search for innovative solutions to enable the 5G era has begun worldwide. In early 2013, the European Commission announced that it would invest €50 million in 2013 for 5G research in multiple projects such as METIS, quickly followed by the formation of the Chinese Government-led IMT-2020 Promotion Group in February 2013, the initiation of the Korean Government-led 5G Forum in May 2013, and the formation of 2020 and Beyond Ad hoc within ARIB (Association of Radio Industries and Businesses), Japan, in October 2013. Recently, the European Commission also announced that it would invest €700 million to 5G research through Horizon 2020 program. Much of the 5G activity in the Americas has been taking place in various universities. These research activities are often joint activities with private industry, funded through government grants, or a combination of the two, such as Berkeley Wireless Research Center (BWRC), NSF Grant for Evaluation of 60 GHz Band Communications, and Polytechnic Institute of New York University (NYU-Poly) Program. From the standardization perspective, 3GPP is currently working on additional 4G enhancements in 3GPP Releases 12 and 13. The ITU has recently initiated activities on defining requirements for International Mobile Telecommunications (IMT)-2020, similar to how ITU has previously defined requirements for IMT-2000 and IMT-Advanced. Eventually, this could lead to what is commonly referred to as “5G.” While the standardization of 5G specifications is still several years away, many share the vision of targeting 2020 for the initial commercialization of 5G cellular with drastically enhanced user experience.

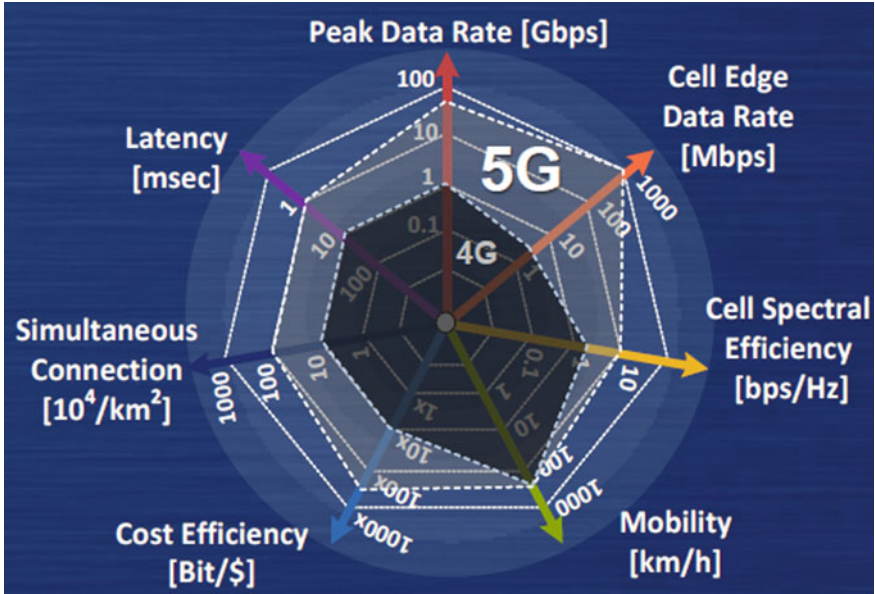


Fig. 2.15 Key requirements of 5G

The high-level key requirements of 5G are summarized in Fig. 2.15. 5G has to be able to manage traffic volume of many orders of magnitude larger than today's networks. It has to provide higher data rates for both peak data rate and user-experienced throughput everywhere. 5G has to allow massive number of devices to be connected simultaneously to the network in order to support all-time connected cloud services and more low-rate and low-power machine type devices for IoT. Reduced latency of less than 1 ms over the RAN is another necessity for future cloud and new services. 5G has also to reduce network cost and be energy-efficient and resilient to natural disasters. Enhanced mobility and spectral efficiency become important for meeting the challenges of future traffic trends.

Several possible technology areas may play a role in meeting these requirements: such as massive MIMO/adaptive beam forming and enhanced MIMO for interference cancellation, flexible full-duplex via the joint operation of FDD&TDD and/or unlicensed spectrum bands (60 GHz), non-orthogonal multiple access (NOMA) with the utilization of power domain, and other advanced modulation and coding technologies. These are all radio access technologies (RAT) from the wireless transmission perspective. Regarding the wireless networking level, centralized radio access network (C-RAN) is gaining great interest because of its potential to bring reduced costs, improved performance, and fixed/mobile convergence. Software-defined networking (SDN) and network function virtualization (NFV) will reshape the entire mobile ecosystem for best utilization of the whole wireless systems [30–33].

## 2.3 Fiber-Wireless Convergence and Technology Evolution

Today's wired networks, based on PON access technologies as discussed in previous sections, have the capability of providing huge bandwidth to end users using optical fiber, but they are not flexible enough to allow convenient roaming connections. On the other hand, wireless-based access solutions offer portability and flexibility to users, but they do not possess abundant bandwidth at lower microwave frequencies or have the difficulties to transmit longer distance at the millimeter-wave frequencies because of high attenuation in the air. To make full use of the huge bandwidth offered by optical fiber and flexibility features presented via the wireless, future broadband access networks will be bimodal, capitalizing on the respective strengths of both optical and wireless technologies and smartly merging them in order to realize future-proof Fiber-Wireless (FiWi) networks that strengthen our information society while avoiding its digital divide [34].

In the following section, some of major fields on the technologies of fiber-wireless convergence are identified and described including both commercial applications and research activities.

### 2.3.1 *Fiber-Based Distributed Antenna Systems (DASs)*

DASs using radio-over-fiber (RoF) links, the dominant market for RoF technology today, have been demonstrated and deployed to achieve broadband wireless access and improve wireless coverage in buildings with the features of low attenuation, large capacity, small-size remote antenna units (RAUs), and centralized management. As shown in Fig. 2.16, a DAS can be designed for use indoors or outdoors and can be used to provide wireless coverage to hotels, subways, airports, hospitals, businesses, roadway tunnels, etc. The wireless services typically provided by a DAS include cellular, Wi-Fi, WiMAX, police, fire, and emergency services. In a RoF-DAS, multiple RAUs are fiber-connected to a center unit where base station facilities are placed. In the downlink, the RAUs receive the optical signals carrying the RF signals from the center unit and convert them into electrical signals and then radiate them into air without any signal processing. A reverse process happens in the uplink. In this field, whether RoF based or not, there are a number of players currently offering DAS system for telecom carriers or enterprises. While Corning Mobileaccess, TE Connectivity, and Commscope dominate the marketplace, ABI Research has identified Axell Wireless, Solid Technologies, Optiway, Alvarion, Zinwave, and Powerwave as the foundation of the next phase of market development. Worldwide DAS Market Size was about \$1.9 Billion in 2012 (Telecomlead). While awareness of small cells is increasing, most DAS vendors do not really see small cells as a threat today. The two technologies, however, are more likely to complement each other rather than compete [35, 36].

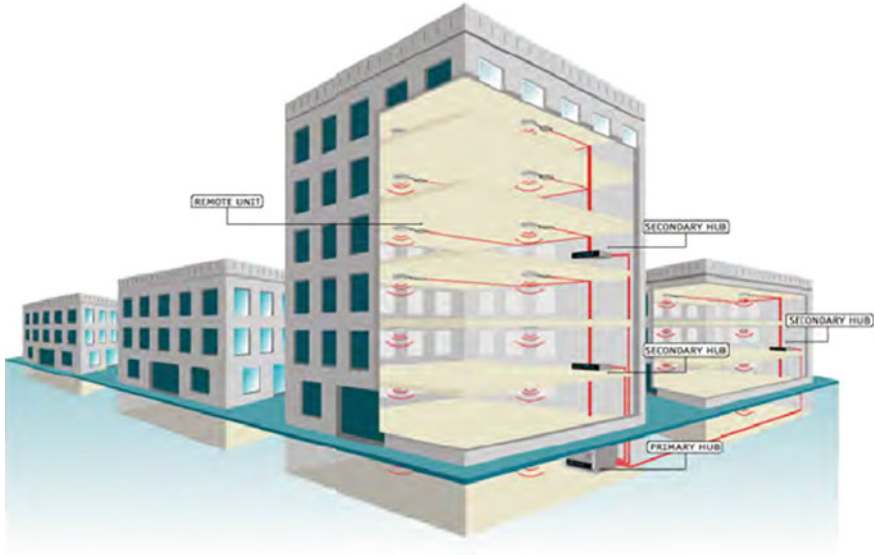


**Fig. 2.16** Fiber-based DAS systems for indoor/outdoor wireless coverage

### ***2.3.2 Ultra-High-Speed Fiber-Wireless Transmission***

With the advent of popular bandwidth-hungry applications such as high-definition (HD) video and high-speed Internet, future wireless systems need to offer data speeds exceeding 1 Gbps. Because of limited frequency spectra at low frequencies, coupled with congestion caused by the large number of consumer products sharing the frequency spectra, it will be necessary to utilize higher carrier frequencies in the future, including mm-waves, to achieve much faster wireless communication at multi-gigabit-per-second speeds. The wireless link speed depends on the frequency and the bandwidth of the wireless carrier. Thus, a high carrier frequency with a large bandwidth is suitable for the realization of a high capacity wireless link. Some wireless link experiments with data rates greater than 10 Gb/s have been performed at a frequency greater than 60 GHz. Multi-Gb/s wireless transmission systems can be constructed by the use of millimeter-wave bands such as V (50–75 GHz), E (60–90 GHz), or W (75–110 GHz) bands, where wide radio frequency resources are available for telecommunications. Unlicensed 60-GHz millimeter wave is very suitable for in-room transmissions due to reduced interference with other systems using the same frequency band. Antenna array and beam-forming technologies are essential avoid blockage due to environment change. In terms of atmospheric attenuation, the use of W-band transmission appears to be suitable, as the attenuation within this band tends to be less than 1 dB/km. However, due to limitation of electric signal processing performance, it is rather difficult to modulate or

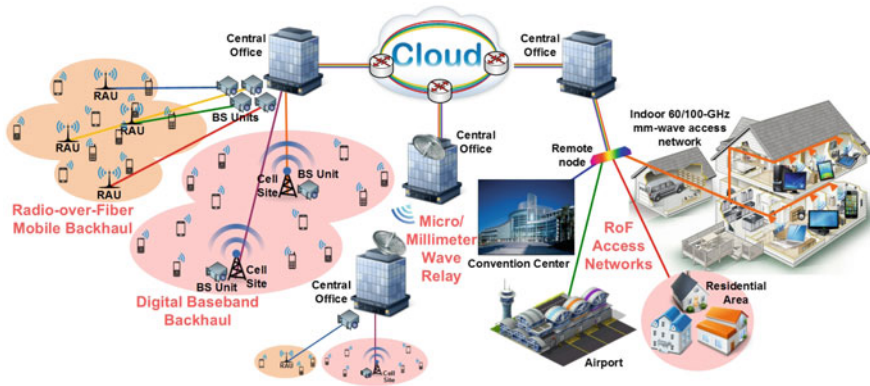


Fig. 2.17 Illustration of convergence of fiber-wireless networks

demodulate wideband millimeter-wave signals by using electric devices designed for narrowband radio systems [37–39].

The generation of wireless signals, based on the RoF technology, is expected to be suitable for high-frequency wireless transmissions as well as in applications involving an optical/wireless seamless network. Generally, the RoF signal is a combination of a RoF local oscillator (LO) carrier component and an optically modulated baseband component. It is easy to convert the optical RoF signal to a wireless signal with a frequency up-conversion technique, which is the so-called direct optical up-conversion technique that utilizes high-speed photodetectors. It is possible that the photodetector, whose frequency is less than the separation frequency between the RoF-LO component and the baseband component, can detect only the baseband components, as in the case as the conventional optical communication scheme. Therefore, the generated RoF signal would be available for the dual services of both optical baseband and wireless communications. The conceptual system block is shown in Fig. 2.17. Recently, large capacity up to 100 Gb/s millimeter-wave wireless links have been demonstrated by the use of RoF technology aided by advanced modulation formats (QPSK/16QAM/64QAM) and MIMO antenna array. Visible light communication (VLC) allows using indoor light-emitting diodes (LEDs) light sources for short-range wireless data transmission and illumination. However, the wireless transmission distance is limited due to inherent characteristics of the light source [40].

### 2.3.3 Fiber-Wireless for Backhaul and the Fronthaul of HetNet

In the past, the relatively low data-rate requirements of backhaul and the relatively large cell sites keep fiber deployment low in wireless backhaul. As the demand for

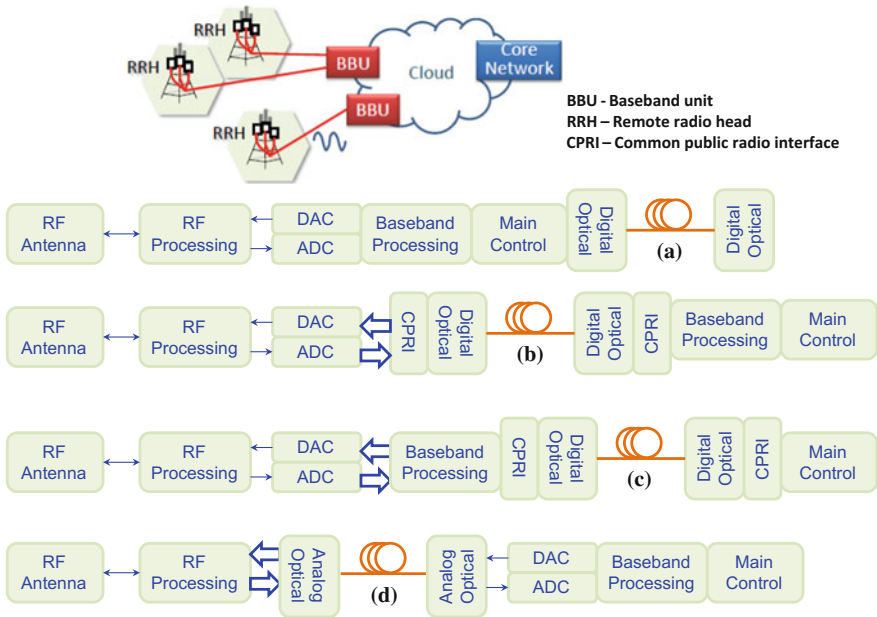


**Fig. 2.18** Potential solution for fronthaul and backhaul implementation by RoF technology

capacity in metropolitan areas has grown, macro cells have reached their limits in terms of the number of locations and/or penetration capability in indoor or densely populated locations. For example, the required total traffic capacity per 1 RU would be approximately 58.9 Gb/s to support LTE-A services employing signal bandwidth of 20 MHz, 2 carrier/antenna, 3 sectors, and  $8 \times 8$  MIMO antennas (data rate = Number of antenna per sector (MIMO) \* number of carriers/antenna \* number of sectors \* sampling rate (30.72Msamples/s/carrier for 20 MHz Channel Bandwidth) \* sample width (16 bit/sample) \* 2 (I and Q) \* 1.25 (overhead)) [41]. Compared with traditional backhaul, fronthaul refers to the interface between the cellular base station’s processing elements (namely, the baseband unit or BBU) and the attached radio units, which is shown in Fig. 2.18.

Small cells, low-powered radio access nodes that have a range of 10 m to 1 or 2 km, are one major innovation that is being currently deployed in larger volumes for capacity enhancements in hotspots in metropolitan areas. A more recent trend has seen mobile operators reconsidering decentralization of the radio-processing resources. This follows global trends of centralization of infrastructure to create a cloud-RAN or C-RAN. To this end, the BS architecture has changed from coax and fiber backhaul to centralize the BBUs and increasing the range of the distribution to RRHs using optical technologies. These techniques create a new paradigm of fronthaul to identify the connection between a baseband unit (BBU) or DU and a remote radio head (RRH) or remote radio unit (RRU) as opposed to backhaul which is from the BBU back into the core network. The pooling of BBUs provides

opportunities to implement dynamic capacity reconfigurability and a reduction in operational expenditure from centralization and consolidation of equipment. It has also been argued that this type of functionality is key in supporting advanced co-processing functions such as Heterogeneous Networks (HetNet) and CoMP, which are hotly tipped to be fundamental features of next-generation wireless networks. It is being predicted that small cells and carrier Wi-Fi deployments will generate nearly \$350 billion of revenue from mobile data services by the end of the decade. Figure 2.18 shows a number of potential implementations that use optical fiber to support the deployment of RANs. Besides the conventional digital connection (a), Digital RoF using the CPRI interface standard with all baseband functions is centralized (b), Digital RoF where the higher layer functions are centralized while radio and lower layer baseband functions remain at the RRH (split eNodeB) (c), analog RoF is also potential solution due to the system simplification, centralized control, and multi-service provisioning. Another potential benefit can be obtained by taking advantage of optical control in CoMP functions [42–44] as shown in Fig. 2.19.

Recently, some research groups have tried to use intermediate frequency over fiber (IFoF) technology as a mobile fronthauling technique to reduce the CAPEX and OPEX. In the IFoF system, it is possible to allocate multi-wireless signals with a particular bandwidth on any IF and then modulate it with a single optical carrier. For MIMO services, multi-wireless signals are assigned with multi-IFs and also multiplexed in the frequency domain [41]. In the meantime, another direction is targeting the convergence of conventional PON access and dedicated wavelengths for mobile traffic fronthaul and backhaul on a single fiber infrastructure. WDM-related access technology (TWDM/WDM-PON) is an attractive candidate for flexibly upgrading the total bandwidth of a mobile network and multiplexing

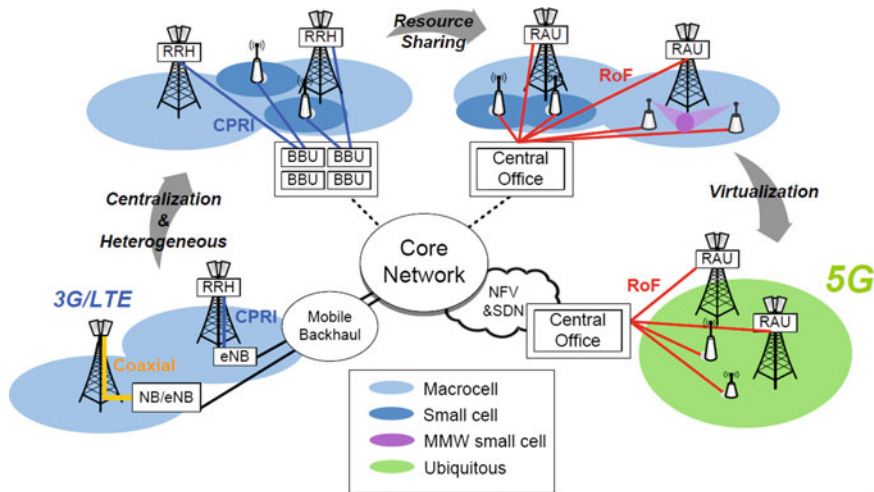


Fig. 2.19 Evolution of CoMP technology

different services on the same optical fiber distribution network. Fiber-wireless convergence will further optimize the use of the most costly part of fixed and mobile networks and drastically decrease cost and energy consumption, thus improving the return on investment of access and aggregation infrastructures: It will also allow central office consolidation of fixed networks to be performed in strong synergy with the development of mobile access infrastructures.

## 2.4 Conclusions

A variety of disruptive technologies are emerging to broaden the data and control plane functionalities of both broadband wireline and wireless access networks to meet the ever-increasing bandwidth requirements. In the meantime, the fiber-wireless convergence continues to evolve from the conventional DAS fiber feeding system and ultra-high optical-based wireless transmission to the architecture innovation in the implementation of fronthaul and backhaul system in mobile networks. Converged fiber-wireless access networks hold great promise to become the most promising solution of broadband access by capitalizing on synergies of two separate systems and are now well recognized for providing realizable service for both fixed and mobile users. It is believed that fiber-wireless system will play more important role in future evolved broadband access networks.

## References

1. (2014) Mobile and wireless communications system for 2020 and beyond (5G), ITU-R 2020 vision workshop
2. (2014) Ericsson mobility report. <http://www.ericsson.com/res/docs/2014/ericsson-mobility-report-june-2014.pdf>
3. (2014) Cisco visual networking index: forecast and methodology, 2013–2018
4. IEEE 802.3ah—Ethernet in the First Mile Task Force archive
5. Kramer G (2005) Ethernet passive optical network. McGraw-Hill. ISBN 0-07-144562-5
6. (2011) 10 Gb/s Ethernet passive optical network. Official working group web site. IEEE 802. Accessed 6 August 2011
7. (2003) Rec. G.984, Gigabit-capable Passive Optical Networks (GPON), ITU-T
8. Recommendation ITU-T G.992.3—Asymmetric digital subscriber line transceivers 2 (ADSL2)
9. tsbmail (2013). G.993.5: Self-FEXT cancellation (vectoring) for use with VDSL2 transceivers. Itu.int. Accessed 4 July 2013
10. UNDERSTANDING CAT—5 CABLES. Satellite & Cable TV. Accessed 5 Jan 2013
11. Cat5 Spec, cat6 specs, cat7 spec—Definitions, comparison, specifications. TEC Datawire. Accessed 5 Jan 2013
12. IEEE P802.3bn, EPON Protocol over Coax (EPoC) Task Force. <http://www.ieee802.org/3/bn/index.html>
13. [www.ovum.com](http://www.ovum.com). Superfast-Access Policy Tracker: 2014
14. <http://www.fcc.gov/>

15. [http://www.gov.cn/zwgk/2013-08/17/content\\_2468348.htm](http://www.gov.cn/zwgk/2013-08/17/content_2468348.htm)
16. [http://www.soumu.go.jp/main\\_content/000030866.pdf](http://www.soumu.go.jp/main_content/000030866.pdf)
17. <http://www.publications.parliament.uk/>
18. [http://www.hoganlovells.com/files/Publication/29686691-4067-49d7-b1e9-0199d2e27d6d/Presentation/PublicationAttachment/3b5ed8c6-f3d0-4b90-ada3-06c886b30387/TMEUpdate\\_Oct2008.pdf](http://www.hoganlovells.com/files/Publication/29686691-4067-49d7-b1e9-0199d2e27d6d/Presentation/PublicationAttachment/3b5ed8c6-f3d0-4b90-ada3-06c886b30387/TMEUpdate_Oct2008.pdf)
19. (2012) Breitbandstrategie [Broadband strategy]. Deutsche Breitbandinitiative. Accessed 19 April 2012
20. OECD Broadband Portal, Dec. 2013
21. Wi-Fi evolution, Qualcomm. <https://www.qualcomm.com/media/documents/files/wireless-networks-wi-fi-evolution.pdf>
22. Gorshe S et al (2014) Broadband access. ISBN: 9780470741801, 2014
23. Labiod H et al (2007) Wi-Fi™, Bluetooth™, Zigbee™ and WiMax™. ISBN-10: 1402053967
24. Wi-Fi Alliance. <http://www.wi-fi.org/>
25. Wi-Fi Timelines. [http://www.ieee802.org/11/Reports/802.11\\_Timelines.htm](http://www.ieee802.org/11/Reports/802.11_Timelines.htm)
26. (2012) Carrier Wi-Fi and Mobile Offload, ABI Research
27. (2014) 802.11ac: the fifth generation of Wi-Fi technical white paper, Cisco
28. Recommendations on 5G requirements and solutions, 4G Americas. [http://www.4gamericas.org/documents/4G%20Americas%20Recommendations%20on%205G%20Requirements%20and%20Solutions\\_10%2014%202014-FINALx.pdf](http://www.4gamericas.org/documents/4G%20Americas%20Recommendations%20on%205G%20Requirements%20and%20Solutions_10%2014%202014-FINALx.pdf)
29. (2011) Introducing LTE-advanced, Agilent
30. (2014) 5G radio access: requirements, concept and technologies, DOCOMO
31. (2014) 5G use cases and requirements, Nokia Solutions and Networks
32. Summary of Global 5G Initiatives, 4G Americas. [http://www.4gamericas.org/documents/2014\\_4GA%20Summary%20of%20Global%205G%20Initiatives\\_%20FINAL.pdf](http://www.4gamericas.org/documents/2014_4GA%20Summary%20of%20Global%205G%20Initiatives_%20FINAL.pdf)
33. Roh W et al (2014) Millimeter-wave beamforming as an enabling technology for 5G cellular communications: theoretical feasibility and prototype results. *IEEE Commun Mag* 52(2):106–113
34. Novak D et al (2013) Emerging disruptive wireless technologies: prospects and challenges for integration with optical networks. In: *OFC 2013, OTu3E.2*
35. Chow B et al (2009) Radio-over-fiber distributed antenna system for WiMAX bullet train field trial. In: *Mobile WiMAX Symposium, MWS '09. IEEE*
36. Gomes N et al (2009) Radio-over-fiber transport for the support of wireless broadband services. *J Optical Netw* 8(2):156–178
37. Anthony N (2013) Radio-over-fiber technologies for multi-Gb/s wireless applications. In: *OFC, OTU3E.3*
38. Kanno A et al (2011) 40 Gb/s W-band (75–110 GHz) 16-QAM radio-over-fiber signal generation and its wireless transmission. *Opt Express* 19(26):B56–B60
39. Jia Z (2008) Optical millimeter-wave signal generation, transmission and processing for symmetric super-broadband optical-wireless access networks. PhD thesis
40. Kawanishi T (2014) Ultra high-speed fiber wireless transport. In: *OFC, M2D.1*
41. Cho S et al (2014) Cost-effective next generation mobile fronthaul architecture with multi-IF carrier transmission scheme. In: *OFC, Tu2B.6*
42. Mitchell J (2014) Integrated wireless backhaul over optical access networks. *J Lightwave Technol* 32(20):3373–3382
43. (2013) Cloud-RAN deployment with CPRI fronthaul technology. JDSU White paper
44. Cheng L et al (2014) Optical CoMP transmission in millimeter-wave small cells for mobile fronthaul. In: *OFC 2014, W2A.43*

# Chapter 3

## The Benefits of Convergence Through Fiber-Wireless Integration and Networking

Gee-Kung Chang and Lin Cheng

**Abstract** A multi-tier radio access network (RAN) combining the strength of fiber-optic and radio access technologies employing adaptive microwave photonics interfaces and radio-over-fiber (RoF) techniques is envisioned for future heterogeneous wireless communications. All-band radio access technologies (RATs) will be used to deliver wireless services with high capacity, high link speed, and low latency. The multi-tier RAN will improve the cell edge performance in an integrated heterogeneous environment enabled by fiber-wireless integration and networking for mobile fronthaul/backhaul, resource sharing, and all-layer centralization of multiple standards with different frequency bands and modulation formats. In essence, for this multi-tier radio access architecture, carrier aggregation (CA) among multiple frequency bands can be easily achieved and seamless handover can be guaranteed through coordinated multi-point (CoMP) transmission among various cells. In this way, current and future mobile network standards such as 4G and 5G can coexist with optimized and continuous cell coverage using multi-tier RoF, regardless of the underlying network topology or protocol. In terms of user's experience, the future-proof approach achieves the goals of increased system capacity and link speed, reduced latency, and continuous heterogeneous cell coverage, while overcoming the bandwidth crunch in wireless communication networks.

### 3.1 Introduction

Driven by video streaming, cloud computing, and Internet of Things (IoT), the overall traffic volume in wireless communication systems has grown tremendously in recent years, fueled primarily by the uptake in mobile broadband [1–3]. This trend is expected to continue into the 5G era in 2020 as predicted by the roadmap of

---

G.-K. Chang (✉) · L. Cheng  
School of Electrical and Computer Engineering, Georgia Institute of Technology,  
Atlanta, USA  
e-mail: Geekung.chang@ece.gatech.edu

**Table 3.1** KPIs for next-generation mobile network [5]

KPI	IMT 2020 PG values
Peak data rate per user	>10 Gb/s
Minimum data rate user	>100 Mb/s
Supported user density	>1,000,000 connections/km <sup>2</sup>
Supported traffic density	>10 Tb/s/km <sup>2</sup>
Latency	<1 ms
Mobility	Up to 500 km/h

3GPP [4]. Based on the predictions of several major equipment suppliers, such as Ericsson, Nokia, and Cisco, it is believed that by 2020 wireless communication systems will have to support more than 1,000 times today’s traffic volume [1–3]. The key performance indices listed by the IMT-2020 promotion group in Table 3.1 foresee a tremendous growth in network performance. Extreme capacity and performance are required for the next-generation wireless access. Moreover, wireless communication trends including machine-type communication (MTC) and IoT require more features for future networks. None of the existing radio access technologies (RATs) will be able to individually provide the capabilities that effectively meet market demands. An evolution from existing and prospective technologies to support the ultimate radio access network (RAN) convergence is currently underway. Figure 3.1 gives an overall map of the various efforts to develop RANs, including raising wireless link performance, spectrum convergence, advanced multi-structure networking, and multi-RAT scenarios to fulfill the user needs for various applications.

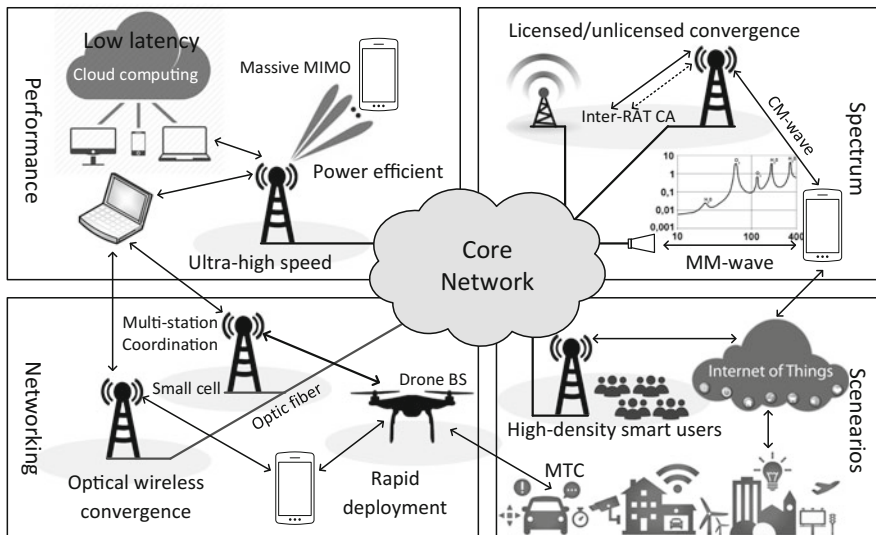


**Fig. 3.1** Future mobile communication system (BS base station, MTC machine-type communication, CA carrier aggregation, RAT radio access technology)

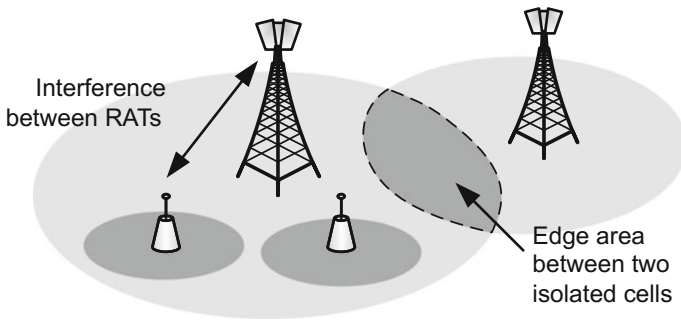
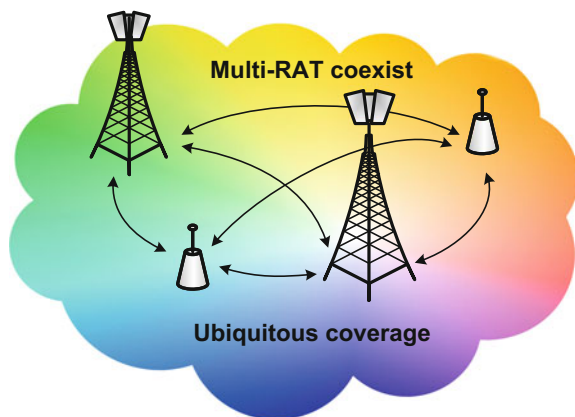


**Fig. 3.2** Current RAN with “walls” between cells and services

In current 4G networks, eNB, OFDMA, IP core, etc., are the major technologies that define the advancement of LTE from previous generations. However, in all generations so far, the network coverage is still composed of almost isolated cells, as illustrated in Fig. 3.2. The “wall” between different cells creates a challenge for both the mobile user’s experience and the backhauling for cell sites. Another “wall” exists among current RAT standards. Though local wireless is possible for traffic handover, users are simply served by independent RANs and unrelated RATs.

This chapter reviews how the convergence happens and what are the benefits for future mobile networks. Convergence is used to break the aforementioned “walls” and essentially merge all “isolated lanes” into a “super high-speed highway” that reaches all users in ubiquitous coverage, as shown in Fig. 3.3. It will be decided on the merits of three objective aspects: RAN architecture, backhaul and fronthaul links, and frequency bands for future mobile networks. This convergence includes fiber-wireless integration as well as multilayer centralization and resource sharing, resulting in seamless coordination among cells and services with accurate synchronization.

**Fig. 3.3** Future ubiquitous coverage enabled by technology convergence



The convergence gives us a vision of future mobile networks. Multi-tier heterogeneous cells with different frequencies converge to a ubiquitous coverage in a mobile network. Carrier aggregation among various bands is arbitrary, handover between various cells is smooth, and coordination at cell edge areas is seamless. Cells from different families coexist and are merged into an optimized continuous coverage distribution when needed. Multi-service coexistence, multi-RAT support, and licensed-assisted access (LAA) allow users to wander previously disparate standards.

## 3.2 Convergence of Architectures

### 3.2.1 Centralization

In traditional architectures deployed in current macrocell RANs, as shown in Fig. 3.4, each base station (BS) can only handle traffic in its coverage area. However, the interference between cells limiting the system capacity can hardly be managed by isolated BSs. Further, the limited communication over X2 links consumes lots of capacity by adding traffic overheads. As the cell size gets reduced and the number of cells increases, it will be too expensive to build, upgrade, and operate the network, as each cell needs its own BS at the cell site. Therefore, centralization is necessary, thus eliminating the BS cost, and consequently allowing multiple heterogeneous services to share the BS [6]. In addition, local small cells can now be connected by mobile midhaul and supported by BSs [7].

Centralized radio access network (C-RAN) architectures have been proposed to extract the baseband signal processing functions from distributed BSs and collocate the baseband units (BBUs) into a pool for centralized signal processing and

**Fig. 3.4** Architecture of traditional distributed RAN (SGW service gateway)

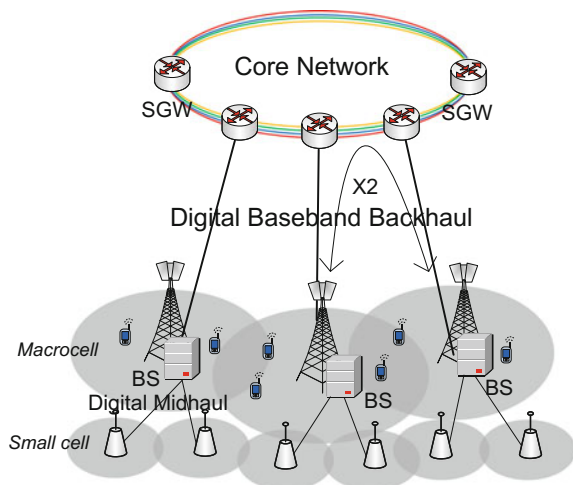
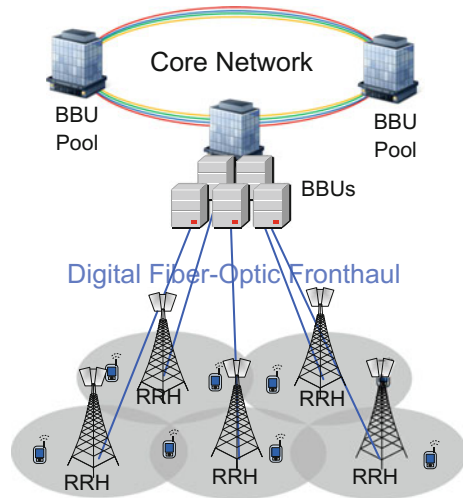


**Fig. 3.5** Architecture of centralized RAN with digital fiber-optic fronthaul



management, as shown in Fig. 3.5 [8]. The centralized BBU and distributed remote radio heads (RRHs) are connected by digital fiber-optic links via standardized digital RF interfaces, such as common public radio interface (CPRI) and open base station architecture initiative (OBSAI) [9, 10]. However, only fundamental centralization is achieved by these techniques and they are limited by their implementation complexity and exceedingly low-spectrum efficiency over the digital fronthaul. Although various optimizations have been proposed to reduce the bandwidth, such as splitting-PHY processing [11], RRHs still encompass a large number of the baseband functions and all of the RF functions.

The convergence of fiber-optic and wireless communications enables radio-over-fiber (RoF) fronthaul as a new form of RAT and hence fully centralized RANs. RoFs can support both digital RoF and analog RoF, but analog RoF will benefit more in terms of convergence and centralization. In the architecture of centralized RANs based on fiber-wireless convergence, all BS functions and most of the RF functions are shifted from cell sites to the BBU pool at the central office (CO) as shown in Fig. 3.6. Different from RRHs, only O/E, E/O, and a few RF components are needed at the end of the fiber fronthaul as the radio access units (RAUs). In other words, RAU is the simplified version of RRH. The comparison between RRH and RAU and other RAN parts is shown in Fig. 3.7. In this architecture, RoF signals carrying multiple services are transmitted from the CO to the RAUs, and directly converted from optical to RF signals for downlinks, while RF signals from the UE are directly carried on light wave at the RAUs for uplinks [12].

This fully centralized RAN architecture based on fiber-wireless convergence provides a solid solution for high-throughput access systems with several advantages [12]:

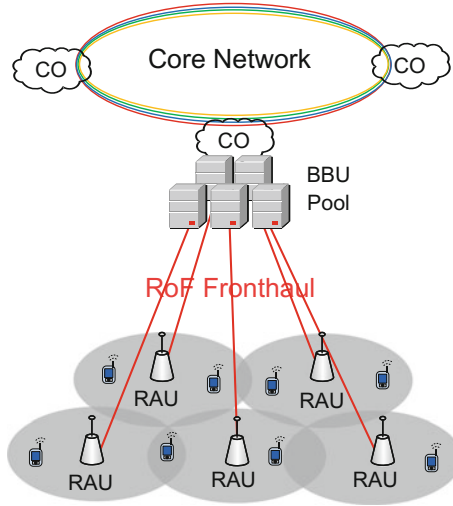


Fig. 3.6 Architecture of centralized RAN with RoF fronthaul

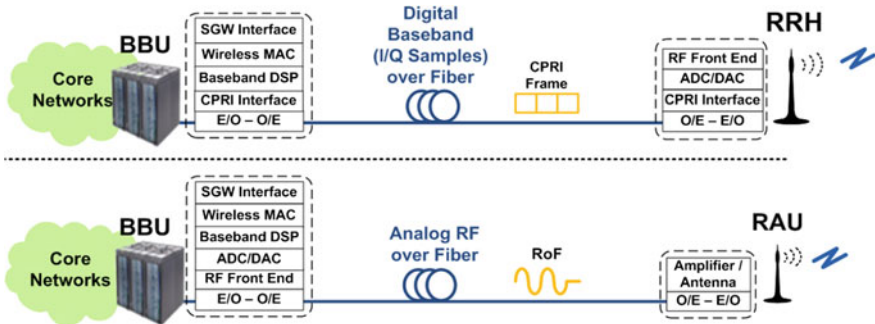


Fig. 3.7 Comparison between two centralized RAN architectures

- RAUs are highly simplified, thus the cell sites' footprint, power consumption, and demands for peripheral and technical support are considerably reduced.
- Cloud BBU pools significantly reduce the number of BSs. Each BBU can serve multiple RAUs to increase the infrastructure utilization rate.
- COs enable centralized processing and more flexible and efficient dynamic bandwidth allocation (DBA) and radio resource management (RRM). As BBUs work together, joint processing and cooperative radio to mitigate inter-cell interference (ICI) provide a higher spectral efficiency.
- Centralization and DBA make the network more adaptive to non-uniform distributed traffic resulting from the inter-cell movement of user equipment (UE).

- RoF fronthaul simplifies the generation and distribution of all frequency signals in a cost-effective way by microwave photonics (MWP) techniques, and provides a seamless integration with centralized RANs.
- The flexibility of centralization supports heterogeneous services and supplies an open platform for operations and maintenance (O&M), upgrade, and service expansion for smooth evolution.
- Most importantly, this centralized RAN architecture can maximize the resource sharing among operators and services over the entire RAN. Especially at the CO, with BBUs integrated inside the same pool, signaling, control, radio, channel state information, as well as physical infrastructures can be efficiently shared.

### 3.2.2 Resource Sharing

Figure 3.8 illustrates the physical resource-sharing hierarchy in centralized RANs where multiple operators and/or multiple services share the same system that includes the CO composed of high-performance BBUs and transceivers, high-bandwidth low-latency fiber links, and distributed RAUs.

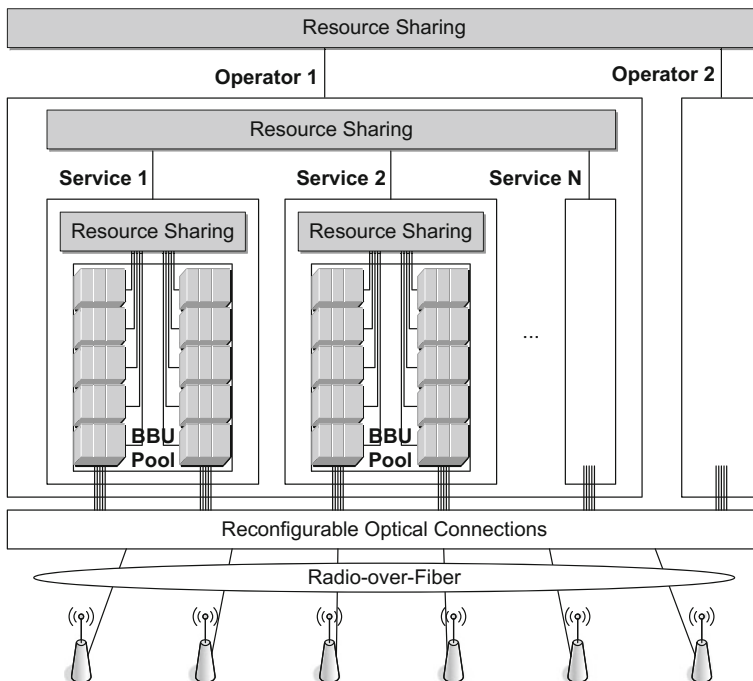


**Fig. 3.8** Resource sharing occurring at different levels in a centralized RAN

Physical resources including laser sources, radio sources, and peripheral equipment can be shared among different operators that provide multiple services. Sharing at this level may include communications between operators inside the CO, thus considerably reducing the core network traffic and improving the efficiency of common services supplied by multiple operators.

For each operator, the sharing among its services involves the physical resources and the O&M. This heterogeneous sharing is especially efficient if the number of cells is high or the services share similar DBA schemes. Further, it also makes direct communication between services possible. Operators can effectively manage the communications between services from the upper layers inside the CO so that the traffic through the SGWs can be eliminated.

For each service from an operator, the sharing inside the BBU pool may occur in Layers 1–3 and also O&M. A set of BBUs and their corresponding E/O transmitters are connected to the service resource-sharing port so as to carry the data, signals, and their processing [8, 13]. Sharing reduces the complexity of each BBU and simultaneously maximizes its utilization. However, resource sharing among BBUs is not only limited to a fixed service, but can also be applied to different services or even to different operators.

Furthermore, sharing occurs not only inside the CO, but also over the entire access infrastructure. At the RAU, the RF access equipment consisting of broadband O/E, E/O converters, and RF components is shared by multiple operators and/or services from the same CO. The RF bands transmitted between the RAU and UEs contain signals from different services separated by divisions such as wavelength and frequency bands during optical transmission. On the other hand, the output from one BBU transmitter can be shared by multiple RAUs. In this case, the virtual BS from each RAU's view is identical. This can be considered as a one-on-N distributed antenna system (DAS) scenario which is likely in small-cell RANs due to the mobility and density of UEs. This infrastructure sharing regime is realized by the reconfigurable optical connections between the CO and fiber link interfaces. Each RAU is virtually connected to all the BBUs in different pools. The reconfiguration manipulated by the upper layers maintains the desired connections between BBUs and RAUs.

### **3.3 Convergence of Links**

#### ***3.3.1 Mobile Backhaul***

Mobile backhaul, midhaul, and fronthaul are the three types of connections in a RAN in terms of the location of the links. Mobile backhaul is the physical link between the core network and the BSs in a distributed architecture as shown in Fig. 3.9. Even though centralization and mobile fronthaul are going to play more and more important roles in the converged architectures, distributed systems and

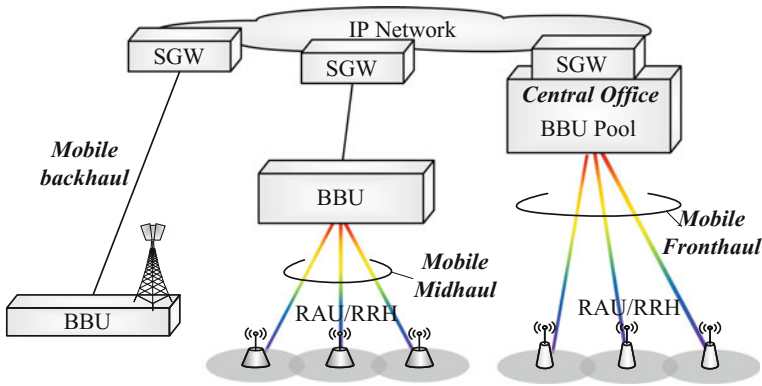


**Fig. 3.9** Mobile backhaul, midhaul, and fronthaul in RANs

mobile backhaul are still necessary to provide a fundamental tier in the heterogeneous network. Further, convergence of technologies will also occur in future mobile backhaul networks.

Historically, the transition to new mobile technologies has resulted in the need for a fourfold to fivefold increase in backhaul capacity. With the advancement from 3G to 4G, RANs reached a capacity of 1–10 Gb/s per cell [14]. Future 5G RANs will increase the requirement for backhaul capacity by at least ten times considering the effective throughput for each user and multi-antenna technologies. Wavelength-division-multiplexed passive optical networks (WDM-PONs) have become a promising solution to alleviate the issue of congested backhaul data traffic [15].

In typical WDM-PON systems, as shown in Fig. 3.10a, optical network units (ONUs) at subscriber ends (BSs in this case) require distributed transmitters, receivers, and other passive components, which greatly increase the OPEX/CAPEX. To reduce the cost of a distributed system, new converged WDM-PON technologies will be adopted to simplify the BS. One of the options is to implement bidirectional transmission systems with non-overlapping downlink and uplink wavelength reuse [16]. By doing so, all the light sources for both downlink and uplink are aggregated at the optical line terminal (OLT) as shown in Fig. 3.10. Assisted by MWP technologies, the converged design enables more efficient management for all the optical sources, e.g., the traditional distributed thermal control at each ONU can be replaced by an economical centralized cooling system at the OLT. Since complexity is centralized at the OLT, the system has the potential to further increase the capacity to adapt to future high-speed WDM-PON applications. In addition, such systems can mitigate troublesome effects such as incomplete data erasing and signal back reflections of traditional reflective WDM-PONs without significantly increasing the cost.

On the other hand, to meet the needs for higher spectral efficiency and bandwidth flexibility, mobile backhaul with more advanced modulation formats will be

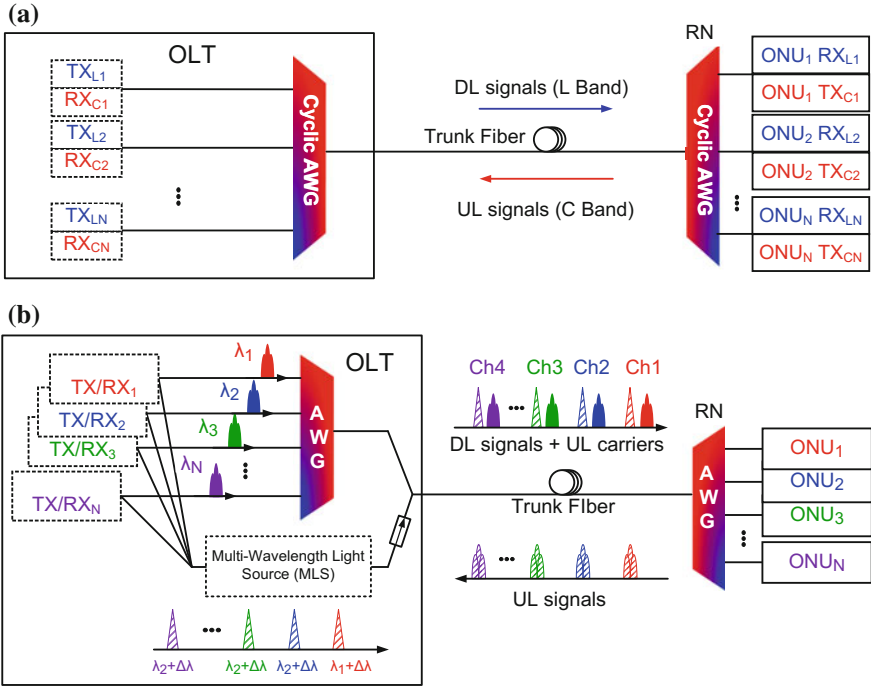


**Fig. 3.10** **a** Traditional WDM-PON structure and **b** non-overlapping wavelength reuse for converged WDM-PON

developed. Currently, orthogonal frequency division multiplexing (OFDM) [17], carrier-less amplitude and phase (CAP) modulation [18], and subcarrier multiplexing (SCM) [19] have been extensively investigated. Similarly, extensive research has been performed on DSP-based modulation formats such as generalized frequency division multiplexing (GFDM), universal filtered multi-carrier (UFMC) and filter bank multi-carrier (FBMC) for high spectral efficiency. The properties for some of these techniques are listed and compared in Table 3.2 below.

**Table 3.2** Advanced modulation formats

	CP-OFDM	FBMC (OQAM)	GFDM	UFMC
PAPR	High	High	Medium	High
CP for dispersion and multipaths	High	0	Reduced	0
OOB	High	Negligible	Reduced	Reduced
Time offset resiliency	Poor	Good	Good	Good
Frequency offset resiliency	Poor	Good	Good	Good
Complexity	Low	High	Medium	High
MIMO	Yes	Yes	Yes	Yes
CoMP	Yes	Excellent	Yes	Yes

In current LTE, OFDM can effectively combat multipath effect and inter-symbol interference (ISI), but it suffers from high peak-to-average power ratio (PAPR) and increases the DSP and synchronization complexities. Combined with quadrature amplitude modulation (QAM), traditional CAP and SCM techniques are more straightforward and can achieve spectral efficiencies (SE) comparable with that of OFDM. However, they still require high-speed DA/AD converters at BSs which in turn reduces the network scalability and tremendously increases the cost. Low-speed DAC/ADCs, with high resolution and reliable performance, can also be utilized to provide an inexpensive option by employing a low-cost intensity modulation/direct detection (IM/DD) scheme for future digitized optical access networks, especially at the BSs. This is now possible as a result of significant technological developments made by wireless service providers and hardware developers, enabling the low-cost and large-scale manufacture of multi-channel low-speed DAC/ADC chips, mixer arrays, and electrical oscillators by the IC industry.

### ***3.3.2 Mobile Midhaul and Fronthaul***

Mobile fronthaul is the physical link between the CO and the RRHs/RAUs in a centralized RAN. As a transient structure between backhaul and fronthaul, mobile midhaul is the link between a macroBBU and its extending RAUs. Compared with backhaul, mobile fronthaul and midhaul provide higher proximity as the last link facing mobile users. Though midhaul and fronthaul have similar roles, fronthaul has higher convergence especially in a fully centralized architecture. More and more mobile fronthaul links will coexist with traditional mobile backhaul and midhaul as the convergence occurs in RANs. The evolution and expansion of mobile fronthaul are directly driven by the exponential growth of the users' demand. A solid fronthaul design is the key approach to build efficient pipes between BBUs and users in terms of coverage, throughput, bandwidth, multi-service, quality, cost, and the compatibility to a long-term convergence. In converged RANs, as the number of cells increases and the average cell size becomes smaller, a huge number of fronthaul links are needed to distribute high-density, high-frequency, high-performance, but lightweight access units. More tiers of different types of cells will coexist in a heterogeneous form to fulfill different demands and provide ubiquitous coverage [20]. Mobile fronthaul supports new-style small cells, as well as inherits legacy cells including macrocells from 4G and small cells from WLAN networks. High-capacity, low-cost, flexible, and transparent services are the metrics for mobile fronthaul design. Furthermore, advanced technologies such as coordinated multi-point (CoMP) transmissions and multi-point carrier aggregation (CA) rely highly on fronthaul characteristics, bringing stringent synchronization and system stability requirements on mobile fronthaul designs [21].

In current RANs, digital fronthaul solutions such as CPRI and OBSAI are straightforward and robust approaches to fulfill basic LTE bandwidth needs. However, their low efficiency will require unaffordable high-speed transceivers and will limit any further bandwidth improvement when they are applied in future high-speed RANs. To fully digitize the RF signals into in-phase and quadrature components, the CPRI interface needs tremendous bandwidth, and any compression method must be developed considering the strict limitation on latency and hardware complexity. In CPRI, a 20 MHz LTE signal, as an example, takes up to 10-Gb/s fronthaul rate. When a 5-channel CA is applied, a 50-Gb/s rate will eventually consume all transceiver capacity. Moreover, in both CPRI and OBSAI, their digital interfaces cause unavoidable delay and jitter, becoming unfriendly to high-speed services that require precise synchronization.

In the next-generation 5G mobile communications, a large number of antennas are needed at the cell site in order to support antenna techniques such as massive MIMO, and each antenna needs a high-capacity stream in the CPRI scheme. Moreover, heterogeneous networks enable the seamless integration of high-frequency small cells with existing cells to support high-speed, low-latency services. As mobile fronthaul networks evolve from 4G–5G, it becomes technically challenging and cost prohibitive to accommodate multiple bands and multiple services into the conventional C-RAN network using digital interfaces.

The convergence over mobile fronthaul itself plays an important role in the universal convergence of RANs. RoF as the core technique to realize fronthaul convergence can solve most of the problems that a distributed digital system may incur. RoF technology is developed as an analog solution that avoids digital components or extra processing overhead over fronthaul. It improves optical spectrum efficiency and simplifies the RAU design. On top of a centralized RAN, RoF provides high-level centralization and minimizes complexity distribution. All baseband functions and most RF signaling are realized in a CO where resources are shared among all fronthaul links even if the links have various structures and serve different types of cells. By centralizing all DSP functions into BBU, downstream RF signals are transmitted as analog signals, where multiple bands of multiple services can be multiplexed in the frequency domain by using band mapping and CA techniques [22]. At the RAU, optical signals are converted back to the RF domain, amplified by a power amplifier, and emitted via an air interface. In addition, RoF facilitates the generation and distribution of high-frequency signals in optical approaches, as high-frequency signaling burdens fronthaul systems much more than low-frequency microwave signals [23].

A versatile multi-structure mobile fronthaul architecture based on RoF technologies and C-RAN hierarchy can converge different access technologies and can provide users proximal access in different environment, as shown in Fig. 3.11. A CO centralizes functions for both macrocells and small cells, including baseband processing as well as radio signaling. It supports both low-frequency (LF) and high-frequency (HF) bands. The LF small cells are normally in unlicensed bands (e.g., 2.4/5 GHz, LTE-U) to provide hot-spot coverage, while the HF small cells

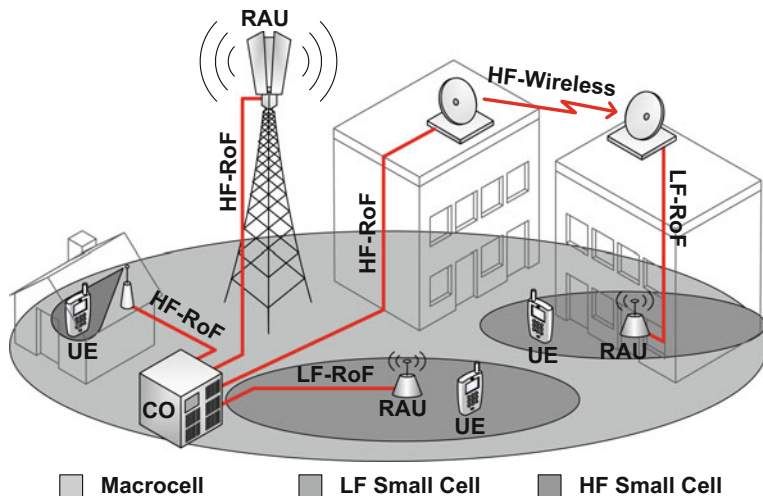


Fig. 3.11 Versatile multi-structure mobile fronthaul architecture

(e.g., 60 GHz) provide very high-throughput coverage for minor-mobility indoor users.

As a result of convergence, no baseband or digital processing exists between the CO and the UE in any fronthaul structure. Besides cost and management savings, this simplification leads to the important property that the propagation delay is only determined by the fronthaul length. For example, a user that is 1 km away from the CO and is covered by a small cell with 2-km fiber fronthaul (including 1 km of detour) has a fixed time offset of 6.7  $\mu$ s without any jitter. This is a promising improvement from traditional CPRI systems where digital processing takes variable delays. Furthermore, in RoF-based fronthaul structures, all latencies are predictable, stable, and easily compensable at the CO so that advance technologies such as CoMP transmission and multi-point licensed-assisted CA can get precise synchronization.

### 3.4 Convergence of Bands

#### 3.4.1 All-Band Coverage

Low-frequency bands (<6 GHz), centimeter-wave (CMW) bands (6–30 GHz), and millimeter-wave (MMW) bands (30–300 GHz) are the three main groups of serving RF bands. Existing cellular systems operating below 6 GHz frequency bands are heavily utilized. There is little space to further increase the transmission rate in these frequency bands. Thus, to reliably support multi-Gbps data rates, high-frequency bands will be exploited for high-capacity access and coverage.

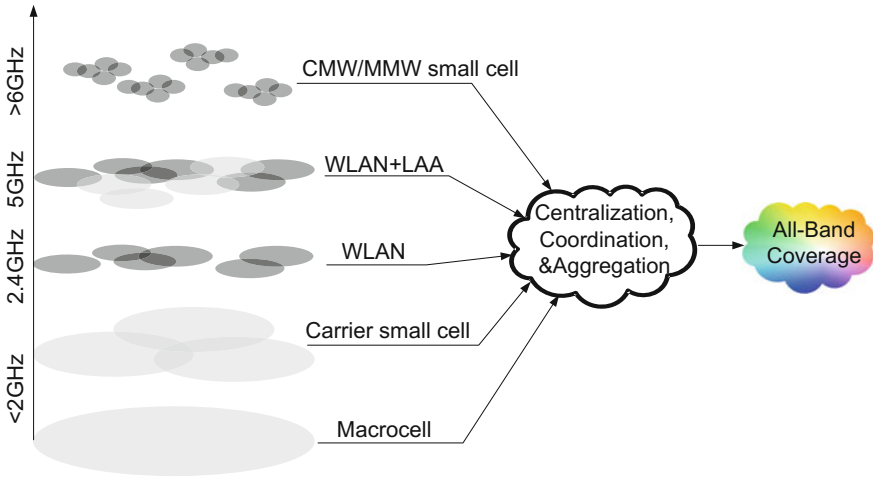


Fig. 3.12 All-band coverage and different service tiers

As shown in Fig. 3.12, on top of traditional low-frequency bands, the exploitation and convergence of CMW and MMW bands can provide potential multi-Gbps wireless links with continuous spectrum. By decoupling control and data channels, multi-RAT access over multiple available bands can boost users' throughput, while still managed by operators' networks. An example is to use WLAN and LAA to associate local unlicensed spectrum to current licensed networks so that two or more spectral channels are aggregated for a certain user. This LAA is also possible for CMW/MMW small cells with higher CA requirement.

However, although the target coverage of CMW and MMW small cells is smaller compared to low-frequency cells, there are several challenges for the deployment of these cells. First, they have to cope with unfriendly high-frequency propagation conditions such as large path loss, blocking object attenuation in real environments, and signal blockage loss due to atmospheric absorptions [24]. Second, considering the mobility of users, they should support dynamic multi-direction signal delivery [25]. Third, CMW and MMW cells should have the functionality to provide flexible support for different service coverage areas including both indoor and outdoor situations [26]. Finally, the high-carrier frequencies, and especially the ultra-wide bandwidths of MMW, have high requirements on hardware for signal generation and distribution.

To solve problems 1–3, MIMO technology is the most effective approach to overcome the inherent drawbacks of high-frequency wireless. Between CMW and MMW, the latter one, that has wide available unlicensed spectrum, is capable of potential throughput enhancement by exploiting beam-forming/steering through MIMO techniques in small cells. Since MMW has small wavelength, massive MIMO technology with beam-forming is promising for high-performance radio

access. Phase antenna arrays are designed for this adaptive beam-forming in different propagation conditions, including single-user and multi-user, NLoS and LoS, static and mobile users. There is considerable research work on beam-forming schemes based on all-electronic or photonic-assisted structures. All-electrical phase-controlled antenna arrays can simultaneously change the amplitude and phase of the signal of each antenna in different RF-chain, which allows for more flexible steering. However, considering the large bandwidth of MMW requiring large numbers of high-speed ADCs and phase shifters, all-electronic control of antennas can cause significant power consumption and has high cost, high complexity, large size, and large weight. Photonic-assisted methods hold a great potential for solving these challenges and enable the use of fiber links with RAU/RRH in a long distance without much loss, as well as fast optical signal processing [27, 28]. In order to change the phase delay of each RF signal, a dispersion medium, such as fiber, fiber Bragg gratings, or other wavelength-selective modules can be used. A photonic amplitude changing module or chip is required to change the intensity of the split optical signals. After the PDs' detection, the mm-wave signals are transmitted by the antenna array with desired beam form. The independent backhauling for each antenna element is solved by the converged fiber-wireless links that conceive and maintain the amplitude and phase information of wireless signals as they are during optical transmissions. In addition, to solve the fourth problem mentioned above, microwave photonic technologies are adopted to ease the generation and distribution of MMW carriers.

In any case, high-frequency bands standing alone have inherent limitations to provide reliable control for mobile networks. By converging traditional low-frequency radio and newly deployed high-frequency radio, RANs can provide an all-band access pipe for the highest channel capacity. The multi-tier coverage for mobile users takes advantage of all the aforementioned potential frequency bands by supporting multiple types of RATs and inter-band CA.

### 3.4.2 *MMW Links*

A multi-structure mobile fronthaul provides system resilience, flexibility, and increased overall bandwidth capacity. The benefits of exploiting MMW for fronthaul transmissions include high capability of wireless data transmission, simple deployment, and adaptive environmental suitability.

To reach high spectral efficiency, advanced MMW technologies are desired for signaling, and this is realized by the supporting fiber-wireless convergence. In fact, many RoF links over MMW bands have been proposed and experimentally demonstrated in recent research efforts. Bit rates above 100 Gb/s have been attained by adopting spectrum-efficient modulation formats and digital coherent detection enabled by fiber-wireless convergence [29–31]. Different approaches for the realization of high-speed fiber-wireless integration systems as mobile backhaul/fronthaul are proposed, including optical polarization division multiplexing

(PDM) combined with MIMO reception [32, 33], advanced multi-level modulation, multi-carrier modulation [31], antenna polarization multiplexing [34, 35], MMW CoMP transmissions [36, 37], and multi-band multiplexing [38]. These approaches can effectively reduce the signal baud rate as well as the required bandwidth for optical and electrical devices. Crosstalk due to polarization rotation and MIMO transmission can be effectively solved based on advanced DSP algorithms including the classic constant modulus algorithm (CMA) [31]. Photonics-aided coordination also improves the MMW transmission stability and mitigates ICI [37].

### 3.5 Conclusion

In this chapter, we have discussed and reviewed the benefits of the convergence of fiber-optic-based optical access networks with radio access networks beyond the current bandwidth crunch. The convergence is used to break these legacy “walls” and merge all isolated and precious bandwidth lanes into a super-speed highway that reaches all users ubiquitously in future mobile data networks. The convergent networks will generate profound changes in RAN architectures, backhaul and fronthaul links, and the way frequency bands are used for future wireless communications. Figure 3.13 summarizes the convergent technologies and directions that will occur in the newly changed RAN architecture. The convergence originates

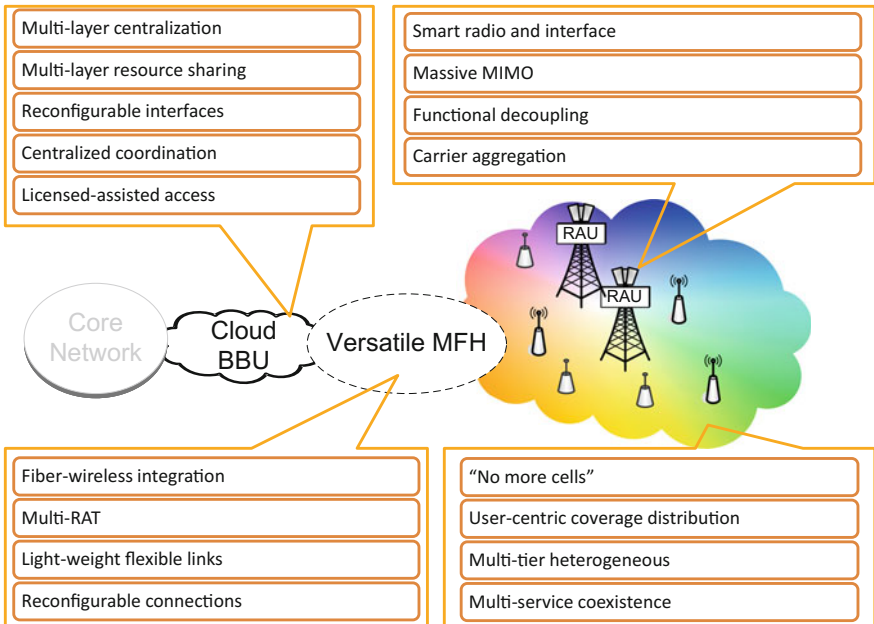


Fig. 3.13 Technology convergence occurring over the entire RAN architecture

from fiber-wireless integration to macro and small cells with multilayer centralization and resource sharing, and results in seamless coordination among cells and services with accurate synchronization in future mobile networks. The convergent networks will usher in a new era for future mobile networks, with integrated multi-tier heterogeneous cells with flexible and user-centric wireless converging to provide a ubiquitous coverage for mobile communications. In this grand unified scheme, carrier aggregation among various bands is flexible and scalable, handover between various cells is smooth, and coordination of user data throughput at cell edges is seamless. Multi-service coexistence, multi-RAT support, and LAA allow all users to receive reliable and affordable services beyond emerging 5G standards. The convergence of fiber-optic and radio access networks will ultimately benefit the future mobile users in a “no more cells” and “no more standards” environment to attain highly rich and reliable experience beyond the capacity crunch.

## References

1. White paper, Cisco visual networking index: forecast and methodology, 2012–2017, Cisco VNI Report, May 2013. [http://www.cisco.com/en/US/solutions/collateral/ns341/ns525/ns537/ns705/ns827/white\\_paper\\_c11-481360.pdf](http://www.cisco.com/en/US/solutions/collateral/ns341/ns525/ns537/ns705/ns827/white_paper_c11-481360.pdf)
2. Rappaport TS et al (2013) Millimeter wave mobile communications for 5G cellular: it will work! IEEE Access 1:335–349
3. DOCOMO 5G White Paper, “5G Radio access: requirement, concept, and technologies”. [https://www.nttdocomo.co.jp/english/binary/pdf/corporate/technology/whitepaper\\_5g/DOCOMO\\_5G\\_White\\_Paper.pdf](https://www.nttdocomo.co.jp/english/binary/pdf/corporate/technology/whitepaper_5g/DOCOMO_5G_White_Paper.pdf)
4. Bertenyi B (2014) 3GPP system standards heading into the 5G era. EURESCOM Message. [http://www.3gpp.org/news-events/3gpp-news/1614-sa\\_5g](http://www.3gpp.org/news-events/3gpp-news/1614-sa_5g)
5. IMT-2020 Promotion Group (2014) White Paper, 5G Vision and Requirements. [http://euchina-ict.eu/wp-content/uploads/2015/03/IMT-20205GPG-WHITE-PAPER-ON-5G-VISION-AND-REQUIREMENTS\\_V1.0.pdf](http://euchina-ict.eu/wp-content/uploads/2015/03/IMT-20205GPG-WHITE-PAPER-ON-5G-VISION-AND-REQUIREMENTS_V1.0.pdf)
6. Liu C, Cvijetic N, Sundaresan K, Jiang M, Rangarajan S, Wang T, Chang G-K (2013) A novel in-building small-cell backhaul architecture for cost-efficient multi-operator multi-service coexistence. In: IEEE/OSA optical fiber communication conference (OFC)
7. MEF 22.1.1, Mobile Backhaul Phase 2, Amendment 1, Jan 27, 2014
8. China Mobile, C-RAN white paper, 2011
9. Common Public Radio Interface (CPRI) specification, V6.1, June 2014
10. Open Base Station Architecture Initiative—BTS System Reference Document, V2.0, 2006
11. Miyamoto K, Kuwano S, Terada J, Otaka A (2015) Split-PHY processing architecture to realize base station coordination and transmission bandwidth reduction in mobile fronthaul. In: IEEE/OSA optical fiber communications conference (OFC), pp 22–26
12. Cheng L, Liu C, Zhu M, Wang J, Chang G-K (2013) Centralized small-cell radio access network with shared millimeter-wave radio-over-fiber resources. In: IEEE global communications conference (GLOBECOM), pp 2448–2453
13. Chang G-K, Liu C, Zhang L (2013) Architecture and applications of a versatile small-cell, multi-service cloud radio access network using radio-over-fiber technologies. In: IEEE international communications conference (ICC)

14. Oliveira RS, Frances CRL, Costa JCWA, Viana DFR, Lima M, Teixeira A (2014) Analysis of the cost-effective digital radio over fiber system in the NG-PON2 context. In: 16th international telecommunications network strategy and planning symposium (Networks), pp 1, 6, 17–19
15. Chang G-K, Chowdhury A, Jia Z, Chien H-C, Huang M-F, Yu J, Ellinas G (2009) Key technologies of WDM-PON for future converged optical broadband access networks. *IEEE/OSA J Opt Commun Netw* 1(4):C35–C50
16. Xu M, Wang J, Zhu M, Cheng L, Alfadhli YM, Dong Z, Chang G-K (2014) Non-overlapping downlink and uplink wavelength reuse in WDM-PON employing microwave photonic techniques. In: European conference on optical communication (ECOC), Sep. 2014, paper P. 7. 17
17. Cvijetic N (2012) OFDM for next-generation optical access networks. *IEEE/OSA J Lightwave Technol* 30(4):384–398
18. Zhang J, Yu J, Li F, Chi N, Dong Z, Li X (2013)  $11 \times 5 \times 9.3$  Gb/s WDM-CAP-PON based on optical single-side band multi-level multi-band carrier-less amplitude and phase modulation with direct detection. *OSA Opt Exp* 21(16):18842–18848
19. Buset JM, El-Sahn ZA, Plant DV (2013) Experimental demonstration of a 10 Gb/s subcarrier multiplexed WDM PON. *IEEE Photon Technol Lett* 25(15):1435–1438
20. Lopez-Perez D, Guvenc I, de la Roche G, Kountouris M, Quek TQS, Zhang J (2011) Enhanced intercell interference coordination challenges in heterogeneous networks. *IEEE Wireless Commun* 18(3):22–30
21. Irmer R, Droste H, Marsch P, Grieger M, Fettweis G, Brueck S, Mayer H-P, Thiele L, Jungnickel V (2011) Coordinated multipoint: concepts, performance, and field trial results. *IEEE Commun Mag* 49(2):102–111
22. Zhu M, Zhang L, Wang J, Cheng L, Liu C, Chang G-K (2013) Radio-over-fiber access architecture for integrated broadband wireless services. *IEEE/OSA J Lightwave Technol* 31(23):3614–3620
23. Yu J, Jia Z, Yi L, Su Y, Chang G-K, Wang T (2006) Optical millimeter-wave generation or up-conversion using external modulators. *IEEE Photon Technol Lett* 18(1):265–267
24. Zhao H et al (2013) 28 GHz millimeter wave cellular communication measurements for reflection and penetration loss in and around buildings in New York City. In: IEEE international communications conference (ICC), June 2013, pp 516–567
25. Azar Y et al (2013) 28 GHz propagation measurements for outdoor cellular communications using steerable beam antennas in New York City. In: IEEE international communications conference (ICC), June 2013, pp 5143–5147
26. Dehos C, González JL, Domenico AD, Ktésas D, Dussopt L (2014) Millimeter-wave access and backhauling: the solution to the exponential data traffic increase in 5G mobile communications systems? *IEEE Commun Mag* 52(9):88–95
27. Pasandi MEM, Sisto MM, Doucet S, Kim Y, Rusch LA, LaRochelle S (2009) Low-distortion optical null-steering beamformer for radio-over-fiber OFDM systems. *IEEE/OSA J Lightwave Technol* 27:5173–5182
28. Cao Z, Lu R, Wang Q, Tessema N, Jiao Y, van den Boom HPA, Tangdiongga E, Koonen AMJ (2014) Cyclic additional optical true time delay for microwave beam steering with spectral filtering. *OSA Opt Lett* 39:3402–3405
29. Li X, Dong Z, Yu J, Chi N, Shao Y, Chang GK (2012) Fiber-wireless transmission system of 108 Gb/s data over 80 km fiber and  $2 \times 2$  multiple-input multiple-output wireless links at 100 GHz W-band frequency. *OSA Opt Lett* 37:5106–5108
30. Yu J, Li X, Chi N (2013) Faster than fiber: over 100-Gb/s signal delivery in fiber wireless integration system. *OSA Opt Express* 21:22885–22904
31. Zhang J, Yu J, Chi N, Dong Z, Li X, Chang G-K (2013) Multichannel 120-Gb/s data transmission over  $2 \times 2$  MIMO fiber-wireless link at W-band. *IEEE Photon Technol Lett* 25(8):780–783

32. Dong Z, Yu J, Li X, Chang GK, Cao Z (2013) Integration of 112-Gb/s PDM-16QAM wireline and wireless data delivery in millimeter wave RoF system. In: IEEE/OSA optical fiber communication conference (OFC) 2013, Anaheim, California, OM3D.2
33. Li F, Cao Z, Li X, Dong Z, Chen L (2013) Fiber-wireless transmission system of PDM-MIMO-OFDM at 100 GHz frequency. *IEEE/OSA J Lightwave Technol* 31 (14):2394–2399
34. Yu J, Zhang J, Xiao J (2014) 432-Gb/s PDM-16QAM signal wireless delivery at W-band using optical and antenna polarization multiplexing. In: European conference on optical communication (ECOC), W.3.6.6
35. Li X, Yu J, Zhang J, Dong Z, Chi N (2013) Doubling transmission capacity in optical wireless system by antenna horizontal- and vertical-polarization multiplexing. *OSA Opt Lett* 38 (12):2125–2127
36. Cheng L, Gul M, Ng'oma A, Lu F, Ma X, Chang G (2015) High-diversity millimeter-wave CoMP transmission based on centralized SFBC in radio-over-fiber systems. In: IEEE/OSA optical fiber communication conference (OFC), paper W3F.5
37. Cheng L, Zhu M, Gul MMU, Ma X, Chang G-K (2014) Adaptive photonics-aided coordinated multipoint transmissions for next-generation mobile fronthaul. *IEEE/OSA J Lightwave Technol* 32(10):1907–1914
38. Li X, Yu J, Zhang J, Dong Z, Li F, Chi N (2013) A 400G optical wireless integration delivery system. *OSA Opt Express* 21(16):18812–18819

**Part II**  
**Novel Systems/Subsystems**  
**for Fi-Wi Networks**

# Chapter 4

## Analog and Digitized Radio-over-Fiber

Maurice Gagnaire

**Abstract** Radio-over-Fiber (RoF) techniques aim to simplify as much as possible the configuration and the cost of the radio terminations of wireless networks. Both wireless LANs (WLAN) and cellular networks can potentially benefit from RoF. In wireless systems, the most costly equipment is the radio oscillators today necessary at each antenna site (called remote access unit or RAU in this chapter). The preprocessing of the radio signal achieved in the electrical domain at each RAU is particularly costly for the operators, both in terms of CAPEX (capital expenditure) and OPEX (operational expenditure). RoF enables a shift of the most sophisticated radio equipment from the RAUs to a central remote site. In the context of public cellular networks, such a central site typically corresponds to a mobile switching center (MSC) with permanent staff. The basic idea of RoF consists in transporting onto standard monomode fibers (SMF) radio frequencies from an MSC to the multiple RAUs under its supervision and vice versa. At the end of the 1990s, the first experimentations of RoF technologies have demonstrated the economic interest of this approach. The fact that the most costly and intelligent equipment originally located at each RAU could be co-located at a same site favors their potential mutualization. This site corresponds typically to a MSC or to a Radio Network Controller (RNC) in the case of public cellular networks. In the case of a private environment, it corresponds to a private branch exchange (PABX) or to an IP router. The benefit of RoF may be considerably increased if point-to-multipoint fiber infrastructures may be deployed between each RNC and its attached RAUs. For the sake of simplicity and coherence with the other chapters of this book, we shall refer in the remaining of this chapter to the term “Central Site” (CS) instead of MSC or RNC.

Around the year 2000, the first RoF systems called **analog radio-over-fiber (A-RoF)** have been developed both in academic and industrial research laboratories. In the mid-2000s, the first returns of experience have pointed out the limits of the A-RoF approach. A-RoF systems are indeed very sensitive to various nonlin-

---

M. Gagnaire (✉)

Institut Mines-Telecom, Telecom ParisTech, 23 avenue d’Italie, Paris 75013, France  
e-mail: maurice.gagnaire@telecom-paristech.fr

earities that may degrade the achievable bit rate for the end-users. To operate optimally, A-RoF systems necessitate a specific tuning proper to each considered environment. Such a constraint has rapidly been considered as unacceptable by the radio mobile operators since it has a non-negligible impact on their OPEX costs. This is why, toward the end of the 2000s, a more robust variant of RoF known as **digitized RoF** (or **D-RoF**) has been introduced. Unlike A-RoF, D-RoF relies on a digitization of the modulated radio carrier frequency at the CS. In comparison with A-RoF, D-RoF presents as its key advantage its compatibility with the existing ITU-T plesiochronous digital hierarchy (PDH) and OTN (optical transport network) encapsulation. OTN is today widely deployed in public fixed optical infrastructures. It is already used for mobile backhauling. D-RoF is much less sensitive than A-RoF to physical layer impairments. Its behavior under various network configurations is then much more predictable.

In summary, this chapter aims to provide a clear view and understanding of the state of the art (SoA) concerning the A-RoF and D-RoF techniques. Very rapidly, D-RoF has been considered as a very promising alternative for the mobile backhaul. This evolution has strongly favored the emergence of two industrial D-RoF standards: OBSAI (Open Base Station Architecture Initiative) [1] and CPRI (Common Public Radio Interface) [2]. The description of these two standards is out of the scope of this chapter. Let us note that, strictly speaking, neither CPRI nor OBSAI are ITU-T standards. CPRI has been proposed as a contribution to ITU-T under the name of “CPRI over OTN (Optical Transport Network)” in 2009. Chapter 5 of this book is totally dedicated to this aspect. It is important to notice that A-RoF has never been subject to a standardization process. We explain in this chapter the reasons why today A-RoF is only considered for private WLAN environment. On the other hand, the CPRI and OBSAI techniques clearly refer to public cellular networks.

## 4.1 Existing Radio Cellular Networks

Existing cellular networks rely on the attachment of a set of Base Transceiver Stations (or Node-Bs in the UMTS taxonomy) to a same radio network controller (RNC). In the 2000s, a RNC controlled typically around ten Node-Bs thanks to point-to-point HDSL symmetrical links. Each HDSL link consists in the transport of a bidirectional E1/T1 digital transmission channel at 2 Mbps in Europe and 1.55 Mbps in North America. In urban areas, these T1/E1 links may rely on two or three pairs of copper wires over a few hundred meters. Beyond such distance, each Node-B is connected to its RNC by means of a pair of T1/E1 links transported on two contradirectional point-to-point optical fiber links. Several factors justify why optical fibers are largely preferred to copper wires in the mobile backhaul in developed countries: their low cost (except the installation cost), their low attenuation, their insensitivity to external noises, and their very large bandwidth. In rural areas, the distance of the digital links between the RAUs and the CS may reach up a few tens of kilometers. In the context of LTE-Advanced, the operators aim to locate

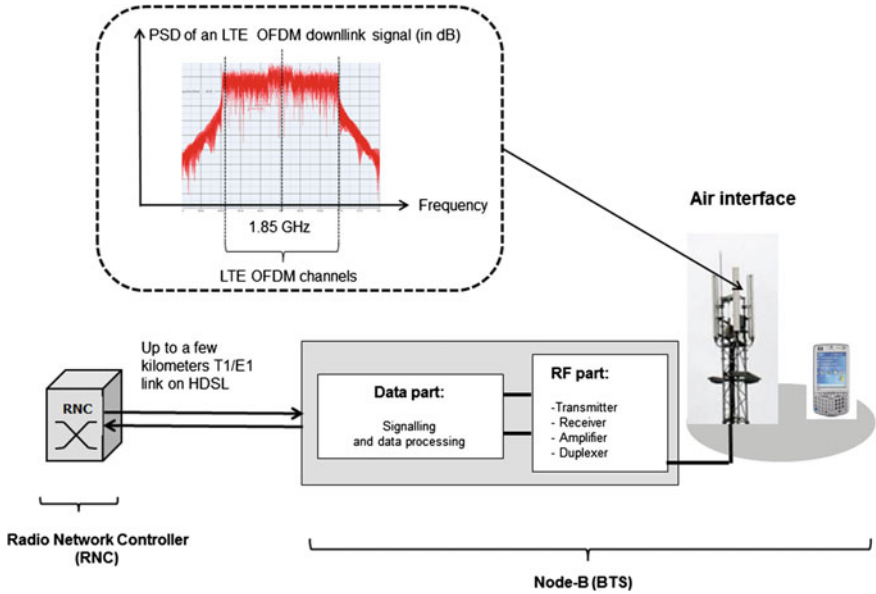


Fig. 4.1 Data part and radio part of a Node-B

the switching nodes in charge of managing radio mobile connections much higher in the infrastructure than it is the case today. Such a strategy reinforces the interest of RoF technologies. Figure 4.1 illustrates the typical configuration of an optical link between a RNC and a Node-B.

Two subsets of equipment are implemented in a Node-B: the data part that corresponds to low-frequency electronics and the radio frequency (RF) part that requires electronic devices operating at much higher frequencies. The data part enables to insert/extract the upstream/downstream data into T1/E1 PDH frames (or OTN frames as it will be depicted in Chap. 5). Mainly, this operation consists in adding to the information data bits redundant bits for synchronization, error detection, and signaling. Figure 4.2 depicts in more detail the elements included in the data part and in the radio part of a Node-B. In the downstream direction (from the CS to a Node-B), the data obtained after HDSL T1/E1 signaling extraction are directed to the radio part. The successive bits of this data flow feed a QAM (quadrature amplitude and phase modulator) centered at an intermediate frequency  $f_i$  of a few hundred MHz. The obtained modulated signal is then transferred at the radio carrier frequency in the GHz range thanks to an RF oscillator at frequency  $f_c$ . The obtained radio signal is filtered by a low-pass filter (LPF) in order to eliminate the useless replicas of the original spectrum. Finally, the useful replica centered on frequency  $f_i + f_c$  is power-amplified and sent to a duplexer. A duplexer consists in a circulator enabling to differentiate the upstream and downstream radio signals sent to or coming from the antenna itself. We assume in this section that the same radio frequency is assigned to the upstream and downstream signals. The differentiation

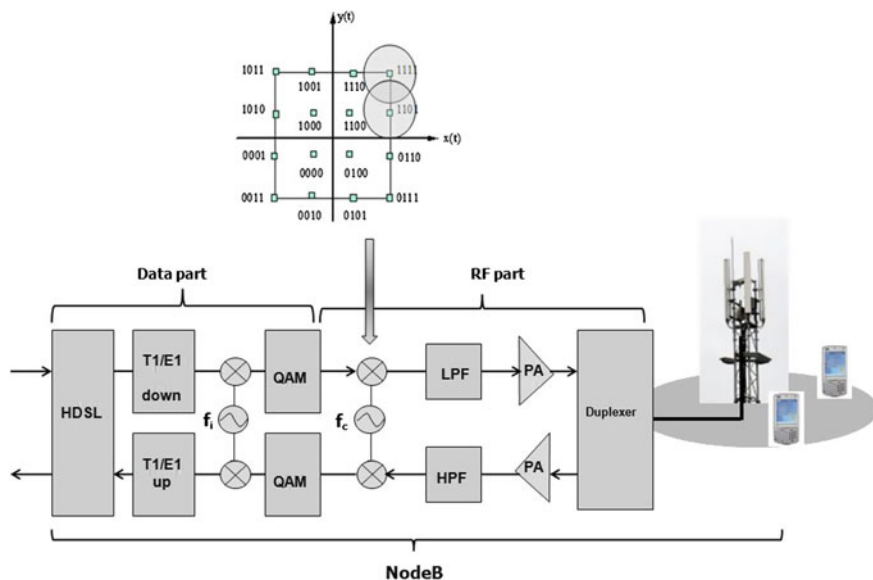
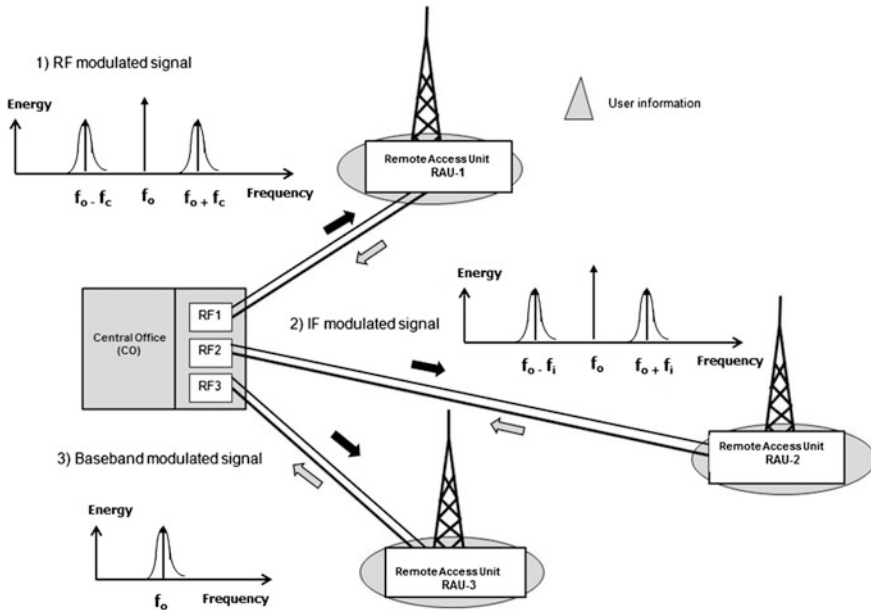


Fig. 4.2 A detailed view of the basic modules of an A-RoF modem

between these two signals can be achieved by adopting time-division multiple access (TDMA) or code-division multiple access (CDMA). The reverse process applies to upstream radio traffic from each Node-B to the CS. It has to be noted that if OFDM modulation is considered (case of LTE or LTE-advanced), the QAM modulator is replaced by an OFDM circuitry achieving the IFFT/FFT (inverse fast Fourier transform/direct fast Fourier transform) operations.

## 4.2 A-RoF Versus Baseband-over-Fiber

As mentioned previously, the main motivation of RoF is to lighten the antennas' sites called remote access unit (RAU) from the costly radio devices such as the oscillators at frequencies  $f_i$  and  $f_c$  and the associated high-speed electronic circuits. For that purpose, a fraction, or ideally all the radio equipment, is transferred from the RAUs to a centralized location (typically the CS) where they can be mutualized and supervised by permanent staff of the operator. In this context, the RAUs of  $N$  remote cells correspond to a set of  $N$  electronic cards placed in the different racks of a chassis. These  $N$  racks are fed locally by a single pair of oscillators at frequencies  $f_i$  and  $f_c$  thanks to short range waveguides. Similarly, a single cooling system can be used for all the RAUs located in the same chassis. In comparison, without RoF,  $N$  pairs of these oscillators are necessary and cannot be under the control of permanent staff. Three approaches are possible to design the communication link between a CS and a RAU. In reference to Fig. 4.3, we describe below these three options. In this figure, the wavelength  $\lambda$  of the optical beam transported



**Fig. 4.3** Three possible techniques to feed a remote access unit (RAU) from a CS (typically a RNC)

on the optical fibers is related to the resonance frequency of the laser cavity used at the transmitter side. The frequency  $f_o$  associated with wavelength  $\lambda$  is linked to the speed of light  $V = C/n$  within the fiber, where  $n$  is the index of the core of the fiber and  $C$  is the velocity (or speed) of light in vacuum.

### 4.2.1 Option 1: RF-Modulated Signals

The first option consists in transporting the downstream modulated radio signal (RF) directly from the CO to the RAU. Such an approach is referred to as “RF-over-Fiber.” This is the most cost-effective option since it does not need any radio oscillator at the RAUs, neither at the intermediate frequency nor at the radio carrier frequency. In Fig. 4.3, we assume that two unidirectional optical fibers are used for downstream traffic (from the CS to a RAU) and for upstream traffic (from a RAU to the CS), respectively. In that case, the same optical channel  $\lambda$  can be used to transport the RF signals in both directions.

### 4.2.2 Option 2: IF Modulated Signals

The second option consists in transporting the pre-modulated signals at the intermediate frequency  $f_i$  from the CO to the RAU. The value of frequency  $f_i$  depends on the considered wireless system. As mentioned in Sect. 4.1, this frequency is the one

at which the radio multiplex is built. According to the considered radio technique, the radio multiplex corresponds typically to either independent QAM channels (case of 3G radio mobile systems) or to interdependent OFDM channels (case of 4G radio mobile systems). The circuitry to be used at frequency  $f_i$  is sensibly less costly than the one operating at frequency  $f_c$ . This second option is referred to as “IF-over-Fiber.”

### 4.2.3 Option 3: Baseband-over-Fiber

Baseband-over-fiber modulation refers to the situation where the data to be transported by the radio carrier frequency are first transported as a baseband signal from the CS to the RAU. At the RAU, after photodetection, the obtained baseband signal modulates an intermediate frequency  $f_i$  much lower than the RF frequency to be radiated in the cell. The basic idea of baseband-over-fiber is to select, utilizing a bypass filter, one of the replicas of this modulated signal located in a frequency region corresponding to the desired radio carrier frequency in the radio cell. This selected replica needs to be amplified before being radiated through the cell. This third option called “Baseband-over-fiber” presents the advantage of using mature and already on-the-shelf electronics for signal processing at the RAU.

### 4.2.4 Conclusion

Option 1 and Option 2 refer to analog RoF (A-RoF). Option 3 differs from the configuration of Fig. 4.2 since one does not need the oscillator at frequency  $f_c$  at each antenna site. In Sects. 4.2.1–4.2.3, we have only considered downstream traffic. Two variants are possible for upstream traffic depending on whether a single or two optical fibers are used between the CS and the RAU. In the case of a single fiber, two distinct optical channels  $\lambda_1$  and  $\lambda_2$  are necessary to distinguish the upstream and downstream signals. If two contradirectional fibers are used between the CS and the RAU, the same type of laser source and photo-detector (operating at the same wavelength  $\lambda$ ) can be used for the upstream and downstream flows.

## 4.3 Transmission of Microwave Signals on Optical Fibers

Three techniques are possible to generate microwave (or millimeter waves) signals at frequencies from a few GHz to a few tens of GHz) over an optical link. The first of these techniques is direct intensity modulation or IM. The second one is external modulation or EM, and the last one is remote heterodyning or RH. This section exploits some of the basic digital communication principles regarding the power

spectral density of narrowband modulated signals [3]. It also uses some of the basic concepts of fiber-optic communications concerning optical modulation and optical detection techniques [4].

### 4.3.1 Intensity Modulation (IM) and Direct Detection (DD)

**IM-DD** is the simplest technique that consists in modulating in intensity a laser source by means of a radio frequency (RF) signal. Figure 4.4 illustrates such a transmission chain.

In the downstream direction, the RF signal centered at frequency  $f_c$  modulates directly in intensity (intensity modulation or IM) the number of photons generated per second by a laser source via dynamically controlling the bias current of this laser. As an illustration, in baseband transmission, the power of the transmitted light beam is centered at wavelength  $\lambda$ . Traditional digital optical transmission consists in modulating via two distinct bias currents the laser source in order to generate a high number of photons during a logical “1” and a low number of photons during a logical “0”. In practice, it is possible to modulate the bias current of a laser source more dynamically by means of an analog signal that induces continuous variations of the bias current. Thus, as it is illustrated in Fig. 4.4, it is possible to modulate a laser diode directly with a modulated RF frequency. At the destination, a photo-detector enables the

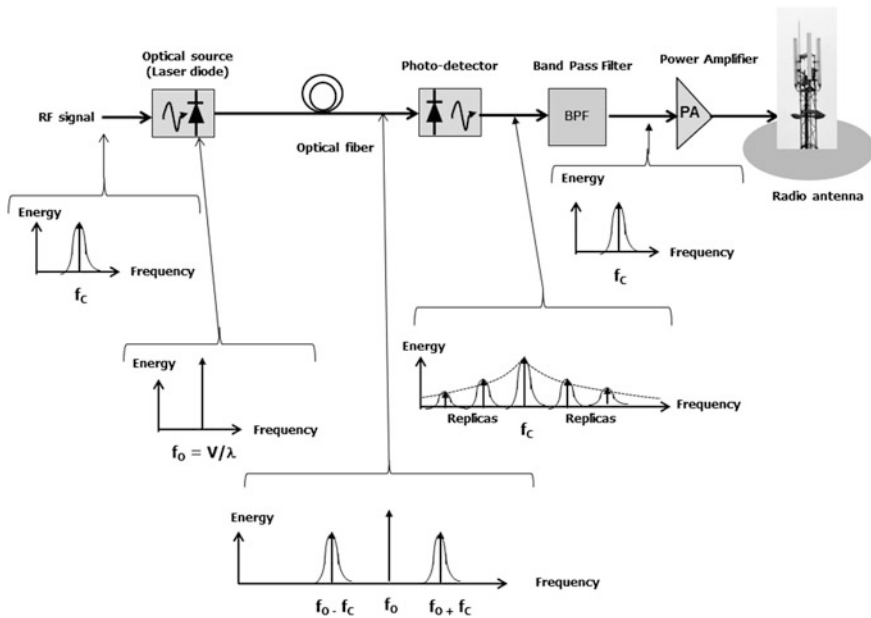


Fig. 4.4 Intensity modulation and direct detection (IM-DD) on an analog optical link

recovery of this modulated radio signal with its replicas by means of a simple “direct detection.” It is then necessary to filter the original pattern from this set of replicas. Mathematically speaking, the number of replicas is infinite. Since these replicas are generated and exploited locally, the attenuation effect of the replicas with their order, as it appears in Fig. 4.4, is in this context negligible. The combination of the IM and DD techniques also known as IM-DD is the most popular approach, mainly for its low cost. Meanwhile, if simple lasers and photo-detectors can be used with IM-DD at frequencies of up to 10 GHz, this is not the case for higher frequencies where external modulation of the laser is necessary. Concerning distance, this is not a real problem up to a few tens of kilometers. Such distances are well suited to mobile backhauling. Without going into the details, let us simply say that at frequencies beyond 10 GHz, chromatic dispersion of the fiber (that is expressed in picosecond per nanometer per kilometer) causes a significant time dilatation of the optical pulses which increases proportionally with distance and that may induce overlap of a pulse with next and/or previous pulses. This phenomenon known as inter-symbol interference (ISI) may induce at the destination erroneous bits after demodulation. The ISI effect increases with distance and bit rate (upper frequency of the baseband signal). In addition, the coherent mixing of sideband replicas of the modulated light may induce transmission zeros. A zero in the optical domain is the equivalent of a notch in the electrical domain. Because of their phase difference in the time domain, the analog summation of the amplitude of various optical pulses belonging to different replicas may result in zero optical power for the resulting signal. According to the large number of base stations to manage in a cellular network, the operators want to keep their equipment simple and cost-effective. This is why IM-DD is preferred in general for low radio frequency RoF transmission systems.

### 4.3.2 *External Modulation and Direct Detection (EM-DD)*

For frequencies above 10 GHz (upper bound of the baseband signal), the bit error rate (BER) observed at the destination of an IM-DD link becomes unacceptable because a permanent regime within the laser cavity is no longer achievable according to the dynamics of the input RF signal. This induces a phenomenon known as “chirp” for which the optical carrier  $\lambda$  fluctuates around its nominal value. This fluctuation degrades the signal-to-noise ratio (SNR) at the destination. External modulation associated with direct detection (**EM-DD**) is then preferable. The principle of EM-DD is illustrated in Fig. 4.5.

A continuous laser source is post-modulated by means of a Mach-Zehnder modulator (MZM) preventing de facto any chirp (the detailed description of a MZM can be found in [4]). At the destination, after demodulation by a photo-detector, the original signal in the radio domain is recovered with its replicas. Similarly to IM-DD, a band-pass filter enables to extract the required modulated RF signal that is finally amplified before being radiated by the antenna.

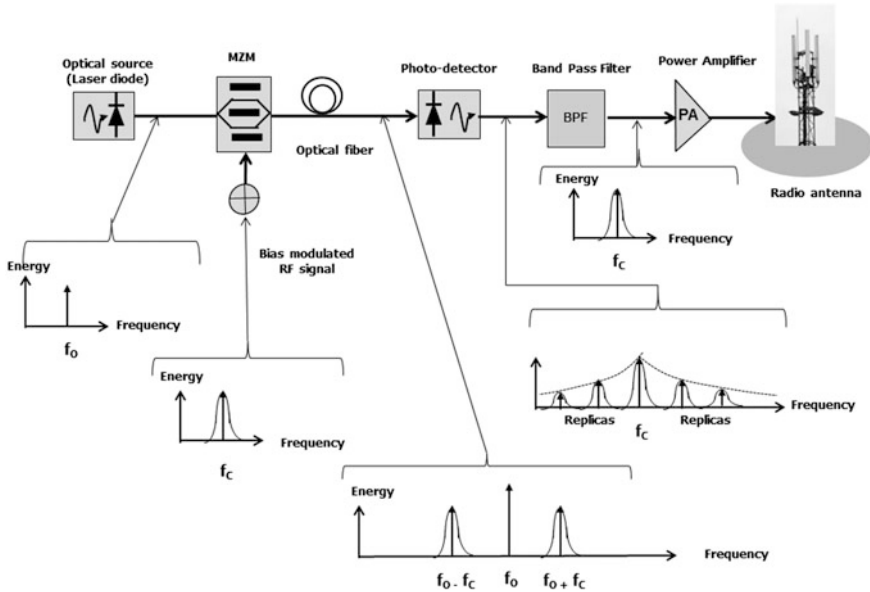


Fig. 4.5 External modulation and direct detection on an analog optical link (EM-DD)

The transport of RF signals on a point-to-point fiber link by means of IM-DD or EM-DD presents advantages and drawbacks. As mentioned previously, both of these techniques are cost-effective as long as they are applied to radio frequencies around the GHz range. An optical fiber is a dispersive medium where the phase speed and the group speed differ more or less depending on the material used for the core and the cladding of the fiber. This means that the various harmonics of a laser beam do not propagate with the same speed because the index of the core varies with the frequency of the propagating beam. In this case, the optical fiber between the CS and the RAU needs to be characterized by low chromatic dispersion in order to prevent its disruptive effect. The main limitation of IM-DD and EM-DD is then that they are effective only for low RF frequencies. In that domain, we must distinguish ultra-high frequencies (UHF) that may reach frequencies up to 10 GHz (or even greater known as super-high frequencies (SHF)).

### 4.3.3 Photo-detector-Based Heterodyning (HE) with Direct Detection (HE-DD)

Remote heterodyning detection (RHD) [5] is a way to improve the radio frequency range of RoF systems. It consists in superimposing on the same fiber between the CS and an RAU two optical fields  $E_1$  and  $E_2$  with close angular frequencies  $\omega_1$  and  $\omega_2$ . Let us consider that  $E_1$  is modulated by the information to be sent from the CS

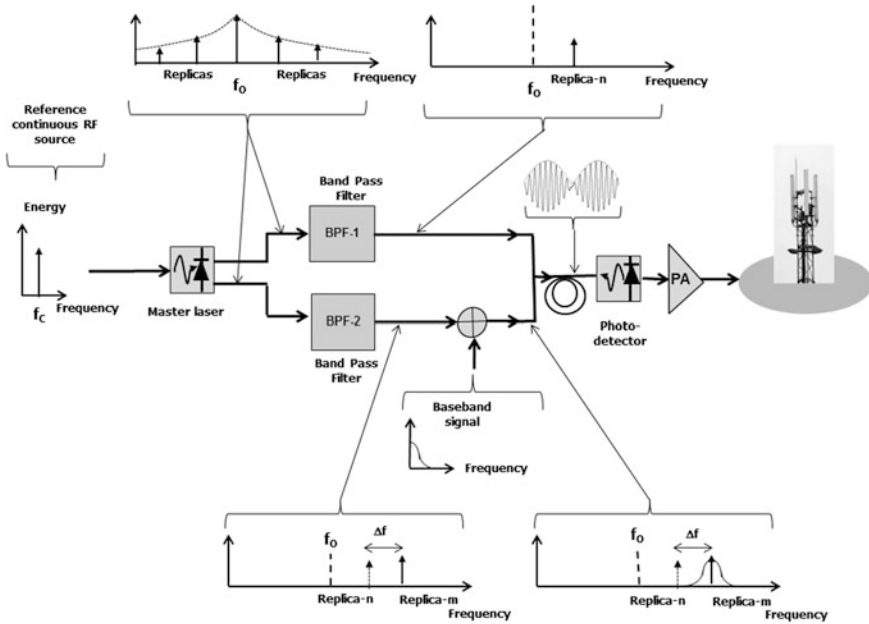


Fig. 4.6 Principle of optical heterodyning with direct detection (HE-DD)

to the RAU, whereas  $E_2$  remains a continuous power wave. Once this composite signal ( $E_1 + E_2$ ) arrives at the RAU, the photo-detector evaluates the optical energy of the received signal corresponding to the square of the amplitude of the induced photocurrent. Two terms constitute this energy: a sinus function with angular frequency  $(\omega_1 + \omega_2)$  and another sinus function with angular frequency  $(\omega_1 - \omega_2)$ . The basic idea of heterodyne transmission is to choose  $(\omega_1 - \omega_2)$  such that it corresponds to the expected RF frequency (beyond 10 GHz). Let us remind that in the C-band (1550 nm), the laser carriers operate around 200 THz. We can then choose, for instance,  $\omega_1$  equal to 193.500 GHz (corresponding to 1549.318 nm) and  $\omega_2$  equal to 193.400 GHz (corresponding to 1550.119 nm) to transport a modulated RF at 100 GHz. Unlike IM-DD and EM-DD, optical heterodyning enables to conceive RoF systems operating at frequencies around 10 GHz or beyond. Figure 4.6 illustrates the principle of a RoF system based on photo-detector heterodyning and direct detection (HE-DD).

A reference master laser at frequency  $f_o$  is modulated by a reference continuous RF frequency  $f_c$ . At the output of the master laser, this frequency  $f_c$  is transposed around the optical carrier  $f_o$  with its periodic replicas. Two copies of this signal are sent to two output branches, one with a band-pass filter that selects, for instance, the replica of order  $n$  for the upper branch and another replica of order  $m$  being selected in the lower branch. All the rationale of optical heterodyning consists in choosing judiciously the value of  $n$  and  $m$  in order that  $(f_o + m \cdot f_c)$  minus  $(f_o + n \cdot f_c)$ , that is a radio frequency at  $(m - n) \cdot f_c$  with  $m > n$  corresponds to the expected RF

frequency to be transmitted in the radio cell, that is 10 GHz or more. Expressed in Hz, the frequencies transported in the two branches are very close because the RF frequencies  $m \cdot f_c$  and  $n \cdot f_c$  are much lower than the optical carrier  $f_o$ . The optical signal modulated with replica  $m$  at frequency  $(f_o + m \cdot f_c)$  is over-modulated with the baseband data flow to be transmitted into the radio cell (the RAU). Frequencies  $(f_o + m \cdot f_c)$  and  $(f_o + n \cdot f_c)$  are numerically sufficiently close to be subject to a beat phenomenon. The resulting beat signal represented in the figure gives after direct detection and filtering the expected RF signal modulated by the downstream data to be radiated in the cell. This signal simply needs to be amplified at the RAU before being sent to the antenna. This approach can then be considered for the next-generation WLAN operating at a few tens of GHz like ultra-wideband (UWB) [6–8].

### 4.3.4 Conclusion

In summary of this section, external modulation with direct detection (EM-DD) is a good alternative to connect a CS to a RAU under two conditions. First, the radio carrier frequencies must be in the GHz range. Between 1 and 5 GHz, the fiber link between the CS and the RAU needs to be characterized by a low chromatic dispersion. Heterodyning is a good alternative for more sophisticated wireless systems operating at higher radio frequencies. Unlike EM-DD, HE-DD is less sensitive to the chromatic dispersion of the fiber. The key benefit of heterodyning is the fact that it allows low-frequency modulation of the optical beam by baseband data or a low-frequency radio signal at the CS [9].

## 4.4 Analog Radio-over-Fiber (A-RoF)

As it has been mentioned previously, the first investigations dedicated to analog RoF (A-RoF) took place in the mid-1990s. In general, the quality of a wireless channel is much less sensitive to the environment if it is transported in a guided fiber link than via free space propagation. In the cellular environment, this could enable much larger distances between the CS and the antennas' sites. In other terms, A-RoF should enable to serve more radio sites with less CSs. Such an evolution could have a strong impact on the CAPEX/OPEX costs for the radio mobile operators. Meanwhile, in practice, things are not so simple due to the strict constraints on the round-trip time required by signaling messages. These constraints mainly concern connection establishment and disconnection but above all, hand-over operations. In practice, two parallel research directions have been considered for A-RoF in the mid-1990s: one for outdoor cellular environment and the other one for indoor WLAN environment. Most of the investigations in this matter consider two separate optical fibers between a CS and its attached remote access units

(RAU) for upstream and downstream traffic, respectively. Thanks to this physical separation, the same class of optical transmission equipment operating with the same wavelength  $\lambda$  can be used for both directions. In practice, two variants of A-RoF corresponding to the two first options mentioned in the precious section have been investigated and demonstrated: “RF-over-fiber” and “IF-over-fiber.”

#### 4.4.1 A-RoF for “RF-over-Fiber”

The “RF-over-fiber” option consists in shifting the two oscillators at frequencies  $f_i$  and  $f_c$ , respectively, from the RAU (a Node-B in the case of LTE cellular networks or a Wi-Fi hotspot in the case of a WLAN) to a central or head-end node (the CS in the case of a cellular network or a Wi-Fi hotspot concentrator in the case of a WLAN). In the WLAN environment, the CS corresponds to the place where the network administrator installs the hotspot concentrator. In the context of domestic usage, a hotspot concentrator is typically an IP router. In the context of a professional environment, a hotspot concentrator is typically an Ethernet switch. Figure 4.7 illustrates the equipment used for a point-to-point A-RoF link.

Thanks to A-RoF, a single pair of oscillators at  $f_i$  and  $f_c$  located at the head of the infrastructure may feed several remote RAUs, since the associated hardware corresponds to electronic cards inserted in the multiple racks of a same chassis. Thanks to the proximity of these opto-electronic cards (a few tens of centimeters), it is possible to feed each of them by means of the same pair of oscillators ( $f_i, f_c$ ) and of a point-to-multipoint waveguide. It has to be noted that the cooling of these electronic cards can also be mutualized. We recognize in Fig. 4.7 some of the equipment mentioned previously in Fig. 4.2. In the downstream direction, the modulated radio signal is used to modulate a laser diode. The obtained intensity-modulated

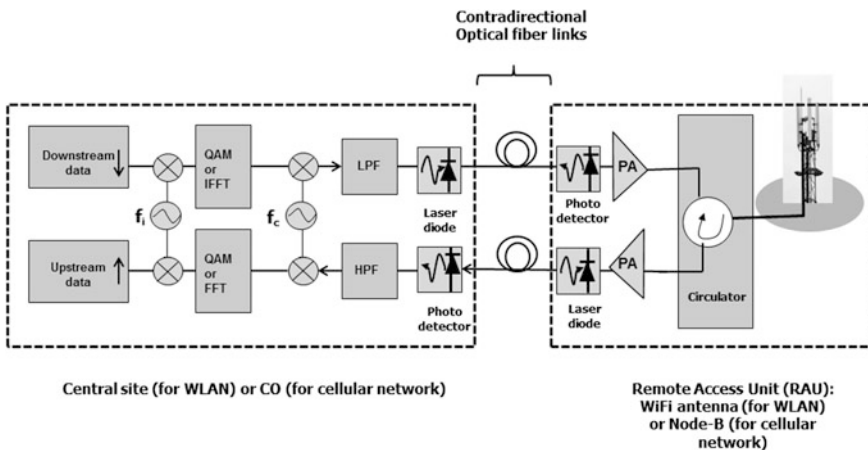


Fig. 4.7 Configuration of a A-RoF point-to-point link

optical signal at wavelength  $\lambda$  located in the C-band (around 1350 nm) is then transmitted to the RAU where the antenna is installed. At the RAU, this optical signal is demodulated thanks to direct detection provided by a PIN photo-detector. The obtained signal centered at frequency  $(f_i + f_c)$  is power-amplified and sent to a circulator. The role of the circulator has already been defined in Sect. 4.1. The gain of the power amplifier is such that the transmitted signal may arrive to the end-user with the expected signal-to-noise ratio (SNR). Let us recall that the expected efficient bit rate offered to the mobile users strongly depends on the effective SNR value. The rationale of the upstream radio channel from the end-user to the CS can then also be easily interpreted from Fig. 4.7.

The approach considered in Fig. 4.7 relies on intensity modulation at the sender and direct detection (IM-DD) at the receiver. While the feasibility of IM-DD A-RoF systems has been demonstrated for cellular networks, it is, however, subject to two drawbacks. First, the quality of the optical signal once modulated by an RF frequency around 2 GHz or above may be subject to physical layer impairments due to the transmitter, the receiver, and the transmission link characteristics. This means that for a given user’s data rate, the reliability of the data extracted from the radio signal at the destination may degrade with distance beyond the acceptable limits, that is beyond the capacity of the error detection and correction techniques adopted in the transmission chain. Second, the cost of the circuitry to operate at such frequencies is quite high. This is why another and less ambitious alternative known as IF-over-fiber is also be considered.

### 4.4.2 A-RoF for “IF-over-Fiber”

Figure 4.8 illustrates the principle of A-RoF operating at the intermediate frequency (A-RoF-IF). In reference to Fig. 4.2, concerning downstream traffic, only the

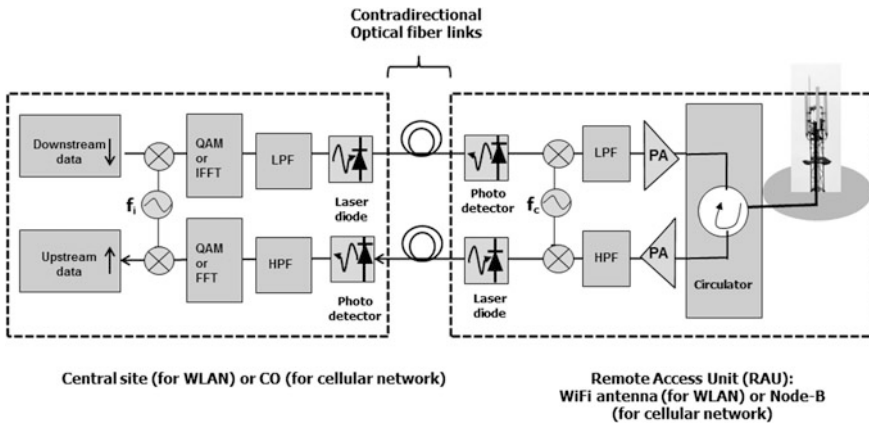


Fig. 4.8 Point-to-point configuration of an A-RoF-IF link

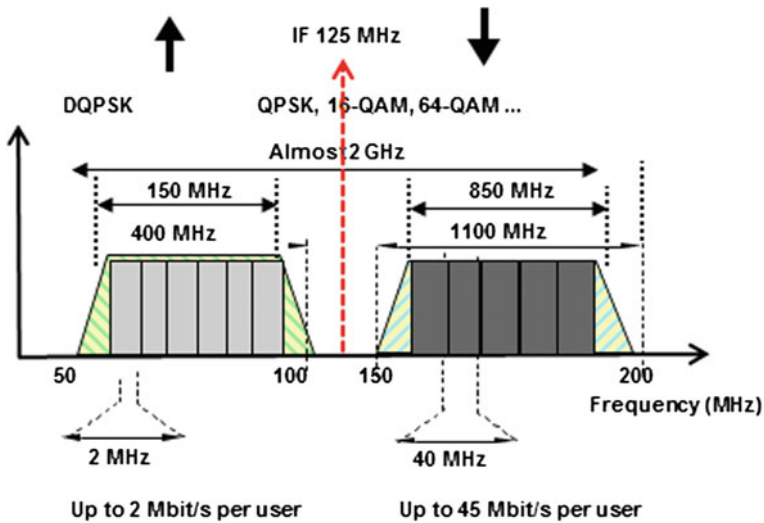


Fig. 4.9 Spectrum occupancy of a replica of a WiMAX QAM-based A-RoF-IF link

multiplex built at the intermediate frequency is in that case transferred from the CS to the RAU. One keeps then the RF oscillator at frequency  $f_c$  at the RAU.

As an illustration, let us consider the case of a WiMAX WLAN based on frequency-division duplexing and QAM modulation. The RF frequency of this system is set to  $f_c = 2$  GHz, whereas the intermediate frequency  $f_i$  is chosen equal to 125 MHz. Several upstream channels using 16-QAM modulation are assigned a 2-MHz bandwidth each. Several downstream channels with 16-QAM modulation are assigned 40 MHz bandwidth each. The resulting spectrum on the received downstream optical channels from the CS to the RAU is made of a number of replicas of the pattern depicted in Fig. 4.9.

#### 4.4.3 A-RoF for Multi-antennas Sites by Means of Sub-carrier Multiplexing (SCM)

In dense urban areas, trisector antennas are adopted at each RAU. The multiplication of antennas at the same site strengthens the interest of RoF technologies. Sub-carrier multiplexing (SCM) is a technique that enables to modulate a same optical carrier with multiple low frequency signals. In our context, these low frequencies may correspond to multiple radio frequencies sent from a CS to a same RAU. Figure 4.10 illustrates an example of application of SCM principles to feed in the downstream direction a trisector antenna.

If the radio frequencies adopted for the trisector antenna are higher than a few GHz, the circuitry described in Fig. 4.10 can be replaced according to the principles

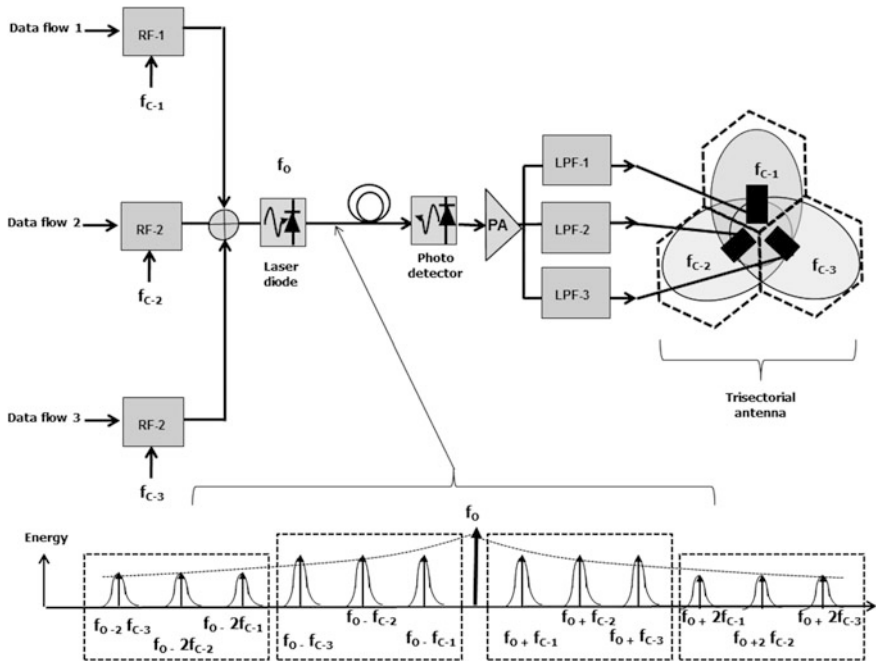
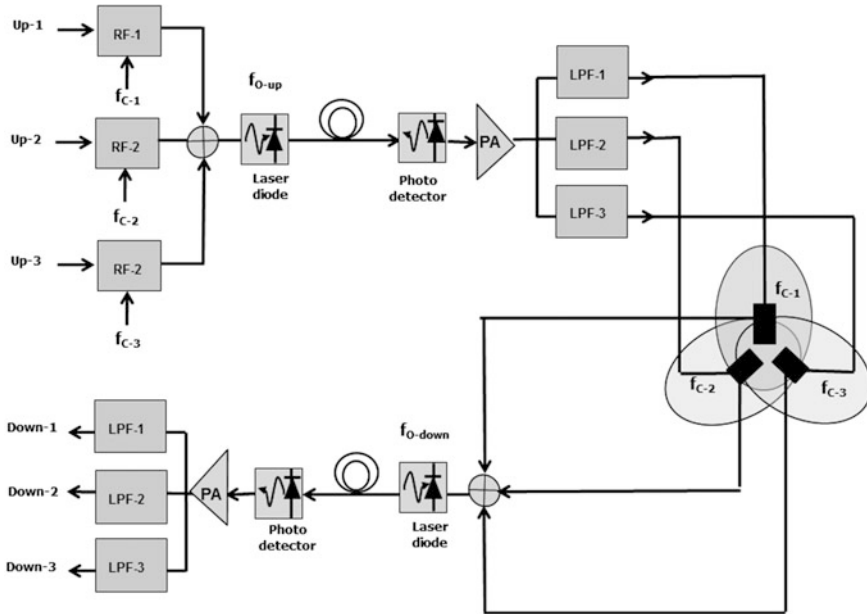


Fig. 4.10 Application of SCM to a trisectorial antenna site

of RHD (Cf. Sect. 4.3.3). Concerning the reverse transmission chain from the trisector antenna to the CS, two options are possible. The first option consists in using two distinct optical fibers between the CS and the RAU for upstream and for downstream traffic respectively. In that configuration, the same optical channel on wavelength  $\lambda$  can be used for upstream and for downstream traffic respectively. The second option consists in using a single optical fiber between the CS and the RAU. In that case, two different optical channels  $\lambda_1$  and  $\lambda_2$  must be adopted for the downstream and for the upstream traffic respectively. This second option is more costly since it needs the usage of WDM multiplexers/demultiplexers at both sides of the optical link and two types of transceivers. In practice, the price of a monomode optical fiber per kilometer is nowadays below the price of a copper wire. Installing two fibers instead of one in the same conduit does not incur any additional civil engineering cost. We can then conclude that the best option to link the CS to the RAU is the one described in Fig. 4.11 with its mirror image, two distinct fibers being used between the CS and the RAU. Although it is not represented on Fig. 4.11, a Power Amplifier must be used on the reverse fiber between the adder and the laser diode for upstream traffic.

The main advantage of SCM is its flexibility of usage. Thus, various types of traffic can be transported by a same optical channel between the CS and the RAU. One of the RF sources may be fed with voice traffic. For instance, in reference to Fig. 4.11, radio channel  $f_{RF-1}$  can be used for transporting multiple low-bit-rate (10



**Fig. 4.11** Application of SCM to a bidirectional A-RoF link between a CO and a trisector antenna site

kbps) circuit-oriented voice connections. Channel  $f_{RF-2}$  can be used for transporting WLAN IP packets at variable bit rates (up to a few Mbps). Finally, channel  $f_{RF-3}$  can distribute CATV channels. Meanwhile, as any analog transmission system, A-RoF SCM is subject to various noise distortion effects inherent to the nonlinearity of the fiber. The impact of these effects on the effective achievable capacity of the wireless systems (its Shannon's capacity) has been deeply investigated in [10, 11].

#### 4.4.4 A-RoF for Multi-antennas Sites by Means of Wavelength-Division Multiplexing (WDM)

SCM can judiciously be associated with wavelength-division multiplexing (WDM) when the A-RoF technique has to serve multiple antennas at a RAU from a CS. In [12], the authors propose a combination of SCM and WDM where WDM is used to separate the downstream A-RoF link (from the CS to the RAU) from the upstream link (from the RAU to the CS). Two different wavelengths are adopted for that purpose:  $\lambda_{up}$  at 1350 nm and  $\lambda_{down}$  at 1310 nm. In the context of the European FUTON (fiber-optic networks for distributed extensible heterogeneous radio architectures and services provisioning) project ended in 2010, a sophisticated experimental setup has been built in using various tools of the MATLAB library in

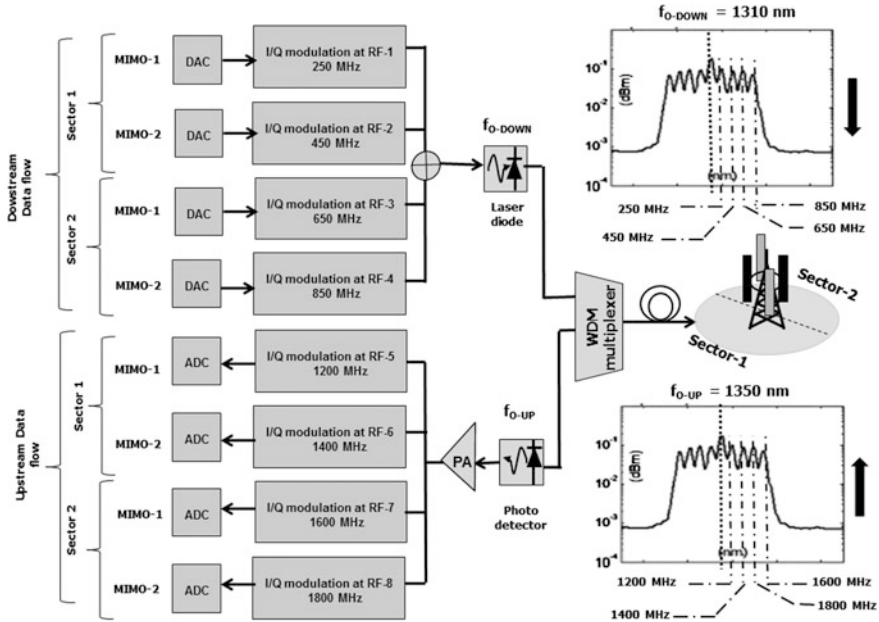


**Fig. 4.12** A-RoF communication system for serving a bisectorial antenna with  $2 \times 2$  MIMO by means of 8 RF sub-channels

order to demonstrate the efficiency of such an approach. The detailed description of this experimental setup goes beyond the objectives of this chapter. Let us simply say that the obtained results are coherent and justify the interest of the design of the system. At the date of publication of this book, one can estimate that these investigations are among the most advanced in matter of A-RoF technologies. Figure 4.12 illustrates a network configuration where a RAU corresponds to a radio cell with two sectors and where each of these sectors exploits  $2 \times 2$  MIMO channels (2 transmitters and two receivers per sector antenna). There are then 4 radio links to establish between the CS and the RAU. Each sector is served by four unidirectional parallel data channels corresponding to the in-phase and quadrature data flows associated with each of the two QAM constellations feeding each antenna.

In the downstream direction, optical wavelength  $\lambda_{\text{down}} = 1310$  nm, referred to as  $f_{o\text{-down}}$  in Fig. 4.12, transports four radio frequency signals at  $f_{c-1} = 250$  MHz,  $f_{c-2} = 450$  MHz,  $f_{c-3} = 650$  MHz, and  $f_{c-4} = 850$  MHz. The first and the second of these radio signals are interpreted correlatively between each other since they apply to the two MIMO antennas serving sector-1 of the cell. Similarly, the third and the fourth of these radio signals are interpreted correlatively between each other since they apply to the two MIMO antennas serving sector-2 of the same cell. In the upstream direction, optical wavelength  $\lambda_{\text{up}} = 1350$  nm, referred to  $f_{o\text{-up}}$  in Fig. 4.12, transports four radio frequency signals at  $f_{c-5} = 1200$  MHz,  $f_{c-6} = 1400$  MHz,

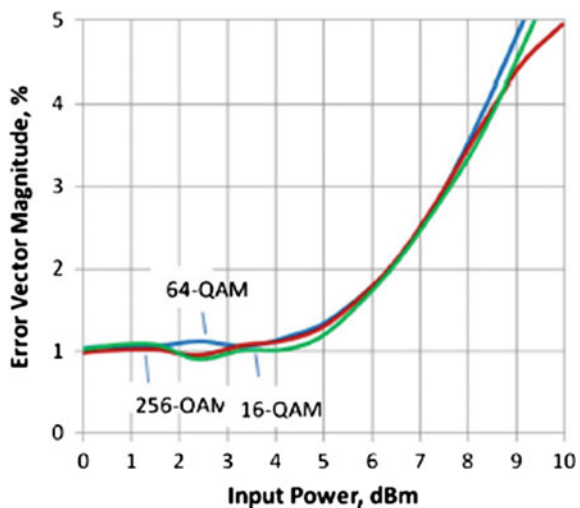
$f_{c-7} = 1600$  MHz, and  $f_{c-8} = 1800$  MHz. With the same rationale as for downstream traffic, radio carriers  $f_{c-5}$  and  $f_{c-6}$  transport the information related to the two MIMO antennas receiving upstream radio signals in sector 1. Radio carriers  $f_{c-7}$  and  $f_{c-8}$  transport the information related to the two MIMO antennas receiving upstream radio signals in sector 2.

It has to be noted that although they are not represented in the figure for the sake of simplicity, two electrical channels are used. A first signaling channel is used for control and monitoring purposes. A second channel is used as a reference tone between the CS to the RAU. Advanced wireless systems, either in WLAN or in cellular environment, rely on OFDM transmission that itself exploits the principles of FFT/IFFT (fast Fourier transform and its inverse operation). Without going into the details, FFT/IFFT may be viewed as a digitized version of QAM modulation. This is why the performance metric of a RoF system where the radio channels exploit OFDM can be based on the evaluation of the numerical value of the error vector magnitude or EVM. The EVM corresponds to the statistical quadratic distance that exists at the destination after demodulation in the I-Q plane between the measured coordinates of a symbol and the original value of these coordinates at the sender. The statistical aspect of the considered data refers to the average gap between the transmitted and received signals associated with the successive transported random QAM symbols. The expression of EVM in percent is given by equation Eq. 2.1:

$$\text{EVM}(\%) = \sqrt{\frac{P_{\text{error}}}{P_{\text{reference}}}} \times 100 \% \quad (2.1)$$

In this equation,  $P_{\text{error}}$  corresponds to the root-mean-square (RMS) of the error vector that separates the original point in the I-Q constellation plane at the sender

**Fig. 4.13** EVM of a RoF link as a function of input power for 2048 IFFT-OFDM signals with 16, 64, and 256-QAM modulation (from [12])



from the measured point in the same I-Q constellation plane at the receiver. The parameter  $P_{\text{reference}}$  stands for the RMS related to the coordinates of the original point of the constellation at the sender.

Figure 4.13 provides as an illustration the evolution of EVM of a RoF link as a function of the input power for a 2048 IFFT-OFDM wireless channels with different QAM constellations (from [12]). One notices that for various types of analog modulation (16-QAM with 4 bits per symbol, 64 QAM with 6 bits per symbol, and 256-QAM with 8 bits per symbol), the quality of the A-RoF channel is acceptable up to 5dBm. Beyond this input power, the nonlinearity of the transmission system degrades regularly with the power of the signal injected into the fiber.

## 4.5 Digitized Radio-over-Fiber (D-RoF)

The empirical Moore's law specifies that the speed of electronic circuits doubles on average every 18 months. Thanks to such an evolution of the technology, various investigations have been carried out in the field of **digitized RoF (D-RoF)**. Two factors have motivated the development of this technique as an alternative to A-RoF. First, as it has been mentioned previously, the quality of A-RoF signals at the RAU is quite unpredictable due the nonlinearities of some of the devices of the transmission chain and of the optical fiber itself. It appears that intermodulation noises occur when SCM is applied to A-RoF. Quantifying and compensating such noises is an achievable but complex and costly task according to the state of the technology [11]. The basic objective of D-RoF consists in enabling, like A-RoF, to prevent the costly usage of two pairs of oscillators at the intermediate frequency ( $f_i$ ) and at the radio carrier frequency ( $f_c$ ) for each radio channel, respectively, at each base station (or RAU). Meanwhile, instead of transporting in the downstream direction RF-modulated signals via an analog modulation, D-RoF assumes a digitization of the modulated radio signal at the CS. The obtained data flow is then transported to the RAU by means of a simple high-bit-rate baseband modulated optical channel. Such an operation should be, in practice, either not feasible or too costly in most cases because of the constraint imposed by the Nyquist sampling theorem in terms of required speed of electronics. This theorem specifies that, to be digitized, an analog signal must be sampled at a frequency at least two times higher than the upper bound of its power spectral density (psd). For instance, a WiMAX 802.16a radio signal operating at a RF frequency of 2.475 GHz should necessitate a digital circuitry operating at almost 5 GHz. Nowadays, such a circuitry is not available at a reasonable price on the shelves of the vendors. Bandpass sampling ([13–16]) is a judicious answer to this problem. We describe in Sect. 4.5.1 the basic principle of band-pass sampling theory that enables the feasibility of a large range of RF signals digitization with current circuitry. The second reason that has motivated the development of D-RoF technologies is the concept of distributed antennas systems (DAS). We mention in Sect. 4.4.4 the MIMO technique. MIMO systems with a size up to  $8 \times 8$  have been developed to increase the capacity of a radio cell. Thus, applied to a trisector antenna, this means that up to 24 antennas could be needed at the center of

the most loaded cells. As already mentioned in the introduction of this chapter, two D-RoF industrial approaches have emerged about 10 years ago: OBSAI [1] and CPRI [2]. These two approaches inspired by two vendors specify cost-effective rules to interconnect the antennas of multiple RAUs to the same CO. In Sect. 4.5.2, we describe an example of D-RoF configuration in the simple case where a single radio antenna is fed with a single radio channel. In Sect. 4.5.3, we consider the case where RoF technology is used to serve a multi-antenna base station.

### 4.5.1 Band-pass Sampling Theory

On the basis of the Nyquist sampling criteria, digitizing a modulated radio signal with a bandwidth  $W$  centered on a radio carrier frequency  $f_c$  in the GHz range requires a very high speed electronics operating at least at twice  $(f_c+W)$  Hz. For instance, a radio frequency at 1 GHz with a bandwidth of  $W$  of 25 MHz necessitates a sampling frequency of at least 2.05 GHz. As mentioned previously, sending a signal at such a high frequency from the CS to a RAU is subject to nonlinearities that strongly degrade the EVM of the received radio signal at the end-user. Band-pass sampling enables to circumvent this practical difficulty. It reuses some of the principles of Discrete Fast Fourier Transform (DFFT). Its principles rely on a seminal paper of R.G. Vaughan, N.L. Scott, and D.R. White published in 1991 [13]. This theory has found its application for D-RoF in the years 2000.

Let us consider the case of an LTE-RAU. The network operator estimates in advance the global intensity in bit per second of the global traffic that must be satisfied within each of his LTE radio cells. This traffic is made of an upstream and of a downstream component from the RAU to the CS, and from the CS to the RAU, respectively. Knowing these two bit rates, it is possible to determine the number of required adjacent LTE channels for both these directions. For a given traffic intensity, one determines the number of LTE channels to affect to upstream and downstream traffic. In addition to the spectrum inherent to each LTE channel, guard bands specified by the LTE standard must be respected. Finally, additional overhead bits are necessary for framing, control sequences and clock management. In other terms, the effective gross bit rate of multiple LTE channels to be transported thanks to D-RoF from the RAU to the CS and vice versa is sensibly higher than the users' data rate. The weight of these various bit rate overheads varies with the adopted transmission data format. Thus, OBSAI and CPRI do not represent the same gross bit rate according to the considered user. On the basis of all these considerations, the choice of the sampling frequency  $f_s$  to be applied at the RAU for downstream (and upstream traffic respectively) depends on the minimum  $f_{min}$  and the maximum  $f_{max}$  frequencies of the global radio signal to be transferred from the CS to the RAU (from the RAU to the CS respectively) [13–15]. Equations 2.2 and 2.3 specify the bound constraints that must be satisfied by the system in order to guarantee the correct reconstruction of the bandpass signal at the RAU (the CS respectively) without spectral aliasing. In Eq. 2.2,  $n_z$  is an integer. The operator

used in the right-hand side of Eq. 2.3 is the floor function of a real number. This real number corresponds to the ratio of  $f_{max}$  divided by  $f_{max}$  minus  $f_{min}$ . In practice, the larger the value of integer  $n_z$ , the lower the required sampling rate  $f_s$ , and then, the lower the required bit rate to be transported between the CS and the RAU (and the RAU to the CS respectively).

$$\frac{2 \cdot f_{max}}{n_z} \leq f_s \leq \frac{2 \cdot f_{min}}{(n_z - 1)} \tag{2.2}$$

$$1 \leq n_z \leq \left\lfloor \frac{f_{max}}{f_{max} - f_{min}} \right\rfloor \tag{2.3}$$

Several investigations have been carried out around the year 2010 to demonstrate the feasibility of D-RoF for existing WLANs or cellular systems. In the remaining of this section, we present the major lessons of recent studies in this matter [14, 15]. In both these papers, the authors apply D-RoF to a WiMAX 802.16a radio channel. The radio carrier frequency of WiMAX 802.16a is equal to 2.475 GHz with a 20-MHz bandwidth. On the basis of the IEEE 802.16a standard, a square-root-raised-cosine filter with a rolloff factor  $\beta = 0.25$  is adopted for pulse shaping. A 15-MHz bandwidth is kept as a guard band on each side of the modulated WiMAX signal. This results, as illustrated in Fig. 4.14, in a channel bandwidth of 50 MHz including left and right guard bands of 15 MHz each. A single channel of that type can be transported as

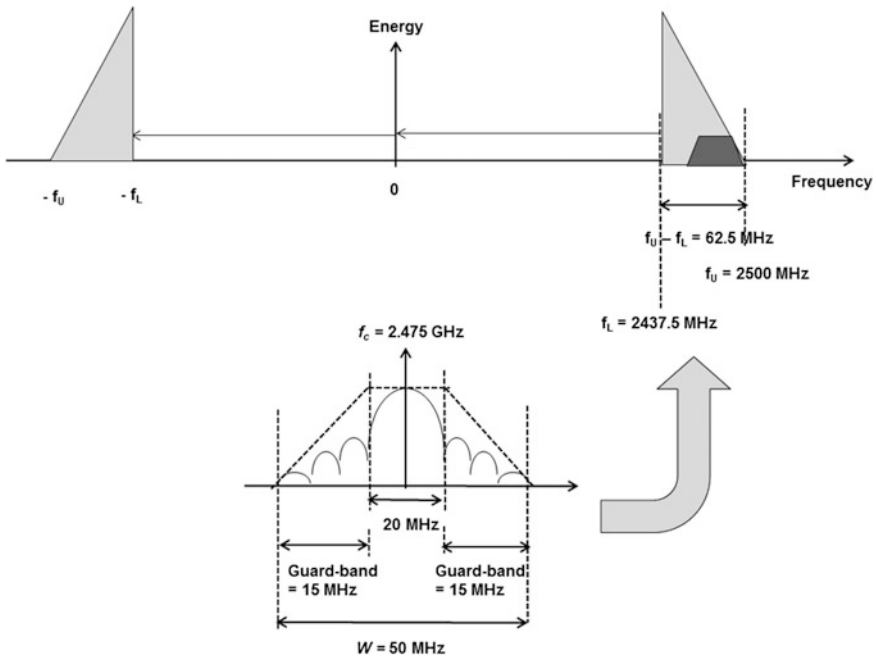


Fig. 4.14 Characteristics of WiMAX IEEE 802.16a WLANs ([17–21])

indicated in Fig. 4.14 in the band  $f_L = 2.4375$  GHz and  $f_U = 2.5$  GHz as it is specified in the WiMAX standard. Figure 4.14 summarizes the characteristics of such a WiMAX IEEE 802.16a system.

On the basis of the provided data, we can deduce from Eq. 2.3 that  $n_z$  must be chosen between 1 and 50. Thus, for  $n_z = 40$ , Eq. 2.2 indicates that a sampling frequency of 125 Msamples/s can be achieved. From Eq. 2.3, we observe that the largest possible value of integer  $n_z$  enables to minimize the sampling frequency  $f_s$ .

In the case of broadband RF signals, the speed of electronics needed for the design of ADC (analog-to-digital converter)/DAC (digital-to-analog converter) may become restrictive. In that case, it is possible to digitize only the pre-modulated IF signal instead of the RF signal. The filtering and amplification of a replica in the desired RF band can be achieved at the destination to up-convert the IF signal to the radio carrier frequency.

### 4.5.2 D-RoF for a Single-Antenna Site

Figure 4.15 illustrates the basic principle of a point-to-point D-RoF link between a CO and a RAU [16]. Band-pass sampling is applied at the level of the ADC converters used at the CS for downstream traffic or at the RAU for upstream traffic, respectively. The ADC of a D-RoF link performs three successive operations: band-pass sampling, quantization, and coding functions. Coupled to the ADC, a DAC is also required either at the RAU for downstream traffic or at the CS for upstream traffic.

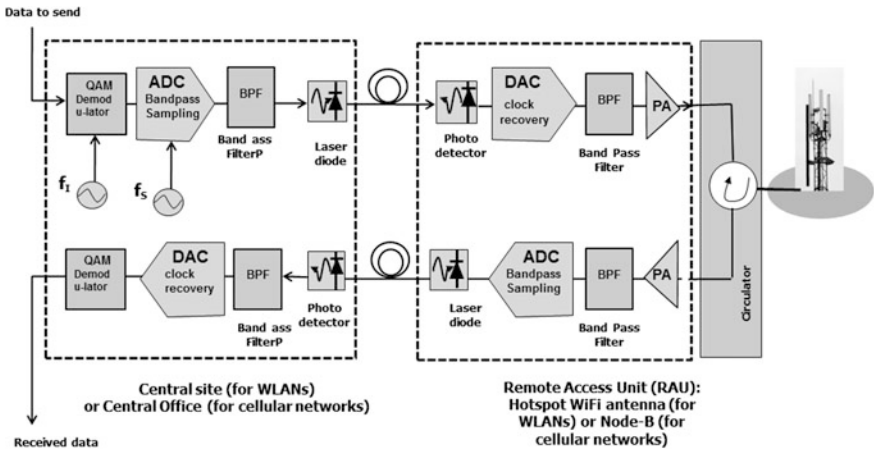


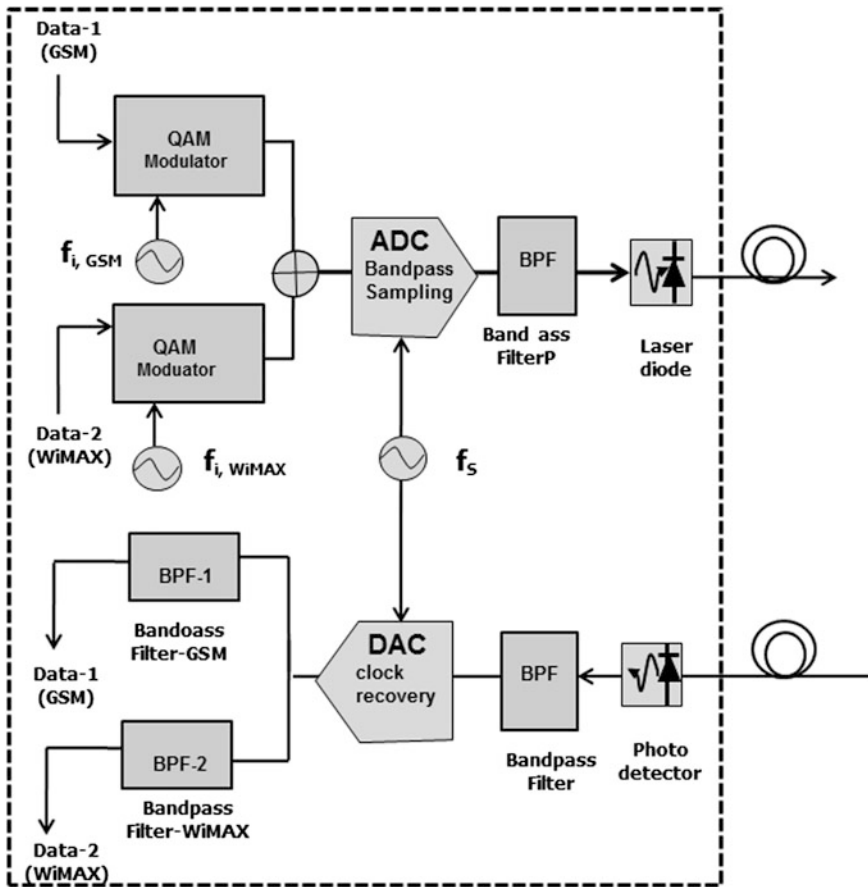
Fig. 4.15 Principle of a D-RoF optical link (from [14])

Downstream data are generated at the CS. These data are first modulated at the IF frequency  $f_i$ , for instance, by means of a QAM modulator. Typically,  $f_i$  is equal to a few hundreds of MHz. This analog QAM signal arrives at the input of the ADC where it is sampled at frequency  $f_s$  and then quantified. The adopted number of bits per sample is an important factor of the quality of the received signal at the destination (typically 8 bits per symbol are adopted for existing cellular systems). The flow of data generated at the output of the ADC is band-pass-filtered in order to suppress eventual noises in the upper frequencies. The resulting baseband signal then modulates a laser diode to be transmitted to the RAU. At the RAU, the optical signal is converted back to baseband by means of a photo-detector. The baseband electrical signal obtained after photodetection feeds a DAC that converts again this signal to analog. The last and essential step of this downlink transmission chain is the usage of a band-pass filter that selects and amplifies among the multiple replicas obtained at the output of the DAC, the one that is located in the frequency region of the desired radio frequency carrier  $f_c$  (around the GHz range, for instance). This outlines the benefit of D-RoF that does not require the use of an oscillator at the radio frequency  $f_c$  or at the intermediate frequency  $f_i$  at the RAU. At the output of the DAC located at the RAU, the obtained analog signal is simply band-pass-filtered for noise suppression, amplified, and radiated by the antenna into the cell. In the reverse direction, the operations carried out by the transmission chain for upstream traffic are simply the inverse of those carried out by the downstream chain.

Building a real test bed of a D-RoF link is a costly operation since it requires the design and manufacturing of dedicated electronic chips and circuits. This is why the most advanced performance evaluation of a realistic D-RoF transmission link has been carried out by means of computer simulations [14, 15]. For that purpose, the authors have considered and formulated analytically the key noise sources that may degrade the SNR (signal-to-noise ratio) of a realistic D-RoF link. Three main noise sources have been considered: the ADC, the optical fiber link, and the DAC. Concerning the ADC, jitter noise and quantization noise have been formulated analytically and expressed in terms of SNR degradation. Concerning the fiber link, the impairment of a 20-km fiber link between the CS and the RAU is mainly due to thermal noise at the receiver and fiber chromatic dispersion. At last, the impact of the DAC consists in clock jitter analysis. Overall, the performance metric of the D-RoF link is summarized in terms of end-to-end root-mean-square error vector magnitude or EVM (Eq. 2.1). Experimental results outline the fact that quantization noise is dominant when the ADC/DAC bit resolution is less than 7. In [15], an 8-bit resolution is considered as acceptable for the transport of a digitized WiMAX signal at 2.475 GHz with 16-QAM modulation, 6 Msymbols/s and an optical link of 20 km.

### 4.5.3 D-RoF for a Multiple-Antenna Site

We have seen in Sects. 4.4.3 and 4.4.4 that it was possible to transmit on the same optical fiber multiple analog radio signals. It has been demonstrated experimentally in [22] that it is also possible to transmit from a CS to a RAU multiple digitized radio signals. In this study, the authors describe the circuitry at the CS and at the RAU enabling the transport of a GSM signal and a WiMAX signal. Figures 4.16 and 4.17 depict the main equipment used at the CS and at the RAU, respectively. In these two figures, both the upstream and downstream traffic are considered. In Fig. 4.16, the downstream GSM and WiMAX signals are first superimposed while they are at their respective intermediate frequencies. The analog summation of these



Central Office (CO) for WiMAX and GSM cellular networks

Fig. 4.16 Operations achieved at the CS for a radio GSM signal and a WiMAX signal destined to the same RAU (inspired from [14])

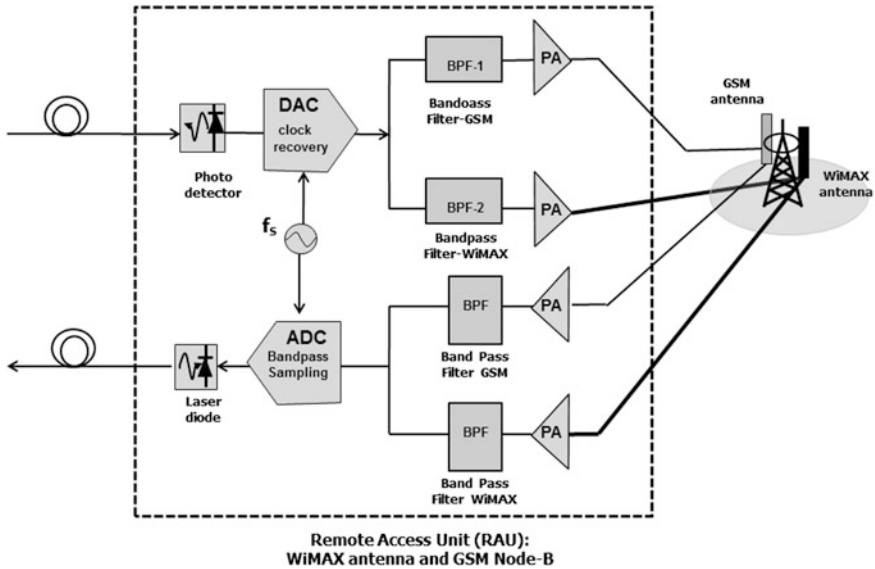


**Fig. 4.17** Operations achieved at the RAU for two radio signals GSM and WiMAX (inspired from [14])

two signals is then digitized by an ADC operating at the sampling frequency  $f_s$  at the CS. It has to be noted that the value of  $f_s$  is sensibly higher in this context than in the context of a single radio channel as it is the case in Sect. 4.5.2. The result of this digitization is then filtered in the frequency domain to modulate directly a laser diode. The corresponding data flow is sent to the RAU by means of an optical carrier. At the RAU (Fig. 4.17), the received optical signal is first demodulated by a photodiode and then treated by a DAC converter operating at the same frequency  $f_s$  as the one used in Fig. 4.16. The obtained electrical signal is duplicated to be sent toward two parallel branches. In the upper and lower branches, a specific filter is applied to isolate the WiMAX and the GSM signals, respectively. Each of these two signals is then amplified and sent to its respective antenna.

A similar treatment is activated for the upstream GSM and WiMAX signals. After having been amplified at the RAU, the analog WiMAX and GSM signals are filtered and recombined to be converted from analog to digital by a common ADC (Fig. 4.17). The output of this ADC corresponds to a data flow that modulates in baseband a laser diode. This optical signal is then demodulated at the CO (Fig. 4.16). After photodetection, the obtained data flow is filtered spectrally to remove undesirable frequencies and converted back to analog by a DAC. The output of the DAC is duplicated. The upper and lower branches at the output of the DAC isolate the GSM data and the WiMAX data, respectively.

It is important to note that, as in the case of Fig. 4.15 referring to a single radio signal and in the case of Figs. 4.16 and 4.17 referring to a dual radio signal (GSM

and WiMAX), none of the GSM or WiMAX radio carrier frequencies are necessary at the RAU. The selection of the suited spectral replicas at the RAU enables such an advantage.

## 4.6 Conclusion

This chapter aimed to describe and explain the basic principles, drawbacks, and benefits of the various A-RoF and D-RoF techniques available as of 2015. We have provided, thanks to an up-to-date bibliography, a picture of the level of advancement of these two techniques.

Concerning A-RoF, the RF-over-fiber approach is clearly the most interesting since it enables to shift all the costly radio equipment today installed at the RAU at a remote site. In the private domain, the possibility to concentrate all the Wi-Fi radio parts close to the Wi-Fi concentrator (an IP router or an Ethernet switch) is cost-effective for the WLAN administrators. Between the years 2000 and 2015, numerous experiments and test beds have demonstrated the technical feasibility of A-RoF for point-to-point and point-to-multipoint configurations. Meanwhile, it appears that A-RoF necessitates a particular attention to distortion effects such as the nonlinearities of the optical fiber (chromatic dispersion, intermodulation noises, etc.). The devices enabling to convert signals from the radio frequency domain to the optical domain are also characterized by a nonlinear behavior with frequency or distance. At the date of publication of this book, we can say that the major drawback of A-RoF is that it needs a form of customization to each environment. The choice of the values of the radio frequencies, the range of the optical link, the number of radio channels transported on the same optical link, the power level of the radio frequencies, etc., need to be dimensioned for each network configuration. Such a customization is not a real problem in the private environment. This is much less admitted by the radio mobile operators that require robust and easy to install equipment. For all these reasons, as of 2015, most of the radio mobile operators have renounced the adoption of A-RoF, benefitting D-RoF. The fact that none of the standards has been considered A-RoF up till now can be viewed as a logical consequence of our previous remark. Since the engineering constraints are less severe in the WLAN environment rather than in cellular networks, A-RoF continues today to motivate new developments, especially for next-generation very-high-speed LANs such as UWB. A-RoF commercial products are now available on the shelves from different vendors. Domestic applications mixing traditional data networking with the interconnection of cameras, sensors, and actuators inside the building are certainly of a great interest for the future of A-RoF. Such applications are directly connected to the concept of Internet of Things (IoT).

D-RoF is clearly viewed by the radio mobile operators as the best solution to upgrade the capacity of their cellular networks. In terms of digital communications, sophisticated techniques (MIMO, turbo-codes, OFDMA, etc.) enable to provide to

the mobile users bandwidth capacities quite close to the Shannon's limit. The available spectrum between 2 and 5 GHz is already well occupied by existing systems. Higher radio frequencies are available, but they impose more costly electronics and higher transmission powers. In other terms, the only way to increase cellular networks capacity is cellular densification. D-RoF appears as the best cost-effective solution in that matter since it enables to federate all the costly radio equipment higher in the infrastructure (at the CO). This characteristic is right in the rationale of the evolution of the mobile backhaul as it is specified by the LTE and LTE-advanced standards. We also estimate that, with the emergence of Cloud Radio Access Network (CRAN) [19], replacing distant and large datacenters by small servers close to the mobile end-users will also boost the emergence of D-RoF technologies.

## References

1. OBSAI: Open Base Station Architecture Initiative. <http://www.obsai.com/members.htm>
2. CPRI: Common Public Radio Interfaces. <http://www.cpri.info/>
3. Proakis JG (2001) Digital communications, 4th edn. McGraw-Hill series in Electrical and Computer Engineering. ISBN 0-07-232111-3
4. Agrawal GP (2010) Fiber-optic communications systems, 4th edn. Wiley. ISBN 978-0-470-50511-3
5. O'Reilly JJ, Lane PM, Capstick MH (1995) Optical generation and delivery of modulated millimeter-waves for mobile communications. Analogue Optical Fibre Communications, The Institute of Electrical Engineers, London
6. Berens F (2009) The European UWB regulation and standardization. In: Proceedings of the UWB workshop, ETSI, Sophia-Antipolis-France
7. Intel White Paper. UWB technology enabling high-speed wireless personal area networks. Intel 2005
8. Allen B et al (2005) Ultra wideband (UWB): applications, technologies and future perspectives. In: Proceedings of the international workshop on convergent technologies (IWCT), Oulu-Finland, 6–10 June 2005
9. Wake D (2003) Optoelectronics for millimeter-wave Radio-over-Fiber systems. In: Wilson B, Ghassemloy Z, Darwazeh I (eds) Analogue optical fiber communications. The Institute of Electrical Engineers, pp 189–192
10. Haddad A, Gagnaire M (2012) Next generation access systems backhauling using Radio-over-Fiber: a prospective approach. IEEE Photonics summer topical meeting series
11. Haddad A, Gagnaire M (2012) PaGeO: Pareto-based Genetic Optimization for LTE radio-over-fiber cellular backhauling. In: Proceedings of the IEEE international conference on wireless and mobile computing, networking and communications (WiMob)
12. Wake D, Nkansah A, Gomes NJ (2010) Radio over fiber link design for next generation wireless systems. IEEE J Lightwave Technol 28(16):2456–2464
13. Vaughan RG, Scott NL, White DR (1991) The theory of bandpass sampling. IEEE Trans Acoust Speech Signal Process 39(9):1973–1984
14. Nirmalathas A, Gamage PA, Lim C, Novak D, Waterhouse R, Yang Y (2009) Digitized RF transmission over fiber. IEEE Microwave Mag 75–81
15. Gamage PA, Nirmalathas A, Lim C, Novak D, Waterhouse R (2009) Design and analysis of Digitized RF-over-Fiber links. IEEE J Lightwave Technol 27(12):2052–2061
16. Ghafoor S, Thomas VA, Hanzo L (2012) Duplex digitized transmission of 64-QAM signals over a single fiber using pulsed laser source. IEEE Commun Lett 16(8)

17. Sesia S, Toufik I, Baker M (2009) LTE, the UMTS Long Term Evolution: from theory to practice. Wiley
18. Wake D, Webster M, Wimpenny G, Beacham K, Crawford L (2004) Radio over fiber for mobile communications. In: Proceedings of the 2004 IEEE international topical meeting on microwave photonics, pp 157–160
19. Arslan H (2007) Cognitive radio, software defined radio and adaptive wireless systems. University of Southern California, signals and communications technology series. Springer
20. Lange C, Kosiankowski D, Von Hugo D, Gladisch A (2014) Analysis of energy consumption in carrier networks. In: Proceedings of the IEEE ONDM conference, Stockholm
21. Yeh S, Talwar S, Lee S-C, Kim H (2008) WiMAX femtocells: a perspective on network architecture, capacity and coverage. IEEE Communications Magazine, pp 58–65, October 2008
22. Gamage PA, Nirmalathas A, Lim C, Novak D, Waterhouse R (2009) Experimental demonstration of the transport of digitized multiple wireless systems over fiber. IEEE Photon Technol Lett 21(11)

# Chapter 5

## Overview of Standardization for D-RoF

Silvano Frigerio, Alberto Lometti and Vincenzo Sestito

**Abstract** The main standard references for Digital Radio over Fiber (D-RoF) transmission are CPRI (Common Public Radio Interface) and OBSAI (Open Base Station Architecture Initiative). OBSAI has a wider extent than CPRI, since it describes not only the interface between the radio base station and the remote radio head, like CPRI, but also the base station system architecture. Nevertheless, CPRI is the technology mostly deployed, both for intra-site connectivity and for front-hauling, a recently developed network paradigm known also as C-RAN (Cloud Radio Access Network), which implies the physical separation of base stations from radio units and their centralization in a central office. This chapter provides the reader with a view on the objectives, the referenced architectures, and the state of the art of the regulations for each of these technologies, with a special attention given to the aspects and standardization activities relative to the possibility of transporting D-RoF over geographical distances, as it is implied by front-hauling. Finally, a brief reference is made to ORI (Open Radio Interface) activity, setup in 2010 by ETSI (European Telecommunications Standards Institute). ORI recognizes that actually neither CPRI nor OBSAI have been designed having in mind full compatibility between equipment from different vendors, and therefore aims at developing a really open D-RoF interface, mainly leveraging on CPRI existing specifications.

---

S. Frigerio (✉) · A. Lometti · V. Sestito  
Alcatel-Lucent Italy, Milan, Italy  
e-mail: silvano.frigerio@sm-optics.com

A. Lometti  
e-mail: alberto.lometti@sm-optics.com

V. Sestito  
e-mail: vincenzo.sestito@sm-optics.com

## 5.1 CPRI

The Common Public Radio Interface is an industry cooperation, operative since 2003 and still active today. Cooperating parties are Ericsson AB, Huawei, NEC, Alcatel Lucent, and Nokia Siemens Networks (Nortel left on 2009). It defines a publicly available specification describing a digital interface for encapsulating the digitized samples of the radio antennas sent between a radio equipment (RE) and a radio equipment control, or baseband unit (REC), which performs the digital processing of those signals. When connecting a REC and a RE with one or several CPRI interfaces, the resulting entity is, e.g., a Node B (or enhanced Node B) in a WCDMA (or LTE/LTE Advanced, respectively) Radio Access Network. Interworking of equipment from multiple vendors is not generally possible although this was the original objective.

More in detail, CPRI can be described as a digitized and serial point-to-point (P2P) radio interface, mapping the sampled antenna signals (I/Q data), possibly related to different mobile technologies, into containers of a synchronous multiplexing digital hierarchy. Key characteristics are:

- the support for different mobile technologies, including: GSM, UMTS, WiMax, LTE, LTE Advanced;
- the allowance for single-hop and multi-hop topologies (between REC and RE);
- the inclusion of three different information flows (user plane data, control and management plane data, and synchronization plane data), which are TDM multiplexed at the CPRI interface;
- the basic assumption of being in a perfectly synchronized environment, without the need for any frequency adjustment mechanisms (e.g., bit or byte stuffing) among the different clients of the digital CPRI stream;
- eight different options for CPRI line bite rates, as multiples of lower line rates: (1) 614.4 Mb/s, (2) 1228.8 Mbit/s, (3) 2457.6 Mbit/s, (4) 3072.0 Mbit/s, (5) 4915.2 Mbit/s, (6) 6144.0 Mbit/s, (7) 9830.4 Mbit/s, (8) 10137.6 Mbit/s.

The CPRI specification covers layers 1 and 2 of the OSI stack. The physical layer (layer 1) supports both an electrical interface (i.e., what is used in traditional base stations), and an optical interface (e.g., for base stations with remote radio equipment). Line coding (8B/10B and 64B/66B) as well as scrambling are foreseen for transmission over a physical medium.

The CPRI was originally designed for point-to-point interconnections; as such it defines maximum latency assuming no intermediate nodes. It assumes near zero jitter and near zero bit error rate. Such assumptions pose quite a few issues, addressed in the following paragraphs, toward CPRI transport over a geographical network, something that is necessary for the exploitation of the front-hauling network paradigm (pre-requisite of C-RAN—Cloud Radio Access network), which is described extensively in several chapters of this book.

### 5.1.1 *Specification Overview*

The first version of the CPRI interface specification was written in order to comply with 3GPP UTRA FDD release 5. The latest version is version 7.0. The main changes introduced for each specification release are listed below:

- Version 2.0 introduced support for networking.
- Version 3.0 added WiMAX and an increase in the line bit rate.
- Version 4.0 extended the specification to encompass the developments for LTE (Long-Term Evolution).
- Version 4.1 added higher line rates for LTE.
- Version 4.2 added one further higher line rate (9.8 Gbps).
- Version 5.0 extended the specification to encompass GSM.
- Version 6.0 has included LTE Advanced and still a higher line rate (10.1 Gbps).
- Version 6.1 added higher line rates for LTE Advanced (8 and 12 Gbps).
- Finally, version 7.0 added still a higher line rate to the previously released 10 Gbps LTE Advanced (24 Gbps).

For a thorough description of all CPRI interface aspects the latest reference is [1] (detailing Version 7.0), to which the reader is directed for any possible detail. What follows is a sum-up of the main interface characteristics along with some considerations about its practical use in the field.

### 5.1.2 *System Description*

The CPRI specification assumes the decomposition of the radio base station into two basic building blocks, the so-called radio equipment control (REC) and the radio equipment (RE) itself. Both parts may be co-located as in a conventional radio base station design or both may be physically separated (i.e., the RE may be close to the antenna, whereas the REC is located in a conveniently accessible site). In the front-hauling paradigm, many RECs from different mobile sites are pooled together in a Central Office located at a distance from the REs that can range from a few km up to possibly 40 km and even beyond.

The REC contains the radio functions of the digital baseband domain, whereas the RE contains the analog radio frequency functions. The functional split between both parts is done in such a way that a generic interface based on In-Phase and Quadrature (IQ) data can be defined.

In addition to the user plane data (IQ data), control and management as well as synchronization signals have to be exchanged between the REC and the RE. All information flows are multiplexed onto a digital serial communication line using appropriate layer 1 and layer 2 protocols. The different information flows have access to layer 2 via dedicated service access points. This defines the Common Public Radio Interface illustrated in Fig. 5.1. Note that the interface definition

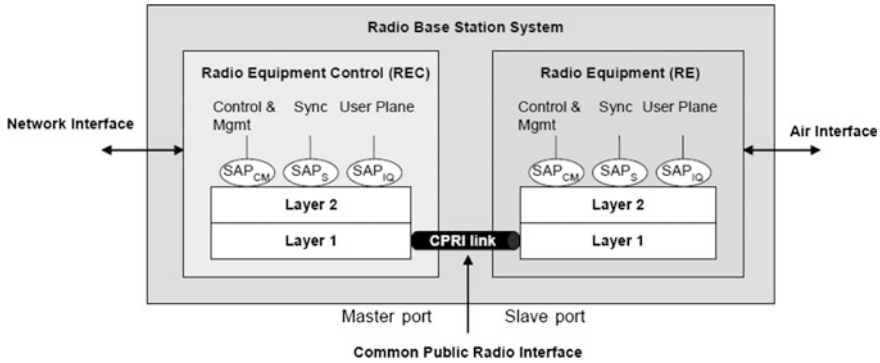


**Fig. 5.1** Basic CPRI system and interface definition (*source* [2])

assumes a “master” side and a “slave” side at the ends of the bidirectional “link” interconnecting two ports, either between REC and RE, or between two nodes, using one transmission line per direction. A working link consists of a master port, a bidirectional cable and a slave port. This master/slave role split is true for different sets of flows of the interface, specifically for start-up and reset sequences, for synchronization, and for control and monitoring during the start-up sequence.

At least one REC in a radio base station shall have at least one master port and optionally may have other ports that may be slave or master. An RE shall have at least one slave port and optionally may have other ports that may be slave or master.

Beyond the basic configuration built with one master, one slave, and one or more interconnecting CPRI, different network topologies can be supported. Specifically:

- Star: multiple slaves RE connected with one or more CPRI to one master REC.
- Chain: with a “head” master REC, a “tail” slave RE and intermediate REs with one master side and one slave side.
- Tree: a mix of chain and star.
- Ring: a slave RE chain closed on the tail REC.

Finally, it is worth noting that also multi-REC configurations, even if less frequently used, can be envisaged, such as different RECs connected to one RE or chains with more than one REC in the sequence.

### 5.1.3 Main Requirements

CPRI requirements, as reported in the CPRI specification [2], delineate the scope of the interface (supported radio technologies, transmission length, network topologies), set bandwidth needs for control and management planes (in the range of hundreds of kbps), indicate basic OAM primitives and needed BER performance

( $10^{-12}$ ), describe auto-negotiation and, most notably, define synchronization and latency aspects. Specifically, CPRI is supposed to convey frequency and time from the REC to the REs with very high accuracy, in order to cope with the synchronization requirements of all involved mobile technologies. Frequency is embedded in the CPRI clock itself, while time is indicated by CPRI framing. Key requirements are:

1. Frequency accuracy from master SAP<sub>S</sub> to slave SAP<sub>S</sub>: 2 ppb (parts per billion)
2. Delay accuracy from master SAP<sub>S</sub> to slave SAP<sub>S</sub> (excluding cable):  $\pm 8.138$  ns
3. Round trip delay accuracy from master SAP<sub>S</sub> to slave SAP<sub>S</sub> (excluding cable):  $\pm 16.276$  ns
4. Round trip cable delay measurement accuracy:  $\pm 16.276$  ns
5. Maximum round trip delay (latency—excluding cable): 5  $\mu$ s

Point 4 refers to the fact that the specification demands for automatic cable delay measurement, which has to be made available to the REC without any manual provisioning.

It is worth noting that those requirements have been defined based on pure point-to-point cable connections; in case of interposition between REC and RE of a geographical network, like in the front-hauling paradigm, it is reasonable to assume that they can be somehow adapted:

- for frequency and time, taking into account overall budgets allowed for the backhauling network (e.g., for LTE the eUTRAN—evolved UMTS Terrestrial Radio Access Network), and
- for latency, considering the 3 ms latency budget between BBU and RRH allowed for HARQ (Hybrid Automatic Repeat Request) by 3GPP.

Figure 5.2 shows a graphical representation of the logical process which can be followed in order to derive CPRI requirements with front-hauling (FH in the figure).

Table 5.1 sums up the resulting budgets that can be applied to the transport network in LTE front-hauling, based on the considerations detailed above.

### 5.1.4 Interface Description

CPRI defines the layer 1 and layer 2 protocols for the transfer of user plane, control and management, and synchronization information between REC and RE as well as between two REs. The interface supports the following types of information flows, as depicted in Fig. 5.3:

- IQ data: user plane information in the form of in-phase and quadrature modulation data (digital baseband signals).
- Synchronization data: used for frame and time alignment.
- L1 in-band protocol: signaling information (e.g., for system start-up) that is related to the link and is directly transported by the physical layer.

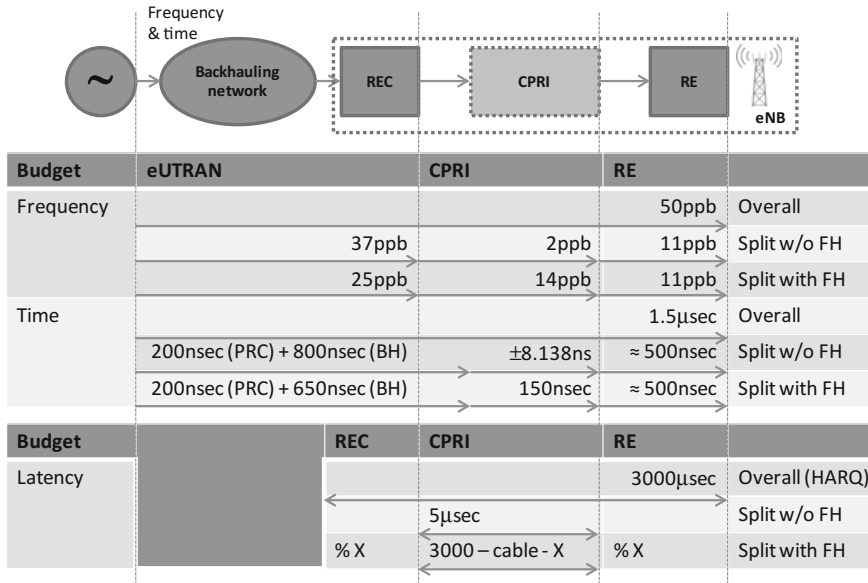


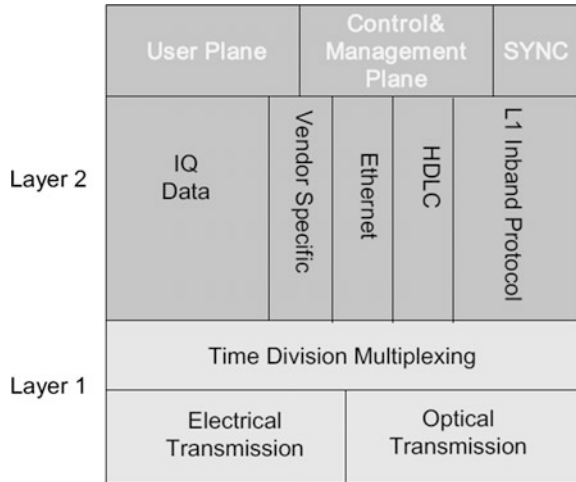
Fig. 5.2 CPRI frequency, time and latency requirements derivation with LTE front-hauling

Table 5.1 Transport budget dimensioning examples for front-hauling

Frequency accuracy: total eUTRAN budget	CPRI budget	Transport budget
LTE FDD/TDD: ±50 ppb	±2 ppb	±14 ppb (as suggested in ITU-T discussions, provided the overall budget is kept)
DL CoMP (coherent): ±5 ppb		±2 ppb
Time accuracy: total eUTRAN budget	CPRI budget	Transport budget
LTE FDD/TDD: ±1.5 μs	±8 ns	±150 ns (set as a rule-of-thumb to 10 % of overall budget)
eMBMS/CoMP: ±1.5 μs		
Latency: 3GPP HARQ budget	eNB budget	Transport budget
LTE FDD: 3000 μs	X μs	= 3000–X–fiber delay (5 μs/Km)
LTE TDD: 3000 μs	Y μs	= 3000–Y–fiber delay (5 μs/Km)

- C&M data: control and management information exchanged between the control and management entities within the REC and the RE. This information flow is given to the higher protocol layers. C&M data are sent either as in-band protocol (for time critical signaling data) or by layer 3 protocols (not defined by CPRI) that reside on top of appropriate layer 2 protocols. Two different layer 2 protocols—a subset of High-level Data Link Control (HDLC) and Ethernet—are supported by CPRI.

**Fig. 5.3** CPRI protocol overview (source [2])



- Protocol Extensions: reserved for future protocol extensions.
- Vendor-Specific Information.

### 5.1.4.1 Layer 1 Interface Specification

As shown in Fig. 5.3, all information streams are multiplexed by a time division multiplexing scheme. Time division multiplexed data are structured into a suitable digital frame, which has a strict time and frequency relationship with the 10 ms WCDMA (Wideband Code Division Multiple Access) frame in air, as depicted in Fig. 5.4. The CPRI specification defines a frame as well as a multi-frame structure; the basic frame contains 16 CPRI “words”, while the CPRI multi-frame, called hyperframe, is built with 256 basic frames; 10 hyperframes coincide with one time slot in the 10 ms WCDMA frame. The different line speeds in the hierarchy are obtained through the usage of different CPRI word lengths, starting from 1 byte (level 1, resulting in 614,4 Mb/s with 8B/10B line coding) up to 20 bytes (level 8, resulting in 10137,6 Mb/s with 64B/66B line coding).

Word “0” is used as a control word, for frame alignment and other control purposes. All information flows, but user plane data, are inserted in the control word by exploiting the hyperframe structure, which allows for a 256 words overall overhead field. The distribution of the different information flows within the 256 words is depicted in Fig. 5.5.

The remaining 15 words in a basic frame are used for IQ user plane data, which are structured in so-called AxC containers. An AxC (Antenna-Carrier) is the amount of digital baseband (IQ) U-plane data necessary for either reception or transmission of only one carrier at one independent antenna element, while an AxC container is a sub-part of the IQ data block of one basic frame. The size of an AxC

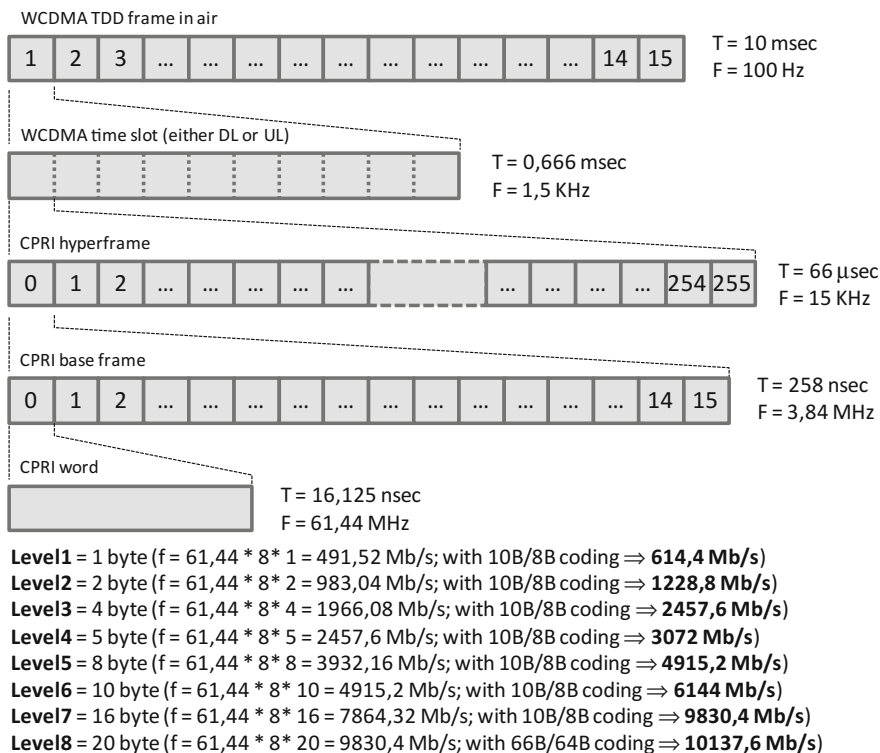


Fig. 5.4 CPRI frame structure

Container is always an even number of bits. A CPRI frame is built via a two step process:

1. Mapping of IQ data within a suitable AxC container;
2. Mapping of AxC containers into the basic frames.

The mapping of AxC containers into the basic frame for both uplink and downlink is based on the following rules:

- Each AxC Container is sent as a block.
- Overlap of AxC Containers is not allowed.
- The position of each AxC Container in the IQ data block is according to one of the following options:
  - Option 1 (packed position): each AxC Container in a basic frame is sent consecutively (without any reserved bits in between) and in ascending order of AxC number.
  - Option 2 (flexible position): for each AxC Container, the application shall decide in which position in the IQ data block the first bit of the AxC Container is positioned.

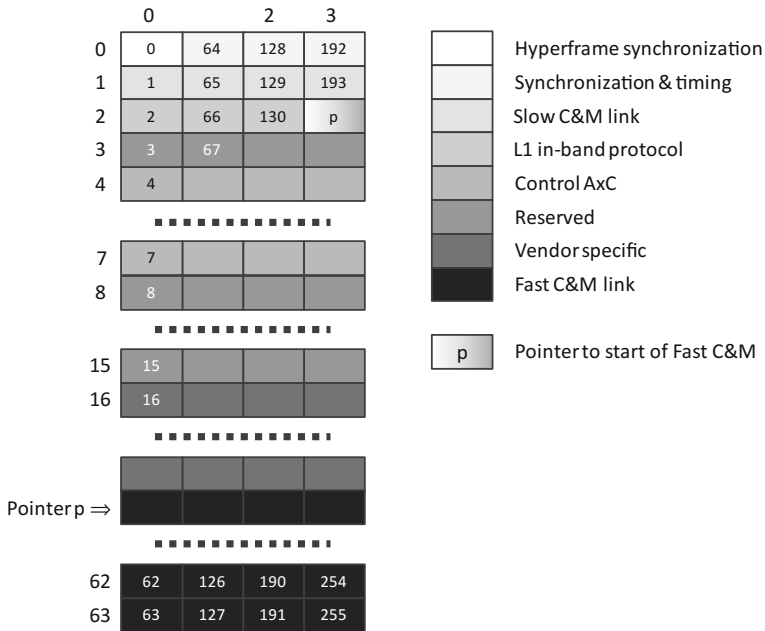


Fig. 5.5 Distribution of overhead within control words in one hyperframe

- The bits not used by AxC Containers in the IQ data block in the basic frame shall be treated as reserved bits (“r”).

Figure 5.6 illustrates these mapping rules for both mapping options.

The mapping of the IQ user plane data within AxC containers follows different rules according to the different mobile technologies. Details are reported in [2]; at any rate, two basic characteristics of the TDM multiplexing process have to be taken into consideration:

1. The frame is fully synchronous, without any means for managing frequency differences between the different user plane information flows (no stuffing mechanisms). This implies that all multiplexed streams have to be traceable to the same frequency reference.

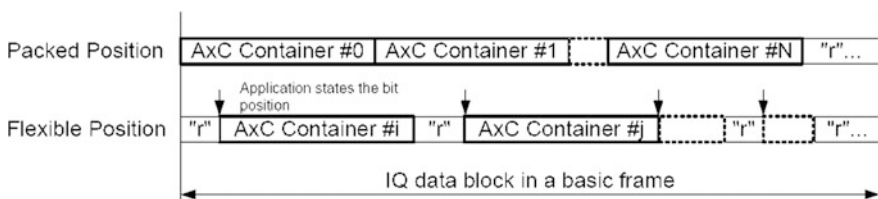


Fig. 5.6 Example of AxC Container mapping in the IQ data block (source [2])

2. The frame is not self-explaining as far as the position of the different AxC containers is concerned (no pointers). This implies that the information for correctly multiplexing and de-multiplexing the different tributaries within a CPRI frame has to be explicitly exchanged between REC and RE, typically using a control channel, the format of which is not specified by the recommendation. This is one of the major obstacles to horizontal compatibility among different vendors.

Layer 1 specification finally includes also the description of link maintenance procedures. They are based on 4 alarm primitives, along with relative consequent actions:

- Loss of Signal (LOS—based on line coding violations and/or loss of optical power for optical interfaces),
- Loss of Frame (LOF—fail of the hyperframe alignment process),
- Remote Alarm Indication (RAI—LOS or LOF signaled back to the remote terminal),
- SAP Defect Indication (SDI—the near end explicitly informs the far end that the link shall not be used for any of the Service Access Points; the detection rule is out of the scope of the specification).

The link maintenance procedures are in line with the requisites of a co-located interface, but are not well-suited for geographical transmission, like it is required by the front-hauling paradigm, due to the lack of any “degrade” information as well as of any formalized protection mechanism. This is one of the main reasons why in the context of front-hauling a traditional and well-proven technology such as OTN [3] is usually taken into account for CPRI transport, as it will be described in Sect. 5.3.

#### 5.1.4.2 Layer 2 Interface Specification

Main contents of the CPRI specification at Layer 2 are:

- slow C&M Data Link Layer
- fast C&M Data Link Layer
- start-up procedures

The slow C&M Data Link Layer is based on HDLC (High-level Data Link Control) standard protocol using the bit-oriented scheme, as described in [4]. Media access, flow control, and data protection, via a 16-bit Frame Check Sequence (FCS), are in accordance with the standard. Retransmission mechanisms are supposed to be accomplished by higher layer signaling.

The fast C&M Data Link Layer follows the Ethernet standard as specified in [5]. Due to the specific CPRI framing, there is no minimum frame length that reasonably matches for CPRI application, moreover CPRI does not require frame padding; as a consequence, the MAC client data + PAD field length ranges from 1 to 1500

octets. The Ethernet MAC frame is encoded using a 4B/5B line code and is delineated by the PCS (Physical Coding Sub-layer) function of 100BASE-X as specified in [5]. No flow control is provided; data protection is based on FCS according to [5], while no retransmission mechanism is specified.

Finally, the start-up procedure accomplishes two main objectives:

1. Synchronization of layer 1: byte and hyperframe alignment.
2. Alignment of capabilities of the master and slave ports: line bit rate, protocol, C&M channel bit rate, C&M protocol, vendor-specific signaling.

As stated above, vendor-specific signaling includes the frame description in terms of IQ data mappings within AxC containers and their position within the CPRI frames.

### 5.1.5 CPRI Compression and CPRI Throughput Examples

One of the main challenges of the front-hauling network paradigm is the large amount of bandwidth to be transported over geographical distances, which is far beyond what is needed with the traditional backhauling approach (from  $n \times 2$  Mb/s for GSM to some hundreds Mb/s for LTE and LTE advanced). That is the reason why the possibility of compressing CPRI has been taken into account in the C-RAN context since the beginning, and relevant algorithms were developed. In general, those algorithms do not compress CPRI as a whole, but act on IQ data and thus require the knowledge of the CPRI frame structure, which at the current status of standardization excludes the possibility for a vendor to compress CPRI signals coming from another vendor, for the reasons detailed above. With standard DSP means, acting on quantization and sampling frequency of IQ flows, a compression capability up to about 2.7 has been demonstrated on LTE signals, with very negligible system performance degradation. In the following, the simple rule to evaluate the bandwidth needed for CPRI is given, along with a table listing some practical cases with and without compression.

If a given IQ signal is characterized by:

$N_{\text{sec}}$	number of sectors in a cell
$N_{\text{MIMO}}$	number of TX antennas in a MIMO (Multiple Input Multiple Output) arrangement
$f_s$	IQ sampling rate
$W_s$	IQ sample width [in bits]
$R_{\text{CPRI}}$	the rate increase due to CPRI redundancy (16/15)
$R_{\text{code}}$	the rate increase due to line coding redundancy (10/8 for 8B/10B; 66/64 for 64B/66B)

**Table 5.2** CPRI equivalent rates for a mix of WCDMA and LTE carriers

5 MHz WCDMA carriers	CPRI equivalent bandwidth (Mb/s)			
	LTE spectral bandwidth (MHz)			
	0	10	20	30
0	0	7.373	14.746	22.152
1	983	8.356	15.729	23.135
2	1.966	9.339	16.712	24.118
3	2.949	10.322	17.695	25.101
4	3.932	11.305	18.678	26.084

**Table 5.3** CPRI equivalent rates for a mix of WCDMA and compressed LTE carriers

5 MHz WCDMA carriers	CPRI equivalent bandwidth (Mb/s)			
	LTE spectral bandwidth (MHz)			
	0	10	20	30
0	0	2.731	5.461	8.204
1	983	3.714	6.444	9.187
2	1.966	4.697	7.427	10.171
3	2.949	5.680	8.410	11.154
4	3.932	6.663	9.393	12.137

then the relevant minimum CPRI equivalent rate is:

$$f_{\text{CPRI}} = N_{\text{sec}} * N_{\text{MIMO}} * f_s * W_s * R_{\text{CPRI}} * R_{\text{code}}$$

Of course, all IQ contributions in the cell need to be evaluated and summed.

In Table 5.2 (uncompressed CPRI) and Table 5.3 (compressed CPRI—LTE only) the CPRI equivalent rates are shown for a mix of a variable number of 5 MHz WCDMA carriers and one LTE carrier, with different spectral widths. Both the huge bandwidth amounts that are possibly reached as well as the positive effect of compression are quite evident.

## 5.2 OBSAI

The Open Base Station Architecture Initiative is an industry agreement, officially established in September 2002 among Hyundai, LGE, Nokia, Samsung, and ZTE, with the aim to create an open market for cellular base stations (Base Transceiver Station—BTS).

The leading idea was to define a reference system architecture and key interfaces, in such a way so as to allow the production of “off-the-shelf” base station modules by wireless OEM’s.

This hardware commoditization should leave, on one side, RAN manufacturers to focus their development efforts on further added value within the base station, in

terms of greater innovation and more cost-effective products. On the other side, it should provide operators with a quicker availability of new BTSs, benefiting at the same time from the competition among base station vendors. The initiative currently involves about one hundred partners including device suppliers, system vendors, testing equipment vendors, and electronics manufacturers.

### **5.2.1 *OBSAI Specifications Status***

OBSAI activity has resulted, through the years, in the definition of a set of public specifications aiming at addressing the following aspects:

- System Specifications, defining the general view on building blocks, functions, and electrical and mechanical requirements for a BTS.
- Reference Point Specifications, defining the characteristics of the interfaces internal to the BTS
- Module Specifications, describing in detail the different building blocks (modules) to be implemented in the BTS.
- Conformance Test Specifications, aiming at providing test procedures for the validation of BTSs, sub-systems (see modules) and interfaces (see reference points), with the basic target to ensure the multi-vendor interoperability.

It is worth noting that the different specifications so far generated are not at the same status. Specifically, documents addressing Reference Points (RP) requirements and associated conformance tests have been sourced in a time window from 2004 to 2010, capturing also recent aspects of technology evolution as the support of IPv6 (for what relates to RP1 and RP2) and the support of LTE as 4G radio technology (for what relates to RP3/RP3-01). Conversely, documents dealing with BTS system specifications, including detailed module descriptions and associated conformance tests, have stopped in 2006, defining requirements for the support of 2G and 3G radio technologies, but with no mention of LTE and LTE Advanced.

### **5.2.2 *System Architecture Overview***

#### **5.2.2.1 Objectives**

OBSAI defines in [6] a modular structure for the open base station, addressing a set of standard BTS modules with required form, fit, and functions. This implies on one side, specific requirements in terms of electrical and mechanical features to be implemented by the target BTS. On the other side, the definition of a target architecture able to match throughput scalability, OAM&P principles, and concurrent operation with different air interface standards.

Similarly, in [7–11], digital interfaces between BTS modules are defined in such a way to assure interoperability and compatibility between different module vendors.

### 5.2.2.2 System Blocks and Interfaces

The OBSAI BTS architecture consists of 4 main blocks (see Fig. 5.7):

- Transport Block (TB).
- Control/Clock Block (CCB).
- Baseband Block (BB).
- RF Block (RFB).

These blocks are connected internally via specified interfaces, called Reference Points (RPs). Namely:

- RP1 used to distribute control and management data and clock signals among all blocks.
- RP2 used to carry user data transport, between Transport Block and Baseband Block.
- RP3 connecting Baseband Block and RF Block for air interface data exchange.
- RP4 providing the power interface between the internal modules and DC power sources.

For external connections, BTS system implements:

- External Network Interface, assumed to connect mobile controllers and gateways systems.
- Air Interface, for connectivity toward User Equipments.
- Power Interface, for powering the BTS.

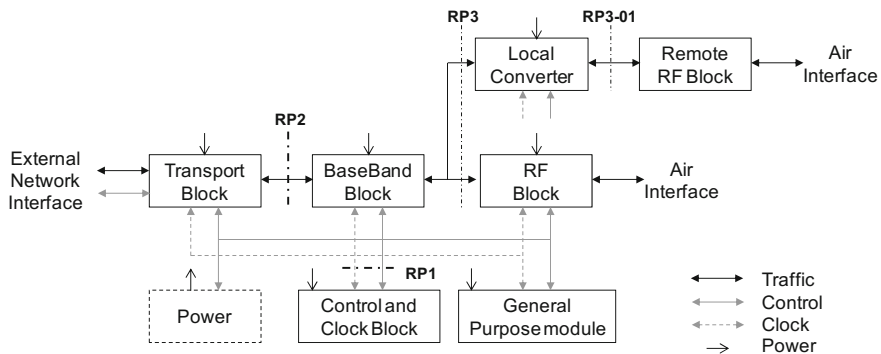


Fig. 5.7 OBSAI BTS reference architecture (source [6])

The **Transport Block** supported functions include:

- External Network Interface termination.
- QoS functions, establishing the required throughput, delay, delay variation, and drop rate limits.
- Synchronization functions, as clock signals extraction from network and SSM handling.
- OAM&P functions.
- Security functions, for OAM&P messages, C-Plane and U-Plane messages exchanged through network interface. IPsec tunneling is referenced as a possible means for security.

Specifically, the External Network Interface may operate with different technologies, depending on the backhaul network connectivity. Examples of this include (not limited to): IP/ATM over PDH (E1, E3), IP/ATM over SDH/SONET (STM1, OC3), IP/ATM over xDSL (HDSL—High-speed Digital Subscriber Line; SHDSL—Symmetrical HDSL; VDSL—Very high-speed DSL), IP over Ethernet (FE, GE). At the same time, it is required to allow for connectivity to various RAN topologies (e.g., star, chain, ring) with no need for additional equipment: this capability implies the support of ATM multiplexing, cross-connection, switching or IP routing, depending on the technology implemented by the backhaul network.

The **Control and Clock Block (CCB)** is the primary control processor for the BTS. The CCB controls BTS resources, supervising all the activities, monitoring BTS status, and reporting status and performance data. The CB specific functions are:

- Congestion Control, related to Transport Block, Baseband Block, and RF Block on the base of pre-defined thresholds.
- Admission Control, toward the air interface, with the purpose to admit or deny new user equipment, new radio access bearers, or new radio links (e.g., due to handover).
- OAM&P Functions.
- Radio Resource Management, i.e., the set of procedures for handling the allocation/de-allocation of radio resources (e.g., call admission, transmit power setting, radio channel rate setting, etc.).
- Multi-vendor Configurations, for allowing interoperability among CCB and modules from different vendors.
- RF Scheduling.
- Network Interface (NI) Signaling Termination, performing the termination of backhaul signaling protocols.
- System Clock Generation and Distribution, including clock monitoring, clock selection and clock switchover. Specifically, the BTS must interoperate with one or more of the following input reference clock and timing sources:
  - GPS-based clock and time reference.
  - Atomic clock locked terrestrial transmission.
  - 10 MHz external reference such as from a rubidium clock.

- 2.048 MHz external reference (typical reference in E1/T1 interface clocking).
- External core network interface.

The **Baseband Block** performs the baseband processing for the air interface signals, related at least to two concurrent radio transmission technologies among the following: GSM, CDMA, WCDMA, HSDPA/HSUPA, WiMAX (licensed/unlicensed bands).

Depending on the specific radio technology implemented, different specific sets of functions are performed, spanning from encoding/decoding, modulation/demodulation, to MIMO handling and interference cancelation procedures. Specifically, the A/D, D/A conversion of signals carrying I/Q components and exchanged with RF Block via RP03, may be implemented in this block or performed via an additional element (see Local Converter, in Fig. 5.7) possibly connected to RF Block via RP03-1 interface.

Note that the OBSAI specification for the BTS system architecture addresses recommendations for 2G and 3G mobile applications, while 4G (LTE) and related technologies (see OFDM, OFDMA, SC-FDMA) are not yet formally included. LTE support is, conversely, included in the specifications for RP03/RP03-1.

The **RF Block** processes air interface signals, consistent with the Baseband Block capabilities and technology support. Supported functions include (not limited to): D/A and A/D conversion, Carrier selection, TX/RX RF filtering, power control, OAM&P, and calibration procedure.

### 5.2.3 *RP3-01 Insight*

Specific attention has to be given to the OBSAI specification for RP3-01, i.e., the interface between Baseband Block and remote RF Block, since its scope is equivalent to the one addressed by the CPRI specification (Fig. 5.8).

In general, the bus interface connecting BB modules to RF modules is a TDM high-capacity, point-to-point serial interface bus assumed to ensure bi-directional exchange of data and control information. Depending on the location of RF modules, the interface is specified as RP3, if RF modules are co-located with BB modules (meaning, same shelf or rack), or as RP3-01, if RF modules are remote with respect to BB modules. In this last case, a Local Converter (LC) Block is included, mainly with the aim to provide the proper media adaptation function for the inter-connections toward RF modules. Depending on the implementation, the LC Block may be collapsed or not into other blocks (e.g., BB block).

RP3-01 is then equivalent to the RP3 protocol except for the technologies used at the physical layer in order to support up to 40 km span reach. Preferred method is, consequently, the optical transmission, but radio and copper technologies are allowed as well, provided they match OBSAI specifications.

RP3-01 operates at line rates defined as multiples ( $i = 1, 2, 3, 4$ ) of the basic module rate (768 Mb/s), specifically: 768, 1536, 3072, and 6144 Mb/s.

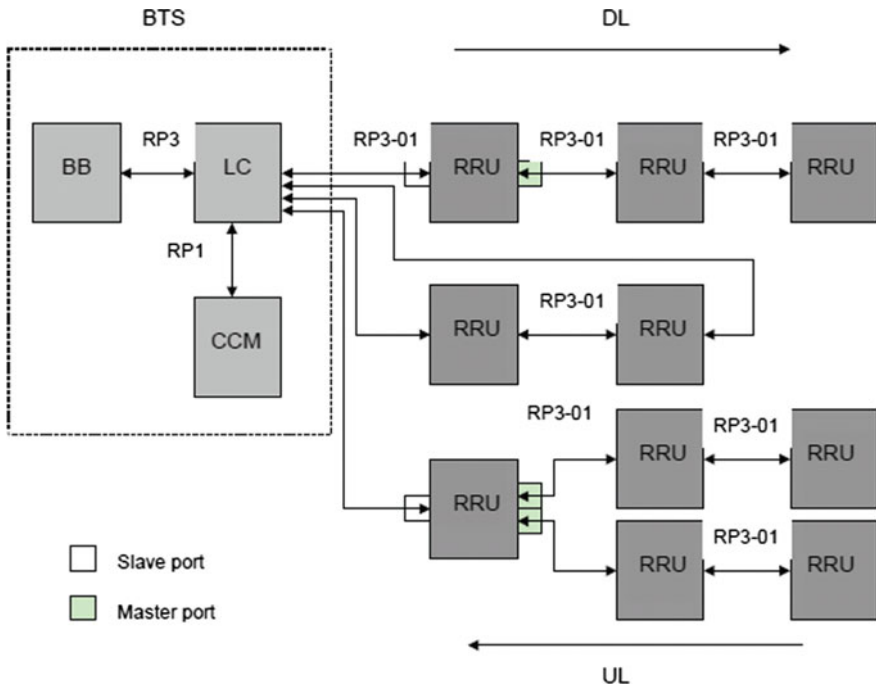
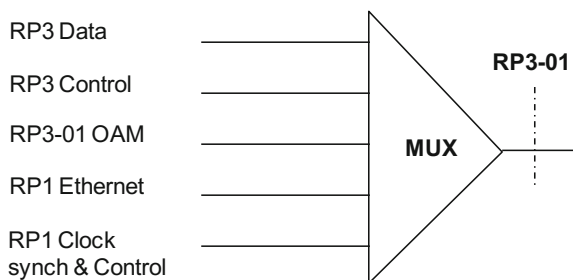


Fig. 5.8 Examples of connectivity for RP3-01 (source [9])

At the link set-up, a dedicated procedure for negotiating the operative transmission rate may be used by BB and RF Blocks (in this case a system operates as a “master” and the opposite one as a “slave”). Alternatively, the operative rate may be provisioned by a management system.

RP3-01 protocol (see Fig. 5.9) provides means for carrying RP3 data and control messages, RP1 Ethernet, RP1 clock bursts (for periodic synchronization of each air interface supported), and RP3-01 OAM data (e.g., RTT measurement, HW reset, loopback).

Fig. 5.9 RP3-01 protocol: carried data



The bus protocol is the result of processing performed at four layers, specifically:

- Application layer, providing the mapping of different types of packets to the payload.
- Transport layer, responsible for the end-to-end delivery of the messages, i.e., responsible for the routing of messages.
- Data link layer, responsible for the framing of messages and message (link) synchronization
- Physical layer, responsible for coding, serialization, and transmission of data.

Figure 5.10 shows the high-level organization and contents of the RP3-01 protocol. The RP3-01 basic module is the “message”, organized on a fixed length of 19 bytes comprising 3 header bytes and 16 payload bytes.

Specifically, the header section comprises:

- Address (13 bits)—The address is used for the routing of messages between RF block and the modules of the BTS system; the connectivity is point-to-point in the downlink direction (i.e., toward RF), while it may be either point-to-point or point-to-multipoint (multicasting) in the uplink direction (i.e., toward BB block).
- Type (5 bits)—It identifies the type of message, i.e., the content of the associated payload data (among Control, Measurement, Data traffic, RP3-01 OAM, Ethernet, Clock synch).
- Timestamp (6 bits)—It provides time information about the associated payload data, with different meanings depending on the direction of transmission (uplink or downlink) and on the specific radio technology carried.

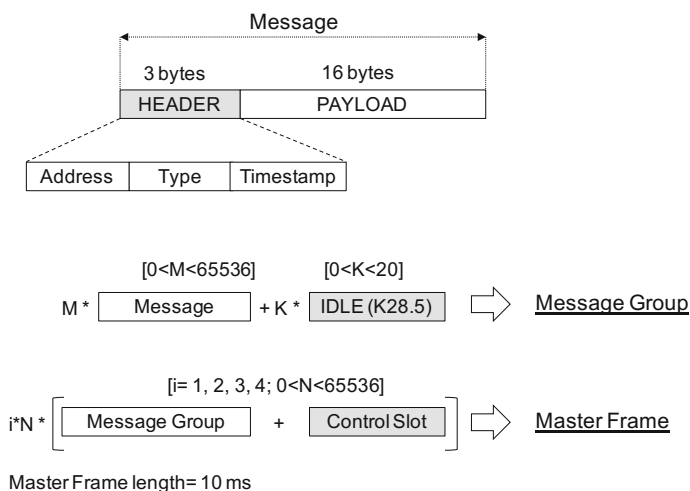
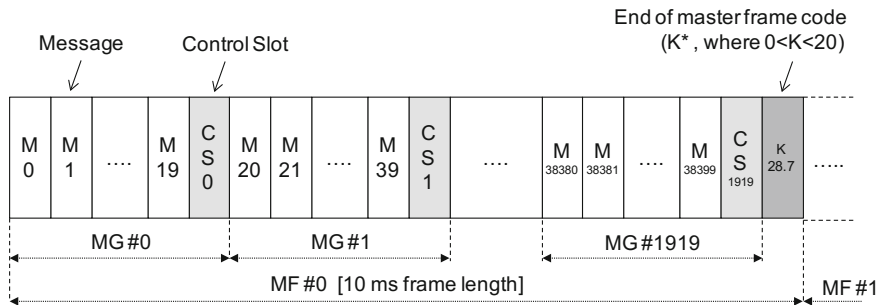


Fig. 5.10 RP3-01 protocol structure



**Fig. 5.11** RP3-01 master frame structure for GSM/EDGE, WCDMA, LTE (with  $M = 21$ ,  $N = 1920$ ,  $K = 1$ ,  $i = 1$ )

The payload field carries the content of the *message* consistent with the *type* field defined (control, measurement, antenna sample (I/Q), or some other data). From the Physical and Transport layer point of view, it is considered to be always full. It is the responsibility of the Application layer to map data to the payload.

As depicted in Fig. 5.10, combination of Message ( $M^*$ ) and Idle code ( $K_{28.5}$ ,  $K^*$ ) results in a Message Group (MG); consequently, combination of Message Group ( $i \cdot N^*$ ) and Control Slot ( $i \cdot N^*$ ) results in a Master Frame (MF). For better demarcation among master frames, consecutive special code  $K_{27.5}$  ( $K^*$ ) are inserted at the end of each MF. Figure 5.11 depicts, as an example, the master frame format applicable to the transport of 2G, 3G, and 4G technologies.

The framed signal is then processed for 8B/10B line encoding (decoding) and reaches the operative line rate (according to the value of the “i” factor ( $i \cdot 768$  Mb/s)). In case of a signal operating at 6144 Mb/s, a scrambling (de-scrambling) operation is performed on the master frames sequence, prior to the 8B/10B encoding (decoding).

### 5.2.4 CPRI Versus OBSAI RP3-01

In order to complete the picture of available technologies for D-RoF, it may be interesting compare the features related to OBSAI RP3-01 frame with the ones associated with the equivalent CPRI format. The aim of this comparison is purely technical and does not imply any judgment about the quality of the considered solutions.

OBSAI RP3-01 is part of a set of specifications aiming at realizing full multi-vendor compatibility for all the components of a base station; the definition of the frame format is consequently done in such a way to include processes from Application layer (layer 4) to Physical layer (layer 1—see Fig. 5.12).

CPRI is designed having as a specific focus the interfacing between BBU and RRU, leaving to the vendors the freedom of implementation for the base station

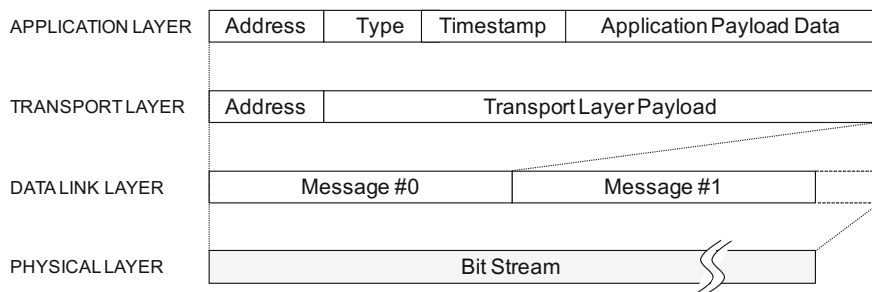


**Fig. 5.12** RP3-01 layered bus protocol (source [9])

building blocks. Consequently, the layers addressed by the specification are limited to Physical (layer 1) and Data-Link (layer 2), with no specific indication for upper layers, as seen in paragraph 2.1.

This leads to the following main considerations:

- The OBSAI RP3-01 frame format includes a percentage of overhead fields, formally higher than the overhead specified for the CPRI frame, with a resulting less bandwidth efficiency for what relates the transport of data traffic.
- The CPRI frame, being specified on the lower layers only, implies that the RRU and BBU blocks belong to the same vendor in order to ensure the proper interoperability at higher layers.

The following table (Table 5.4) summarizes, then, the main points of the comparison.

### 5.3 D-RoF Transport Over Optical Networks

In traditional RAN (Radio Access Network) architectures, baseband units are located in close proximity or even integrated with the RF assets, while packet networking technologies, like Ethernet or IP/MPLS, are used for interconnection with the packet core, as depicted in Fig. 5.13.

In the C-RAN architecture based on D-RoF, shown in Fig. 5.14, the centralized baseband processing (pool of RECs) is geographically separated from multiple antennas (REs) and the volume of IQ data transmitted between REC and RE, carried by interfaces like OBSAI or CPRI, is by far larger than the one transferred in the usual backhauling from conventional macro base stations. The network segment between the centralized baseband processing and geographically separated antennas is conventionally addressed as front-hauling. In this segment, due to the very stringent latency and clock synchronization requirements, traditional packet-based solutions are no longer practicable, while the use of circuit-based transport technologies can help service providers to accelerate the time-to-service, improve the

**Table 5.4** CPRI and OBSAI RP3-01 features comparison

Features		CPRI	OBSAI RP3-01
Link bandwidth allocation (for 3.072 Gb/s link)	Payload data	~ 94 %	80 %
	Overhead	~ 6 %	20 %
Carriers capacity		Air interface programmable IQ sample size, from 8 to 20 bits, any carrier type (4 bits size foreseen for specific cases)	Air interface fixed IQ sample size, 8 or 16 bits depending on the carrier type
Physical layer	Line rate	614 Mb/s, 1228 Mb/s, 2457 Mb/s, 3072 Mb/s, 4915 Mb/s, 6144 Mb/s, 9830 Mb/s, 10137 Mb/s	768 Mb/s, 1536 Mb/s, 3072 Mb/s, 6144 Mb/s
	Line coding	8B/10B	8B/10B (w/scrambling for 6144 Mb/s rate)
Data link layer	Frame length	10 ms	10 ms
	Frame module	Frame: 1 OH(control word) + 15 payload words Variable word length: from 8 bits (614 Mb/s) to 160 bits (10137 Mb/s)	Message: 3 OH + 16 payload bytes Fixed byte length: 8 bits
	Frame contents	IQ data (payload), Synchronization, L1 in-band protocol (OAM link), C&M (control and management) data, protocol extensions, vendor-specific information	RP3 data (payload), RP1 synch (synchronization), RP3-01 (OAM link), RP3 control/RP1 Ethernet (control and management)
Transport layer		Not specified	Address/type message fields filtering (for routing purpose)
Application layer		Not specified	Address/type/timestamp/payload message generation and transmission rules

overall performance, and simplify operations for a lower Total Cost of Ownership (TOC).

The most basic and simple C-RAN solution utilizes one fiber link per RE connected to the centralized REC. However, as more and more RECs and REs are deployed, many optical fibers have to be used; considering that the access network fiber resources are not infrequently scarce, such an approach is quickly running out of steam. As a consequence all those technologies that can improve the fiber's

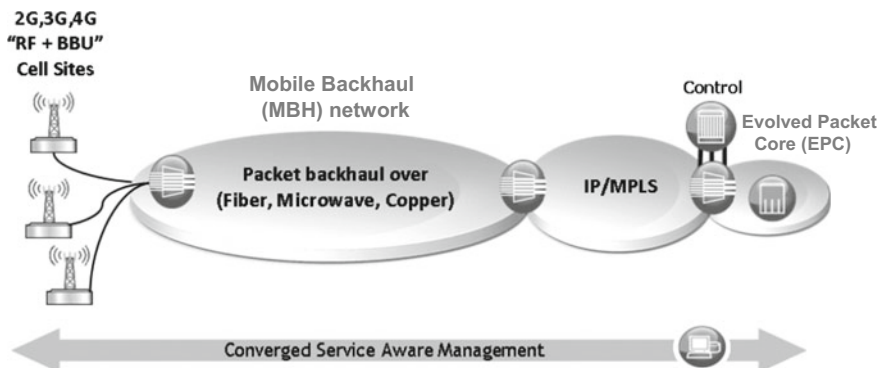


Fig. 5.13 Traditional RAN architecture (source [14])

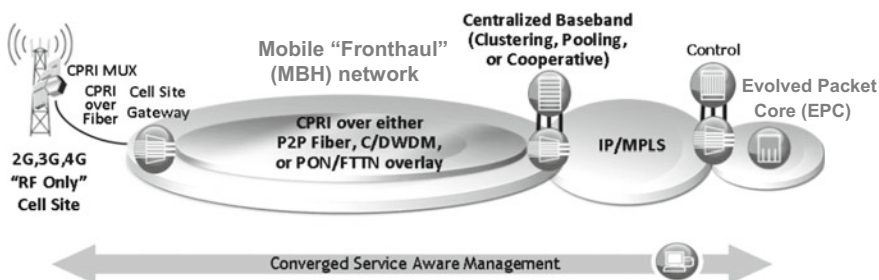


Fig. 5.14 Cloud/centralized RAN (C-RAN—source [14])

capacity usage in the front-haul segment of the network are becoming increasingly important for the deployment of C-RAN. The following ones are considered among the most promising:

- CPRI (or OBSAI) directly over wavelength, in a Wavelength Division Multiplexed (WDM) transmission environment; each CPRI channel will occupy one lambda over 16 (Coarse WDM) or over 40–80 (Dense WDM) in the fiber.
- CPRI (or possibly OBSAI) over OTN; the currently in-force ITU-T recommendation G.709 (02/2012) [3] already contains precise guidance for CPRI over OTN, while OBSAI over OTN has not been addressed so far. Several CPRI channels are Time Division Multiplexed (TDM) and mapped into a high-capacity ODU<sub>k</sub> container ( $n \times$  CPRI over one ODU/OTU uplink) to improve the transmission efficiency.
- CPRI over WDM-PON; non-standard type of optical passive networking where a dedicated wavelength is assigned to each ONT (Optical Line Terminal).

In general, CPRI multiplexing is deemed as essential for the mass deployment of C-RAN networks and in this context electrical multiplexing of CPRI signals, whenever applicable, is considered more advantageous than pure WDM techniques

in terms of number of required optical transceiver modules as well as optical spectrum occupancy.

Furthermore, the CPRI (or OBSAI) signal is not by itself well suited for transmission, because it does not provide adequate support for link monitoring, protection, and maintenance (functions such as BER detection, Trace Identifier Mismatch etc. are not supported, as well as any self-healing algorithms). CPRI over OTN complements such deficiencies and noticeably improves the transport features thanks to:

- strong OTN OAM and resiliency mechanisms (sub-50 ms protection), fully standardized;
- efficient network resource utilization, since OTN enables the multiplexing of multiple clients together;
- strong or interoperable low latency RS(255, 239) FEC, enabling 10G DWDM metro deployment and reach enhancement;
- timing transparent service transport, and
- flexibility for switched, ring, mesh, and point-to-point topologies.

### 5.3.1 CPRI Over OTN

In the next paragraphs we focus on CPRI over OTN and specifically on key technical and standardization aspects that can allow for the transport of the raw radio digital data over an optical network. Basic OTN concepts, which in the following are given for known, can be found in [3].

#### 5.3.1.1 Client Mapping Over OTN

The CPRI specification version 6.0 [2] defines 8 CPRI rates while the latest published ITU-T G.709 Recommendation [3] describes the way of transporting CPRI over OTN just for 6 of them, as shown in Table 5.5.

The 7th rate (9830.40 kbit/s) and the 8th rate (10137.60 kbit/s), though not yet considered by ITU-T, could be carried using either ODUflex in a similar manner as rates 4, 5, and 6 (with BMP mapping) or ODU2 and ODU2e, respectively, (with GMP mapping).

From the viewpoint of operators, the multiplexing of CPRI signals is a key feature to reduce the number of optical fibers needed in the mobile front-hauling. Table 5.6 synthesizes the applicable LO ODU into HO OPU mappings defined in ITU-T G.709 Appendix X as far as the CPRI client transport is concerned. The regular multiplexing architecture for CPRI over OTN in accordance with Table 5.6 is depicted in Fig. 5.15. Note that an OPU1 corresponds to a line rate of about 2.5 Gb/s, OPU2 to about 10 Gb/s, OPU3 to about 40 Gb/s, and OPU4 to about 100 Gb/s.

**Table 5.5** Currently specified CPRI over OTN mapping

CPRI signal	Nominal rate (kb/s)	Mapping procedure	LO ODU container
1	614.40	GMP	ODU0
2	1228.80	GMP	ODU0
3	2457.60	GMP	ODU1
4	3072.00	BMP	ODUflex
5	4915.20	BMP	ODUflex
6	6144.00	BMP	ODUflex

Abbreviations and acronyms

*AMP* Asynchronous Mapping Procedure

*GMP* Generic Mapping Procedure

*ODU<sub>k</sub>* Optical channel Data Unit-k

*ODUflex* flexible Optical channel Data Unit

**Table 5.6** Overview of LO ODU into HO OPU mapping types, as far as the CPRI signal is concerned

	2.5 G tributary slots		1.25 G tributary slots			
	OPU2	OPU3	OPU1	OPU2	OPU3	OPU4
ODU0 (CPRI Option 1 or 2)	–	–	ODTU01 AMP (PT = 20)	ODTU2.1 GMP (PT = 21)	ODTU3.1 GMP (PT = 21)	ODTU4.1 GMP (PT = 21)
ODU1 (CPRI Option 3)	ODTU12 AMP (PT = 20)	ODTU13 AMP (PT = 20)	–	ODTU12 AMP (PT = 21)	ODTU13 AMP (PT = 21)	ODTU4.2 GMP (PT = 21)
ODUflex (CPRI Option 4)	–	–	–	ODTU2.3 GMP (PT = 21)	ODTU3.3 GMP (PT = 21)	ODTU4.3 GMP (PT = 21)
ODUflex (CPRI Option 5)	–	–	–	ODTU2.4 GMP (PT = 21)	ODTU3.4 GMP (PT = 21)	ODTU4.4 GMP (PT = 21)
ODUflex (CPRI Option 6)	–	–	–	ODTU2.5 GMP (PT = 21)	ODTU3.5 GMP (PT = 21)	ODTU4.5 GMP (PT = 21)

Abbreviations and acronyms

*AMP* Asynchronous Mapping Procedure

*GMP* Generic Mapping Procedure

*ODTUG* Optical channel Data Tributary Unit Group

*ODTU<sub>jk</sub>* Optical channel Data Tributary Unit j into k

*ODTU<sub>k.ts</sub>* Optical channel Data Tributary Unit k with ts tributary slots

*ODU<sub>k</sub>* Optical channel Data Unit-k

*OPU<sub>k</sub>* Optical channel Payload Unit-k

*OTU<sub>k</sub>* completely standardized Optical channel Transport Unit-k

*PT* Payload Type

• PT = 20 indicates an ODU multiplex structure supporting ODTU<sub>jk</sub> only (AMP only)

• PT = 20 indicates an ODU multiplex structure supporting ODTU<sub>k.ts</sub> or ODTU<sub>k.ts</sub> and ODTU<sub>jk</sub> (GMP capable)

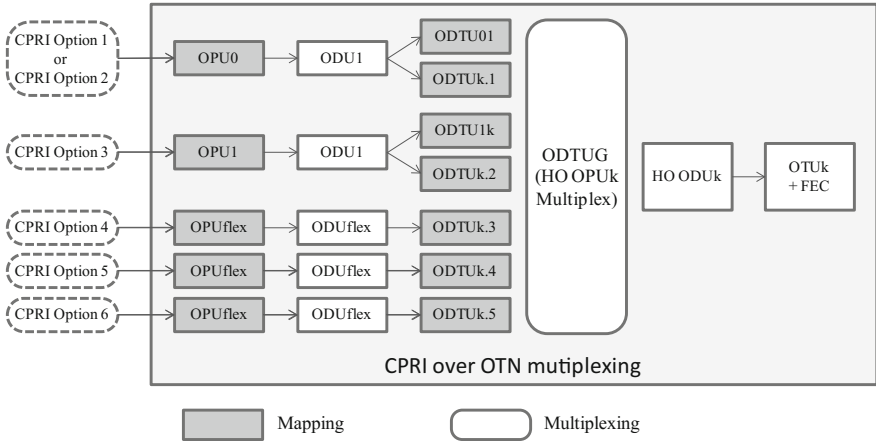


**Fig. 5.15** Regular multiplexing architecture for CPRI over OTN

**Table 5.7** Number of CPRI signals per ODU<sub>k</sub>/OTU<sub>k</sub> ( $k = 2, 3, 4$ ) either transparently mapped in ODUflex or without 8B/10B line code (figures into brackets)

CPRI signal	CPRI per ODU2/OTU2	CPRI per ODU3/OTU3	CPRI per ODU4/OTU4
4	2 (4)	10 (16)	26 (40)
5	2 (2)	8 (8)	20 (20)
6	1 (2)	6 (8)	16 (20)
7	1 (1)	4 (4)	10 (11)

It is worth noting that in order to improve the efficiency of the transport, it is possible to apply some form of rate reduction before the mapping and the multiplexing of the CPRI signals, the easiest of which is the simple removal of the line coding redundancy. Table 5.7 describes the improvement that can be obtained with such an approach just considering the CPRI options based on the 8B/10B line code and mapped in ODUflex.

More sophisticated compression techniques for a more drastic bandwidth reduction can be directly applied to I/Q samples exploiting the intrinsic redundancies in the signal structure of the LTE/LTE-A uplink and downlink data flows. As elsewhere noted, achievable compression ratios without any unacceptable degradation in system performance are positioned in the range from 1.5:1 to 3:1.

### 5.3.1.2 Client Jitter and Wander Accumulation Over OTN

Any digital mapping and multiplexing procedure based on digital justification is inevitably adding some noise on the recovered clock of the returned client signal. Specifically, the OTN generates and accumulates jitter and wander on its client

signals due to the buffers for mapping into ODUk and for ODUk multiplexing. The limits for such accumulation are related to the specific timing requirements of the client signal (typical references are for examples ITU-T G.825 for SDH clients or ITU-T G.8261 for Synchronous Ethernet). These ones and all the other timing aspects associated to OTN are summed up in ITU-T G.8251 [12].

The standpoint of whether OTN can meet the CPRI timing requirements has extensively been analyzed inside ITU-T. The main outcomes have been documented in ITU-T G.709 Annex VIII for the following transport cases:

- (a) CPRI Option 2 (GMP)  $\leftrightarrow$  LO-ODU0 (GMP)  $\leftrightarrow$  HO-ODU2/OTU2
- (b) CPRI Option 3 (GMP)  $\leftrightarrow$  LO-ODU1 (AMP)  $\leftrightarrow$  HO-ODU2/OTU2
- (c) CPRI Option 3 (GMP)  $\leftrightarrow$  LO-ODU1/OTU1
- (d) CPRI Option 4 (BMP)  $\leftrightarrow$  LO-ODUflex (GMP)  $\leftrightarrow$  HO-ODU2/OTU2

In this context it is interesting to highlight that cases (a) and (b) are characterized by 2 digital justification stages, one for the mapping of the CPRI to ODUk and another one for ODUk multiplexing, while cases (c) and (d) are characterized by one single justification stage (note that BMP in case d) is basically a simple 239/238 constant multiplication factor applied to the received CPRI bit rate).

The results summarized in Table 5.8 indicate that the short term CPRI RMS frequency offset requirement of 2 ppb is very difficult to be met and indeed is not. That is why the CPRI mappings are still kept in an Appendix of ITU-T G.709, which is not an integral part of the Recommendation (it will not be moved in the main body until all CPRI performance specifications can be formally respected).

Setting the bandwidth of the client de-synchronizer in the range 100–300 Hz (current OTN client de-synchronizers are 300 Hz or, in a few cases, 100 Hz or 200 Hz) the RMS frequency offset spans in the range 113–317 ppb for the examined cases (a) and (b) with 2 justification stages or in the range 29–130 ppb for the cases (c) and (d) with 1 justification stage.

**Table 5.8** CPRI timing performances for the four transport cases analyzed

CPRI transport case	Desync bandwidth (Hz)	Demapper with 1 UI phase info (see Note 1)	RMS frequency offset (ppb)	Peak-to-peak jitter (UI)
a.	100	Yes	113	6.9
	300	No	190	14.2
b.	100	Yes	156	6.7
	300	No	317	14.1
c.	100	Yes	29	0.8
	300	No	116	7.2
d.	100	Yes	32	0.76
	300	No	130	7.2

*Note 1* The insertion of CBR client data into the payload area of the OPUk frame (and the insertion of LO-ODUj data into the payload area of the ODTUk.ts multiframe) via GMP is performed in M-byte data entities ( $M = ts$ ). The remaining data entities can be signaled in the justification overhead as additional timing/phase information expressed in bits or byte

The situation could be significantly improved by narrowing the bandwidth of the desynchronizers well below 100 Hz; however, the full compliance to the 2 ppb limit would call for the inclusion of very high-quality oscillators never used so far in the OTN User-Network Interface (UNI) cards. Possibly, in order to ease the compatibility with the OTN transport, the CPRI REs should be designed for tolerating and cleaning up the possible residual noise on the CPRI signal present at the output of the OTN network, currently not budgeted by the CPRI specification, when not properly filtered out by the OTN desynchronizer.

Additional sources of noise may also exist that have to be taken into account. Specifically, the OTN network should be designed in order to meet the applicable CPRI stringent symmetry requirements and the absolute delay propagation limits. The mobile front-haul networks essentially will not be too large, and for this purpose, OTUk interfaces with no FEC or low latency FEC, such as Reed-Solomon RS (255, 239), are surely practical.

In conclusion, ITU-T G.709 by a note in Annex VIII clarifies that “OTN transport of CPRI is intended for use within an administrative domain. Users of this Recommendation [3] should not assume that the required performance for the CPRI client is met. It is the responsibility of the network operator to determine whether the required performance can be met. The noise generated by the OTN would have to be handled by the CPRI system in order to meet the application requirements. This is considered as a complex task according to the current OTN specification. The OTN network should also be designed in order to meet the applicable symmetry requirements.”

The persistent operators’ concerns about latency and synchronization requirements are reviving the debate around possible CPRI-specific OTN enrichments with the introduction of peculiar solutions avoiding mapping/de-mapping processes based on digital justification. The fact that CPRI signals originating from REs are typically synchronized in “loopback timing” mode to a common clock delivered from the REC, may indeed enable some form of byte synchronous multiplexing, cutting down the jitter and possibly increasing at the same time the efficiency of the mapping.

### ***5.3.2 Viable Network Applications for CPRI Over WDM/OTN***

The CPRI interface according to CPRI specification must support a continuous range of distances between the CPRI master and slave, i.e., cable lengths, from 0 km (lower limit) to an upper limit >10 km (the actual number is vendor-specific).

With that type of distance limitation, the most likely network applications (see Fig. 5.16) are essentially restricted to the metro access area including:

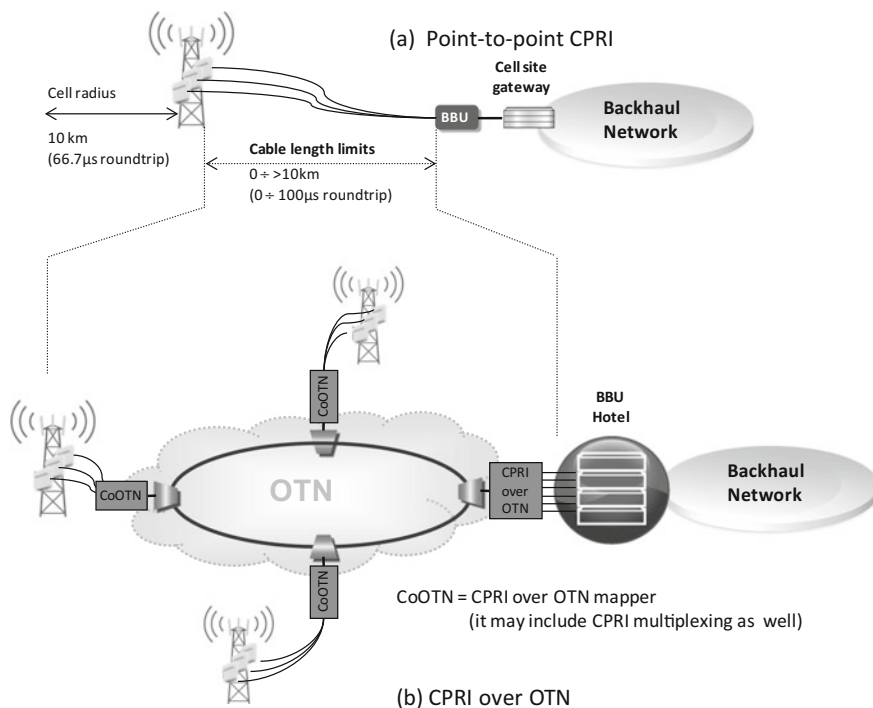


**Fig. 5.16** From point-to-point CPRI (a) to CPRI over OTN (b)

- point-to-point WDM or ROADM ring with optical pass through at intermediate nodes;
- electrical muxing/demuxing only at the ingress/egress nodes to the ring; because of the delay constraints, there would hardly be room for muxing/demuxing stages and LO-ODU electrical switching at the intermediate nodes of the ring.

The increase of the roundtrip delay between CPRI master and slave (length of the transmission link and/or U-plane IQ data interface processing time), although possible, must be carefully weighed since it comes at the expense of a reduced processing time in the eNodeB (as also addressed in previous Fig. 5.2 and Table 5.1).

## 5.4 ORI

In May 2010, a new ETSI Industry Specification Group (ISG) was created to develop an interface specification enabling inter-vendor interoperability between elements of base stations of cellular mobile network equipment. This ETSI ISG on Open Radio equipment Interface (ISG ORI) is specifying an open interoperable

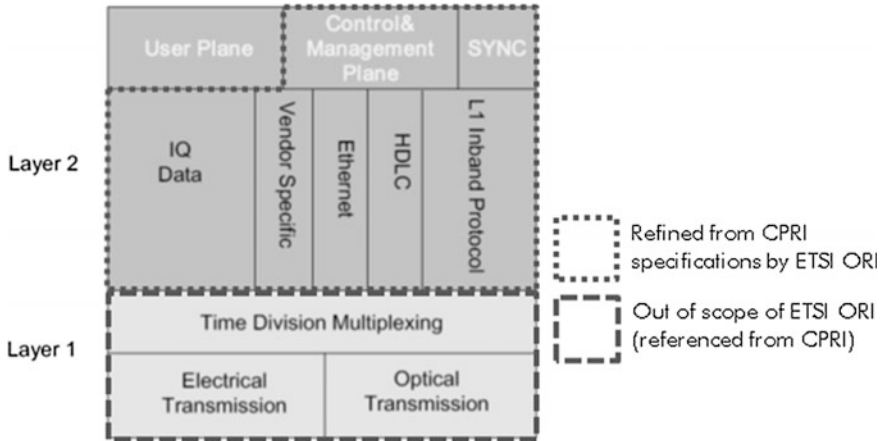


Fig. 5.17 ORI and CPRI relationships

interface for radio equipment in distributed mobile cellular base stations—GSM, UMTS, and LTE. Such a specification is intended to cover those layers of the OSI stack, which are required to enable interoperability, and may refer to appropriate publicly available specifications. In fact, the interface is built on top of the CPRI; however, options are removed and functions are added with the objective of making the interface fully interoperable. A synthesis of the CPRI reuse methodology is described in Fig. 5.17.

The ETSI ORI Industry Specification Group is a direct result of requirements work undertaken by the NGMN (Next-Generation Mobile Networks) Alliance, in their OBRI (Open BBU RRH Interface) project. As a consequence, the ISG is strongly supported by the NGMN Alliance, and leading mobile network operators and telecommunication equipment vendors are among the ISG's founding members. Nonetheless, the real in-field adoption of the ORI is at the moment of writing at a very early stage.

References on ORI work and relevant specifications can be found in the ETSI website [13].

## 5.5 Conclusions

This chapter has introduced the reader to the main standardization activities related to D-RoF, namely those relating to the definition of the digital interface between radio unit and base station (CPRI, OBSAI, ORI) and those aimed at allowing for the transport of such interfaces over a geographical network. The latest aspect is specifically important in view of a modern network paradigm, currently being analyzed by many operators in the world, usually addressed as front-hauling or

C-RAN. This paradigm is based on the removal of base band units from mobile sites and their centralization, or pooling in a central office. It is aimed at saving OPEX at the expense of CAPEX, since the transport network connecting mobile sites to the central office need to convey a by far larger bandwidth than with the traditional backhauling approach, and with very severe limitations in terms of jitter/wander and latency.

**Acknowledgment** The research leading to these results has received funding from the European Community's Seventh Framework Programme FP7/2013–2015 under grant agreement no. 317762 COMBO project.

## References

1. Common Public Radio Interface (CPRI) (2015) Specification—V7.0, 09 Nov 2015
2. Common Public Radio Interface (CPRI) (2013) Specification—V6.0, 30 Aug 2013
3. Recommendation ITU-T G.709/Y.1331 (2012) Interfaces for the optical transport network
4. ISO/IEC (200) Information technology—telecommunications and information exchange between systems—high-level data link control (HDLC) procedures. International Standard ISO/IEC 13239, 3rd edn, Reference number: ISO/IEC 13239:2002(E), 15 July 2002
5. IEEE Std 802.3-2005 (2005) Part 3: carrier sense multiple access with collision detection (CSMA/CD) access method and physical layer specifications, 12 Dec 2005
6. OBSAI (2006) BTS system reference document—version 2.0
7. OBSAI (2008) Reference point 1 specification—version 2.1
8. OBSAI (2008) Reference point 2 specification—version 2.1
9. OBSAI (2010) Reference point 3 specification—version 4.2
10. OBSAI (2009) RP3/ RP3-01 interface profile document—version 1.0
11. OBSAI (2004) Reference point 4 specification—version 1.1
12. Recommendation ITU-T G.8251 (2010) The control of jitter and wander within the optical transport network (OTN)
13. [www.etsi.org](http://www.etsi.org)
14. Colombo C, Sfameni G (2012) Optical access network architecture based on WDM-PON technique for backhauling traffic of mobile cell-sites. *Fotonica*

# Chapter 6

## Wireless Delivery of over 100 Gb/s mm-Wave Signal in the W-band

Jianjun Yu

**Abstract** We summarize several different approaches for the realization of large capacity (>100 Gb/s) fiber wireless integration system, including optical polarization-division multiplexing (PDM) combined with multiple-input multiple-output (MIMO) reception, advanced multi-level modulation, optical multi-carrier modulation, electrical multi-carrier modulation, antenna polarization multiplexing, and multi-band multiplexing. These approaches can effectively reduce the signal baud rate as well as the required bandwidth for optical and electrical devices. We also investigate problems, such as wireless multi-path effects due to different wireless transmission distances, existing in large-capacity fiber wireless integration systems. We demonstrate that these problems can be effectively solved based on advanced digital signal processing (DSP) algorithms including classic constant modulus algorithm (CMA). Moreover, based on the combination of these approaches as well as advanced DSP algorithms, we have successfully demonstrated a 400G fiber wireless integration system, which establishes a new record for delivered wireless capacity and ushers in a new era of ultra-high bit rate (>400 Gb/s) optical wireless integration and communications at mm-wave frequencies.

### 6.1 Introduction

As the next major phase of mobile telecommunications standards beyond the current 4G/IMT-Advanced standards, 5G requires data rates of 100 Mb/s for ten thousands of users in a km<sup>2</sup> coverage area and promotes a substantial increase in throughput over existing 2G, 3G, and 4G cellular systems. A converged fiber-wireless network, as one kind of very distinct 5G network visions having emerged by 2014, demands the support of peak data access speeds of up to 10 Gb/s [1]. At the same time, wireless devices with the bit rate of 1 Gb/s and beyond have been commercially available since 2013 using a variety of techniques. Adopting high-frequency

---

J. Yu (✉)  
Basking Ridge, USA  
e-mail: jianjun@fudan.edu.cn; yu.jianjun@ztetx.com

millimeter-wave (mm-wave) frequency bands as well as high-speed wireless devices, some wireless systems can realize 10-Gb/s and even 40-Gb/s signal delivery over short wireless distances. Such high-rate wireless delivery can truly be described as comparable to or perhaps faster than fiber. Meanwhile, smart mobile and fixed terminals have recently been equipped with very-high-definition (HD) cameras, such as 8k video, compared with the current 1k version. For example, advanced companies, such as Nokia and Samsung, have introduced 8k and 4k super HD (SHD) video cameras in their smartphones that require transmission speeds, for uncompressed SHD video images, of 60 and 30 Gb/s, respectively [2]. Evidently, it is not desirable to require such thin and light-weight mobile terminals to install heavy, high-definition multimedia interfaces (HDMIs) or fiber cables.

On the other hand, due to the wider bandwidths available at higher frequencies, wireless delivery at mm-wave frequencies is expected to provide multi-gigabit mobile data transmission and has been intensively studied in the research community [3–52]. Furthermore, 100-Gb/s and beyond wireless mm-wave signals can be achieved based on photonic mm-wave techniques, in which the ultra-high-speed optical baseband signal is first generated by externally modulating a continuous-wavelength (CW) lightwave. Consequently, beating or heterodyning the modulated wavelength with another CW lightwave at a different wavelength is utilized to generate the ultra-high-speed wireless mm-wave signal. The photonic mm-wave technique thus further promotes the seamless integration of wireless and fiber-optics networks.

However, photonic mm-wave generation based on the fiber wireless integration system, as shown in Fig. 6.1a, is different from that based on a traditional radio-over-fiber (RoF) system as shown in Fig. 6.1b [53]. For the latter, the optical mm-wave or microwave wave (at lower frequencies) is generated at the optical line terminator (OLT) or central office, and thus, the optical carrier and the optical baseband signal are simultaneously transmitted over the fiber [54], while in the former case, the optical baseband signal is up-converted at the remote station and only the optical baseband signal is transmitted over the fiber. Compared to the traditional RoF system, the fiber wireless integration system will suffer less from linear fiber transmission impairments [such as chromatic dispersion (CD) and polarization mode dispersion (PMD)] and nonlinear fiber transmission impairments at the expense of a more complex optical up-converter. Thus, the fiber wireless integration system can realize longer-haul fiber transmission.

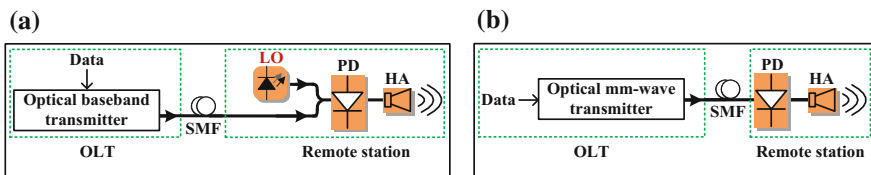


**Fig. 6.1** Photonic mm-wave generation based on **a** fiber wireless integration system and **b** traditional RoF system. *OLT* optical line terminator

Based on photonic mm-wave techniques, the required bandwidth for optical and electrical devices in the large capacity (>100 Gb/s) fiber wireless integration system can be reduced by reducing the signal baud rate, for which, as shown in Fig. 6.2, several different approaches can be adopted. The first approach is optical polarization-division multiplexing (PDM) together with multiple-input multiple-output (MIMO) reception, which can effectively double the transmission bit rate [30–37]. The second approach is advanced multi-level modulation, such as 16-ary quadrature amplitude modulation (16QAM) and 64QAM, but higher receiver sensitivity is required [37]. The third approach is optical multi-carrier modulation, such as optical orthogonal frequency-division multiplexing (OFDM) and Nyquist wavelength-division multiplexing (WDM), which also gives the possibility for optical sub-carrier optimization [38–41]. The fourth approach is electrical multi-carrier modulation, such as electrical OFDM, which is robust against

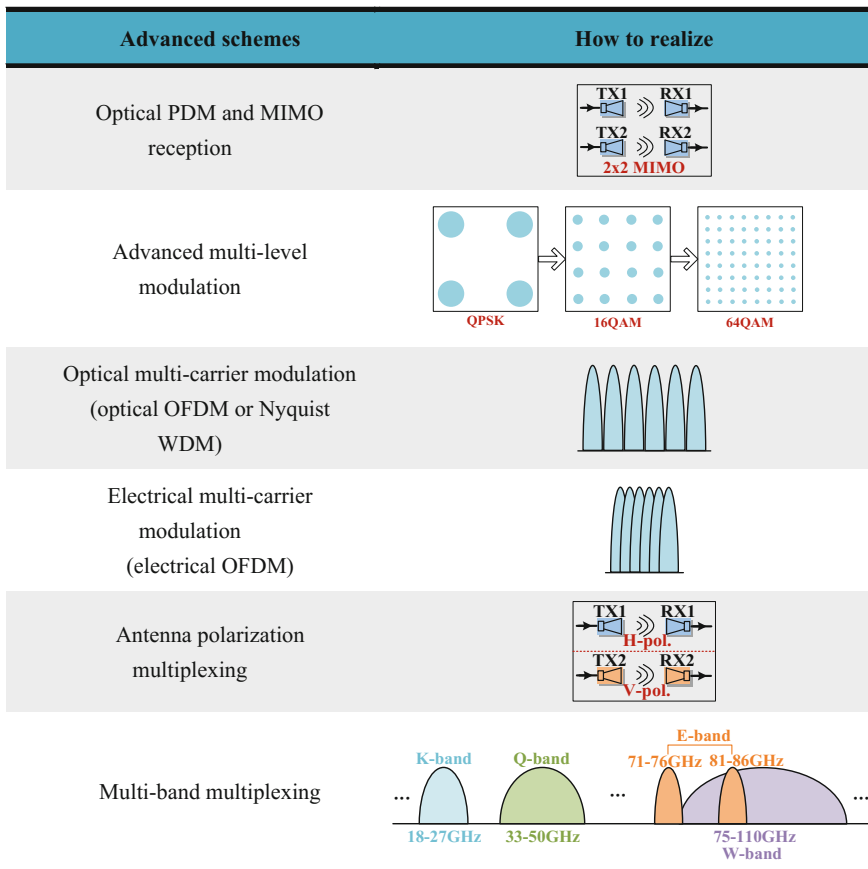


**Fig. 6.2** Different approaches for the realization of large-capacity (>100 Gb/s) fiber wireless integration system

fiber CD and PMD [42–48]. The fifth approach is antenna polarization multiplexing, but more optical and electrical devices are required [49]. Finally, multi-band multiplexing [39–41] can be used to simultaneously deliver ultra-high-speed wireless signals at 40-, 60-, 80-, and 100-GHz mm-wave frequencies. It is worth noting that multi-band multiplexing, to some degree, is similar to optical and electrical multi-carrier modulation, but the multiple mm-wave frequencies simultaneously adopted in optical and electrical multi-carrier modulation are generally located at the same mm-wave band, while those in multi-band multiplexing can be located at several different mm-wave bands (similar to WDM). A series of problems, such as wireless multi-path effects due to different wireless transmission distances, nonlinearity, component filtering, and so on, exist in large capacity fiber wireless integration systems. We have demonstrated that these problems can be effectively solved based on advanced digital signal processing (DSP) algorithms including classic constant modulus algorithm (CMA) [35–37].

In this paper, we summarize several different approaches for the realization of large capacity (>100 Gb/s) fiber wireless integration systems, including optical PDM combined with MIMO reception, advanced multi-level modulation, optical multi-carrier modulation, electrical multi-carrier modulation, antenna polarization multiplexing, and multi-band multiplexing. These approaches can effectively reduce the signal baud rate as well as the required bandwidth for optical and electrical devices. We also investigate problems, such as multi-path effects due to different wireless transmission distances that exist in large-capacity fiber wireless integration systems. We demonstrate that these problems can be effectively solved based on advanced DSP algorithms including classic CMA. Moreover, based on a combination of these approaches as well as advanced DSP algorithms, we have successfully demonstrated a 400G fiber wireless integration system, which benchmarks a capacity record for wireless delivery and ushers in a new era of ultra-high bit rate (>400 Gb/s) optical wireless integration and communications at mm-wave frequencies.

## **6.2 Approaches for the Realization of Large Capacity (>100 Gb/s) Fiber Wireless Integration System**

As mentioned in the introduction, several approaches, such as optical PDM combined with MIMO reception, advanced multi-level modulation, optical multi-carrier modulation, electrical multi-carrier modulation, antenna polarization multiplexing, and multi-band multiplexing, can be adopted to reduce the signal baud rate and the required bandwidth for optical and electrical devices and thus achieve large capacity (>100 Gb/s) fiber wireless integration systems. The following part of this section is the detailed introduction of these approaches as well as the corresponding experimental demonstrations.

### 6.2.1 Optical PDM Combined with MIMO Reception

Figure 6.3 shows a schematic diagram for a fiber wireless integration system adopting optical PDM combined with MIMO reception, including an optical baseband transmitter to generate optically modulated PDM baseband signals, an optical heterodyne up-converter to up-convert the optical PDM baseband signal into the mm-wave frequency band, and a wireless mm-wave receiver to down-convert the received wireless mm-wave signal into the baseband.

At the optical baseband transmitter, the CW lightwave from a laser is modulated by an optical external modulator and then polarization-multiplexed by a polarization multiplexer to generate the optical PDM baseband signal. The optical external modulator is driven by the transmitter electrical data. After fiber-optic transmission, the optical PDM signal is received by the optical heterodyne up-converter. The optical heterodyne up-converter consists of a laser which provides the optical local oscillator (LO), an optical  $180^\circ$  hybrid, two fast-response photo detectors (PDs), and two transmitter horn antennas (HAs). Here, the LO is used as the reference carrier-frequency generating source. The frequency spacing between the LO and the light carrying the optical baseband data is located in the mm-wave frequency band, and heterodyning generates the mm-wave central carrier frequency of the up-converted wireless signal. The optical  $180^\circ$  hybrid includes two polarization beam splitters (PBSs) and two optical couplers (OCs) and is used to implement polarization diversity of the received optical signal and the LO in the optical domain before heterodyne beating. Next, two fast-response PDs, function as two photo-mixers and directly up-convert each X- and Y-polarization component of the optical PDM signal into two coherent mm-wave signals at the same frequency. It is worth noting that the polarization of the light in front of the PBS, which the received optical signal is sent into, is arbitrary due to fiber transmission. Thus, the X- or Y-polarization component at the output port of the PBS contains an uncertain mix of the data which is simultaneously encoded on the X- and Y-polarization at

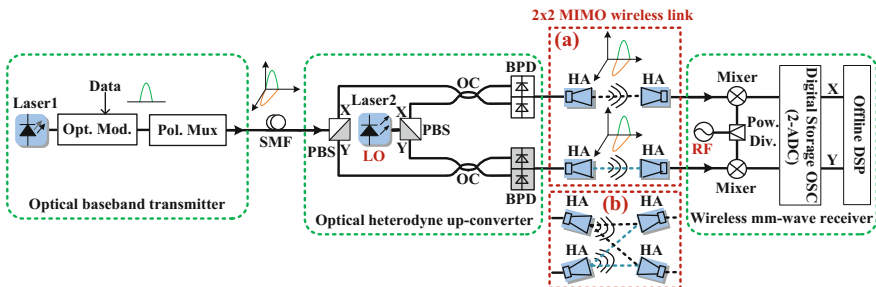


**Fig. 6.3** Schematic diagram for a fiber wireless integration system adopting optical PDM combined with MIMO reception. **a**  $2 \times 2$  MIMO wireless link without interference. **b**  $2 \times 2$  MIMO wireless link with large interference. *Opt. Mod.* optical modulator, *Pol. Mux* polarization multiplexer, *Pow. Div.* power divider

the transmitter and thus also has an arbitrary polarization state. In this paper, we define one output port of each PBS as the X-polarization component and the other as the Y-polarization for convenience. Then, the X- and Y-polarization components are up-converted at the same time and independently sent into free space by two transmitter HAs. The transmission is subsequently received by two corresponding receiver HAs, which makes up a  $2 \times 2$  MIMO wireless link based on microwave polarization multiplexing. At the wireless mm-wave receiver, there is a two-stage down converter. In the first-stage analog conversion, the X- and Y-polarization components are, respectively, down-converted to a lower intermediate frequency (IF) in the analog domain by a balanced mixer and a sinusoidal radio-frequency (RF) LO signal. The IF signal is subsequently sent into a digital storage oscilloscope (OSC) to implement analog-to-digital conversion. Finally, IF down conversion and data recovery is realized with DSP in the digital domain.

In the  $2 \times 2$  MIMO wireless link shown in Fig. 6.3a, there is negligible wireless MIMO interference because of spatial separation and good directionality of transmitter and receiver HAs. However, when wireless interference does exist, as in the  $2 \times 2$  MIMO wireless link shown in Fig. 6.3b, each receiver HA can receive wireless power from two transmitter HAs, and thus, there exists large wireless MIMO interference. The unwanted interference can be suppressed by frequency-domain equalization proposed by [55]. However, in view of the built-in optical polarization de-multiplexing, a uniform method for the fiber wireless integration system is preferred. The polarization PDM signal carried on the fiber link and the  $2 \times 2$  MIMO signal carried on the wireless link can both be treated in the same  $2 \times 2$  MIMO model formalism. Thus, the equalization of the wired and wireless integrated  $2 \times 2$  MIMO channels can be uniformly realized by classic CMA based on DSP. The overall transfer function for the fiber-wireless  $2 \times 2$  MIMO transmission can be expressed as

$$\begin{pmatrix} r_x \\ r_y \end{pmatrix} = \begin{pmatrix} H_{xx} & H_{yx} \\ H_{xy} & H_{yy} \end{pmatrix} \cdot \begin{pmatrix} s_x \\ s_y \end{pmatrix} + \begin{pmatrix} n_x \\ n_y \end{pmatrix}. \quad (6.1)$$

where  $(r_x \ r_y)^T$  denotes the received PDM signal after both fiber and wireless transmission, while  $(s_x \ s_y)^T$  and  $(n_x \ n_y)^T$  denote the transmitted PDM signal and the noise, respectively. In Eq. 6.1, the Jones matrix includes the lumped channel response describing both the fiber link and the  $2 \times 2$  MIMO wireless link, that is,

$$\begin{pmatrix} H_{xx} & H_{yx} \\ H_{xy} & H_{yy} \end{pmatrix} = H_{fiber} \cdot H_{wireless} = \begin{pmatrix} m_{xx} & m_{yx} \\ m_{xy} & m_{yy} \end{pmatrix} \cdot \begin{pmatrix} h_{xx} & h_{yx} \\ h_{xy} & h_{yy} \end{pmatrix}. \quad (6.2)$$

where  $(m_{xx}, m_{yy}, m_{yx},$  and  $m_{xy})$  and  $(h_{xx}, h_{yy}, h_{yx},$  and  $h_{xy})$  are the Jones transfer matrix elements for fiber and wireless links, respectively. Thus, in order to recover the transmitted PDM signal  $(s_x \ s_y)^T$ , the task is to estimate the total Jones matrix and to obtain its inverse. As in digital coherent communication, four

butterfly-configured adaptive digital equalizers based on CMA can be used to de-multiplex the received PDM signal.

Correspondingly, we have experimentally demonstrated a fiber wireless integration system adopting optical PDM combined with MIMO reception, which can deliver 108-Gb/s PDM quadrature-phase-shift-keying (PDM-QPSK) signal through 80-km single-mode fiber-28 (SMF-28) and a 1-m  $2 \times 2$  MIMO wireless link at 100 GHz [35]. The X- and Y-polarization components of the PDM-QPSK optical baseband signal are simultaneously up-converted to 100-GHz wireless carrier by optical polarization-diversity heterodyne beating and then delivered over a  $2 \times 2$  MIMO wireless link. At the wireless receiver, a two-stage down conversion first takes place in the analog domain by balanced mixer down conversion using a sinusoidal RF LO signal, followed by digital domain DSP baseband recovery. The classic CMA equalization based on DSP is used to realize polarization de-multiplexing. The bit error ratio (BER) for the 108-Gb/s PDM-QPSK signal is under the pre-forward-error-correction (pre-FEC) threshold of  $3.8 \times 10^{-3}$  [56] after both the 80-km SMF-28 transmission and the 1-m MIMO wireless delivery at 100 GHz.

Figure 6.4 shows the experimental setup for the seamless integration of 108-Gb/s PDM-QPSK 80-km SMF-28 transmission and 1-m MIMO wireless delivery at 100 GHz. At the optical baseband transmitter, there is an external cavity laser (ECL) at 1558.51 nm with linewidth less than 100 kHz and output power of 14.5 dBm. The CW lightwave from the ECL is modulated by an in-phase/quadrature (I/Q) modulator. The I/Q modulator is driven by a 27-Gbaud electrical binary signal, which, with a pseudo-random binary sequence (PRBS) length of  $2^{15} - 1$ , is generated from a pulse pattern generator (PPG). For optical QPSK modulation, the two parallel Mach-Zehnder modulators (MZMs) in the I/Q modulator are both biased at the null point and driven at the full swing to achieve zero-chirp 0- and  $\pi$ -phase modulation. The phase difference between the upper and lower branches of the I/Q modulator is controlled at  $\pi/2$ . The polarization multiplexing is realized by a polarization multiplexer, comprising a polarization-maintaining OC to split the signal into two branches, an optical delay line (DL) to provide a 150-symbol delay, an optical attenuator to balance the power of two branches, and a polarization beam combiner (PBC) to recombine the signal. The generated signal is launched into 80-km SMF-28, which has 18-dB average loss and 17-ps/km/nm CD at 1550 nm without optical dispersion compensation. An erbium-doped fiber amplifier (EDFA) is used to compensate for the fiber loss. The launch power (after the EDFA) is 0 dBm.

At the optical heterodyne up-converter, an ECL with linewidth less than 100 kHz is used as LO at 1557.71 nm, which has 100-GHz frequency offset (FO) relative to the received optical signal. Two PBSs and two OCs are used to implement polarization diversity of the received optical signal and LO in the optical domain before heterodyne beating. Two single-ended PDs, each with 75-GHz 3-dB bandwidth and 7.5-dBm input power, directly up-convert the X- and Y-polarization components of the optical PDM-QPSK signal into W-band wireless signals, respectively. The X- and Y-polarization up-converted components carried by 100-GHz wireless carrier independently pass through two 100-GHz narrowband

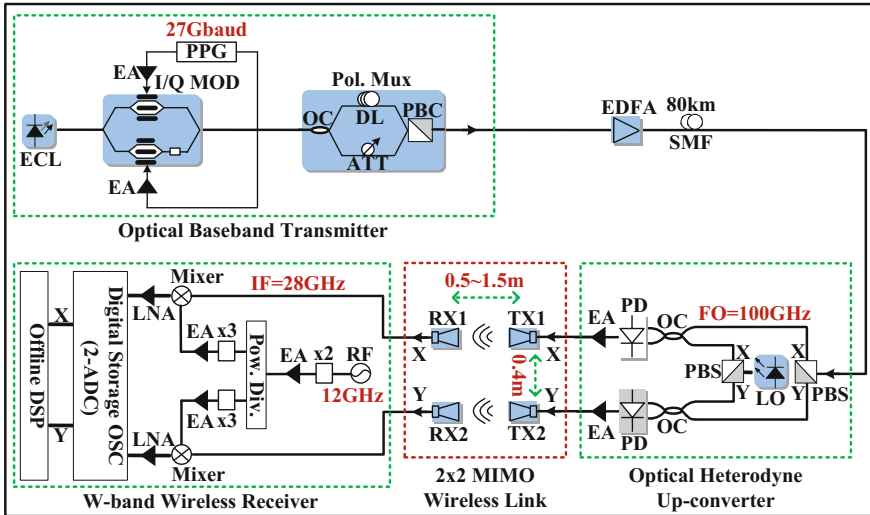


**Fig. 6.4** Experimental setup for the seamless integration of 108-Gb/s PDM-QPSK 80-km SMF-28 transmission and 1-m MIMO wireless delivery at 100 GHz

electrical amplifiers (EAs) with 32-dB gain and, then, are simultaneously sent into a  $2 \times 2$  MIMO wireless air link. The pairs of transmitter and receiver HAs are separated by a link distance of 0.5–1.5 m and each is laterally separated from its counterpart by 40 cm. Each HA has a 25-dBi gain. Almost no wireless MIMO interference exists because of the good directionality of transmitter and receiver HAs.

Two-stage down conversion is first implemented at the W-band wireless receiver. A 12-GHz sinusoidal RF LO signal source is frequency-doubled ( $\times 2$ ), amplified (EA), and split into two branches by a power divider, and each is further amplified. Next, each branch is frequency-tripled and amplified to generate a sinusoidal mm-wave LO at 72 GHz for the down-conversion double-balanced mixer. Therefore, the X- and Y-polarization components with 28-GHz IF are obtained after first-stage down conversion. Each band-pass low-noise amplifier (LNA) after the mixer is centered on 100 GHz and has a 5-dB noise figure. The analog-to-digital conversion is realized in the digital storage OSC with 120-GSa/s sampling rate and 45-GHz electrical bandwidth.

Figure 6.5 shows a functional block diagram for DSP processing after analog-to-digital conversion. Firstly, the clock is extracted using the “square and filter” method, and then, the digital signal is re-sampled at twice the baud rate based on the recovered clock. Secondly, the received signals are down-converted to the baseband by multiplying synchronous cosine and sine functions, which are generated from a digital LO for down conversion [57]. Thirdly, a T/2-spaced time-domain finite impulse response (FIR) filter is used for CD compensation, where the filter coefficients are calculated from the known fiber CD transfer

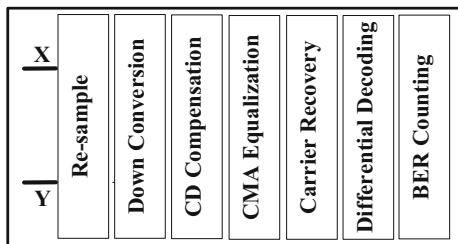


Fig. 6.5 Functional block diagram for DSP processing after analog-to-digital conversion

function using the frequency-domain truncation method. Fourthly, two complex-valued, 13-tap, T/2-spaced adaptive FIR filters, based on the classic CMA, are used to retrieve the modulus of the PDM-QPSK signal and realize polarization de-multiplexing. The subsequent step is carrier recovery, which includes FO estimation and carrier phase estimation. The former is based on a fast Fourier transform (FFT) method, while the latter is based on a fourth-power Viterbi–Viterbi algorithm. Finally, differential decoding is used to eliminate the  $\pi/2$  phase ambiguity before BER counting.

Figure 6.6a shows the X-polarization optical spectrum after polarization-diversity splitting at the optical heterodyne up-converter. The frequency spacing and power difference between the LO and the received optical signal are 100 GHz and 20 dB, respectively. Figure 6.6b shows the electrical spectrum with 28-GHz IF after the first-stage analog down conversion at the W-band wireless receiver. Figure 6.7 shows the X-polarization received constellations at the BER of  $1.2 \times 10^{-3}$ .

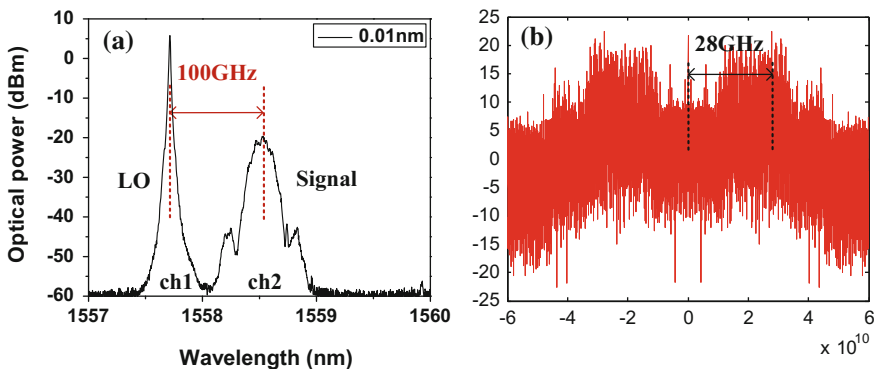
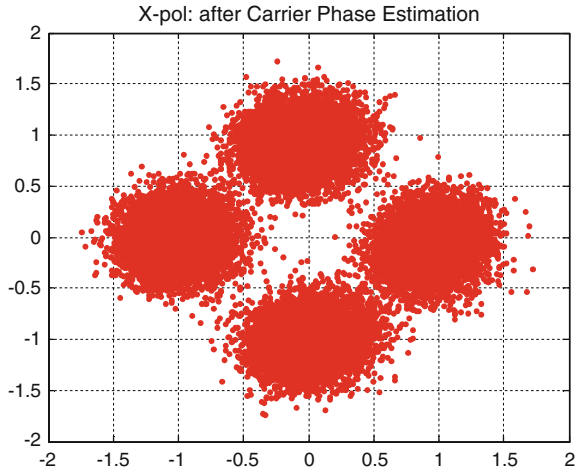


Fig. 6.6 a X-polarization optical spectrum (0.01-nm resolution) after polarization-diversity splitting. b Electrical spectrum after first-stage analog down conversion

**Fig. 6.7** Received QPSK constellation



## 6.2.2 Advanced Multi-level Modulation

High-order I/Q modulation schemes are traditionally used to increase spectral efficiency, for example, 16QAM can carry four bits per symbol. We have experimentally demonstrated a fiber wireless integration system adopting optical PDM combined with MIMO reception, which can deliver 14-Gbaud (112-Gb/s) PDM-16QAM signal through 400-km SMF-28 and a 0.5-m  $2 \times 2$  MIMO wireless link at 35 GHz [37]. In the demonstration experiment, the 14-Gbaud PDM-16QAM optical baseband signal is first transmitted over a 400-km SMF-28 optical link to a radio head, whereupon it is up-converted to 35-GHz mm-wave frequency and delivered over a 0.5-m  $2 \times 2$  MIMO wireless link. At the wireless receiver, DSP processing is used for mm-wave down conversion, CD compensation, polarization de-multiplexing, and carrier recovery, after analog-to-digital conversion. The BER is less than the pre-FEC threshold of  $3.8 \times 10^{-3}$  after both 0.5-m MIMO wireless delivery at 35 GHz and 400-km SMF-28 transmission.

Figure 6.8 shows the experimental setup for the seamless integration of 112-Gb/s PDM-16QAM 400-km SMF-28 transmission and 0.5-m MIMO wireless delivery at 35 GHz. At the optical baseband transmitter, the CW lightwave at 1549.8 nm is generated from an ECL and then modulated by an I/Q modulator. The 14-Gbaud electrical four-level signal with a PRBS length of  $2^{15} - 1$  is generated from an arbitrary waveform generator (AWG) to drive the I/Q modulator. It is worth noting that before I/Q modulation, the two middle levels of the 14-Gbaud electrical four-level signal are pre-compensated by multiplying the two middle levels by 0.89 to overcome the nonlinear characteristics of the two parallel MZMs in the I/Q modulator. Subsequent polarization multiplexing is realized by a polarization multiplexer identical to that adopted in Fig. 6.4. The generated PDM-16QAM optical

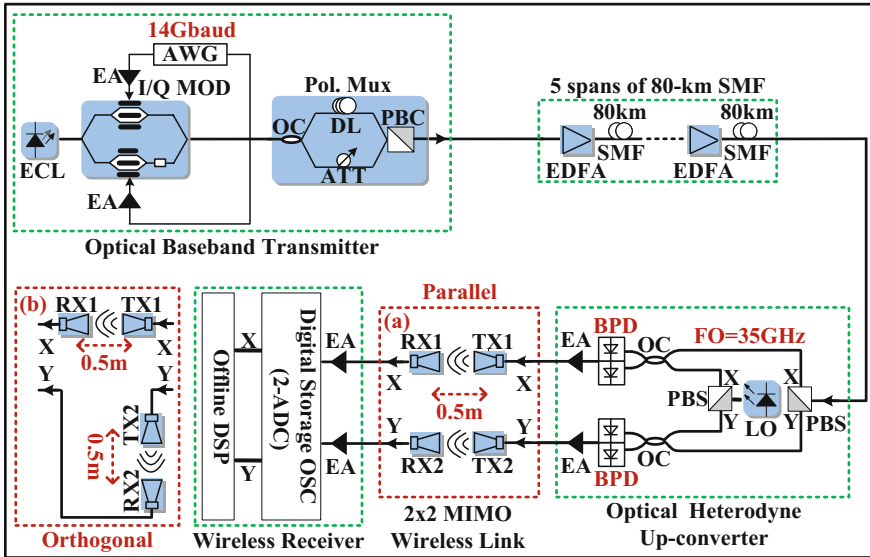


**Fig. 6.8** Experimental setup for the seamless integration of 112-Gb/s PDM-16QAM 400-km SMF-28 transmission and 0.5-m MIMO wireless delivery at 35 GHz

baseband signal is launched into a straight line optical link consisting of 5 spans, each of 80-km SMF-28. An EDFA is used to compensate for the loss of each span. The total launch power (after the EDFA) into each span is 1 dBm.

The optical heterodyne up-converter is similar to that adopted in Fig. 6.4, except that in this case, the FO between the LO and the received optical signal is 35 GHz, and two balanced PDs (BPDs), instead of two single-ended PDs, are used for photonic up-conversion. The generated two 35-GHz mm-wave signals are independently power-amplified by two EAs with 10-GHz 3-dB bandwidth and then broadcasted by two transmitter HAs with 25-dBi gain. Insets (a) and (b) in Fig. 6.8 show the parallel and orthogonal HA arrays, respectively. Each wireless link is 0.5 m whether parallel or orthogonal. The crosstalk is acceptable because of good HA directionality. It is noted that greater crosstalk is expected to be acceptable when blind equalization based on CMA is used to realize polarization de-multiplexing in the DSP baseband recovery process.

Analog-to-digital conversion is realized in the digital storage OSC with 120-GSa/s sampling rate and 45-GHz electrical bandwidth. Figure 6.9 shows the details of DSP processing after analog-to-digital conversion. The first three steps, i.e., time recovery, IF down conversion, and CD compensation, are identical to that discussed in conjunction with Fig. 6.4. This is followed by two complex-valued, 13-tap, T/2-spaced adaptive FIR filters that are used to retrieve the modulus of the 16QAM signal. The two adaptive FIR filters are based on the classic CMA followed by three-stage CMA, to realize multi-modulus recovery and polarization de-multiplexing [58, 59]. The carrier recovery, including residual FO estimation

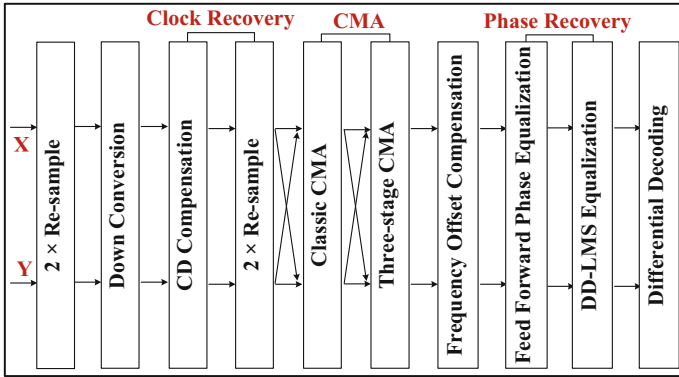


Fig. 6.9 Functional block diagram for DSP processing after analog-to-digital conversion

and carrier phase estimation, is performed in the subsequent step. A fourth-power Viterbi-Viterbi algorithm is used to estimate the FO between the LO and the received optical signal. The phase recovery is obtained by feed-forward and least-mean-square (LMS) algorithms. Finally, differential decoding is used to eliminate the  $\pi/2$  phase ambiguity before BER counting.

Figure 6.10a shows the X-polarization optical spectrum after polarization-diversity splitting at the optical heterodyne up-converter, where the optical signal-to-noise ratio (OSNR) difference of the LO and the received optical signal is larger than 20 dB. Figure 6.10b shows the electrical spectrum after analog-to-digital conversion at the wireless receiver. It can be seen that the central frequency is 35 GHz. An obvious frequency dip appears at 45 GHz, which is the limit of the analog-to-digital converter (ADC) bandwidth. Figure 6.11a, b shows the recovered constellations in the case of back-to-back (BTB) (OSNR = 28 dB) transmission and after 400-km SMF-28 transmission (OSNR = 28 dB), respectively. BTB denotes no fiber transmission. Because of the adoption of conventional

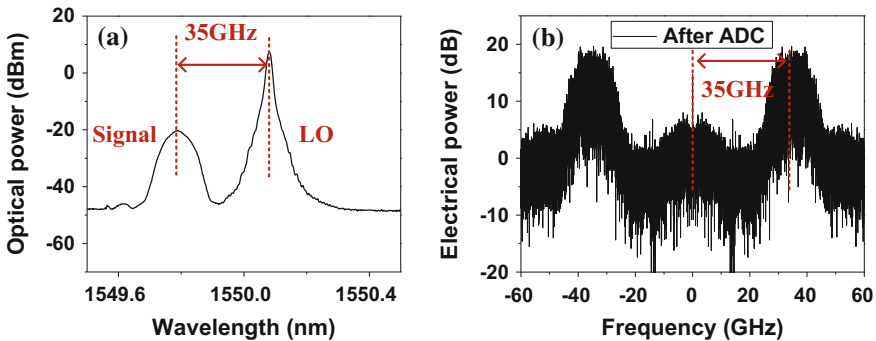
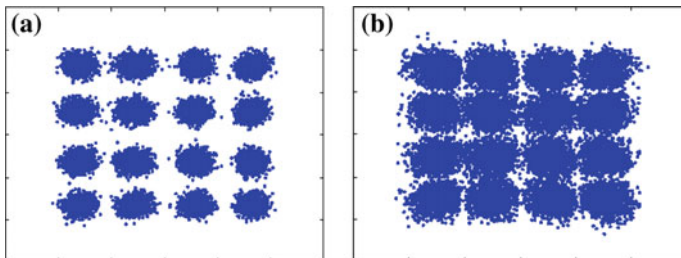


Fig. 6.10 a X-polarization optical spectrum after polarization-diversity splitting. b Electrical spectrum after analog-to-digital conversion



**Fig. 6.11** Recovered 16QAM constellations in the case of **a** BTB (OSNR = 28 dB) and **b** 400-km SMF-28 transmission (OSNR = 28 dB)

digital coherent demodulation algorithms (particularly CMA), the multiplexing effect caused by both fiber and  $2 \times 2$  MIMO wireless links can be mostly compensated for, leaving fiber nonlinearity as the remaining key factor that influences the transmission performance. Nevertheless, although the 112-Gb/s PDM-16QAM signal is quite sensitive to fiber nonlinearity, compared to the BTB case, only 3.5-dB OSNR penalty is observed after 400-km SMF-28 transmission [37]. Considering the observed very small penalty after 400-km SMF-28 transmission, the feasibility of this  $2 \times 2$  MIMO wireless transmission system is clearly demonstrated.

### 6.2.3 Optical Multi-carrier Modulation

Compared to optical single-carrier modulation, optical multi-carrier modulation can also effectively reduce the transmission baud rate. Figure 6.12 shows the schematic diagram of the proposed multi-carrier optical heterodyne up-converter and wireless mm-wave receiver with joint-channel DSP. The technique can be demonstrated by a simple dense WDM (DWDM) experiment exemplified by three optical carrier channels (ch1, ch2, and ch3). The frequency spacing between LO and ch2 is used to

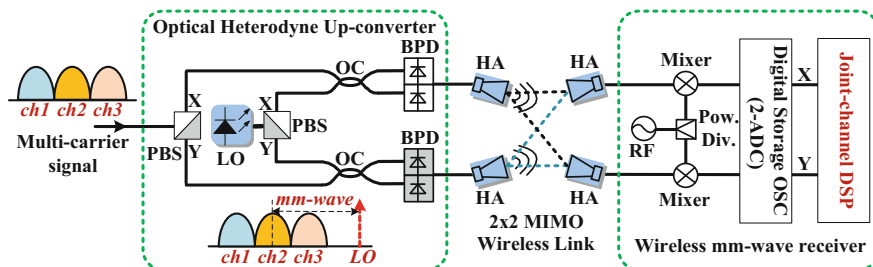


**Fig. 6.12** Schematic diagram of the proposed multi-carrier optical heterodyne up-converter and wireless mm-wave receiver with joint-channel DSP

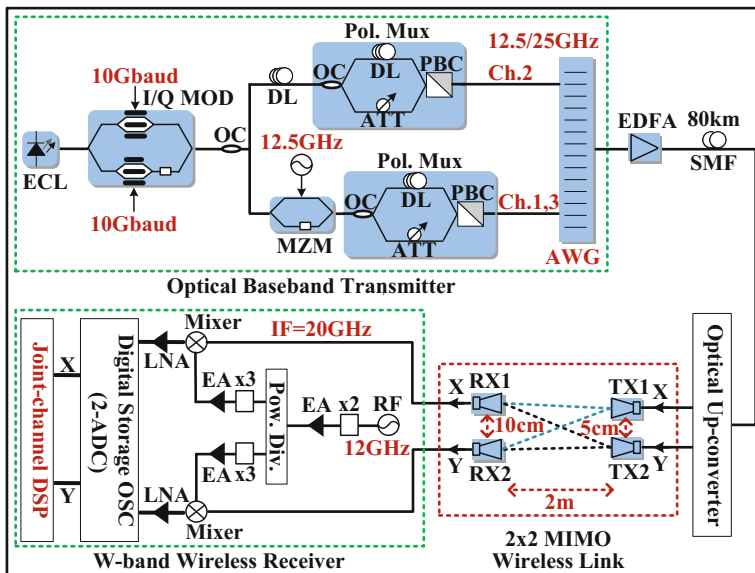
generate the wireless mm-wave carrier frequency. The optical heterodyne up-conversion and wireless mm-wave reception for the three-channel DWDM signal is quite similar to that previously described for the single-carrier signal. Moreover, after analog-to-digital conversion, the generated digital signal, with full channel information, can be processed by joint-channel DSP, which is described in detail in the following.

Based on the optical multi-carrier modulation technique, we have experimentally demonstrated a fiber wireless integration system that delivers 120-Gb/s multi-channel PDM-QPSK signal through 80-km SMF-28 and a 2-m  $2 \times 2$  MIMO wireless link at 92 GHz [41]. In this experiment, the  $3 \times 40$ -Gb/s three-channel PDM-QPSK signal has 12.5-GHz neighboring frequency spacing. Each receiver HA can receive signals from two transmitter HAs, and thus, there exists wireless MIMO interference in the  $2 \times 2$  MIMO wireless link. At the wireless receiver, the classic CMA equalization based on DSP is used to realize polarization de-multiplexing and suppress MIMO interference. In [41], we have also experimentally demonstrated that more CMA taps are required for this system with the additional  $2 \times 2$  MIMO wireless link.

Figure 6.13 shows the experimental setup for the seamless integration of  $3 \times 40$ -Gb/s multi-channel PDM-QPSK signal transmission through 80-km SMF-28 and 2-m  $2 \times 2$  MIMO wireless link at 92 GHz. At the optical baseband transmitter, an ECL at 1554.43 nm is used with linewidth less than 100 kHz and output power of 14.5 dBm. For optical QPSK modulation, the I/Q modulator is driven by a 10-Gbaud electrical binary signal with a PRBS length of  $2^{10} - 1$ . After I/Q modulation, the 20-Gb/s optical QPSK signal is split into two branches. One branch is polarization-multiplexed to generate even-channel PDM-QPSK signal (channel 2), while the other is injected into a MZM. The MZM is driven by a 12.5-GHz RF signal and biased at the null point, in order to implement optical carrier suppression (OCS) modulation [60]. After OCS modulation, the two sidebands of 25-GHz channel spacing are polarization-multiplexed to generate two odd-channel PDM-QPSK signals (channel 1 and channel 3). Both the I/Q modulator and the polarization multiplexer are identical to those adopted in Fig. 6.4. The odd and even channels are combined by a 12.5/25-GHz arrayed waveguide grating before fiber transmission. The generated 120-Gb/s multi-channel signal is launched into an 80-km-long SMF-28. An EDFA is used to compensate for the fiber loss.

The optical heterodyne up-converter is similar to that adopted in Fig. 6.4, except that in this case, the FO between the LO and the received optical signal is 92 GHz. The generated  $3 \times 40$ -Gb/s three-channel PDM-QPSK wireless signal at 92 GHz is delivered by a  $2 \times 2$  MIMO wireless link. The pairs of transmitter and receiver HAs are separated by a link distance of 2 m, while the separation between two transmitter HAs and two receiver HAs are 5 and 10 cm, respectively. Each HA has a 25-dBi gain. Each receiver HA can receive signals from two transmitter HAs, and thus, there exists wireless MIMO interference in the  $2 \times 2$  MIMO link.

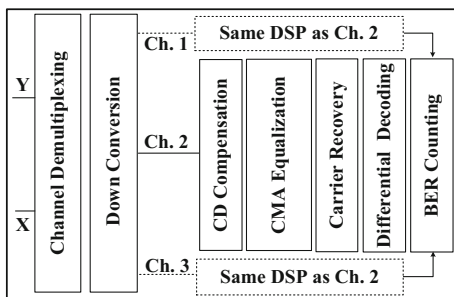
At the wireless receiver, the first stage of the two-stage down conversion is identical to that adopted in Fig. 6.4. The three-channel PDM-QPSK signal centered around 20 GHz is obtained after the first-stage analog down conversion. The



**Fig. 6.13** Experimental setup for the seamless integration of  $3 \times 40$ -Gb/s multi-channel PDM-QPSK signal transmission through 80-km SMF-28 and 2-m  $2 \times 2$  MIMO wireless link at 92 GHz

analog-to-digital conversion is realized in the digital storage OSC with 120-GSa/s sampling rate and 45-GHz electrical bandwidth. Figure 6.14 shows the DSP modules used after the analog-to-digital conversion. Firstly, the received three-channel PDM-QPSK signal is de-multiplexed in the electrical domain, which is realized by a digital fifth-order Bessel filter. Then, three sub-channels are simultaneously down-converted to the baseband by multiplying synchronous cosine and sine functions at different frequencies, i.e., 32.5, 20, and 7.5 GHz for channel 1, channel 2, and channel 3, respectively. The frequencies are generated by a digital LO used for down conversion. The subsequent CD compensation, CMA equalization, carrier recovery, differential decoding, and BER counting are similar to those discussed in conjunction with Fig. 6.4. Here, two complex-valued, 25-tap,

**Fig. 6.14** Functional block diagram for DSP processing after analog-to-digital conversion



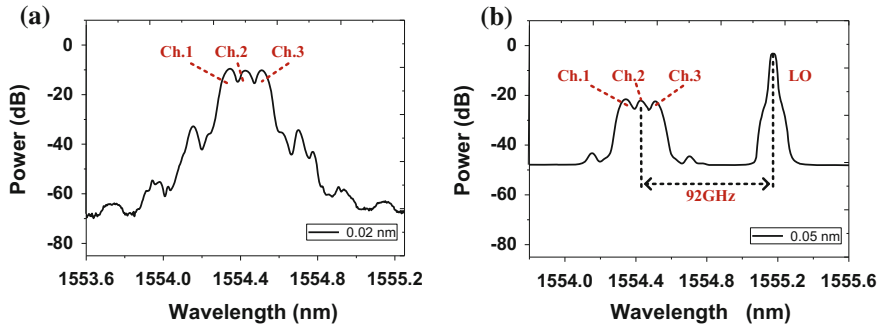
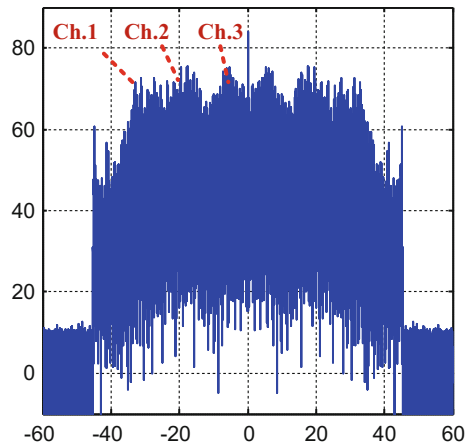


**Fig. 6.15** **a** Optical spectrum (0.02-nm resolution) after arrayed waveguide grating. **b** Optical spectrum (0.05-nm resolution) after polarization-diversity splitting

$T/2$ -spaced adaptive FIR filters, based on the classic CMA, are used to retrieve the modulus of the PDM-QPSK signal, to affect polarization de-multiplexing and wireless interference suppression [36].

Figure 6.15a, b shows the optical spectra after the 12.5/25-GHz arrayed waveguide grating and polarization-diversity splitting, respectively. The frequency spacing and power difference between channel 2 and LO are 92 GHz and 20 dB, respectively. Figure 6.16 shows the electrical spectrum of the three-channel signal with 20-GHz IF. We can see that, due to the low-pass frequency response of wireless and electrical devices, channel 1 and channel 2 have a lower power compared to channel 3. Figure 6.17a, b shows the constellations with CMA tap number of 13 and 25, respectively. The constellation for the 25-tap CMA length is much clearer than that for the 13-tap CMA length. To our knowledge, the CMA tap for PDM-QPSK in most coherent systems is around 13, which means that more taps are required for this system with the additional  $2 \times 2$  MIMO wireless link.

**Fig. 6.16** Electrical spectrum of the three-channel signal with 20-GHz IF



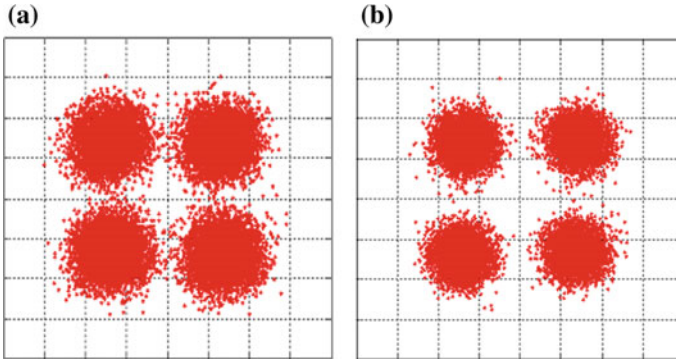


**Fig. 6.17** Received QPSK constellations with **a** 13 taps and **b** 25 taps

### 6.2.4 Electrical Multi-carrier Modulation

As one kind of electrical multi-carrier modulation, OFDM has been widely used in optical networks because of its high immunity to fiber CD and PMD as well as high spectral efficiency. OFDM can also be used in the fiber wireless integration system to reduce the transmission baud rate as well as to improve performance and spectral efficiency [42–48].

Correspondingly, we have experimentally demonstrated a fiber wireless integration system adopting optical PDM combined with MIMO reception, which can deliver 30.67-Gb/s PDM OFDM signal through 40-km SMF-28 and a 2-m  $2 \times 2$  MIMO wireless link at 100 GHz [48]. In this experiment, there also exists wireless MIMO interference in the  $2 \times 2$  MIMO wireless link. At the wireless receiver, de-multiplexing is realized by channel estimation based on a pair of time-interleaved training sequences (TSs). The BER for the 30.67-Gb/s PDM OFDM signal is less than the pre-FEC threshold of  $3.8 \times 10^{-3}$  when the OSNR is larger than 17 dB after both 40-km SMF-28 transmission and 2-m wireless delivery at 100 GHz.

The experimental setup for the 30.67-Gb/s PDM OFDM optical baseband transmitter is similar to that shown in Fig. 6.4, except that in this case, the I/Q modulator is driven by an electrical baseband OFDM signal. The electrical OFDM signal is generated by an AWG at a sampling rate of 11.5 Gsa/s. For electrical OFDM modulation, as shown in Fig. 6.18a, the inverse FFT (IFFT) size is 256. Among the 256 subcarriers, 192 subcarriers are allocated for data transmission with 4QAM, 8 subcarriers are used as pilots for phase estimation, the first subcarrier is set to zero for DC-bias, and the remaining 55 null subcarriers at the edge are reserved for oversampling. After IFFT, a cyclic prefix (CP), which is 1/8 of IFFT size, is added in the OFDM symbol. Two types of TSs are added at the front of the data stream. The first type includes only one TS used for time and frequency synchronization, while the other is comprised of one TS surrounded by two null symbols in order to construct a pair of time-interleaved TSs after polarization multiplexing. These are used for channel estimation. As shown in Fig. 6.18b, the Y-polarization is delayed

by exactly one symbol relative to the X-polarization after the polarization multiplexer, which is used to construct a pair of time-interleaved TSs for de-multiplexing. The total bit rate is 30.67 Gb/s ( $11.5 \times 192/288 \times 2 \times 2$  Gb/s = 30.67 Gb/s) after the polarization multiplexer. The generated signal is launched into a 40-km SMF-28. The launch power (after the EDFA) is 0 dBm.

The operation of the optical heterodyne up-converter is identical to that adopted in Fig. 6.4, that is, the received 30.67-Gb/s PDM OFDM optical baseband signal is up-converted to the 30.67-Gb/s PDM OFDM wireless signal at 100 GHz. In the  $2 \times 2$  MIMO wireless link, each pair of transmitter and receiver HAs have a 2-m wireless link, while the separation between two transmitter HAs and receiver HAs are 8 cm and 10 cm, respectively. Interference exists in the  $2 \times 2$  MIMO link. At the wireless receiver, the first stage of the two-stage down conversion is also identical to that adopted in Fig. 6.4. Figure 6.18c shows details of the DSP processing after the analog-to-digital conversion. Firstly, the 30.67-Gb/s PDM OFDM wireless signal with 28-GHz IF is down-converted to baseband with the RF pilot, which is the DC component of the signal injected into the I/Q modulator. Secondly, time synchronization is accomplished by placing the conjugate symmetric OFDM symbol, in the time domain, at the front of the frame as the first type of TS at the transmitter. Thirdly, channel estimation for the MIMO channel is implemented by a pair of TSs set as the second type of TS at the transmitter in two polarizations, and then, de-multiplexing can be realized in order to minimize crosstalk between the two branches. Fourthly, phase noise cancelation in the two branches is implemented with the pilots inserted in each OFDM symbol, and after the decision and de-mapper procedure, the feedback algorithm is applied to improve the accuracy of the phase noise estimation. The final step is BER counting. It is noted that an intra-symbol frequency-domain averaging (ISFA) algorithm is applied to improve the accuracy of the channel estimation. The subcarrier number used for ISFA is 13.

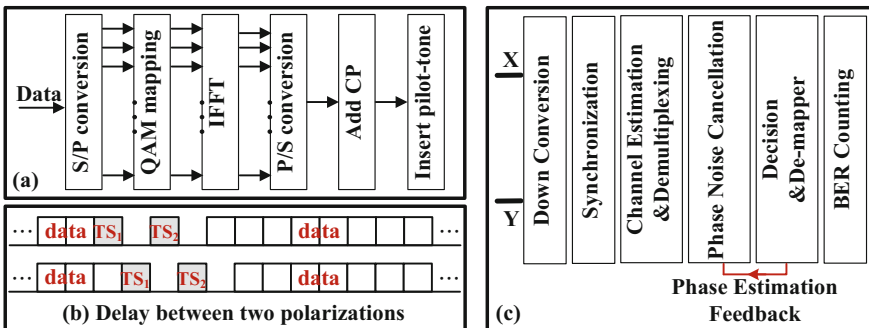


**Fig. 6.18** a Electrical OFDM modulation. b Delay between two polarizations. c Detailed DSP after analog-to-digital conversion

### 6.2.5 Antenna Polarization Multiplexing

Antennas generally display a greater or lesser degree of polarization (polarization is understood to refer to the direction of the electric field), and HAs can display a substantial gain, referred to as isotropic. The two states of polarization are E- and H-polarization, or sometimes more conveniently but less precisely simply called the horizontal-polarization (H-polarization) state and vertical-polarization (V-polarization) state. Figure 6.19 shows the schematic diagram of the fiber wireless integration system adopting antenna polarization multiplexing. In the case of a two-channel DWDM signal (ch1 and ch2), for example, the optical heterodyne up-conversion stage contains an additional wavelength selective switch (WSS) to de-multiplex the two DWDM channels which are independently but simultaneously up-converted by optical heterodyning. The heterodyne up-conversion of ch1 or ch2 is quite similar to that adopted in Fig. 6.4. The MIMO wireless link includes four transmitter HAs and four receiver HAs. The upper two transmitter HAs and two receiver HAs are all horizontally polarized and thus form an H-polarization HA array to deliver ch1. The lower two transmitter HAs and two receiver HAs are all vertically polarized and thus form a V-polarization HA array to deliver ch2. After MIMO wireless delivery, the received wireless two-channel signal is sent into a digital storage OSC, and offline DSP is implemented after analog-to-digital conversion. The signal baud rate and performance requirements for optical and wireless devices can be reduced by adopting antenna polarization multiplexing at the expense of doubling the number of antennas and devices. The adoption of antenna polarization multiplexing can also increase wireless transmission capacity at the cost of stricter requirements for V-polarization.

Correspondingly, we have experimentally demonstrated the  $2 \times 56\text{-Gb/s}$  two-channel PDM-QPSK signal delivery based on antenna polarization multiplexing over 80-km SMF-28 and a 2-m Q-band (33–50 GHz) wireless link [49]. At the wireless receiver, the classic CMA equalization based on DSP can realize polarization de-multiplexing and remove the crosstalk at the same antenna polarization. For 2-m wireless delivery, the BER of each channel after 80-km SMF-28 transmission can be under  $3.8 \times 10^{-3}$ , while the BER without fiber transmission

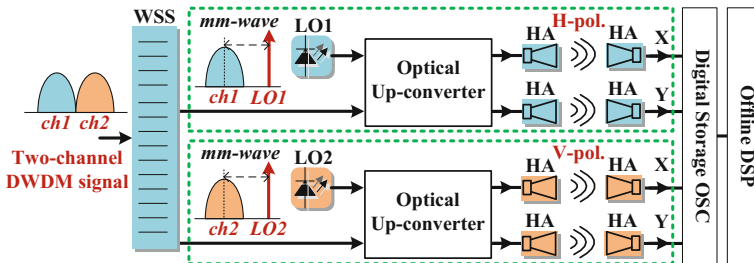


Fig. 6.19 Schematic diagram of a fiber wireless integration system adopting antenna polarization multiplexing

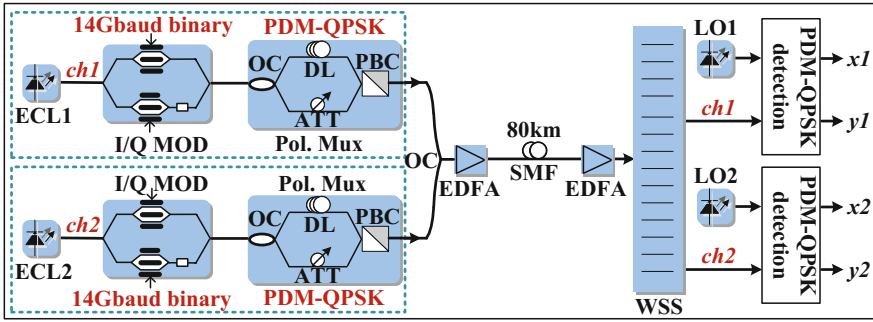
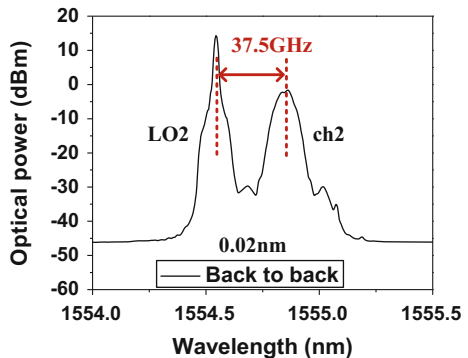


Fig. 6.20 Experimental setup for optical mm-wave generation

under  $1 \times 10^{-5}$ . We also have experimentally demonstrated that the isolation is only about 19 dB when the V-polarization deviation approaches  $10^\circ$ , which will affect the wireless delivery for high-speed ( $>50$  Gb/s) signals.

Figure 6.20 shows the experimental setup for the optical mm-wave generator for the  $2 \times 56$ -Gb/s two-channel, Q-band, PDM-QPSK wireless signal. The optical baseband transmitter contains two ECLs, each with linewidth less than 100 kHz. In the upper path, the CW lightwave from ECL1 has a wavelength of 1554.43 nm and is modulated by an I/Q modulator. The I/Q modulator is driven by a 14-Gbaud electrical binary signal with a PRBS length of  $2^{15} - 1$ , generated by a PPG. The optical PDM-QPSK modulation is realized by the I/Q modulator and the subsequent polarization multiplexer, which is identical to that adopted in Fig. 6.4. The same operation is implemented in the lower path except that the CW lightwave from ECL2 has a wavelength of 1554.83 nm. An OC is then used to combine the two 56-Gb/s PDM-QPSK optical baseband channels, separated by 50-GHz channel spacing. The optically combined channels are amplified by an EDFA and then launched into an 80-km SMF-28. The second EDFA is used to compensate for the fiber loss. The total optical power after the first and second EDFAs is 4 and 10 dBm, respectively. In the subsequent portion of this section, ch1 and ch2 are used to denote the two channels at 1554.43 and 1554.83 nm, respectively.

Fig. 6.21 Optical spectrum (0.02-nm resolution) for ch2 after polarization-diversity splitting



In optical heterodyne up-conversion, a  $1 \times 2$  programmable WSS is first used to separate ch1 and ch2 as well as suppress the amplified spontaneous emission (ASE) noise from the EDFAs. Another two ECLs with linewidth less than 100 kHz are used as LOs. LO1 and LO2 have 37.5-GHz FO relative to ch1 and ch2, respectively. The heterodyne up-conversion of ch1 or ch2 is similar to that adopted in Fig. 6.4, except that in this case, two single-ended PDs, each having 60-GHz 3-dB bandwidth and a linearity input power limit of 7.5 dBm, are used to directly up-convert the PDM-QPSK optical signal into the wireless signal at 37.5 GHz. Figure 6.21 shows the BTB optical spectrum for ch2 (0.02-nm resolution) after polarization diversity.

Figure 6.22 shows the Q-band HA array including four transmitter HAs (TX1–TX4) and four receiver HAs (RX1–RX4). TX1, TX2, RX1, and RX2 are vertically polarized, while TX3, TX4, RX3, and RX4 are horizontally polarized. The V- and H-polarization HA arrays are used to deliver ch1 and ch2, respectively. The isolation between H- and V-polarization HA arrays is 33 dB, but there exists large crosstalk at the same antenna polarization due to the deliberate HA arrangement in which receiver HAs subtend power from each transmitter HA. Each HA has 25-dBi gain, useful frequency range of 33–50 GHz, and follows, or is followed by, a 60-GHz EA with 30-dB gain and 24-dBm saturation output power. After a 2-m wireless delivery, the received two-channel PDM-QPSK wireless signal at

**Fig. 6.22** Experimental setup for Q-band HA array

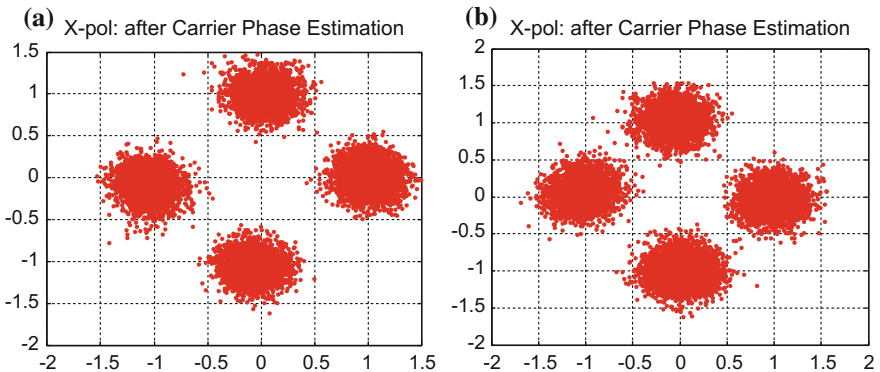
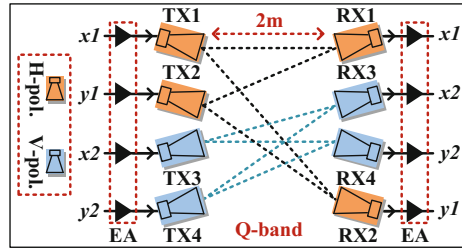


**Fig. 6.23** **a** X-polarization constellation after 80-km SMF-28 transmission. **b** X-polarization BTB constellation

37.5 GHz is first amplified by four parallel 60-GHz EAs and then directly sent to the digital storage OSC with 120-GSa/s sampling rate and 45-GHz electrical bandwidth. Subsequent DSP processing is similar to that discussed in conjunction with Fig. 6.4. It is worth noting that, here, CMA equalization with 53 T/2 taps is used to realize polarization de-multiplexing and remove the crosstalk at the same antenna polarization [36]. Figure 6.23a shows the X-polarization constellation after 80-km SMF-28 transmission and 2-m wireless delivery at the BER of  $4 \times 10^{-4}$  at 24-dB OSNR. Figure 6.23b shows the X-polarization BTB constellation after 2-m wireless delivery when no crosstalk exists and the BER is  $1 \times 10^{-5}$ .

### 6.2.6 Multi-band Multiplexing

Similar to antenna polarization multiplexing, the adoption of multiple frequency bands can also effectively reduce the signal baud rate and performance requirements for optical and wireless devices, but at the cost of more antennas and devices. We have experimentally demonstrated an optical wireless integration system simultaneously delivering  $2 \times 112$ -Gb/s two-channel PDM-16QAM wireless signal at 37.5 GHz and  $2 \times 108$ -Gb/s two-channel PDM-QPSK wireless signal at 100 GHz, adopting two mm-wave frequency bands, two orthogonal antenna polarizations, MIMO, photonic mm-wave generation, and advanced DSP [52]. In the case of no fiber transmission, the BERs for both the 112-Gb/s PDM-16QAM signal after 1.5-m wireless delivery at 37.5 GHz and the 108-Gb/s PDM-QPSK signal after 0.7-m wireless delivery at 100 GHz are under the pre-FEC threshold of  $3.8 \times 10^{-3}$ . To our knowledge, this is the first demonstration of a 400G optical wireless integration system in mm-wave frequency bands and also a capacity record of wireless delivery.

Figure 6.24 shows the experimental setup for the optical mm-wave generator for  $2 \times 108$ -Gb/s two-channel PDM-QPSK wireless signal in the W-band and  $2 \times 112$ -Gb/s two-channel PDM-16QAM wireless signal in the Q-band. The optical baseband transmitter contains four ECLs, each with linewidth less than 100 kHz and output power of 14.5 dBm. For optical PDM-QPSK modulation, the two CW lightwaves from ECL1 at 1553.22 nm and ECL2 at 1553.82 nm are first combined by an OC and then modulated by an I/Q modulator. The I/Q modulator is driven by a 27-Gbaud electrical binary signal, with a PRBS length of  $2^{15} - 1$ , generated by a PPG. The operation of the I/Q modulator and the subsequent polarization multiplexer is identical to that adopted in Fig. 6.4. Thus, the  $2 \times 108$ -Gb/s two-channel PDM-QPSK optical baseband signal is generated with 75-GHz channel spacing. Similarly, in the optical PDM-16QAM modulation, two CW lightwaves from ECL3 at 1554.43 nm and ECL4 at 1554.83 nm are combined by an OC, and modulated by an I/Q modulator and polarization-multiplexed. What is different in this case is that the I/Q modulator is driven by a 14-Gbaud electrical four-level signal, generated by an AWG, likewise with a PRBS length of  $2^{15} - 1$ . Thus, the  $2 \times 112$ -Gb/s two-channel PDM-16QAM optical baseband signal is

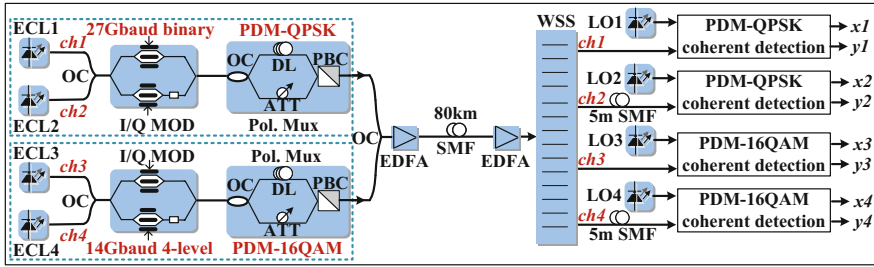


Fig. 6.24 Experimental setup for optical mm-wave generation

generated with 50-GHz channel spacing. The generated  $2 \times 112$ -Gb/s two-channel PDM-16QAM and  $2 \times 108$ -Gb/s two-channel PDM-QPSK optical signals are further combined by an OC, amplified by an EDFA, and launched into 80-km SMF-28. The second EDFA is used to compensate for the fiber loss. The total optical power after the first and second EDFAs is 15 and 18 dBm, respectively. In the subsequent portion of this section, ch1, ch2, ch3, and ch4 are used to denote the four channels at 1553.22, 1553.82, 1554.43, and 1554.83 nm, respectively.

In optical heterodyne up-conversion, a  $1 \times 4$  programmable WSS is first used to separate ch1–ch4 as well as suppress the ASE noise from the EDFAs. Another four ECLs with linewidth less than 100 kHz are used as LOs. LO1 and LO2 have 100-GHz FO relative to ch1 and ch2, respectively. LO3 and LO4 have 37.5-GHz FO relative to ch3 and ch4, respectively. Here, 5-m SMF is used to de-correlate ch1 and ch2 or ch3 and ch4. The heterodyne up-conversion of ch1 or ch2 is similar to that adopted in Fig. 6.4, except that in this case, two PDs, each with 90-GHz 3-dB bandwidth and 7.5-dBm input power, directly convert the PDM-QPSK optical signal into the PDM-QPSK wireless signal at 100 GHz. The heterodyne up-conversion of ch3 or ch4 is similar to that adopted in Fig. 6.8, except that in this case, two BPDs directly up-convert the PDM-16QAM optical signal into the PDM-16QAM wireless signal at 37.5 GHz. Each BPD has a 10-dBm input power. Figure 6.25a, b shows the optical spectra (0.1-nm resolution) after the first and second EDFAs, respectively. Figure 6.25c–f shows the optical spectra (0.02-nm resolution) after polarization diversity corresponding to ch1–ch4, respectively.

Figure 6.26 shows the HA system including a W-band HA array and a Q-band HA array. Each HA array includes four transmitter HAs and four receiver HAs. The two pairs of transmitter and receiver HAs in the middle of the W-band HA array are in H-polarization state, while the other two pairs are in V-polarization. The  $2 \times 108$ -Gb/s two-channel PDM-QPSK wireless signal at 100 GHz is delivered by the W-band HA array, with ch1 and ch2 corresponding to the H- and V-polarization, respectively. For the W-band HA array, each receiver HA can only receive wireless power from the corresponding transmitter HA as shown by the black dashed lines, because the link distance between the HAs is much larger than the wavelength of about 3 mm corresponding to the 100-GHz carrier wave. Thus, there hardly exists crosstalk at the same polarization (H or V) for the W-band HA array if the HAs are

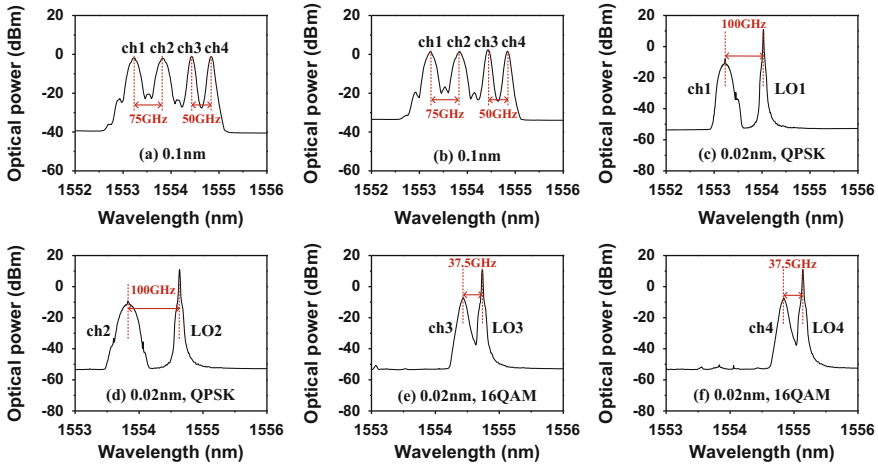


Fig. 6.25 a, b Optical spectra (0.1-nm resolution) after the first and second EDFAs. c-f Optical spectra (0.02-nm resolution) after polarization diversity corresponding to ch1-ch4

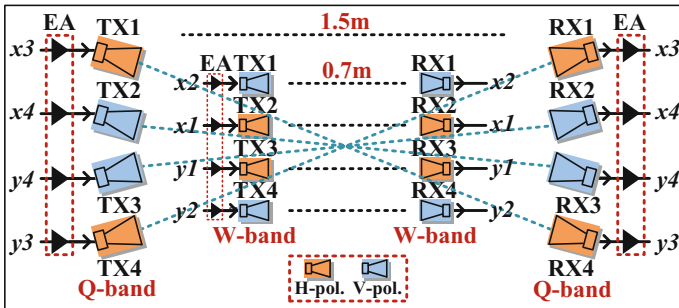
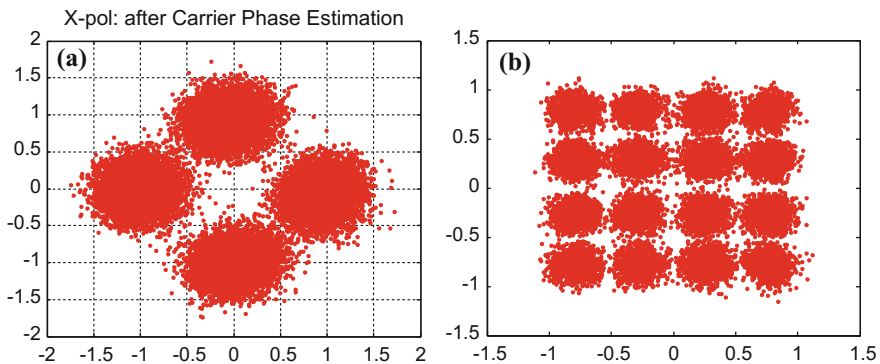


Fig. 6.26 Experimental setup for Q-band and W-band HA system

sufficiently separated from one another. Moreover, the crosstalk, even if it exists, can be compensated by a long-tap constant modulus algorithm (CMA) [36]. On the other hand, the two pairs of transmitter and receiver HAs in the middle of the Q-band HA array are vertically polarized, while the other two pairs are horizontally polarized. The  $2 \times 112$ -Gb/s two-channel PDM-16QAM wireless signal at 37.5 GHz is delivered by the Q-band HA array, with ch3 and ch4 corresponding to the H- and V-polarization, respectively. For the Q-band array, RX2 or RX3 can receive the same wireless power from TX2 and TX3, while RX1 or RX4 can receive the same wireless power from TX1 and TX4, as shown by the blue dashed lines. Thus, there exists a large crosstalk at the same polarization (H or V) for the Q-band HA array. The crosstalk depends on the beam width of the 37.5 GHz mm-wave signal, the relative inclination of the HAs as well as the relative distance between the HAs.

The distance is 0.7 m for the wireless transmission links at W-band, while it is 1.5 m at Q-band. Each HA has a 25-dBi gain. Each Q-band HA follows, or is followed by, a 60-GHz EA with 30-dB gain and 24-dBm saturation output power, while each W-band transmitter HA follows a 100-GHz EA with 30-dB gain and 10-dBm saturation output power. The 3-dB beam width at the input of each receiver HA is about  $10^\circ \times 10^\circ$ . The transmitted and received RF power is about 9 and  $-10$  dBm, respectively. The isolation between H- and V-polarization HA array is 33 dB. Thus, the crosstalk between H- and V-polarization signals can be ignored, and other arrangements apart from H-V-V-H and V-H-H-V are also feasible for the HA system.

For the received 100-GHz PDM-QPSK wireless signal (corresponding to ch1 or ch2), analog down conversion is first implemented at the wireless receiver, which is identical to that adopted in Fig. 6.4. The 28-GHz IF signals after the first-stage analog down conversion are amplified by two 40-GHz EAs and then sent to the digital storage OSC with 120-GSa/s sampling rate and 45-GHz electrical bandwidth. The subsequent digital DSP, similar to that discussed in conjunction with Fig. 6.4, includes IF down conversion, CD compensation, CMA equalization, carrier recovery, differential decoding, and BER counting. Here, CMA equalization with 53 T/2 taps is used to realize polarization de-multiplexing and remove the crosstalk in the wireless delivery [36]. Analog down conversion is unnecessary for the received 37.5-GHz PDM-16QAM wireless signal (corresponding to ch3 or ch4), which is amplified by 60-GHz EAs and then directly sent to the real-time OSC with 120-GSa/s sampling rate and 45-GHz electrical bandwidth. The subsequent DSP, similar to that discussed in conjunction with Fig. 6.8, includes IF down conversion, CD compensation, cascaded multi-modulus algorithm (CMMA) equalization, carrier recovery, differential decoding, and BER counting. Here, CMMA equalization is used to realize multi-modulus recovery and polarization de-multiplexing. Figure 6.27a shows the X-polarization constellation for the 108-Gb/s PDM-QPSK signal after 80-km SMF-28 transmission and 0.7-m wireless delivery when the OSNR is 36 dB and the CMA tap number is 53. Figure 6.27b



**Fig. 6.27** a X-polarization QPSK constellation. b X-polarization 16-QAM constellation

shows the X-polarization constellation for the 112-Gb/s PDM-16QAM signal after 80-km SMF-28 transmission and 1.5-m wireless delivery at the BER of  $9 \times 10^{-4}$  at 33-dB OSNR.

### 6.3 Problems Existing in the Large Capacity Fiber Wireless Integration System and Corresponding Solutions

#### 6.3.1 *Wireless Multi-path Effects Due to Different Wireless Transmission Distances*

Due to the wireless multi-path effects, wireless interference exists in the MIMO wireless transmission. We have experimentally investigated the MIMO wireless interference in a 100-GHz optical wireless integration system, which can deliver 50-Gb/s PDM-QPSK signal over 80-km SMF-28 and a  $2 \times 2$  MIMO wireless link [36]. In the parallel MIMO wireless link, each receiver HA can only receive wireless power from the corresponding transmitter HA, and thus, there is no wireless interference. However, for the cross-over cases, the receiver HA can see wireless power from two transmitter HAs, giving rise to interference. Polarization de-multiplexing is realized by CMA-based processing at the DSP level. Compared to the parallel case, about 2-dB OSNR penalty at a BER of  $3.8 \times 10^{-3}$  is caused by wireless interference for the cross-over cases if similar CMA taps are employed. The increase in tap length can reduce wireless interference and improve BER performance. More taps should be adopted when two pairs of transmitter and receiver HAs have different link distances. But more taps also means more calculation time during the DSP processing.

The experimental setup for the 100-GHz 50-Gb/s PDM-QPSK optical wireless integration system is similar to that shown in Fig. 6.4, except that in this case, the I/Q modulator at the optical baseband transmitter is driven by a 12.5-Gbaud electrical binary signal with a PRBS length of  $2^{15} - 1$ , and the  $2 \times 2$  MIMO wireless link has a deliberate HA arrangement in order to investigate the effects of MIMO wireless interference. Figure 6.28 shows one parallel and three cross-over MIMO wireless links by fixing the locations of two receiver HAs and adjusting the positions of the transmitter HAs. There exists an 80-km SMF-28 transmission with 2-dBm launched power into the fiber (after the EDFA), and the two receiver HAs have a 10-cm separation. The 3-dB beam width at the input of the receiver HA is  $40^\circ \times 40^\circ$ . For Case 1, shown in Fig. 6.28a, each pair of transmitter and receiver HAs has a 0.6-m wireless distance and two transmitter (receiver) HAs have a 10-cm separation. In this case, there is no wireless interference due to high directionality. For Case 2, shown in Fig. 6.28b, two transmitter HAs are both moved to the location that has the same wireless distance from two receiver HAs, and each pair of transmitter and receiver HAs has a 0.6-m wireless distance horizontally. Thus, each

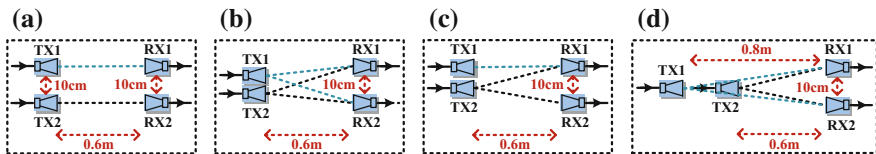
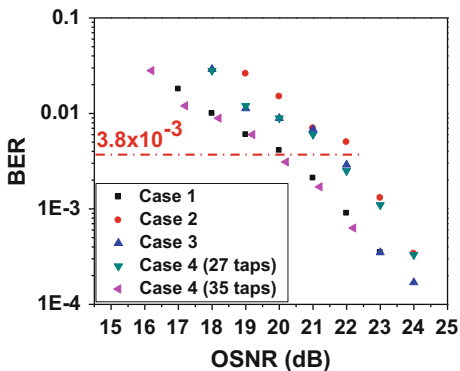


Fig. 6.28 MIMO wireless links. a–d Cases 1–4

receiver HA can receive the same wireless power from two transmitter HAs. For Case 3, shown in Fig. 6.28c, transmitter HA1 is fixed, transmitter HA2 is moved to the location that has the same wireless distance from two receiver HAs, and each pair of transmitter and receiver HAs has a 0.6-m wireless distance horizontally. Thus, receiver HA2 can only receive signal from transmitter HA2, whereas receiver HA1 can receive the same wireless power from two transmitter HAs. For Case 4, shown in Fig. 6.28d, two transmitter HAs are both moved to locations that have the same wireless distance from two receiver HAs, and the horizontal wireless distance is 0.6-m between transmitter HA2 and receiver HA2, while it is 0.8 m between transmitter HA1 and receiver HA1. Thus, each receiver HA can also receive the same wireless power from two transmitter HAs. The block effect of transmitter HA2 is removed by locating transmitter HA2 a little lower than transmitter HA1, that is, two transmitter HAs have different heights on the optical table. Because receiver HA can receive power from two transmitter HAs, there exists wireless interference for these cross-over cases.

Figure 6.29 shows BER versus OSNR for Cases 1–4. The CMA tap number is 19 for Cases 1–3, while it is 27 and 35 for Case 4 because the BER performance is very poor if only 19 taps are used in this case. The reason more taps are required for Case 4 is that two pairs of transmitter and receiver HAs have different link distances, which is equivalent to a large differential group delay (DGD) effect existing in the transmission fiber. The wireless interference in Case 4 can be nearly completely removed when the tap number is 35. Compared to Case 1, only about 2-dB OSNR penalty is caused at the BER of  $3.8 \times 10^{-3}$  by the wireless interference for

Fig. 6.29 BER versus OSNR for Cases 1–4



Cases 2–4 if similar CMA taps are employed, which shows the uniform equalization of the wired and wireless integrated  $2 \times 2$  MIMO channel can be well realized by classic CMA.

Relative to Case 1, the optimal additional tap number in Case 4 can be calculated as follows

$$\Delta n = 2nlb/c = 2 \times 1 \times 0.2 \times 12.5 \times 10^9 / (3 \times 10^8) \approx 16.7. \quad (6.3)$$

where  $n$  is the medium index ( $=1$  in the air),  $l$  is the link distance difference between two pairs of transmitter and receiver HAs,  $c$  is the speed of light in vacuum, and  $b$  is the baud rate. The optimal tap number for Case 4 will be about  $19 + 16 = 35$  if that for Case 1 is 19. When the adopted tap number is 35 for Case 4, we can get a BER curve similar to that of Case 1 as shown in Fig. 6.29. Thus, the increase in tap length can overcome the wireless interference and improve the BER performance. More CMA taps should be adopted when two pairs of transmitter and receiver HAs have different link distances, and the interference can be nearly completely removed if the tap number is large enough. But more taps also means more calculation time during the DSP processing.

### 6.3.2 Advance Algorithms Based on DSP

In the large-capacity fiber wireless integration system, the signal quality degradation due to the limited bandwidth of optical and electrical components can be pre-compensated by high-speed digital-to-analog converter (DAC) based on advanced DSP [61]. Furthermore, if the bandwidth of optical and electrical components is narrow enough, the QPSK signal will be converted into 9QAM-like, and thus, the digital post filter combined with 1-bit maximum likelihood sequence estimation (MLSE) [62, 63] can be adopted to improve the signal quality. On the other hand, the high peak-to-average power ratio (PAPR) characteristic of OFDM modulation will also degrade the performance of the fiber wireless integration system [64], for which discrete Fourier transform (DFT) [65–68] can be introduced to reduce PAPR and thus improve the system performance. Many related investigations are currently being carried out.

## 6.4 Conclusion

We have summarized several different approaches for the realization of large capacity ( $>100$  Gb/s) fiber wireless integration systems, including optical PDM combined with MIMO reception, advanced multi-level modulation, optical multi-carrier modulation, electrical multi-carrier modulation, antenna polarization multiplexing, and multi-band multiplexing. These approaches can effectively

increase both optical and electrical spectral efficiency as well as reduce the required bandwidth for optical and electrical devices. We have also investigated problems such as multi-path effects due to different wireless transmission distances, existing in the large-capacity fiber wireless integration system. We have demonstrated that these problems can be effectively solved based on advanced DSP algorithms including classic CMA. Moreover, based on the combination of these approaches as well as advanced DSP algorithms, we have successfully demonstrated a 400G fiber wireless integration system, which established a capacity record for wireless delivery and ushers in a new era of ultra-high bit rate (>400 Gb/s) optical wireless integration and communications at mm-wave frequencies. We believe that, in the near future, 1 Tb/s and beyond fiber wireless integration system can be realized either by adopting more optical/electrical carriers, more frequency bands, higher-level modulation, and so on, or by introducing more emerging techniques, such as orbital angular momentum (OAM).

## References

1. What is 5g, 5g visions. GSM history: history of GSM, mobile networks, vintage mobiles
2. Fitzsimmons M (2013) Sharp dazzles with 8 K TV prototype, VP says production about 4 years off (CES 2013). <http://www.techradar.com/us/news/television/hdvt/sharp-dazzles-with-8k-tv-prototype-vp-says-production-about-4-years-off-1124330>
3. McKenna TP, Nanzer JA, Clark TR (2014) Experimental demonstration of photonic millimeter-wave system for high capacity point-to-point wireless communication. *J Lightwave Technol* 32(20):3588–3594
4. Kitayama K, Maruta A, Yoshida Y (2014) Digital coherent technology for optical fiber and radio-over-fiber transmission systems. *J Lightwave Technol* 32(20):3411–3420
5. Li X, Zhang J, Xiao J, Zhang Z, Xu Y, Yu J (2015) W-band 8QAM vector signal generation by MZM-based photonic frequency octupling. *IEEE Photon Technol Lett* 27(12):1257–1260
6. Yu J, Li X, Zhang J, Xiao J (2014) 432-Gb/s PDM-16QAM signal wireless delivery at W-band using optical and antenna polarization multiplexing. In: Proceedings of the ECOC 2014, Cannes, France, We.3.6.6
7. Li X, Yu J, Xiao J, Xu Y (2014) Fiber-wireless-fiber link for 128-Gb/s PDM-16QAM signal transmission at W-band. *IEEE Photon Technol Lett* 26(19):1948–1951
8. Li X, Yu J, Zhang J, Li F, Xu Y, Zhang Z, Xiao J (2014) Fiber-wireless-fiber link for 100-Gb/s PDM-QPSK signal transmission at W-band. *IEEE Photon Technol Lett* 26(18):1825–1828
9. Xiao J, Yu J, Li X, Xu Y, Zhang Z (2015) 20-Gb/s PDM-QPSK signal delivery over 1.7-km wireless distance at W-band. In: Proceedings of the OFC 2015, Los Angeles, California, W4G.4
10. Xiao J, Li X, Yu J, Xu Y, Zhang Z, Chen L (2015) 40-Gb/s PDM-QPSK signal transmission over 160-m wireless distance at W-band. *Opt Lett* 40(6):998–1001
11. Li X, Yu J, Xiao J, Zhang Z, Xu Y, Chen L (2015) Field trial of 80-Gb/s PDM-QPSK signal delivery over 300-m wireless distance with MIMO and antenna polarization multiplexing at W-band. In: Proceedings of the OFC 2015, Los Angeles, California, Th5A.5
12. Li X, Yu J, Zhang J, Li F, Xiao J (2014) Antenna polarization diversity for 146 Gb/s polarization multiplexing QPSK wireless signal delivery at W-band. In: Proceedings of the OFC 2014, San Francisco, California, M3D.7

13. Chang CH, Peng PC, Lu HH, Shih CL, Chen HW (2010) Simplified radio-over-fiber transport systems with a low-cost multiband light source. *Opt Lett* 35(23):4021–4023
14. Yu J, Chang GK, Jia Z, Chowdhury A, Huang MF, Chien HC, Hsueh YT, Jian W, Liu C, Dong Z (2010) Cost-effective optical millimeter technologies and field demonstrations for very high throughput wireless-over-fiber access systems. *J Lightwave Technol* 28(16):2376–2397
15. Pang X, Caballero A, Dogadaev A, Arlunno V, Borkowski R, Pedersen JS, Deng L, Karinou F, Roubeau F, Zibar D, Yu X, Monroy IT (2011) 100 Gbit/s hybrid optical fiber-wireless link in the W-band (75–110 GHz). *Opt Express* 19(25):24944–24949
16. Kanno A, Inagaki K, Morohashi I, Sakamoto T, Kuri T, Hosako I, Kawanishi T, Yoshida Y, Ki-tayama KI (2011) 40 Gb/s W-band (75–110 GHz) 16-QAM radio-over-fiber signal generation and its wireless transmission. In: *Proceedings of the ECOC 2011, Geneva, Switzerland, We.10.P1.112*
17. Chow CW, Kuo FM, Shi JW, Yeh CH, Wu YF, Wang CH, Li YT, Pan CL (2010) 100 GHz ultra-wideband (UWB) fiber-to-the-antenna (FTTA) system for in-building and in-home networks. *Opt Express* 18(2):473–478
18. Zibar D, Sambaraju R, Caballero A, Herrera J, Westergren U, Walber A, Jensen JB, Martí J, Monroy IT (2011) High-capacity wireless signal generation and demodulation in 75- to 110-GHz band employing all-optical OFDM. *Photon Technol Lett* 23(12):810–812
19. Zibar D, Antonio C, Yu X, Pang X, Dogadaev AK, Monroy IT (2011) Hybrid optical fibre-wireless links at the 75–110 GHz band supporting 100 Gbps transmission capacities. In: *Proceedings of the MWP/APMP 2011, Singapore*, pp 445–449
20. Ye C, Zhang L, Zhu M, Yu J, He S, Chang GK (2012) A bidirectional 60-GHz wireless-over-fiber transport system with centralized local oscillator service delivered to mobile terminals and base stations. *IEEE Photon Technol Lett* 24(22):1984–1987
21. Cvijetic N, Qian D, Yu J, Huang YKK, Wang T (2010) Polarization-multiplexed optical wireless transmission with coherent detection. *J Lightwave Technol* 28(8):1218–1227
22. Ghazisaidi N, Maier M (2011) Fiber-wireless (FiWi) access networks: Challenges and opportunities. *IEEE Netw* 25(1):36–42
23. Jia Z, Yu J, Agarwal A, Chien HC, Chowdhury A, Ellinas G, Jackel JL, Chang GKK (2010) Photonic generation and processing technologies for converged ultra-high throughput fiber-wireless systems. In: *Proceedings of the OFC/NFOEC 2010, San Diego, California, OTuF6*
24. Lebedev A, Pham T, Beltrán M, Yu X, Ukhanova A, Deng L, González NG, Llorente R, Monroy IT, Forchhammer S (2011) Optimization of high-definition video coding and hybrid fiber-wireless transmission in the 60 GHz band. In: *Proceedings of the ECOC 2011, Geneva, Switzerland, We.10.P1.97*
25. Dogadaev AK, Monroy IT (2011) Challenges and capacity analysis of 100 Gbps optical fibre wireless links in 75–110 GHz band. In: *Proceedings of the IEEE photonics conference, Arlington, VA*, pp 268–269
26. Islam AHMR, Bakaul M, Nirmalathas AT, Town GE (2012) Simplified generation, transport, and data recovery of millimeter-wave signal in a full-duplex bidirectional fiber-wireless system. *Photon Technol Lett* 24(16):1428–1430
27. Pinter SZ, Fernando XN (2010) Estimation and equalization of fiber-wireless uplink for multiuser CDMA 4G networks. *IEEE Trans Commun* 58(6):1803–1813
28. Lim C, Nirmalathas AT, Bakaul M, Gamage PA, Lee K-LL, Yang YM, Novak D, Waterhouse RB (2010) Fiber-wireless networks and subsystem technologies. *J Lightwave Technol* 28(4):390–405
29. Pang X, Caballero A, Dogadaev AK, Arlunno V, Deng L, Borkowski R, Pedersen JS, Zibar D, Yu X, Monroy IT (2012) 25 Gbit/s QPSK hybrid fiber-wireless transmission in the W-band (75–110 GHz) with remote antenna unit for in-building wireless networks. *Photon J* 4(3):691–698

30. Lin C, Ng'oma A, Lee W, Wei CC, Wang CY, Lu TH, Chen J, Jiang WJ, Ho CH (2012)  $2 \times 2$  MIMO radio-over-fiber system at 60 GHz employing frequency domain equalization. *Opt Express* 20(1):562–567
31. Zhao Y, Pang X, Deng L, Othman MB, Yu X, Zheng X, Zhang HY, Monroy IT (2011) Experimental demonstration of 5-Gb/s polarization-multiplexed fiber-wireless MIMO systems. In: Proceedings of the MWP/APMP 2011, Singapore, pp 13–16
32. Kanno A, Kuri T, Hosako I, Kawanishi T, Yasumura Y, Yoshida Y, Kitayama K (2012) Optical and radio seamless MIMO transmission with 20-Gbaud QPSK. In: Proceedings of the ECOC 2012, Amsterdam, The Netherlands, We.3.B.2
33. Tao L, Dong Z, Yu J, Chi N, Zhang J, Li X, Shao Y, Chang GK (2012) Experimental demonstration of 48-Gb/s PDM-QPSK radio-over-fiber system over 40-GHz mm-wave MIMO wireless transmission. *Photon Technol Lett* 24(24):2276–2279
34. Li X, Yu J, Dong Z, Cao Z, Chi N, Zhang J, Shao Y, Tao L (2012) Seamless integration of 57.2-Gb/s signal wireline transmission and 100-GHz wireless delivery. *Opt Express* 20(22):24364–24369
35. Li X, Dong Z, Yu J, Chi N, Shao Y, Chang GK (2012) Fiber wireless transmission system of 108-Gb/s data over 80-km fiber and  $2 \times 2$  MIMO wireless links at 100 GHz W-Band frequency. *Opt Lett* 37(24):5106–5108
36. Li X, Yu J, Dong Z, Zhang J, Chi N, Yu J (2013) Investigation of interference in multiple-input multiple-output wireless transmission at W band for an optical wireless integration system. *Opt Lett* 38(5):742–744
37. Dong Z, Yu J, Li X, Chang GK, Cao Z (2013) Integration of 112-Gb/s PDM-16QAM wireline and wireless data delivery in millimeter wave RoF system. In: Proceedings of the OFC 2013, Anaheim, California, OM3D.2
38. Kuri T, Toda H, Olmos JJV, Kitayama KI (2009) Fiber-wireless DWDM networks and radio-over-fiber technologies. In: Proceedings of the MWP 2009, Valencia, pp 1–4
39. Luizink M, Steenbergen CAM, Koonen, Antonius MJT (1999) Capacity allocation using WDM in fiber-wireless access networks. In: Proceedings of the OFC/IOOC 1999, San Diego, California, pp 61–63
40. Nirmalathas AT, Lim C, Novak D, Castleford D, Waterhouse RB, Smith GH (2000) Millimeter-wave fiber-wireless access systems incorporating wavelength division multiplexing. In: Proceedings of the microwave conference 2000, pp 625–629
41. Zhang J, Yu J, Chi N, Dong Z, Li X, Chang G-K (2013) Multichannel 120-Gb/s data transmission over  $2 \times 2$  MIMO fiber-wireless link at W-band. *Photon Technol Lett* 25(8):780–783
42. Deng L, Beltrán M, Pang X, Zhang X, Arlunno V, Zhao Y, Caballero A, Dogadaev AK, Yu X, Llorente R, Liu D, Monroy IT (2011) Fiber wireless transmission of 8.3-Gb/s/ch QPSK-OFDM signals in 75–110-GHz band. *Photon Technol Lett* 24(5):383–385
43. Cao Z, Zou L, Chen L, Yu J (2011) Impairment mitigation for a 60 GHz OFDM radio-over-fiber system through an adaptive modulation technique. *J Opt Commun Netw* 3(9):758–766
44. Yu J, Hu J, Qian D, Jia Z, Chang GKK, Wang T (2008) 16 Gbit/s super broadband OFDM-radio-over-fibre system. *Electron Lett* 44(6):450–451
45. Cao Z, Yu J, Xia M, Tang Q, Gao Y, Wang W, Chen L (2010) Reduction of intersubcarrier interference and frequency-selective fading in OFDM-ROF systems. *J Lightwave Technol* 28(16):2423–2429
46. Liu C, Chien HC, Gao Z, Jian W, Chowdhury A, Yu J, Chang GKK (2011) Multi-band 16QAM-OFDM vector signal delivery over 60-GHz DSB-SC optical millimeter-wave through LO enhancement. In: Proceedings of the OFC/NFOEC 2011, Los Angeles, California, OTHJ2
47. Tao L, Yu J, Yang Q, Shao Y, Zhang J, Chi N (2013) A novel transform domain processing based channel estimation method for OFDM radio-over-fiber systems. *Opt Express* 21(6):7478–7487

48. Li F, Cao Z, Li X, Dong Z, Chen L (2013) Fiber-wireless transmission system of PDM-MIMO-OFDM at 100 GHz frequency. *J Lightwave Technol* 31(14):2394–2399
49. Li X, Yu J, Zhang J, Dong Z, Chi N (2013) Doubling transmission capacity in optical wireless system by antenna horizontal- and vertical-polarization multiplexing. *Opt Lett* 38(12):2125–2127
50. Chowdhury A, Chien HC, Fan SH, Yu J, Chang GKK (2010) Multi-band transport technologies for in-building host-neutral wireless over fiber access systems. *J Lightwave Technol* 28(16):2406–2415
51. Hsueh YT, Jia Z, Chien HC, Chowdhury A, Yu J, Chang GKK (2011) Multiband 60-GHz wireless over fiber access system with high dispersion tolerance using frequency tripling technique. *J Lightwave Technol* 29(8):1105–1111
52. Li X, Yu J, Zhang J, Dong Z, Li F, Chi N (2013) A 400G optical wireless integration delivery system. *Opt Express* 21(16):18812–18819
53. Yu J, Jia Z, Chang GK (2006) Optical millimeter wave generation or up-conversion using external modulator. *IEEE Photon Technol Lett* 18(1):265–267
54. Jia Z, Yu J, Chang GK (2006) A full-duplex radio-over-fiber system based on optical carrier suppression and reuse. *IEEE Photon Technol Lett* 18(16):1726–1728
55. Lin C, Ng'oma A, Lee W, Wei C, Wang C, Lu T, Chen J, Jiang W, Ho C (2012)  $2 \times 2$  MIMO radio-over-fiber system at 60 GHz employing frequency domain equalization. *Opt Express* 20(1):562–567
56. (2004) ITU-T Recommendation G.975.1. Forward error correction for high bit-rate DWDM submarine system
57. Zhang J, Dong Z, Yu J, Chi N, Tao L, Li X, Shao Y (2012) Simplified coherent receiver with heterodyne detection of eight-channel 50 Gb/s PDM-QPSK WDM signal after 1040 km SMF-28 transmission. *Opt Lett* 37(19):4050–4052
58. Dong Z, Li X, Yu J, Chi N (2012)  $6 \times 128$ -Gb/s Nyquist-WDM PDM-16QAM generation and transmission over 1200-km SMF-28 with SE of 7.47b/s/Hz. *J Lightwave Technol* 30(24):4000–4005
59. Dong Z, Li X, Yu J, Yu J (2013) Generation and transmission of  $8 \times 112$ -Gb/s WDM PDM-16QAM on a 25-GHz grid with simplified heterodyne detection. *Opt Express* 21(2):1773–1778
60. Liu C, Chien HC, Fan SH, Yu J, Chang GK (2012) Enhanced vector signal transmission over double-sideband carrier-suppressed optical millimeter-waves through a small LO feedthrough. *Photon Technol Lett* 24(3):173–175
61. Li X, Yu J, Dong Z, Zhang J, Tao L, Chi N, Shao Y (2013) Performance improvement by pre-equalization in W-band (75–110 GHz) RoF system. In: *Proceedings of the OFC 2013, Anaheim, California, OW1D.3*
62. Li X, Yu J, Chi N, Dong Z, Zhang J, Yu J (2012) The reduction of the LO number for heterodyne coherent detection. *Opt Express* 20(28):29613–29619
63. Li X, Dong Z, Yu J, Yu J, Chi N (2013) Heterodyne coherent detection of WDM PDM-QPSK signals with spectral efficiency of 4b/s/Hz. *Opt Express* 21(7):8808–8814
64. Li F, Yu J, Cao Z, Xiao J, Chen H, Chen L (2012) Reducing the peak-to-average power ratio with companding transform coding in 60 GHz OFDM-ROF systems. *J Opt Commun Netw* 4(3):202–209
65. Tao L, Yu J, Fang Y, Zhang J, Shao Y, Chi N (2012) Analysis of noise spread in optical DFT-S OFDM systems. *J Lightwave Technol* 30(20):3219–3225
66. Yang Q, He Z, Yang Z, Yu S, Yi X, Shieh W (2012) Coherent optical DFT-spread OFDM transmission using orthogonal band multiplexing. *Opt Express* 20(3):2379–2385
67. Tang Y, Shieh W, Krongold BS (2010) DFT-Spread OFDM for fiber nonlinearity mitigation. *Photon Technol Lett* 22(16):1250–1252
68. Tao L, Yu J, Yang Q, Luo M, He Z, Shao Y, Zhang J, Chi N (2012) Spectrally efficient localized carrier distribution scheme for multiple-user DFT-S OFDM RoF-PON wireless access systems. *Opt Express* 20(28):29665–29672

# Chapter 7

## Systems Challenges for SDN in Fiber Wireless Networks

Neda Cvijetic and Ting Wang

**Abstract** This chapter will introduce and discuss important system-level challenges for software-defined networking (SDN) in fiber wireless networks, particularly in light of recent networking trends such as 5G mobile networks and the Internet of Things (IoT) paradigm. The presented discussion will cover vital aspects from both the control and data plane perspectives. In the data plane, recent fiber wireless trends surrounding the increasingly strong reliance of advanced mobile systems on fiber-optic networks and the emergence of cloud radio access network architectures with fiber-optic links to/from remote wireless cell sites will be covered in particular detail. Specifically, the high-speed, low-latency optical fronthaul architecture will be regarded as the baseline for future fiber wireless networks, and system-level challenges related to signaling formats, network densification and topology, and optical component selection will be considered. Moreover, the requirements for and ramifications of SDN-based control in fiber wireless networks will be examined. A survey of recent R&D advances in SDN for fiber wireless will also be presented. As potential solutions to important system-level challenges, efficient signaling across the optical network, flexibility in the selection of wavelength division multiplexing (WDM)-based optics components, and support for a dynamic physical-layer topology will be highlighted. In terms of network control and management, a centralized, programmable SDN-based control plane is regarded as an attractive approach to bring about a fiber wireless network evolution featuring automated, programmable end-to-end resource orchestration and ultimately a high quality-of-experience (QoE) for end users.

---

N. Cvijetic · T. Wang (✉)  
NEC Laboratories America, Princeton, NJ, USA  
e-mail: ting@nec-labs.com

*Present Address:*  
N. Cvijetic  
Tesla Motors Inc., Palo Alto, CA, USA

## 7.1 Introduction

The convergence of fixed and mobile networks has been attracting significant attention for years and is a particularly compelling challenge from the systems perspective due to the heterogeneity of underlying technologies [1]. Moreover, as wireless transceivers become part of arbitrary machines and devices (e.g., various smart mobile devices, household appliances, vehicles, distributed sensors, etc.), enabling high-speed, low-latency connectivity between these devices and the Internet through fixed–mobile convergence becomes vital to provisioning new and important services beyond traditional wireless cellular and data connectivity [2]. In this so-called Internet of Things (IoT) networking paradigm [3], the ability to not only interconnect and manage fiber wireless network segments, but also a plurality of mobile devices/connections per person will emerge as a very important performance metric [1, 4]. Consequently, the IoT-based fiber wireless network future will likely not revolve primarily around a data rate increase. Although data rates will certainly continue to climb to multi-Gb/s at the mobile user end, the overall quality-of-experience (QoE) will become just as important. For example, supporting fluid handoffs between services, spectral bands, and mobile devices, and providing a quality-of-service (QoS) hierarchy for dynamic network- and traffic-aware data flow differentiation can be regarded as an important future fiber wireless network QoE criterion. Additionally, more traditional metrics such as network capacity, latency, outage, spectral efficiency, network coverage, and battery longevity will also play a role in the future fiber wireless network performance optimization. This new system-level fiber wireless dynamic thus poses new challenges that require a new set of technology solutions that can enable an overall network evolution from a “cell-centric” to a “device-centric” platform.

In terms of technical solutions, powerful new mechanisms are arising both in the control plane and in the data plane that will have significant system-level impact on the fiber wireless network. From the data plane perspective, massive multiple-input multiple-output (MIMO) systems are a prime example of a powerful new technique with far reaching system-level implications. While MIMO already plays a key role in existing wireless standards, including 4G and Wi-Fi networks, massive MIMO is an orders-of-magnitude scaled-up version of its predecessor, involving hundreds of antenna elements. By spacing transmitter and receiver antennas such that the channel path gains between antenna pairs are independent, theoretical capacity gains that are linearly proportional to the number of transmitter and receiver antenna elements become feasible. In other words, 100 total antennas can translate to  $100\times$  capacity gain. Moreover, by exploiting high radio frequency (RF) signals, such as millimeter-wave carriers, the required antenna element spacing can be reduced to the order of centimeters. In an early demonstration of 5G mobile technology [5], for example, 128 antennas (64 transmitters, 64 receivers) and a 28-GHz RF carrier were exploited to realize up to 1 Gb/s transmission over last-mile access distances. While this is quite impressive, it also has significant system-level ramifications on the fiber wireless network, which will be discussed in

this chapter. Moreover, next to antenna densification through massive MIMO, network densification through a significantly higher number of increasingly smaller and smaller cells is also a new data plane-related technology that is both expected to enhance QoE of future fiber wireless networks and have significant system-level effects on the network. In terms of enhancing QoE, massive MIMO and dense small/pico/femto cells [6, 7] can jointly enable highly advanced enhanced inter-cell interference cancellation (eICIC) and spatially distributed coordinated multipoint (CoMP). These techniques have been shown to dramatically increase both uplink and downlink throughput, with uplink throughput gains reaching the 40–100 % range and downlink throughput gains of 30 % becoming feasible through CoMP techniques, given that centralized processing and very low latency can be provided by the network [6]. On the fixed side of the fiber wireless network, data plane advances have also been tremendous. Specifically, with the advent of increasingly sophisticated multi-level optical modulation, coherent detection, and advanced coding strategies, highly spectrally efficient fiber-optic transmission at terabit-scale data rates have been experimentally demonstrated across fiber-optic network segments [8–10].

In addition to breakthroughs in the data plane, there has also been an advent of control plane innovations for fiber wireless networks. A key motivating factor for this technical trend has been the growing gap that is arising between transmission capacity growth and revenue growth, particularly in fixed networks that support the mobile network front end. This growing and precarious gap has largely been attributed to network management inefficiencies as well as limitations in the ability to support bandwidth on-demand networking that is becoming increasingly important in arbitrary network monetization [11–15]. While it has been noted that these trends apply to all optical network segments, since the heterogeneity of services, traffic pattern dynamicity, cost constraints are highest in the edge-facing fixed portion of fiber wireless networks, the exploration of novel control plane solutions for better orchestrating and managing network resources is perhaps most compelling in this networking context. To this end, software-defined networking (SDN) [16] presents a uniquely valuable opportunity for addressing system-level challenges in fiber wireless networks. In this chapter, the extension of SDN principles to address system-level fiber wireless network challenges will be discussed in detail, with a particular focus on the unique traits of this networking environment and some particular considerations for SDN in this domain. One such consideration is the unprecedented level of heterogeneity of mobile devices and underlying network technologies that future fiber wireless networks may need to address. In such an environment, a centralized intelligent and dynamic SDN-based network management framework optimized for somewhat unpredictable device and traffic dynamics can be regarded as highly valuable. In other words, a device-oriented SDN-based network policy that can differentiate between arbitrary devices and data flows so as to automate hierarchical QoS and enforce network security in a “bring your own device” setting may be regarded as a control plane solution that is just as important to overall QoE as a high-speed, low-latency data plane solution.

In this chapter, the focus will lie on examining system-level challenges for SDN in fixed–mobile convergence ramifications from both the control and data plane perspectives. In the data plane, natural fiber wireless convergence is already happening as advanced mobile techniques are already immutably relying on fixed optical networking through the emergence of cloud radio access network architectures [17–19] in which fiber-optic links to/from remote wireless cell sites are being regarded as the leading solution for sufficiently high-speed, low-latency connectivity. By adopting this architecture as the baseline for future fiber wireless networks, this chapter will explore the system-level challenges related to signaling formats, optical component selection, and physical-layer topology. In terms of system-level solutions, enabling efficient signaling by enhancing common public radio interface (CPRI)-based solutions, enabling support for arbitrary wavelength division multiplexing (WDM) optics components, and enabling a dynamic physical-layer topology are all envisioned to bring about significant benefits. In terms of network control and management approaches, enabling SDN-based control plane is very well positioned to bring about a fiber wireless network evolution and enables a seamless user experience with a high degree of QoE.

The rest of the chapter is organized as follows. Section 7.2 will take a detailed look at the system-level challenges in fiber wireless networks, including signaling formats, network densification, and topology, and propose some corresponding solutions. Section 7.3 will consider the requirements and ramifications of introducing an SDN-based control plane in fiber wireless networks, while Sect. 7.4 will survey recent advances and progress in SDN for fiber wireless networks. Finally, Sect. 7.5 will conclude the chapter.

## 7.2 System-Level Fiber Wireless Network Challenges

In this section, key system-level challenges for fiber wireless network evolution are discussed in greater detail. Each fixed network challenge will be related to an underlying cause in the mobile network segment, with a set of potential solutions also presented. In terms of signaling formats, massive MIMO is regarded as the vital motivating factor for moving beyond CPRI-based signaling across the fixed network. Mobile network densification in terms of the number of cell sites per unit area is treated as a key motivator for the rise of WDM-based networking in the fixed optical network segment. Finally, fixed network topology evolution to a more dynamic networking fabric is discussed as a promising way of supporting all WDM optics types and enabling new features in future fiber wireless networks. Figure 7.1 illustrates the fiber wireless network architecture that serves as the baseline for the discussion of system-level aspects in this chapter.

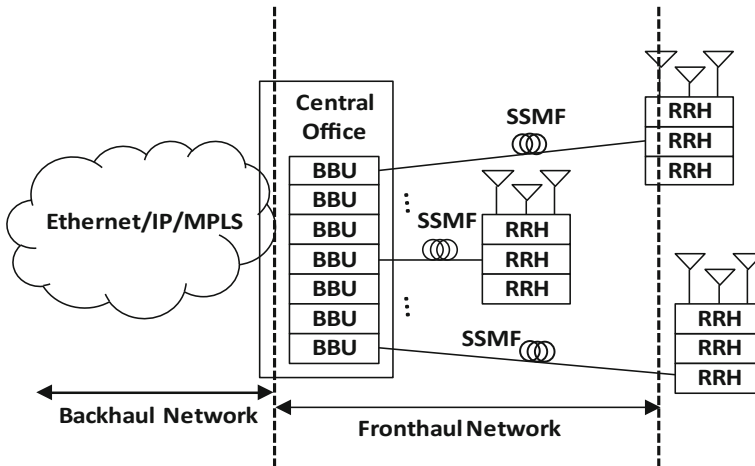


**Fig. 7.1** System-level fiber wireless network architecture featuring centralized/cloud processing and optical fronthaul networks [20]. *IP* Internet Protocol; *MPLS* Multiprotocol Label Switching; *BBU* baseband unit; *SSMF* standard single mode fiber; *RRH* remote radio head

### 7.2.1 Signaling Formats

As shown in Fig. 7.1, the fiber wireless network architecture features centralized cloud processing and a standard single mode fiber (SSMF) optical fronthaul network. It is noted that in optical fronthaul networks, which are currently regarded as a highly attractive solution for the fiber networking part of fiber wireless, one CPRI stream per antenna is to be transmitted across the fixed/optical network. The reasoning for this is that such an approach most comprehensively unleashes the benefits of fully centralized baseband processing, such as the ability to implement advanced downlink and uplink CoMP, for example. However, this approach is also known to exert a very high penalty in terms of bandwidth overhead. As an example, digitizing a 100-MHz signal (e.g., LTE) using 16 bits/sample resolution mandated by CPRI [21], adopting a 30 % compression ratio, and assuming only  $M = 2$  antennas per cell site, the required data rate that needs to be supported for CPRI transmission of digital samples over the optical network is 20.644 Gb/s [22]. Compared to the original signal bandwidth, this represents a two-order-of-magnitude increase. Moreover, since CPRI mandates that the underlying analog radio waveform must be continuously digitized whether it is modulated or not, a high bandwidth overhead is incurred whether the signal is carrying data or not, which prevents the ability to statistically multiplex traffic in the electrical domain. Moreover, while it is conceivable that the large bandwidth consumption penalty can be tolerated for a dual antenna system, in the massive MIMO case with  $M = 100$  rather than  $M = 2$  antennas and all other parameters unchanged, the CPRI bandwidth expansion in the aforementioned example grows to  $\sim 2.1$  Tb/s per cell site, which becomes unsustainable. In terms of optical transmission requirements, more than twenty 100 Gb/s/ $\lambda$  optical transceivers

per cell site would be needed to handle the resulting data rate requirement, which is prohibitive. Some additional bandwidth savings (e.g., up to 50 %) could be gained by increasing the CPRI compression ratio, yet the trade-off for this advantage is the increase in processing latency, which can grow to tens of microseconds [23]. For a total latency budget of  $\leq 150 \mu\text{s}$  in an optical fronthaul fiber wireless network [19], tens of  $\mu\text{s}$  is not an insignificant fraction. Moreover, the fractional bandwidth reduction that can be gained by higher CPRI compression ratios is largely overshadowed by the enormous increases in the number of antennas,  $M$ . For these reasons, advanced techniques for bandwidth efficiency improvement are currently being investigated for future fiber wireless networks [18, 20]. Currently, technology candidates in this space include electrical domain CPRI-to-Ethernet mapping, optical domain CPRI-to-optical transport network (OTN) mapping, and baseband processing function re-allocation between the centralized and distributed units. With electrical domain CPRI-to-Ethernet mapping, multiple variable-rate CPRI channels can be multiplexed via Ethernet to increase bandwidth efficiency. CPRI-to-OTN mapping operates on a similar multiplexing premise in the optical domain. A key advantage of both the electrical and optical domain multiplexing approaches lies in their compliance with mature and commercially proven standards. A disadvantage of both is that they do not in themselves address the inherent CPRI-based bandwidth penalty that arises from high-resolution digitization of an analog waveform. Moreover, additional multiplexing and/or overlays could potentially increase latency in a highly latency-sensitive setting. New CPRI compression algorithms and alternative centralized-versus-distributed processing splits are currently under discussion with the goal to address these challenges.

### 7.2.2 *Network Densification*

In the previous subsection, massive MIMO was discussed as the primary cause for the dramatic increase in the number of antennas per cell site in future mobile systems that will have a strong impact on the fixed network portion. Moreover, in addition to antenna densification, future mobile systems will also feature network densification: a notable increase in the number of cell sites per unit area motivated by the need for spatial reuse of spectrum and improving signal strength coverage through shorter reach cell-to-device transmission. As the number of cell sites grows, the number of connections between the cell sites and the fixed network will also need to follow suit (Fig. 7.2).

The extensive use of WDM technologies in the optical network segment of future fiber wireless networks becomes inevitable, particularly in areas with limited optical fiber connectivity. On the other hand, while trends clearly point to a more extensive use of WDM in future fiber wireless networks, precisely which type of WDM optics should be selected remains largely unclear. Part of the reason for this uncertainty is the high variability in underlying physical-layer optical connectivity

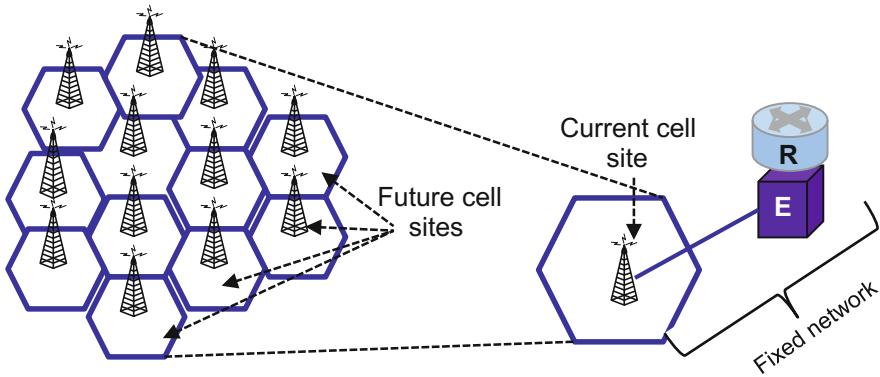


**Fig. 7.2** Illustration of network densification through an increase in the number of cell sites per unit area. *R* router; *E* Ethernet switch

for mobile systems support which can range from point-to-point, to point-to-multipoint/passive optical network (PON), to hybrid topology scenarios. Depending on the underlying topology and required channel count, coarse WDM, dense WDM, colorless WDM, coherent WDM, or a combination of the aforementioned solutions may emerge as the optimal WDM optics selection. Consequently, a single universal WDM optics solution may not be feasible since the relevant deciding metrics exhibit high case-by-case variability. The needed wavelength channel count, for example, can vary significantly depending on the deployment location (i.e., urban vs. suburban vs. rural) and network topology. Indoor versus outdoor environments may also impose a very different set of requirements on WDM optics (e.g., with respect to temperature control), yet both environments will be important to future fiber wireless networks. The need for and degree of per-cell-site coexistence between legacy 2G, 3G, 4G, and emerging, e.g., 5G systems is also an important system-level aspect that may impose potential back-compatibility constraints on WDM optics selection, such as wavelength selection and range. Finally, it is noted that ongoing parallel developments and advances in WDM optics for other short-reach fixed optical network segments, such as datacenter applications, for example, as well as state-of-the-art advances in silicon photonics could also have a strong impact on WDM optics selection in future fiber wireless networks.

### 7.2.3 Network Topology

Network topology is another key system-level challenge for future fiber wireless networks. Echoing the discussion of the previous subsection, it can be stated that certain WDM optics types are naturally better suited for certain fixed network topologies (e.g., PON versus point-to-point architectures). However, given the high

degree of variability expected in future fiber wireless network deployments, rather than placing a priori restrictions on WDM type selection, a more accommodating and comprehensive approach could be to pursue a network topology evolution approach that encompasses all WDM types. The motivation for this approach lies in the fact that WDM-based optical connectivity can be established either by tuning optical transceivers to a common wavelength (e.g., as in a potential scenario using wavelength-tunable optical network units), or routing/switching a common wavelength to a desired optical transceiver set (e.g., as in a potential scenario using fixed wavelength ONUs). The routing/switching approach, which essentially results in a reconfigurable optical network topology, is attractive in that it enables dynamic WDM-based connectivity that does not necessarily depend on the optics type adopted in legacy optical transceivers. In addition to promoting an inclusive WDM optics model, topology re-configurability is also naturally amenable to more mesh-like decentralized networking, with significant benefits to be gained through such network topology evolution. Specifically, a mesh-like topology is advantageous in that it can provide support for on-demand high-speed data flow transfer with a high degree of higher-layer legacy network bypass. In enabling such dynamic network bypass, transmission latency can be notably reduced, improving QoE. Since cost considerations call for efficient reuse of deployed fiber, and deployed fiber links feature fixed topologies, optical topology evolution and re-configurability will require a mix of physical-layer techniques as well as network virtualization/abstraction mechanisms. From the physical-layer perspective, exploiting electrical and optical switching elements can be a promising way to overcome fixed topology limitations and provide support for on-demand connectivity between desired network nodes. In a recent demonstration [4], the first SDN-controlled optical topology-reconfigurable optical mobile fronthaul architecture was proposed and experimentally verified. Specifically, in [4], SDN-based control was used to dynamically configure optical and electrical switching elements for dynamic instantiation of bidirectional CoMP and inter-cell D2D features through match/action combinations in OpenFlow-based control plane flow tables. Dynamic topology reconfiguration was thus enabled, while maintaining back-compatibility with legacy fiber deployments. The results of the demonstration of [4] are discussed in greater detail in Sect. 7.4, while the principles, advantages and system-level challenges of a SDN-based control in fiber wireless networks are overviewed in the following section.

### 7.3 SDN-Based Control Plane

Before delving into the details of system-level challenges for SDN-based control in fiber wireless networks, it is worthwhile to discuss the fundamentals of SDN, as they can help elucidate the role SDN can play in this network segment. Figure 7.3 illustrates the control and data plane architectures for non-SDN and SDN control paradigms. As shown in Fig. 7.3, the term SDN refers to a network in which: (a) the

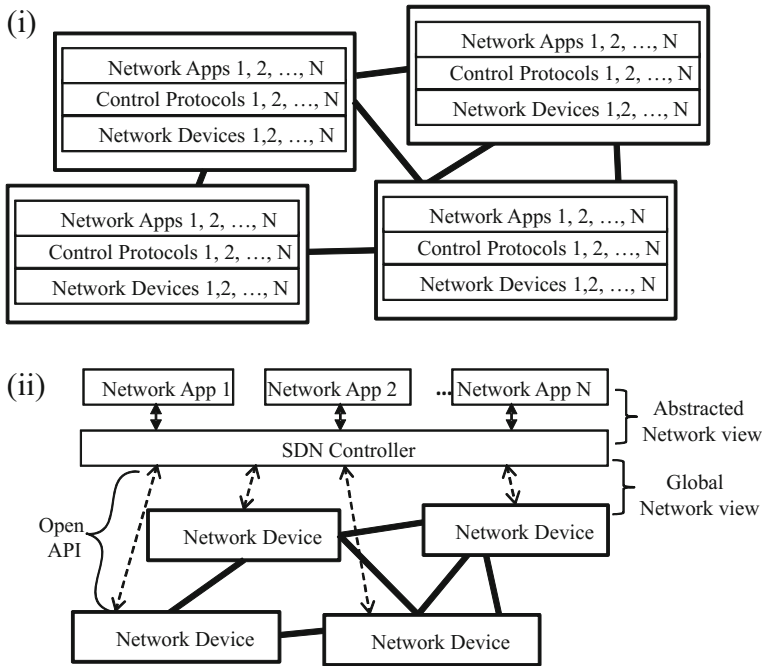


**Fig. 7.3** Control and data plane architectures for: (i, *top*) legacy non-SDN control; and (ii, *bottom*) SDN control

control plane is physically separated from the data (forwarding) plane and (b) a single control plane controls a plurality of devices [16]. It is noted that all the key features associated with SDN—logically centralized control with a global network view, a programmable control plane supporting event-driven network behavior, automated network response, flow-specific traffic differentiation, and multi-vendor interworking using open protocols and interfaces—are in fact ramifications of this definition. It is also noted that the requirement for a unified control plane that is separate from the data plane is fully agnostic to the underlying network type and technologies. Owing to this agnosticity, SDN has been able to rapidly migrate from intra-datacenter, to inter-datacenter, to wide area networks (WAN), as well as to optical transport and mobile/wireless network segments, with the transition to each application domain fueled by the discovery of valuable use cases that feature unique challenges for which an SDN-based approach is well suited. The relevance of SDN to a particular network is thus not a function of network topology or technology, but on the existence of compelling use cases and challenges that SDN is uniquely qualified to address [24].

We can take legacy optical transport networks and fiber wireless networks as an example of the applicability of SDN across seemingly disparate network segments due to the existence of compelling native use cases and challenges in each.

Specifically, in multilayer, multi-segment optical transport networks, manual intervention is currently needed both on the same layer between network domains, and between different layers in the same domain [11–13]. These challenges are known to notably drain profitability, limit dynamic end-to-end resource orchestration, and form a set of highly compelling use cases for SDN-based control in optical transport networks. Moreover, although at first glance, this set of challenges and use cases may seem unique to optical transport, strong analogies can be drawn to challenges and use cases for fixed/mobile and access/aggregation networks that are vital for future fiber wireless systems. In current fixed/mobile and access/aggregation networks, there are simply too many networks/domains such that CAPEX and OPEX are high and end-to-end resource provisioning is not seamless. The promise of SDN in multilayer, multi-segment optical networking, whether it be in the context of optical transport or fiber wireless, lies in a unified, physically separate control plane that can more intelligently and efficiently manage the entire network. An analytical model for this perspective of system-level challenges for SDN was proposed in [25] and evaluated in terms of its ability to minimize latency and cost in multilayer, multi-segment networks with variable degrees of SDN functionality. As was shown in [25], minimizing both latency and energy consumption can be accomplished by minimizing the number of hops between different layers by performing the switching and routing functionality on the lowest network layer whenever possible. A ramification of this observation is that the optical layer should be involved in SDN-based control, such that optical technology can enable both dynamic high-speed transmission and energy-efficient switching while also reducing latency via higher-layer by-pass. However, to do so, the SDN controller must speak the language of the optical layer. Else, mismatches between network resources and applications and/or an overly complicated network management scheme may persist. From a practical perspective, optical-layer SDN control may be implemented by expanding the adopted SDN language to include a standardized, concise optical-layer parameter set. As an example, in [26], the L2–L4 OpenFlow matching rules were extended to include optical-layer parameters (i.e., optical wavelength and modulation format), enabling application-aware, on-demand wavelength provisioning. Such SDN-enabled dynamic optical resource allocation is perhaps particularly compelling in optical access/aggregation networks where dynamic optical-layer circuits can be used to quickly deploy new fiber wireless network services, including mobile fronthaul/backhaul overlays, on-demand enterprise connectivity, and support for datacenter/cloud networking. SDN-based control can thus go a long way in better monetizing existing fixed networks with large prior infrastructure investments (Fig. 7.4).

### ***7.3.1 SDN-Based Control in Fiber Wireless Networks***

It is noted that the technology-agnostic nature of SDN is quite important in SDN applications to fiber wireless networks since they can rely on a plethora of

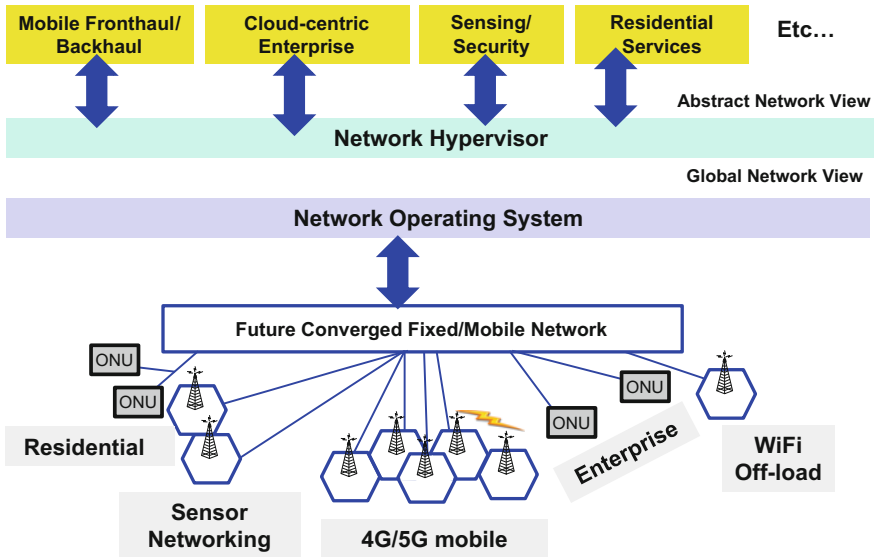


Fig. 7.4 SDN-based control for future fiber wireless systems

underlying fixed network topologies and technologies, including more and more prominently, optical access networks [27–29]. In the optical access networks context, however, there exists a tendency to equate this networking segment with PONs deployed for residential services. However, if optical access is equated only with PON, the first thought on the matter might be that SDN may not be needed for a variety of reasons. First, in certain cases, the PON might be a single domain, single operator, often single vendor network that is too small for SDN to make a significant impact. Secondly, there may not always be a need for network abstraction/virtualization as the underlying services often tend to be homogeneous. For Ethernet-based bit stream services, for example, there may not be an urgent need to differentiate between data flows beyond what is already done in legacy PON. And finally, in legacy PONs, there is no out-of-band control plane with north/south-bound management interfaces to remote optical network units (ONUs).

On the other hand, it can be argued that even if optical access networks are circumscribed to legacy PON, SDN can still introduce valuable benefits into the network, by evolving the degree of programmability in both the optical line terminal (OLT) and the ONUs beyond what is achievable with legacy management and protocols. As an example, it is noted that conventional ONUs do not support the dynamic modification of the high-level network policy that determines how incoming data flows are mapped to logical connections. Instead, these mapping rules are hard-coded and vendor proprietary. Introducing the capability for programmable modification of these rules and policies as a service and implementing it through an open, vendor-agnostic interface such as OpenFlow could create new revenue streams in PON-based fiber wireless networks. Specifically, since legacy

PON technologies already provide quality-of-service (QoS) support by mapping incoming flows into queues, it becomes possible to exploit SDN to map traffic into specific service classes at the OLT and ONU ports, effectively treating the OLT and ONUs of the PON as the backplane of a distributed SDN switch. The resulting data flow differentiation can be attractive across customer verticals including content providers, mobile operators, as well as enterprise and residential customers, and has no dependence on underlying PON technology type. It would, however, require a physically separate control plane. To implement this, exploiting existing centralized OLT-side control that governs ONU bandwidth allocation and management, and extending existing mechanisms, such as the ONU management and control interface (OMCI), could be a promising approach.

Moreover, a more broad future-oriented perspective can also be adopted under which optical access is not equated only to PON, but is regarded as the short-reach optical network infrastructure that will increasingly be needed to handle new traffic types, particularly from mobile applications. Recent trends of short-reach fiber-optic connections to a highly diverse set of end users are becoming increasingly pervasive, such that novel optical access network segments continue to emerge, including mobile fronthaul/backhaul and cloud/data-centric enterprise connectivity, which will feature different traffic dynamics and technology requirements compared to legacy counterparts, and will also unleash new opportunities for the optical access infrastructure, particularly in the fiber wireless networking context [30–34]. These trends underscore the need for a unified, programmable control plane across optical access segments and layers and emerge as a key motivating factor for extending SDN to the future fiber wireless space. Without unified SDN-based control, running multiple control and management planes in parallel will continue to be inevitable, resulting in bandwidth/resources orchestration challenges typical for legacy multilayer, multi-segment networks, as discussed above. Under the more broad future fiber wireless networking oriented perspective, a clear need exists for underlying network abstraction and virtualization, more nuanced traffic differentiation, and more advanced control mechanisms, all of which form compelling use cases for SDN in fiber wireless systems. We recall that for future fiber wireless networks, optimizing user QoE will be regarded as a key performance metric, such that the ability to dynamically and efficaciously share the network among competing services, prioritize important traffic flows, and quickly provide new services will become vital. It is thus highly desirable to implement the dynamic topology-reconfigurable approach discussed in Sect. 7.2.3 through SDN-based control of optical and electrical switching elements. In this context, SDN offers a highly attractive system-level solution for centralized, unified, protocol- and vendor-agnostic control that effectively realizes a dynamic mesh-like architecture which incorporates legacy fiber links. In addition, from a network policy perspective, SDN-based control is a very good fit for increasingly unpredictable “bring your own device” (BYOD) networking environments in which both security and QoE would need to be correctly enforced amidst growing device heterogeneity. By binding packets with a common logical association (i.e., data flows) to a specific device with a unique high-level name, rather than binding them to a lower level



OOK signals without tunable optical filtering or optical coherent detection. In the control plane, the motivation for adopting an SDN-based approach in [26] lies with the introduction of software-reconfigurable flex-grid (or grid-less)  $\lambda$  planning at the OLT side rather than defining a fixed physical  $\lambda$  plan, as has been done in previous PON generations. Consequently, through the SDN-based approach of [26], wavelengths can be made available on-demand without requiring a single universally agreed upon physical wavelength plan, which can be attractive for future fiber wireless systems that will need to support arbitrary and often unpredictable emerging applications requiring dynamic optical-layer circuit overlays. With the flex-grid SDN-based approach, a centralized controller with a global view of the  $\lambda$ -space would compute customized on-demand  $\lambda$ -provisioning metrics, use these to determine a wavelength plan, and communicate the results to software-defined optical transceivers tasked with implementing them using an OpenFlow-based application programming interface (API). The OpenFlow-based API can thus serve to provide both external interoperability and agile, customized physical  $\lambda$  plans. From a practical perspective, the OLT-side  $\lambda$ -space virtualization can be supported by widely tunable distributed feedback (DFB) lasers, for which notable cost reduction in the C-band has been observed, bringing cost points very close to those of fixed wavelength lasers. Moreover, in [26], an SDN-based control approach was also proposed for the upstream through the adoption of software-controlled flex-grid filters designed to track upstream wavelengths and create dynamic, spectrally efficient pass-bands for them, which can effectively relax ONU-side upstream tunable laser requirements and also reduce the required upstream spectral band size. The experimental verification of [26] featured an OpenFlow 1.0-based flex-grid  $\lambda$ -flow architecture for 150 Mb/s per-cell OFDMA mobile backhaul overlays onto PONs consisting of bidirectional 10 Gb/s OOK channels. By extending OpenFlow 1.0 to control OLT-side tunable lasers, dynamic optical-layer flows were created to enable joint downstream transmission of OFDMA and OOK signals at software-variable flex-grid  $\lambda$  channel spacings ranging between 41.25 and 141.25 GHz. Both the OFDMA and OOK signals were directly photodetected without receiver-side optical filtering, optical amplification, or coherent detection over 20 km SSMF with a 1:64 passive split. In the upstream, OpenFlow 1.0 was extended to control an OLT-side flex-grid wavelength selective switch (WSS), creating a software-tunable passband for spectrally efficient upstream transmission in the presence of ONU-side upstream laser wavelength drift. The reach and split ratio of this approach were both subsequently doubled in [30, 32] to 40 km SSMF with a 1:128 passive split by applying optical Nyquist filtering on the 10 Gb/s OOK signals to reduce the post-detection spectral overlap between the downstream OFDMA and OOK signals. A software-defined throughput optimization algorithm was proposed in [33], while a software-defined transceiver architecture that enables reconfigurable dual-mode CPRI versus OFDMA mobile fronthaul/backhaul over PON was also introduced in [34]. Software-defined advanced modulation and bit labeling for coexistence between legacy OOK and next-generation DSP-based OLTs and ONUs and optical access network virtualization were discussed in [35, 36], respectively. The first real-time OFDM-PON platform with OpenFlow-based dynamic control of OFDM signal parameters, including OFDMA subcarrier allocation and modulation

format selection, was presented in [37], with SDN control of 100 Gb/s OFDM transceivers demonstrated in [38].

From the control plane perspective, novel centralized resource allocation and network management algorithms were proposed and evaluated in [31, 39]. In [31], optical network virtualization was considered through the novel “meta-MAC” concept introduced to abstract physical-layer differences between heterogeneous flows in the same network through a virtual sub-wavelength frequency domain mapping. In other words, the goal of the software-defined OFDMA-based “meta-MAC” concept is to overcome the inherent physical-layer differences and disparate bandwidth requirements between different technologies and traffic flows expected to coexist in future access and fiber wireless systems. At the core of the OFDMA meta-MAC concept proposed in [31] is a centralized bandwidth arbitration process with a global network view that manages the medium access control (MAC) protocols of several “virtual PONs” (VPONs) under its domain, and exploits virtualized OFDMA subcarrier units for dynamic bandwidth provisioning. To do so, a sophisticated three-stage dynamic bandwidth allocation scheme was presented in [31], comprising: VPON admission, bandwidth assignment, and spectrum allocation. The first step—i.e., VPON admission—was analytically formulated as a multiple knapsack problem for finding the optimal solution for a number of admitted VPONs, while a load-balancing heuristic was subsequently proposed to further increase spectrum utilization. A bandwidth provisioning arbitration method was also proposed to ensure fair bandwidth allocation among VPONs. Finally, two schemes for the third step (i.e., spectrum allocation) were discussed in [31], one featuring compact spectrum assignment and one featuring free-range (scattered) spectrum allocation, with each scheme targeting a different service type. All of the approaches proposed in [31] were verified via custom real-time traffic simulations under many different network scenarios. The results indicated that adopting a flexible, software-defined resource allocation approach can be highly advantageous for maximizing spectrum utilization in future multi-technology and multi-service fiber wireless networks. More recently, a joint bandwidth provisioning and cache management scheme for software-defined PON building on the meta-MAC concept was introduced and evaluated in [39].

As mentioned earlier in this chapter, mobile systems will continue to evolve to their fifth-generation (5G), such that the QoE, as measured by the capability to efficaciously interconnect and manage a plurality of mobile connections per person as a device-centric “Internet of Things” will become increasingly important [1–4]. To achieve this goal, 5G networking is expected to strongly rely on advanced techniques, such as massive MIMO, as well as on decentralized device-to-device (D2D) connectivity that can effectively bypass the network to achieve ultra-low-latency short-range transmission. To enable optical fronthaul architectures that can flexibly interconnect many remote radio heads (RRH), BBU pooling and virtualization have been proposed to overcome topology limitations through a centralized processing approach in which resources are dynamically moved across a single virtual BBU platform that manages many spatially distributed RRHs

[17, 18]. Centralized BBU processing, along with efficient usage of BBU processing resources, will be crucial for enabling bidirectional CoMP in future 5G fiber wireless networks. However, to virtualize physically distinct BBUs into a single platform, ultra-low-latency connectivity between them will be needed. To achieve this goal, centralized rather than distributed control may be more attractive. Moreover, under its current formulation, D2D communication cannot exploit the fixed network and is limited to wireless communication between parties that are in very short range of each other. To overcome these limitations that can strongly affect QoE, centralized SDN-based control of optical and electrical switching can be introduced into the optical mobile fronthaul network, evolving it into a novel topology-reconfigurable fiber wireless network architecture that is both back-compatible with legacy fiber and can support high-speed and low-latency inter-BBU connectivity, efficient bidirectional CoMP, and inter-cell D2D with a high degree of network bypass. It is noted that both electrical and optical switching are incorporated into the architecture to enhance flexibility by routing flows along different paths based on their granularity and/or QoE requirements, as well as to increase redundancy by supporting multiple potential paths in case of failure. Finally, with an open SDN-based centralized control interface such as OpenFlow, advanced features can be implemented in a dynamic fashion through match/action combinations in control plane flow tables. The SDN-based OpenFlow approach thus boasts transparency across protocols, switch types, and vendors.

Figure 7.6 illustrates the topology-reconfigurable optical mobile fronthaul architecture recently proposed and demonstrated in [4]. As shown in Fig. 7.6, at the central office, the BBU pool is linked to the electrical SDN-controlled OpenFlow switch, as well as  $10^+$  Gb/s software-defined optical transceivers, and an any-to-any optical switch. The optical and electrical switches and the optical transceivers are all under the domain of an SDN controller featuring an OpenFlow-based API. Through software-defined control of optical and electrical switch ports (a)–(f) and software-defined optical Tx ports (1)–(9), advanced features such as CoMP, low-latency inter-cell device-to-device (D2D) connectivity and inter-BBU transmission can be enabled in support of future fiber wireless networks. As illustrated in Fig. 7.6, a *FlowMod* control message comprising a single-match and two actions can be used to implement downlink CoMP, by which the downlink user data from BBU A is sent from transmitter port (a) of the OpenFlow switch to dual receiver ports (i) and (k). This scenario models both downlink CoMP from two transmitters to a single user at the aggregate peak rate, as well as downlink CoMP of the same aggregate message to multiple users at sub-peak per-user rates. Next, as shown in Fig. 7.6, two single-match, single-action *FlowMod* messages can be invoked to merge uplink traffic from transmitter ports (j) and (l) onto a common receiver port (d) for processing in BBU B to model uplink CoMP from a single user to two transmitters featuring comparable uplink channels. Finally, a single-match-action *FlowMod* interconnecting designated BBU transmitter and receiver ports can be exploited to support low latency, high-speed inter-BBU connectivity, and also enable inter-BBU load balancing. Optical downlink CoMP, in which the downlink user data from BBU A is sent from transmitter port (a) of the OpenFlow switch to

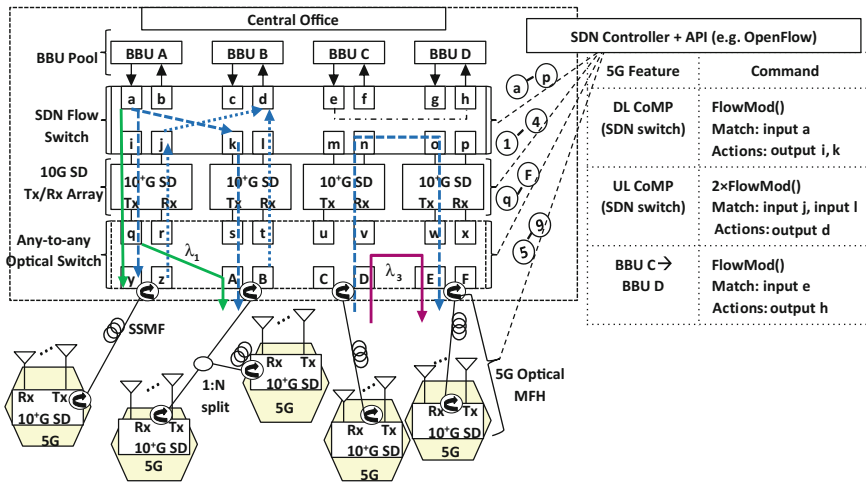


Fig. 7.6 Proposed SDN-controlled topology-reconfigurable optical MFH architecture for bidirectional CoMP and low-latency inter-cell D2D [4]. Tx transmitter; Rx receiver

an optical input port (q) and subsequently multicast to optical output ports (y) and (A) of Fig. 7.6 can moreover be supported via SDN control of an optical switch. An any-to-any optical switching architecture capable of supporting this feature is shown in detail in Fig. 7.7 for a  $4 \times 4$  structure with downlink and uplink tunable wavelength sets  $\lambda_1-\lambda_4$  and  $\lambda_5-\lambda_8$ , respectively. As observed from Fig. 7.7, the any-to-any optical switch differs from a conventional optical switch in its capability to support optical downlink multicasting as well as loopback functionality. It is noted the optical switch port labels in Fig. 7.7 are matched to those of Fig. 7.6. To enable optical downlink CoMP, the SDN controller configures port A of the 1:2 WSS in Fig. 7.7 to output downlink wavelength  $\lambda_1$  instead of the inactive downlink wavelength  $\lambda_4$  by using a *FlowMod* control message extended to support  $\lambda$ -based WSS pass-band tuning. By deactivating the downlink wavelength  $\lambda_3$  and re-tuning the uplink wavelength  $\lambda_5-\lambda_3$  using an extended *FlowMod* message, a low-latency loopback path for inter-cell D2D can moreover be created in the optical switch through the 1:2 colorless optical couplers (Fig. 7.7). Low-latency, energy-efficient inter-cell D2D can thereby be achieved by optical loopback through ports D and E without needing to access higher network layers. Inter-cell D2D connectivity can likewise be implemented by linking transmitter and receiver ports (n) and (o) of the electrical SDN switch (Fig. 7.7), yet this would yield higher latency due to the multilayer optical-to-electrical-to-optical data path. In the experimental evaluation of the architecture of Fig. 7.6 and the optical switch of Fig. 7.7 in [4], it was found that 10 Gb/s peak per-cell rates can be supported with  $<7 \mu\text{s}$  back-to-back transmission latency and a 29.6 dB power budget, corresponding to 10 km SSMF reach with a 1:512 passive split. In terms of latency, the optical switching approach enabled  $\leq 4 \mu\text{s}$  latency even with maximum 10 Gb/s Ethernet packet size (1518

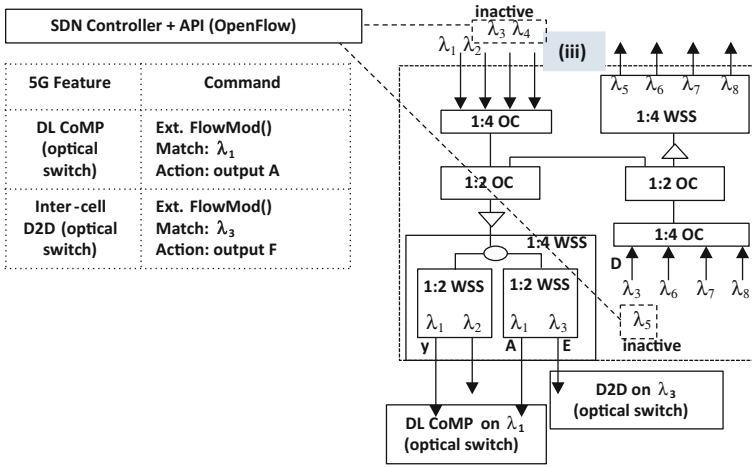


Fig. 7.7 Any-to-any optical switch architecture for optical multicast and loopback functions [4]. OC optical coupler; WSS wavelength selective switch

bytes), while in the electrical switching case, latency rose to 6.3  $\mu$ s, which was attributed to buffering delay that grows with packet size in the SDN electrical switch. By enabling advanced networking features, this new approach is promising for future fiber wireless systems with SDN control.

### 7.5 Conclusions

The above work has introduced the reader to system-level challenges for SDN in fiber wireless networks, including important aspects from both the control and data plane perspectives. In the data plane, organic fiber wireless convergence is already under way as advanced mobile technologies are more prominently relying on fiber-optic networks through the emergence of cloud radio access network architectures in which fiber-optic links to/from remote wireless cell sites are emerging as the leading solution for high-speed, low-latency fronthaul, and backhaul connectivity. By adopting the optical fronthaul architecture as the baseline for future fiber wireless networks, this chapter has examined the system-level challenges related to signaling formats, optical component selection, and physical-layer topology, as well as their ramifications on SDN-based control in fiber wireless systems. As potential solutions, efficient signaling across the optical network, flexibility in the selection of wavelength division multiplexing (WDM)-based optics components, and support for a dynamic physical-layer topology are all envisioned to introduce significant benefits. In terms of network control and management, a centralized, programmable SDN-based control plane is very well positioned to bring about a fiber wireless

network evolution featuring automated, on-demand end-to-end resource orchestration and ultimately a high degree of QoE for end users.

## References

1. Okumura Y, Terada J (2014) Optical network technologies and architectures for backhaul/fronthaul of future radio access supporting big mobile data. In: Proceedings of 2014 IEEE/OSA optical fiber conference (OFC), San Francisco, CA, March 2014, paper Tu3F.1
2. Bangerter B, Talwar S, Arefi R, Stewart K (2014) Networks and devices for the 5G era. *IEEE Commun Mag* 51(2)
3. Gubbi J, Buyya R, Marusic S, Palaniswami M (2013) Internet of things (IoT): a vision, architectural elements, and future directions. *Future Gener Comput Syst* 29(7):1645–1660
4. Cvijetic N, Tanaka A, Kanonakis K, Wang T (2014) SDN-controlled topology-reconfigurable optical mobile fronthaul architecture for bidirectional CoMP and low latency inter-cell D2D in the 5G mobile era. *OSA Opt Express* 22(17):20809–20815
5. <http://www.technologyreview.com/news/515631/samsung-says-new-superfast-5g-works-with-handsets-in-motion/>. Accessed June 2013
6. Parsons G, Ruffini S, Pearson T (2013) Mobile backhaul for small cells. IEEE Communication Society webinar. <http://webcast.you-niversity.com/comsoc>. Archived Nov 20 2013
7. Bojic D, Sasaki E, Cvijetic N, Wang T, Kuno J, Lessmann J, Schmid S, Ishii H, Nakamura S (2013) Advanced wireless and optical technologies for small-cell mobile backhaul with dynamic software-defined management. *IEEE Commun Mag* 51(9):86–93
8. Qian D et al (2011) 101.7-Tb/s ( $370 \times 294$ -Gb/s) PDM-128QAM-OFDM transmission over  $3 \times 55$ -km SSMF using pilot-based phase noise mitigation. In: Proceedings of the 2011 IEEE/OSA optical fiber conference (OFC), paper PDPB5
9. Huang YK et al (2012) Real-time transoceanic transmission of 1-Tb/s Nyquist superchannel at 2.86-b/s/Hz spectral efficiency. In: Proceedings of the ACP 2012, paper PAF4C.2
10. Cvijetic N, Cvijetic M, Huang M-F, Ip E, Huang Y-K, Wang T (2012) Terabit optical access networks based on WDM-OFDMA-PON. *IEEE/OSA J Lightwave Technol* 30(4)
11. Gringeri S, Bitar N, Xia TJ (2013) Extending software defined network principles to include optical transport. *IEEE Commun Mag* 51(3)
12. Simenidou DE, Nejabati R, Channegowda M (2013) Software defined optical networks technology and infrastructure: enabling software-defined optical network operations. In: Proceedings of the 2013 IEEE/OSA optical fiber conference (OFC), Anaheim, CA, March 2013, paper OTh1H.3
13. Liu L et al (2012) First field trial of an OpenFlow-based unified control plane for multi-layer multi-granularity optical networks. In: Proceedings of the 2012 IEEE/OSA optical fiber conference (OFC), Los Angeles (CA), March 2012, paper Tu3F.1, paper PDP5D.2
14. Woesner H, Fritzsche D (2013) SDN and OpenFlow for converged access/aggregation networks. In: Proceedings of the OFC 2013, paper OTu3E.4
15. Cvijetic N (2013) Software-defined optical access networks for multiple broadband access solutions. In: Proceedings of the OECC 2013, paper TuP2-1
16. Open Networking Foundation. [www.opennetworking.org/](http://www.opennetworking.org/)
17. China Mobile Research Institute. C-RAN the road toward green RAN. White Paper v2.5. [http://labs.chinamobile.com/cran/wpcontent/uploads/CRAN\\_white\\_paper\\_v2\\_5\\_EN.pdf](http://labs.chinamobile.com/cran/wpcontent/uploads/CRAN_white_paper_v2_5_EN.pdf)
18. Chanclou P et al (2013) Optical fiber solution for mobile fronthaul to achieve cloud radio access network. In: Proceedings of the 2013 future network and mobile summit, July 2013

19. Nishimura K, Agata A, Nanba S, Optical access technologies for rapidly expanding mobile data traffic accommodation. In: Proceedings of the 2013 optoelectronics and communications conference (OECC), Kyoto, Japan, July 2013, paper WP4-3
20. Cvijetic N (2014) Optical network evolution for 5G applications and SDN control. In: Proceedings of the Networks 2014, paper Thu.18.4
21. Common Public Radio Interface. <http://www.cpri.info/>
22. Cvijetic N, Tanaka A, Cvijetic M, Huang Y-K, Ip E, Shao Y, Wang T (2013) Novel optical access and digital processing architectures for future mobile backhaul. *IEEE J Lightwave Technol* 31(4)
23. Samardzija D, Pastalan J, MacDonald M, Walker S, Valenzuela R (2012) Compressed transport of baseband signals in radio access networks. *IEEE Trans Wireless Commun* 11(9)
24. Cvijetic N, Tanaka A, Ji P, Sethuraman K, Murakami S, Wang T (2014) SDN and OpenFlow for dynamic flex-grid optical access and aggregation networks. *IEEE J Lightwave Technol* 32(4)
25. Cvijetic N, Angelou M, Patel AN, Ji PN, Wang T (2013) Defining optical software-defined networks (SDN): from a compilation of demos to network model synthesis. In: Proceedings of the OFC 2013, paper OTh1H.1
26. Cvijetic N, Tanaka A, Ji PN, Murakami S, Sethuraman K, Wang T (2013) First OpenFlow-based software-defined  $\lambda$ -flow architecture for flex-grid OFDMA mobile backhaul over passive optical networks with filterless direct detection ONUs. In: Proceedings of the OFC 2013, paper PDP5B.2
27. Cvijetic N (2014) SDN for optical access networks. In: Proceedings of the 2014 OSA photonics in switching, San Diego, CA, paper PM3C.4, July 2014
28. Bitar N (2014) SDN and potential applicability to access networks. In: Proceedings of the OFC 2014, paper Th1G.4
29. Parol P, Pawlowski M (2013) Towards networks of the future: SDN paradigm introduction to PON networking for business applications. In: Proceedings of the IEEE FedCSIS 2013, pp 829–836
30. Tanaka A, Cvijetic N, Wang T (2013) First optical Nyquist filtering of 10G OOK for OFDMA  $\lambda$ -overlays on 40 km and 1:128 split PON. In: Proceedings of the OECC 2013, Kyoto Japan, paper PD3-1, July 2013
31. Kanonakis K, Cvijetic N, Tomkos I, Wang T (2013) Dynamic software-defined resource optimization in next-generation optical access enabled by OFDMA-based meta-MAC provisioning. *IEEE/OSA J Lightwave Technol* 31(14)
32. Tanaka A, Cvijetic N (2014) Software defined flexible optical access networks enabling throughput optimization and OFDM-based dynamic service provisioning for future mobile backhaul. *IEICE Trans Commun* E97-B(7):1244–1251
33. Cvijetic N, Wang T (2013) Software-defined throughput optimization for next-generation optical mobile backhaul. In: Proceedings of the OECC 2013, paper TuP1-4
34. Cvijetic N, Tanaka A, Kanonakis K, Huang YK (2012) Software-defined heterogeneous 100 Gb/s mobile backhaul with 1000<sup>+</sup> per-fiber cell counts. In: Proceedings of the OECC 2012, paper PDPD1-2
35. Iiyama N, Kim SY, Shimada T, Kimura S, Yoshimoto N (2012) Co-existent downstream scheme between OOK and QAM signals in an optical access network using software-defined technology. In: Proceedings of the OFC 2012, paper JTh2A.53
36. Yoshimoto N, Kani J, Kim SY, Iiyama N (2013) DSP-based optical access approaches for enhancing NG-PON2 systems. *IEEE Commun Mag* 51(3)
37. Johnson S, Mo W, Cvijetic M, He J, Wissinger J, Willner A (2014) Real-time software-defined dynamic resource allocation using OpenFlow for next-generation OFDM-based optical access networks. In: Proceedings of the OFC 2014, paper Tu2F.5

38. Yoshida Y et al (2014) First international SDN-based network orchestration of variable-capacity OPS over programmable flexi-grid EON. In: Proceedings of the OFC 2014, paper ThA.2
39. Li X, Kanonakis K, Cvijetic N, Tanaka A, Qiao C, Wang T (2014) Joint bandwidth provisioning and cache management for video distribution in software-defined passive optical networks. In: Proceedings of the OFC 2014, paper Tu3F.5

**Part III**  
**Novel Network Architectures**  
**for Fi-Wi Networks**

# Chapter 8

## Architectural Evolution and Novel Design of Fiber-Wireless Access Networks

Cheng Liu

**Abstract** As the industrial trend is moving toward 5G wireless technology, the important role that optical fiber plays in high-speed mobile backhaul and fronthaul networks is becoming more essential. In this chapter, we introduce several key enabling technologies for 5G, with emphasis on the role of optical fibers in access networks. Existing and emerging fiber-wireless (Fi-Wi) access network architectures (e.g., macrocells, small cells, distributed antenna systems (DAS), and cloud radio access networks (C-RANs)) are reviewed. A novel Fi-Wi access network design based on cloud radio-over-fiber (cloud-RoF) architecture is also introduced and experimentally demonstrated.

### 8.1 Introduction

Mobile data traffic growth due to the proliferation of smart mobile devices and bandwidth-demanding applications is accelerating the evolution of radio access networks (RAN) from 2G, 3G to 4G and beyond. Looking into the future, 5G wireless technology is on the horizon. The exact definition of 5G is still under active discussions with many on-going activities in both industry and academia [1–3]. However, a consensus has been reached on the basic requirements of future wireless communication systems: (1) support for the massive growth in the number and evolving diversity of emerging devices (e.g., connected cars, Internet of Things (IoT), machine-to-machine communications); (2) support for the continuous growth in data traffic especially due to real-time and bandwidth-demanding applications (e.g., video traffic, online gaming); and (3) support for diverse applications with various requirements (e.g., latency, data rate, mobility, user density, power consumption, always-on applications). It is to be noted that all of the aforementioned requirements have to be realized in an affordable and sustainable way which, in of itself, is the biggest challenge for network operators and system vendors.

---

C. Liu (✉)  
AT&T Labs, Atlanta, USA  
e-mail: cl906f@att.com; lch.ian12@gmail.com

Considering the evolution of key enabling technologies for 5G, future directions are listed as summarized in [4] and shown in Fig. 8.1. To maximize link spectral efficiency, existing wireless technologies for point-to-point transmission within a given RF bandwidth have been pushed very close to the Shannon theoretical limit by using high-level modulation formats (e.g., 64-QAM-OFDM), multiple-input and multiple-output (MIMO) techniques, and advanced channel coding schemes (e.g., low-density parity-check (LDPC) and turbo codes). However, there is great potential for enhancing the spectral efficiency of the system as a whole. For example, techniques such as cognitive radio that allocates underused or “white space” spectrum dynamically can improve the system spectrum efficiency [5]. In addition, by coordinating adjacent cells to jointly transmit/receive signals to/from cell-edge users, coordinated multi-point transmission (CoMP) [6] can significantly improve throughput for the cell-edge user, thus enhancing the overall system spectral efficiency. In another dimension, there is always demand for more RF spectrum. Notwithstanding the release of obsolete lower-frequency analog TV bands, further available spectrum is mostly confined to higher radio frequencies (i.e., millimeter-wave bands [7, 8]). Finally, small cells are expected to be a key component of future wireless communication network topologies. By reducing the cell size, limited spectral resources can be reused aggressively among the small cells, thus enhancing the total system capacity. However, managing inter-cell interference and reducing cost are key issues associated with small cell deployment. In addition, a WLAN (e.g., Wi-Fi) hot spot can be considered as a special case of a “small cell,” and its integration with cellular systems can provide seamless roaming and enhance user experience. For this reason, WLAN-cellular integration has drawn significant interest and is being considered as a basic requirement for 5G [9].

From the network architecture perspective, the design of a 5G network should consider how to incorporate the billions of emerging (IoT) devices and to support

	<b>Future Potential</b>	<b>Example Techniques</b>
<b>Link spectrum efficiency</b>	<i>near limit</i>	<i>massive MIMO, new waveforms, etc.</i>
<b>system spectrum efficiency</b>	<i>great potential, but challenging</i>	<i>cognitive radio, CoMP, SON, etc.</i>
<b>more spectrum</b>	<i>mostly in higher frequencies</i>	<i>mm-wave, microwave, white spaces, etc.</i>
<b>smaller cells</b>	<i>almost unlimited potential, but expensive</i>	<i>femtocell, picocell, microcell, nanocell, etc.</i>

Fig. 8.1 Directions for 5G radio access networks [4]

them in a scalable and cost-effective way. This may lead to significant changes in the architecture of mobile networks and related mobility management mechanisms [10]. In addition, new techniques such as software-defined networks [11] and network function virtualization [12] have shown great potential to simplify and scale the network, increase flexibility, facilitate innovation, and lower the cost [13]. These emerging techniques can be used as building blocks and supporting platforms for the design of future networks.

To support the ever-increasing data rate in 5G radio links, the design of high-speed and cost-effective backhaul and fronthaul networks, which connect cell sites to the core network, is of paramount importance. In today's cellular network, various types of backhaul/fronthaul networks are used. They differ in terms of both the underlying transport media (e.g., electrical cable, fiber, and microwave) and carried signal transmission format (T1 (transmission system 1), Ethernet, CPRI (common public radio interface), etc.). Given the fact that higher and higher data rates will be transported over the backhaul/fronthaul network, optical fibers have been considered as the ultimate wired solution to provide sufficient bandwidth for future backhaul/fronthaul demands. Therefore, the integration of fiber-optic networks and wireless access networks has become an important topic requiring interdisciplinary research efforts.

In this chapter, consistent with the development of 5G wireless technology, we emphasize the important role that fiber optics play in future integrated fiber-wireless access networks. An overview of existing and emerging fiber-wireless access network architectures is given, including conventional macrocells and small cells, distributed antenna systems, and emerging cloud-RAN architectures. Finally, a novel cloud radio-over-fiber architecture is introduced as a promising candidate for future fiber-wireless access systems.

## **8.2 Overview of Existing Fiber-Wireless Access Architectures**

### ***8.2.1 Macrocell and Small Cell with Fiber-Optic Backhaul***

In this section, existing macrocell and small cell architectures are briefly reviewed with emphasis on backhaul networks and on the role that fiber optics play in existing networks.

Cellular networks were originally designed to cover a large cell area using low frequencies that carried only voice services. However, as new services emerged and cellular technologies continued to evolve, the conventional macrocell architecture could no longer meet the bandwidth load, especially with the emergence of smart phones. Over the years, the cell size of macrocell systems in the suburban/urban areas has decreased significantly, from 10 to 20 km radius in the 1990s–2000 time period, to today's 500 m–1 km radius. In some ultra-dense urban areas

(e.g., Manhattan, New York City), the cell size can be as small as  $\sim 100$  m radius. Higher overall system capacity is attained through more aggressive spectral reuse inherent in smaller macrocell topologies.

Different from the macrocell, but following the same trend of reducing the cell size, the “small cell” concept emerged around 2008 that aims at enhancing capacity at “HOT spots” or providing coverage at “NOT spots.” Today, the “small cell” is used as an umbrella term for operator-controlled, low-powered radio access nodes, including those that operate in a licensed spectrum and unlicensed carrier-grade Wi-Fi [14]. Small cells typically have a range from 10 to 700 m and are usually deployed as separate networks on top of macrocell systems.

Since the network architecture and backhaul requirements for macrocells and small cells differ substantially, we will review them separately as follows.

Macrocells have evolved with time and can therefore be characterized by succeeding generations of cellular systems that have different system architectures, names, and different associated backhaul networks. A high-level overview of different cellular network architectures and backhaul techniques is shown in Fig. 8.2. A typical cellular system consists of three major parts: the radio link, the backhaul network, and the mobility core network. The first two parts are usually considered together and referred to as the radio access network (RAN). The radio link starts from the user equipment (UE) and terminates at cell sites. Each cell site is connected to the mobility core network through a backhaul network. Different cellular generations have different names for the cell site equipment (e.g., base transceiver station (BTS), NodeB, eNodeB), RAN equipment (e.g., base station controller (BSC), radio network controller (RNC)), and the core network equipment (mobile switching center (MSC), serving/gateway GPRS support node (SGSN/GGSN),

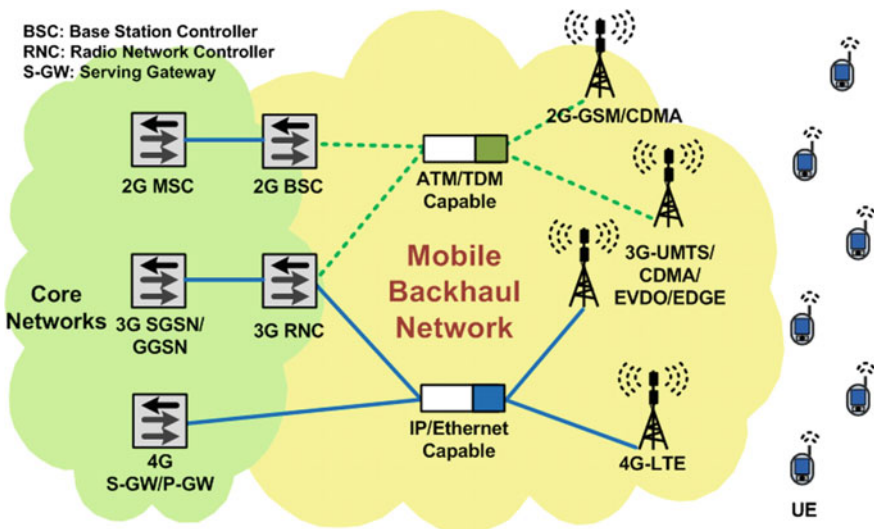


Fig. 8.2 Macrocell backhaul networks overview

serving gateway/packet data network gateway (S-GW/P-GW), etc. In addition, the technologies and functions of the equipment across different generations are very different. While a detailed summary of the technology differences between cellular generations is not the focus of this chapter, it is nevertheless worth it to include a brief synopsis that can facilitate the comparison of generational backhaul networks and emphasize the importance of optical fibers in macrocell backhaul networks.

In today's networks, the backhaul network for most of the 2G systems and for a small number of 3G systems is T1-based, utilizing a time-division multiplexing (TDM) technique. For most of the 3G systems and all of the 4G systems, Ethernet/IP-based backhaul transmission is used. Considering the underlying transport media, T1 lines are natively copper-based transmission lines. But when optical fibers are available to those 2G/3G cell sites, T1 signals can be mapped into other signal formats to be carried over optical fibers. Ethernet/IP-based backhaul primarily uses optical fibers as the transport medium. The shift from copper-based backhaul to fiber-based backhaul is due to the significant advantages of optical fiber in capacity, range, and reliability. Therefore, looking into the future, the backhaul networks of 5G macrocells will be all fiber based.

As noted above, the term "small cell" is used broadly to designate low-powered radio access nodes that operate in a licensed or unlicensed carrier-grade Wi-Fi spectrum, with a range of several meters up to several hundred meters. There are many types of small cells including femtocells, picocells, nanocells, microcells, and metrocells. They are designed for different application scenarios, as illustrated in Fig. 8.3 [14] and described below.

**Femtocell:** A low-power, short-range, self-contained base station is initially used to describe consumer units intended for residential homes. The term has expanded to encompass higher-capacity units for enterprise, rural, and metropolitan areas. Key attributes include IP backhaul, self-optimization, low power consumption, and ease of deployment.

**Picocell:** It is typically used to describe low-power compact base stations, used in enterprise or public indoor areas. The term is sometimes used to encompass outdoor small cells as well. Some care is required in selecting the number and location of these cells for indoor use, although the self-optimizing features of newer picocells, borrowed from femtocell technology, reduce the number of trained technicians required.

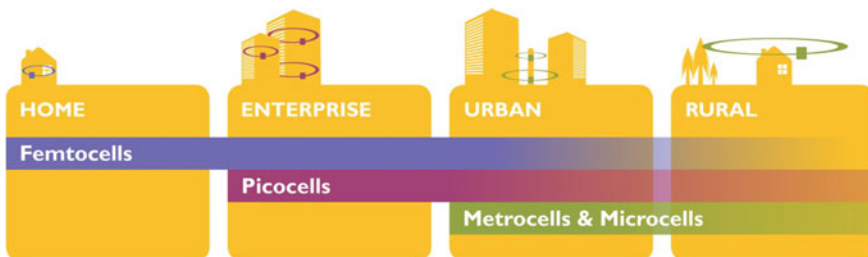


Fig. 8.3 Small cell application scenarios [14]

**Nanocell:** A newly developed small cell concept that integrates cellular small cells (e.g., picocell, femtocell, etc.) with carrier-grade Wi-Fi access points (APs). It is generally deployed in enterprise, hot spots, and home scenarios.

**Microcell:** It is typically used to describe an outdoor short-range base station designed to enhance coverage for both indoor and outdoor users where macrocell coverage is insufficient. It is occasionally installed indoors to provide coverage and capacity in areas above the scope of a picocell.

**Metrocell:** A recent term used to describe small cell technologies designed for high-capacity metropolitan areas. Such devices are typically installed on building walls or street furniture (e.g., lampposts and utility poles). This category can include technologies such as femtocells, picocells, and microcells that meet these deployment criteria.

Because there are many different types of small cells that are deployed in different scenarios for different purposes, there are many choices for their backhaul solutions depending on the specific deployment scenario.

A high-level view of the backhaul networks for different types of small cells is shown in Fig. 8.4 [14]. In general, small cells can use any type of Internet connection to backhaul traffic between the radio access node and the mobile operator's core network. The backhaul connection can be a wire-based solution [e.g., direct fiber, passive optical networks (PON), digital subscriber lines (xDSL), hybrid fiber-coaxial (HFC) cable, etc.] or a wireless-based solution (e.g., microwave, millimeter wave, TV whitespace, satellite) [15]. The backhaul network can be owned by the mobile network operator or provided by a 3rd Party Internet Service Provider (ISP). For example, the indoor femtocell deployment for residential homes typically leverages the existing high-speed Internet connection to the home. The connection may be based on fiber to the home (FTTH), xDSL, or cable access, which may be provided by a 3rd Party ISP. Therefore, in this case, the femtocell backhaul traffic first traverses the 3rd Party ISP's network and then connects to the mobile operator's core network. In the case of outdoor microcells and metrocells, a typical deployment practice is to leverage existing macrocell backhaul toward the core network. The challenge is in the last mile between the street-level microcells/metrocells and the local "aggregation point" (as explained below). The backhaul solutions for such deployment scenario can be categorized into two types: wired backhaul solutions and wireless backhaul solutions. For wireless backhaul solutions, it is suggested that in many cases the macrocell site itself may be used as an aggregation point, as it is generally well positioned to provide coverage down to the street level. For wired backhaul solutions, the aggregation point is likely to be a street cabinet or an exchange building.

In general, if optical fibers are available to a small cell site, optical fiber-based backhaul is ideal due to its high capacity, low latency, and high reliability. Otherwise, other backhaul solutions may be used according to the specific environment. In future small cell systems, we can expect that more small cells will use optical fiber-based backhaul as the penetration of optical fibers in the last-mile access network is gaining momentum.

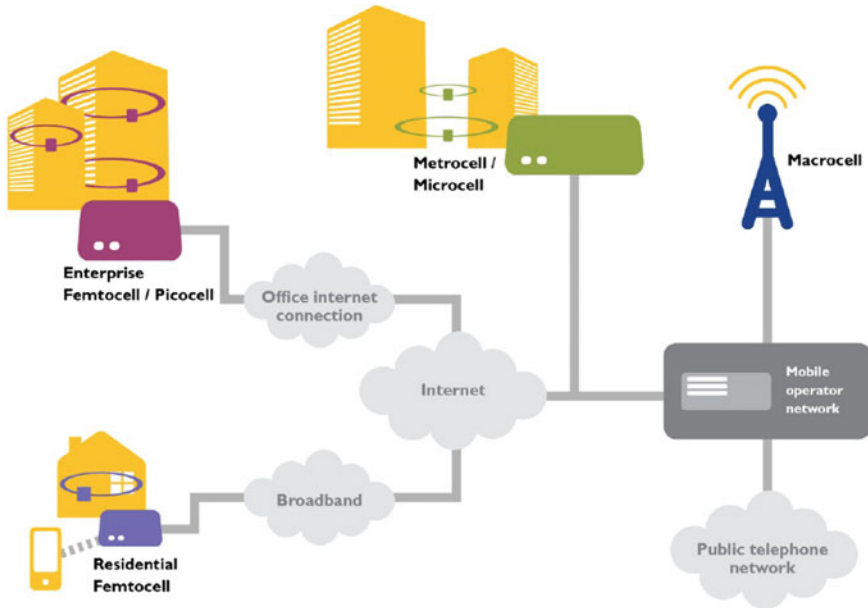


Fig. 8.4 Small cell backhaul overview [14]

## 8.2.2 Distributed Antenna System

In addition to small cells, distributed antenna system (DAS) networks are often deployed by mobile network operators to provide coverage in targeted locations as well as to provide additional capacity in areas with concentrated demands for wireless services. Before we introduce the details of a typical DAS network design, a comparison between DAS and small cell networks is given below, because these two terms are often used interchangeably with some degree of confusion.

There are several similarities between DAS nodes and small cell nodes. For example, they both transmit at much lower power levels than those transmitted by macrocells, and they are both physically much smaller than macrocell nodes. However, DAS networks and the various types of small cells differ greatly with respect to functionality, capacity, complexity, and cost, among other things [16]. Their network architectures and technologies are not interchangeable, and each is suitable only for the particular purpose and deployment environment that each is designed to address.

In contrast to DAS, small cells are typically deployed gradually (piece by piece) to provide coverage or enhance capacity in much smaller areas with a single wireless communications technology for a single wireless carrier. While each small cell installation is similar to a single DAS node installation, an appropriately

configured small cell can generally be deployed quickly to provide an immediate solution to a smaller and more isolated coverage/capacity challenge in a manner that requires much less upfront design work, planning, and capital investment than a DAS facility. More importantly, DAS networks differ from small cells because the distributed architecture of a DAS network—including the design and configuration of the high-capacity fiber-optic network providing interconnectivity and the ability to operate large numbers of DAS nodes from a central hub location—makes the typical DAS network a much more robust, scalable, flexible, and efficient solution to a range of capacity and coverage challenges compared to small cells. For example, a DAS network can be deployed to simultaneously accommodate multiple wireless frequencies and technologies for two or more wireless service providers. A DAS network can also be designed or relatively easily retrofitted to handle 2G, 3G, and 4G commercial frequencies that operate in a large range of spectra.

An example of a neutral-host DAS network that supports multiple generations of wireless technologies (e.g., 2G, 3G, 4G) from multiple mobile operators (MO) is shown in Fig. 8.5. In general, a DAS network consists of three primary components: (i) a number of remote communications nodes [DAS node(s)], each including at least one antenna for transmitting and receiving RF signals to and from mobile user equipment; (ii) a high-capacity signal transport medium (typically optical fiber) connecting each DAS node back to a central communications hub site; and (iii) radio transceivers or other head-end equipment located at the DAS hub site that propagates, converts, and processes the communication signals transmitted and received through the DAS nodes. In the example of a neutral-host DAS network shown in Fig. 8.5, at the DAS hub site multiple generations of wireless signals from multiple mobile operators are sent to a neutral DAS hub. The wireless signal source may be a macrocell sector, a small cell, or an RF repeater (note: An RF repeater uses rooftop antennas to draw capacity from a nearby macrocell and rebroadcasts the RF signal. Its capacity is shared with the donor cell). The neutral DAS hub then processes, multiplexes, and distributes the signal to DAS nodes over optical fiber or copper cable (optical fiber is preferred). The signal transmission format in the transport network is either digital baseband or analog RF. At the DAS node, the signal is sent to mobile users through an RF antenna. The same procedure applies to the reverse link.

DAS networks can require significant upfront capital investment because of the size and complexity of the network. The initial up-front cost includes installation, equipment, system configuration, bringing power to multiple DAS nodes, and the extensive fiber-optic cabling or other transport links that provide high-capacity connectivity between each of the DAS nodes and the central hub site. It is this initial investment in careful network design and the construction of high-capacity network connectivity, as well as the significant investment in central hub and DAS node equipment that makes DAS networks a flexible and scalable long-term solution. However, amortization of the initial investment and profitability for the DAS network provider and mobile operators may be many years in the making.

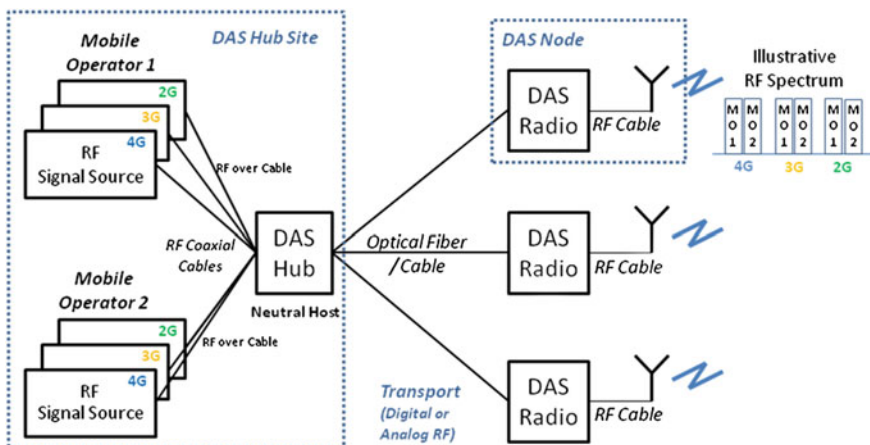
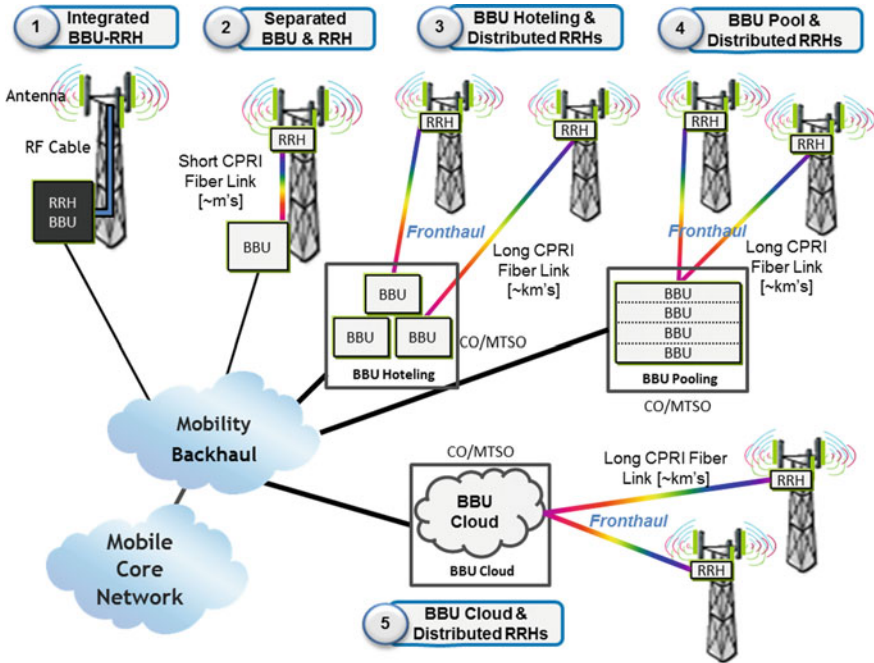


Fig. 8.5 Neutral-host DAS network architecture [16]

### 8.2.3 Cloud Radio Access Network (C-RAN)

Cloud radio access network (C-RAN) is a relatively new cellular network architecture first proposed by China Mobile [17] around 2010. The basic concept of cloud-RAN is to separate the digital baseband processing units (BBUs) of conventional cell sites, from the largely analog remote radio heads (RRHs), and move the BBUs to the “cloud” (BBU hotel, BBU pool, and cloud datacenter) for centralized signal processing and management. Therefore, conventional complicated and power-hungry cell sites can be simplified to RRH only, which reduces capital expenditures (CAPEX) and operational expenditures (OPEX) related to power consumption and site maintenance. In addition, from the performance perspective, the centralized BBU processing simplifies network management and enables more advanced and efficient coordination among cells, thus providing enhanced overall system performance.

The evolution from a conventional macrocell to a C-RAN-based network is illustrated in Fig. 8.6. Early generation macrocells include integrated BBU and RRH equipment located at the bottom of a cell tower with heavy RF electrical cables connecting to RF antennas at the top of the tower (Step 1 in Fig. 8.6). Due to the significant RF signal propagation loss in the electrical cable feed, resulting in degraded signal transmission/reception power and quality, a separated BBU and RRH scheme was widely adopted and is used in most of today’s macrocell site designs (Step 2). In this scheme, the BBU equipment that deals with network layers 2–3 (MAC and IP layer) and some part of layer 1 (PHY layer, e.g., pre-coding and data modulation) is located at the bottom of the cell tower. I/Q samples of the modulated data stream generated by the BBU are carried over a high-speed fiber-optic interface to the RRH at the top of the tower. CPRI (common public radio interface) is the most commonly used fiber-optic interface protocol today. At the



**Fig. 8.6** Evolution path from conventional macrocell to C-RAN-based architecture

RRH, the I/Q samples are multiplexed, digital-to-analog converted (DAC), filtered, RF upconverted, amplified, and transmitted to the mobile users through RF antennas (the reverse procedure applies to the reverse link). Optical fibers are used as the only practical media to carry the high-bit-rate CPRI I/Q samples between the BBU and RRH due to its high-bandwidth, low-loss, and low-weight nature. Typically, the CPRI fiber link distance is short (less than one hundred meters to cover the height of the cell tower). If the separation between BBU and RRH is further extended and several BBUs are centralized at one location, as shown in Steps 3–5, they are considered as C-RAN architectures.

Steps 3 and 4 are considered to be the predecessor of the ultimate cloud-based RAN architecture (Step 5). Step 3 is sometimes also referred to as BBU centralization or BBU hoteling (see Chap. 3.3), in which many BBUs are co-located at a central office (CO) or mobile telephone switching office (MTSO), but each of the BBUs is independent and running on specialized hardware, as is the case today. The connections between the BBU hotel and RRHs are based on long-distance CPRI fiber links, which are typically referred to as the “fronthaul,” as opposed to the backhaul link between the MTSO and core networks. Various fronthaul topologies are feasible, including point-to-point fiber links, daisy chains, and ring topologies.

Signals transmitted on the fronthaul links are CPRI-based I/Q samples, same as the Step 2 case. Regarding the distance limitations of long CPRI links, in the current 4G-LTE system, the CPRI link is typically limited to around 20 km due to the latency requirement of the uplink synchronous hybrid automatic repeat request (HARQ) defined in the LTE protocol.

Step 4 is called BBU pooling, where BBU hardware (HW) resources are shared among the co-located BBUs. But the shared platform is still based on dedicated HW. The final step, Step 5, is the “cloud-based” RAN, where the BBUs’ functions are running on commercial off-the-shelf (COTS) hardware in the data center “cloud.” The last two steps are aligned with the current trend of network functions virtualization (NFV) [12] in wide area networks (WAN) and data centers. The concept of NFV is to share network resources through the abstraction and isolation of network functionalities, a concept adapted from server virtualization, which has achieved great success in the evolution of cloud-based data centers. In the context of radio access network virtualization (RAN virtualization), in order to share hardware resources among different cells and eventually virtualize them to run on general purpose processors (GPPs), the centralization of baseband processing functions is the first step.

The benefits of C-RAN and RAN virtualization include reduced OPEX and CAPEX and improved system performance by centralized processing and management. However, the major challenge of C-RAN deployment is the cost and availability of high-speed fiber-optic fronthaul networks. Even though most of the macrocell sites are currently connected with optical fiber links, the signal transmission format in the conventional fiber-optic backhaul (Ethernet-based frames) is very different from the signal format in CPRI-based fronthaul. CPRI-based fronthaul architectures use much higher data rates (typically 10 times higher) due to the nature of the digitized I/Q samples and have more stringent latency requirements. This requires upgrade of existing backhaul transport interface devices or sometimes a separate wavelength service.

It is to be noted that the C-RAN architecture can be applied to small cells as well. In the small cell environment, the BBU hotel/pool/cloud can be located at the “aggregation point” of the small cell network and can be connected with many small cell RRHs through high-speed CPRI fiber links. From the system performance perspective, the implementation of C-RAN architecture over small cells [or heterogeneous network (HetNet) environment] is very attractive because of the simplified small cell radio nodes and the enhanced interference management capability provided by the C-RAN architecture. The only implementation hurdle is the requirement for a high density of dedicated high-speed CPRI fiber links for the fronthaul. Given the fact that fiber penetration is gaining momentum, we can expect that the C-RAN-based network architecture will prevail in the future for both macrocell and small cell systems, as well as in the coordinated HetNet environment.

### 8.3 Novel Cloud Radio-Over-Fiber Access Architecture

#### 8.3.1 Generic Cloud-RoF Architecture and Operational Principle

After a brief recapitulation of existing fiber-wireless access networks, this section will introduce a novel cloud radio-over-fiber access network architecture. This proposed architecture is aligned with the centralized BBU concept in the C-RAN architecture. It can further simplify the RRH and can provide infrastructure-sharing capability among multiple wireless services [18].

A comparison between the network architectures of conventional macrocell, emerging cloud-RAN, and cloud-RoF is illustrated in Fig. 8.7. As discussed in the C-RAN architecture, the C-RAN cell sites are simplified to RRH only by shifting layer 2–3 functions and some layer 1 baseband signal processing functions to a centralized location (e.g., at the CO or MTSO). By doing so, the conventional Ethernet-based backhaul is changed to CPRI-based fronthaul. The transport media are also changed from various choices of cable, fiber, or microwave to the optical fiber, exclusively.

The transition from C-RAN to cloud-RoF can occur by simplifying the RRH through shifting DAC/ADC and RF frontend functions to the BBU. Therefore, only optical-to-electrical (O/E) and electrical-to-optical (E/O) conversion modules and RF antennas are needed in the modified RRH, which is now referred to as the remote antenna unit (RAU). Since the RF frontend is now shifted to the BBU, the RF signals are generated at the BBU and transmitted to RAUs through the fiber-optic fronthaul network. Therefore, the signal transmission format in the fronthaul network is analog radio, hence the name “radio-over-fiber.”

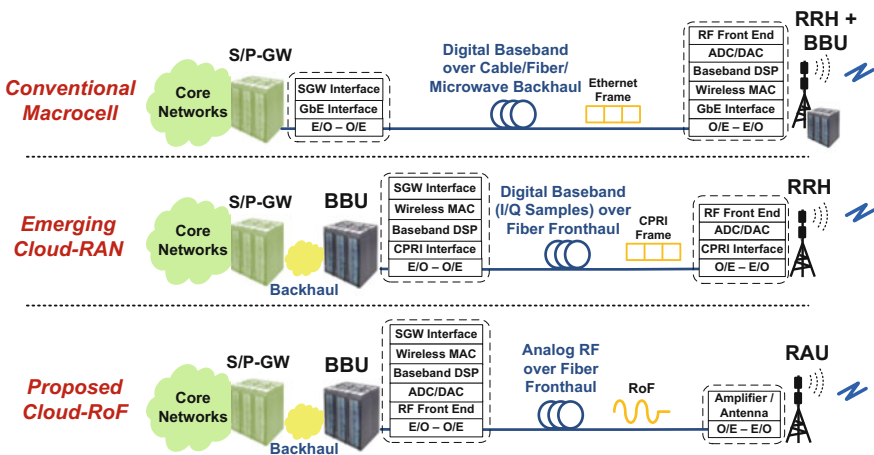


Fig. 8.7 Comparisons between conventional macrocell, C-RAN, and cloud-RoF [18]

The advantages of this new cloud-RoF architecture are multifold: (1) RAUs are greatly simplified and wireless standard agnostic. Conventionally, the transition of wireless standards from 2G to 3G and from 3G to 4G requires upgrade of both BBU and RRH. However, in the cloud-RoF system, since the modified BBU takes all the signal processing responsibilities including RF generation, the RAU is protocol agnostic and transparent to any wireless technologies. When a wireless technology upgrade is needed, the upgrade operation only needs to be done in the central office without a site visit. In addition, since BBUs are implemented in the cloud environment by running dedicated software over COTS hardware through NFV, we can expect that the transition and upgrade of wireless standards can be done by a simple software upgrade in the “cloud.” This provides significant OPEX and CAPEX savings compared to the traditional approach. (2) Due to the protocol-independent feature of the cloud-RoF system, multi-band, multi-service, and multi-operator wireless services can coexist in the system by sharing the RoF fronthaul network and RAUs. This infrastructure-sharing feature can help reduce the cost related to system deployment and utilization and also provide versatility to the cloud-RoF access network. (3) The bandwidth requirement of O/E and E/O modules in the cloud-RoF system is less compared to the C-RAN system for conventional wireless services below the millimeter-wave band. Since signals are transmitted in analog RF form in the cloud-RoF fronthaul, the required bandwidth that O/E and E/O modules have to cover is the highest carrier frequency of the wireless signal (typically below 5 GHz for conventional wireless services). Also, this bandwidth requirement remains the same regardless of the RF bandwidth in each band and of the number of RF bands that need to be simultaneously transported. In contrast, in CPRI-based C-RAN fronthaul, the typical bandwidth requirement of an O/E and E/O module for current LTE system with 20 MHz RF bandwidth, 3 sectors, and  $4 \times 4$  MIMO antenna, is around 10 Gb/s. In addition, this bandwidth requirement increases linearly when a wider LTE channel bandwidth is used or multiple wireless services (e.g., 3G and 4G) are transmitted simultaneously. (4) Similar to the centralized BBU concept in C-RAN, cloud-RoF maintains the separation between BBUs and RAUs, thus maintaining the performance advantages of effective network management and inter-cell coordination. In addition, cloud-RoF systems can leverage BBU pooling and cloud-based virtualization techniques that are being developed in C-RAN systems.

Nevertheless, notable challenges remain for the implementation of cloud-RoF access networks. First of all, the design requirements of analog O/E and E/O interfaces at both the BBU and RAU sites are different from the conventional digital baseband-over-fiber system. High linearity is required for optical signal generation, detection, and in the fiber channel. Nonlinearity-induced interference in radio-over-fiber systems is an important issue which has been investigated in some recent works [19, 20]. In addition to supporting both legacy wireless services and future-proof wireless services at higher carrier frequencies (e.g., millimeter-wave band), the bandwidth requirement of the analog RoF interface becomes much higher.

In the following sections, two proof-of-concept experimental demonstrations of cloud-RoF systems are presented. The first demonstrates the feasibility of multi-operator coexistence and infrastructure sharing in a cloud-RoF system based on RoF and WDM techniques, while the second introduces two types of interface design that support the coexistence of legacy services and future-proof millimeter-wave services in a cloud-RoF access system.

### 8.3.2 Reconfigurable Cloud-RoF Architecture with WDM Techniques

In this section, a proof-of-concept experiment based on an in-building small cell cloud-RoF test bed is presented. The work is briefly introduced here, and it is shown how WDM techniques can be utilized in a cloud-RoF system to provide re-configurability and flexibility. Additional details about this work can be found in [21].

A schematic diagram of the small cell cloud-RoF test bed is shown in Fig. 8.8, where an example of two-operator coexistence in the cloud-RoF system is illustrated. At the BBU pool, where the centralized digital processing power is located, baseband data traffic from core networks is processed and up-converted to RF via base stations (BSs), where a BS here includes both BBU and RRH functions. Since different operators and/or wireless services occupy different RF spectral bands,  $f_1$ ,  $f_2$ , and  $f_3$  represent the RF carrier frequencies of signals from different BSs. Each downstream RF signal is then intensity modulated onto a different CWDM optical wavelengths,  $\lambda_1$ ,  $\lambda_2$ , and  $\lambda_3$ , respectively, using integrated off-the-shelf optical transceivers (Tx/Rx in Fig. 8.8, where Tx/Rx are E/O and O/E modules, respectively, as mentioned in the previous section) for bidirectional intensity modulation

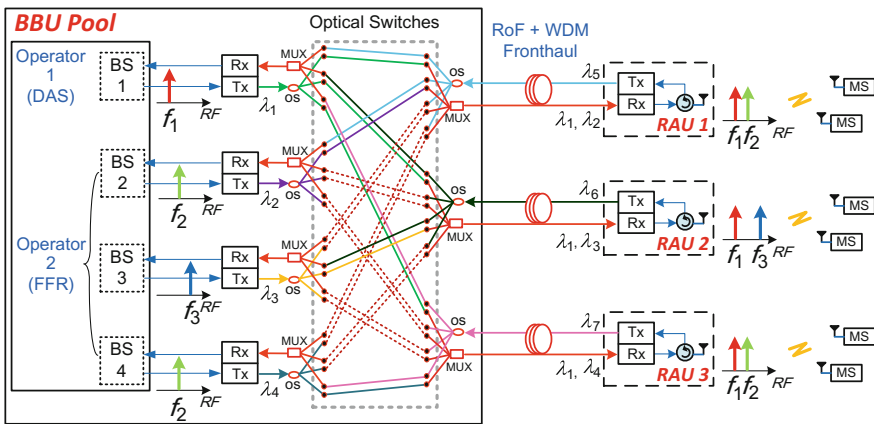


Fig. 8.8 System diagram of cloud-RoF access network using WDM techniques [21]

and direct detection (IM-DD). Optical splitters (OS) and CWDM multiplexers (MUX) are used at the BBU pool to split and multiplex the downlink and uplink signals. An off-the-shelf optical switch with built-in independent on-off sub-switches is used to establish reconfigurable fiber-optic fronthaul connections between the centralized BBUs and distributed RAUs. Notice that the reconfigurability of the network architecture is done in the optical domain by using optical switches in this proof-of-concept experiment. However, the reconfigurability can also be realized in the electrical domain within the BS pool.

Two system configurations are considered for two hypothetical operators: distributed antenna system (DAS) and fractional frequency reuse (FFR) [22]. The term “DAS” as used here refers to the signal distribution scheme rather than the particular architecture and technology that has been implemented in the field today (as introduced in the previous sections). In the DAS scenario, the same signal from a single BS is distributed to all three RAUs to extend coverage, especially for mobile users. However, all mobile subscribers (MS) in the coverage area share the total bandwidth. On the other hand, in the FFR scenario, different signals from 3 BSs are transmitted to different RAUs to exploit frequency reuse. In this particular example (frequency reuse factor of 2), RAU1 and RAU3 will reuse the same spectrum ( $f_2$ ) in nonoverlapping geographic regions without interference. Therefore, MSs occupy the dedicated bandwidth of each RAU. While DAS provides less hand-off complexity and better power efficiency to mobile users, FFR increases total system capacity especially for static users. In this example, Operator 1 uses the DAS scheme to serve mobile users, while Operator 2 adopts the FFR scheme to serve static users. The two operators share the same fiber-optic fronthaul as well as the same RoF transceivers at RAUs. This is enabled by the combination of RoF and WDM techniques.

Based on this system architecture, an in-building WiMAX small cell cloud-RoF test bed was set up as shown in Fig. 8.9a. Four WiMAX BSs were centralized at the BBU pool, while three RAUs were distributed in the building and connected to the BBU pool using standard single-mode fiber (SSMF) as shown by the red line on the floor plan in Fig. 8.9a. As shown in Fig. 8.9b, one WiMAX BS ( $f_1$ ) is used in the DAS configuration to serve two mobile users MS1 and MS2 along a moving path, denoted by checkpoints L1–L7 (dashed green line). The remaining WiMAX BSs are used in the FFR configuration ( $f_2$  and  $f_3$ ; reuse  $f_2$  for BS2 and BS4), serving two static users (SS1 and SS2). Both DAS and FFR configurations were running simultaneously. The output RF signals of four BSs are carried on four CWDM wavelengths with 4 dBm per- $\lambda$  optical launch power. The measured downlink throughputs for the DAS and FFR scenarios are shown in Fig. 8.9c, d, respectively. For Operator 1, since the DAS configuration is used, the mobile users experience no degradation in the steady 6 Mb/s throughput while moving across three small cells (L1–L7 and back), even at the cell edges, highlighting the key coverage benefits of DAS. For Operator 2, since FFR with a reuse factor of 2 was exploited for static users, the system throughput is doubled to 12 Mb/s for each user, which demonstrates the capacity benefits of the FFR scheme. Consequently, this architecture enables both operators to simultaneously run different network configurations by sharing the in-building fronthaul and RAU infrastructure, without interference.

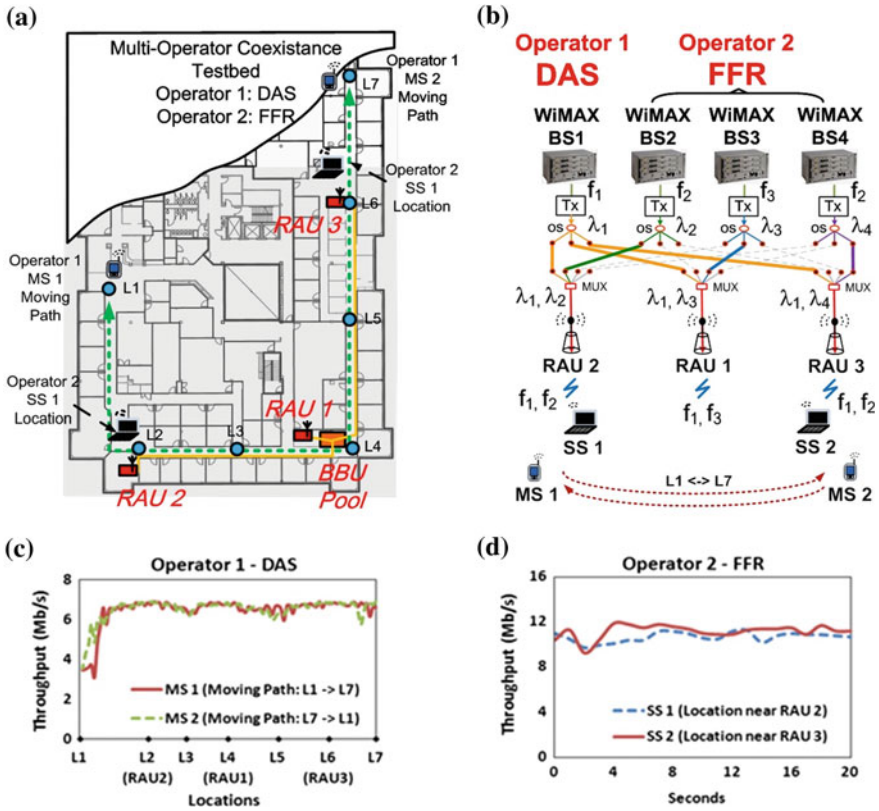


Fig. 8.9 a In-building cloud-RoF test bed showing multi-operator coexistence capability; b detailed network configuration (with only downlink shown here); c measured downlink throughput of mobile users of Operator 1 at different locations; d measured downlink throughput over time for static users of Operator 2 [21]

### 8.3.3 Multi-Service Delivery Including Future-Proof Millimeter-Wave Services

In addition to supporting the coexistence of multiple operators using the same wireless technology, the cloud-RoF system is capable of delivering different generations of wireless services carried on different radio frequencies in a shared infrastructure.

As mentioned in the introduction, short-reach, higher radio frequencies are the new frontier for 5G wireless communication. The RF spectrum, with some examples of existing services, is shown in Fig. 8.10. We can see that the lower microwave band (300 MHz–3 GHz) where conventional cellular services reside has become very congested. However, the higher end of the microwave band, in particular the millimeter-wave (mm-wave) band (30–300 GHz), is attracting

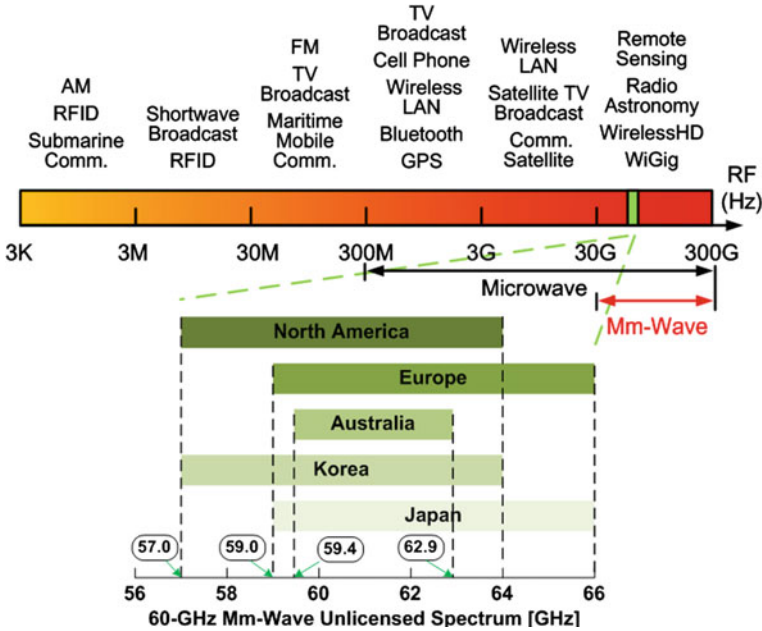


Fig. 8.10 RF spectrum and 60-GHz millimeter-wave band [18]

increased attention due to its abundant spectral resources to potentially deliver 1000× throughput over short distances, suitable in an urban environment, as required by 5G. Within the mm-wave band, the 60-GHz band with 7-GHz license-free bandwidth, in particular, has been a fertile R&D ground for many start-ups over the last decade. Many organizations are working on the standardization of the 60-GHz band for high-speed wireless communications, including wireless local area network (WLAN) [23] and wireless personal area networks (WPAN) [24]. However, a millimeter-wave killer application suitable for cellular communication is still at an early research stage [25–27]. Of course, there are many challenges with mm-wave cellular communications. For example, the line-of-sight (LOS) channel requirement may limit the use of mm-wave radio for short-range semi-static use cases only. Also, high-speed but low-cost fronthaul/backhaul networks to support many mm-wave small cells are critical for the success of mm-wave cellular implementation.

Due to the analog nature of radio-over-fiber techniques, different wireless services including future-proof mm-wave services can coexist in the cloud-RoF system. Two possible implementations (all-band RoF and band-mapped 60-GHz RoF systems) are considered as shown in Fig. 8.11.

In the all-band RoF scheme (Fig. 8.11a), existing lower-RF services and mm-wave services are transmitted at their original carrier frequencies, providing backward compatibility and simplicity. The whole RF spectrum is modulated and transmitted in the RoF fronthaul link. On the other hand, the band-mapped mm-wave

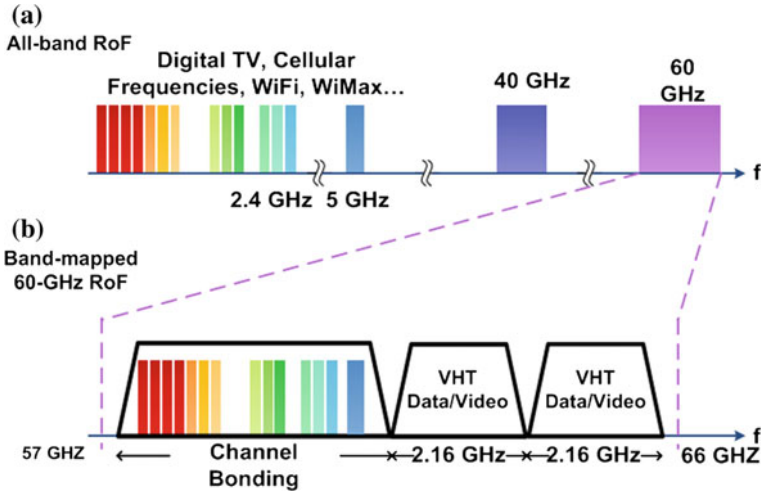
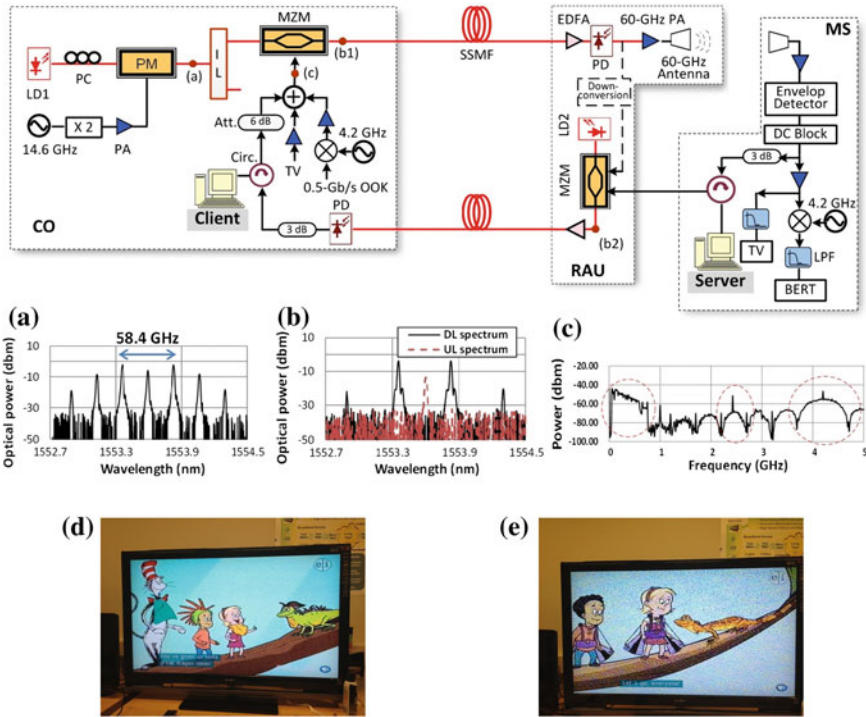


Fig. 8.11 Spectrum allocations in **a** all-band RoF and **b** band-mapped 60-GHz RoF systems [28]

RoF scheme (Fig. 8.11b) fully utilizes the wide 7-GHz bandwidth at 60 GHz and divides it into several sub-bands to deliver band-mapped existing services and high-speed data services in separate sub-bands. Therefore, only the spectrum around 60 GHz is modulated and transmitted in the fronthaul link, which may provide better performance with less cost since narrow-band RoF transceivers can be used.

In the following section, a proof-of-concept band-mapped 60-GHz cloud-RoF access system is described. Three real-time services (TV, Wi-Fi, and high-speed data) are mapped into 60-GHz sub-bands and delivered to end users through a converged cloud-RoF platform.

The experimental setup is shown in Fig. 8.12. Three services represent three distinct signal types: broadcast television (TV) signal in analog form, Wi-Fi as high-level modulated vector signal, and very high-throughput (VHT) data service in digital binary bits. At the central office (CO), an optical phase modulator (PM) is driven by a 29.2-GHz sinusoidal wave to generate multiple optical sub-carriers, shown as inset (a) in Fig. 8.12. A 33/66-GHz interleaver (IL) is used to separate the first-order sidebands from other sub-carriers in order to generate the 60-GHz mm-wave carrier in a microwave-photonic way. A Wireless-G Adapter in a client computer is used to transmit and receive 802.11 g Wi-Fi signals of 22-MHz channel bandwidth carried on 2.4 GHz. The 0.5 Gb/s OOK data are firstly upconverted to an intermediate frequency (IF) at 4.2 GHz and combined with Wi-Fi and TV signal (combined RF spectrum shown in Fig. 8.12c) to drive an intensity modulator (MZM). The downstream optical spectrum is shown as the solid black line in Fig. 8.12b. After standard single-mode fiber (SSMF) fronthaul transmission, the lightwave is pre-amplified by an EDFA in the RAU and detected by a 60-GHz PD to optically upconvert the three services to 60-GHz sub-bands. At the mobile subscriber (MS), an envelope detector (ED) downconverts the received 60-GHz band-mapped signal to their original carrier



**Fig. 8.12** Experimental setup and results of the band-mapped 60-GHz cloud-RoF system for TV, Wi-Fi, and VHT data. **a, b** Optical spectra measured at location a, b1, and b2; **c** electrical spectrum measured at location c; **d** received TV signal (transmitted alone) after band-mapped 60-GHz RoF transmission; **e** received TV signal after co-transmission with Wi-Fi signal and VHT data in band-mapped 60-GHz cloud-RoF system [28]

frequencies. After 60-GHz wireless transmission through a pair of mm-wave horn antennas, the downlink (DL) Wi-Fi signal is received by a wireless PCI (peripheral component interconnect) adapter in a server computer. Circulators and a 3-dB attenuator are used to isolate the uplink (UL) and DL signals. The 2.4-GHz Wi-Fi UL is directly modulated and delivered back to the CO. Note that the central wavelength of the DL can be reused for upstream transmission, thus avoiding the need for additional laser and IL resources for a simpler RAU.

The DL 0.5 Gb/s OOK signal is downconverted and filtered by a 1-GHz low-pass filter (LPF) before it is sent to a bit error rate tester (BERT) for BER measurement. Meanwhile, after a 1-GHz LPF, the analog TV signal is displayed by a TV. The Wi-Fi signal throughput is measured by *Iperf* (a TCP/UDP throughput measurement tool) in various conditions. The detailed measurement results of OOK data and Wi-Fi service can be found in [28]. Figure 8.12d, e shows the received TV signal after band-mapping 60-GHz RoF transmission without and with OOK and Wi-Fi service co-transmission. Since the TV signal used in the test is analog, any interference or distortion imposed on it will be observed. The observed interference

from neighboring OOK and Wi-Fi signals is due to the nonlinear transfer function of the optical modulator used in the multi-band 60-GHz cloud-RoF system [29]. To solve this issue, pre-distortion techniques can be used for distortion-sensitive signals like analog TV.

Overall, in this proof-of-concept experiment, the feasibility of multi-service transmission in a band-mapped 60-GHz cloud-RoF system is demonstrated. It is to be noted that the band-mapped mm-wave transmission is just one of the possible schemes to support multi-service delivery. Other schemes, such as all-band RoF transmission, are also capable of delivering multiple services in the cloud-RoF platform.

## 8.4 Summary

In this chapter, we reviewed several existing and emerging fiber-wireless access networks including macrocells, small cells, distributed antenna systems, and cloud radio access networks. A novel cloud radio-over-fiber (cloud-RoF) access network is introduced as a promising Fi-Wi access architecture for future 5G networks. Proof-of-concept experiments are presented to demonstrate multi-operator/multi-service infrastructure-sharing capabilities in the cloud-RoF systems.

## References

1. Osseiran A, Braun A, Hidekazu T, Marsch P, Schotten H, Tullberg H, Uusitalo MA, Schellman M (2013) The foundation of the mobile and wireless communications system for 2020 and beyond challenges, enablers and technology solution. In: Proceedings of the vehicular technology conference (VTC2013-Spring), Dresden, Germany, June 2013
2. European Union Mobile and wireless communications Enablers for the Twenty-twenty Information Society (METIS) Project. <https://www.metis2020.com/>
3. NGMN (Next Generation Mobile Networks) 5G Initiative Work Program. <http://www.ngmn.org/workprogramme/5g-initiative.html>
4. Alamouti S (2012) Networks of the future—some challenges ahead. In: Keynote speech, WCNC 2012, Paris, France
5. Akyildiz IF, Lee W-Y, Vuran MC, Mohanty S (2006) Next generation/dynamic spectrum access/cognitive radio wireless networks: a survey. *Comput Netw* 50:2127–2159
6. Lee D, Seo H, Clerckx B, Hardouin E, Mazzaresse D, Nagata S, Sayana K (2012) Coordinated multipoint transmission and reception in LTE-advanced: deployment scenarios and operational challenges. *IEEE Commun Mag* 50(2):148–155
7. Pi Z, Khan F (2011) An introduction to millimeter-wave mobile broadband systems. *IEEE Commun Mag* 49(6):101–107
8. Yu J, Chang G-K, Iia Z, Chowdhury A, Huang M-F, Chien H-C, Hsueh Y-T, Jian W, Liu C, Dong Z (2010) Cost-effective optical millimeter technologies and field demonstrations for very high throughput wireless-over-fiber access systems. *IEEE/OSA J Lightwave Technol* 28(16):2376–2397
9. GPP TS 24.312: Access network discovery and selection function (Andsf) management object

10. Kim B-J, Henry P (2012) Directions for future cellular mobile network architecture. First Monday 17
11. McKeown N, Anderson T, Balakrishnan H, Parulkar G, Peterson L, Rexford J, Shenker S, Turner J (2008) Openflow: enabling innovation in campus networks. SIGCOMM Comput Commun Rev 28(2):69–74
12. Network Functions Virtualization: An introduction, benefits, enablers, challenges and call for action. Introductory White Paper, SDN and OpenFlow World Congress, Oct 2012
13. AT&T Domain 2.0 Vision White Paper [http://www.ece.cmu.edu/~ece739/papers/att\\_whitepaper.pdf](http://www.ece.cmu.edu/~ece739/papers/att_whitepaper.pdf)
14. Small Cell Forum, Small cells—big ideas: how small cells left home and where they’re going next. Document SCF030.03.03, 2014
15. Small Cell Forum, Backhaul technologies for small cells: use cases, requirements and solutions. Document SCF049.03.01, 2013
16. HetNet Forum, Distributed antenna systems (DAS) and small cell technologies distinguished, White Paper, 2013
17. China Mobile, C-RAN: The road towards green ran, White Paper, 2011
18. Liu C, Zhang L, Zhu M, Wang J, Cheng L, Chang G-K (2013) A novel multi-service small-cell cloud radio access network for mobile backhaul and computing based on radio-over-fiber technologies. IEEE/OSA J Lightwave Technol 31(17):2869–2875
19. Yang H, Zeng J, Zheng Y, Jung HD, Huiszoon B, van Zantvoort JHC, Tangdionga E, Koonen AMJ (2008) Evaluation of effects of MZM nonlinearity on QAM and OFDM signals in RoF transmitter. In: Proceedings of the microwave photonics conference, pp. 90–93
20. Wang J, Liu C, Zhu M, Yi A, Cheng L, Chang G-K (2014) Investigation of data-dependent channel cross-modulation in multiband radio-over-fiber systems. IEEE/OSA J Lightwave Technol 32(10):1861–1867
21. Liu C, Cvijetic N, Sundaresan K, Jiang M, Rangarajan S, Wang T, Chang G-K (2013) A novel in-building small-cell backhaul architecture for cost-efficient multi-operator multi-service coexistence. In: Proceedings of the IEEE/OSA Optical Fiber Communication Conference (OFC) 2013, Paper OTh4A.4
22. Liu C, Sundaresan K, Jiang M, Rangarajan S, Chang G-K (2013) The case for re-configurable backhaul in cloud-RAN based small cell networks. In: Proceedings of the IEEE INFOCOM 2013, pp 1124–1132
23. IEEE 802.11 WLAN Task Group ad
24. IEEE 802.15 WPAN Task Group 3c
25. Rappaport TS, Sun S, Mayzus R, Zhao H, Azar Y, Wang K, Wong G, Schulz J, Samimi M, Gutierrez F (2013) Millimeter wave mobile communications for 5G cellular: it will work! IEEE Access 1:335–349
26. Jia Z, Yu J, Ellinas G, Chang G-K (2007) Key enabling technologies for optical-wireless networks: optical millimeter-wave generation, wavelength reuse, and architecture. IEEE/OSA J Lightwave Technol 25(11):3452–3471
27. Koonen A, Garcia L (2008) Radio-over-mmwave techniques-part II: microwave to millimeter-wave systems. IEEE/OSA J Lightwave Technol 26(15):2396–2408
28. Zhu M, Zhang L, Wang J, Chen L, Liu C, Chang G-K (2013) Radio-over-fiber access architecture for integrated broadband wireless services. IEEE/OSA J Lightwave Technol 31(21):3614–3620
29. Wang J, Liu C, Zhu M, Chang G-K (2013) Investigation of intra/inter-band cross-modulation in multiband radio-over-fiber systems. In: Proceedings of the IEEE international conference on communications (ICC), pp 843–847

# Chapter 9

## Advanced Architectures for PON Supporting Fi-Wi Convergence

Georgios Ellinas, Kyriakos Vlachos, Chrysovalanto Christodoulou  
and Mohamed Ali

**Abstract** The phenomenal growth of mobile backhaul capacity required to support the emerging mobile traffic including cellular Long-Term Evolution (LTE), and LTE-Advanced (LTE-A) requires rapid migration from today's legacy circuit-switched T1/E1 wireline and microwave backhaul technologies to a new fiber-supported, all-packet-based mobile backhaul infrastructure. Mobile backhaul is utilized to backhaul traffic from individual base stations (BSs) to the radio network controller (RNC), which then connects to the mobile operator's core network or gateway. Many carriers around the world are considering the potential of utilizing the fiber-based passive optical network (PON) access infrastructure as an all-packet-based converged fixed-mobile optical access networking transport architecture to backhaul both mobile and typical wireline traffic. This chapter details the case for backhauling wireless traffic utilizing an optical access network, the various standards and technology options for passive optical networks (PONs), as well as the design of a novel, fully distributed, ring-based WDM-PON architecture that could be utilized for the support of a converged next-generation mobile infrastructure. Further, as in 4G and 5G the radio access network (RAN) becomes a broad concept that describes network transport systems including mobile backhaul, mobile fronthaul, and wireless connections between radio equipment and user devices, a fiber-wireless integrated system is nowadays not only limited to mobile backhaul, which is mainly composed of fixed wires, but also includes mobile fronthaul. Thus, a discussion is also added at the end of this chapter on mobile fronthaul utilizing PON infrastructures.

---

G. Ellinas (✉) · C. Christodoulou  
University of Cyprus, Nicosia, Cyprus  
e-mail: gellinas@ucy.ac.cy

K. Vlachos  
University of Patras, Patras, Greece

M. Ali  
City College of New York, New York, USA

## 9.1 Introduction

Advances in optical networking technologies over the last two decades have provided tremendous growth in both backbone and MAN communication capacity, and at the same time, enterprise local area networks (LANs) have scaled tributary speeds progressively from 10 to 100 Mb/s toward multi-gigabit speeds (e.g., 1 and 10 Gb/s Ethernet, or GbE/10 GbE). The last front of this evolution is the access technology so as to address the bottleneck in bandwidth and service quality between a high-speed residential/enterprise network and a largely overbuilt core backbone network. This in turn will enable the support of more bandwidth-intensive networking applications, as well as the support of end-to-end QoS for a wide variety of applications, particularly non-elastic applications such as voice, video, and multimedia that cannot tolerate variable or excessive delay or data loss.

Bridging this gap between the capacity provided by the backbone and metro networks on one side, and the actual capacity experienced by end users on the other, is a significant challenge that is currently being addressed by service providers and local carriers. The introduction of optical technologies solutions in the access network is one way to address this acute need for bandwidth. This need is exacerbated, as discussed in detail in Sect. 9.2 that follows, by the additional requirement imposed on the access network to backhaul wireless traffic.

Fiber-to-the-home (FTTH) access systems are considered the ultimate level of access bandwidth. Further, to lower the cost and expedite the implementation of FTTH, passive optical network (PON)-based solutions have been proposed. PONs are point-to-multi-point (P2MP) fiber optical networks with no active elements in the signal's path. Deployment of PONs as architectures for FTTH access networks is viewed as a future-proof last mile technology that has enough flexibility to support new and unforeseen applications. The rest of this chapter details the case for backhauling wireless traffic utilizing an optical access network, the various standards and technology options for passive optical networks (PONs), as well as the design of a novel, fully distributed, ring-based WDM-PON architecture that could be utilized for the support of a converged 4G/5G mobile infrastructure. The chapter ends with a short discussion on fronthauling mobile traffic.

## 9.2 Backhauling Wireless Traffic

The current standardized mobile telecommunication system, universally recognized as 4G, provides increased capacity and reliable wireless communications. Wireless access architectures such as Mobile WiMAX and LTE are two competing technologies that achieve data rates beyond 100 Mb/s per end user. Unlike WiMAX, LTE uses an evolution of the existing universal mobile telecommunication system (UMTS) infrastructure, used by over 80 % of the mobile operators [1]. Thus, it is

not necessary to build a new network infrastructure, making LTE more popular with operators worldwide. In addition, LTE-Advanced, which can be seen as an enhancement to LTE, offers a clear upgrade path to mobile carriers. This makes it more cost effective for vendors to offer LTE and then upgrade to LTE-Advanced. Furthermore, LTE and LTE-Advanced can also make use of additional spectrum and multiplexing to achieve higher data speeds. Coordinated multi-point (CoMP) transmission (as discussed in various other chapters of this book) can also allow for more system capacity to help handle the enhanced data speeds, something that is a necessity for the optical-wireless architecture convergence.

The demand for high-bandwidth access networks is expected to grow continuously, due to the increased expansion of innovative and high-bandwidth applications like Web 2.0, mobile TV, and streaming content, that will be the dominant application in LTE/LTE + networks. Thus, current backbone standards are expected to become less effective for building mobile access networks. Specifically, legacy technologies such as circuit-switched T1/E1 wireline or microwave used for existing 3G network infrastructures cannot scale to the capacity requirements of new 4G (and 5G) access architectures [1]. Thus, mobile operators are investing heavily in upgrading their backhaul infrastructure, with fiber-optic deployments to the LTE base stations (“fiber to the cell”). Due to their compelling advantages, many works have addressed the need for building access architectures for LTE networks, such as [2, 3]. However, LTE/LTE + technologies possess specific requirements, when considering issues like intercommunication of base stations, traffic roaming, and end-to-end service provision across heterogeneous networks. Therefore, it is worth looking into the enhanced base stations called “evolved node Bs (eNBs),” before identifying the needs of the LTE network for backhauling network traffic. The LTE network architecture consists of an all-IP core network, called Enhanced Packet Core or in short EPC. The eNBs are connected by means of the S1 interface to the EPC, whose logical components are the Mobility Management Entity (MME), the Serving Gateway (S-GW), and the Packet Data Network gateway (P-GW), together also known as the Access Gateway (AGW) (see Fig. 9.1). LTE also introduced support for inter-BS connectivity via the X2 interface, to support handover operations. Recent studies have estimated traffic traversing the X2 interface to reach 4–10 % of traffic traversing the S1 interface [3]. Thus, it is important for an efficient converged architecture to support at least partial meshing of eNBs, so that X2 traffic does not flow through the AGW, which would waste resources and significantly increase packet delay. With respect to the eNB architecture, ASIC and/or FPGA are used to implement the PHY, DSPs for lower layer protocols (i.e., MAC and RLC), and CPUs or network processors for the upper layers of the protocol stack. The MAC sublayer is responsible for QoS-aware downstream/upstream packet scheduling. For downlink traffic, the scheduler decides which packets to be sent to the intended user equipment (UE).

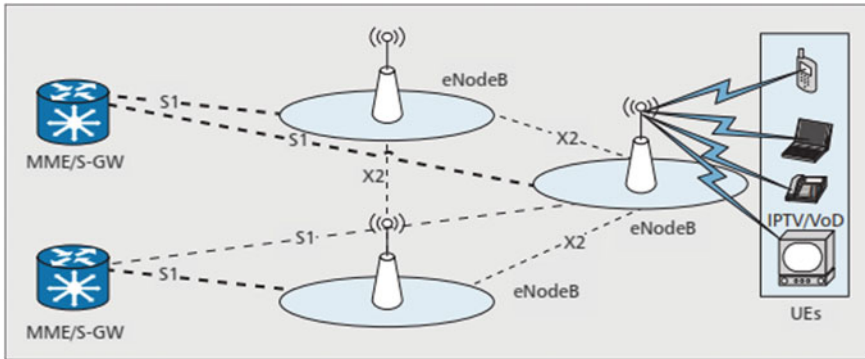


**Fig. 9.1** LTE network architecture

Uplink scheduling results in resource grants being sent to UEs. Each UE is responsible for determining, which data to transmit within the granted resources. A QoS-aware MAC Scheduler at the eNB aims to distribute the available air interface resources to the UEs within the cell, supporting QoS guarantees. The Bearer information (QoS mapping) must be carried on all system interfaces and mapped to pre-configured QoS parameters regarding priority, packet delay, and packet loss. This includes RAN elements that might be prone to congestion-related losses or excess packet forwarding delay. QoS mapping (bearer information) and X2 traffic are two key issues that the backhaul network should handle, apart from the general support of high-speed connection.

It is generally accepted that fiber deployment to cell towers (“fiber to the cell”) is the only future-proof solution to build mobile backhalls, which will scale to the increased capacity requirements of future NG-WBAN technologies [1]. It will alleviate the need of using expensive RF point-to-point links (i.e., 26 GHz) or even the unlicensed 60-GHz Wi-Fi band. Apart from requiring additional RF circuits and antennas, they lack the high capacity, inherent resilience, and the ubiquity offered by optical fiber networks. Therefore, the implementation of an optical network supporting the fiber-enabled cell towers is the only viable solution. Among the optical network architectures, passive optical networks (PONs) meet the needs for such high-capacity access architecture. PONs have been proposed in the past 10 years as an access technology, bearing (a) low deployment costs, avoiding active components in the field, (b) bandwidth sharing between the end users, (c) scalability in terms of users and points of presence, as well as (d) bandwidth granularity. Different variants of PONs have been proposed, but most were conceived based on the demands and bandwidth prospects of the past. PONs architectures have slightly changed since then and only the technology (i.e., TOSA/ROSA) has changed. These are discussed in detail in the sections that follow.

### 9.3 Passive Optical Network (PON): Standards and Technology Options

Passive optical network (PON) technology has been widely considered for building mobile access networks. The mobile backhaul portion of 4G telecommunication networks, or radio access network (RAN), interconnects the Enhanced Packet Core (EPC) with the edge section of the wireless domain and transports traffic from individual base stations (BSs) to the access gateway (AGW). However, it must be noted that with peak per-edge cell downlink throughput of 1 Gbit/s and uplink of 500 Mbit/s in the case of LTE-Advanced, 4G base stations are expected to be densely populated to achieve high spectral efficiency and require high bandwidth and cost-effective backhauling.

A PON consists of three parts: (i) an optical line terminal (OLT) that is located at the operator's central office and hosts the active equipment. In particular, it hosts the laser TRx banks depending on the standard deployed. (ii) A set of optical network units (ONUs) that communicate with the OLT either directly with a separate wavelength or over a passive splitter. The number of ONUs deployed determines the splitting ratio and thus the power budget of the system. The ONUs are located near end users, either in multi-tenant buildings, businesses, or individual houses. Further, the ONU provides the required service interface to all operator's customers. (iii) A passive feeder network, also called optical distribution network (ODN) that is utilized to interconnect the OLT and ONUs. The ODN uses simple optical fiber and a power splitter and typically is in the form of a tree network architecture. Depending on how data are multiplexed and transmitted, in downstream (from OLT to ONU) and upstream (from ONUs to OLT) mode, there exist three different technology options. The most popular one is time division multiplexing (TDM) PON, where traffic from/to the OLT to multiple ONUs is TDM multiplexed over a single (or more) wavelength(s). Wavelength division multiplexing (WDM) PON (also called PtP-WDM-PON) uses discrete wavelength channels, one per ONU. In this, capacity is not shared as in TDM-PON and each OLT-ONU link uses a different wavelength. A third option is orthogonal frequency division multiplexing (OFDM) PON, where a number of orthogonal subcarriers are employed to transmit traffic from/to the ONUs. With the WDM and OFDM technology, PONs are capable of providing data rates of up to 40 Gb/s.

## 9.4 Technology Options

### 9.4.1 TDM-PON

TDM-PONs (sometimes referred to as *power-splitting* PONs (PS-PONs) since the branching device used in the outside plant is a  $1 \times N$  power splitter) utilize a single wavelength containing downstream information that is shared by  $N$  users. Upstream

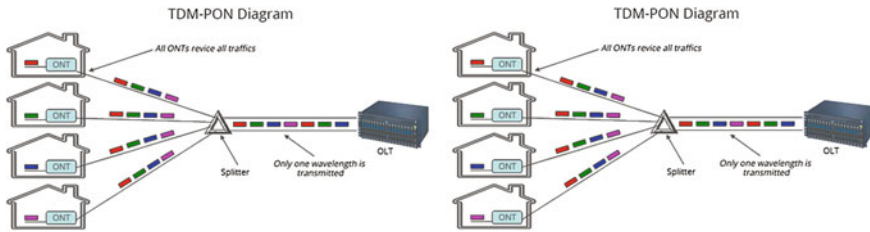


**Fig. 9.2** Time-division-multiplexed passive optical network architectures

information is provided by a low-cost transmitter placed in the ONU. Coarse wavelength division multiplexing is used to separate the upstream and downstream transmissions.

Figure 9.2 illustrates a typical tree-based TDM-PON architecture. The ONUs terminate all traffic and constitute the service interface for end users such as DSL or coaxial cable. In contrast, OLT constitutes the gateway interface of the entire PON to the (outside) IP core network and is commissioned to forward IP traffic over standard interfaces, i.e., SDH/SONET or Ethernet. Downstream traffic is forwarded by broadcasts from the OLT to all connected ONUs, while in the upstream direction an arbitration mechanism is employed, so that data packets from the ONUs do not overlap at a given time frame (slot). The start time and length of each transmission time slot for each ONU is scheduled using a bandwidth allocation scheme, which is executed at the OLT. In order to achieve a high degree of bandwidth utilization, with a notion of fairness among the ONUs, a dynamic bandwidth allocation (DBA) technique is employed that can adapt to the current traffic demand if required. To facilitate bandwidth sharing as well as ONU registration and service discovery, a multi-point control protocol (MPCP) has been proposed and designed, consisting of five basic messages: (a) REGISTER REQ, REGISTER, and REGISTER ACK for discovering and registering new ONUs at the network and (b) REPORT and GATE for facilitating centralized medium access control. Upon receiving ONUs buffer sizes, the OLT executes the dynamic bandwidth allocation (DBA) and communicates via a GATE message to all ONUs the granted transmission window (number of slots) as well as the starting time.

Since the OLT and the ONUs can be separated by  $\sim 10$  km and the distance from each ONU to the OLT is not the same, a TDM-PON architecture suffers from switchover shortfalls. Interleaved polling is subsequently used to mitigate the large propagation delays. With interleaved polling, the next ONU to be polled is issued a GATE message giving transmission access, while the previous ONU is still transmitting. Guard band times are used between ONU transmissions to avoid any overlap in data transmission as well as to allow each to switch ON and OFF its lasers, thus preventing CW spurious transmission in the network (upstream traffic). Data from the ONUs arrive at the OLT at different power levels, and thus the OLT must adjust its threshold and decision criteria to receive data without errors.

Therefore, the OLT should keep a record of all ONU transmissions over time (something that is not the case in downstream traffic).

Various bandwidth allocation schemes have been devised for the efficient usage of available bandwidth as well as making allocation decisions computationally light [4]. Grant sizing can be divided into four major categories: *Fixed*, where the grant size is fixed for each ONU every cycle; *Gated*, where the granted size equals the queue size of the ONU; *Limited*, where the grant size is set between the reported buffer size and a maximum one, specified for that ONU; and *Limited with Excess Distribution*, which is based on the *Limited* grant size with the excess bandwidth being distributed to the “overloaded” ONUs. Both the *Limited* and the *Limited with Excess Distribution*, approaches prevent bandwidth monopolization by a certain ONU, which is the case for the *Fixed* granting scheme.

The execution of the DBA algorithm at the OLT, once per cycle, poses computation overhead. Therefore, both the algorithms and the MPCP messages should be kept simple for fast execution to avoid delays in packet transmissions.

TDM-PONs, though cost-effective, have some limitations for future access network demands. TDM-PONs place a lot of stress on the electronic and optoelectronic components in the OLT and ONU, since these components have to operate at the aggregate bit rate. Also, the insertion loss of the power splitter increases with increasing number of subscribers. In addition, privacy is limited in TDM-PONs since all the downstream information is broadcast to all ONUs.

The currently deployed PON systems are mostly TDM-PON systems, which include ATM-PON (APON), Broadband PON (BPON), Ethernet PON (EPON), Gigabit PON (GPON), 10G EPON, and Next-generation PON (NG-PON) [4–16] to provision different data rates up to 10 Gbps. APON/BPON, GPON, and NG-PON architectures were standardized by the Full Service Access Network (FSAN), which is an affiliation of network operators and telecom vendors. Since most telecommunications operators have heavily invested in providing legacy TDM services, these PON architectures are optimized for TDM traffic and rely on framing structures with a very strict timing and synchronization requirements. EPON and 10G-EPON are standardized by the IEEE 802 study group. They focus on preserving the architectural model of Ethernet. No explicit framing structure exists in EPON, and Ethernet frames are transmitted in bursts with a standard inter-frame spacing. The above-mentioned standards are further discussed in the sections that follow.

## 9.4.2 WDM-PON

Another PON variant is the wavelength division multiplexing PON, or WDM-PON (or Pt-to-Pt WDM-PON). In this architecture, ONUs do not share wavelength capacity, but each ONU possesses its own wavelength, directly routing its traffic to the OLT (as Fig. 9.3 illustrates). The different wavelengths may coexist on the same fiber or may be router over different ones. WDM-PONs offer the advantage of higher speed, as well as scalability in capacity and network size, simply by adding

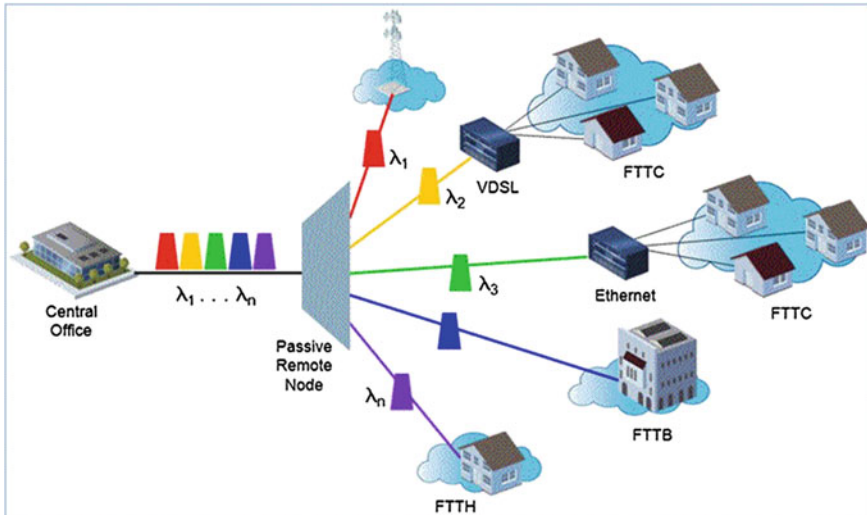


**Fig. 9.3** Wavelength-division-multiplexed passive optical network architecture

more wavelengths and more ONUs, respectively. However, this bears the disadvantage of deploying more WDM active components, yielding a higher cost of initial setup. This should not be ignored, having in mind the relative low (<1 Gbps) bit rate service that access networks provide to their end users.

In either case, WDM-PONs have several advantages compared to their TDM counterparts. Apart from their higher bandwidth, WDM-PONs entail protocol, modulation format, and rate transparency. Furthermore, WDM-PONs provide a higher notion of security, since data are not broadcast to all ONUs, but each ONU receives its own dedicated data. In terms of the split ratio that determines the power budget and PON reach in TDM-PONs, this is now not as significant in WDM-PONs, since the employment of more ONUs actually means the addition of extra wavelengths. In addition, no arbitration is required for upstream transmission, and thus the need for the P2MP media access control is no longer required. Finally, system speeds can now be increased in a pay-as-you-grow fashion, whereas in a TDM-PON an upgrade of the OLT would create the need to upgrade the entire set of ONUs. Nevertheless, WDM-PONs also present some disadvantages, such as increased deployment costs due to the WDM components required (AWG, MUX/DMUX, tunable sources, etc.), increased temperature sensitivity, which entails the need for temperature control (temperature control is costly and requires active electronic parts in the optical distribution network or alternatively temperature-insensitive WDM components), as well as increased operational expenditures in terms of maintenance, spare parts, inventory stocks, and production lines since ONUs are now  $\lambda$ -specific (creating the need for “colorless ONUs”).

Therefore, WDM-PON resembles a typical point-to-point optical network, where reach and optical transmission is mainly determined by the type of laser

source (WDM sources can achieve >80-km repeater-less transmission). Finally, the control layer and the bandwidth allocation mechanism are much simplified, compared to typical G(E)PON. In essence, there is no need for DBA algorithms, and OLT-ONUs communicate in a point-to-point fashion.

Despite these attractive features, WDM-PON installation is costly, mainly because of the use of active WDM sources. These must be anchored on the ITU grid, with proper thermal management, a fact that also increases power consumption. Many different solutions have been proposed in the literature. Among these are solutions where the ONUs are employed with tunable laser sources, so as to tune each ONU to the proper wavelength. However, tunable sources are relative expensive and thus do not constitute a viable solution. Another solution is to equip each subscriber with a wavelength transparent optical modulator, and the OLT with a bank of all lasers. In such a case, the OLT can send the downstream data with a low modulation index. The signal will be split at each ONU for data reception of the downstream traffic and modulation of the upstream traffic. The technique is known as *reflective modulation*, and either optical modulators or SOAs can be used to implement it. SOAs provide the advantage of optical signal amplification, bearing in mind the extra losses incurred due to the doubling of transmission reach. Alternatively, the ONUs may employ a fixed but different wavelength optical source (ONUs are not colorless in this case), while the OLT will have a bank of fixed-wavelength sources for all ONUs connected to it. Further, the OLT will also employ the same number of fixed-wavelength (or broadband) optical receivers.

Various WDM-PON architectures have been proposed in the research literature over the years, with different variations for the optical sources at the OLT and ONUs, as well as different OLT and ONU architectures [17]. As an example, the Composite PON (CPON) architecture utilized a single-wavelength, burst-mode receiver at the OLT to receive the upstream signal. Even though it avoided the drawbacks of upstream WDM, it was cost prohibitive, as it was limited to the use of a single-frequency laser, such as a distributed feedback (DFB) laser diode (LD) at the ONU. The Local Access Router Network (LARNET) architecture, on the other hand, employed a broad-spectrum source at the ONU, in order to avoid the limitations of CPON, using an inexpensive light-emitting diode (LED) whose spectrum was sliced by the AWG-based router into different optical bands in the upstream direction. However, spectrum slicing with AWG may lead to high-power loss. Therefore, the distance from the OLT to the ONU utilizing this architecture was considerably reduced. For the Remote Interrogation of TErminAl NETWORK (RITENET) architecture, at the ONU, the light was split by a passive tap, with a portion of the light detected by the receiver, while the remainder was looped back toward the CO through a modulator. The signal from the OLT was shared for downstream and upstream transmission through time sharing. Another type of WDM-PON architectures is the multistage AWG-based WDM-PON architectures that exploit the periodic routing property of the AWG so that the reuse of a given wavelength for more than one subscriber is possible. These architectures provide scalability in bandwidth as well as in the number of users, either by employing additional wavelengths at the CO or by cascading multiple stages of AWGs with

increasing AWG coarseness at each stage. Further, architectures such as super-PON (SPON) proposed a solution that covers a range of over 100 km with a splitting ratio reaching 2000 with the usage of optical amplifiers (OAs) placed in the long feeder and after the first splitting stage, while architectures such as SUCCESS-DWA separated the upstream and downstream traffic by a wideband WDM filter residing between the AWG and the PON, aiming to offer scalability by employing dynamic wavelength allocation.

### 9.4.3 OFDM-PON

Orthogonal frequency division multiplexing (OFDM) PONs or in short OFDM-PONs use a number of orthogonal subcarriers assigned to different ONUs. Figure 9.4 displays sub-carrier allocation to the ONUs for such an OFDM-PON implementation. OFDM-PONs bear all the advantages of OFDM transmission, namely enhanced spectral efficiency and superior transmission performance (extended reach, dispersion, polarization and noise tolerance, power budget requirements, lower nominal repetition rates, etc.). As in xDSL technology, each sub-carrier is modulated with a conventional m-QAM scheme at a lower symbol rate. Thus, bandwidth (as well as transmission) reach can be increased with a negligible effect of chromatic and/or polarization mode dispersion. Albeit OFDM-PON is considered for future deployment (NG-PON2), it possesses some significant advantages. First, transmission reach has been extended to beyond 100 km without the use of specialty fibers, optical amplification, or expensive laser sources. Such an extension can be beneficial, when connecting distant users and/or

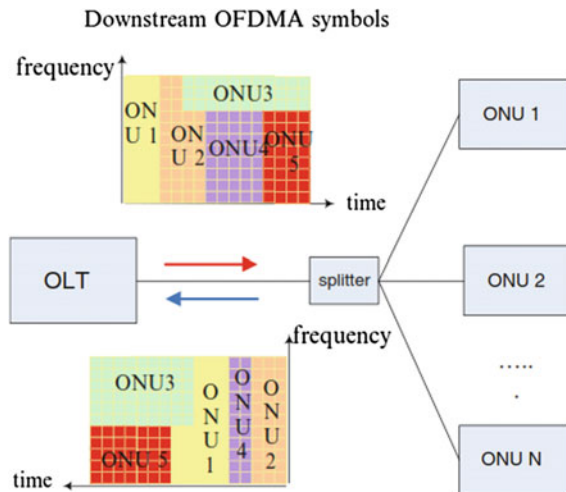


Fig. 9.4 Time-division-multiplexed passive optical network architectures. RE-DRAWN

designing PONs that cover a large geographical scale. Further, OFDM relies on low-cost ASICs for advance signal processing and not on optical components (WDM lasers) that are more expensive and have stringent requirements in terms of packaging, thermal management, etc. Another advantage of OFDM-PON is that bandwidth allocation per user can differ, by simply changing the subcarrier modulation frequency and/or modulation scheme. Thus, different services can be provided with no extra components or complex control plane algorithms.

Even though OFDM-PON has significant advantages, it still is a premature technology, mainly due to the high cost and requirement of high-speed ADC/DACs, and is currently being considered as a research topic for potential future deployment.

### 9.4.4 Hybrid PONs

Hybrid PONs refer primarily to a TDM-WDM co-design of PONs and secondarily to OFDM-WDM. In the first case, hybrid WDM/TDM-PON bridges the gap between TDM-PON and pure WDM-PON and can be deployed for a smooth migration of the currently deployed TDM-PONs. There are different concepts of hybrid TDM-WDM-PONs. One such concept is illustrated in Fig. 9.5 [18], where the number of available wavelengths to all ONUs/end users is simply increased. Such an approach invests on scheduling bandwidth requests, originating from ONUs, to a larger pool of shared wavelengths, thus increasing PON capacity. Another approach relies on a joint ring/tree architecture [19], where a WDM ring serves distant remote nodes with a separate wavelength, whereas remote nodes serve multiple ONUs over the same wavelength. Such an approach constitutes a

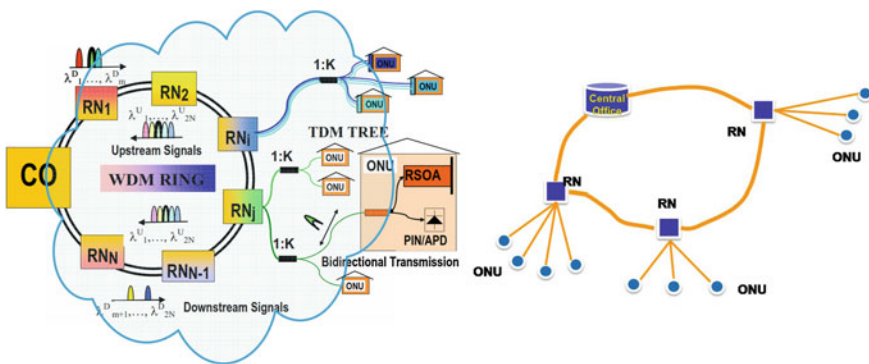


Fig. 9.5 Implementation of hybrid WDM-TDM-PON networks in the ACCORDANCE project [20]

smooth migration from currently deployed PONs (mainly GPON) with increased scalability and backwards compatibility.

Overall, looking at all different types of PON architectures, the major issue of PONs is that they are purely digital systems. They are bandwidth consuming and lack flexibility and scalability as the data rates and system capacity of 4G/5G systems increasing exponentially. To support future multi-tier, carrier aggregated heterogeneous mobile data networks, PONs should be service/format agnostic. Combination of Digital and Analog Radio-over-Fiber RANs can be a future-proof solution, and many research works have been carrying out on this approach as discussed in various chapters of this book.

## 9.5 PON Standards

### 9.5.1 GPON/EPON

Most advances on PONs were carried out upon ITU standardization of the older ITU-T G.983 standard based on Asynchronous Transfer Mode (known also as ATM-PON (or simply APON)). Due to the low penetration of the ATM protocol, the ITU developed the final version of ITU-T G.983 widely known as Broadband PON, or simply BPON. BPON was initially designed to offer 622 Mbit/s (OC-12) of downstream bandwidth and 155 Mbit/s (OC-3) of upstream traffic. Soon, ITU finalized G.984 Gigabit-capable passive optical networks (GPONs) representing a smooth upgrade in terms of upstream/downstream speeds (2.488/1.244 Gbit/s). GPON has and still is the most successful implementation in fiber access networks. Among the implementations, the Ethernet PON (or in short EPON or GEAPON) has been the successful candidate due to the ease that the Ethernet protocol offers in layer 2 networking, as well as the fact that Ethernet has emerged as the frontrunner technology for transporting data, video, and voice services over a single platform (the great majority of all installed connections of all LANs is Ethernet based).

The initial EPON standard 802.3ah has evolved since 2004 from symmetric 1–10 Gbit/s (10G-EPON standard is IEEE 802.3av). Both standards use separate wavelengths for downstream and upstream traffic (1.5/1.3  $\mu\text{m}$ ). The GEAPON standard continues to evolve, bearing in mind the advances in GEthernet interfaces. The IEEE 802.3 working group is commissioned with the task of maintaining and extending speeds beyond 10Gbps. To this end, the 802.3ba standard describes 40- and 100-Gbit/s connection speeds for a variety of connection reaches spanning from a few meters to beyond 40 km. Discussions for 400 GbE and 1 TbE are also currently under way.

## 9.6 10G-PON

As demand for network speed continues to grow, new and faster technologies are spawned from the existing standards. 10G-PON is the next-generation ultra-fast capability for G-PON providers, designed to coexist with installed G-PON user equipment on the same network. To this end, ITU-T in 2010 completed the G.987 standard, also known as 10G-PON or XG-PON, defining shared network access rates up to 10 Gbit/s over existing fiber, specifically for last mile, access networks. Initially, G.987 was designed for multi-tenant buildings, where 10G capacity is shared by all end users. ITU-T defined two variants in the G.987 standard. The first concerns asymmetric 10G-PON (also known as XG-PON1) with 10 Gbit/s downstream and 2.5 Gbit/s upstream line rates and the second concerns symmetric 10G-PON (also known as XG-PON2), where both downstream and upstream speeds are 10 Gb/s (the nominal rates are 9.95328 and 2.48832 Gbit/s, respectively). 10G-PON and G-PON are similar with respect to framing and protocols but differ in the operating wavelengths (10G-PON uses wavelengths of 1577 and 1270 nm for downstream/upstream traffic, while GPON and EPON use wavelengths of 1490 and 1310 nm). This was decided so as to allow coexistence of 10G-PON and GPON over the same access network. It should be noted that symmetric operation of an access networks implies a stringent requirement; the ONUs must employ expensive high-speed burst-mode lasers, while the OLT must employ expensive burst-mode receivers.

ITU is now developing 40/80G PON standards (also noted as NG-PON2), based on a multi-wavelength scheme (similar to 100 GbE). The primary solution that is considered is a hybrid time/wavelength division multiplexing (TWDM) scheme, while an optional evolutionary scenario concerns a pure point-to-point wavelength division multiplexing (PtP-WDM) scheme. Both schemes use colorless power splitters in the feeder network and “colorless” ONUs.

## 9.7 10G-Epon

As mentioned previously, GEAPON is a variant of GPON based on Ethernet protocol. As in 10G-PON, 10G-EPON supports both symmetric at 10 Gbit/s and asymmetric 10G/1G downstream/upstream operation (as per the 802.3av standard). Specific attention has been given to the coexistence of 1G and 10G-EPON, again by using different wavelengths but only in the downstream direction. In this case, 1G-EPON uses the 1480–1500 nm band, while 10G-EPON uses the 1575–1580 nm band. In the upstream direction, the 1G-EPON and 10G-EPON upstream bands overlap. 1G-EPON uses the 1260–1360 nm band, while 10G-EPON uses the 1260–1280 nm band. This is feasible since the upstream communication is separated over time and thus GEAPON and 10G-PON packets do not overlap in time. The 10G-EPON standard also defined different link classes and power budget for

different fiber reach and splitting ratios. The min class “ $\times 10$ ” defines a 10-km reach with a 1:16 split ratio and a 20-dB power budget, while the maximum “ $\times 40$ ” a 20-km reach with a 1:64 split ratio and a 33-dB power budget.

### 9.7.1 NG-PON2

To enable cutting-edge standardization of future optical access systems, the Full Service Access Network forum and ITU-T Study Group 15 are currently discussing the specifications of a 40-Gigabit-capable PON, which employs wavelength division multiplexing (WDM) technology, for the purpose of enabling cost-effective 40-Gigabit-capable transmission capacity and multiple service capability. It is worth noting that the term NG-PON1 is used for the evolutionary growth of EPON/GPON, which supports coexistence with EPON/GPON on the same feeder network, while the term NG-PON2 represents the revolutionary change in NG-PON, with disruptive technologies, such as optical code division multiplexing (OCDM), with no requirement of coexistence with EPON/GPON. The NG-PON2 standard, ITU-T G.989, emerged in 2015 and details the architectural and technology features for network throughput of 40 Gbps, corresponding to up to 10-Gbps symmetric upstream/downstream speeds available at each end user.

An example of NG-PON2 system architecture is shown in Fig. 9.6. Although the previous PON systems offer broadband service only for residential users,

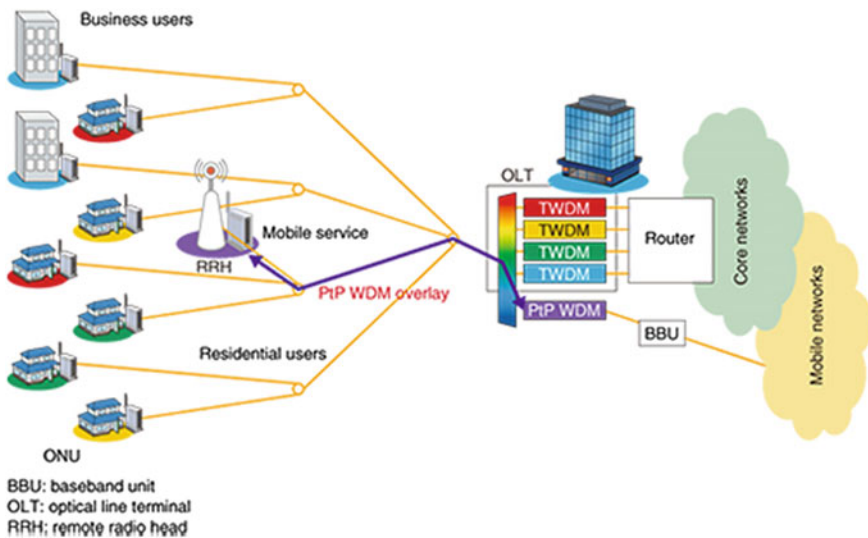


Fig. 9.6 NG-PON2 system architecture. RE-DRAWN

NG-PON2 systems are expected to accommodate business users and mobile users in addition to residential users. The primary NG-PON2 solution is called TWDM (time and wavelength division multiplexing)-PON, which is a hybrid of conventional TDM (time division multiplexing) and WDM technologies. Optionally, NG-PON2 also supports point-to-point (PtP) WDM overlay, which is expected to be suitable for mobile services that require low latency. In NG-PON2, colorless optical network units (ONUs) are mandatory for reducing system operating expenses because they can eliminate the complicated inventory management of ONUs.

In TWDM-PON, there are four (with an option to deploy eight) multiplexed wavelengths for upstream and downstream transmission. In addition, NG-PON2 envisages the use of three line rates for each wavelength, particularly symmetric 2.5 and 10 Gbit/s, as well as 2.5 and 10 Gbit/s for upstream and downstream, respectively. Therefore, the transmission capacities for each line rate are symmetric 10 and 40 and 10/40 Gbit/s for upstream/downstream. The symmetric 40 Gbit/s is expected to be used by business users, while the 10/40 Gbit/s asymmetric one by plain residential users. In TWDM-PON upstream traffic, time division multiplexing is supported through the use of tunable burst-mode lasers at each ONU. Wavelengths are dynamically assigned, through the use of burst lasers at each ONU, and thus it is important that wavelengths do not overlap over time. In the downstream direction, wavelength division multiplexing is supported by combining four fixed-wavelength lasers, hosted at the OLT and combined with a wavelength MUX filter before launching to the feeder network. At each ONU, the MUXed signal (4 or 8 wavelengths) is actively filtered with a tunable filter that forwards only the appropriate wavelength.

The NG-PON2 wavelength assignment plan uses the 1524–1544 nm band for upstream transmission and the 1596–1602 nm band for downstream transmission. The G.989.2 standard also specifies two other options with a reduced spectrum band for upstream traffic: 1528–1540 and 1532–1540 nm. Wavelengths used are anchored on the 50-, 100-, or 200-GHz grid spacing, matched with the corresponding tunable components employed at each ONU. Attention is given to dispersion compensation and polarization maintaining techniques, especially for 40 Gbit/s-capable NG-PON2 access networks.

The case of WDM-PON is simpler, as the wavelengths used cover the expanded spectrum 1524–1625 nm, with no specification on the number of wavelengths and the exact allocation for upstream/downstream traffic. This is because the number of wavelengths specifies the number of supported ONUs and it is a choice of the operators. For supporting backward compatibility with other PON standards, the spectrum band is narrowed to 1603–1625 nm only. Figure 9.7 illustrates the complete wavelength allocation plan for all PON standards.

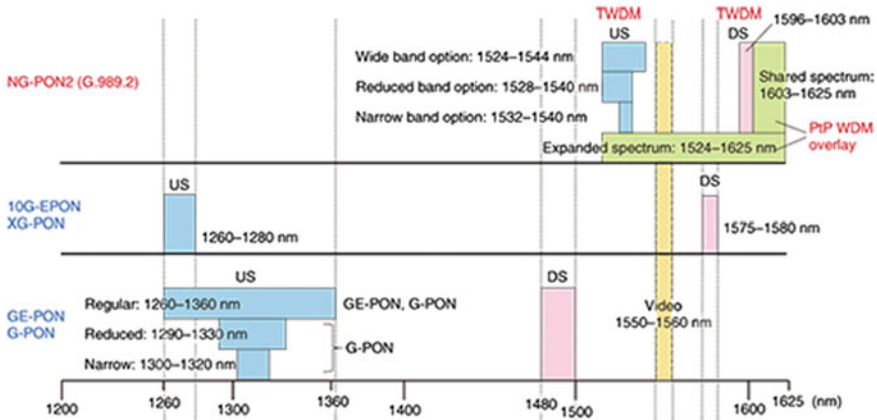


Fig. 9.7 Wavelength allocation plan for PON standards for backwards compatibility

### 9.7.2 Evolution Scenarios

Market opportunities for 10G-PON rely on the penetration of next-generation multimedia rich applications. These span from typical triple play services (voice, video, and Internet), to interactive ones, and to remote storage cloud services. Examples of bandwidth-hungry applications include IPTV, online gaming, video-conferencing, and interactive video. Further, the rapidly increasing use of advance cloud services for storage and processing (either from typical PCs or handheld devices) has further fueled traffic in the access networks. Soon, the explosive growth of access traffic together with the wide usage of real-time services with strict quality-of-service (QoS) requirements (e.g., low packet delay and jitter, and bandwidth guarantee) will justify the need of Next-generation PON standards, such as NG-PON2 and beyond [21].

The reader should also note that 100G-EPON is currently the up-to-date PON standard and it has attracted significant research attention. The objectives of the standardization work being carried out on 100G-EPON include defining the specifications for physical layers operating over a single fiber strand and supporting symmetric and/or asymmetric data rates of 25, 50, and 100 Gb/s (note that the specified data rate should be supported in the downstream direction and less than or equal to the specified data rate should be supported in the upstream direction), with a BER better than or equal to  $10E-12$  at the MAC/PLS service interface, and supporting coexistence with 10G-EPON. Due to the several technology, interoperability, and economical issues raised for this technology, 100G-EPON has attracted interest across the entire optical communications field, including network operators, system and device vendors, as well as researchers working on issues such as optical fiber transmission and the application of signal processing techniques.

## 9.8 Challenges in PON Design

With the emergence of LTE/LTE + networks, PONs have been revisited as viable architectures for also backhauling wireless traffic. Among the most important challenges are the extension of the PON reach and the development of burst-mode receivers. PON operators are mainly interested in increasing the PON reach instead of deploying new feeder networks. Similarly, they prefer to increase the split ratio, which limits reach, for adding new ONUs. Among the options for how to extend reach, Raman amplification has been proposed, especially for the upstream traffic. In order to maintain the feeder network completely passive, a Raman pump can be placed at the OLT for providing distributed gain in the feeder fiber for the upstream signal, while a high-power signal source, EDFA or SOA, can be employed at the OLT for amplifying the downstream signal. Work presented in [22] demonstrated a GPON extension system of 60-km reach and 1:128 split ratio, employing Raman amplification.

Another important challenge is the design and development of high-speed, low-cost burst-mode receivers. As mentioned before, upstream packets from ONUs are asynchronous and may travel different distances before arriving at the OLT. Thus, they may enter the OLT with different optical power, as well as with different amplitude and phase noise. It is therefore essential that the OLT has a burst-mode receiver that can receive such optical burst signals and instantaneously amplify them to a fixed amplitude in the electrical domain. Furthermore, for backward compatibility issues, a burst-mode receiver must support more than one rate. For example, GEAPON and 10G-EPON customers are both connected to the same OLT's burst-mode receiver. Therefore, the design of a reliable burst-mode receiver is challenging and requires high-sensitivity, a wide dynamic range, as well as short setting times in order to meet PON specifications. Of particular importance is the response time for clock and data recovery, which must be below 400 ns for GEAPON and 10G-EPON.

Currently research focuses on developing 40G burst-mode receivers using discreet IC designs of broadband transimpedance and limited amplifiers (TIA/LA), as well as clock and data recovery CDR circuits.

## 9.9 Distributed Ring-Based WDM-PON Architecture

As previously described, traditional WDM-PON systems allocate a separate pair of dedicated upstream and downstream wavelength channels to each subscriber, enabling the delivery of a symmetric 1 Gbps or more of dedicated bandwidth per subscriber/ONU in each direction, with bit rate and protocol transparencies, guaranteed quality of service (QoS), and increased security. Despite these numerous crucial advantages, traditional tree-based WDM-PON architectures suffer from several inherent limitations that must be addressed first before WDM-PON evolves

as the dominant NG broadband access infrastructure able to efficiently backhaul wireless traffic. These include (i) the inability to efficiently utilize limited available network resources and to cope with the dynamic and bursty traffic patterns of the emerging services [23, 24]. The former limitation is exacerbated when some wavelength channels are heavily loaded, while others are underutilized or are totally idle. Since bandwidth is dedicated on a point-to-point basis, there is no way to dynamically move capacity from a heavily loaded channel to another lightly loaded/idle channel, leading to the waste of scarce network resources. Therefore, to increase the total throughput, it is essential that future WDM-PON access architectures must support dynamic bandwidth allocation (DBA) and sharing; (ii) the inability to support a truly shared LAN capability among end users (end users attached to these PONs cannot directly communicate with each other, and thus the need for meshing of the eNBs as previously described cannot be accommodated). This LAN capability also provides the ability to support a distributed control architecture. Mainstream PON dynamic bandwidth allocation (DBA) schemes have been centralized, relying on a component at the distant OLT to arbitrate upstream transmission. In addition to the typical single point of failure problem, the centralized processes of upstream bandwidth allocation at the distant OLT are lengthy and complex and require many changes at each ONU.

Numerous WDM-PON architectures have been proposed in the literature to address the aforementioned limitations of traditional WDM-PONs [8, 9, 23–29]. To address the former problem, several WDM-PON architectures and protocols that dynamically manage and allocate bandwidth in both time and wavelength dimensions have been proposed [8, 9, 23–29]. Most of these schemes, however, are costly, require many redundant components, and assume complex OLT and ONUs setups, which require tunable transceivers, or an array of fixed transceivers, or both, WDM filters, and wavelength/waveband-selective receivers at both the OLT and ONUs. Furthermore, schemes that support dynamic wavelength sharing, where additional wavelength channels are added to accommodate the fraction of bursty downstream traffic that may exceed the user's dedicated downstream wavelength channel rate, are still falling short of addressing the fundamental problem of the inefficient utilization of network resources [23, 24]. This is because unused capacities of those lightly loaded, or even idle dedicated downstream wavelength channels are being wasted. Overall, each of these complex architectures has only targeted a single limitation and applied specific solutions and workarounds to traditional WDM-PONs, mostly resulting in increased cost and complexity.

The latter problem has received considerable attention due to the rising importance of supporting virtual private connections among end users (for instance, branch sites in a business enterprise). In this regard, several physical layer LAN emulation schemes have been proposed to achieve intercommunication among the ONUs, but only within the context of TDM-PONs. Fewer schemes have also been proposed to achieve intercommunication among the ONUs within a WDM-PON infrastructure. In addition to the added cost and complexity, most of these schemes, however, suffer from poor scalability due to high splitting losses as the redirected LAN signals traverse through the star coupler/AWG once or twice, resulting in

lower power budget that limits the number of ONUs that can be attached to a single PON. In general, achieving intercommunication among subscribers within a tree-based WDM-PON setup is a lengthy and complex process that requires much more resources than those needed for a TDM-PON.

In this section, we examine a simple and cost-effective local access WDM-PON architecture that addresses some of the limitations of conventional tree-based WDM-PON architectures including supporting dynamic allocation of network resources as well as a truly shared LAN capability among end users. The proposed architecture combines the salient features of both traditional static WDM-PON (i.e., dedicated connectivity to all subscribers with bit rate and protocol transparencies, guaranteed QoS, and increased security) and dynamic WDM-PON (i.e., efficiently utilizing network resources via dynamic wavelength allocation/sharing among end users).

As 4G is a distributed architecture where, in particular, the 4G LTE standard requires a new distributed mobile backhaul radio access network (RAN) architecture and further creates a requirement for fully meshing the BSs (as previously mentioned the X2 interface for LTE BS-BS handoffs requires a more meshed architecture), a PON-based mobile backhaul RAN must be capable of supporting a distributed architecture as well as distributed network control and management (NCM) operations. The proposed architecture eloquently complies with both requirements via a purposely selected simple ring topology, which enables direct intercommunication/connectivity among the access nodes (ONUs/BSs), allowing for the support of a distributed PON-RAN access architecture as well as for simply meeting the stringent requirement to fully meshing the ONUs/BSs. Thus, the proposed ring-based architecture may provide a simple and cost-effective mobile backhaul RAN solution. Note that the proposed ring-based architecture can also be evolved to an all-packet-based converged fixed-mobile optical access networking transport infrastructure by simply interconnecting (overlying) the ONUs with the 4G/5G BSs.

## 9.10 Architecture Design

Unlike a typical WDM metro access ring network, where the feeder fiber of a PON is replaced with a metro fiber ring that interconnects the hub and access nodes, the proposed architecture interconnects WDM ONUs via a short distribution fiber ring in the local loop but allows them to share the feeder fiber for long reach connectivity to the OLT (Fig. 9.8). Specifically, the OLT is connected to the ONUs via a 20-km trunk feeder fiber, a passive three-port optical circulator, and a small fiber ring. To cover the same local access area as in a similar tree-based architecture, the small ring at the end of the trunk is assumed to have a 1–4 km diameter. The ONUs are joined by point-to-point links in a closed loop around the access ring. The links are unidirectional: Both downstream and upstream signals (combined signal) are transmitted in one direction only. Each ONU is assigned a single dedicated

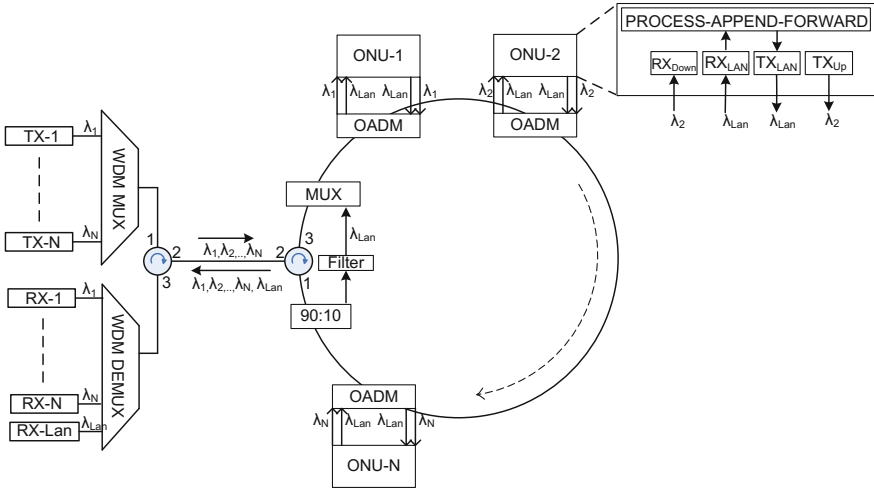


Fig. 9.8 Ring-based C/DWDM-PON architecture [32]

wavelength for both downstream and upstream transmissions. Direct intercommunication among ONUs is achieved via an additional local control/LAN wavelength channel,  $\lambda_{LAN}$ , which is terminated, regenerated, and retransmitted at each ONU [30, 31].

Downstream/upstream wavelengths as well as the LAN wavelength are spaced 200 GHz apart in the 1530–1565 nm standard C-band. For example, for an architecture supporting 16 ONUs, the total number of required wavelength channels would be 17 (corresponding to 16 downstream/upstream wavelength channels plus an additional local control/LAN wavelength channel) and these channels could also be allocated over the 1270–1610 nm CWDM spectrum that can offer up to 18 available channels with 20-nm spacing, as defined in ITU TG.694.2. Thus, the overall system cost could potentially be reduced via the utilization of low-cost commercially available CWDM components. To scale beyond 16 ONUs, the number of downstream/upstream wavelength channels could be doubled or quadrupled by reducing the channel spacing in the C-band to 100 or 50-GHz, respectively (provided, of course, that the overall system power budget would still be satisfactory).

The OLT houses an array of  $N$  fixed transmitters (Tx) and another array of  $N + 1$  fixed receivers (Rx), a passive three-port optical circulator, and a commercially available low-cost thin-film-based DWDM multiplexer/demultiplexer. Each Tx/Rx pair corresponds to one ONU and utilizes the same wavelength for transmitting and receiving downstream and upstream traffic, respectively. The extra receiver ( $N + 1$ ) located at the OLT is used to detect the local control/LAN channel. Each ONU has a Tx/Rx pair which is matched to the corresponding pair at the OLT and another Tx/Rx pair for transmitting and receiving the local LAN channel,  $\lambda_{LAN}$ . In addition, each ONU houses a commercially available low-cost four-port thin film

filters-based fixed optical add-drop multiplexer (OADM), where two wavelengths (corresponding downstream/upstream and LAN wavelengths) are dropped and added at each node.

The DWDM downstream signal is coupled to the ring via port 3 of the optical circulator. After recombining it with the re-circulated LAN signal via a  $2 \times 1$  WDM combiner (placed on the ring directly after the optical circulator), the combined signal then circulates around the ring (ONU<sub>1</sub> through ONU<sub>N</sub>) in a drop/add and go-through fashion. Finally, at the last node (ONU<sub>N</sub>), wavelengths  $\lambda_N$  and  $\lambda_{LAN}$  are dropped/added. Thus, the DWDM downstream signal is terminated at the last node.

The combined DWDM upstream and LAN signals emerging from the last ONU at the end of the ring are split into two components via a (10:90)  $1 \times 2$  passive splitter placed on the ring directly after the last ONU. The first component (90 %) is directed toward the OLT via circulator ports 1 and 2, while the second component (10 %) passes first through a band rejection filter that terminates the DWDM upstream signal. The second component emerging from the band rejection filter, the LAN signal, is allowed to re-circulate around the ring after recombining with the downstream signal (originating from the OLT) via the  $2 \times 1$  WDM combiner (multiplexer). The first component of the combined DWDM upstream and LAN signal is received and processed by an array of  $N + 1$  fixed optical receivers (housed at the OLT). Specifically, each one of the  $N$  upstream optical receivers detects the corresponding upstream signal and recovers the MAN/WAN traffic, while the LAN optical receiver, as will be explained below, processes the control messages and may discard or process the LAN traffic provided that, as will be shown below, it carries upstream traffic as well [32].

## 9.11 Allocation of Network Resources

The potential of this architecture is further explored below in terms of its capability to support distributed and dynamic allocation/sharing of overall network resources among the access nodes (ONUs). As previously mentioned, direct communication among ONUs is achieved via the LAN/control channel, which is terminated, processed, regenerated, and retransmitted at each ONU. Since control messages are processed and retransmitted at each node, the ONUs can directly communicate their LAN queue status and exchange signaling and control information with one another in a fully distributed fashion. The control plane utilized among the ONUs can thus support a distributed PON architecture, where each access node (ONU) deployed around the ring has now a truly physical connectivity and is capable of directly communicating with all other access nodes. Supported by the distributed control plane, each ONU can now independently provision both upstream and LAN traffic and can further collaborate with the OLT to dynamically provision downstream traffic as well.

### ***9.11.1 Dynamic Bandwidth Allocation***

The proposed scheme utilizes a fully distributed time division multiple access (TDMA) arbitration scheme in which the OLT is excluded from the arbitration process. This work utilizes the control and management messages defined by the IEEE 802.3ah multi-point control protocol (MPCP) standard that were previously described in Sect. 9.4.1. It further assumes a cycle-based LAN link, where the cycle size can be either fixed or variable length confined within certain lower and upper bounds to accommodate the dynamic LAN traffic conditions. During each LAN cycle, the ONUs transmit their control (REPORT) messages along with LAN data sequentially in an ascending order within their granted time slots around the ring from one node to the next, where each REPORT message is finally removed by the source ONU after making one trip around the ring. ONUs sequentially and independently run instances of the same LAN-DBA algorithm outputting identical bandwidth allocation results each cycle [33, 34]. The execution of the algorithm at each ONU starts immediately after the collection of all REPORT messages. Thus, all ONUs must execute the DBA algorithm prior to the expiration of the current cycle so that bandwidth allocations scheduled for the next cycle are guaranteed to be ready by the end of the current cycle. An execution of the DBA algorithm produces a unique and identical set of ONU assignments. Once the algorithm is executed, the ONUs sequentially and orderly transmit their data without any collisions, eliminating the OLT's centralized task of processing requests and generating grants for LAN bandwidth allocations. It is important to emphasize that maintaining accurate time synchronization between the ONUs is essential for the appropriate operation of the distributed DBA algorithm. In general, this is always the case, as all ONUs are synchronized to a common reference clock extracted from the OLT downstream traffic.

This architecture can also be utilized for implementing an efficient dynamic wavelength assignment/sharing strategy for upstream and downstream traffic (implemented jointly at both the OLT and ONUs).

### ***9.11.2 Upstream Traffic Flows Rerouting and Sharing***

Analogous to traditional WDM-PONs, each ONU in the proposed architecture is assigned a dedicated wavelength for upstream transmission. However, if the incoming user's bursty traffic flows exceed its dedicated upstream wavelength channel rate for some interval, the corresponding upstream queue becomes congested. In this case, the flow scheduler at that ONU may redirect one or more of the user's excess upstream service flows to the local LAN queue, provided that this LAN queue has some available space that can accommodate one or more of the upstream excess flows. More details on the proposed techniques can be found in [32].

## 9.12 Wavelength Assignment/Sharing for Downstream Traffic

Each OLT downstream queue is assigned to a specific ONU and is connected to a dedicated downstream wavelength. Each ONU houses two queues: One queue is assigned to a dedicated upstream wavelength, while the other queue is assigned to the LAN/control traffic. The process of dynamically assigning/sharing downstream wavelengths is implemented jointly at both the OLT and ONUs as follows: If a dedicated downstream wavelength channel,  $\lambda_i$ , with traffic destined to ONU<sub>*i*</sub> is overloaded (i.e., incoming bursty traffic flows may exceed the dedicated channel rate for some interval, so that its corresponding queue is congested), the following steps are executed [31]: (i) The scheduler at the OLT searches for another underutilized/idle downstream wavelength channel, i.e., a channel  $\lambda_j$  whose corresponding queue has some available space that can accommodate one or more excess flows (i.e.,  $Q_j$ ). (ii) If the search is successful, the available channel is selected if and only if its corresponding LAN queue at the corresponding ONU (ONU<sub>*j*</sub>) is also available. (iii) The scheduler redirects one, some, or all of the excess flows to  $Q_j$ , where it is then transmitted, along with ONU<sub>*j*</sub>'s native downstream traffic, to ONU<sub>*j*</sub> over its dedicated wavelength channel  $\lambda_j$ . (iv) The  $\lambda_j$ -downstream optical receiver housed at ONU<sub>*j*</sub> terminates all  $\lambda_j$ 's downstream traffic, including both native downstream traffic destined to ONU<sub>*i*</sub> and traffic destined to ONU<sub>*i*</sub>. It examines the destination MAC address of each detected Ethernet frame and then performs the following two functions: (a) Native downstream traffic that matches ONU<sub>*j*</sub>'s MAC address is copied and delivered to end users; (b) traffic destined to ONU<sub>*i*</sub> (whose MAC address does not match that of ONU<sub>*j*</sub>) is redirected to ONU<sub>*j*</sub>'s LAN queue and then retransmitted, along with ONU<sub>*j*</sub>'s own local LAN traffic, as LAN traffic around the ring to its final destination (ONU<sub>*i*</sub>), within the proper designated LAN timeslot of ONU<sub>*j*</sub>.

Various resource allocation schemes that efficiently support dynamic and fair allocation of wavelengths and sharing traffic among PON end users have been developed for this architecture and can be found in [32, 35, 36]. Performance results on link throughput and delay as detailed in the aforementioned works demonstrate that the proposed methodologies can meet the capacity requirements of the dynamic and highly fluctuant traffic pattern of the emerging multimedia applications and services.

## 9.13 Fault Detection and Recovery

While the economics for commercially deploying WDM-PONs in the access arena for backhauling wireless traffic or as a converged fixed-mobile optical networking transport infrastructure are quite compelling, however, several key outstanding technical hurdles must be further addressed. The key stumbling block has been, and

certainly remains to be, the inherent lack of simple and efficient resilience capabilities in mainstream tree-based PON topologies, which guarantee the reliable delivery of the massive amount of fixed-mobile traffic, specifically, against failures in the distribution network. Since a single-wavelength channel failure may affect the premium services delivered to thousands of fixed-mobile end users, the reliability offered by such an access networking transport infrastructure to the services and customers it supports is one of the most important considerations in designing and deploying such a PON-based converged architecture. Thus, given the unique advantages provided by the aforementioned ring-based WDM-PON architecture, it was also imperative to introduce efficient resilience mechanisms for such architecture.

Figure 9.9 illustrates the proposed fully distributed self-healing WDM-PON architecture. The solid lines (working fiber) represent the normal state architecture, while the dotted lines (protection fiber) represent the redundant protection components. The protected architecture is identical to that of the normal working architecture (as explained in Sect. 9.10) except for the following additional components (dotted lines): (i) a redundant short distribution fiber ring and a trunk fiber; (ii) two  $2 \times 1$  optical switches located at the OLT; (iii) an automatic protection switching (APS) module located at each ONU.

The APS module attached to each ONU is the basic building block of the proposed self-healing mechanism that monitors the state of its adjacent distribution fiber paths and its own state and performs both fault detection and automatic switching process. The APS module connects to both incoming and outgoing working and protection fibers. Each APS module houses a commercially available low-loss  $4 \times 4$  bidirectional optical switch (OS) that is capable of switching from any input port to any output port [37]. It also includes two detection circuits, where each circuit comprises a band splitter (to separate the combined downstream/upstream/LAN signal into its constituents LAN and downstream/upstream signals), control circuit to configure the OS, and a PIN

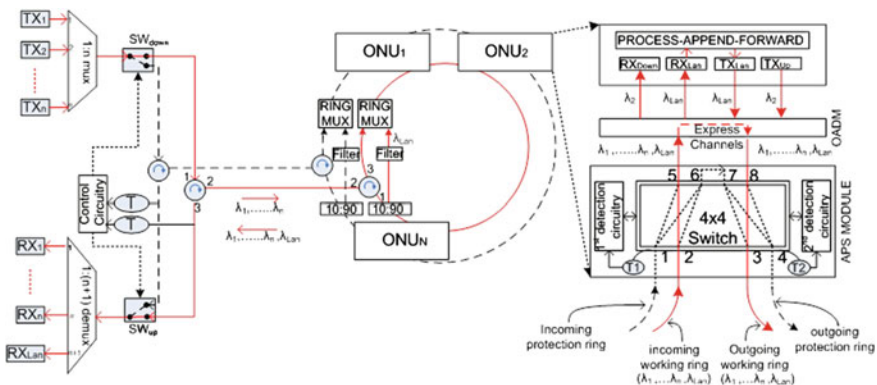


Fig. 9.9 Self-healing ring-based C/DWDM-PON architecture [38]

detector. Under normal operation, as shown in Fig. 9.9, the combined signal traverses the incoming and outgoing working fibers via ports 2–5 and 8–3, respectively.

### 9.13.1 *Fault Detection*

If a failure occurs in the network, the REPORT message transmitted by the affected ONU typically contains a failure indication alarm message that includes specific instructions to both the OLT and a remote node that will be involved in the recovery process. Since the LAN signal is always present on the ring and trunk (cyclic control message is always transmitted independent of the presence or absence of LAN data), general failure detection scenarios (general distribution link and node failures) will primarily be based on detecting the absence/presence of the LAN signal only. Thus, all ONUs are continuously monitoring the status of the LAN signal on both incoming and outgoing fibers. If, for example, the first control circuit of a given ONU<sub>*n*</sub> detects the absence of the LAN signal on its incoming working fiber, a general distribution link failure is assumed. This is the link that interconnects ONU<sub>*n-1*</sub> with ONU<sub>*n*</sub>. On the other hand, if the first control circuit of a given ONU<sub>*n*</sub> detects presence of the LAN signal on its incoming working fiber, while the second control circuit detects absence of same signal (after being processed, regenerated, and retransmitted by ONU<sub>*n*</sub>) on its outgoing working fiber, a node (ONU<sub>*n*</sub>) failure is assumed. While ONU<sub>*n*</sub> detects its own failure (via an APS module attached to it), however, managing the failure is delegated to the next node on the ring (ONU<sub>*n+1*</sub>). Complete details on the detection of all types of failures in this architecture can be found in [38].

### 9.13.2 *Fault Recovery*

In general, the recovery process is implemented via the participation of three cooperating network nodes including the affected node (ONU<sub>*n*</sub>), OLT, and either ONU<sub>*n-1*</sub> (in the case of a link failure) or ONU<sub>*n+1*</sub> (in the case of a node failure). As an example below the general link failure recovery is described. A detailed description of all failure recovery mechanisms for any other type of failure can be found in [38]. These protection schemes are capable of protecting against both node and distribution/trunk fiber failures, and they enable the recovery of all network traffic including upstream, downstream, and LAN data. In addition, these schemes can also protect against any combination of concurrent double failures including trunk/distribution fiber breaks and node failures.

*General Link Recovery:* The successful completion of the recovery process of a given general link failure scenario involves the following steps: (i) To avoid false failure detection, once the affected node (for instance ONU<sub>*n*</sub>) detects a given link

failure (e.g., fiber cut), it must wait for a predetermined timeout. (ii)  $ONU_n$  then stops both LAN and upstream transmissions, switches to the incoming protection fiber, and floods the network with a failure indication alarm message (first REPORT message) that includes specific instructions to  $ONU_{n-1}$  (to switch its transmission from outgoing working fiber to outgoing protection fiber), each and every other ONU (to stop both LAN and upstream transmissions), and OLT (to stop downstream transmission). (iii)  $ONU_n$  keeps flooding the network with the failure message expecting its failure frame to loop back to it via  $ONU_{n-1}$ 's outgoing protection fiber. (iv) Upon receiving the failure message, each and every ONU on the ring stops LAN and upstream transmissions; likewise, OLT stops downstream transmission. (v) Once  $ONU_n$  receives back its failure frame (assuming  $ONU_{n-1}$  has already switched to the outgoing protection fiber), it starts flooding the OLT with a second REPORT message requesting downstream resynchronization frames. (vi) Once the OLT receives a resynchronization request from  $ONU_n$ , it resumes all downstream transmissions. (vii) Once  $ONU_n$  receives resynchronization frames from the OLT, it initiates a new cycle (recovery process is now complete) by transmitting its normal REPORT control message to all other ONUs. Then, all ONUs sequentially send their REPORTs; once all reports are exchanged for LAN-DBA calculation of the new cycle, new grants are calculated and normal operation resumes.

Performance results as illustrated in [38] demonstrate that the recovery time associated with any and all different distribution network/trunk failures is still within the delay bound limit required for delivering guaranteed triple play services.

## 9.14 Fronthauling Mobile Traffic

As previously explained in various other chapters of this book, to increase efficiency in LTE and LTE-Advanced systems, an important feature is the distributed radio access network (RAN) architecture that includes remote radio heads (RRHs) (comprising of the radio, amplification, filtering, and the antenna) connected to the baseband unit (BBU) (utilized for the centralized signal processing functions) using the Common Public Radio Interface (CPRI) standard (a digital interface standard for encapsulating radio samples between a radio and a BBU). This CPRI traffic must be fronthauled efficiently, following tight quality constraints (in terms of maximum latency, jitter, and bit error rate) between the RRH and BBU locations. It should be noted here that CPRI requires significantly higher data transmission rates than the payload it is carrying (fronthaul carries uncompressed digital data—the digitally sampled analog radio signal with error correction and encapsulation on top).

There are several options for CPRI fronthaul, including utilizing dedicated fiber links (albeit a costly solution), the OTN (that can potentially add latency into the system), microwave links (only for short distances and a subset of the CPRI bit rate options), as well as PONs. In general, fiber connections are the best choice for this

applications, partly because of the long reach and capacity that they can provide, and partly because of their characteristics (weight, ice loading, wind resistance, etc.) that make them ideal for running up the tower.

Fronthauling mobile traffic utilizing PONs is a potentially attractive solution for CPRI transport as the data-rate requirement of CPRI matches the development of PON technologies. Further, the stringent delay requirements of the CPRI protocol are also well supported by using PONs, as the only source of transport-incurred latency is due to signal propagation (allowing the maximization of the distance between the RRH and BBU). Nevertheless, if PONs are utilized to fronthaul mobile traffic, careful engineering is required to accommodate for the power loss budget and prevent additional latency being incurred which would limit the cell radius.

Further, looking at the PON technologies and standards described previously in this chapter, NG-PON2 can easily support the required fronthaul speeds and distances; however, for the TWDM-PON implementation of NG-PON2 it could potentially be very challenging to meet the strict latency and jitter requirements imposed. Other potential techniques to implement fronthaul utilizing PONs include dedicating one of the wavelengths in the TWDM-PON implementation of NG-PON2 for fronthauling mobile traffic or utilizing a WDM-PON (that has a large number of available dedicated 1G/10G wavelengths). There are a number of recent research efforts on utilizing WDM-PONs for mobile fronthauling, including the 5G-XHaul initiative, a project that is part of the EU Horizon 2020 5G Infrastructure Public-Private Partnership (5G PPP).

Finally, the reader should note that as the choice of technology for mobile fronthauling is still an open issue, the Full Service Access Network (FSAN) forum has set up a Mobile Fronthaul Study Group to collect mobile fronthaul requirements from operators, evaluate possible solutions, and present recommendations on the technology best suited to be used for mobile fronthauling.

## 9.15 Conclusions

This chapter motivates the need for utilizing fiber-based passive optical network (PON) access infrastructure to backhaul mobile traffic and subsequently describes the various standards and technology options for this type of networks. It also describes a novel, fully distributed, ring-based WDM-PON architecture that could be utilized for backhauling wireless traffic, as well as supporting a converged next-generation mobile infrastructure. This architecture can support dynamic allocation of network resources as well as a truly shared LAN capability among end users, combining the salient features of both traditional static and dynamic WDM-PON. Efficient distributed QoS-aware resource allocation schemes were developed for this architecture, guaranteeing the delivery of delay and jitter-sensitive real-time applications. The ring architecture design also provides simple and cost-effective resilience capabilities against any and all kinds of

networking failures, enabling the recovery of all network traffic including upstream, downstream, and LAN data.

Finally, as in 4G and 5G the radio access network (RAN) becomes a broad concept that also includes mobile fronthaul, a discussion is also added at the end of this chapter on mobile fronthaul utilizing PON infrastructures.

## References

1. Dahlman E, Parkvall S, Skold J, Beming P (2008) 3G evolution: HSPA and LTE for mobile broadband, 2nd edn. Academic Press
2. Ali M, Ellinas G, Erkan H, Hadjiantonis A, Dorsinville R (2010) On the vision of complete fixed-mobile convergence. *IEEE/OSA J Lightwave Technol* 28(16):2343–2357
3. Ranaweera C, Wong E, Lim C, Nirmalathas A (2012) Next generation optical-wireless converged network architectures. *IEEE Network* 26(2):22–27
4. Kramer G (2005) Ethernet passive optical networks. McGraw-Hill
5. Kramer G, Pesavento G (2002) Ethernet passive optical network (EPON): building a next generation optical access network. *IEEE Commun Mag* 40(2):66–73
6. Shumate PW (2008) Fiber-to-the-home: 1997–2007. *IEEE/OSA J Lightwave Technol* 26(9):1093–1103
7. Lee C-H, Sorin WV, Kim BY (2006) Fiber to the home using a PON infrastructure. *IEEE/OSA J Lightwave Technol* 24(12):4568–4583
8. Kazovsky LG, Shaw W-T, Gutierrez D, Cheng N, Wong S-W (2007) Next-generation optical access networks. *IEEE/OSA J Lightwave Technol* 25(11):3428–3442
9. Effenberger F, Cleary D, Haran O, Kramer G, Li RD, Oron M, Pfeiffer T (2007) An introduction to PON technologies. *IEEE Commun Mag* 45(3):S17–S25
10. Effenberger F, El-Bawab T (2009) Passive optical networks (PONs): past, present, and future. *Opt Switch Netw* 6(3):143–150
11. Skubic B, Chen J, Ahmed J, Wosinska L, Mukherjee B (2009) A comparison of dynamic bandwidth allocation for EPON, GPON, and next generation TDM PON. *IEEE Commun Mag* 47(3):S40–S48
12. Roy R, Kramer G, Hajduczenia M, Silva H (2011) Performance of 10GEPON. *IEEE Commun Mag* 49(11):78–85
13. Aurzada F, Scheutzw M, Reisslein M, Ghazisaidi N, Maier M (2011) Capacity and delay analysis of next-generation passive optical networks (NG-PONs). *IEEE Trans Commun* 59(5):1378–1388
14. Kani J-I, Bourgart F, Cui A, Rafel A, Campbell M, Davey R, Rodrigues S (2009) Next-generation PON—part I: technology roadmap and general requirements. *IEEE Commun Mag* 47(11):43–49
15. Rujian L (2008) Next generation PON in emerging networks. In: *Proceedings IEEE/OSA optical fiber communication/national fiber optic engineers conference (OFC/NFOEC)*, pp 1–3
16. Tanaka K et al (2010) IEEE 802.3av 10G-EPON standardization and its research and development status. *IEEE/OSA J Lightwave Technol* 28:651–661
17. Gutierrez L, Garfias P, De Andrade M, Cervello-Pastor C, Sallent S (2010) Next Generation Optical Access Networks: from TDM to WDM. In: Bouras CJ (ed) *Trends in telecommunications technologies*, InTech
18. Banerjee A et al (2005) Wavelength-division-multiplexed passive optical network (WDM-PON) technologies for broadband access: a review. *OSA J Opt Netw* 4(11):737–758
19. Zhang J, Ansari N (2011) Scheduling hybrid WDM/TDM passive optical networks with nonzero laser tuning time. *IEEE/ACM Trans Netw* 19(4):1014–1027
20. <http://www.ict-sardana.eu>

21. [www.ict-accordance.eu](http://www.ict-accordance.eu)
22. Maier M (2014) The escape of Sisyphus or what “Post NG-PON2” should do apart from never-ending capacity upgrades. *Photonics* 1(1):47–66
23. Leng L, Le T (2012) A Raman amplified GPON reach extension system using parameters of a deployed fiber. *OSA Opt Express* 20(24):26473–26479
24. Song H, Mukherjee B, Park Y, Yang S (2006) Shared-wavelength WDM-PON access network for supporting downstream traffic with QoS. In: *Proceedings of IEEE/OSA optical fiber communication conference (OFC)*, Anaheim, CA, March 2006
25. Song H, Park Y, Banerjee A, Mukherjee B (2010) Shared wavelength WDM-PON access network. In: *Proceedings international conference on the optical internet (COIN)*, Jehu, Korea
26. An F-T, Kim KS, Gutierrez D, Yam S, Hu E, Shrikhande K, Kazovsky LG (2004) SUCCESS: a next-generation hybrid WDM/TDM optical access network architecture. *IEEE/OSA J Lightwave Technol* 22(11):2557–2569
27. Maier M, Herzog M, Reisslein M (2007) STARGATE: the next evolutionary step toward unleashing the potential of WDM EPONs. *IEEE Commun Mag* 45(5):50–56
28. McGarry M, Reisslein M, Maier M (2006) WDM ethernet passive optical networks. *IEEE Commun Mag* 44(2):15–22
29. Dhaini A, Assi C, Maier M, Shami A (2007) Dynamic wavelength and bandwidth allocation in hybrid TDM/WDM EPON networks. *IEEE/OSA J Lightwave Technol* 25(1):277–286
30. Hsueh Y-L, Rogge MS, Yamamoto S, Kazovsky LG (2005) A highly flexible and efficient passive optical network employing dynamic wavelength allocation. *IEEE/OSA J Lightwave Technol* 23(1):277–286
31. Hossain ASM D, Dorsinville R, Hadjiantonis A, Ellinas G, Ali M (2007) A simple self-healing ring-based local access PON architecture for supporting private networking capability. In: *Proceedings of IEEE global communications conference (GLOBECOM)*, Washington DC, November 2007
32. Erkan H, Hossain ASM D, Dorsinville R, Ali MA, Hadjiantonis A, Ellinas G, Khalil A (2008) A novel ring-based WDM-PON access architecture for the efficient utilization of network resources. In: *Proceedings of IEEE ICC*, pp 5175–5181
33. Erkan H, Ellinas G, Hadjiantonis A, Dorsinville R, Ali MA (2013) Dynamic and fair resource allocation in a distributed ring-based WDM-PON architectures. *Comput Commun Spec Issue Progr Broadband Access Netw Opt-Wirel Converg* 36(14):1559–1569
34. Sherif S, Hadjiantonis A, Ellinas G, Assi C, Ali MA (2004) A novel distributed Ethernet-based PON access architecture for provisioning differentiated QoS. *IEEE/OSA J Lightwave Technol* 22(11):2483–2497
35. Delowar A, Dorsinville R, Ali MA, Shami A, Assi C (2006) Ring-based local access PON architecture for supporting private networking capability. *OSA J Optical Netw* 5(1):26–39
36. Ramantas K, Vlachos K, Bikos AN, Ellinas G, Hadjiantonis A (2014) A new unified PON-RAN access architecture for 4G LTE networks. In: *IEEE/OSA Journal of Optical Communications and Networks*, vol 6, no 10, pp 890–900
37. Christodoulou C, Manousakis K, Ellinas G (2016) Optimization algorithm for downstream wavelength sharing and scheduling in Mobile Backhaul networks. In: *Proceedings of IEEE 18th Mediterranean electrotechnical conference (Melecon)*, Limassol, Cyprus
38. Erkan H, Ellinas G, Hadjiantonis A, Dorsinville R, Ali MA (2010) Native ethernet-based self-healing WDM-PON local access ring architecture: a new direction for supporting simple and efficient resilience capabilities. In: *Proceedings of IEEE international communications conference (ICC)*, Cape Town, South Africa, May 2010

# Chapter 10

## BBU Hotelling in Centralized Radio Access Networks

Nicola Carapellese, M. Shamsabardeh, Massimo Tornatore  
and Achille Pattavina

**Abstract** This chapter focuses on the role of BBU hotelling in converged network architectures. The main motivations behind this technique are described, and the critical drawbacks are detailed, mainly related to the transport of the new “fronthaul” traffic over the network infrastructure. A classification of the various architectural solutions for BBU hotelling is detailed, regarding BBU placement and implementation, and fronthaul transport. Finally, a specific example of converged network architecture is presented, which is based on an optical WDM aggregation network supporting both fronthaul and backhaul traffic. We discuss also a novel network optimization problem, the BPTR (BBU Placement and Traffic Routing), whose objective is the minimization of a generic cost/energy metric. The problem is solved through a heuristic algorithm, and a numerical evaluation is carried on over randomly generated multi-stage aggregation networks. The main result is that the achievable BBU consolidation into a few hotel nodes is considerably high for realistic geographic scenarios, justifying the evolution toward converged networks.

### 10.1 Introduction

The current explosion of traffic generated by mobile devices (e.g., smartphones, tablets, USB dongles) requires some radical changes to existing mobile network technologies and architectures. Some changes are being already introduced, for instance, adopting novel radio access technologies (e.g., LTE) to increase spectrum efficiency and deploying additional cells to serve high traffic density areas (e.g., micro-cells, small cells). Several other improvements are under investigation by academic and industrial research. The “BBU hotelling” (sometimes written as “BBU hostelling”) is one of the ways to evolve mobile networks. It is not a single technique, but a family of technological and architectural concepts that radically

---

N. Carapellese · M. Shamsabardeh · M. Tornatore (✉) · A. Pattavina  
Politecnico di Milano, Department of Electronics, Information and Bioengineering (DEIB),  
Milan, Italy  
e-mail: massimo.tornatore@polimi.it

change the way in which mobile networks are implemented. For this reason, in order to understand the motivations behind BBU hotelling and its potential benefits over conventional architectures, it is important to briefly describe how a typical mobile network is structured and how it works. Therefore, in Sect. 10.2 the fundamentals of mobile networks are presented, while in Sect. 10.3 details of the implementation of base stations are given, which lead to the definition of BBU hotelling and its main advantages in Sect. 10.4. The challenges of BBU hotelling, regarding the new “fronthaul” traffic, are described in Sect. 10.5. In Sect. 10.6, several possible BBU hotelling architectures are discussed. Section 10.7 introduces a new possible converged aggregation architecture, and Sect. 10.8 describes the optimization problem (BPTR) associated with the design of this proposed network architecture. Finally, in Sect. 10.9 a heuristic algorithm for BPTR is presented and in Sect. 10.10 a case study analysis is given. Section 10.11 concludes the chapter.

## 10.2 Mobile Network

A typical mobile network can be divided into three parts: Radio Access Network, Backhaul Network, and Core Network (the reader can refer to Chap. 2 for a high-level example of mobile network architecture). The Radio Access Network (RAN) includes all the systems performing radio-access-related functions, i.e., directly managing radio transmission and reception toward/from mobile devices. Note that the standard that defines the network architecture and specifies functions, interfaces, and protocols assigned to RAN nodes and mobile devices is called the Radio Access Technology (RAT) (e.g., WCDMA/HSPA, LTE, WiMax). The Backhaul Network performs traffic aggregation and transport between the RAN and the Core Network. For this reason, its architecture and implementation can be almost agnostic with respect to radio access and core architectures, so they are not covered by RAT standards, given that adequate transport capacity and QoS (e.g., latency) requirements are guaranteed. Finally, the Core Network is in charge of all remaining non-radio-access-related functions and acts as a gateway toward all other mobile and fixed networks, i.e., toward the Internet. Some core network functions and interfaces are standardized too, in most of cases accordingly to the adopted RAT.

The RAN directly interfaces to mobile devices (UE, User Equipment) via radio links established toward the Base Stations (BS). Each BS manages the transfer of user and control data toward (downlink) and from (uplink) several UEs simultaneously, by means of physical layer and multiple access protocols, according to the so-called radio, or air interface. Some higher-layer radio access functions (e.g., radio resource control) can be either performed by other network nodes (e.g., Base Station Controllers, BSC, or Radio Network Controllers, RNC) that manage several BSs, or directly embedded into the BSs themselves (e.g., eNodeB). Each BS manages UEs belonging to a specific coverage area, denoted as “cell”, and the RAN

also coordinates the procedures for user mobility, i.e., allowing UEs to move across adjacent cells (handovers), without losing data connection.

BSs are placed into premises denoted as “cell sites”, whose geographic coordinates are influenced by many different factors, most notably coverage, capacity planning, and infrastructural/cost constraints. To save costs, a consolidated practice is implementing more than one BS into a single cell site, thus dividing the coverage area into up to three cells, denoted also as “sectors”. For the same reason, BSs of different RATs and different mobile operators often share the same cell site. A typical cell site consists of a tower or a mast, on top of which there are installed BS directional antennas (at least one per sector), and a cabinet, or shelter, where the remaining BS equipment is installed. The cabinet also hosts collateral systems which do not perform network functions, but ensure proper BS operation. They typically consist of power supply equipment (AC/DC converters, backup batteries) and cooling systems (fans, air conditioners).

### 10.3 Evolving the Base Station: BBU and RRH

The fundamental enabler of BBU hotelling is a recent evolution on how BSs are physically implemented.

Traditionally, the BS consisted in an all-in-one solution produced by a single manufacturer, performing all functions and interfacing to both the backhaul network and the antennas via coaxial cables. With time, manufacturers have found it more convenient to adopt a modular architecture, i.e., separating some functions in different subsystems. This trend eventually led to a well-consolidated solution, in which the BS is divided into two separate kinds of modules:

- BaseBand Unit (BBU), which performs physical layer digital processing of the baseband version of the radio signals, includes all functions of the upper layers (e.g., wireless MAC, radio link control), and interfaces with the backhaul network;
- Radio Resource Head (RRH), which performs the remaining physical layer functions (i.e., Digital-to-Analog (DA)/Analog-to-Digital (AD) conversion of the baseband signals, frequency up/down conversion, power amplification, and some measures on the received analog signal) and interfaces with antennas via coaxial cables.

The data exchanged between BBU and RRH consist in a digitized baseband version of the radio signals received and transmitted by the antennas, respectively, for the uplink and downlink direction. This data communication is enabled by an ad hoc transport interface established between BBU and RRH. Since the physical connection between them typically consists of an optical fiber link, such kind of transport is known as Digitized Radio-over-Fiber (D-RoF). Another widely used denomination is the “fronthaul”, as a contraposition to the backhaul.

As an alternative to different proprietary fronthaul interfaces, some consortia of manufacturers have defined public interfaces, of which the most established in the market are CPRI and OBSAI. It is important noting that such interfaces were initially defined for short-range connection of BBUs and RRHs located in the same cell site, and later they were considered as natural solutions for fronthaul transport in BBU hotelling architectures. Both standards define different fronthaul transport formats and protocols, covering all the configurations of the main radio access technologies. CPRI is currently the most commercially adopted solution, although it still has some vendor-specific implemented features, which prevent a full multi-vendor interoperability. More details about CPRI, OBSAI, and other in-progress fronthaul standardization activities can be found in Chap. 5.

## 10.4 Advantages of BBU Hotelling

Splitting BSs into BBUs and RRHs and defining open public interfaces for fronthaul has some valuable benefits. In fact, it facilitates the design and implementation of evolved features, because each module can be separately updated, and it also enables the interoperability between different manufacturers and opens the market to smaller newcomers. As a consequence, substantial cost savings can be achieved by both manufacturers and network operators. However, the most important innovation is that BBUs and RRHs are no longer seen as different parts of the same BS, but as distinct network nodes. In fact, they can be independently placed over the infrastructure and exploit the existent RAN to transport the fronthaul. The BBU hotelling is a family of different techniques that take advantage of such physical separation between the BBU and the RRH. At a basic level, it consists in placing the BBUs of a set of cells no more in their respective cell sites, but centralizing them into a single shared site, denoted as “BBU hotel”, or simply “hotel”. This can be done in two main ways: by “stacking”, i.e., purely grouping the BBUs; or by “pooling”, i.e., re-implementing their functions in fewer devices that are designed to share (“pool”) some of their hardware/software resources.

With respect to the traditional architecture, BBU hotelling solutions promise various kinds of advantages, regarding cost, energy consumption, and radio performance [1].

### 10.4.1 Cost Reduction

Costs faced by network operators are typically classified as: Capital Expenditures (CapEx), paid once for purchasing sites and premises, deploying the support infrastructure, and buying/installing network equipment; Operational Expenditures (OpEx), paid continuously over time, to ensure the proper operation of the network, and including lease fees, electricity bills, control/management, repair costs, and

updating costs. For CapEx, it is interesting to note that, while network equipment makes up only 35 %, the cost of site acquisition, civil works, and support (non-RAN) equipment is more than 50 % of the total cost. Also, for OpEx, a relevant part, around 30 %, is needed for site rent [1]. Installing BBUs in a few centralized hotel sites rather than in every cell site can substantially reduce the required space and the installation times, therefore the relative purchase/rent cost. In addition, the BBU centralization into hotels allows sharing some collateral subsystems (e.g., power supplying, cooling, air conditioning, control/monitoring servers, in-site interconnection backplanes), instead of deploying an independent subsystem for every cell site, thus gaining benefit from some “economies of scale”. As a consequence, it gets less expensive to manage the maintenance, repair of failures, and hardware/software updates, because most of the critical equipment is centralized in single hotel sites, which are often more easily and quickly accessible.

### ***10.4.2 Energy Savings***

The energy consumption of the RAN is of primary interest for operators, mainly because it heavily impacts on OpEx. It is estimated that around 40 % of their OpEx comes from electricity bills [1]. Another aspect of interest is the increasing concern toward environmental issues, which motivate the efforts for a reduction of the carbon footprint. BBU hotelling has a great potential for reducing the energy consumption, as a direct consequence of the sharing of collateral subsystems into hotel sites. Differently from cell sites, whose equipment rooms are mostly obtained from existent premises used for other purposes, hence not energy optimized, hotel sites can be conveniently adapted from already deployed telecom offices or cabinets, taking advantage of existent cooling and power management systems [2]. A further energy consumption reduction is expected by BBU “pooling”, with respect to simple “stacking”, because, thanks to an accurate optimization of the pool, an overall better resource utilization can be achieved. For instance, when the traffic load of some cells is low, fewer resources can be shared and the rest of resources can be released and put in “sleep mode”, thus reducing energy consumption. It is also expected that the achievable amount of pooling gain increases when a larger number of cells is managed by a single hotel, which could be a strong push toward massive BBU centralization (up to hundreds of BBUs per hotel).

### ***10.4.3 Improved Radio Performance***

The radio performance of a RAN, i.e., the average bitrate and Quality-of-Service (QoS) delivered to customers, strongly depends on the capability of the signal processing techniques used to cope with the wireless channel, which is characterized by multi-user interference and harsh radio propagation conditions. To improve

radio performance by increasing the spectrum efficiency, especially for UEs located at cell edges, recent RATs (e.g., LTE, LTE-A) are adopting advanced processing schemes that operate jointly on several cells and/or users. Some examples are: multi-cell packet scheduling, enhanced Inter-Cell Interference Coordination (eICIC), and Coordinated MultiPoint transmission and reception (CoMP). Since these schemes require exchange of end-user data and uplink/downlink channel state information among different BSs, LTE introduces a new logical interface (X2) to interconnect different BSs in a logical peer-to-peer topology. In general, a very tight coordination between different cells is needed, translating to low latency and high-capacity constraints on the X2 interface, which might not be generally met in some RAN scenarios and for specific joint processing schemes. BBU centralization makes available a virtually zero latency and extremely high-capacity backplane among all BBUs hosted in the hotel site, thus enabling some advanced features, such as the Joint Transmission/Joint Reception in CoMP, and also serves as a future-proof solution for further advances (see Chap. 13). For the same reason, implementing BBU pooling can further enhance the radio performance, because some processing functions can be implemented into single hardware parts, thus gaining more computational power and even less latency.

## 10.5 Challenges of BBU Hotelling: Fronthaul

Fronthaul traffic has radically different features compared to those of backhaul traffic, and it poses specific challenges to the transport network. There are three main critical characteristics.

### 10.5.1 *High, Constant Bitrate*

Fronthaul flows have a very high bitrate, on the order of a few to tens of Gb/s for a cell site, as resulting from aggregating flows of one or more antennas, sampling their baseband signals with bandwidths around tens of MHz, and quantizing their I (In-phase) and Q (Quadrature) components with about 10–20 bits per sample. The specific values depend on the fronthaul interface, RAT typology and configuration [3, 4]. For instance, an LTE sector configured as  $2 \times 2$  MIMO with 20 MHz bandwidth requires approximately 2.5 Gb/s, which gives 7.5 Gb/s total fronthaul for a typical 3-sector cell site. Normally, such bitrates do not scale with the varying traffic load condition of the cell, resulting in a fully non-elastic traffic. These features constitute a relevant problem for the traditional access infrastructures, which are designed to transport much lower bitrates and to massively exploit the statistical multiplexing gain (i.e., the fact that networks can be under-dimensioned with respect to the peak traffic values, because of their statistical variability). As a consequence, a practical and future-proof transport solution for fronthaul traffic is

given by optical access networks, but this requires a capillary rollout of optical fiber links, needing the corresponding investment by network operators. As an attempt to mitigate this issue, some of the recent research is focusing on alternative solutions. For instance, advanced compression schemes for fronthaul are under study, in order to reduce the bitrate by a factor 2–4 [5]. Also, thanks to the reduced bitrate, ways to transport the fronthaul over point-to-point microwave or millimeter wave links are being investigated [6]. Another solution to cope with the fronthaul bandwidth requirement is currently being investigated, which relies on a redefinition of the functional split between the RRH and the BBU modules. This means that some BBU physical layer functions (e.g., FFT/IFFT, channel coding) are moved to the RRH to reduce the required fronthaul bandwidth, while maintaining the centralized joint processing functions to achieve radio benefits. Apart from deciding exactly which functions to place in each module, that is not trivial, such solution would require brand-new interfaces to be defined between the new RRHs and BBUs.

### ***10.5.2 Maximum End-to-End Latency***

RAT standards specify strict timing conditions for some physical layer procedures between the BS and the UEs. Most of them explicitly pose bounds on the “BS latency”, i.e., the latency due to internal processing of radio frames by the BS. In BBU hotelling, the BS functions are actually “spread” between BBUs and RRHs potentially located very far apart from each other; therefore, the “fronthaul latency”, i.e., the delay contribution due to the transport of fronthaul signals along the RAN infrastructure, has a relevant impact on the total latency budget inside the BS. As a result, given that the total BS latency budget is fixed by the standard and the internal processing delays of BBU and RRH are dependent on the specific hardware/software implementation, there is an upper limit on the tolerable fronthaul latency. Such latency can be further divided into two parts. The first one is due to the adaptation of fronthaul signals into the RAN transport service and it is purely technology dependent, e.g., caused by CPRI or OBSAI transmission/reception interfaces and additional functions required by optional lower-layer transport technologies, e.g., buffering, reframing, mu/demultiplexing, error correction. The second contribution is due to the signal propagation along the RAN, and it constitutes a fundamental limitation for BBU hotelling, because it constrains the maximum geographic distance between hotel sites and controlled cell sites, with a relevant impact on architectural choices. To provide some illustrative numerical values, we consider the LTE Frequency Division Duplexing (FDD) radio interface. In this case, the tightest BS latency limitation is due to the timing of the synchronous uplink Hybrid Automatic ReQuest (HARQ). Specifically, once the uplink data packet at radio frame number  $i$  is received, the BS must send back the corresponding ACK/NACK indication at frame number  $(i + 3)$  [7]. This gives exactly

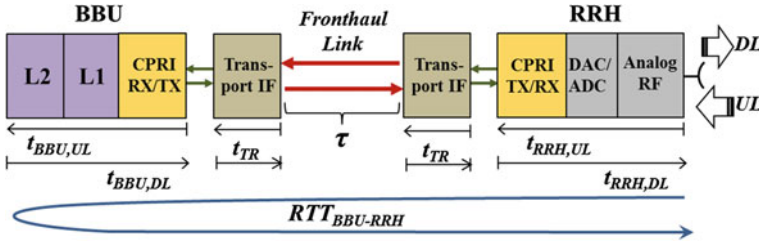


**Fig. 10.1** Delay contribution of  $RTT_{\text{BBU-RRH}}$  along the fronthaul processing chain

3 ms of latency budget for the BBU-RRH round trip time ( $RTT_{\text{BBU-RRH}}$ ), i.e., the time difference between the complete reception of the data frame and the start of transmission of the ACK/NACK indication. All delay contributions having impact on this quantity are summarized in Fig. 10.1.

Hence, the following must hold:

$$RTT_{\text{BBU-RRH}} = 2\tau + t_{\text{RRH,UL}} + t_{\text{BBU,UL}} + t_{\text{BBU,DL}} + t_{\text{RRH,DL}} + 4t_{\text{TR}} \leq 3 \text{ ms}$$

As a consequence, the maximum value of the one-way propagation delay along the fronthaul link ( $\tau$ ) depends on the remaining processing times. Regarding the internal BBU and RRH processing times in uplink (UL) and downlink (DL), there are no universal values, because they largely depend on the vendor implementation. By averaging over currently typical commercial equipment implementing CPRI interfaces, the following approximate values can be given:  $t_{\text{RRH,UL}} \cong 12 \mu\text{s}$ ,  $t_{\text{BBU,UL}} = t_{\text{BBU,DL}} \cong 1.3 \text{ ms}$ ,  $t_{\text{RRH,UL}} \cong 21 \mu\text{s}$ . The processing time introduced by the transport end node ( $t_{\text{TR}}$ ) also depends on the specific transport technology. For instance, typical values for OTN wrappers can be in the range 28–41  $\mu\text{s}$ . Considering a basic fronthaul implementation, in which the fronthaul is transported “as it is”, for instance, as dedicated CPRI links, there is no latency contribution caused by the fronthaul transport over a lower-layer technology ( $t_{\text{TR}} = 0$ ); therefore, the previous numbers lead to a value of maximum one-way fronthaul latency equal to about 184  $\mu\text{s}$ , which is equivalent to a maximum fronthaul link distance of about 37 km (assuming the classical value of 5  $\mu\text{s}/\text{km}$  for fiber propagation delay). However, in case of OTN transport such values reduce to 128–102  $\mu\text{s}$ , which correspond to a range of 20–26 km for the maximum distance. These values are in accord with the typical range of 20–40 km reported in the recent literature [1]. However, since a precise characterization of such quantity is extremely important for BBU hotelling deployment, further investigation is also being performed by standardization bodies (see Chap. 5).

### 10.5.3 *Strict QoS Requirements*

Digitized baseband radio signals are very sensitive to received bits errors, mismatches between transmitter and receiver clock frequencies, and random variations of the instantaneous received clock phase (jitter).

In fact, differently from traditional BSs, in which a single clock generator feeds both colocated BBU and RRH, in BBU hotelling the fronthaul transports not only the baseband data in both directions, but also the clock signal, generated at the BBU, toward the RRH. In order to meet the requirements imposed by RAT standards on accuracy and stability of radio interface, BBUs and RRHs must be precisely synchronized to each other. As a consequence, fronthaul has strict QoS requirements, in terms of Bit Error Rate (BER), frequency, and phase synchronization. As an example, CPRI specifies that BER must not be greater than  $10^{-12}$  and that the jitter introduced by the CPRI link can contribute a quantity not greater than 2 parts per billion (ppb) to the BS frequency accuracy budget [3]. While such requirements are satisfied in a BBU hotelling scenario in which fronthaul is transported over dedicated point-to-point optical links automatically meeting the CPRI specification, they are critical whenever fronthaul exploits an underlying transport technology.

In principle, the constraint on BER is less problematic, because it can be met by adjusting the transmission power budget, in order to increase the received Signal-to-Noise Ratio (SNR), and/or adopting more powerful Forward Error Correction (FEC) algorithms. It is worth noting that such algorithms generally increase the signal processing latency, thus reducing the maximum tolerable fronthaul latency. The synchronization constraints are more critical. For instance, they make unfeasible the transport over Ethernet today, even though Ethernet standards are continuously evolving to include advanced carrier-grade QoS features (e.g., Carrier Ethernet Transport [8]). The transport over Optical Transport Networks (OTNs) is seen as a more feasible solution, because it defines a fully synchronous optical signal hierarchy, with embedded advanced features for mu/demultiplexing and controlling several fronthaul flows into a single optical signal. For this purpose, the ITU-T G.709 standard specifies a set of recommendations for mapping CPRI flows into various OTN signals [9]. However, the effects on synchronization are still not completely investigated and they are currently the focus of the next standard releases.

## 10.6 RAN Architectures Based on BBU Hotelling

There are various proposed RAN architectures, employing BBU hotelling principles with different flavors. To get some type of an ordered survey of the main solutions, we propose a classification by some key features, namely the BBU placement, the fronthaul transport solution, and the BBU implementation. To limit

the number of possible architecture variations and at the same time present the more realistic cases, we consider a pure LTE and macro-cell based coverage scenario. The same considerations can be also easily extended to other RATs. The extension to heterogeneous coverage, featuring mixed macro-, micro-, and femto-cell deployment, deserves a separate specific treatise.

### 10.6.1 Classification on BBU Placement

We classify four main options to place BBUs across a RAN infrastructure, that reflect the progressive evolution from a traditional BS (i.e., not employing BBU hotelling), toward most advanced hotelling solutions [10]. The four architectures are depicted in Fig. 10.2 and described in the following.

#### 10.6.1.1 All-in-One BS (No Hotelling)

This is the traditional widely deployed macro-cell RAN architecture. The BS is placed in the cell site, so no BBU hotelling is performed. It can be implemented either as a single form factor device or, more frequently, as separated BBUs and RRHs, both located in the same cell site cabinet. Since they are connected by dedicated short-range D-RoF links, no fronthaul transport is needed over the RAN. The RRHs are connected to respective transmission and reception antennas via dedicated coaxial cables, which carry the radio-frequency analog signals. Their lengths can be up to a few meters or tens of meters, depending on the type of cell site and the distance between the antennas and the equipment cabinet. As a result, they experience a non-negligible power loss, which must be properly taken into

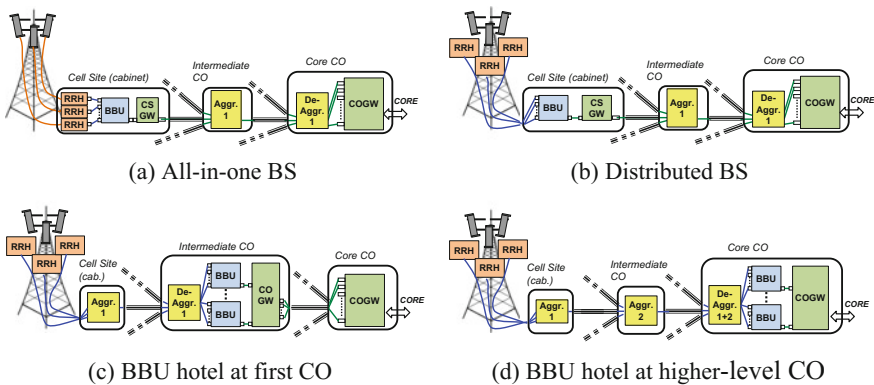


**Fig. 10.2** Four architectures for the BBU placement across the RAN infrastructure

account by increasing the output power of RRHs (approximately 3 dB of margin is reported as average value in the literature [11]).

The backhaul traffic generated by every BBU in the cell site is aggregated by a Cell Site GateWay (CSGW), and sent toward the core, through the remaining RAN portion. Traditionally, such gateway implemented legacy transport technologies, e.g., SDH/SONET signals, but currently a shift to Ethernet transport solutions is taking place, pushed by their lower costs and higher capacities.

### 10.6.1.2 Distributed BS (No Hotelling)

This is a first preliminary step toward BBU-RRH splitting, serving as a basis for all BBU hotelling solutions, though it is not a hotelling architecture. In fact, BBUs remain in cell site cabinets, while RRHs are moved outside the cell site cabinets and are directly attached to the antennas. To do this, RRHs must be implemented as Remote Radio Heads, i.e., stand-alone devices (embedding their own power and cooling subsystems) designed for operating in outdoor environmental conditions. Placing RRHs closer to antennas enables the reduction of their power consumption with respect to the all-in-one BS architecture, because the power margin for the short coaxial cable losses is much lower (virtually negligible). In addition, the equipment located in the site cabinet is partially reduced, with consequent benefits due to the smaller required space occupancy. Although this architecture features no BBU hotelling yet, its benefit in reducing the relevant coaxial cable losses has been one of the main reasons that triggered in the first place the implementation of BSs as separated BBUs and RRHs by manufacturers, thus opening the door to subsequent hotelling solutions.

### 10.6.1.3 BBU Hotel at First CO

This is the basic BBU hotelling solution. Through the RAN infrastructure, each cell site is directly connected to a first-hop CO, here denoted as “first” CO. BBUs of different cell sites are placed in their first COs, which become hotel sites, while RRHs are placed at remote locations, directly connected to antennas (as in the Distributed BS case). The RAN portion between cell sites and first COs is used to transport the fronthaul, with different possible solutions, depending on fiber availability and required costs. For instance, instead of dedicating a separate point-to-point connection for each fronthaul flow, it is possible to multiplex into few optical links several flows generated by a cell site, toward the first CO. A more detailed discussion of fronthaul transport is reported in the dedicated subsection.

A very important consequence of this architecture is that the cell site cabinet space occupancy is greatly reduced, while the CO can more efficiently manage a large number of hotels, resulting in relevant benefits on energy consumption and cost savings, as previously described.

#### **10.6.1.4 BBU Hotel at Higher-Level CO**

BBUs can also be placed at higher-level COs, instead of at first COs. With respect to the previous case, the architecture of cell sites and hotel sites is unchanged, but there can be different solutions for the fronthaul transport. In fact, first COs become intermediate “transit” nodes for fronthaul; hence, their implementation is an additional degree of freedom, depending on how the fronthaul is aggregated toward higher-level COs.

In general, this architecture allows higher concentration of BBUs into single hotels, that leads to more energy and cost savings (reduction of the number of hotel sites) and potentially higher pooling gains. For these reasons, such solution is greatly relevant to the concept of Fixed–Mobile Convergence (FMC), because the reduction of the number of hotels can be seen as part of the more general reduction of the number of active nodes, also known as “node consolidation”, which is one of the key enablers of FMC. In this case, this makes the implementation of intermediate COs as completely passive nodes possible, with great reduction of energy and cost. Also, the fronthaul latency constraint plays a critical role, more critical than in the previous first-CO hotelling architecture, because of the higher distances between cell sites and hotel sites. This could make this solution infeasible in some scenarios featuring a greater geographic distribution of COs, for instance, rural coverage cases.

### ***10.6.2 Classification on Fronthaul Transport***

In BBU hotelling architectures, the fronthaul can be transported over the RAN by using existing network infrastructure at different levels, e.g., cable, wavelength, sub-wavelength (bitstream). To do so, a transport technology can be used (e.g., OTN, Ethernet). A distinction is made between passive and active solutions, where passive means that no additional energy-consuming equipment is needed at end-points or intermediate nodes, and active indicates the converse. Passive solutions lead to lower operational costs, because they require less maintenance and they are more robust against failures. In the following, we present a general classification of the main transport solutions, but it is implied that more cases can be obtained by mixing together some of these solutions.

#### **10.6.2.1 Dedicated Point-to-Point**

In this case, fronthaul is transported by Point-to-Point (PtP) dedicated links, possibly reusing existing RAN infrastructure elements, as trenches, ducts, and multi-fiber cables. Although any fronthaul interface can be used, already defined public standards are preferred (mostly, CPRI). If intermediate nodes are present, PtP connections are routed via passive interconnection fabric, namely Optical

Distribution Frames (ODF). With these assumptions, this method is classified as passive. The main drawback is in the high number of required fibers (each carrying a separate flow for each RRH-BBU CPRI port pair).

### 10.6.2.2 Passive WDM

Fronthaul flows are transmitted on separate wavelength channels, by means of transceivers that operate according to the Wavelength Division Multiplexing (WDM) technology. This makes possible to multiplex several wavelengths into a few fibers, via a passive WDM multiplexer placed in each cell site. At the hotel site, the incoming wavelengths are separated by passive demultiplexers and sent to separate CPRI ports of BBUs, equipped with WDM transceivers. Among the different WDM technologies, Coarse WDM (C-WDM) is regarded as the most practical, because it is best suited for outdoor equipment (it does not require temperature control) and has lower costs, with respect to Dense WDM (D-WDM) solutions. With C-WDM, up to about 16 wavelengths can be multiplexed into a single fiber. Since the maximum number of RRHs in a cell site (considering several sectors, RATs, antennas) is in most cases smaller than this, it is possible to aggregate the whole cell site fronthaul into a single fiber.

This solution exhibits advantages with respect to dedicated PtP, because the amount of fiber is reduced with no impact on energy consumption. A drawback is that a proper inventory management is needed, in order to align wavelengths of endpoint transceivers to each fronthaul flow.

### 10.6.2.3 TDM-over-WDM (OTN)

In this solution, several fronthaul flows are end-to-end mapped into wavelengths, by Time Division Multiplexing (TDM), over WDM. One of the best ways to do this is by employing the OTN (Optical Transport Network) technology. At both cell sites and hotel sites, there are OTN mu/demultiplexers (commercially denoted also as “wrappers”), which transport fronthaul flows over the OTN signal hierarchy, i.e., CPRI signals are mapped into OTN low-level containers, which are multiplexed into high-layer signals and transmitted on different wavelengths.

Differently from the previous passive case, this solution can easily manage DWDM transport, in which each fiber can carry up to about 40–90 wavelengths, even with bidirectional transmission. Moreover, it is automatically endowed with control and management functions, without having to resort to external monitoring devices. In the presence of intermediate nodes, the fronthaul infrastructure becomes a complete OTN network, in which cross-connect devices can be added, in order to get more advanced transport functions, e.g., reconfiguration of routes, protection with redundant paths. They can be implemented as either electronic switches (i.e., OTN wrappers) or all-optical switches, e.g., Arrayed Wavelength Grating

(AWG) or Optical Add/Drop Multiplexers (OADM), whose energy consumption is much lower.

Unfortunately, the drawback of such active architecture is the relevant additional energy consumption due to OTN devices and, particularly, the much higher costs. These features make it unattractive for operators, at least for a short-term deployment and for smaller RAN instances. Nevertheless, they are promising future-proof solutions in the long term.

### ***10.6.3 Classification on BBU Implementation***

#### **10.6.3.1 BBU Stacking**

This is the basic case, in which original BBUs simply are placed in centralized hotel sites, rather than cell sites, without changes on their implementation. Thanks to the centralization into the hotel site, collateral systems, i.e., cabinets, racks, power supply equipment (voltage transformers, rectifiers, back-up batteries), cooling (ventilation or air conditioning), backplanes, aggregation gateways, can be re-implemented in a way such that relevant energy and cost savings can be achieved. If the association between each BBU and its cell site is preserved, the BBUs replacement does not modify their number, so their cost and energy contribution is unchanged. However, commercial BBUs have a capacity, in terms of maximum number of CPRI flows, therefore in terms of maximum number of managed RRHs, which is designed to serve maximum-configuration cell sites, such that a single BBU is sufficient for every cell site, for each RAT. This leads to a capacity underutilization, because some CPRI ports are not used for typical cell configurations. In case of BBU stacking, the 1:1 association between BBUs and cell sites can be relaxed (within certain limits), thus achieving a higher BBU capacity utilization. The consequence is that the total number of BBUs can be reduced, with further cost and energy gains.

#### **10.6.3.2 BBU Pooling**

In this architecture, BBUs placed at hotel sites are radically different from BBUs at cell sites. They can be implemented in several ways (for instance, maintaining a modular structure, or as monolithic devices), but the main feature is that they share some portion of their hardware resources. For this reason, we refer to the BBUs in a single hotel as a single BBU “pool”. Resource pooling can be of two kinds: static or dynamic. Static pooling occurs when a processing function is performed by a single resource element, rather than replicating it across many separate elements. For instance, some low-level physical layer functions requiring intensive vector-based processing (typically joint multi-cell and multi-user algorithms) are often performed by dedicated hardware. By consolidating such hardware, it is possible to improve

computational performance and in some cases reduce energy consumption. The pooling is static, because these functions are fixedly assigned to hardware, at the design stage. Dynamic pooling consists in allocating computational resources “on demand” for processing signals of different cells. In this way, to some extent, resource usage can be adapted to the load of each controlled cell, i.e., reserving more resources to high-loaded cells with respect to low-loaded ones. In this way, differently from a traditional BBU exhibiting almost constant energy consumption as function of the load, the BBU pool energy can better scale with it. Adapting the RAN consumption to the traffic load is seen as the most promising way of improving energy efficiency. For non-pooling based BBUs (i.e., traditional no hotelling and pure BBU stacking), “sleep-states” techniques are being investigated. They consist in entirely switching off some cells (both BBUs and RRHs) when they are off-peak and providing them coverage through adjacent cells. BBU pooling can provide a smoother adaptation, thanks to dynamic pooling, without sacrificing coverage, because critical RRHs can be kept in on-state while corresponding BBU resources are drastically reduced. Pooling techniques can be further differentiated by their adaptation time scale. For instance, by slow reconfiguration of pool resources (order of minutes or hours) it is possible to adapt to predictable periodic variations of traffic load occurring at daily or weekly periods, denoted as “tidal effect”. For instance, a well-known tidal effect is due to the almost complementary traffic load patterns experienced by residential and office areas, during the day. If the network planning is such that each BBU manages both kinds of areas, relevant pooling gains can be achieved. On the other side, by fast reconfiguration of the pool (orders of seconds, or comparable with radio frames) it is possible to adapt resources to quasi-instantaneous unpredictable traffic variations, for instance, caused by user behaviors and/or packet schedulers that operate according to the instantaneous channel conditions. Even higher pooling gains are expected in this case, of course at the expense of much more complex BBU hardware.

### 10.6.3.3 BBU Virtualization

This approach is envisioned as the future evolution of BBU hotelling, commonly denoted as Cloud RAN (C-RAN). BBU processing functions are fully virtualized over a distributed hardware/software platform decentralized over several hotel sites, hence the term “cloud”. In this way, the resources assigned to each cell are no more statically located inside a fixed hotel, but can be dynamically re-assigned to different hotels, thus implementing a kind of inter-hotel BBU pooling [12, 13]. Such paradigm can be seen as a particular case of a more general concept, denoted as Network Function Virtualization (NFV) [14]. For this architecture, an advanced underlying RAN transport infrastructure is required, which allows inter-hotel communication with very low latencies and high reliability, and online traffic reconfiguration. BBU virtualization is regarded as a way to further reduce RAN costs, because the virtualized platform can be built over general-purpose commodity equipment, instead of specialized hardware, potentially increasing the

competition in the market and enabling multi-vendor interoperability. The strong point of BBU virtualization is enabling full load adaptation and balancing of BBU processing. For instance, if some cells are heavily loaded, more resources can be reserved, possibly involving more than one hotel location. Similarly, during off-peak periods, the entire fronthaul of a certain area can be re-routed toward a single hotel site and remaining hotels can be switched off. From these considerations, even bigger energy gains are expected with respect to single-hotel pooling solutions. However, differently from pooling, for which some commercial solutions are starting to be deployed, BBU virtualization is still a purely research topic.

## 10.7 An FMC Network Architecture for BBU Hotelling

As seen in the previous sections, BBU hotelling in centralized radio access networks brings several benefits in terms of cost, energy consumption, and network performance improvements. However, it also imposes strict requirements to the RAN infrastructure, particularly regarding the transport of fronthaul traffic between BBUs and RRHs. Therefore, to fully enable the potential of BBU hotelling, not only BBU implementation, but also the underlying RAN must be properly designed and optimized. Many different optimization problems originate, covering various technological and architectural issues (e.g., [10, 15, 16]).

In this section, we present a network optimization problem, featuring the placement of BBUs over a fixed/mobile converged WDM network acting at the same time as a backhauling/fronthauling RAN for mobile traffic and metro/aggregation for fixed traffic.

### 10.7.1 General Network Architecture

The considered aggregation network offers transport of traffic between a single Point of Presence (PoP), which is the edge node toward the core network, and two types of clients spread across a metropolitan or regional area: Central Offices (CO), which are the Fixed clients collecting the backhaul of various kinds of last-mile fixed access technologies (e.g., xDSL, TDM-PON), and Cell Sites (CS), which are the Mobile clients collecting backhaul/fronthaul traffic of mobile users. Some CO and CS may be co-located, and in this case they are Fixed/Mobile clients. An illustrative example of such network is shown in Fig. 10.3.

The physical infrastructure consists of mono-fiber optical links connecting the PoP with network clients, through some intermediate nodes. As physical topology, the most straightforward is a multistage tree, but more complex topologies are possible as well, for instance, including rings and meshed connections. The network is based on WDM, i.e., fiber spectrum is divided into a number of independent optical signals at different wavelengths. The capacity of each wavelength is shared

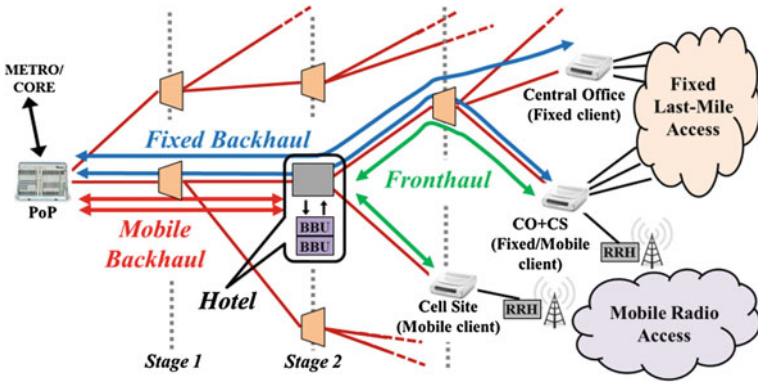


Fig. 10.3 Illustrative example of a FMC optical aggregation network, employing BBU hotelling

by multiple traffic flows, by means of electrical domain multiplexing schemes (typically based on TDM). For this reason, at the PoP and at network clients, where optical signals are terminated via “colored” transceivers, there are also electronic switches that perform mu/demultiplexing of different flows in/from the wavelength signals.

Besides increasing the system capacity, WDM allows to route some traffic flows directly in the optical domain, i.e., without performing optical/electrical/optical signal conversion. To do this, intermediate nodes are equipped with optical wavelength routers, i.e., devices that are capable of cross-connecting wavelengths at certain inputs toward different outputs, without performing wavelength conversion (e.g., AWG, OADM). Installing optical wavelength routers instead of electronic switches in intermediate nodes allows to greatly reduce energy consumption and operational costs for such nodes.

### 10.7.2 BBU Placement

The proposed WDM network serves not only as converged network for fixed and mobile backhaul, but also as infrastructure for a centralized radio access network, by means of BBU hotelling. This means that every network node becomes eligible for hosting one or more BBUs, so the BBU associated with a RRH can be placed at any node along the path from the CS to the PoP. Considering a generic BBU, there are three cases for its placement: at the CS, at the PoP, or at one of the intermediate nodes. Placing the BBU at its CS is equivalent to the distributed BS architecture, i.e., an intra-CS optical connection transports the D-RoF signals between the BBU, located at the CS cabinet, and the RRHs, directly attached to antennas on the tower. In this case, the CS does not require fronthaul transport from the network. If the BBU is placed at the PoP, the network transports fronthaul up to the CS cabinet,

where the switch extracts the D-RoF signals to be sent toward the RRHs. Therefore, the CS does not require backhaul transport from the network.

If the BBU is placed at an intermediate node, the same network transports both backhaul, toward the PoP, and fronthaul, toward the CS. The node becomes a hotel, and it can host collateral equipment, which requires higher energy and operation/management costs than non-hotel intermediate nodes. In order to save switch processing resources (thus, energy consumption), some of the transit traffic can be directly routed by wavelength routers, without passing through the electronic switch. This technique is known as “optical bypass”.

### 10.7.3 Traffic Routing

As a result of the BBU placement, in general three types of traffic coexist in the aggregation network: Fixed backhaul between COs and the PoP, Mobile backhaul between CSs or hotels and the PoP, and CPRI (fronthaul) between CSs and hotels. Differently from fixed and mobile backhaul, which is packet-based, asynchronous, and latency-tolerant, CPRI consists of constant bitrate flows, which require accurate synchronization and a constrained end-to-end latency. In order to effectively route such different traffic flows over the same network, a two-layer transport hierarchy is adopted.

At the lower layer, the basic element is the “lightpath”, which is a wavelength-routed circuit established between two nodes equipped with optical line terminations, which only traverses optical wavelength routers along its path. Every lightpath is uniquely identified by its wavelength and physical path and provides a fixed capacity equal to the wavelength signal bitrate. All lightpaths whose propagation delay (i.e., total length) is not bigger than a threshold value are denoted as delay-limited lightpaths, or “D-lightpaths”. Each CPRI flow is end-to-end transported over a single D-lightpath. Preventing the flow to be split among or traverse multiple lightpaths is necessary to meet fronthaul synchronization and latency requirements. For this purpose, the delay threshold of D-lightpaths is calculated as the fronthaul maximum latency minus the processing delays introduced by electronic equipment at lightpaths terminal nodes. Of course, more than one CPRI flow can be multiplexed into the same D-lightpath.

In our assumption, several lightpaths, including also D-lightpaths, can be established from a source to a destination node, in general routed over different paths and wavelengths. They constitute a single “virtual link” between these nodes, with capacity equal to the sum of capacities of all component lightpaths. Many backhaul flows can be transported in a virtual link, via inverse multiplexing techniques, i.e., splitting them in any proportion across multiple component lightpaths. Allowing the backhaul flows to be splitted at the lower layer enables more flexible routing, but different lightpath delays increase transport latency due to buffering and reordering. However, unlike fronthaul, this does not critically impact on backhaul requirements. Virtual link capacity can be actually shared among backhaul and

fronthaul, because some component D-lightpaths are filled with CPRI flows. The spare capacity of D-lightpaths, plus the capacity of regular lightpaths, is used for backhaul.

## 10.8 The BPTR Optimization Problem

We propose a network optimization problem, denoted as BPTR (BBU Placement and Traffic Routing), which addresses two main questions: where to place the BBU for each CS, and how to route traffic flows having as objective the minimization of a suitable global “cost” function. The right cost function would result from a proper mix of CapEx, OpEx, and energy consumption, but it is difficult to characterize it in a precise manner, as it largely depends on specific implementation details (e.g., used technologies) and other features which are difficult to generalize (e.g., economic ecosystem surrounding the network operator). In the following numerical evaluation, we choose a generic cost characterization, which is based on the following observations.

- Placing BBUs in the PoP has zero cost, because its premises are already optimized for hosting network systems, so its cost is virtually unaffected by additional hotelling equipment.
- Placing BBUs in any intermediate node has a fixed cost, say  $A$ , independent of how many BBUs are hosted, because the fixed costs due to the hotel installation should be dominant.
- Placing a BBU in its CS has also cost equal to  $A$ . This derives from the assumption that a CS cabinet is similar to other intermediate sites. In fact if it is equipped with the BBU, it requires approximately the same CapEx/OpEx (that dominates over energy). If the BBU is not installed, the cabinet hosts only the terminal electronic switch, with a negligible cost.
- Establishing a lightpath has another cost, say  $B$ . It includes the cost for activating the pair of WDM interfaces but it can be dominated by other costs related to “resource utilization” (for instance, if dark fiber capacity is bought from another operator, in units of used lightpaths). For this reason, giving  $B$  an absolute value is not trivial, but we can safely assume that it is much smaller than  $A$  (say,  $B = A/100$ ).

Therefore, the BPTR problem can be described as follows:

**given:** the network topology (nodes connectivity and links lengths), the set of traffic demands, link capacity (number of wavelengths), traffic capacity (bitrate) of each wavelength, maximum number of BBUs that can be hosted in each intermediate node (hotel capacity), and the maximum fronthaul length;

**decide:** the placement of each BBU, and the routing of traffic requests, that includes lightpath establishment (path and wavelength assignment) and mapping of flows into lightpaths;

**to minimize:** the global cost, which, following from the previous observations, can be written as:

$$Z = A \times (n_{HI} + n_{BC}) + B \times n_{EL}$$

where  $n_{HI}$  is the number of hotels placed at intermediate nodes,  $n_{BC}$  is the number of CSs equipped with their BBU (i.e., featuring the regular BS architecture), and  $n_{EL}$  is the number of established lightpaths.

The defined problem can be interpreted as a non-trivial combination of two well-known network optimization problems, namely the Grooming, Routing and Wavelength Assignment (GRWA) problem typical of core/backbone WDM networks [17] and the Facility Location Problem (FLP) [18]. However, here the two problems are not independent, since the placement of BBUs influences both the source/destination nodes of mobile backhaul and fronthaul and consequently their routing. In addition, the additional constraints on fronthaul transport make the problem more complex. Both GRWA and FLP are known to be NP-hard; therefore, our defined problem is NP-hard too, because it contains both of them as sub-problems. In practice, it means that all known algorithms can find the optimal solution with complexity that grows exponentially as a function of the size of the network instance. This prevents us to obtain exact solutions for realistic network sizes, so we must resort on heuristic algorithms, which exhibit reasonable complexity, but do not guarantee that the optimal solution will be obtained. In the following, we propose a heuristic formulation of the problem.

## 10.9 A Heuristic Greedy Algorithm for BPTR

Considering the fact that the cost of housing a BBU at CS dominates compared to the cost of establishing lightpaths, the focus of proposed greedy heuristic is on FLP. The strategy to minimize the global cost consists of the following principles (in decreasing order of priority): (a) to open as few intermediate hotels as possible; (b) to locate as many as possible BBUs at intermediate hotels; and (c) to activate as few lightpaths as possible. Fronthaul has more priority in routing, with respect to backhaul, because it cannot be split among different wavelengths and it is delay-sensitive, so it exclusively requires D-lightpaths.

### 10.9.1 Notation and Input Data

- $N$  is the set of network nodes, partitioned into: the PoP, the subset  $N_I$  of intermediate nodes, and the subset of clients, which can be Fixed ( $\in N_F$ ), i.e., COs; Mobile ( $\in N_M$ ), i.e., CSs; or both ( $\in N_F \cap N_M$ ), i.e., CSs collocated with COs.

- $E$  is the set of physical links, with a length associated to each physical link.
- $V$  is the set of virtual links, indexed by  $(i, j)$ , with  $i, j \in N$ ,  $i \neq j$ .
- $R$  is the set of connection requests, partitioned into: Fixed backhaul ( $R_F$ ), Mobile backhaul ( $R_M$ ), and Fronthaul, e.g., CPRI ( $R_C$ ). For each request,  $r \in R$ ,  $t_{(i)}^{(r)}$  is the traffic demand of node  $i$ .
- $\Lambda$  is the set of wavelengths.
- $C$  is the traffic capacity of each wavelength.
- $L_D$  is the maximum fronthaul length, i.e., the maximum length of D-lightpaths.

### 10.9.2 Heuristic Subroutines

- *Initialization*: For each node pair  $(i, j)$ ,  $i \neq j$  a number  $\Omega_{i,j}$  of D-paths (i.e., paths from  $i$  to  $j$  with physical length not exceeding  $L_D$ ) is calculated. For each mobile client  $i \in N_M$ , a first-fit decreasing bin packing heuristic [19] is solved to calculate  $NUM_{FH}^{(i)}$  = the number of D-lightpaths that the client needs for fronthaul if its BBU is placed at a hotel. For each  $i \in N_M$ , the Residual Fixed Traffic is defined as:  $RFT^{(i)} = \sum_{r \in R_F} t_{(i)}^{(r)} - \lfloor t_{(i)}^{(r)} \rfloor$ , i.e., the amount of fixed traffic modulo the single wavelength capacity.
- *BestFeasible*: Given a candidate hotel node  $j$ , a mobile client  $i$  is said to be reachable from  $j$  if there are enough D-lightpaths for accommodating the total fronthaul traffic requested by  $i$ . The set of reachable mobile clients, denoted as  $P_C^{(j)}$ , is computed for each candidate hotel  $j$ . The candidate hotel with the highest cardinality  $|P_C^{(j)}|$  is selected, and feasibility of the routing of the traffic associated with reachable mobile clients is checked. If the routing is not feasible, then the next highest-cardinality candidate hotel is checked, until a feasible routing is found. In this case, the relative candidate hotel is opened.
- *Stop*: break if no other candidate hotel can host at least two BBUs.
- *Groom&Route*: *D-lightpaths for fronthaul are established, choosing, among free D-lightpaths, those with the smallest hop-distance and randomly assigning the wavelengths. If  $RFT^{(i)}$  is less than the spare capacity of established D-lightpaths, then it is groomed in those D-lightpaths up to the hotel node. All groomed RFTs and mobile traffic demands associated with  $P_C^{(k)}$  are further groomed together and routed from the PoP to the hotel. For each mobile client  $i$  in  $P_C^{(k)}$ , the remaining fixed traffic, i.e., the RFTs which have not been groomed plus all the traffic which fits into an integer number of wavelengths, is routed from PoP to  $i$ . The routing phase is performed in such way that any active node is bypassed. Physical layer routing is implemented by shortest path.*
- *Update*: remove  $k$  and  $P_C^{(k)}$  from  $N$ .

- *RemainedBBUs&Routing*: BBUs of remaining mobile clients are placed at CSs. Traffic of these mobile nodes and of the nodes with pure fixed traffic ( $N_F \setminus N_M$ ) is routed from PoP to client nodes.

### 10.9.3 Heuristic Scheme

```

begin {
  Initialization {
    extract all D – paths;
    calculate  $NUM_{FH}^{(i)}, \forall i \in N_M$ ;
    calculate  $RFT^{(i)}, \forall i \in N_M$ ;
  }end Initialization
  do {
     $(k, P_C^{(k)}) = \text{BestFeasible}(N, \text{Free } D\text{-lightpaths}, \text{Free lightpaths}, NUM_{FH}^{(\forall i)});$ 
    Stop( $|P_C^{(k)}|$ );
     $(\text{Routing of } P_C^{(k)}) = \text{Groom \& Route}(P_C^{(k)}, \text{Free lightpaths}, \text{Free } D\text{-lightpaths});$ 
     $(N) = \text{Update}(N, P_C^{(k)}, k);$ 
  }end do
   $(\text{RemainedRouting, BBUs at CSs}) = \text{RemainedBBUs \& FinalRouting}(N);$ 
} end begin

```

## 10.10 A Case Study for the BPTR

As a case study for numerical evaluation, we performed multiple optimization runs over synthetic network instances based on multistage tree topologies, which are randomly generated according to the model summarized in the following (a more detailed description can be found in [10]). Three typical geotypes are considered: “Dense Urban”, “Urban” and “Rural”, featuring different values of the size of the coverage area and of the spatial densities of network clients (CSs and COs). Clients’ coordinates are randomly scattered over the coverage area, according to a uniform distribution. A multistage tree graph is constructed by performing a hierarchical clustering, via the k-means algorithm with city block (also known as “Manhattan”) distance metric. The number of stages is fixed to 3, and the numbers of clusters for each stage are such that the corresponding split ratio is approximately constant.

After this process, the physical topology and all links' lengths of the instance are obtained.

The traffic associated with each network client is generated according to the following assumptions. Traffic requests are rounded to integer multiples of the gross bitrate of the SONET/SDH OC-3 signal (155.52 Mb/s); hence, they can be quantified in terms of “OC-3” units. Each CS provides LTE coverage of 3 sectors, with 20 MHz carrier bandwidth and  $2 \times 2$  MIMO configuration. Using the CPRI interface, the required fronthaul bitrate can be computed as 6.29 Gb/s (41 OC-3 s), not including the CPRI line code overhead, which is not needed if fronthaul is mapped on an underlying transport network. Required mobile backhaul bitrate is uniformly distributed in the range 300–750 Mb/s (2–5 OC-3 s), which is typical for such macro-CS configuration. Each CO collects fixed access traffic from approximately 800 households, each requiring a typical bitrate uniformly distributed from 12.5 to 25 Mb/s. Therefore, each CO requires fixed backhaul bitrate uniformly distributed in the range 10–20 Gb/s (64–128 OC-3 s). In the following results, the number of wavelengths per link is 80 and each wavelength has a capacity equal to 64 OC-3 s (around 10 Gb/s). Each plotted point results from the average of 10 randomly generated instances, according to the previously described model and the BPTR problem input parameters.

Figures 10.4, 10.5, and 10.6 show a metric that quantifies the consolidation of BBUs into shared hotels, as opposed to being placed into CSs. It is denoted as “BBU consolidation factor”, and it is defined as the first term contributing to the global cost, namely the sum of the number of intermediate hotels and the number of CSs equipped with their BBU ( $n_{HI} + n_{BC}$ ), normalized to the number of CSs ( $n_{CS}$ ). The metric is shown as a function of the maximum fronthaul length ( $L_D$ ), in km. For all geotypes, it is evident that the metric rapidly decreases when the maximum fronthaul length ( $L_D$ ) increases, because higher values of  $L_D$  allow BBUs to be placed at highest nodes of the multistage tree hierarchy (i.e., closer to the PoP), thus enabling a bigger number of CSs to be controlled by a single hotel site. The case  $L_D = 0$  reduces to the conventional no hotelling network architecture, in which all

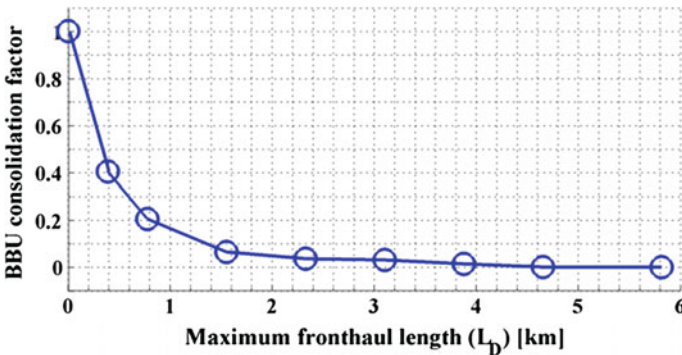


Fig. 10.4 Dense-Urban geotype: BBU consolidation factor versus maximum fronthaul length

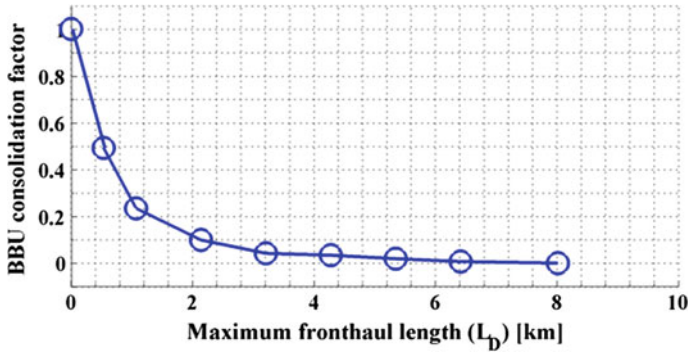


Fig. 10.5 Urban geotype: BBU consolidation factor versus maximum fronthaul length

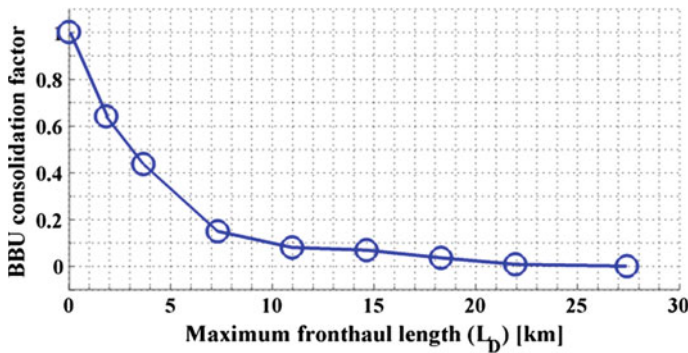


Fig. 10.6 Rural geotype: BBU consolidation factor versus maximum fronthaul length

BBUs are located in respective CSs and no fronthaul is transported (zero BBU consolidation), i.e., the metric assumes the highest value, equal to the number of CSs to which the network provides coverage. It can be observed that the metric reduces to 20 % of the maximum value after  $L_D$  reaches a few kms (around 1 km for Dense-Urban and Urban scenarios, around 6 km for the Rural scenario). It also gets the minimum value, which is 0 (maximum BBU consolidation, corresponding with all BBUs placed in the PoP premises), for  $L_D$  values larger than about 10 km for Dense-Urban and Urban and about 25 km for the Rural scenario. Such values are considerably below the classical 40 km limit; hence, they indicate not only that BBU hotelling is a feasible solution for the proposed network architecture, but also that relevant amount of latency budget is available for adding more complexity to the transport architecture. This strongly justifies, as a possible next step, the investigation of long-reach architectures, that feature regional coverage areas (characterized by a mixture of different geotypes) and distances from the PoP to clients up to hundreds of kilometers. In this case, the longer optical distances require more advanced signal processing in order to overcome propagation

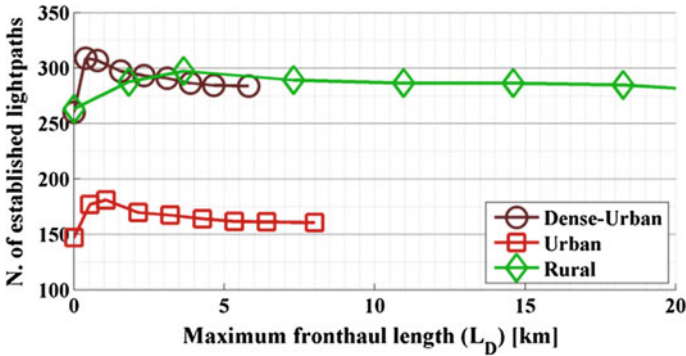


Fig. 10.7 All geotypes: number of established lightpaths versus maximum fronthaul length

impairments, with an impact on the available fronthaul latency budget and therefore with an impact on the achievable BBU consolidation.

Figure 10.7 shows the second metric contributing to the global cost, namely the number of established lightpaths ( $n_{EL}$ ). For every geotype, it can be observed that such metric stays almost constant for all values of  $L_D$ . The only remarkable difference is the case  $L_D = 0$ , in which, as intuition suggests, the architecture reduces to a pure no hotelling network; hence, the total amount of traffic significantly reduces as there is no fronthaul traffic to be transported.

## 10.11 Conclusion and Open Issues

This chapter starts with a survey of BBU hotelling techniques in converged network architectures. The main current trends of mobile radio access networks are surveyed to motivate the application of BBU hotelling solutions. BBU hotelling introduces a new kind of network traffic, called fronthaul traffic, which has radically different features compared to backhaul traffic and enforces strict transport requirements. How and where to place the BBUs and which transport technology to use for fronthaul are important questions in the design of future converged network architectures.

In the second part of the chapter, we have proposed a possible WDM network architecture for a Fixed/Mobile Converged aggregation network, where a (possibly minimized) subset of the network nodes could be used to host a BBU hotel. Fronthaul and fixed/mobile backhaul coexist in the same converged network in a cost/energy efficient manner, because an electronic transport layer above WDM enables different flows to be aggregated in few wavelengths, and optical bypass of some transit traffic can be adopted in intermediate hotel nodes. We have presented a network optimization problem for the design of this network, namely the BPTR (BBU Placement and Traffic Routing), and a heuristic algorithm has been devised

to solve the problem. Finally, a numerical illustrative evaluation has been carried out over randomly generated multistage tree networks, for different geographic scenarios. Results clearly indicate that BBU consolidation into fewer hotel nodes is the key principle for reducing the overall cost/energy and justifies the evolution toward converged architectures. The BBU placement formalized and solved in this chapter is only one of many different problems that can be identified in the context of C-RAN and FMC. However, it is apparent that its underlying optimization structure is enough general and powerful to be easily adapted to some correlated problems that are recently arising. Among such open issues, the most relevant one involves the adoption of CoMP strategy in a distributed (non-hotelling) RAN architecture. In CoMP schemes, a centralized controller is needed to switch and process the common data shared by a cluster of cooperative cells via X2 interfaces (for more details, refer to Chap. 14). Since such data are subject to some range of latency/bandwidth constraints (depending on the implemented CoMP features), there is a tradeoff between placing the controller close enough to cell sites to satisfy such constraints, and move it far to cover larger cell clusters and get more efficient joint processing. Such tradeoff quite resembles that of BBU placement, so a similar optimization problem can be devised, with potentially interesting insights on the evolution of mobile access network architectures in the next future.

**Acknowledgment** The research leading to these results has received funding from the European Community's Seventh Framework Programme FP7/2013–2015 under grant agreement no. 317762 COMBO project.

## References

1. (2013) China Mobile White Paper. C-RAN, The Road Towards Green RAN, v. 3.0
2. Carapellese N, Pizzinat A, Tornatore M, Chanclou P, Gosselin S (2014) An energy consumption comparison of different mobile backhaul and fronthaul optical access architectures. In: ECOC
3. (2014) CPRI (Common Public Radio Interface) Specification V6.1, July 1, 2014
4. OBSAI (Open Base Station Architecture Initiative) Specification RP3\_V4.2
5. Lorca J, Cucala L (2013) Lossless compression technique for the fronthaul of LTE/LTE-advanced cloud-RAN architectures. In: 2013 IEEE 14th international symposium and workshops on a world of wireless, mobile and multimedia networks (WoWMoM), pp 1–9, 4–7 June 2013
6. Ghebretensae Z, Laraqui K, Dahlfors S, Chen J, Li Y, Hansryd J, Ponzini F, Giorgi L, Stracca S, Pratt AR (2012) Transmission solutions and architectures for heterogeneous networks built as C-RANs. In: 2012 7th international ICST conference on communications and networking in China (CHINACOM), pp 748–752, 8–10 Aug 2012
7. 3GPP (Third Generation Partnership Project) TS-36.213, Physical Layer Procedures
8. Reid A, Willis P, Hawkins I, Bilton C (2008) Carrier ethernet. *IEEE Commun Mag* 46(9):96–103
9. ITU-T Recommendation G.709. Interfaces for the optical transport network (OTN)
10. Carapellese N, Tornatore M, Pattavina A (2013) Energy efficient baseband units placement in a fixed/mobile converged WDM aggregation network. Energy-efficiency in optical networks. *IEEE J Sel Areas Commun (J-SAC)*

11. Saadani A, El Tabach M, Pizzinat A, Nahas M, Pagnoux P, Purge S, Bao Y (2013) Digital radio over fiber for LTE-advanced: opportunities and challenges. In: 2013 17th international conference on optical network design and modeling (ONDM), pp 194–199, 16–19 April 2013
12. Rost P, Bernardos CJ, Domenico AD, Girolamo MD, Lalam M, Maeder A, Sabella D, Wübben D (2014) Cloud technologies for flexible 5G radio access networks. *IEEE Commun Mag* 52(5):68–76
13. Haberland B, Derakhshan F, Grob-Lipski H, Klotsche R, Rehm W, Schefczik P, Soellner M (2013) Radio base stations in the cloud. *Bell Labs Tech J* 18(1):129–152
14. Jain R, Paul S (2013) Network virtualization and software defined networking for cloud computing: a survey. *IEEE Commun Mag* 51(11):24–31
15. Iida D, Kuwano S, Kani JI, Terada J (2013) Dynamic TWDM-PON for mobile radio access networks. *Opt Express* 21(22):26209–26218
16. Sundaresan K, Arslan MY, Singh S, Rangarajan S, Krishnamurthy SV (2013) FluidNet: a flexible cloud-based radio access network for small cells. In: Proceedings of the 19th annual international conference on Mobile computing and networking. ACM, pp 99–110
17. Zhu K, Mukherjee B (2002) Traffic grooming in an optical WDM mesh network. *IEEE J Sel Areas Commun* 20(1):122–133
18. Laoutaris N, Smaragdakis G, Oikonomou K, Stavrakakis I, Bestavros A (2007) Distributed placement of service facilities in large-scale networks. In: 26th IEEE international conference on computer communications, INFOCOM 2007, 6–12 May 2007. IEEE, pp 2144–2152
19. Coffman Jr, Edward G, Garey MR, Johnson DS (1996) Approximation algorithms for bin packing: a survey. In: Approximation algorithms for NP-hard problems. PWS Publishing Co., pp 46–93

# Chapter 11

## Rethink Ring and Young: Green and Soft RAN for 5G

Chih-Lin I, Jinri Huang, Ran Duan, Gang Li and Chunfeng Cui

**Abstract** This chapter discusses one of the key design principles for 5G systems: “No More *Cells*” (NMC) [1]. NMC transfers the traditional cell-centric network design to a user-centric design principle. It is pointed out that NMC realization could be facilitated by the Cloud RAN (C-RAN) architecture which pools the processing resources and virtualizes “soft” BBUs and various applications on demand. The major challenges for C-RAN, including the transport networks to connect the resource pool and the remote sites as well as virtualization with potential solutions, are analyzed in detail. Various fronthaul solutions, including Common Public Radio Interface (CPRI) compression, single-fiber bi-direction, as well as wavelength division multiplexing (WDM) technology, are demonstrated and verified through our extensive field trials. In addition, the feasibility of general purpose processor (GPP) platform adoption in baseband processing with optimized virtualization implementation is functionally demonstrated and initially verified in terms of interruption time through prototype development implemented with a commercial LTE protocol stack.

### 11.1 Introduction

The concept of cellular systems was proposed in 1947 by two researchers from Bell Labs, Douglas H. Ring and W. Rae Young. Since the first generation of cellular standards, this cell-centric design has been maintained through every new generation of standards including 4G. The nature of a homogeneous cell-centric design is that cell planning and optimization, mobility handling, resource management, signaling and control, coverage, and signal processing are all assumed to be done either for or by each base station (BS) uniformly.

---

C.-L. I (✉) · J. Huang · R. Duan · G. Li · C. Cui  
Green Communication Technology Research Center,  
China Mobile Research Institute, Beijing, China  
e-mail: icl@chinamobile.com

To meet the rapid traffic growth (potentially  $1000\times$  by 2020), network densification is viewed as a major way to achieve the targeted increase in throughput. Further, heterogeneous network (HetNet) deployment is widely adopted. Thus, from the network's perspective, diverse types of BSs with different coverage, transmit power, frequency bands, etc., are introduced, such as Macro, Micro, Pico, and Femto. Also, from the users' perspective, traffic fluctuation is more significant than before, taking into account the emerging millions of mobile data applications. Therefore, in practical deployment, it is clear that the current system design for homogeneous networks is not compatible with traffic variations and diverse radio environments. Conventionally, radio resources are allocated semi-statically from the standpoint of the network rather than the user equipment (UE). This approach lowers resource utilization and wastes power. Poor performance at the cell edge also severely influences the consistency of the user experience. In addition, user mobility causes handover to occur frequently, especially under dense small cell deployment [2]. Consequently, radio resources are re-assigned with complex neighboring cell monitoring algorithms and a high signaling overhead. Moreover, frequent handover failures degrade the user experience significantly.

Relays, distributed antenna systems (DASs), coordinated multipoint processing (CoMP), and HetNets have been implemented as short-term solutions for these issues. While relays and DASs are mainly used for coverage extension, HetNets are deployed mainly for capacity improvement. CoMP has been intensively investigated by academia, industries, and standard bodies like 3GPP and WiMax, in which inter-BS joint processing and/or coordination is sought for enhanced cell-edge and cell-average performance. Note that in the above initial efforts, the cell-centric network operation was hardly changed.

## 11.2 No More Cells: One Key 5G Vision

Recently, Beyond Cellular Green Generation (BCG2) [3], liquid cells, soft cells, and phantom cells [4] have surfaced as potential radio access architectures. These paradigms all lead to the principle of "No More Cells" [1]. Different types of information can come from different sites, and the set of sites used for transmission is transparent to the UE.

5G design of the user-centric radio network should start with the principle of "No More Cells," departing from cell-based coverage, resource management, and signal processing. User demand, rather than cell, should be centric to network radio resource assignment and processing. All nearby radio access points with diverse frequency bands, transmit power, and coverage could serve one user. Moreover, the available radio resources from multiple access points could be dynamically scheduled for coordinated multipoint transmission, and the selection of control/user plane and uplink (UL)/downlink (DL) channels, respectively.

The concept of "No More Cells" (NMC) is user-centric with amorphous cells, decoupled signaling and data, and decoupled DL and UL. For example, a macro-BS

with lower frequency and wider coverage would become a signaling BS, while small cells with higher frequency and overlapped coverage would be data-only BSs [5, 6]. In a HetNet scenario, the small cell is within the coverage of a macrocell. Even if the small cell has no traffic, it cannot be turned off in the traditional cell paradigm. But with a control and data decoupling scheme, the macrocell is responsible for control and the small cell only for data. Thus, when there is no data traffic in the small cell, it can be completely turned off to save energy. New users can access the macrocell, and then the macrocell can coordinate with the small cell for possible data transmission. With signaling and data decoupled, the mobility robustness can be improved since handover signaling overhead is reduced with a more stable signaling connection when employing a macrosignaling BS. Additionally, spectrum usage in small cells will be significantly enhanced, due to the relaxed need for transmission of control information and reference signals from small cells.

NMC is also user-centric with decoupled UL and DL. This decoupling is deemed to facilitate better resource allocation between cells. This can be illustrated in the following example: Consider two cells where cell 1 is heavily loaded in the DL and cell 2 overloaded in the UL. In the traditional cell concept, if a UE is located at the cell boundary with symmetric data requirements, and the serving cell is cell 1, its DL requirement may not be satisfied. Conversely, if the UE device's serving cell is cell 2, its UL requirement may not be satisfied.

This situation of UL/DL asymmetry is becoming even worse under HetNet deployment since UL is always associated with DL based on the measurement of "best DL" reference signals. However, the nearby small cells with less reference signal power may be likely to provide a better UL connection. If there is a user-centric network design, the UE's DL can be from one radio access point and the UL from another access point, meeting the UE device's data requirement for symmetric transmission.

Moreover, CoMP with coordinated scheduling and multipoint transmission can be utilized to improve the split of the control/user planes and UL/DL channels. For example, under dense HetNet deployment, UE may anchor to one macro/signaling BS to establish a stable signaling connection and attach to small cells for data connections. Furthermore, UE may select UL and DL data connections separately from different radio access points and the DL data connection may be served dynamically by multiple radio access points.

With the introduction of ultra dense network (UDN) in 5G, the radio environment is becoming more complicated than ever due to extensive overlapped coverage. Thus, more radio channel information between radio access points nearby should be shared in real-time and more joint cooperation between neighboring access points is required to implement control/user plane and UL/DL channel selection from one or multiple points. This is not feasible in a traditional radio access network, because too much inter-BS information sharing is incurred, including dynamic user channel state information and scheduling information. Fortunately, with the emergence of C-RAN [7, 8] as shown in Fig. 11.1, many technologies necessary for the realization of the NMC concept can be facilitated. In addition, system-level and even multi-radio access technology (multi-RAT) optimization can also be made possible.

In the following sections, the concept of C-RAN will be elaborated with its key features and advantages. The major challenges and potential solutions will also be discussed. Finally, we will present recent progress in this area in terms of extensive C-RAN field trials and prototype development.

## 11.3 Cloud RAN: The Key Enablers to NMC

### 11.3.1 The Concept of C-RAN

Figure 11.1 shows the basic concept of C-RAN, while Fig. 11.2 illustrates more architecture details. A C-RAN system centralizes different processing resources to form a pool in which the resources could be managed and dynamically allocated to different applications on demand. The key design principle of C-RAN is to support various kinds of applications running on the same hardware platform. The key enabler for this is the virtualization technology widely used in modern data centers. With virtualization, standard IT servers are used as the general platform with computation and storage as the common resources. As shown in Fig. 11.2, a C-RAN system runs different applications on top of the servers in the form of virtual machines (VMs). The indispensable applications in C-RAN are those that can realize different radio access technologies (RATs) including 2G, 3G, 4G, and,

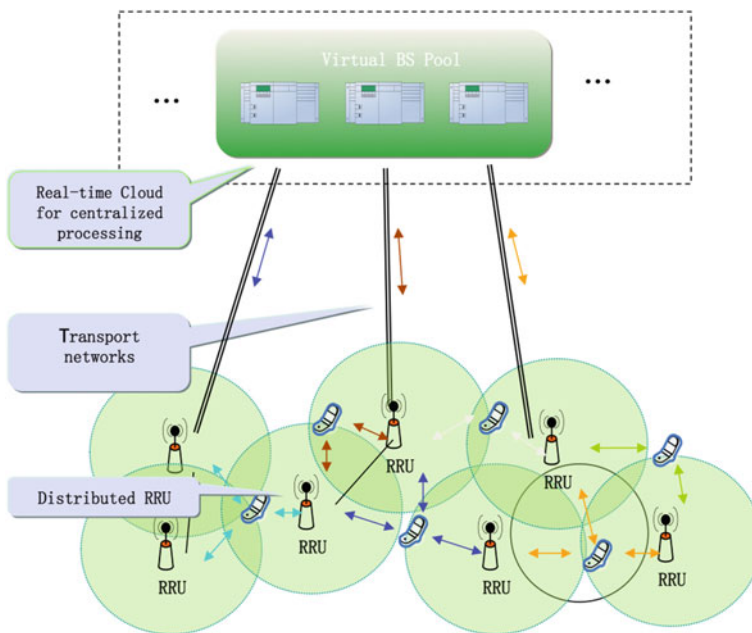


**Fig. 11.1** Illustrative C-RAN concept

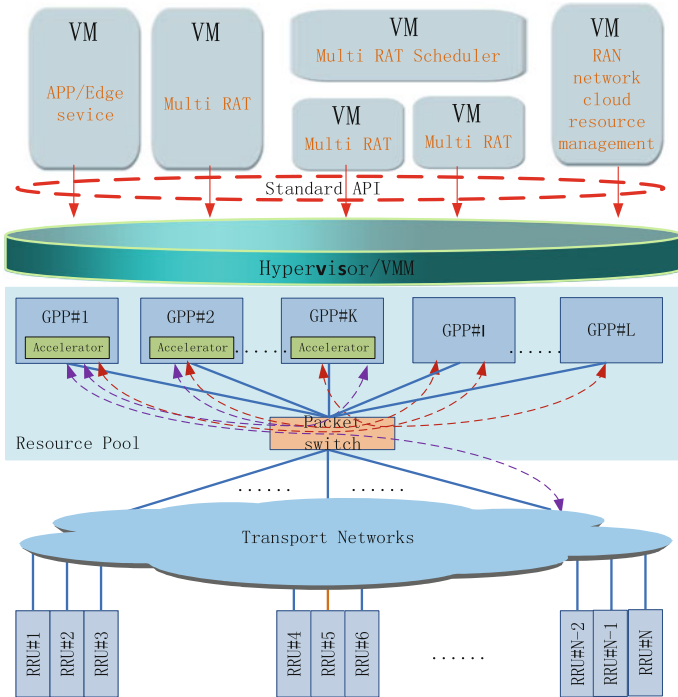


Fig. 11.2 C-RAN architecture

eventually, 5G. Additional user applications such as content delivery networks (CDN) and web caches can also be deployed on the open virtualized platform. In addition, the C-RAN platform provides a set of standard application program interfaces (APIs), which open the opportunity for new service provisioning and deployment. In this way, C-RAN is no longer a single RAT processing entity but rather a platform for the co-existence of diverse services.

The C-RAN architecture consists mainly of three parts.

- **Resource pool:** In C-RAN, all the resources are pooled and virtualized so that they can be delegated for use in different applications. One indispensable application in C-RAN is “soft” BBU. A soft BBU is a BBU instance in a traditional network where processing resources and capabilities are dynamically allocated and reconfigured based on real-time conditions (e.g., traffic status). In addition, a prerequisite for a pool in C-RAN is an inter-connection switching network of high bandwidth and low latency. This switching mechanism realizes an inter-connection of different computation nodes and enables efficient information exchange among them.
- **Remote Radio Units (RRU)/antenna sites:** Design of RRU or antenna networks is relatively independent of the central pool. The remote RRU networks could be the same as those in traditional systems for easiest migration.

Alternatively, potential 5G antenna or RRU technologies such as large-scale antenna systems (LSASs) could also be supported in C-RAN. In that case, there may be an impact on the interface between the central pool and the remote sites.

- **Transport networks:** A transport network provides a connection between the resource pool and the remote sites. It could be of different forms depending on practical situations and scenarios. Some examples include direct fiber connection via dark fiber, microwave transmission, and fiber transport networks.

Traditional wireless systems can easily migrate into a C-RAN architecture in two stages. The first stage realizes centralization by aggregating existing BBUs from different locations into one equipment room. In the second stage, virtualized general purpose platforms (GPPs) should be introduced to replace vendor-specific platforms.

### 11.3.2 C-RAN Features

Although C-RAN might at first appear to be nothing more than the centralization of BBU, centralization is just the first step toward a complete C-RAN that includes several other features:

- **Advanced Technology Facilitation:** The high-bandwidth and low-latency inter-connection switching network facilitates the efficient and real-time information exchange among different computation nodes. As a result, many technologies that are difficult to implement in traditional architectures, especially joint processing and cooperative radio, can benefit from this feature and thus will become viable in a C-RAN context.
- **Resource Virtualization/Cloudification:** Unlike traditional RAN systems in which computation resources are limited within one BBU and therefore cannot be shared with other nodes, in C-RAN these resources are aggregated on a pool level and can be flexibly allocated on demand. This feature, very similar to the cloud and virtualization concepts in data center, is called resource “cloudification.”
- **“Soft” BBU:** Traditional wireless equipment is developed based on proprietary platforms and possesses only “hard” fixed capabilities designed for carrying peak traffic. Contrary, in a C-RAN BBU pool, through resource cloudification, a BBU is of a soft form, which means that the capability of a soft BBU could be dynamically reconfigured and adjusted. In this way, resource utilization efficiency can be increased considerably.
- **Generalization of platform:** Generalization of platform is another essential feature of C-RAN. The use of GPPs not only reduces the procurement cost for operators but more importantly lays down the basis for the implementation of virtualization technology.
- **Openness:** C-RAN is also “open” in the sense that C-RAN is designed to provide a set of standard APIs to outside parties to encourage new service development on the edge and to provide interoperability.

### 11.3.3 *Advantages of C-RAN*

Several advantages can be directly derived from the C-RAN architecture:

- **Total cost of ownership (TCO) reduction:** TCO reduction mainly comes from two sources. Firstly, centralization allows the aggregated computation nodes to share the same facilities, such as air-conditioning, which reduces the power consumption and therefore operating expenses (OPEX). Power consumption by air-conditioning usually accounts for over half of the total power consumption for operators. Secondly, centralization makes it easier to find a smaller number of central offices to accommodate the BBU node pool, which in turn can speed up network construction. Improved resource utilization efficiency due to resource cloudification also contributes to TCO reduction.
- **Improved system performance:** Internal high-bandwidth low-latency switching networks enable implementation of advanced joint processing techniques, which leads to system performance improvement.
- **Energy saving:** Similarly to TCO reduction, energy saving is attributed to two factors: centralization and resource cloudification. First, facility sharing in the same central office helps to reduce energy consumption. Second, reduction in equipment usage due to improved resource utilization efficiency by cloudification reduces the total power consumption.
- **Improved resource utility efficiency:** This benefit is mainly from resource cloudification.
- **Facilitation of service deployment on the edge:** A C-RAN network covers a larger area and serves more users than a traditional single BS. Making use of this, it is possible to move services to or directly deploy new services on the RAN side. In this way, user experience could be improved and backhaul pressure could be relieved.

## 11.4 Challenges and Potential Solutions for C-RAN Realization

### 11.4.1 *Challenges on Transport Networks for Centralization*

Centralization is the critical first step required in order to realize all the features of C-RAN. Centralization aggregates different BBUs which traditionally are located in geographically disparate places into one central office with shared facilities.

Centralization of certain carriers may consume a significant number of fiber resources if using a dark fiber solution, i.e., direct fiber connection. For example, in a Time Division Long-Term Evolution (TD-LTE) system with 20 MHz bandwidth and RRUs equipped with 8 antennas (most common scenario in the China Mobile (CMCC)'s network), the CPRI [9] data rate between one BBU and one RRU for

one TD-LTE carrier transmission is as high as 9.8 Gbps. When considering both UL and DL, then 4 fiber connections would be required with 6-Gbps optical modules. Since usually one site consists of three sectors with each supporting at least one carrier, the number of fiber connections for one site is as high as 12. When the centralization scale becomes larger, the amount of fiber needed will be greatly increased, resulting in an implementation which is difficult to achieve for most operators due to limited fiber resources. As a result, a dark fiber solution is usually not recommended. Instead, an efficient transport solution is needed to address the fiber consumption issue in order to achieve C-RAN large-scale deployment.

When a transport network is adopted, there will be a new challenge resulting from the dynamic BBU-RRU mapping requirement. In C-RAN, the BBU is soft and can be dynamically changed. The relationship between the BBU and RRU is no longer a fixed one-to-one correspondence as in traditional RAN systems. Therefore, the transport network should be able to support dynamic mapping and routing for data between the pool and the remote RRU. Software-defined networks (SDNs) could be one of the promising technologies to provide this capability. The basis of SDN is to separate the control plane from the forwarding plane and change the forwarding behavior through programming on the control plane [10]. In this way, SDN greatly improves the transport efficiency and flexibility.

## 11.4.2 Potential Fronthaul Solutions

In the subsequent subsections, the transmission between the BBU and the RRU in C-RAN is defined as fronthaul transmission (compared with traditional backhaul transmission between the BBU and the core network).

The fronthaul transmission technology is of decisive significance to C-RAN large-scale deployment. As more operators are paying attention to C-RAN, more resources are being committed to the issue. There have been some notable breakthroughs recently:

- **CPRI compression.** With the maturity of CPRI compression, several vendors have commercially realized 2:1 compression with lossless performance, potentially reducing fiber consumption by 50 %. In addition, single-fiber bi-direction (SFBD) technology allows simultaneous UL/DL transmission on a single fiber, which further halves fiber consumption. Combining CPRI compression and SFBD can reduce fiber consumption threefold. CMCC has successfully verified both technologies in C-RAN TD-LTE field trials. More information can be found in Sect. 11.5.1.
- **WDM solutions.** Since WDM technology is sufficiently mature, vendors can develop WDM equipment tailored to fronthaul transmission within a short period of time. Currently, a few operators have adopted this solution to enable the large-scale C-RAN deployment. Some commercial products can support as many as 60 2.5-Gbps CPRI links in one pair of fibers. 1+1 or 1:1 ring protection

is also supported and several low-data-rate links can be multiplexed into one high-data-rate link. The main issue with the solution lies in its high cost, which hinders its large-scale deployment.

- **OTN (optical transport network) solutions.** Compared with a WDM solution, OTN provides more powerful O&M capability, longer reach and flexible routing. In addition, the open interface and standard protocols of OTN help to lower the cost and decrease development time. Some vendors have suggested integrating OTN functions into optical modules rather than using active line cards, which can simplify network deployment and maintenance to a large extent.
- **Millimeter microwave transmission.** In some scenarios, it is too expensive, or even impossible to deploy fiber. In that case, microwave transmission may come to play a role as the last-100-m fronthaul solution. 60 GHz is currently the most common frequency band for millimeter microwave and can be implemented under loose regulation in many countries. 60 GHz offers wide bandwidths, and thus it is easy to get channels with 250 MHz or greater bandwidth. With simple modulation techniques, it is easy to achieve over 1-Gbps transmission rate within the 100–400 m range. For LTE RRU with 20 MHz bandwidth and 2 antennas, the data rate after 2:1 compression is less than 1 Gbps and can be transmitted via millimeter microwave. 5 GHz millimeter microwave products have recently entered the market and can support the fronthaul transmission of 20 MHz LTE with 8 antennas.
- **CPRI redefinition.** The basic idea behind CPRI redefinition is to move a partial set of physical-layer functions to the RRU side in order to reduce the required data rate between the BBU and the RRU. There can be several possibilities for the partition of functions. By carefully designing the partition scheme, the data rate between the BBU and the RRU can become elastic and vary with real user traffic, as opposed to the traditional case in which the I/Q stream is constant even when there is no real traffic. This feature helps not only to reduce the capacity requirement on the switching network within the BBU pool but also to reduce the switching latency. In addition, the data can now be encapsulated in the form of packets rather than a constant stream and therefore can be transmitted by a packet switching protocol, such as Ethernet which enjoys the benefits of improved flexibility and improved switching efficiency. In Sect. 11.6.2, this idea is expanded.
- **Wavelength Division Multiplexing-Passive Optical Network (WDM-PON).** Using WDM-PON as a C-RAN, fronthaul has recently been discussed as an alternative in the Full Service Access Network (FSAN) and ITU-T Q2 working group. The basic idea is to make use of the rich fiber resource deployed for Fiber-to-the-x (FTTx) and design a new technology based on the combination of the low-cost PON and WDM for CPRI transmission. WDM solutions adopt colored optical modules, which raise the bar in installation of optical modules, maintenance, and storage. In comparison, WDM-PON targets use of colorless optical modules, which helps to greatly simplify installation, maintenance, and storage. In addition, WDM-PON claims such advantages as cost reduction,

saving on fiber consumption, and flexible topology support. Despite being at its initial stage, WDM-PON can become one of the most efficient fronthaul solutions for C-RAN in the long run.

### ***11.4.3 Challenges on Virtualization Implementation to Realize Resource Cloudification***

C-RAN's core feature is resource cloudification in which processing resources can be dynamically allocated to form various functional nodes (e.g., BBU). In addition, with C-RAN, all the diverse applications and services should operate independently and simultaneously on the same platform in the form of software. To enable this, it is widely believed that virtualization is one of the key components. In fact, this design philosophy is exactly the same as that employed in network function virtualization (NFV). Proposed by China Mobile and 12 other operators in a joint white paper under ETSI NFV ISG [11], NFV has been widely accepted in industry as one of the most important technologies in order to realize 5G. Incorporating C-RAN as an essential part, the basic idea of NFV is to "consolidate many network equipment types onto industry-standard high-volume servers, switches and storage, which could be located in data centers, network nodes and in the end-user premises" [11]. Prior to the establishment of the NFV ISG (Industry Specification Groups) under ETSI (European Telecommunications Standards Institute), its original defined scope focused on core networks. We propose instead that it should be extended to include RAN, which would make the NFV concept be truly end to end.

Virtualization, in its simplest form, is a mechanism to abstract hardware and system resources from a given operating system (OS). This is usually performed via hypervisor which separates an OS from the underlying hardware resources. Certain functionalities usually run in the form of VMs on top of the hypervisor. VMs are separated from each other and this separation provides independence and ensures security.

Despite the simplicity of the idea of using virtualization, the implementation is more difficult in practice. Wireless communication is distinct from IT data centers in that wireless communication has extremely strict requirements on real-time processing. For example, for LTE systems it is required that an acknowledgement/negative acknowledgement (ACK/NACK) must be produced and sent back to the UE/eNodeB (eNB) within 3 ms after a frame is received. Traditional data center virtualization technology with GPP cannot meet this requirement. Therefore, applying virtualization to BSs requires careful design and special optimization of key functional blocks.

To better describe the issues, let us take LTE C-RAN as an example. Then these challenges include, but are not limited to the following:

- **Meeting the real-time (RT) constraint for system performance:** The biggest challenge for RAN virtualization is to meet the strict RT constraint imposed by mobile signal processing. To partially address this, from the physical (PHY) layer perspective, a dedicated hardware accelerator is proposed to process computation-intensive function modules such as channel coding and decoding. However, when it comes to L2 and L3, this constraint still holds. Since L2 and L3 are mainly processed on GPP platforms with the software layers of hypervisors and OSs, the issue can then be translated to the optimization of the hypervisor and OS. The optimization of these components is not only to fulfill the RT requirement but also to minimize the overhead and guarantee system performance.
- **Meeting the RT requirement for VM management, especially for live migration:** In traditional live migration, the workload of one VM can live migrate to another. Although this idea still applies to C-RAN systems, it would become much more difficult when it comes to mobile communication implementations. The main issue lies with the high arrival rate of wireless frames, for example, one subframe per millisecond in LTE systems. This is often shorter than the migration interval from one VM to another. This will lead to a non-convergence of migration, resulting in failure. Moreover, when a source VM is switched off and the destination VM takes over, it usually requires an interruption of several hundred milliseconds, which, from a wireless communication point of view, means the inevitable loss of several hundred subframes. This is obviously intolerable for wireless systems.
- **I/O virtualization:** As mentioned above, C-RAN requires the use of an L1 accelerator to partially solve the RT problem. The data exchange between the accelerator and the upper-layer software could result in high I/O requirements. In a traditional virtualization environment, the data communication between the VM and the underlying hardware needs the hypervisor's intervention, which brings additional overhead and therefore results in further degradation of I/O performance, particularly the I/O throughput and the latency. Therefore, I/O virtualization techniques should be introduced to improve system I/O performance. Moreover, it is possible that VMs outnumber accelerators in C-RAN. In this case, a mechanism of I/O virtualization is needed to enable different VMs to share the accelerators without degraded performance.
- **Design on virtualization granularity:** There are several possible ways to compose a VM. Taking LTE L2/L3 virtualization as an example, there could be as many VMs as carriers, each VM dealing with one carrier. Alternatively, there could also only be two VMs with one dealing with all L2 functions and the other dealing with all L3 processing. Even a VM for one UE is possible. It is obvious that the VM granularity, or composition, can have different impacts on system performance and VM management and is thus worth careful study.
- **Evaluation of different hypervisor alternatives:** There exist in industry various hypervisor products including Xen, Vmware ESX, Oracle VirtualBox, and KVM [12]. Different hypervisors differ from each other in many aspects such as the supporting virtualization types, OS, architecture, core count, memory

capacity, and live migration. It would be of great value to evaluate which hypervisors are more suitable for RAN virtualization and how.

## 11.5 Recent Progress on C-RAN from China Mobile

In this section, we will introduce the recent progress on C-RAN activities at China Mobile. We have conducted extensive field trials, some of which being commercial LTE networks, to verify various fronthaul solutions. In addition, we also developed several sets of prototypes to evaluate the implementation of virtualization technology for wireless communication.

### 11.5.1 *Field Trials on Centralization with Different FH Solutions*

The first step toward C-RAN is BBU centralization which is relatively easy to implement and can be tested with existing 2G, 3G, and 4G systems. In the past few years, extensive field trials have been carried out in more than 10 cities in China using commercial 2G, 3G and pre-commercial TD-LTE networks with different centralization scales. The main objective of C-RAN deployment in 2G and 3G is to demonstrate deployment benefits by centralization, including site construction speed-up and power consumption reduction.

In the city of Changchun, 506 2G-BSs in five counties were upgraded to a C-RAN-type architecture, centralized into several central sites. In the largest central site, 21 BSs were aggregated to support 101 RRUs with a total of 312 carriers. It was observed that power consumption was reduced by 41 % due to shared air-conditioning. In addition, system performance in terms of call drop rate as well as downlink data rate was increased using same frequency network (SFN) technology. More details on 2G and 3G C-RAN trials can be found in [7, 8].

While C-RAN trials in 2G and 3G demonstrated the viability and advantages of centralization, C-RAN trials in TD-LTE aimed to verify availability of technologies to reduce fiber consumption, including CPRI with 2:1 compression and SFBD which, as described in Sect. 11.4.2, allows simultaneous UL/DL transmission within the same fiber core.

When combining 2:1 CPRI compression and SFB together, fiber resources could be saved threefold with lossless performance.

To verify the two technologies in real networks, three field trials were carried out in three cities with similar configurations to each other as shown in Table 11.1. In these trials, commercial eNBs and Evolved Packet Core (EPC) were used together with test UEs.

**Table 11.1** System configuration of TD-LTE C-RAN field trial

Frequency	2.85 GHz
Bandwidth	20 MHz
Frame structure	UL/DL configuration type 1 • Normal CP • Special subframe configuration type 7 (DwPTS:GP:UpPTS = 10:2:2) • DwPTS for data transmission
CPRI	2:1 compression
Optic module	Single-fiber bi-direction
UL	SIMO
DL	Adaptive MIMO
QCI	9
Scheduler	PF

**Table 11.2** Throughput comparison b/w with and without compression plus SFBD

	RSRP*	SINR** (dB)	DL (Mbps)		UL (Mbps)	
			w/	w/o	w/	w/o
Near point	(-75, -85)	>22	50.57	48.71	18.38	18.06
Middle point	(-90, -100)	(10, 15)	21.01	24.09	18.02	17.93
Edge point	<-105	<5	12.66	10.18	7.92	6.24

\*RSRP Reference Signal Receiving Power

\*\*SINR Signal to Interference plus Noise Ratio

**Table 11.3** Coverage comparison (*unit* m)

DL coverage		UL coverage	
w/	w/o	w/	w/o
600	607	598	607

Extensive test cases were performed to compare the system performance with and without the two technologies. In Tables 11.2 and 11.3, the coverage and throughput are compared. It can be seen that the performance difference is almost negligible after the adoption of both compression and SFBD.

Test results verified that compression (with a 2:1 compression ratio) and SFB are mature enough and the system performance is almost the same as without the adoption of the two technologies.

Despite the fact that combination of compression and SFBD can reduce fiber usage by 75 %, it is still far from enough for the large-scale deployment of C-RAN. From a future system upgrade perspective, it is obvious that capacity expansion and upgrade should not depend on the upgrade of fiber transport infrastructure since it would be too costly. Instead, it should rely on equipment updates. In this sense, WDM is a promising solution.

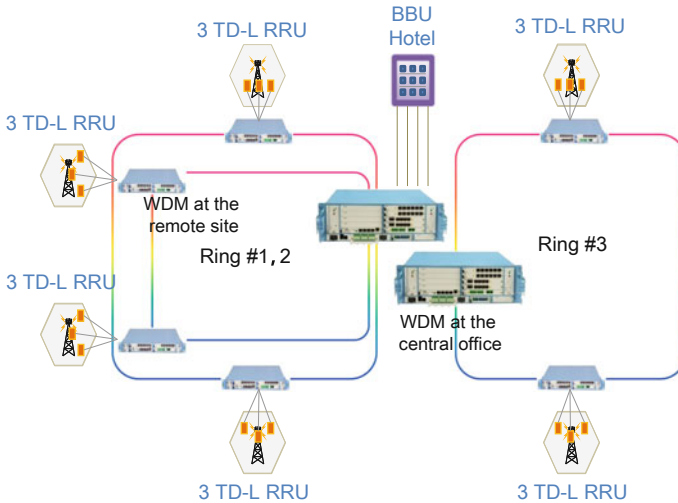


**Fig. 11.3** C-RAN field trial with WDM solution

The basic introduction of a WDM solution has been described in Sect. 11.4.2. So far in the industry, there have already been several vendors who claim to provide mature WDM fronthaul solutions. To further qualify the solution, based on the previous field trial in Fuzhou City (one of the three field trials for CPRI compression and SFBD), we reconstructed the C-RAN fronthaul utilizing WDM equipment. The network topology is shown in Fig. 11.3.

In this field trial, six remote WDM setups are installed at the remote RRU sites, each supporting one site, i.e., three LTE carriers. The BBU pool is connected with the local WDM equipment in the central office. Several WDM nodes are connected in a ring, with SFBD implemented. Due to power budget constraints, one such ring consists of only two WDM nodes. As a result, three fiber cores are needed for three rings of six WDM nodes. The number of supported LTE carriers is still 18, the same as in the previous trial. Compared with the previous test with compression and SFB which consumes 18 fiber cores (one fiber core per carrier), the reduction in the fiber consumption with WDM in this trial is fivefold.

The processing delay of the WDM nodes is empirically observed to be less than  $1 \mu\text{s}$ , which is small enough to have no impact on CPRI transmission.

Another key feature of this WDM solution is protection switch (PS) capability. The operators' requirement in this case is less than 50 ms. In this field trial, both active and passive PSs are carefully examined. In active PS, we launched the switch command through a management system and found that the latency is only around 12 ms. Further, in the case of a passive PS, in which the fiber is pulled out to simulate link failure, the switch time is around 36 ms, meeting the requirement with room to spare.

To verify the maturity of the solution, we executed many O&M functions such as remote software download, remote system update, system backup and restoration, verifying that they all worked well.

In addition to the performance on the WDM network itself, we further tested the entire wireless system performance in terms of throughput, coverage, end-to-end latency, handover success rate and so on (the same tests as in the previous field trials for compression and SFBD). The key finding is that all the performance metrics are almost the same as in the previous trials. There is no impact with the introduction of WDM. Furthermore, the network continued to run for 3 months as a commercial trial network without failure.

## ***11.5.2 Exploitation of C-RAN Virtualization***

### **11.5.2.1 Accelerator Design**

In our first endeavor in C-RAN virtualization, we first developed a Proof of Concept (PoC) to evaluate the feasibility of baseband processing based on a GPP. There is further elaboration on this in [8]. Although the feasibility is verified, it is also found that almost 10 CPU cores are needed to process one 8-antenna 20-MHz TD-LTE carrier physical layer. Accordingly, the performance-to-power ratio of pure software BBU is relatively low. Based on these observations, we then conclude that a hardware accelerator should be used to speed up physical-layer processing so that more carriers can be handled with the same processing resources, and the performance-to-power ratio will be improved significantly. In this section, we introduce a design scheme for the accelerator. The design principles are as follows:

According to our evaluation and assessment on a preliminary pure software prototype, in DL, processing modules of high computation load include Fast Fourier Transformation (FFT), 8-antenna precoding and turbo encoding. The other modules, including scramble, modulation, and layer mapping, do not require high computation capability. They can be performed by GPPs as the latency is not critical. However, it is more reasonable to also incorporate these functions on the hardware accelerators from an interface data traffic point of view.

For each user's DL, Physical Downlink Shared Channel (PDSCH) processing not only requires a pending data block from the MAC layer of the user, but also needs the corresponding physical-layer configuration parameters of the user. The physical-layer DL processing modules on the hardware platform will process the MAC data on PDSCH according to the configured physical-layer parameters. On the other hand, the algorithms for bit-level processing and symbol-level signal processing of Physical Downlink Control Channel (PDCCH) are of low complexity and can be completed by a GPP. In order to call the physical-layer DL processing function modules, subcarrier mapping location information is required.

Similarly, in UL, processing modules of heavy computation are: Inverse Fast Fourier Transformation (IFFT), channel estimation, equalization, and turbo



servers. In each modem server, several CPRI Peripheral Component Interconnect express (PCIe) plug-in cards are equipped for TD-LTE CPRI link termination. In the control servers, there are two kinds of VMs running, i.e., GSM VM and TD-LTE L3 VM. Control servers have external Ethernet connections to the EPC and the base station controller (BSC). Those external connections are used by the VMs for backhaul connection. For GSM VM, there are no dedicated accelerator cards. It is worth pointing out that in our demo except for the accelerator, all the other realizations in both GSM and LTE are based on commercial protocol stacks.

The prototype is first tested from a functional perspective. A GSM call is made between two GSM UEs, while an LTE terminal is simultaneously accessing the LTE VM and downloading files. The services ran well for at least 1 h.

In addition, we further evaluated the processing benchmark as well as interruption time performance with the following results:

- **Processing benchmark**

The processing benchmark for key L1 functions are calculated and shown in Table 11.4.

**Table 11.4** Benchmark for physical functions processing (*unit*  $\mu\text{s}$ )

		20 MHz	
		2 Ant. ( $\mu\text{s}$ )	8Ant. ( $\mu\text{s}$ )
<i>Uplink processing</i>			
PUSCH (single UE with UL 100 PRB)7	7.5 K shift + FFT	105.9	189.9
	Channel evaluation (IRC)	147.7	524
	PUSCH frequency domain processing	52	218
	MIMO/EQU	179.8	384
	IDFT	34.6	34.6
	Demodulation	71.9	71.9
	HARQ merge	59.7	59.7
	Turbo decode	113	113
	CRC	9.6	9.6
PUSCH	PUCCH format 1 per UE	2.3	4.1
	PUCCH format 2 per UE	9.7	17.2
<i>Downlink processing</i>			
PDSCH (single UE, 200 PRB, TM3/TM8, peak throughput)	CRC	13.8	13.8
	Turbo encode	70	70
	Scrambling	14.9	14.9
	Mod.	36.4	36.4
	Power control, precode, BF	21	190
	iFFT	32	116

From the test results in Table 11.4, it can be calculated that on average 4 Sandy Bridge CPU cores are required for one 8-antenna cell with a specified level of code optimization for the commercial capacity requirement.

- **Evaluation of interruption time**

To further investigate the virtualization performance, the interruption time, which is a key indicator of the response time that a GPP system can have, is tested with the test results shown in Table 11.5. Both the internal interruption time triggered by the application and the external interruption time which is triggered by an external PCI card are tested. Thanks to the joint optimization on the virtualization systems such as the hypervisor and the OS, the interruption time is greatly reduced. It can be seen from the table that the maximum internal and external interruption times are 23 and 40  $\mu$ s, respectively, while the averages are around 17 and 10  $\mu$ s. By comparison, for a general Linux-based GPP platform, the typical interruption time ranges from 50 to 1000  $\mu$ s. These results indicate that the system has the determinism required by hard RT applications. Considering that LTE processing usually has a 1 ms processing time budget, we then conclude that such latency is tolerable for LTE baseband processing.

## 11.6 Evolving Toward 5G

### 11.6.1 C-RAN to Enable Key 5G Technologies

As described at the beginning of this chapter, in the 5G vision the network should evolve from cell-centric to user-centric, i.e., “No More Cell.” This idea means that users should be provided with not only much higher data rate services but also experience less difference between the cell-center and cell-edge regions. To achieve this goal, the severe interference experienced by the cell-edge users should be alleviated. Thus, coordination among multiple cells is necessary. In 5G networks, various coordination techniques have been proposed to solve the interference problem. However, algorithms such as Joint Transmission [2] cannot achieve maximum performance gain under the traditional architecture, e.g., LTE with an X2 interface which is of high latency and low bandwidth [13, 14]. C-RAN, on the other hand, thanks to the strong inherent central processing capability, provides an ideal structure to facilitate the implementation of coordination technologies with full or partial channel state information. In fact, it has been demonstrated that C-RAN can

**Table 11.5** Interruption time of the prototype (*unit*  $\mu$ s)

	# of interrupts	Min	Max	Ave.
Internal interruption time	95,309,564	15	23	17
External interruption time	217,587,258	5.59	40.01	10.19

greatly improve CoMP performance in terms of cell-edge spectrum efficiency by 119 % over non-cooperative transmission mechanisms [8].

C-RAN is also an ideal match for the deployment of an UDN which is deemed to be a promising solution for highly dense user traffic. The design of UDN involves joint consideration of many issues, including the control and user plane decoupling, inter-site carrier aggregation and coordination, and interference mitigation in a heterogeneous network. In this case, C-RAN can play an important role, with its internal high-speed low-latency switching mechanism and the central processing, for the implementation of those key technologies.

Finally, C-RAN provides a unique opportunity to support multi-RAT with the adoption of GPP and virtualization technology. In C-RAN, different RATs can be virtualized in the form of VMs and operate separately and independently on the same platform. Thanks to highly efficient VM communication, C-RAN can further help with multi-RAN coordination.

### ***11.6.2 Rethink CPRI: CPRI Redefinition***

CPRI, the most common transmission protocol between BBU and RRU, has several disadvantages, which may make it not suitable for 5G networks:

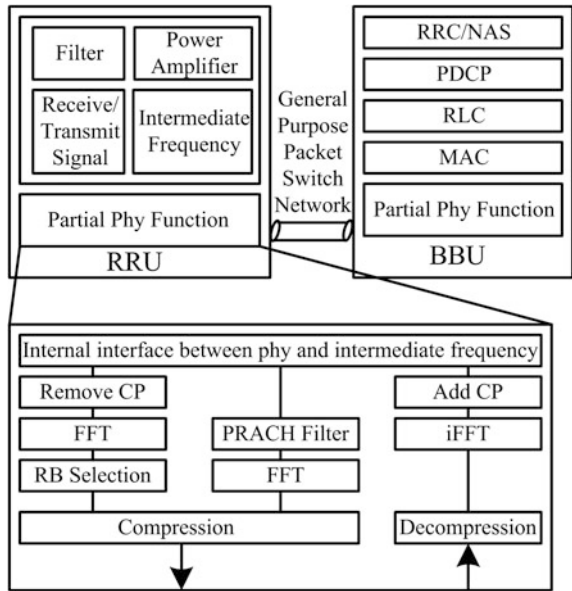
- The CPRI data rate is exceedingly high. One typical example is as described in Sect. 11.4.1; up to 9.8 Gbps is required for just one 20-MHz TD-LTE carrier with 8 antennas. It could be foreseen that in 5G, when large-scale antenna technology is introduced, the data rate will increase significantly.
- The CPRI data rate is constant, regardless of the real amount of user traffic. This makes the transmission extremely inefficient.
- The current CPRI link is point to point. However, in C-RAN with soft BBU pool, as pointed out before, there is no longer one-to-one correspondence between the BBU and RRU, and therefore a flexible fronthaul with multi-point to multi-point mapping capability is required.

CPRI redefinition aims at overcoming these shortcomings so as to have a better fronthaul interface for future 5G evolution. The basic idea of CPRI redefinition is to move a partial set of physical-layer functions to the RRU side and to realize packet transmission. Take LTE as an example. There are several possibilities on the function partition, and one example is shown in Fig. 11.5. In this scheme, the function set is comprised of the major PHY functions such as FFT/IFFT and Cyclic Prefix (CP) addition/removal. A new function block called Resource Block Selection (RB Selection) is implemented which only selects the scheduled (i.e., occupied) RBs to be placed into the compression module.

This scheme has several advantages:

- (1) The data rate between the BBU and the RRU could be significantly reduced. As an example, an 8-antenna 20-MHz TD-LTE carrier without this scheme

**Fig. 11.5** Example of CPRI redefinition in LTE



has an I/Q bandwidth requirement of 9.8 Gbps. With this new scheme, the maximum bandwidth can be reduced to around 2.2 Gbps.

- (2) CoMP implementation can still be supported since no CoMP-needed information is processed and terminated on the RRU.
- (3) Due to the RB selection, the data rate between the BBU and the RRU is now elastic and varies with real user traffic, which is the opposite of the traditional case where the I/Q stream is constant even when there is no real traffic. This feature not only helps to reduce the capacity requirement on switching networks within the BBU pool but also reduces the switching latency. In addition, the data can now be encapsulated in the form of packets rather than a constant stream and therefore can be transmitted by a suitable packet switching protocol, such as Ethernet (which enjoys the benefits of improved flexibility and improved switching efficiency). Furthermore, statistical multiplexing gain can be used to improve the transmission efficiency.

The major problem with this idea is that it may require a major overhaul of existing standards. In addition, it will increase the complexity of RRU equipment due to the implementation of functions in the RRU. This in turn may make future system upgrades more difficult. Moreover, some key features such as support of CoMP may be lost. In the future, however, the idea of interface redefinition still becomes critical for some 5G technologies such as LSAS where there are a number of antennas on one RRU. It would be of interest to explore redesigning the BBU-RRU interface to achieve packetized fronthaul transmission while still keeping the RRU as simple as possible.

### 11.6.3 Edge Application on C-RAN

With the large-scale commercialization of LTE networks, a wide variety of bandwidth-hungry and latency-sensitive mobile data applications are expected to emerge. For operators, the profit margins of traditional telecom services (e.g., voice and SMS) have been going down continuously. Despite the heavy investment of operators in network construction and maintenance, mobile networks tend to become “dumb pipes” of over-the-top (OTT) Internet companies. In addition, self-operated data services are also facing fierce, homogeneous competition, which makes the existing mobile business model hard to sustain in the near future. It is critical for operators not only to reduce network expansion cost, but also to provide differentiated QoE for mobile subscribers.

On the other hand, mobile base stations, as operators’ important and differentiated assets, have not been utilized to their full capacity. The idea of combining C-RAN with applications is to exploit their unique advantage by building applications over the edge of mobile networks, especially the C-RAN BBU pool. It is expected that, in this way, operators can take full advantage of distributed computation and storage capabilities to reduce network congestion and latency and also provide differentiated QoE to improve subscriber loyalty.

As shown in Fig. 11.6, edge applications and BBU pool software are deployed over the same hardware platform and isolated from each other via VMs. It is expected not only to reduce backbone traffic and latency, but also to provide rapid

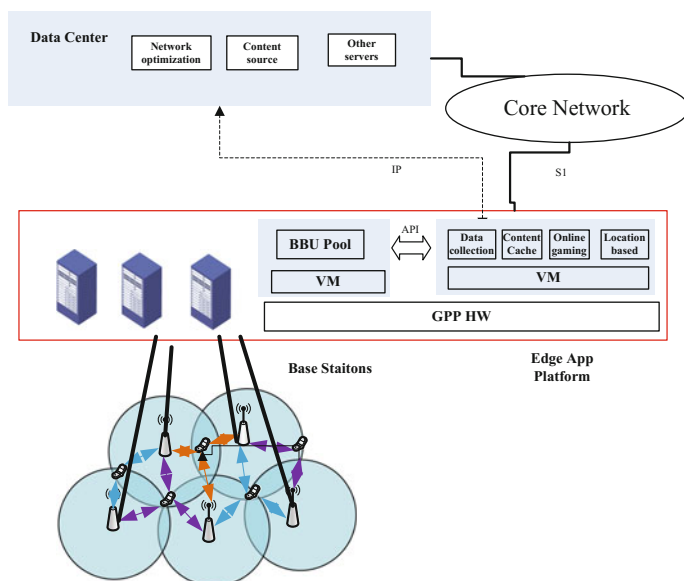


Fig. 11.6 Edge applications architecture over C-RAN GPP BBU pool

time-to-market deployment via GPP platforms and virtualization technologies. The architecture has the following characteristics:

- (1) **Distributed computation and storage:** User plane traffic can be locally cached and processed. If we deploy applications over a C-RAN BBU pool serving 5000–1000 users, the hit rate of content retrieval can be guaranteed and deployment costs can be reduced as well.
- (2) **Radio API:** By providing real-time and refined radio network information, e.g., RT loading and radio link status, applications on edge can be improved further.
- (3) **GPP platform and IT technologies:** Low cost and faster development, release, and maintenance can be achieved with mature development toolkits when using GPP platforms.
- (4) **Collaboration with cloud data centers:** Applications in cloud data centers and over the edge can collaborate and complement each other to build a smarter pipe.

## 11.7 Conclusions

Traditional network design is cell-centric, which has become more and more unsuitable for future 5G systems, since it fails to take into account traffic variation and diverse environments. It is well recognized that 5G should be designed starting with a paradigm shift from cell-centric design toward “*No More Cells*,” i.e., user-centric design in order to better deal with tidal effects and improve system efficiency. The realization of “*No More Cells*” can be facilitated by C-RAN which virtualizes the processing resources in a pool and is capable of dynamically allocating the resources on demand.

C-RAN is a revolutionary evolution of radio access network. It is not only a key enabling element of future 5G systems but also offers a significant enhancement path to all existing systems including 2G, 3G, and 4G. In this chapter, a comprehensive study of C-RAN was provided. Due to the inherent high-speed, low-latency nature within the C-RAN resource pool, different information such as the channel state information and scheduling information can be shared among different nodes in a timely manner. Consequently, key enabling technologies toward user-centric networks, such as CoMP, can be realized efficiently.

However, two major kinds of challenges need to be addressed for C-RAN realization: an efficient fronthaul solution as well as real-time virtualization implementation. For the former challenge, we demonstrated through various field trials different approaches, including CPRI compression, single-fiber bi-direction, and WDM. It is verified that WDM-based fronthaul significantly reduces fiber

consumption, supports flexible topology, and facilitates future system upgrade along with mature management capability. In one of the field trials, only three fiber cores are used to aggregate 6 sites of 18 TD-LTE carriers. Thus, existing WDM solutions are mature enough to enable large-scale C-RAN deployment in existing systems such as 4G.

On the road toward C-RAN cloudification, it is found that an accelerator is still currently necessary. Moreover, virtualization implementation imposes several challenges, including optimization on hypervisor and OSs, management functions, and I/O virtualization. A prototype with commercial LTE protocol stack implemented on GPP was developed. It successfully demonstrated multi-RAT support, i.e., GSM voice calls and LTE data services, as well as satisfactory performance in interruption latency. Further evaluation showed that 4 Sandy Bridge cores are needed to process a 20-MHz TD-LTE carrier with 8 antennas.

In the long run, C-RAN will not only facilitate the realization of “No More Cells” for a user-centric 5G system, but also remain an integral part of future greener and softer systems.

**Acknowledgments** We would like to express our sincere gratitude to all of our partners, including Alcatel-Lucent, Intel, and Wind River for the development of the GPP-based C-RAN prototype. We would also like to thank all C-RAN and 5G team members in China Mobile for their helpful discussion and valuable comments.

## References

1. Chih-Lin I, Rowell C, Han S, Xu Z, Li G, Pan Z (2014) Toward green and soft: a 5G perspective. *IEEE Commun Mag* 52(2):66–73
2. 3GPP TR 36.819 (2011) Coordinated multi-point operation for LTE physical layer aspects (Release 11). Version 11.1.0
3. <http://www.greentouch.org>
4. Kishiyama Y, Benjebbour A, Nakamura T, Ishii H (2013) Future steps of LTE-A: evolution toward integration of local area and wide area systems. *IEEE Wirel Commun* 20(1):12–18
5. Chen Y, Li G, Cui C (2014) Macro assisted ultra-lean data carrier and architectural design. *ZTE Technol J* 2:17–21
6. Marzetta T (2010) Noncooperative cellular wireless with unlimited numbers of base station antennas. *IEEE Trans Wirel Commun* 9(11):3590–3600
7. Wu J, Rangan S, Zhang H (2013) Green communication. CRC Press
8. C. M. R. Institute (2013) C-RAN white paper 3.0: the road towards green ran. <http://labs.chinamobile.com/cran>
9. <http://www.cpri.info/>
10. Sezer S et al (2013) Are we ready for SDN? Implementation challenges for software-defined networks. *IEEE Commun Mag* 51(7):36–43
11. ETSI NFV ISG (2012) Network functions virtualisation. <http://portal.etsi.org/portal/server.pt/community/NFV/367>

12. Younge AJ et al (2011) Analysis of virtualization technologies for high performance computing environments. In: IEEE international conference on cloud computing. Washington DC, USA, pp 9–16
13. CMCC. Simulation results for CoMP Phase I (2011) Evaluation in homogeneous network. R1-111301, 3GPP TSG-RAN WG1 #65, Barcelona, Spain
14. Wang QX, Jiang DJ, Liu GY, Yan ZG (2009) Coordinated multiple points transmission for LTE-advanced systems. In: Proceedings of 5th international conference on wireless communications, networking and mobile computing, pp 1–5

**Part IV**  
**Novel Management Strategies**  
**for Fi-Wi Networks**

# Chapter 12

## Next-Generation PoP with Functional Convergence Redistributions

Philippe Bertin, Tahar Mamouni and Stéphane Gosselin

**Abstract** The current level of convergence between fixed and mobile infrastructures is not sufficient to allow the most efficient use of heterogeneous access network resources (fixed, mobile, Wi-Fi) while facing the exponential growth for data traffic demand. Pooling or sharing of fixed and mobile network infrastructures is already possible in the present mode of operation; however, there is still a long way to go before reaching an effective convergence leading toward common network functions, nodes, and gateways. In this chapter, we discuss how to realize convergence in the framework of the next-generation point of presence (NG PoP). The NG PoP introduces the new concept of a flexible platform in the Telco's network hierarchy that combines aggregation of fixed and mobile access traffic, IP edge routing, and the ability to host additional network functions and services. In the NG PoP framework, different types of networking as well as service and application functions can be hosted at the IP edge, starting with virtual residential gateway, broadband network gateway, and evolved packet core. Likewise, we introduce two other important concepts which we consider essential in the path toward convergence: the converged subscriber data and session management and the universal access gateway. Such a truly converged approach will naturally leverage on NG PoP. Furthermore, we introduce some design principles and initial dimensioning figures, privileging the NG PoP realization as an open and flexible platform benefiting from network function virtualization and software-defined networking concepts.

### 12.1 Introduction

Today's telecommunication networks are facing major evolutions with the deployment of very high bandwidth access technologies, such as fiber to the home (FTTH) in the fixed network and long-term evolution (LTE) in the mobile network.

---

P. Bertin · T. Mamouni · S. Gosselin (✉)  
Orange Labs, Rennes & Lannion, France  
e-mail: stephane.gosselin@orange.com

These evolutions and the constant need for cost reduction stimulate operators to find new ways to streamline their infrastructures, by making broadband networks generic for fixed and mobile usages and by optimizing traffic management.

Regarding the access network infrastructure, with current gigabit-capable passive optical network (GPON) technology, an optical line termination (OLT) can reach customers located up to 20 km from the first central office, compared to a few kilometers in the case of copper and asynchronous digital subscriber line (ADSL). Fiber is also an enabler for simplifying base stations deployment: as far as point-to-point fiber is available, the base band unit (BBU) function of the base station can be hosted remotely from the antenna site, in a central office. Such BBU hosting in the central office allows for the management of several cellular base stations and radio cells in a coordinated manner. When chosen appropriately, central offices can host both the OLT and the BBU hosts. The expected advantages are a massive reduction on the number of network central offices to be managed by the operator, as well as better infrastructure sharing between fixed and mobile access networks (for a more detailed description of BBU hosting architectures, please refer to Chap. 10).

In parallel to the process of access node consolidation, we observe a growing interest in deploying advanced networking and service functions at the edge of the IP network. Expected benefits are the provisioning of services with the best expected quality of service (QoS) for the end user in terms of bandwidth and latency, as well as the reduction of traffic at the transport network, core network, and peering levels. Such network edge deployments are particularly relevant for content caching facilities in content delivery network (CDN) and, more generally, to new content distribution paradigms like information-centric network (ICN). Traffic accelerator solutions or even end-user applications such as personal cloud and virtual office suites can also be considered as functions to be moved toward the edge.

The combined need for optimizing the access infrastructure and hosting network functions and services at the network edge has led us to the *next-generation point of presence (NG PoP)* concept [1]. It is a new type of operator's network platform, whose location can vary from central offices to regional PoP in the Telco's network architecture. The NG PoP introduces a flexible point in the operator's network hierarchy, providing aggregation of both fixed and mobile access traffic, IP edge routing, and the ability to host additional network functions and services, for providing best-in-class QoS to the customer.

On the one hand, implementing the NG PoP raises several challenges regarding the functional level, the network dimensioning, the interworking with core nodes, the distribution of cloud components. On the other hand, the emergence of software-defined networking (SDN) and network function virtualization (NFV) approaches brings new opportunities for designing programmable network devices with software-based appliances hosting network or service functions that can significantly facilitate the deployment of the NG PoP.

Implementation of the NG PoP concept would thus foster two types of convergence for fixed and mobile networks:

- The convergence of fixed and mobile network functions, called **functional convergence**, defined as the implementation of generic functions to realize similar goals in different network types (fixed, Wi-Fi, mobile). This includes the moving of functions in order to merge specific fixed, mobile, and Wi-Fi functions into some generic functions;
- **Structural convergence** defined as pooling/sharing of network and infrastructure resources (cable plants, cabinets, buildings, sites, equipment, links, technologies) for several network types (fixed, mobile, Wi-Fi). It aims at defining joint fixed/mobile equipment and infrastructures for access and aggregation networks, thus allowing streamlining of broadband network infrastructures.

In this chapter, we discuss specifically how to realize network functional convergence in the framework of the NG PoP. The first section introduces the main networking services being envisaged at the network edge. The second section addresses the path toward fixed and mobile convergence through converged subscriber management and universal access gateway. The last section provides guidelines for implementing the NG PoP.

## 12.2 What Services at the Network Edge?

The opportunity to locate in the same central office aggregation/routing functions (such as switches, routers) together with IP edge service capabilities, such as user's session management, is expected to foster the emergence of a new network element, the NG PoP, as mentioned in Introduction and proposed in [1]. Furthermore, considering that current large-scale data centers may face scalability issues due to new usage paradigms and due to the steep increase in the data traffic that new access technologies enable (LTE, FTTH), in-network support of mini data centers would allow the distribution of cloud functions into more distributed servers deployed at the edge of the network. Such mini data centers are typically located at current regional PoPs or below in the aggregation network at the level of enhanced edge nodes, which is consistent with the NG PoP model. These servers, based on commodity/on-the-shelf IT servers (e.g.,  $\times 86$ ), will provide processing and storage capacities for hosting network functions and services.

Several types of applications and services could be implemented at the network edge level; however, it is not trivial to identify univocally which applications/services should or should not be hosted in highly distributed small servers at the edge of the IP network, and there is certainly a limit to such cloud distribution. The gain in latency, bandwidth, and/or cost will drive such service migration toward the edge, and the NG PoP shall be seen as a natural extension to traditional datacenters for hosting local content and services whenever appropriate. In the remainder of this section, we focus on the description of some of the key applications (broadband network gateway (BNG) and packet data network gateway (P-GW), virtual residential gateway, CDN, and caching) that could be hosted in the NG PoP and provide some arguments for justifying their hosting at the network edge.

### 12.2.1 Virtual Residential Gateway

The current home-triple-play offers (Internet, VoIP, and IP-TV) are based on a model in which many network functions are located in the home premises, i.e., in a residential gateway, also known as a device called “box.” Typically, the operator controls IP addressing and routing and is able to propose value-added services in the customer’s LAN (e.g., IP-TV). However, this model suffers from a lack of flexibility since the box is a compromise between cost and performance and might be hardware limited for any new additional service. Moreover, the number of hardware/software (firmware) combinations can be very large and extremely difficult to manage, slowing down time to market for new services.

The virtual residential gateway (vRGW) approach allows for the hosting of most of the legacy residential gateway functions in the operator’s network, while keeping in the home-network premises only a basic CPE (customer-premises equipment): typically, the modem, the Wi-Fi card, and other necessary hardware. It leads therefore to a new functional distribution model, where the subscriber’s LAN is extended to the network. The control plane will then be hosted in the operators’ network, but should stay at the edge of the network, closer to the customer premises, because of the high constraints in terms of latency and bandwidth that the remote management of a home network would impose. NG PoP provides an adequate location for hosting such function.

In terms of architecture, the vRGW shifts most of the networking and service-related functions from the residential gateway to an entity called the vG (virtual gateway) and keeps a light physical device at the customer premises, called the broadband residential gateway (BRG). Typically, the vG hosts functions such as routing, network address translation (NAT), and IP addressing-related functions. The BRG, the remaining physical device in customer premises, would essentially have to support the physical interfaces (Wi-Fi, RJ-45, network uplink) as well as layer 2 forwarding, Wi-Fi management, and upstream QoS. The BRG is configured in bridged mode between its LAN interfaces and the vG in the operator’s network.

Figure 12.1 depicts the high-level vRGW architecture. In the Broadband Forum, this architecture is called NERG, for network enhanced residential gateway [2].

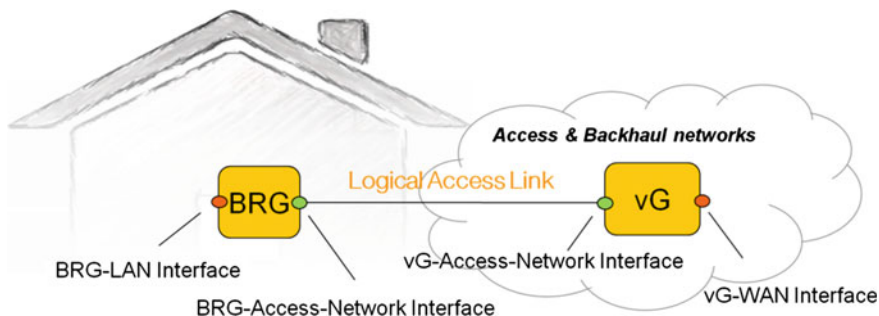


Fig. 12.1 The vRGW high-level architecture

Different implementation approaches are considered for vG support in telecommunication networks, from leveraging on BNG infrastructure to a full IT approach.

### 12.2.1.1 Implementing Virtual Gateway with a Physical BNG

This approach considers the location of the vG in NG PoP. In fact, the vG can be split into two entities: the network vG (N-vG), integrated in the core router, and the service vG (S-vG) that can be hosted in a virtual machine at the mini data center part of the NG PoP (Fig. 12.2).

The main function of the vG is to provide enhanced and personalized services from the network, meaning that the vG has to apply subscriber policies (e.g., QoS per device, service chaining) that can be provided thanks to AAA (authentication, authorization, and accounting) mechanisms.

This requires the N-vG to be in charge of terminating all customer sessions: both the subscriber session and additional sessions for selected devices. The N-vG is also required to support NAT and firewall functions; it is in charge of forwarding the subscriber traffic to selected services, according to the subscriber policies provided by the AAA mechanism. Such service chaining capability is initiated by the NG PoP and can be performed thanks to a programmable switching function. The S-vG can be realized through software appliances deployed in IT servers, e.g., allocating a dedicated resource or application per customer in virtual machines. Each application contains several services: DHCP server for the LAN devices, LAN topology discovering mechanism, proxies for media discovering, etc.

Almost all traffic goes directly through the N-vG toward the core network. The S-vG is optimized for supporting only required services. Other appliances may be implemented in this architecture at the same level as S-VG in the NG PoP, not specific to the v-RGW architecture; it could be, for example, a parental control platform or an antivirus platform.

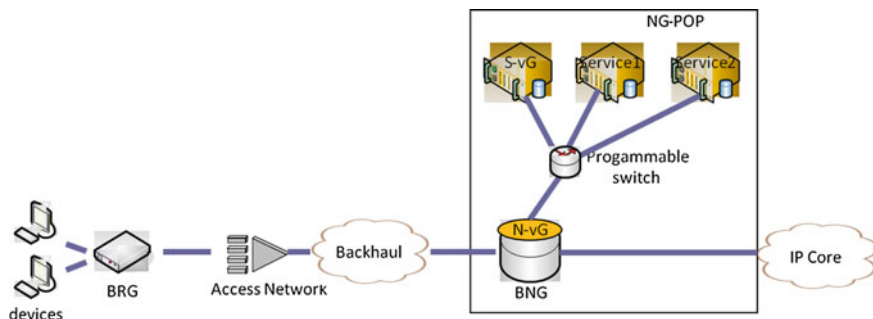


Fig. 12.2 vG implementation in NG PoP

Regarding the dimensioning of the IT part, dedicating one virtual machine for each S-vG (i.e., each subscriber) is very expensive in terms of resource usage. Rather, virtualization in containers seems more appropriate, as a single file system is shared between containers, allowing drastic resource savings.

In this approach, the vG is fully implemented in IT servers. This requires processing 100 % of the subscriber’s traffic (LAN ↔ WAN), for both the data and control planes. Recent progress on network function virtualization, especially improved packet processing on ×86 processors, should allow decent performances for such implementation.

### 12.2.2 Broadband Network Gateway

The broadband network gateway, standardized by the Broadband Forum, can be seen as an evolution of the BRAS (broadband remote access server) in today’s fixed networks. It is a key function for fixed access networks, dealing with subscriber session management. The BNG performs network authorization in order to grant, block, or limit the access to the network according to the subscriber’s subscriptions or limitations (for legal reasons for example). Beyond authentication and authorization, the BNG also performs accounting per subscriber, depending on the business model of the operator. The BNG can also enforce some forwarding policies per subscriber in order to enable advanced service chaining such as restricted access, lawful intercept, or parental control.

Different implementation approaches of the BNG can be considered; the following paragraph introduces three of them as depicted in Fig. 12.3.

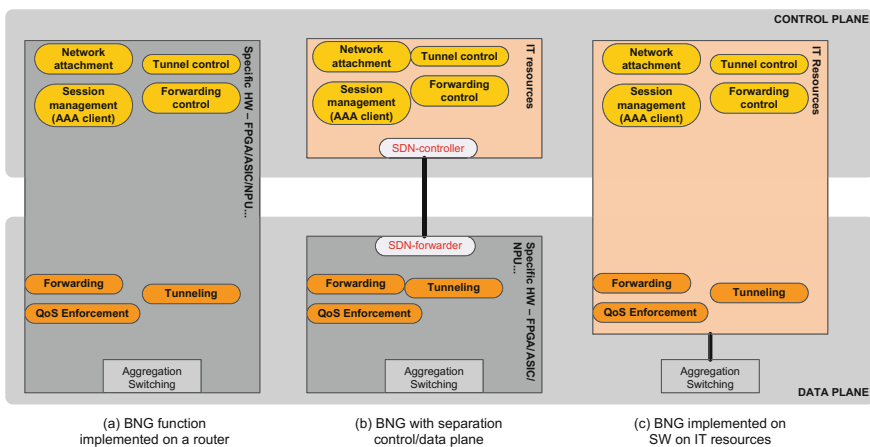


Fig. 12.3 Possible implementations for the BNG function

### 12.2.2.1 BNG Function Implemented in Hardware on an Existing Network Element

In this approach, the vendor implements the BNG function on its edge router portfolio, which already supports access node aggregation, IP routing, and L2/L3 VPN. The BNG-enabled access cards may need specific hardware compared to the classical IP/VPN access cards which manage the subscriber sessions and the associated hierarchical QoS.

### 12.2.2.2 Pure Soft BNG: Implementation on IT Servers

Building on a well-established trend in the IT industry, virtualization is rapidly entering the telecom industry, with NFV being its latest incarnation. Leveraging cloud computing technologies, NFV is currently a topic of much hype; however, due to the huge ecosystem exploring the subject, there is a strong indication that it may become a rapidly adopted paradigm in telecom operator networks. Currently, most telecom equipment is sold in the form of integrated vertical systems (sometimes referred to as network appliances) with applications running on purpose-built middleware and hardware. The proposition of NFV is a paradigm shift, from the current situation to a cloud model where telecom functions are virtualized and run on virtual machines in pools of commodity servers. This approach already found its way in the IT industry. What makes NFV a challenge in this application is the telecom industry's demanding requirements for five-nines availability and for predictable real-time performances.

The term NFV was coined by a group of tier-1 telecommunication operators and introduced via the ETSI standards organization in a white paper published in October 2012 [3] (see also Fig. 12.4). Network function virtualization is defined as the process of “*implementing network functions in software that can run on a range of industry standard server hardware, and that can be moved to, or instantiated in, various locations in the network as required, without the need to install new equipment.*” Such locations include—but are not limited to—highly centralized data centers or smaller data centers in network points of presence like the NG PoP.

The ETSI-NFV performance group [4] provides some results on the virtualization of the BRAS function, which in terms of performance requirements is similar to the BNG function. Both control and data planes are implemented on  $\times 86$  servers, using hardware acceleration features available in new general-purpose processors and latest software optimization for such hardware (DPDK libraries). The virtualization of the BNG might be feasible in the near future, but aggregation network equipment is still required in front of the soft BNG.

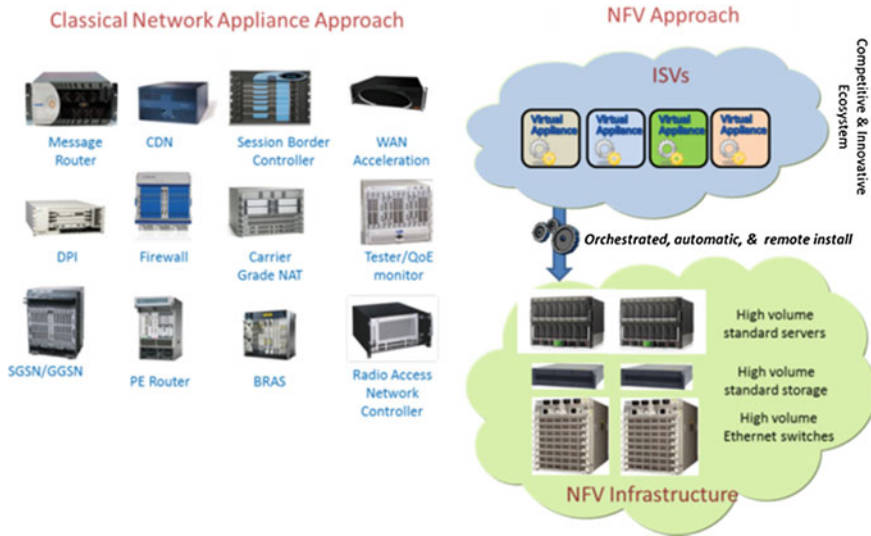


Fig. 12.4 A network function virtualization overview [3]

### 12.2.2.3 BNG Function Implemented with Both IT Resources and Dedicated Hardware Resources

In parallel to the NFV work, telecommunication vendors also consider another path for evolving network equipment and especially equipment having to support high-performance data transport. This work encompasses evolution of core routers, high-density BNG, and security gateways for which integrated boxes and embedded application-specific integrated circuits (ASICs) may be still relevant.

If vendors invoke performance issues, we can also imagine that pure NFV solutions threaten their business model. Rather, vendors envision a SDN solution where the control plane is separated from the data plane. The idea is to provide a flexible control plane which will be implemented on IT resources and a programmable data plane which is still implemented in hardware in order to maintain high-performance network functionalities.

### 12.2.3 Distributed Evolved Packet Core

In legacy LTE networks, a small number of evolved packet core (EPC) nodes hosting serving gateways (S-GW) and P-GW (the mobile core gateways) seem enough to address core network data traffic requirements on a country-wide scale. However, such centralized EPC architecture is not optimal for some key use cases:

- For content delivery network (CDN), deploying CDN for the mobile network with caching functions at the edge is not allowed as far as the EPC is centralized. The CDN caching servers should be hosted at least behind the PDN Gateway, where the data traffic is removed from the general packet radio service tunnelling protocol (GTP) tunnels.
- For communication and services established among participants located in the same area with high real-time requirements, such as online gaming or the sharing of user-generated content.
- When services can be hosted locally, very close to the end users, optimizing bandwidth use and delays, such as personal cloud services (online personal content storage and applications execution).

Enabling the traffic to escape to the Internet via a nearby gateway without having to cross the entire mobile core network is also known as *local breakout* and should be applied for these cases. The 3GPP managed to address this issue in Release 10 selected IP traffic offload (SIPTO), but the proposed solution requires the definition of a specific gateway utilized for the breakout traffic (in 3GPP, the gateway is identified with a particular access point name—APN). This APN needs to be appropriately selected depending on the type of traffic or application (Fig. 12.5).

Thus, an alternative would be to consider distribution of mobile gateways (S-GW and P-GW) and adapting the GW selection process, anchoring the traffic at

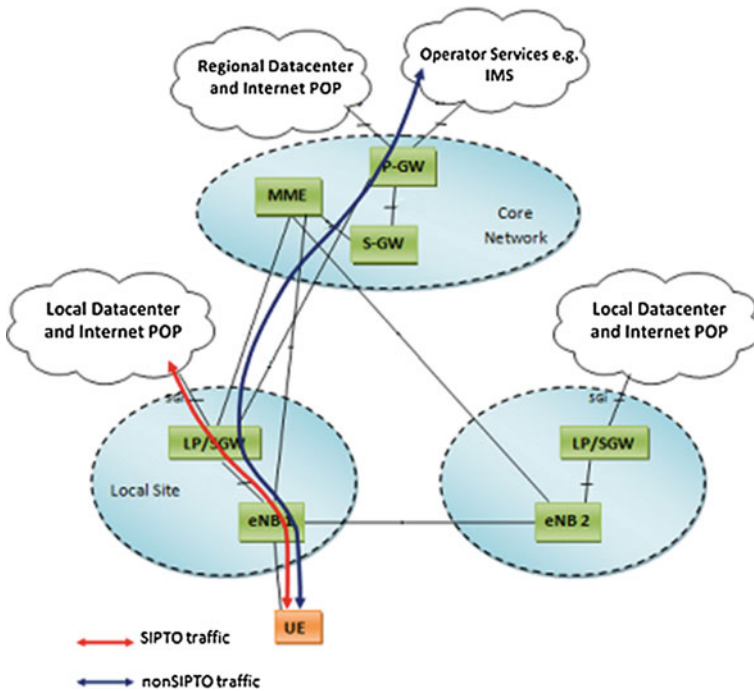


Fig. 12.5 Local breakout with SIPTO

the most appropriate P-GW, for instance based on user's location. The P-GW could then be hosted at the NG PoP level, allowing standard IP traffic routing and steering as close as possible to the end user.

### 12.2.4 Highly Distributed Content Delivery Networks

A content delivery network refers to a large network of servers deployed across multiple networks in several data centers, often geographically distributed. CDNs are employed by companies across many industries to deliver HTTP content, rich media content such as streaming audio and video, and downloadable files. CDNs are optimized to provide higher speed and greater scalability and availability compared to the case of a standalone server deployment. CDN caches distribution closer to the end user, at network's edge, and allows for an optimal content delivery, as far as many similar contents are consumed in the area covered by the NG PoP. Its dimensioning is a trade-off between content availability and storage capacities at the edge. In general, it is considered that a 20 % distribution of the most popular content allows to serve 80 % of the users' requests. Figure 12.6 shows the different traffic paths with caching servers located at a regional PoP; if the mobile core gateways (P-GW) are hosted in the regional PoP (right figure), the benefits are obvious in terms of transport savings and effectiveness of content caching.

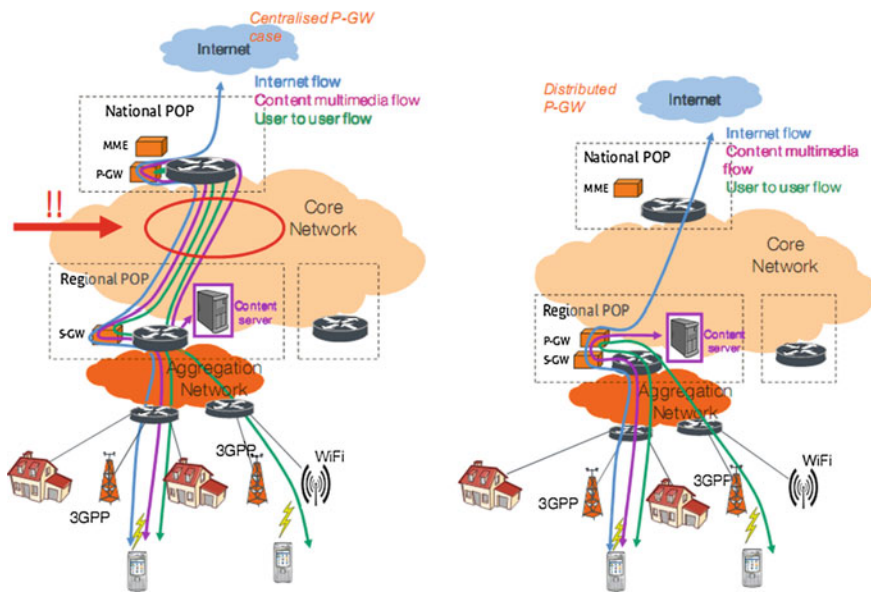


Fig. 12.6 Local breakout with distributed EPC

## 12.3 The Path Toward Fixed and Mobile Convergence

To a minor extent, pooling of fixed and mobile infrastructures is already implemented today in access and aggregation networks. For example, mobile base stations and business customer premises as well as the first access node as seen from most residential customers are already connected via fiber, while the aggregated traffic is transported via Ethernet infrastructure. Also, common backbone is generally based on IP and MPLS. Furthermore, Wi-Fi hot spots are generally gathered through fixed access lines like residential/business customers. As a final example, access control functionality to grant connectivity to Internet or dedicated services may be shared with mobile core control, e.g., in providing AAA information.

However, the current level of convergence between fixed and mobile infrastructures is not sufficient to allow the most efficient use of network resources, whether fixed, mobile, or Wi-Fi. The need for actual fixed and mobile convergence (FMC) will soon become more pressing due to the steep traffic growth fostered by the increasing number of connected devices, higher-speed connections, and bandwidth hungry applications and services [5, 6]. FMC will help to manage traffic more efficiently, providing more capacity to end users through a single network infrastructure with seamless multiple accesses.

Different use cases can be identified for FMC, and various technical solutions can be considered to address these use cases [5]. This section focuses here on two important concepts which are believed to be essential in the path toward FMC and are able to leverage on NG PoP flexibility, namely

- a universal AAA function implementing a converged subscriber data and session management
- the convergence of the fixed, mobile, and Wi-Fi IP edge functionalities into a universal access gateway (UAG).

### 12.3.1 *Converged Subscriber Data and Session Management*

Today, users hold different subscriptions and identities for fixed and mobile telecommunication services. One highly desirable feature of future FMC networks is a converged subscriber data and session management, with the objective to unify the AAA functionalities of fixed, mobile, and Wi-Fi.

In the mobile network, as it is utilized for personal communication services, the subscriber is generally also identifying the user and even to some extent his personal device. In fixed access networks, the situation is different; one can find behind a subscriber many different users and devices. So a clear distinction has to be made between subscribers and users.

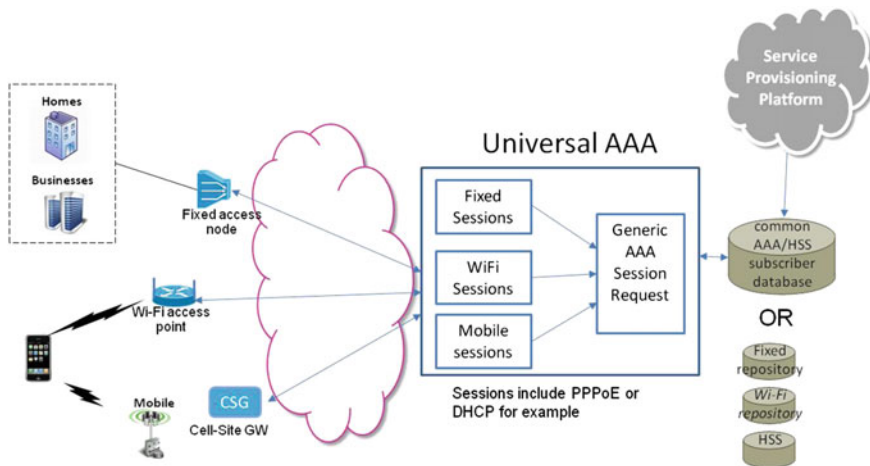


Fig. 12.7 Conceptual view of universal AAA

At the network level, a universal AAA infrastructure is required as a common user access control entity for any kind of access network used. Such a converged AAA function should be also capable of providing service-level adaptation information based on access network capabilities and type, resulting in better end-user quality of experience (QoE). We envisage a step-by-step introduction of converged AAA functions.

In a first step toward universal AAA, each access network can still rely on its own authentication methods, while an additional common subscriber session database is introduced in order to keep track of the access network used. The main concept of this universal AAA is depicted in Fig. 12.7. The different sessions managed can include, for example, PPP over Ethernet (PPPoE) or dynamic host control protocol (DHCP). The universal AAA will allow further service adaptation, common subscriber session management, and common charging whatever the access network is in use.

In a second step, a fully converged AAA infrastructure requires the introduction of a single universal user identity, managed by a single AAA/HSS (home subscriber server) database. As a matter of fact, the HSS of mobile networks is just a particular AAA server based on the Diameter protocol.

Note that, even if there is a single logic subscriber database, there should be, for redundancy reasons, different physical locations that host synchronized copies of the database and that can take over the traffic in case of an outage of the main node.

### 12.3.2 *Universal Access Gateway*

Functionalities implemented at the IP network edge (typically located at the boundary between core and metro networks) are extremely important in broadband networks, as the IP edge node is the first network node. The IP edge is an important functionality of broadband networks, as this is the first network node where IP traffic from the end user is treated and routed or forwarded through IP backbones (and the other way round). In other words, it acts as an anchor point for user's data traffic, allowing access to several IP networks, including the public Internet. This IP edge is typically implemented as an IP router with additional specific functionalities. In legacy networks, IP edges are specific to given types of networks (fixed, mobile, Wi-Fi) and can be implemented at very different locations:

- In the fixed network, the Internet service provider (ISP) terminates user IP traffic together with the user point-to-point protocol (PPP) tunnel at a label edge router called LNS (L2TP network server). When the ISP and the access provider are the same, this function is generally combined with the broadband remote access server (BRAS) which terminates the Ethernet section of the aggregation network and also acts as a L2TP access concentrator (LAC). An evolution of the fixed IP edge functionality is called broadband network gateway (BNG) and would result in a greater distribution of the fixed IP edge entities compared to the BRAS/LAC/LNS model (see Sect. 12.2.2 for more details on BNG). The BNG typically includes forwarding functions of layers 2 and 3 and also functions related to resilience, security as well as network management;
- In the 4G mobile network, user IP data traffic is terminated at the P-GW, a key equipment of the EPC. In general, between the user equipment and the P-GW, private IP addresses are used. Thus, the IP edge also includes network address translation (NAT) functionality, in addition to many other functions such as deep packet inspection (DPI), lawful interception (LI), accounting for inter-operator charging, and service-level rate enforcement;
- In Wi-Fi networks, various implementations of the IP edge are possible. Basically, IP edge functionalities can be distributed in network nodes, including Wi-Fi access points, or centralized in a so-called Wi-Fi gateway, i.e., a centralized node which hosts IP forwarding functions as well as some other key functions such as advanced subscriber management, policy-based routing, data filtering, QoS, NAT, DPI, and LI.

A converged IP edge is thus a desirable target for future FMC networks. This converged IP edge, which we call the universal access gateway (UAG), integrates fixed, mobile, and Wi-Fi gateway functionalities in the same network entity. One could consider gathering in the same node the various specific functions of fixed and mobile IP edges, but we preferably target the definition of a common (generic)

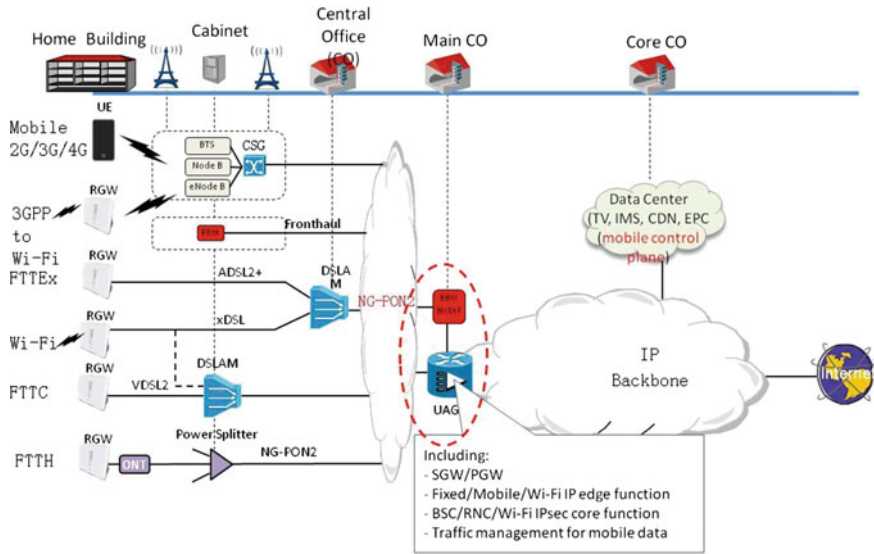


**Fig. 12.8** Concept of universal access gateway

set of IP edge functionalities. This promises a more efficient operation of transport and control functionalities within the aggregation network and reduces the number of network elements. A joint operation of mobile core functionalities (e.g., EPC gateways) and aggregation for 2G/3G/Wi-Fi, together with IP edge functions, can also improve the routes of service specific traffic flows (e.g., through local breakout of mobile Web or content delivery network access). More efficient data transport may also improve QoS (reduced delay) for customers and save operator resources. The UAG concept is applicable to operators with fixed, mobile, and/or Wi-Fi infrastructures, as well as multi-operator network sharing where the same UAG is shared by multiple operators.

The concept of UAG is depicted in Fig. 12.8. An UAG would encompass functions for mobile aggregation routers and data plane EPC gateways, BNG, and security gateways and would be located typically in aggregation networks in the main central office (main CO). Some BBU radio processing units of base stations may also be part of it, depending on the location of the main CO.

The UAG innovative concept takes advantage of SDN, which uses a single control protocol for multiple simple network devices. Furthermore, NFV brings the required flexibility to encompass the functions in an effective way into such a node with adapted scaling.

## 12.4 Implementing the NG PoP

In this section, we further discuss design principles for NG PoP implementation as well as dimensioning figures.

### 12.4.1 Design Principles

The NG PoP is the network node where fixed and mobile accesses are aggregated and where the first IP router is located. It leverages on the most appropriate central offices for hosting network functions and services at the network's edge. This first IP router would enable flexible traffic forwarding policies, e.g., forwarding Internet traffic to the nearest peering point. Subscribers' session management functions would be supported through the hosting of standard gateway functions (e.g., the BNG for fixed users and the P-GW for mobile users), or preferably a UAG, and their interconnection with legacy, preferably unified, control infrastructures (AAA, HSS, mobility management entity, etc.).

In addition, the broadband fixed and mobile traffic can be handled following differentiated policies (routing, forwarding, access to local services, etc.). The NG PoP behaves as a mini data center with storage and processing capabilities in addition to the classic forwarding functions. It enables the distribution of contents and applications closer to the end users, reducing latency and optimizing bandwidth use. The NG PoP enables the network to progressively evolve toward an open and programmable infrastructure. Last but not least, it can behave as a mediator/proxy for the network, between users and service providers (machine-to-machine, over-the-top, etc.), and is preparing the functional and organic convergence of fixed and mobile nodes.

Implementing the NG PoP requires taking into consideration different types of functions, which are traditionally supported by separate entities in current networks, such as

- Access nodes aggregation, for fixed, optical, and mobile access;
- Networking functions, at and beyond the first IP router;
- Access selection functions, for a cooperation between fixed and mobile networks;
- Security functions;
- Subscriber's session management;
- Virtual CPE functions;
- In-networks caching facilities for CDN;
- Service appliances platform hosting.

Instead of considering a dedicated NG PoP specification with a complete list of functions, we favor defining an open platform able to host different kinds of services, from low-level forwarding to content or applicative servers. We foster then an IT-oriented approach relying on commodity on-the-shelf hardware instead of

specific network devices hardware. Most functions could be brought as software building blocks, possibly virtualized following NFV principles, even if compliance with carrier grade requirements needs to be verified, particularly in terms of capacity, latency, bandwidth, and availability. Forwarding elements may be also virtualized or, more probably, supported via dedicated switching devices.

Secondly, the NG PoP will need to adapt traffic flow management to different services or users' requirements. For example, it could consider some traffic redirection to local caches when content is stored locally or to a traffic inspection function for parental control. Thus, traffic steering policies need to be implemented and adapted to each traffic flow, following a service chaining approach.

This leads to the consideration for the separation of the control plane from the data plane with programmable interfaces following an SDN design. The controller could be logically centralized, either dedicated to a single NG PoP or managing several instances distributed in the network. The NG PoP data plane functions will naturally be provided on infrastructures deployed at the NG PoP location, i.e., at the first access router level in the Telco network. Firstly, we consider an Openflow-based interface between the NG PoP controller and forwarding instances. Thus, the NG PoP controller dynamically triggers traffic flow forwarding through the different network services by controlling forwarding rules.

The deployment of local content caches into an NG PoP is allowed through dedicated software appliances and local storage facilities, with the related traffic flow redirection rules being provisioned through the controller. Similarly, different types of applications can be hosted for providing end-user services, such as gaming, personal cloud, and communication suites.

Lastly, NG PoP application programming interfaces would allow different types of openness, from a low-level access to forwarding/storage/processing resources to high-level appliances activation. This will allow new business cases for Telcos' infrastructure valorization, through business-to-business and business-to-business-to-customer models.

### ***12.4.2 Dimensioning the NG PoP***

Several dimensioning factors need to be taken into consideration, like number of subscribers, session distribution, network function processing, appliances requirements, storage size, switching capabilities, number and configuration of virtual machines. Such figures need to be factored in for each deployment scenario and adapted to foster scalability. Depending on their real-time requirements, some software appliances will benefit from a cloud-based approach to be deployed and scaled out/in between neighboring NG PoPs and more traditional data center facilities at a regional or nationwide level. However, at least access control functions, traffic forwarding capabilities, and vRG functions need to be hosted in the NG PoP managing the area because of the requirements of such functions in terms of bandwidth and latency. Considering the case of a convergent operator, we estimated

that different deployment options for NG PoP might require a total aggregated bandwidth between 30 and 60 Gbit/s, corresponding to the support of about 60.000 fixed access lines (FTTH and xDSL) and around 30 mobile base stations needed to cover the NG PoP area. This figure provides only a rough estimation.

## 12.5 Conclusions

The NG PoP concept brings a flexible point in the operator's network, where access, networking, and services features could be hosted in a coherent architecture. It is an enabler for functional convergence between fixed and mobile networks capable, e.g., of implementing the necessary building blocks for Converged Subscriber Management and Universal Access Gateway. As a mini data center, it facilitates the distribution of content caches and the hosting of applications closer to the user, thus reducing latency and increasing bandwidth. By allowing several applications and networking services sharing, a common IT platform thanks to virtualization, and by separating the controller from forwarding facilities through programmable interfaces (thanks to the Software-Defined paradigm), it enables the network to progressively evolve toward an open and programmable platform. Moreover, the NG PoP can behave as a mediator/proxy for the network, between users and service providers (machine-to-machine, over-the-top, etc.) allowing infrastructure valorization through new business-to-business and business-to-business-to-customer business models.

Obviously, several technical aspects need to be addressed in order to make the NG PoP a real convergent, flexible, and cost-effective network node: the rationale for hosting a given application at the edge of the network, instead of in a centralized network site or data center, needs to be addressed on a case-by-case basis with evaluation of benefits in terms of latency, bandwidth, energy savings, and obviously cost. A smooth move from telecom-specific devices to IT ones is a current trend, but hosting network functions in virtual machines still raises questions in terms of performance and energy efficiency. Some functions would still need hardware acceleration for instance. SDN adoption on a large network scale will depend on standards adoption and interoperability between equipment from different vendors. For example, an open-source approach should help meet such interoperability requirements.

Lastly, the NG PoP should not be designed as a closed component with a restricted list of functionalities. Indeed, we strongly believe that an open model will stimulate innovation for new types of applications and services that are not yet imaginable and that will benefit from the cooperation with various components (e.g., users' profiles, context awareness, content, QoS monitoring, processing and storage facilities, incremental deployment from cloud components).

**Acknowledgments** This work was supported by several colleagues from Orange and from partners of European project COMBO and has received funding from the European Union's seventh framework program (FP7/2007–2013) under grant agreement no. 317762.

## References

1. Gosselin S, Mamouni T, Bertin P, Torrijos J, Breuer D, Weis E, Point J-C (2013) Converged fixed and mobile broadband networks based on next generation point of presence. Future Network Mobile Summit (FutureNetworkSummit) 2013:1–9
2. Broadband Forum Working Text WT-317
3. Network Functions Virtualisation. An introduction, benefits, enablers, challenges & call for action. October 22–24, 2012 at the SDN and OpenFlow World Congress, Darmstadt-Germany
4. ETSI DGS/NFV-PER001 network function virtualization, performance & portability, NFV performance & portability best practices, September 2013 (draft)
5. Gosselin S, De Biasio J, Feknous M, Mamouni T, Torrijos J, Cucala L, Breuer D, Weis E, Geilhardt F, Hugo D, Bogenfeld E, Hamidian A, Fonseca N, Liu Y, Kuehrer S, Gravey A, Mitsenkov A, Galán JV, Masgrau E, Gómez L, Alonso L, Höst S, Magee A (2014) Fixed and mobile convergence: needs and solutions. In: Proceedings of the European Wireless 2014, session A4, Barcelona, Spain
6. Feknous M, Gravey A, Houdoin T, Le Guyader B, De Biasio J, Torrijos J (2014) Internet traffic analysis: a case study from two major European operators. In: Proceedings of the IEEE symposium on computers and communications 2014 session 8, Madeira, Portugal

# Chapter 13

## Coordinated Multi-point (CoMP) Systems

Yizhuo Yang, Christina Lim and Ampalavanapillai Nirmalathas

**Abstract** This chapter first gives a brief introduction on the coordinated multi-point (CoMP) technologies and the backhaul requirements for enabling CoMP techniques in LTE-A. As fiber–wireless integration (also known as radio-over-fiber (RoF)) is introduced to next-generation mobile backhaul networks as a promising technology to meet the critical backhaul requirements, in this chapter, the CoMP backhaul architectures and BS/RAU configurations based on various RoF technologies are also presented.

### 13.1 Introduction on CoMP

With exploding demand for mobile broadband services and the emergence of new high-capacity mobile devices and data-intensive applications, mobile networks have to continuously evolve, incorporating the latest technological capabilities, so as to meet the capacity and coverage demands. LTE-Advanced with high spectral efficiency and improvements in mobile cells makes higher network capacity possible. As the cell continues to grow smaller and the frequency reuse factor gets closer to 1, the cell performance is significantly limited by the inter-cell interference (ICI). More advanced wireless communication techniques are thus required to mitigate the inter-cell interference and increase the throughput of cell-edge users. One such approach is a base stations (BSs) cooperation technique, also referred to as coordinated multi-point (CoMP) transmission and reception, is proposed in LTE-Advanced (as shown in Fig. 13.1). CoMP utilizes the multiple transmit and receive antennas from multiple antenna sectors, which may or may not belong to the same physical cell, to enhance the received signal quality, decrease the received interference, as well as improve the channel capacity of cell-edge users in the network.

---

Y. Yang (✉) · C. Lim · A. Nirmalathas  
Department of Electrical and Electronic Engineering, The University of Melbourne,  
Melbourne, Australia  
e-mail: yyz3309@gmail.com

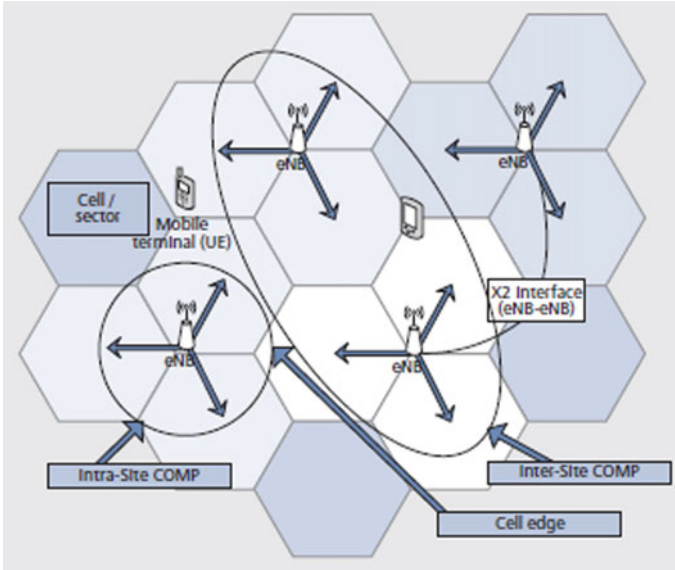


**Fig. 13.1** Base station cooperation: intra-site and inter-site CoMP

CoMP techniques are generally categorized into the following types (as shown in Fig. 13.2): coordinated scheduling and coordinated beamforming (CS/CB), joint processing (JP), and transmission point (cell) selection (TPS). In CS/CB, multiple coordinated transmission points (antenna sectors or base stations) share only channel state information (CSI) for multiple user equipment (UE) terminals, while data packets that need to be conveyed to a user equipment terminal are only available at one transmission point. In JP, the same data are transmitted from multiple coordinated transmission points with appropriate beamforming weights, and users can simultaneously receive/transmit signals from/to multiple transmission points. TPS can be regarded as a special form of JP, where transmission of beamformed data for a given UE terminal is performed at a single transmission point at each time instance, while the data are available at multiple coordinated transmission points.

The applicability of the CoMP functionality depends to a great extent on the backhaul characteristics (latency and capacity), which condition the type of CoMP processing that can be applied and the associated performance. Both CoMP techniques are supported by means of coordination message exchanges between base stations (eNodeBs in LTE) via a logical interface named X2. In CS/CB, an X2 interface with a data rate below 1 Mbps will be enough for exchanging channel state information between transmission points. In JP, adjacent transmission points share the data packet to be transmitted to particular user equipment, which requires exchanging large volumes of information, including unprocessed I/Q samples

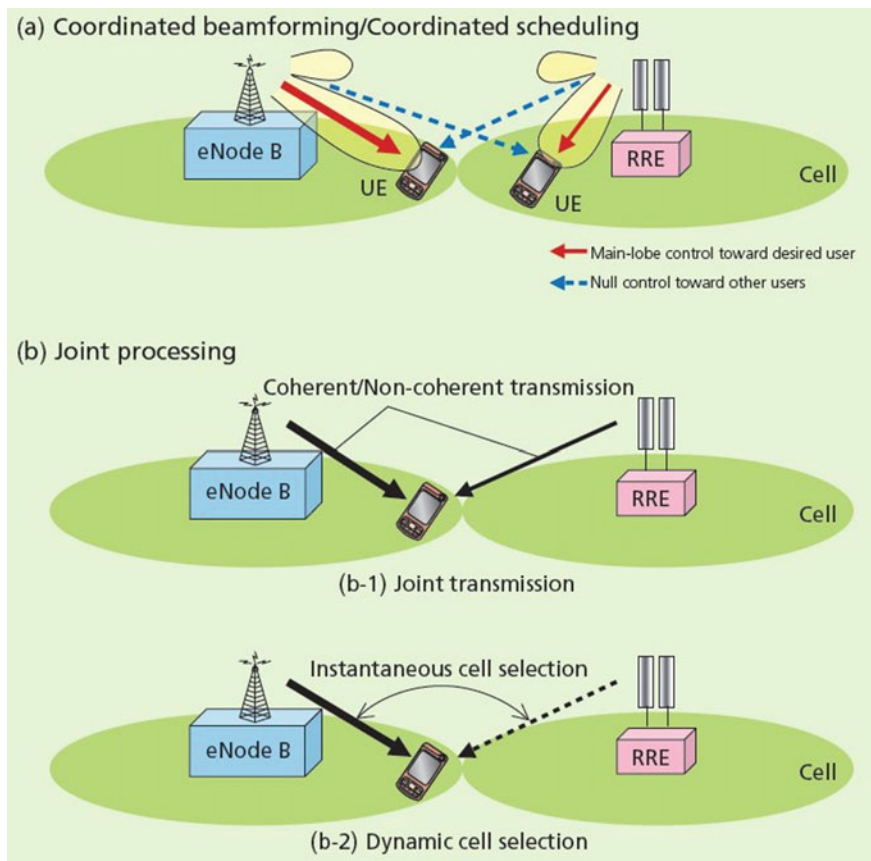


**Fig. 13.2** Downlink CoMP transmission (*RRE* remote radio equipment, *eNodeB* evolved node B, *UE* user equipment)

before demodulation. In return, the JP technique generally gives greater performance benefit compared to the CS/CB technique.

### 13.2 Requirements on the Backhaul Network

Here, we take a look inside the backhauling of the X2 interface in terms of bandwidth, latency, and development requirements. It should be noted that the X2 interface does not require physical connections between all eNodeBs, as it is a “logical” interface between only neighboring transmission points (eNodeBs) and can be switched over the existing transport network.

### **13.2.1 Latency**

X2 assists in optimizing handover performance when direct connectivity exists between the source and target eNodeBs with X2 interfaces. X2 handover is no more sensitive to latency than S1 signaling or user traffic, so the same requirements apply. Next-generation mobile network (e.g., LTE-A) requirements are 10 ms end-to-end round-trip delay, and 5 ms is recommended. When used for data forwarding, the X2 delay must be added onto the S1 delay, and thus it should be as small as possible. The X2 backhaul latency, or more generally latency between eNodeBs or RRE, is highly deployment dependent (e.g., it will be different for a dedicated X2 fiber network and for a generic IP network). An X2 latency value of about 1 ms is suggested in 3GPP.

### **13.2.2 Synchronization**

In addition to low-latency connections, the clocks at cooperating base stations need to be in phase to enable proper operation of inter-cell interference coordination (ICIC) and CoMP. This leads to highly accurate phase or time-of-day synchronization. Most 3GPP base station clocks are currently synchronized on frequency only, since accurate phase synchronization was not a requirement until now. The new LTE-Advanced functions, however, require base stations to be in phase with an accuracy of 500 ns to efficiently operate ICIC and CoMP. This is nearly impossible to achieve without on-path support. Therefore, the backhaul network needs to support the timing distribution architecture actively and ensure the synchronous exchange of I/Q data samples and channel state information (CSI) between eNodeBs over the X2 interface.

### **13.2.3 Capacity**

Besides key challenges, such as latency and synchronization, a major concern is the demand for additional capacity which is found to limit the performance of inter-site CoMP. CoMP schemes in LTE-Advanced may require considerably more bandwidth; an analysis of the CS/CB scheme suggests as much as 770 kbps of signaling would be needed for an X2 interface for three-sector eNodeBs.

Though the joint processing (JP) scheme generally gives a greater performance benefit compared to the CS/CB scheme, the requirements on backhaul network are more stringent. Joint processing (JP) differs in that the user data are present at multiple eNodeBs. Transmission or reception can be coordinated to rapidly select the best cell or combine signals from multiple cells coherently. As a result, the JP scheme requires additional sharing of user data over the X2, which for the cell-edge

UE requiring coordination could be of the order of several Mbps per user. According to a recent study on backhaul capacity estimation in CoMP, for an LTE link with 10 MHz bandwidth using  $8 \times 8$  MIMO, the backhaul requirements vary from a few Mbps to around 4 Gbps. Thus, JP requires significantly more backhaul bandwidth than the CS/CB scheme.

### 13.3 Backhaul Architecture

Since further increasing radio access network performance will be achieved by very tight coordination between base stations, the backhaul architecture of the radio access network is foreseen to change as well. Developing means of sufficient connectivity between adjacent BSs via a centralized architecture is preferred as it would exploit the existing backhaul connectivity and thus offer cost-effectiveness and ease of deployment. It is predicted that future wireless networks will have to handle data rates in the orders of hundreds of Mbps and beyond where current microwave backhaul will not be able to cope with the growing capacity. Meanwhile, governments around the world have recognized the broadband network as a key infrastructure for the emerging digital economy and are willing to invest or directly assist in an accelerated deployment of broadband optical access networks capable of providing broadband connectivity. The access to optical fiber networks will become much easier. High-capacity fiber-optic backhaul will eventually replace microwave backhaul to overcome this traffic bottleneck and provide the needed capacity.

With a centralized backhaul, the BSs can be relieved from the duty of performing signal processing and this will in turn reduce the scale, cost, and energy consumption compared to traditional fully functional base stations. The BSs become remote antenna units (RAUs), which consist of only an analog RF unit and in some cases analog-to-digital and digital-to-analog converters (ADCs and DACs), as well as a digital interface. Thus, the deployment and maintenance now become much easier and it is more feasible to install a large number of RAUs to provide broadband services for mobile users.

Integrated fiber-wireless networks, the so-called radio-over-fiber (RoF) networks, have attracted much attention over the past two decades in the development of wireless backhuls, with a promised centralized control architecture and simple BS configuration. Analog RoF-based hybrid optical-radio architecture with its simplified RAU configuration has been proposed and studied for future mobile backhaul network by some research groups. Digitized IF-/RF-over-fiber with centralized signal processing functionality incorporating digital optical link has also been studied with demonstrated high flexibility. Further, the Common Public Radio Interface (CPRI) and the Open Base Station Architecture Initiative (OBSAI) have standardized the digital interface between the central baseband module and the remote RF module, fueling the use of digital optical links. In the

following, we will review some mobile backhaul architectures based on fiber–wireless integration technologies enabling CoMP.

### 13.3.1 GROW-Net Architecture

GROW-Net (grid reconfigurable optical and wireless network) is a hybrid optical–wireless approach (more specifically digitized IF-/RF-over-fiber) designed specifically for high-density intra-city networks. GROW-Net adapts the street layout in a city or downtown environment and leverages potentials to reuse available dark fibers available in these regions. A grid cell in GROW-Net (as shown in Fig. 13.3) provides the backbone fiber connectivity to wireless gateway through an ultra-scalable grid infrastructure. This infrastructure is scalable because it provides WDM scalability through an evolvable optical backbone, shown in Fig. 13.4. The GROW-Net architecture consists of the following nodes:

- Optical central hub that connects optical–wireless gateways to the wide area network;
- Optical–wireless gateways that send data to a nearby wireless mesh router on a wireless link or to another optical–wireless gateway on an optical link, depending on the routing needs;
- Wireless mesh routers connected to the end users with wireless links.

In the downlink, shown in Fig. 13.5, a tunable laser is employed at the hub and thin-film filter (TFF)-based filters are employed at the receivers. In the uplink, shown here in Fig. 13.6, each optical terminal is colorless by employing a reflective semiconductor optical amplifier (RSOA). Combining the colorless terminals with

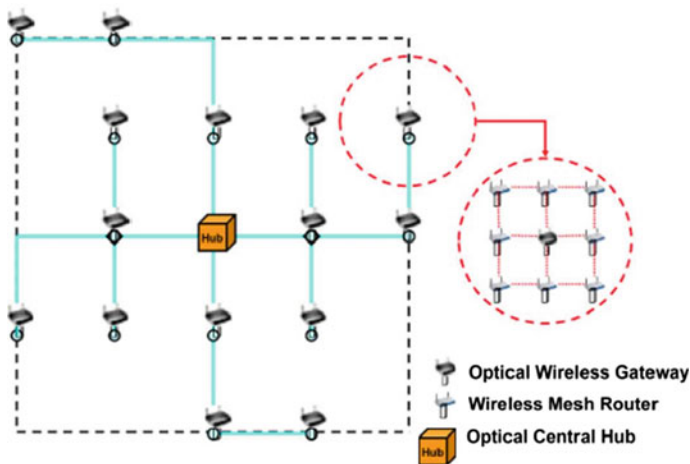


Fig. 13.3 GROW-Net topology and grid cell

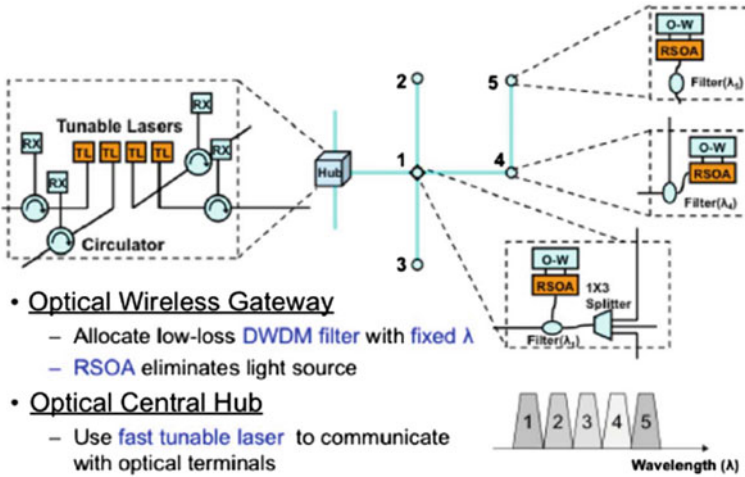


Fig. 13.4 GROW-Net optical subnetwork

the dynamic backbone allows higher wavelength insertion and assignment flexibility to accommodate for future demand growth. Based on this architecture, CoMP can be enabled by leveraging the high-capacity and low-latency backhaul infrastructure and coordinating wireless transmissions to enhance network throughput.

Figure 13.7 illustrates the new network scenario with a central processor (CP) reaching a cluster of cells through the GROW-Net backbone. It does this to implement a CoMP in order to serve many sets of user equipment (UE) in a given geographical region covered by that cluster. The term “base station” also corresponds to optical–wireless gateways. In a CoMP cell, the CP coordinates the transmission and reception of all K user equipment (UE) from/to all N base stations

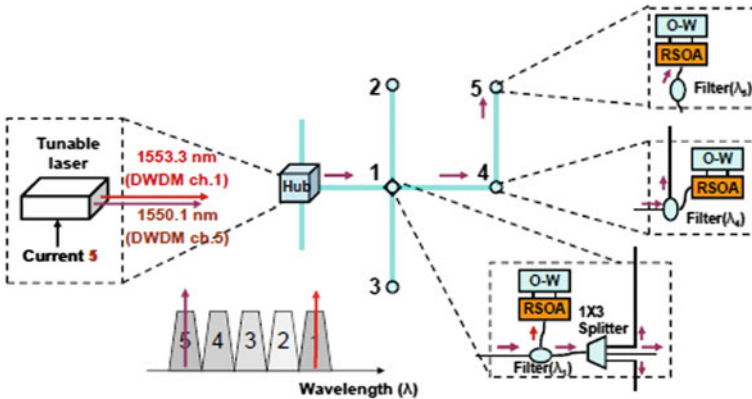


Fig. 13.5 GROW-Net grid cell downlink transmission

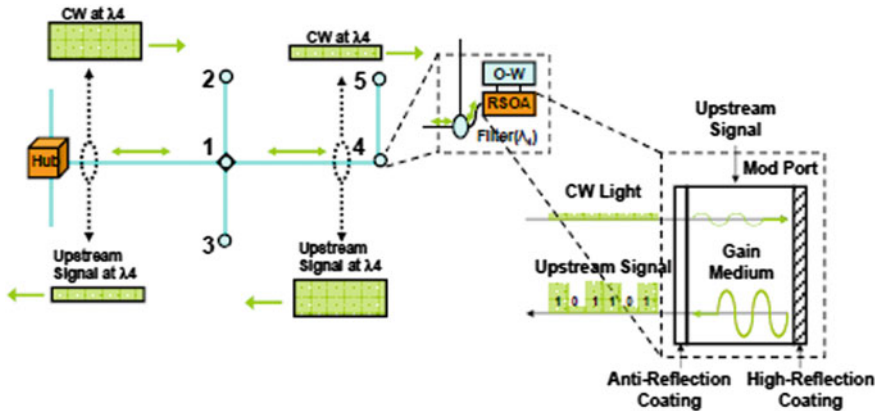


Fig. 13.6 GROW-Net grid cell uplink transmission

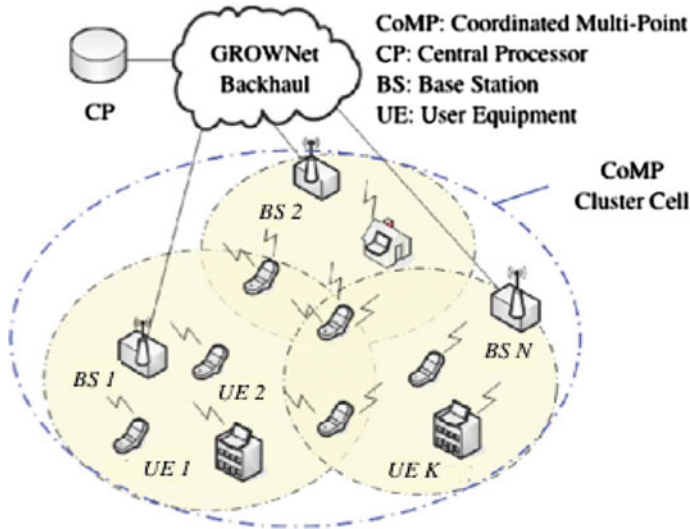


Fig. 13.7 GROW-Net CoMP cluster

(BSs). The performance of CoMP in the GROW-Net architecture has been investigated for the case where all baseband signal processing functions are deferred from the BS to the CP. The potential throughput performance improvement is substantial when combining multiple spatial antennas per node using the JP-CoMP scheme. While significant throughput improvements are enabled by coherent RF signal combining techniques, a disproportionately large volume of backhaul capacity is required when a digitized backhaul interface is used. In such a system, the large varying dynamic range in the upstream direction imposes the large number of bits

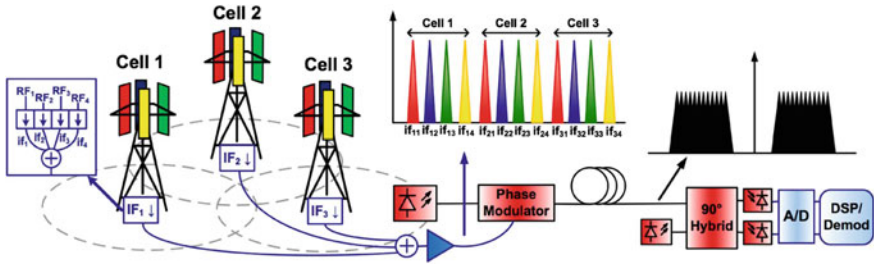


Fig. 13.8 GROW-Net backhaul using an IF-ROF link

required to quantize the RF samples. As discussed previously, the peak backhaul data rate is at around 4 Gbps for each BS/RAU, and the number is expected to grow if more antenna sectors or higher-order modulation schemes are employed. For a cluster size of  $N$ , the central processor/hub needs to support downlink transmission at more than  $N \times 4$  Gbps, and each BS/RAU needs to provide a uplink  $>4$  Gbps. The GROW-Net architecture, the tunable lasers in downlink, and RSOA in uplink could hardly reach such high speed while maintaining a reasonable cost. Therefore, it is still very challenging for GROW-Net to fully support JP-CoMP, especially when with large numbers of cell-edge users.

In order to relax the potentially huge demand on the backhaul and scale with the number of antennas in the network, GROW-Net using analog interfaces to replace digital ones is also proposed and investigated. To support multiple antenna technology, coherent optical transmission links and subcarrier multiplexing (SCM) techniques are adopted. Phase-modulated analog RoF for an upstream distributed antenna subsystem (DAS) is shown in Fig. 13.8. The phase of the optical carrier is recovered there using coherent detection. Most of the transmission impairments from electrical and optical components can be compensated by digital signal processing. The required receiver sensitivity is significantly reduced, making use of optical amplification or high-power laser sources unnecessary. The architecture can be easily scaled to a wavelength-division-multiplexed (WDM) system, using different wavelengths for different groups of cells. The main limitations for a PM-RoF system are the modulation index of the electrical signal and the induced phase noise due to the linewidth of the transmitter and local oscillator lasers.

### 13.3.2 FUTON Prototype

In the FUTON (Fiber Optic Networks for Distributed and Extendible Heterogeneous Radio Architectures and Service Provisioning) architecture, low-complexity remote antenna units (RAUs) are transparently connected via optical links to a central unit (CU), where joint signal processing and resource management are performed. Figure 13.9 depicts the system architecture. As the

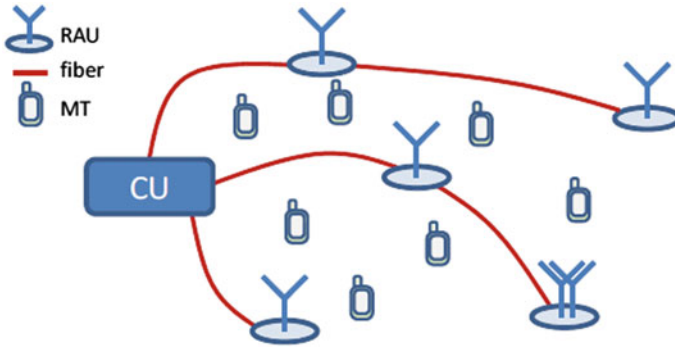


Fig. 13.9 FUTON architecture

RAUs form a distributed antenna system (DAS), this infrastructure allows to employ various CoMP techniques and multi-user MIMO to greatly enhance throughput and coverage in the service area. The RAUs in the FUTON architecture are connected to the CU via analog radio-over-fiber (RoF) link, which is similar to the analog RoF-based GROW-Net architecture. The advantages of analog fiber transmissions are that they support high bandwidths and are cost-efficient. Signals from the CU to different antennas of a site and to different RAUs can be multiplexed onto the same optical fiber by employing WDM and SCM. As digital-to-analog conversion (DAC) and IQ modulation components are not required at the RAUs, it further shifts complexity from the RAUs to the CU. Throughout the development of this architecture, economic viability has been one of the focus areas. It is delivered through low-complexity hardware, great flexibility, and compatibility with existing radio access technologies. Also, the possible convergence of wireless and wired services that can capitalize on the increasing penetration of fibers for fixed access services is a viable prospect to cut the network TCO (total cost of ownership).

However, analog optical transmission limits the achievable dynamic range performance in wideband systems and nonlinear distortions degrade the signal quality. In the RAUs, uplink power control and automatic gain control are preferred to assist meeting the dynamic range requirements, and additional digital signal processing is needed to compensate the nonlinear distortions introduced in the analog RoF link.

The FUTON prototype comprises a collection of MAC-, PHY-, and cross-layer algorithms that utilize the FUTON architecture to deliver the high data rates envisaged for future wireless systems. One of the key performance enablers is the usage of CoMP techniques to exploit spatial degrees of freedom. Figure 13.10 depicts all components of the demonstration setup. The main functional blocks are described in detail below:

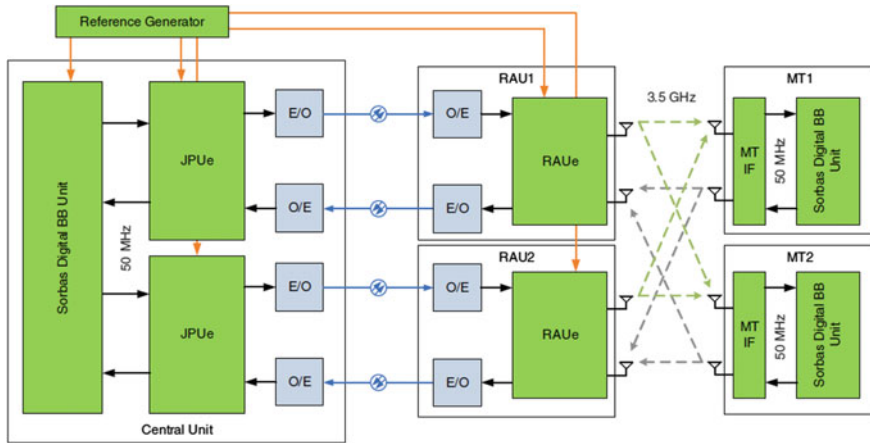
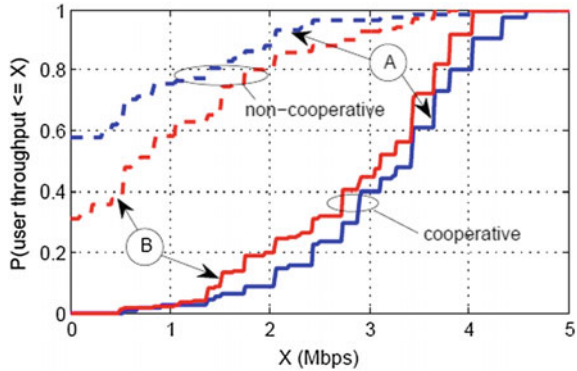


Fig. 13.10 FUTON prototype

- **Sorbas digital baseband unit:** All required signal processing at the CU and MTs (mobile terminals) is implemented on the Sorbas digital baseband radio platform.
- **JPUe:** The function of the electrical joint processing unit (JPUe) is to connect the CU to a subset of RAUs. To serve multiple RAUs with a single fiber, it is capable of multiplexing several radio signals (designated to different antennas of an RAU and/or different RAUs) onto a single fiber and performing the reverse function in the uplink direction. At the interface between CU and JPUe, the analog radio signals of each antenna served by the JPUe are exchanged on an intermediate frequency of 50 MHz. At the interface to the optical fibers, E/O components perform the electrical/optical conversion.
- **RAUe:** The electrical part of the remote antenna unit (RAUe) is capable of multiplexing signals from the receive antennas onto the fiber in the uplink and demultiplexing signals from the fiber to different transmit antennas in the downlink. Furthermore, it amplifies the signals and performs the frequency conversion of the radio signals to be transmitted at the desired RF bands (here 3.5 GHz is used).
- **MT IF:** The mobile terminal interface (MT IF) performs up- and down-conversion as well as amplification of the radio signals. At the interface to the digital baseband unit at the MT, analog radio signals are exchanged at a frequency of 50 MHz.
- **Reference generator:** The reference signal generator ensures synchronous transmission and reception on the CU side. This is especially important to guarantee that the employed oscillators are not impaired by different phase noise processes, which can lead to severe performance degradations.

The FUTON prototype system has been tested in a laboratory environment. Measurement data were collected for two different positions of the RAUs in the

**Fig. 13.11** User throughput CDF for both users sharing a frequency allocation of 1.8 MHz



laboratory. Two mobile terminals were then moved to various locations within the room to collect measurement data. The observed channels can be classified into two groups: A, symmetric channels (for cell-edge users), and B, asymmetric channels (for non-cell-edge users), where the link to the MT's respective RAU is stronger than the link to the interfering RAU. For each measurement, incoming baseband samples for 100 TTIs (transmission time intervals) were collected once for the coordinated mode and once for the non-coordinated mode with a time delay of 2 s between the modes. The statistics of the throughput measurements (both users) for both modes and channel types are depicted in Fig. 13.11 in the form of a cumulative distribution function (CDF). The results illustrate that the coordinated mode provides a large overall throughput gain compared to the non-coordinated mode. By comparing the results for the two different channel types, a second observation could be made; as expected, cell-edge users (group A) benefit more from the joint processing than cell-center users (group B). Note that the system throughput is calculated as the sum of the user throughputs depicted here.

### 13.3.3 Adaptive Photonics-Aided CoMP for MMW Small Cells

An adaptive photonics-aided CoMP architecture (Fig. 13.12) based on RoF techniques is proposed for millimeter wave (MMW) small cells over a fronthaul level or an in-home fiber distribution, which extends from the BBU/HGW to the RAUs of the RoF system. The fronthaul and in-home distributions are functionally centralized, avoiding distribution complexity and reducing system cost. Thus, CoMP functions can also be realized at a central location with traffic overhead reduced over the entire network. Figure 13.12 depicts the main functional structure of the adaptive photonics-aided CoMP architecture based on RoF. At the central office (CO), one optical mm-wave generation module is shared by all transmitters to

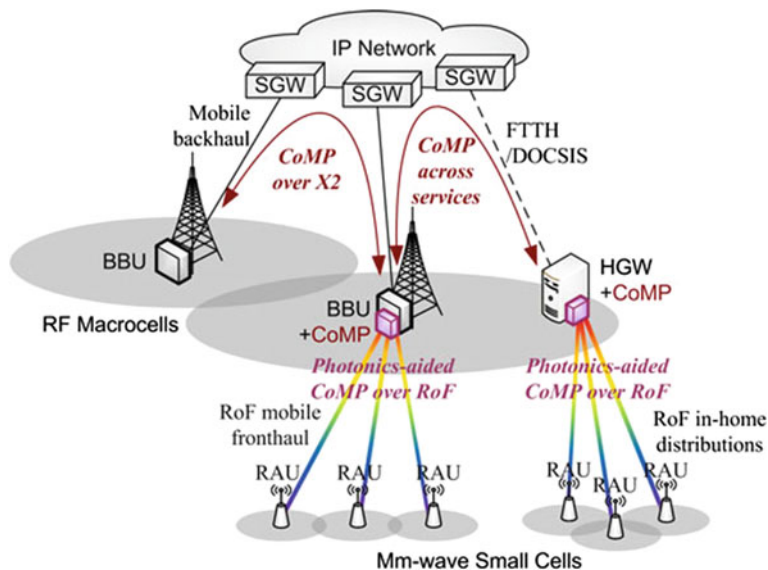


**Fig. 13.12** Adaptive photonics-aided CoMP for MMW small cells (SGW service gateway, FTTH fiber to the home, DOCSIS data over cable service interface specification, BBU baseband unit, HGW home gateway)

guarantee the coherency of mm-wave signals during both optical and wireless transmissions. After independent modulation and processing at the transmitters, the output optical signals are jointly processed inside a photonics-aided CoMP module over the fiber links at the frontend of the CO. The module realizes amplitude and/or phase adjustment on each link and its branches.

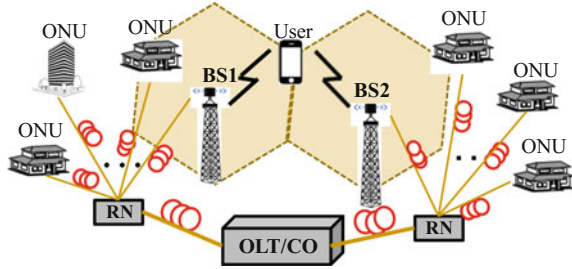
This architecture is designed only for small-cell applications using MMW frequency, which may be an interesting research direction for next-generation access network. However, it does not directly solve the current backhaul in LTE-Advanced with JP-CoMP operation.

### 13.3.4 Converged Fiber–Wireless Architecture

The convergence of mobile wireless backhaul with optical access networks is foreseen as the future for mobile telecommunication networks. In order to provide sufficient backhauling for future mobile networks using CoMP and to maximize the usage of existing fiber-optic network infrastructure, a hybrid mobile and fiber access network based on fiber–wireless integration technologies and passive optical networks (PONs) is proposed and studied as a possible solution.

In this architecture (Fig. 13.13), mobile BSs/RAUs are connected with the nearest remote node (RN) in PON and use the same optical feeder as the optical

**Fig. 13.13** Converged mobile backhaul and optical access networks



network units (ONUs) to connect to the central office (CO) which is in the same physical location as the optical line terminal (OLT). As the OLT is connected with multiple remote nodes and ONUs, the CO will support multiple BSs and will provide centralized signal processing functionality. In Fig. 13.13, the signal from the cell-edge user will be received by both BS1 and BS2 simultaneously and will be sent to the same CO using RoF technology via different fiber feeders. These received signals will then be used for joint processing in the CO. Both analog and digitized RoF technologies are capable of sending the unprocessed signals from users to the CO for joint processing, though the corresponding configurations of BSs and the requirements on the optical links are quite different. To realize the convergence of mobile backhaul and optical access networks, a dedicated wavelength is necessary for both TDM- and WDM-based PONs using analog RoF technologies; on the contrary, digitized RoF technologies can easily integrate with existing TDM-PONs by sharing the bandwidth with ONUs, as well as with WDM-PONs by using an assigned wavelength.

## 13.4 Fiber–Wireless Integration Schemes Enabling CoMP

### 13.4.1 BS Configuration

Figure 13.14a–c illustrates the BS configurations enabling CoMP based on analog RF-over-fiber (a), digitized RF-over-fiber based on bandpass sampling (b), and digitized IF-over-fiber with OBSAI/CPRI interfaces (c). Although analog RoF suffers from nonlinear effects of the optical link and lacks control and management capability, the direct transmission of the analog RF signals over optical links without any processing (Fig. 13.14a) is still the simplest scheme for transporting wireless signals. This approach leads to a simple base station design which only requires optical-to-electrical conversion and RF amplification while enabling centralized control and management of the wireless signals. However, to support MIMO transmission in 4G mobile technologies, a subcarrier multiplexing technique is used, where MIMO signals at the same RF frequency are down-converted to

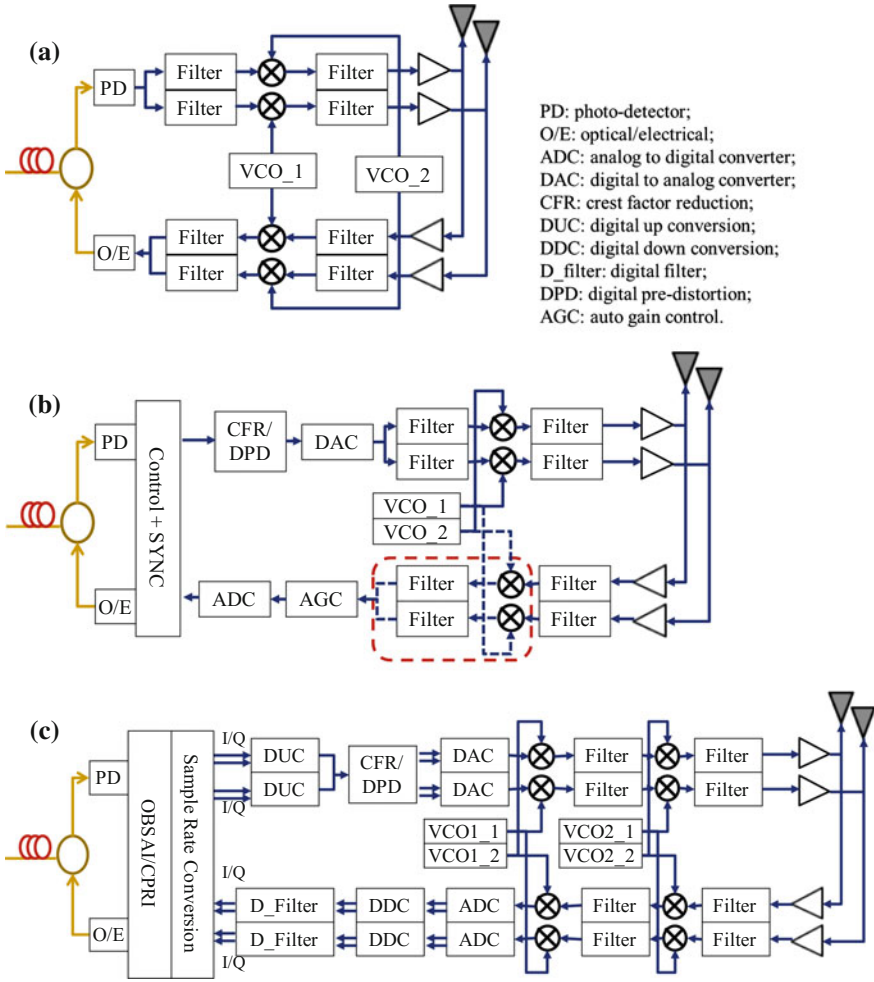


Fig. 13.14 BS configurations

different IF frequencies before modulating the same laser source. Additional electronics functions such as mixer, local oscillator, and filter are also necessary.

Figure 13.14c shows the BS configuration using digitized IF-over-fiber. The configuration is based on super-heterodyne RF receiver and simply keeps the radio functions of a traditional BS with additional processing implementing the OBSAI/CPRI interface. The following functions are performed in such BS: (1) antenna interface, RF combining, RF filtering; (2) power amplification; (3) two stages of frequency up-/down-conversion; (4) D/A and A/D conversion with auto-gain control; (5) carrier selection; (6) digital predistortion; (7) OFDM peak power reduction; (8) control and management; (9) optical interface. To support

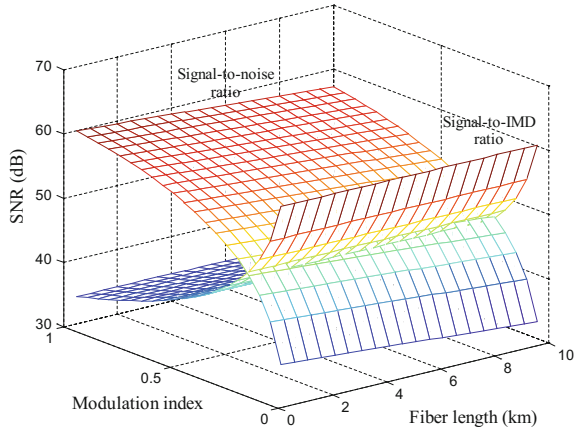
MIMO transmission, most of these functions must be performed in parallel for each MIMO signal.

To further simplify the BS, digitized RF-over-fiber based on bandpass sampling using low-IF architecture with minimal amount of digital signal processing is also proposed (Fig. 13.14b (without red dashed box)). In the uplink, the RF signal is down-converted and digitized at the same time by the bandpass ADC after amplification and filtering. The ADC will first transfer the radio signal from RF to the desired IF frequency according to the sampling rate and then digitize the IF frequency signal. In the control and management block, the quantized samples are coded and sent with control/sync overhead to the central office. Reverse functions are performed for downlink transmission. Parameters such as VCO control voltage, ADC/DAC sampling rate, amplification gain are remotely controlled by the CO via the downlink transmission. One stage of frequency conversion is employed in downlink, since the conversion efficiency from IF to RF using bandpass sampling is not sufficient. With the second frequency conversion removed, frequency conversion between IF and baseband takes place in the central office in the digital domain. For MIMO signals at a same frequency, either multiple AD/DA converters or frequency mixing (red dashed box) are necessary for signal separation. In the former configuration, signals received from different MIMO antennas are digitized using separate ADCs and combined digitally before sending to the central office. The latter approach converts the MIMO signals to different IF frequencies without overlapping and digitizes them by a single ADC with a higher sampling rate.

### 13.4.2 Performance Analysis

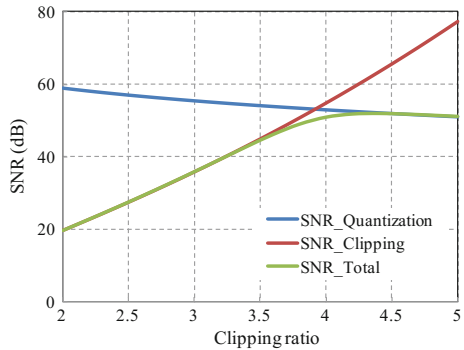
It is well established that in a wireless access network with a multi-carrier environment, linearity plays an important role in the achievable system dynamic range. It has been shown that the nonlinearity of the optical frontend in a fiber distributed wireless network limits the overall system dynamic range. In analog RoF systems, the nonlinearity is mainly contributed by third-order inter-modulation (IMD) of the optical frontend. Given an analog RoF link, the level of IMD varies with the modulation depth. Another factor limiting the performance of an analog RoF link is the receiver noise, including photodiode thermal noise, shot noise and TIA, and post-amplifier noise. Figure 13.15 shows the SNR and signal-to-IMD ratio varying with the modulation depth and transmission distance, in a direct-modulation RoF link. The signal-to-IMD ratio becomes worse, while the SNR improves with modulation depth; the signal-to-IMD ratio is independent of the transmission distance, while the SNR decreases with fiber length. The interplay between these two factors restrains the modulation depth to a certain range and limits the transmission distance of an analog RoF link. To ensure a sufficient SNR (above 40 dB), modulation depth should be around 0.3 and the fiber length should be limited to within a few kms. In external-modulation RoF systems, similar results can be obtained.

**Fig. 13.15** Performance estimation of analog RoF link



Digital optical links have much better performance in terms of nonlinear effects and noise tolerance. In digitized IF/RF-over-fiber systems, as digital data are transmitted and used to reconstruct the analog signal, it lowers the SNR requirement on the optical link and removes the constraints on modulation depth and fiber length. In such systems, the dominant noise arises from the AD/DA conversion process determined by the effective number of bits (ENOB). On the other hand, as the ADC has a limited range, in order to handle 4G wireless signals with high PAPR (peak-to-average-power ratio), clipping is necessary and clipping noise is inevitable. A clipping ratio  $\gamma$  is normally defined as  $A_{\text{clipping}}/\sigma$ , where  $A_{\text{clipping}}$  is equal to the full scale of the ADC and  $\sigma^2$  is the variance of the wireless signal. The noise introduced by clipping can be calculated using the power of the clipped portion of the wireless signal. The signal-to-clipping-noise ratio ( $\text{SNR}_C$ ) and ADC noise ( $\text{SNR}_{\text{ADC}}$ ) are shown in Eq. 13.1.  $\text{SNR}_C$  increases with the clipping ratio, while  $\text{SNR}_{\text{ADC}}$  decreases with it. An optimum clipping ratio exists for a certain ADC. Figure 13.16 shows SNR versus clipping ratio when ENOB is 10 bits, and the optimum clipping ratio is 4.3.

**Fig. 13.16** Performance estimation of digitized RoF link



$$\text{SNR}_c = \sqrt{\frac{8}{\pi}} \gamma^3 e^{\gamma^2/2} \quad \text{SNR}_{\text{ADC}} = \frac{3 \cdot 2^{2n}}{\gamma^2} \quad (13.1)$$

In digitized RoF systems based on bandpass sampling, spectral aliasing introduces additional aliasing noise. The SNR of the bandpass-sampled signal is poorer compared to the conventional sampling system due to noise aliasing from the bands between DC and the passband. Under the assumption that the introduced thermal noise in a sampling device is an additive white Gaussian noise (AWGN) with zero mean, the power spectral density (PSD) of the aliasing noise is  $M$  times the thermal noise, where  $M$  is the number of Nyquist regions between DC and the passband. Another issue with bandpass sampling is the imperfect frequency response. In the digitized RF-over-fiber systems, frequency conversion is realized by selecting the appropriate images from a particular Nyquist region of the sampled signal. The amplitude in each Nyquist region is very different and is shaped by a sinc function response. After bandpass sampling, we choose the signal at the first Nyquist region to realize frequency down-conversion. The RF signal is not only relocated to the lower frequency, but also filtered by an equivalent lowpass filter governed by the sinc function. Due to the uneven frequency response of the lowpass filter, the signal is shaped and distorted. A frequency domain equalizer may be needed to compensate for this signal distortion.

### 13.4.3 Implementation of CoMP

In this architecture (Fig. 13.13), the signal from the cell-edge user is sent to the CO via two neighboring BSs. At the CO, two “copies” of the signal are received after being transmitted through two different channels (each channel comprises a wireless link and an optical link). Channel estimation is performed after FFT for each channel. To facilitate channel estimation, reference OFDM symbols are embedded in the transmitted signal. After channel estimation, linear combination of the two “copies” with different weights will yield a single output signal. The key issue is to determine the proper weights to be used to determine the output signal. With the knowledge of the channel gains, the weights are adjusted to maximize the effective SNR of the output signal. Note that these weights were updated frequently to accommodate the change of channel conditions. CoMP with joint processing is proposed to improve the channel capacity of cell-edge users only. However, for cell-center users it will not provide significant benefit. Therefore, as the user is moving toward/away from the cell edge, JP-CoMP should be turned on/off according to the achievable capacity improvement for this user. Assuming  $h_{i,1}$  and  $h_{i,2}$  are the complex channel gains via two neighboring BSs and  $N_0$  is the noise power, the information theoretic capacity (in the unit of bits/subcarrier/OFDM symbol) is given by Eq. 13.2. Figure 13.17a, b illustrates the channel capacity improvement by CoMP, when SNR of channel 1 (SNR1) is fixed (5 and 20 dB) and

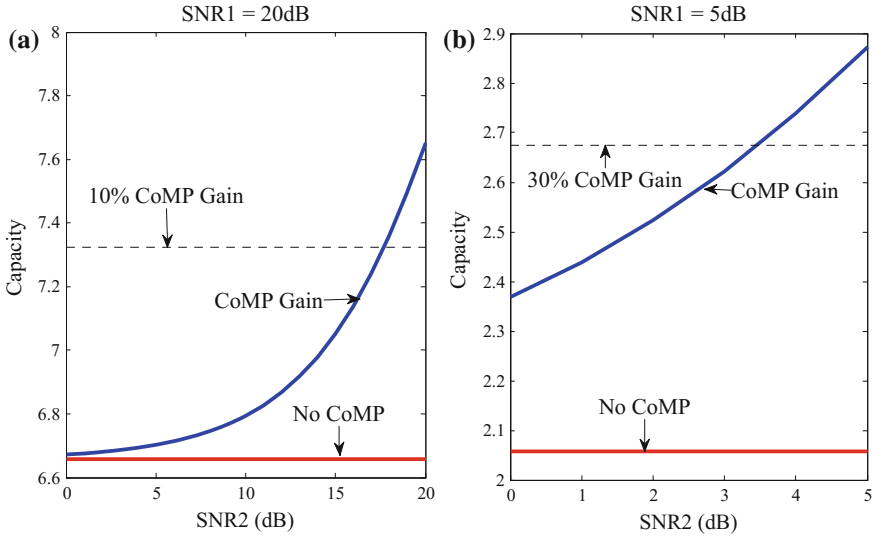


**Fig. 13.17** Capacity improvement by CoMP (**a** SNR1 = 5 dB, **b** SNR1 = 20 dB)

SNR of channel 2 (SNR2) varies between 0 and SNR1. It is shown that (1) large CoMP gain can be achieved when the SNRs of the two channels are comparable; (2) with lower channel SNR, CoMP gain is more significant. In the case where the CoMP gain is not significant (e.g., less than 30 %), CoMP can be disabled to reduce the processing overhead.

$$C(H_{I,1}, H_{I,2}) = \text{LOG}_2 \left( 1 + \frac{|H_{I,1}|^2 + H_{I,2}^2}{N_0} \right) \quad (13.2)$$

### 13.4.4 Experimental Demonstration

The three RoF-based mobile backhaul schemes enabling CoMP have been experimentally demonstrated. An OFDM signal at 2.4 GHz carrier frequency with 100 MHz bandwidth is used to emulate the signal of the cell-edge user. Due to the low antenna gain and space limitation of our laboratory, the distance between the transmitting antenna and the receiving antenna was set to 2 m. The experimental setups of the BSs were in accordance with the configurations in Fig. 13.14.

Figure 13.18a–c shows the error vector magnitude (EVM) performance of analog RoF, digitized IF, and digitized RF technologies, respectively. The solid lines represent the results of CoMP with joint processing, while the dashed lines represent the results of single BS processing. Regardless of whether CoMP is used or not, the performance of analog RoF decreases rapidly as a function of decreasing

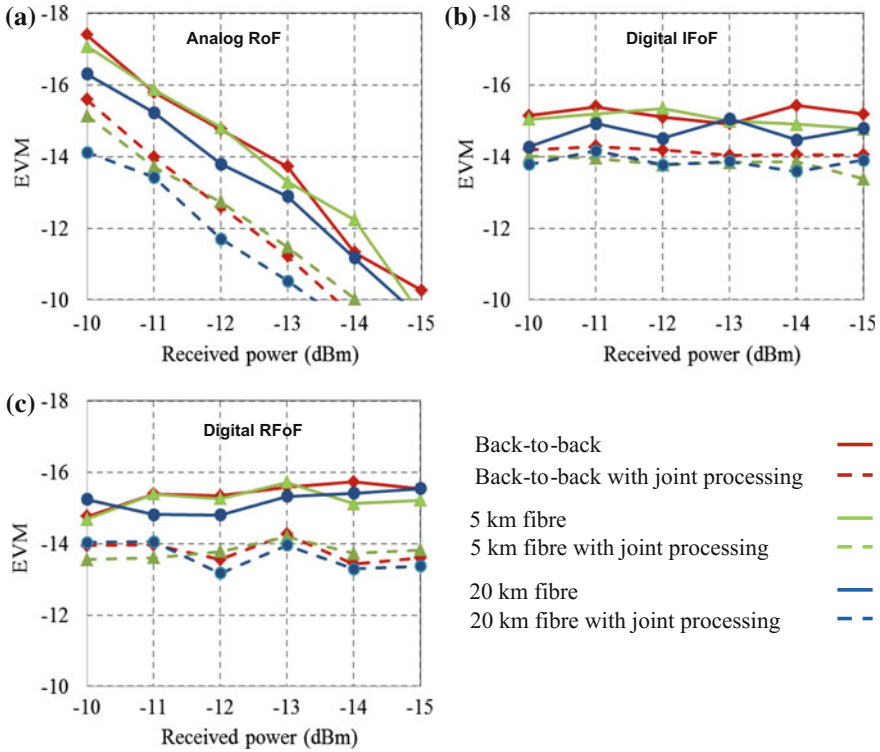


Fig. 13.18 EVM performance of RoF technologies for JP-CoMP

received power; in addition, 1.5-dB EVM deterioration due to chromatic dispersion is observed when the fiber length increases from 0 to 20 km. However, in digitized RF/IF schemes, digital optical transmission ensures that the performance is relatively stable as a function of received power. By using CoMP, an average gain of more than 2 dB can be achieved for all three RoF schemes. Further, the acceptable received power and transmission distance can also be extended for analog RoF schemes because of the improved performance.

### 13.5 Summary

Base stations (BSs) cooperation techniques, also referred to as coordinated multi-point (CoMP) in 3GPP terminology, promise significant performance improvements in future 4G and beyond mobile systems. CoMP allows cell-edge users to simultaneously receive/transmit signals from/to multiple BSs and dramatically improves the channel capacity of cell-edge users in the network. To facilitate coordinated signal processing in CoMP, adjacent BSs are required to

exchange large volumes of information, such as unprocessed I/Q samples before demodulation. Besides key challenges, such as latency and synchronization, a major concern is the demand for additional capacity in the uplink and it is found to limit the performance of inter-site CoMP.

It is predicted that future wireless networks will have to handle data rates on the orders of hundreds of Mbps and beyond where current microwave backhaul will not be able to cope with the growing capacity. High-capacity fiber-optic backhaul has to eventually replace microwave backhaul to overcome this traffic bottleneck and provide the needed capacity. Integrated fiber–wireless networks, also called radio-over-fiber (RoF) networks, have attracted much attention over the past two decades for the development of next-generation mobile backhauls, with a promised centralized control architecture and simple BS configuration. Analog RoF-based hybrid optical-radio architecture has shown its advantage in the backhaul architecture, while digital RoF, with centralized signal processing functionality incorporating digital optical link, has also been studied with demonstrated high flexibility. Further, the Common Public Radio Interface (CPRI) and the Open Base Station Architecture Initiative have standardized the interface between the central baseband module and the remote RF module of the aforementioned digital RoF architecture.

## References

1. GPP TS 36.300, V8.9.0 (2009) Evolved universal terrestrial radio access (EUTRA) and Evolved universal terrestrial radio access network (EUTRAN): overall description
2. Akyildiz IF et al (2010) The evolution to 4G cellular systems: LTE-advanced. *Phys Commun* 3:217–244
3. Irmer R et al (2011) Coordinated multipoint: concepts performance and field trial results. *IEEE Commun Mag* 49(2):102–111
4. Lee D et al (2012) Coordinated multipoint transmission and reception in LTE-advanced: deployment scenarios and operational challenges. *IEEE Commun Mag* 50(2):148–155
5. Jungnickel V et al (2013) Backhaul requirements for inter-site cooperation in heterogeneous LTE-advanced networks. In: *IEEE international conference on communications (ICC)*
6. Sawahashic M et al (2010) Coordinated multipoint transmission/reception techniques for LTE-advanced [Coordinated and Distributed MIMO]. *IEEE Wireless Commun* 17(3)
7. (2008) Next generation mobile networks optimised backhaul requirements. NGMN Alliance
8. Brück S et al (2013) Backhaul requirements for centralized and distributed cooperation techniques
9. Kazovsky L et al (2012) Hybrid optical-wireless access networks. *Proc IEEE* 100(5)
10. Diehm F et al (2010) The FUTON prototype: proof of concept for coordinated multi-point in conjunction with a novel integrated wireless/optical architecture. In: *IEEE wireless communications and networking conference (WCNC)*
11. Shaw W-T et al (2009) An ultra-scalable broadband architecture for municipal hybrid wireless access using optical grid network. In: *Conference on optical fiber communication (OFC)*
12. Wake D et al (2009) A comparison of remote radio head optical transmission technologies for next generation wireless systems. In: *LEOS annual meeting*
13. Mola DD et al (2011) Photonic integrated technologies for optical backhauling. In: *International conference on transparent optical networks (ICTON)*

14. Lim C et al (2010) Fiber-wireless networks and subsystem technologies. *IEEE/OSA J Lightwave Technol (JLT)* 28(4):390–405
15. Wake D et al (2010) Radio over fiber link design for next generation wireless systems. *IEEE/OSA J Lightwave Technol (JLT)* 28(16):2456–2464
16. CPRI specification v4.0 at [www.cpri.info](http://www.cpri.info)
17. OBSAI specification v2.0 at [www.obsai.com](http://www.obsai.com)
18. Santiago C et al (2009) Next generation radio over fiber network management for a distributed antenna system. In: International conference on wireless communication, vehicular technology, information theory and aerospace and electronics systems technology
19. Lometti A et al (2012) Network architectures for CPRI backhauling. In: International conference on transparent optical networks (ICTON)
20. Li H et al (2011) Efficient HetNet implementation using broadband wireless access with fiber-connected massively distributed antennas architecture. *IEEE Wireless Commun* 18(3)
21. Xu X (2011) Imperfect digital-fiber-optic-link-based cooperative distributed antennas with fractional frequency reuse in multicell multiuser networks. *IEEE Trans Veh Technol* 60(9)
22. Yang Y et al (2011) Experimental demonstration of multi-channel hybrid fiber-radio system using digitized RF-over-fiber technique. *IEEE/OSA J Lightwave Technol (JLT)* 29(9):2130–2137
23. Chowdhury et al (2009) Advanced system technologies and field demonstration for in-building optical-wireless network with integrated broadband services. *IEEE/OSA J Lightwave Technol (JLT)* 27(12):1920–1927
24. Vaughan RG et al (1991) The theory of bandpass sampling. *IEEE Trans Signal Process* 39(9):1973–1984
25. Yang Y et al (2012) A full-duplex digitized RoF system for millimeter-wave OFDM transmission. In: ECOC
26. Lim et al (2007) Intermodulation distortion improvement for fiber radio applications incorporating OSSB + C modulation in an optical integrated-access environment. *IEEE/OSA J Lightwave Technol (JLT)* 27(6)
27. Yariv et al (1984) Intermodulation distortion in a directly modulated semiconductor injection laser. *Appl Phys Lett* 1034–1036
28. Mestdagh JG (1993) Effect of amplitude clipping in DMT-ADSL transceivers. *Electron Lett* 29(15)
29. Sun Y (2004) Effects of noise and jitter on algorithms for bandpass sampling in radio receivers. *ISCAS* 1:761–764
30. Diniz PSR (2010) *Digital signal processing: system analysis and design*. Cambridge University Press
31. Yang Y, Lim C, Nirmalathas A (2011) Comparison of energy consumption of integrated optical-wireless access networks. In: OFC
32. Tse D et al (2005) *Fundamentals of wireless communications*. Cambridge University Press
33. Cheng L, Zhu M, Gul MMU, Ma X, Chang G-K (2014) Adaptive photonics-aided coordinated multipoint transmissions for next-generation mobile fronthaul. *IEEE/OSA J Lightwave Technol* 32(10):1907–1914

# Chapter 14

## Converged Wireless Access/Optical Metro Networks in Support of Cloud and Mobile Cloud Services Deploying SDN Principles

**Anna Tzanakaki, Markos Anastasopoulos, Bijan Rofoee, Shuping Peng, George Zervas, Reza Nejabati, Dimitra Simeonidou, Giada Landi, Giacomo Bernini, Roberto Monno, Nicola Ciulli, Gino Carrozzo, Kostas Katsalis, Thanasis Korakis, Leandros Tassiulas, Georgios Dimosthenous, Dora Christofi, Jordi Ferrer Riera, Eduard Escalona, Jacopo Pianigiani, Dirk Van Den Borne and Gert Grammel**

**Abstract** This chapter proposes a next-generation ubiquitous converged infrastructure to support cloud and mobile cloud computing services. The proposed infrastructure facilitates efficient and seamless interconnection of fixed and mobile end users with computational resources through a heterogeneous network integrating optical metro and wireless access networks. To achieve this, a layered architecture which deploys cross-domain virtualization as a key technology is presented. The proposed architecture is well aligned and fully compliant with the Open Networking Foundation (ONF) Software-Defined Networking (SDN) architecture and takes advantage of the associated functionalities and capabilities. A modeling/simulation framework was developed to evaluate the proposed architecture and identify planning and operational methodologies to allow global

---

A. Tzanakaki (✉) · M. Anastasopoulos · B. Rofoee · S. Peng · G. Zervas · R. Nejabati · D. Simeonidou

High Performance Networks Group, University of Bristol, England, UK  
e-mail: anna.tzanakaki@bristol.ac.uk

G. Landi · G. Bernini · R. Monno · N. Ciulli · G. Carrozzo  
Nextworks, Busto Arsizio, Italy

K. Katsalis · T. Korakis · L. Tassiulas  
University of Thessaly, Thessaly, Greece

G. Dimosthenous · D. Christofi  
Primetel, Limassol, Cyprus

J.F. Riera · E. Escalona  
I2CAT, Barcelona, Spain

J. Pianigiani · D. Van Den Borne · G. Grammel  
JUNIPER, California, USA

optimization of the integrated converged infrastructure. A description of the tool and some relevant modeling results are also presented.

## 14.1 Introduction

Big data, Internet of Things, and Content Delivery Services are driving the dramatic increase of the global Internet traffic, which is expected to exceed 1.6 zettabytes by 2018. These new and emerging applications collect, process, and compute massive amounts of data, and require efficient management and processing of very large sets of globally distributed unstructured data. To support these services, the concept of cloud computing, where computing power and data storage are moving away from the end user to remote computing resources, has been introduced. To enable this, there is a clear need for a next-generation ubiquitous converged infrastructure. This infrastructure needs to facilitate the interconnection of data centers (DCs) with fixed and mobile end users.

In this environment, optical network solutions can be deployed to interconnect distributed DCs, as they provide abundant capacity, long reach transmission capabilities, carrier-grade attributes, and energy efficiency [1], while spectrum-efficient wireless access network technologies such as Long Term Evolution (LTE) can be effectively used to provide a variety of services to a large pool of end users. In this context, interconnection of DCs with fixed and mobile end users can be provided through a heterogeneous converged network integrating optical metro and wireless access network technologies.

However, to address limitations and inefficiencies of current optical and wireless network solutions optimized for traditional services, novel approaches that enable cost-efficiency and utilization efficiency through multi-tenancy and exploitation of economies of scale need to be developed. Toward this direction, infrastructure virtualization that allows physical resources to be shared and accessed remotely on demand has been recently proposed as a key enabling technology to overcome the strict requirements in terms of capacity sharing and resource efficiency in cloud and mobile cloud environments. Given the heterogeneous nature of the infrastructures suitable to support cloud and mobile cloud services described above, it is clear that cross-technology and cross-domain virtualization is required. In this context, the introduction of mobile optical virtual network operators (MOVNOs) facilitates the sharing of heterogeneous physical resources among multiple tenants and the introduction of new business models that suit well the nature and characteristics of the Future Internet and that enable new exploitation opportunities for the underlying physical resources.

Existing mobile cloud computing solutions commonly allow mobile devices to access the required resources by accessing a nearby resource-rich cloudlet, rather than relying on a distant “cloud” [2]. In order to satisfy the low-latency requirements of several content-rich mobile cloud computing services, such as high-definition video streaming, online gaming, and real-time language translation [3], one-hop,

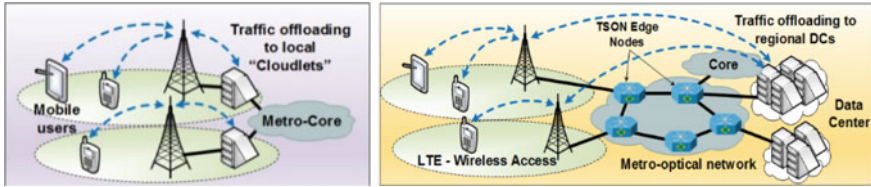


**Fig. 14.1** **a** *Cloudlet* approach: micro-DCs in the wireless access to support mobile cloud traffic and large DCs in the core to support fixed cloud traffic, **b** *CONTENT* proposed approach: shared DC infrastructure fully converged with the broadband wireless access and the metro optical network

high-bandwidth wireless access to the cloudlet is required. In the case where a cloudlet is not available nearby, traffic is offloaded to a distant cloud such as Amazon's Private Cloud, GoGrid [4], or Flexigrid [5]. However, the lack of service differentiation mechanisms for mobile and fixed cloud traffic across the various network segments involved, the varying degrees of latency at each technology domain, and the lack of global optimization tools in the infrastructure management and service provisioning make the current solutions inefficient.

In response to these observations, this chapter is focusing on a next-generation ubiquitous converged network infrastructure [6]. The infrastructure model proposed is based on the Infrastructure as a Service (IaaS) paradigm and aims at providing a technology platform interconnecting geographically distributed computational resources that can support a variety of cloud and mobile cloud services (Fig. 14.1).

The proposed architecture addresses the diverse bandwidth requirements of future cloud services by integrating advanced optical network technologies offering fine (sub-wavelength) switching granularity with a state-of-the-art wireless access network based on hybrid LTE and Wi-Fi technology, supporting end user mobility. However, in these converged cloud computing environments, management and control information needs to be exchanged across multiple and geographically distributed network domains, causing increased service setup and state convergence latencies [7]. Given the complexity of the overall infrastructure, additional challenges that need to be addressed include the high probability of management/control data loss [8], often leading to violation of quality-of-service (QoS) requirements as well as impractical and inefficient collection of control data and management of network elements due to scalability issues [9]. Finally, these are highly dynamic environments where service requests can have big and rapid variations that are not known in advance.

To address the challenge of managing and operating this type of complex heterogeneous infrastructures in an efficient manner, Software-Defined Networking (SDN) and network function virtualization have been recently proposed [10, 11]. In SDN, the control plane is decoupled from the data plane and is moved to a logically centralized controller that has a holistic view of the network. At the same time, to enable sharing of the physical resources the concept of virtualization across heterogeneous technology domains has been recently proposed. Taking advantage

of the SDN concept and the benefits of cross-technology virtualization solutions, we propose and present a converged network infrastructure and architecture able to efficiently and effectively support cloud and mobile cloud services. The benefits of the proposed approach are evaluated through a modeling tool that allows the comparison of the performance of the proposed solution compared to alternative state-of-the-art solutions, extending the work presented in [6]. Our modeling results identify trends and trade-offs relating to resource requirements and energy consumption levels across the various technology domains involved that are directly associated with the services' characteristics.

The remaining of this chapter is structured as follows: Sect. 14.2 describes the relevant state-of-the-art. Section 14.3 provides a functional description together with a detailed structural presentation of the proposed architecture. This includes the details of the individual layers involved as well as a description of the interaction between the different layers. Section 14.4 includes a discussion on the modeling framework that is being developed with the aim to evaluate the architecture and propose optimal ways to plan and operate it, while Sect. 14.5 summarizes the conclusions.

## **14.2 Existing Technology Solutions Supporting Cloud and Mobile Cloud Services**

### ***14.2.1 Physical Infrastructure Solutions Supporting Cloud Services***

#### **14.2.1.1 State of the Art in Metro Optical Network Solutions**

Recent technological advancements in optical networking are able to provide flexible, efficient, ultra-high data rate, and ultra-low-latency communications for DCs and cloud networks. Optical transmission solutions offering high data rate and low latency have been reported as field trial deployments of 400 Gb/s channels [12], while research on 1 Tb/s per channel is already in progress [13, 14]. However, beyond high capacity, optical networks need to address the requirement for fine granularity to enable efficient utilization of network resources both for service providers and end users. Optical orthogonal frequency division multiplexing (OFDM) [15], optical packet switched networks [16], and optical burst switching [17] technologies are examples of providing such fine granularity. These advanced novel optical network technologies offer the flexibility and elasticity required by the diverse, dynamic and uncertain cloud and mobile cloud services.

Time Shared Optical Networks (TSON) is a dynamic and bandwidth-flexible sub-lambda networking solution that has been introduced to enable efficient and flexible optical communications by time-multiplexing several sub-wavelength connections in a WDM-based optical network [17]. TSON allocates time slices over

wavelengths to satisfy the bandwidth requirements of each request, and statistically multiplexes them exploiting each wavelength channel capacity to carry data for as many requests as possible. In TSON, the electronic processing and burst generation is performed at the edge of the network, and the data of several users are transferred transparently in the core between TSON edge nodes in the form of optical bursts. The proposed infrastructure deploys TSON as it can be used to efficiently interconnect wireless networks with datacenters exploiting its fine granularity to accommodate the granularity mismatch inherent between the wireless and optical network domains.

### **14.2.1.2 State of the Art in Wireless Technologies Solutions**

High-speed wireless access connectivity is provided by three prominent technologies: cellular LTE networks, WiMAX, and Wi-Fi. These technologies vary across a number of distinct dimensions [18], including spectrum, antenna characteristics, encoding at the physical layer, sharing of the available spectrum by multiple users, as well as maximum bit rate and reach. Femtocells appear to be a promising solution as they allow frequent spectrum reuse over smaller geographical regions with easy access to the network backbone. On the other hand, Wi-Fi networks are readily available and are easy to install and manage [19]. In this study, the proposed architecture relies on a converged 802.11 and 4G—Long Term Evolution (LTE) access network used to support cloud computing services.

## ***14.2.2 Infrastructure Management***

Heterogeneous infrastructure management has been already addressed by several research projects and commercial systems. Traditionally, infrastructure management is vertically separated, i.e., each technological segment has its own management system. Thus, the management of the different essential operation components (e.g., policies, processes, or equipment) was performed in a per-domain basis. As such, there are clearly differentiated network management systems and cloud management systems.

Network management has been addressed following two approaches depending on the context and requirements of the network owners. On the one hand, centralized management assumes the existence of a single system that controls the entire network of elements, each of them running a local management agent. On the other hand, distributed management approaches introduce the concept of management hierarchies, where the central manager delegates part of the management load among different managers, each responsible for a segment of the network.

Most of the network infrastructure management systems are proprietary, since there are no common interfaces at the physical level. Each management solution depends on each equipment vendor. However, ISO Telecommunications

Management Network defines the Fault, Configuration, Accounting, Performance, Security (FCAPS) model [20], composed of fault, configuration, accounting, performance monitoring/management, and security components, which is the global model and framework for network management. Apart from the general network management model in [20], there are some standard network management protocols. Most relevant are the SNMP and NetCONF. SNMP is standardized by the IETF in RFCs 1157, 3416, and 3414. NetCONF is also an IETF network management protocol defined in RFC 4741 and revised later in RFC 6241. Its specifications mainly provide mechanisms to install, handle, and delete network device configurations. However, as the network grows, SNMP-based solutions that have limited instruction set space and rely on the connectionless UDP protocol, are inefficient. In the proposed cloud computing systems, information needs to be exchanged across multiple, heterogeneous, and geographically distributed network domains, causing increased service setup and state convergence latencies. At the same time, in such highly complex environments the probability that management/control data are lost is high, leading often to violation of quality-of-service (QoS) requirements. These challenges introduce a clear need for alternative management solutions.

To address these challenges in an efficient manner and also support multi-tenancy requirements inherent in cloud infrastructures, optical network virtualization becomes a key technology that enables network operators to generate multiple coexisting but isolated virtual optical networks (VONs) running over the same physical infrastructure (PI) [21]. Optical network virtualization in general adopts the concepts of abstraction, partitioning, and aggregation over node and link resources to realize a logical representation of network(s) over the physical resources [22]. Virtualization of optical networks is one of the main enablers for deploying software-defined infrastructures and networks in which, independently of the underlying technologies, operators can provide a vast array of innovative services and applications with a lower cost to the end users. Network management solutions focusing on optical network resources include the EU project GEYSERS (<https://www.geysers.eu>) which introduced the Logical Infrastructure Composition Layer (LICL) [23]. The LICL is a software middleware responsible for the planning and allocation of virtual infrastructures (VIs) composed of virtualized network and IT resources.

On the other hand, IT/server virtualization has reached its commercial stage, e.g., VMWare vSphere. In order to better serve the dynamic requirements that arise from the IT/data center side, coordinated virtualization of both optical network and IT resources in the data centers is desired. Joint allocation of the two types of resources to achieve optimal end-to-end infrastructure services has been investigated in the literature, but the reported work concentrates mostly on optical infrastructures supporting wavelength switching granularity [1, 24]. However, solutions addressing optical network technologies supporting sub-wavelength granularity, such as the CONTENT proposed approach [6], are still in their early stages.

In wireless networks, significant management challenges exist because of the system complexity and a number of inter-dependent factors that affect the wireless

network behavior. These factors include traffic flows, network topologies, network protocols, hardware, software, and most importantly, the interactions among them [25]. In addition, due to the high variability and dependency on environmental conditions, how to effectively obtain and incorporate wireless interference into network management remains an open problem. Similar to the optical domain, multi-tenancy in wireless networks can be provided through virtualization. Virtualization and slicing in the wireless domain can take place in the physical layer, data link layer (with virtual Mac addressing schemes and open-source driver manipulation), or network layer (VLAN, VPN, label switching). In [26], the SplitAP architecture is proposed in order for a single wireless access point to emulate multiple virtual access points. Clients from different networks associate corresponding virtual access points (APs) through the use of the same underlying hardware. The approach of creating multiple virtual wireless networks through one physical wireless LAN interface, so that each virtual machine has its own wireless network, is proposed in [27]. In [28], the CellSlice is proposed, focusing on deployments with shared-spectrum RAN sharing. The design of CellSlice is oblivious to a particular cellular technology and is equally applicable to LTE, LTE-Advanced, and WiMAX. CellSlice adopts the design of NVS for the downlink but indirectly constrains the uplink scheduler's decisions using a simple feedback-based adaptation algorithm.

The decoupling of the control from the data plane, supported through the emergence of the SDN paradigm, introduces the need for unified southbound interfaces and thus an abstraction layer that in turn helps to simplify network operation and management. In this context, suitable frameworks have been developed including OpenNaaS (<http://www.opennaas.org>) that provides a common lightweight abstracted model at the infrastructure level enabling vendor-independent resource management. Similarly, the OpenDaylight (<http://opendaylight.org>) platform aims at providing a software abstraction layer of the infrastructure resources that allows geographically distributed network domains to be unified and operated as a single network [29].

Management of IT resources in the context of a converged network/IT infrastructure is commonly performed using modern platforms based on web services (e.g., REST APIs). A typical example is the Open Grid Forum (OGF) Open Cloud Computing Interface (OCCI) [30], which comprises a set of open community-led specifications delivered through the OGF. Well-known cloud management system (CMS) implementations of OCCI-compliant application programming interfaces (APIs) include OpenStack, OpenNebula, and CloudStack.

### ***14.2.3 Service Provisioning***

The service provisioning and orchestration of IT resources (computing and storage) located in geographically distributed DCs, seamlessly integrated with inter-DC networking in support of a variety of cloud services, has been addressed in several

European projects. A number of technical solutions have been investigated and proposed for a variety of scenarios spanning from multi-layer architectures enabling the inter-cooperation between cloud and network domains, up to procedures, protocols, and interfaces allowing integrated workflows to support delivery and operation of joint cloud and network services.

The FP7 GEYSERS project has developed a framework for on-demand provisioning of inter-DC connectivity services, specialized for cloud requirements, over virtual optical infrastructures [1]. Following similar inter-layer approaches, some IETF drafts [31] have proposed cross-stratum solutions for the cooperation between application (service) and network layers in path computation for inter-DC network services, potentially combined with stateful path computation element (PCE) mechanisms [32]. Other relevant research efforts include the FP7 projects SAIL and BonFIRE.

In terms of infrastructure service provisioning, following the Network as a Service (NaaS) paradigm, the OpenNaaS framework has been recently proposed. It is an open-source framework that provides tools to manage the different resources present in any network infrastructure (including virtual infrastructures). The tools enable different stakeholders to contribute and benefit from a common software-oriented stack for both applications and services. Currently, OpenNaaS supports on demand both network and cloud service provisioning.

Emerging cloud applications such as real-time data backup, remote desktop, server clustering, etc., require more traffic being delivered between DCs. Ethernet remains the most used technology in the DC domain, but the end-to-end provisioning of Ethernet services between remote DC nodes poses a big challenge. Central to this capability is the SDN-based service and network orchestration layer [33]. This layer (a) is aware of the existing background and existing practices and (b) applies new SDN principles to enable cost reduction, innovation, and reduced time-to-market of new services, while covering multi-domain and multi-technology path—packet networks. This layer provides a network-wide, centralized orchestration. This high level, logically centralized entity exists on top of and across the different network domains and is able to drive the provisioning (and recovery) of connectivity across heterogeneous networks, dynamically and in real time.

## 14.3 Proposed Converged Network Architecture

### 14.3.1 *Vision and Architectural Approach*

As already discussed in the introduction, the infrastructure model proposed in this chapter is based on the IaaS paradigm. To support the IaaS paradigm, physical resource virtualization plays a key role and is enabled by using a cross-domain infrastructure management layer in the proposed architectural structure. Connectivity services are provided over the virtual infrastructure slices, created by

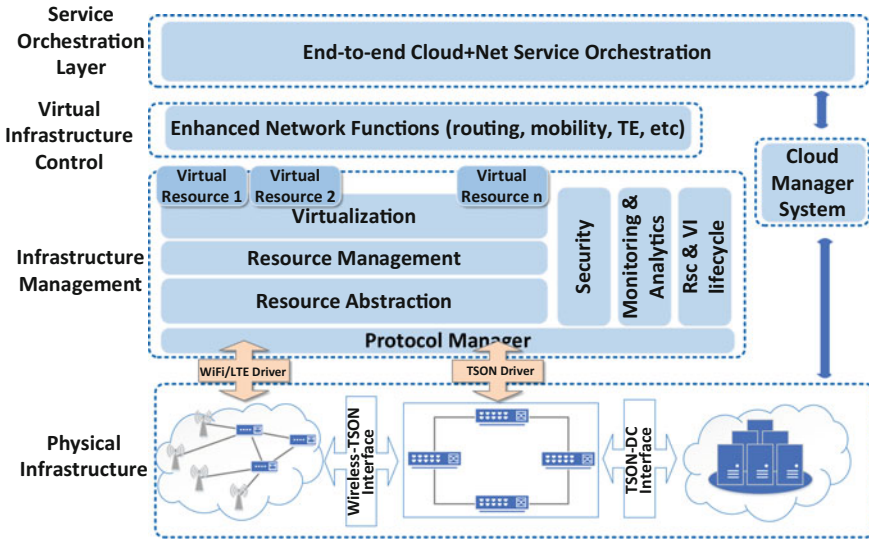


Fig. 14.2 Overall cross-domain, cross-layer architecture

the infrastructure management layer, through the virtual infrastructure control layer. Integrated end-to-end network, cloud, and mobile cloud services are orchestrated and provisioned through the service orchestration layer. The details of the proposed cross-domain, cross-layer architecture are discussed in Fig. 14.2.

The **physical infrastructure layer (PIL)** comprises an optical metro network and a hybrid Wi-Fi/LTE wireless access system. The optical metro network supports frame-based sub-wavelength switching granularity and is used to interconnect geographically distributed DCs.

The **infrastructure management layer (IML)** is responsible for the management of the network infrastructure and the creation of virtual network infrastructures over the underlying physical resources. This involves several functions, including resource representation, abstraction, management, and virtualization across the heterogeneous TSON and the wireless access network domains. An important feature of the functionalities supported is orchestrated abstraction of resources across domains, involving information exchange and coordination across domains. The IML functional architecture can be mapped over the SDN architecture as defined by the ONF. The IML comprises mainly the infrastructure segment of the SDN architecture and the associated management.

The **virtual infrastructure control layer (VICL)** is responsible to provision IT and (mobile) connectivity services in the cloud and network domains, respectively. The VICL is structured in two main levels of functionality. The lower-layer functions, implemented within one or more SDN controllers, deal with the details of each technology deployed at the data plane in the wireless access and TSON-based metro network segments, as exposed in the associated virtual resources through the

IML. These functions provide elementary services with a per-domain scope and are specialized to operate on top of specific (virtual) technologies. On top of the basic services offered by the SDN controller(s), further enhanced functionalities are developed in order to operate the entire heterogeneous infrastructure in a unified manner. These functions manage more abstracted entities (e.g., “per-domain TSON paths”) that summarize the results of the configuration actions performed by the lower-level functions directly on the virtual resources. The VICL architecture is fully compliant with the SDN architecture defined by the ONF.

The *service orchestration layer (SOL)* is responsible for the converged orchestration of cloud and network services, with the automated and cloud-aware setup and adjustment of the user-to-DC and inter-DC network connectivity. Furthermore, it is used for the composition and delivery of multi-tenant chains of virtualized network functions from a service provider’s perspective.

The proposed architecture is fully compliant with the SDN architecture defined by the ONF shown in Fig. 14.3. As it can be seen, the ONF architecture is structured in a data plane, a controller plane, and an application plane together with a transversal management plane. More detailed discussion on the commonalities of the two architectures is provided in Sects. 14.3 and 14.4 that follow.

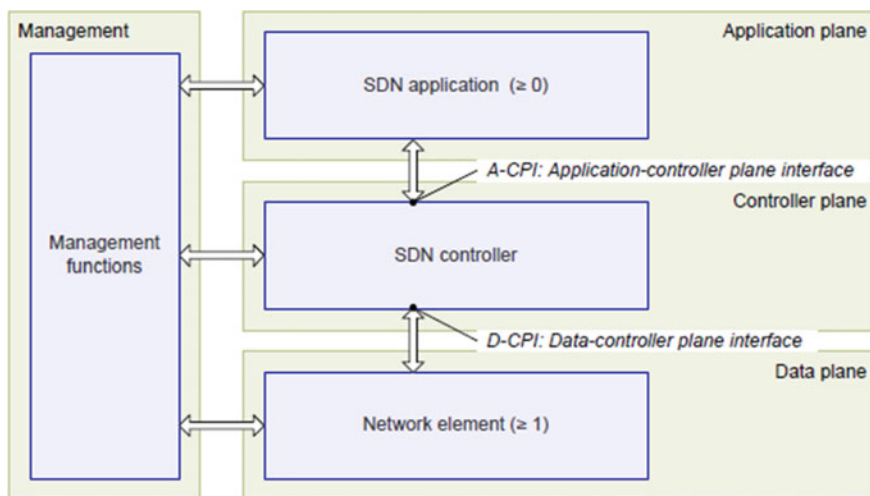


Fig. 14.3 SDN architecture defined by ONF

### 14.3.2 Physical Infrastructure Layer

#### 14.3.2.1 Optical Physical Infrastructure

The optical metro network solution adopted supports frame-based sub-wavelength switching granularity and implements time-multiplexing of traffic flows, offering dynamic connectivity with fine granularity of bandwidth in a connectionless manner [17]. This technology can efficiently support connectivity between the wireless access and DC domains by providing flexible rates and a virtualization-friendly transport technology. It can also facilitate the seamless integration of wireless and IT resources to support a converged infrastructure able to provide end-to-end virtual infrastructure delivery.

A typical scenario of an optical network interconnecting the wireless access with distributed DCs is shown in Fig. 14.4. The optical network comprises FPGA platforms (to receive the ingress traffic and convert it into optical bursts), and 10-ns optical switches (to route them within the TSON core to the final destination all-optically). The routing at each node is performed using the allocation information displayed as matrices on top of each link.

The operational architecture of the optical nodes follows the generic approach presented in [34] and can be structured in three layers. The optical network data plane consists of FPGA nodes for high-speed data processing in rates of 10 Gb/s/λ. Ethernet traffic from the client sides in the wireless network and in the data centers is the ingress traffic to the optical network. At the optical network edge, this tributary traffic is processed and converted into optical bursts, which are then sent to fast switches and, from there, they are routed all optically to the destination nodes. The optical network uses 10GE SFP+ modules, and, by using extended FPGA features, the edge nodes can process any combination of Ethernet header information including MAC address and VLAN IDs.

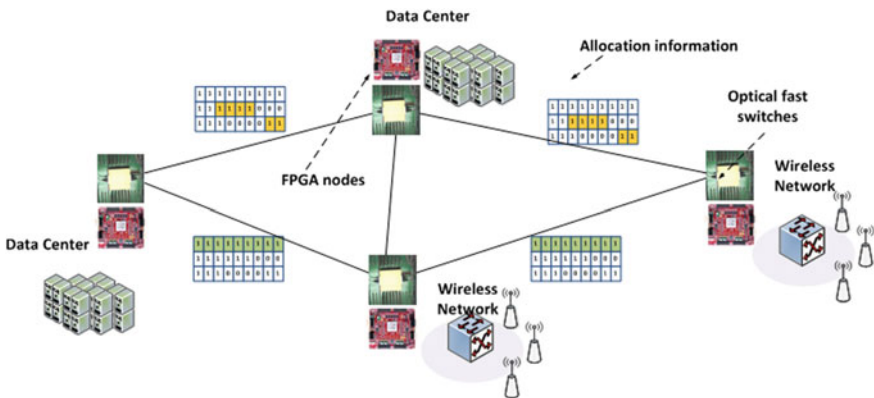


Fig. 14.4 Optical network interconnecting DC and wireless access networks

### 14.3.2.2 Wireless Physical Infrastructure

The wireless network consists of a hybrid IEEE 802.11 and LTE network and a wired backhaul OpenFlow-enabled packet core network that will interact with the optical domain through a Wireless Domain Gateway. A high-level overview of the wireless network architecture is presented in Fig. 14.5. In this work, the LTE network utilizes a commercially available EPC solution and an Orbit Management Framework (OMF) Aggregate Manager service that enables control of the LTE femtocells and the EPC network.

### 14.3.2.3 Integrated Infrastructure

The integration of the two physical infrastructures creates a datapath across multiple technology domains including DC, optical, and wireless access networks (Fig. 14.6). The wireless network is equipped with OpenFlow-based backhaul switches which can apply policies to the ingress traffic and redirect them to different access points. Wi-Fi and LTE access points are available in the test bed and provide connectivity to the end users.

The horizontal connectivity between the different technologies is based on the Ethernet protocol and uses MAC addressing, VLAN IDs, and also specific priority bits [35]. For instance, in a simple case VLAN IDs can be identified end-to-end when transporting different flows across the optical and wireless backhaul. When more complicated grooming is the objective, the optical network can classify and transport traffic based on a set of Ethernet bits, and the traffic on the wireless side

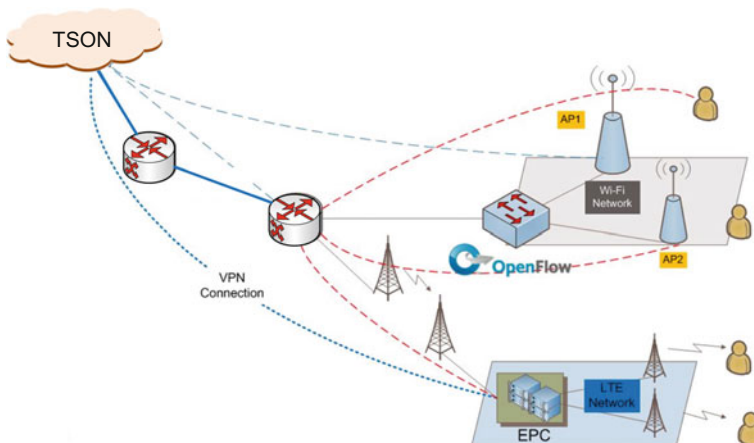


**Fig. 14.5** Wireless access network. The OMF aggregate manager service is running at a dedicated server for each AP

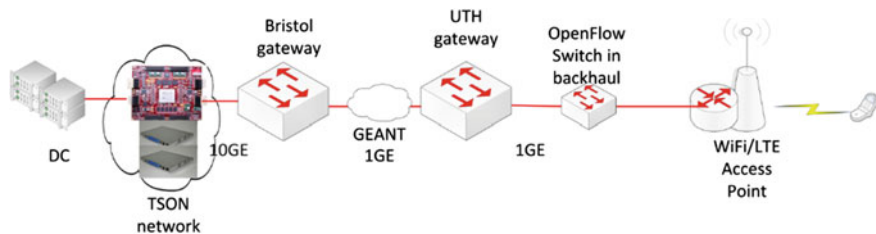


**Fig. 14.6** Integrated physical infrastructures with end-to-end datapath

can apply its own forwarding policies using, e.g., OpenFlow layer 2 on either the downlink or uplink.

### 14.3.3 Infrastructure Management

The IML is devoted to the converged management of resources of the different technology domains and is responsible for the creation of isolated virtual infrastructures composed of resources from those network domains.

The overall IML architecture is shown in Fig. 14.7. The bottom part of the IML contains the components (i.e., drivers) that are responsible for retrieving information and communicating with each one of the domains. Once the information has been acquired, the resources are abstracted and virtualized. Virtualization is the key functionality of the infrastructure management layer. This layer of the architecture provides a cross-domain and cross-technology virtualization solution, which allows the creation and operation of infrastructure slices including subsets of the network connected to the different computational resources providing cloud services. From the architectural and functional perspective, the design of the IML is capable of covering and addressing the set of specific requirements identified for physical resource management and virtualization.

The IML functional architecture can be mapped over the SDN architecture defined by the ONF as depicted in Fig. 14.8. The IML comprises mainly the infrastructure segment of the SDN architecture and the associated management. The virtual slices created by the IML are seen as actual network elements by the corresponding controller deployed on top of the IML. The IML is also responsible for composing the virtual resources created and offering them as isolated virtual infrastructures. The virtual resources will hold operational interfaces, which will be used by the VICL in order to configure and provision dynamic connectivity services.

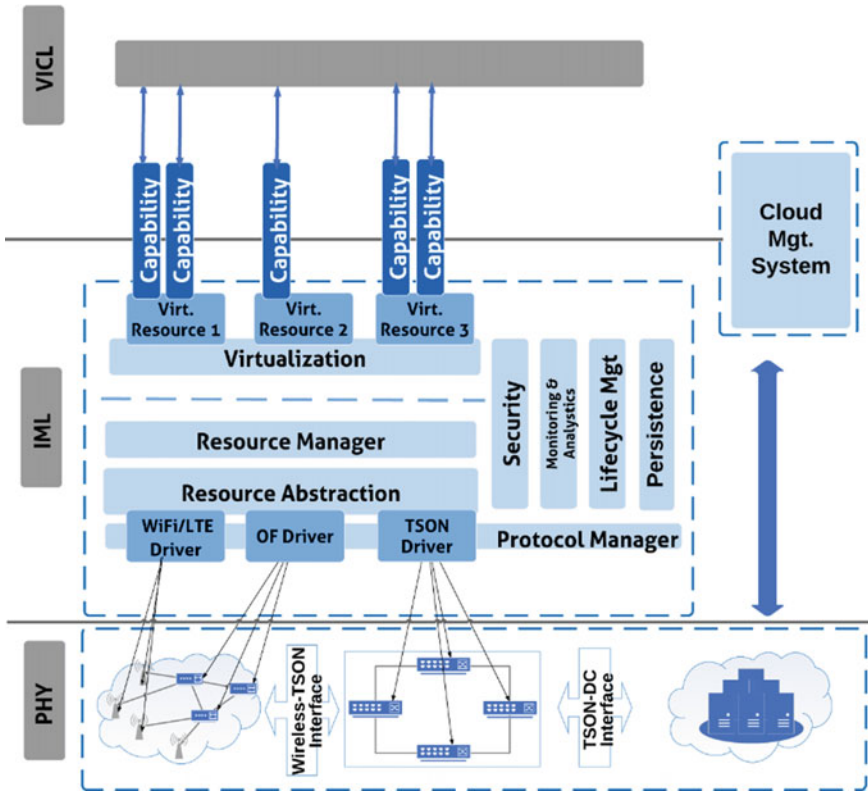


Fig. 14.7 IML overall architecture

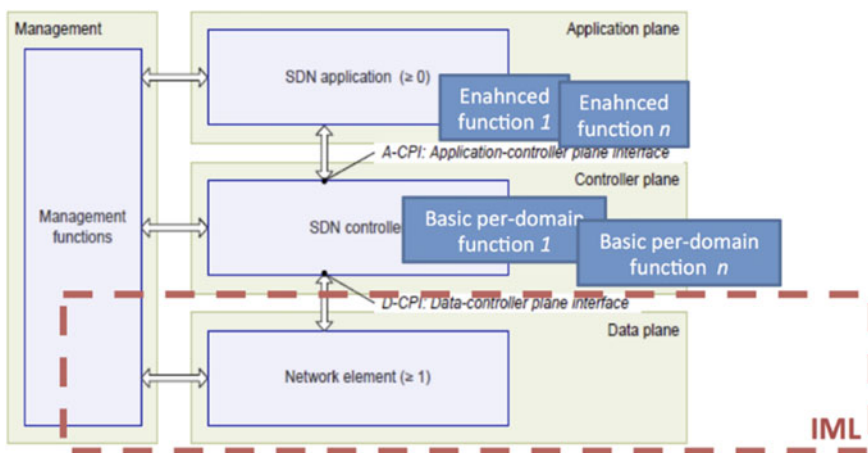


Fig. 14.8 IML mapping over the SDN ONF architecture

### 14.3.4 Virtual Infrastructure Control Layer

The architecture design of the VICL is structured in two main levels of functionalities, as shown in Fig. 14.9. Lower-layer functions, implemented within one or more SDN controllers, deal with the details of each technology deployed at the data plane in the wireless access and optical metro network segments, as exposed in the associated virtual resources through the IML. These functions provide elementary services with a per-domain scope and are specialized to operate on top of specific (virtual) technologies: radio, L2 wireless backhaul, and optical virtual resources. On top of the basic services offered by the SDN controller(s), further enhanced functionalities are developed in order to operate the entire heterogeneous infrastructure in a unified manner, without dealing with the specific constraints of the virtual resources exposed by the IML. These functions manage more abstracted entities (e.g., “per-domain TSON paths”) that summarize the results of the configuration actions performed by the lower-level functions directly on the virtual resources. Some examples of enhanced functions are the provisioning of end-to-end, multi-domain connectivity crossing wireless and metro domains or the re-optimization of this connectivity based on current traffic load and characteristics of the cloud services running on top. The cooperation of these enhanced functions allows MOVNOs to operate efficiently their entire infrastructures and dynamically establish the connectivity between users and DCs, or between DCs, that is required

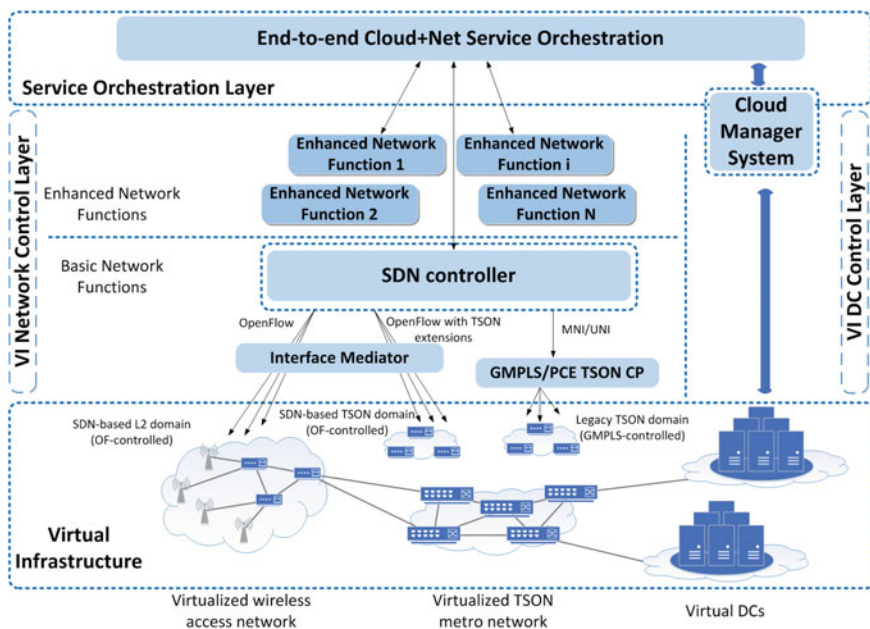
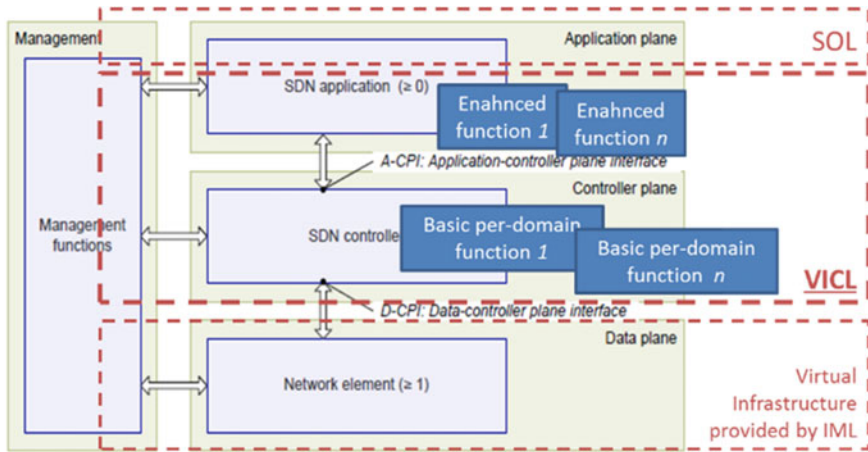


Fig. 14.9 High-level architecture of virtual infrastructure control layer



**Fig. 14.10** Mapping between the proposed VICL architecture and SDN architecture defined by ONF

to properly execute and access the cloud applications running on the distributed IT resources at the virtual DCs.

The VICL architecture is fully compliant with the SDN architecture defined by the ONF shown in Fig. 14.3. Following the VICL perspective, the data plane corresponds to the virtual infrastructure exposed by the IML, the SDN controller offers the basic per-domain functions, while the enhanced application for provisioning and optimization of cloud-aware multi-domain connectivity operates at the application plane (Fig. 14.10).

Here, a single SDN controller is deployed to control the whole infrastructure, with specific plug-ins for the different virtual technologies. A unified resource control layer is responsible to create an abstracted internal information model, properly extended to cover the technological heterogeneity of the virtual infrastructure. However, the MOVNO may decide to deploy the VICL following a distributed approach, with different SDN controllers dedicated to each single technology domain and an upper layer SDN controller implementing the cross-domain enhanced functions. Other applications may run on top of this controller in order to manage the interaction with the cloud environments.

This model is compliant with the recursive hierarchical distribution of SDN controller defined by ONF (Fig. 14.11), with two levels of controllers. On the lower side, the “child” controllers are able to manage the specific granularity of each technology and have a geographical scope limited to the topology of the wireless access or metro domains. On the upper side, the “parent” controller operates on more abstracted resources, as exposed by the child controllers, but with a wider geographical scope, managing the entire virtual infrastructure (Fig. 14.12).

The ONF architecture defines two main interfaces, the Application-Controller Plane Interface (A-CPI) and the Data-Controller Plane Interface (D-CPI). In the

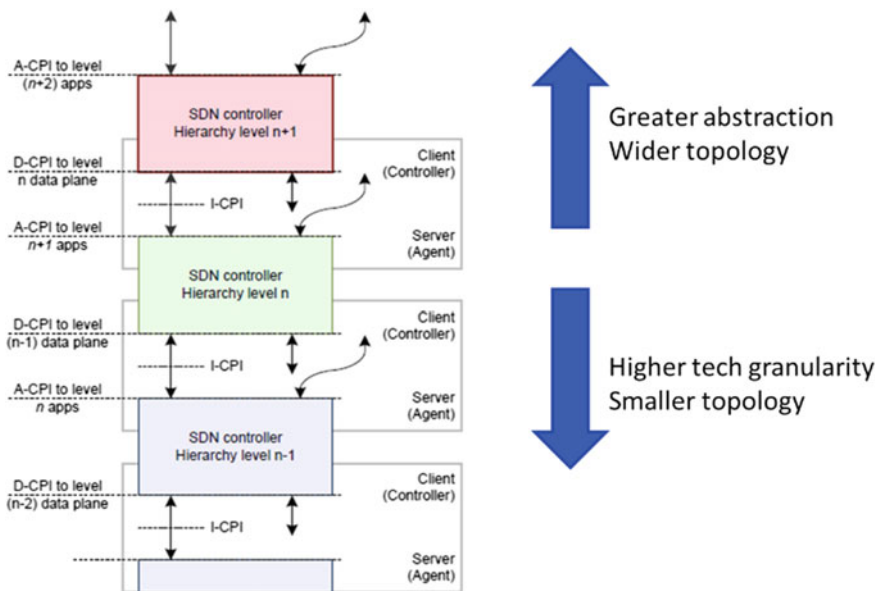


Fig. 14.11 Recursive hierarchical distribution of SDN controller, as defined by ONF

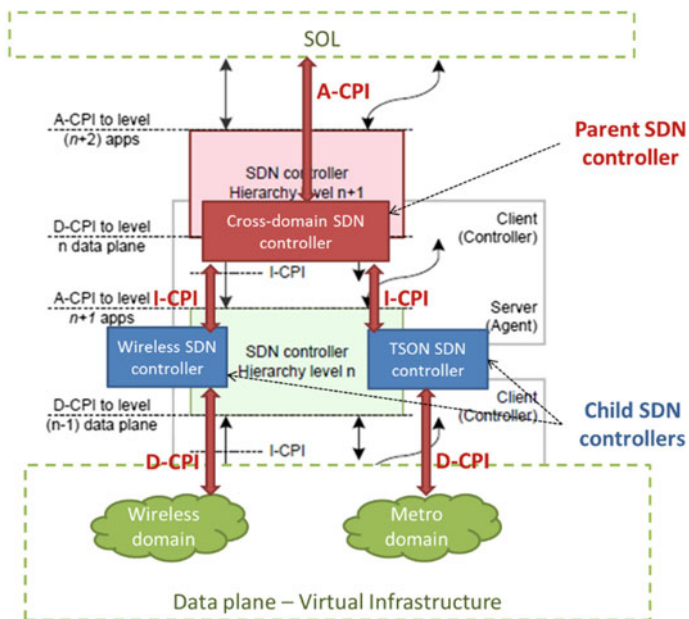


Fig. 14.12 Mapping of VICL distributed deployment model with the recursive hierarchical distribution of SDN controllers defined by ONF

proposed architecture, the D-CPI corresponds to the interface between the IML and the VICL and provides all the functionalities related to discovery, configuration, and monitoring of the virtual resources belonging to the virtual infrastructure under control of a given SDN controller (of the lower layer) deployed in the VICL. The protocol adopted at this interface is OpenFlow for the operation of layer 2 resources and an extended version of OpenFlow for the operation of optical resources. The extensions introduced in OpenFlow allow handling the specific granularity and characteristics of optical resources, through modeling of wavelengths and the related time slots available for each port. Similar extensions could not be adopted in the OF protocol in the case of wireless resources, since real-time response to channel configuration request is not feasible, in terms of acceptable time, in reaction to packet-in events. Thus, in the wireless domain, the OF protocol is used for the operation of OF systems (e.g., Open vSwitch (OVS) instances in the access points and the backhaul network) and Representational State Transfer (REST)-based management interfaces for the management and control of other types of resources.

The A-CPI is considered at two different levels. The former is the interface between the SDN controller providing the elementary per-domain functionalities and the cross-domain applications running on top of that for the operation of the entire infrastructure. A second level of A-CPI is the interface between the entire VICL and the SOL, responsible for the management of the end-to-end cloud services. It should be noted that, from the SOL perspective, the actual deployment of the VICL is completely transparent and the VICL itself can be considered as a single SDN controller that exposes some services on its A-CPI to control the end-to-end multi-domain connectivity. In this sense, the components of the SOL act as SDN applications which operate on the most abstracted level of the resources managed at the VICL (i.e., the end-to-end connections). The A-CPIs in the proposed architecture are based on the REST paradigm and allow to manage the associated resources through create, read, update, and delete (CRUD) operations (Fig. 14.13).

#### 14.3.4.1 Provisioning of Cross-Domain Connectivity

The dynamic provisioning of cross-domain connectivity is handled through a set of cooperating enhanced functions, implemented as SDN applications that run on top of the SDN controller and makes use of the basic per-domain services offered through the A-CPI REST interface of the controller (see Fig. 14.10). Part of these applications offers a north-bound interface to be invoked by the SOL at the upper level, while other applications are related to the internal management of the virtual infrastructure and are not consumed by external entities.

Figure 14.14 shows an example of interaction between some cross-domain enhanced services at the SDN application plane and per-domain basic services implemented at the SDN controller plane. When a new multi-domain connection,

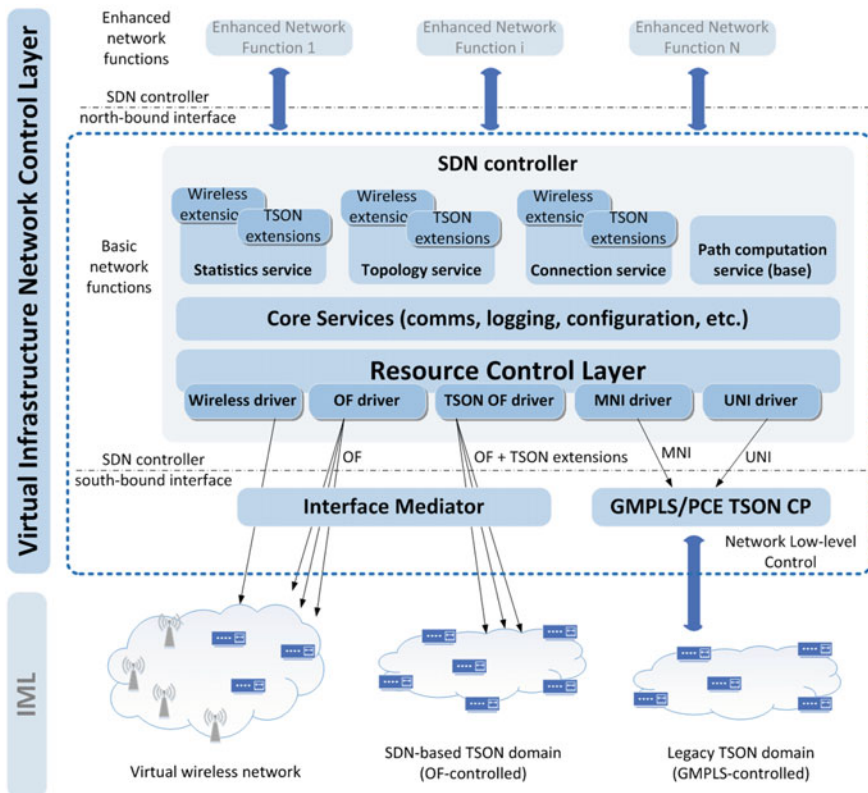


Fig. 14.13 Low-level control functions in the SDN controller

spanning from the wireless access to the metro optical domain, must be established to connect a cloud mobile user to a DC, the SOL sends a request to the end-to-end (E2E) Multi-domain Connection Service. This service acts as a consumer of the E2E Multi-layer Path Computation Service, which is a sort of parent PCE specialized in the elaboration of multi-layer, multi-technology paths. The E2E Multi-layer Path Computation Service elaborates a path which specifies just the edge nodes of the domains traversed by the flow, together with the ports and resources to be used at the inter-domain links. This information is used by the E2E Multi-domain Connection Service to trigger the creation of per-domain connections between these edge nodes, consuming the wireless access and TSON connection services provided by the SDN controller.

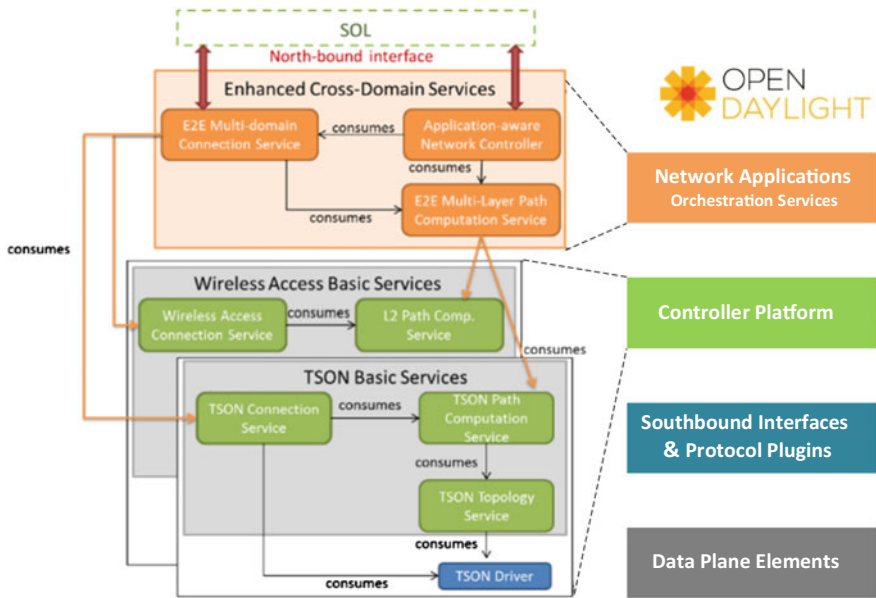


Fig. 14.14 Example of interaction between cross-domain enhanced services and per-domain basic services

### 14.3.5 Converged Service Orchestration

The mechanisms for the converged orchestration of cloud and network services, with the automated and cloud-aware setup and adjustment of the user-to-DC and inter-DC network connectivity, are implemented at the SOL.

Figure 14.15 shows the SOL architecture together with the interaction between the SOL and the entities responsible to manage, control, and operate cloud and network resources. As analyzed in previous sections, the network control layer is provided through the combination of one or more SDN controllers (based on the OpenDaylight platform) and additional SDN applications developed on top of them. These applications provide enhanced functions for end-to-end provisioning of multi-domain connectivity, as required to support a suitable access and execution of distributed cloud-based applications. REST APIs are available to allow the interaction between SOL and VICL, from the basic requests for creation, tear-down, and modification of user-to-DC and inter-DC connections to more advanced bidirectional communications to collect monitoring metrics or cross-layer information to take joint decisions about the evolution of the cloud service. The cloud management system can adopt several open-source solutions to control the different types of cloud resources (computing and storage), together with the internal connectivity of the data center. An example is OpenStack, a flexible cloud management platform widely used in cloud environments to deliver multi-tenant services.

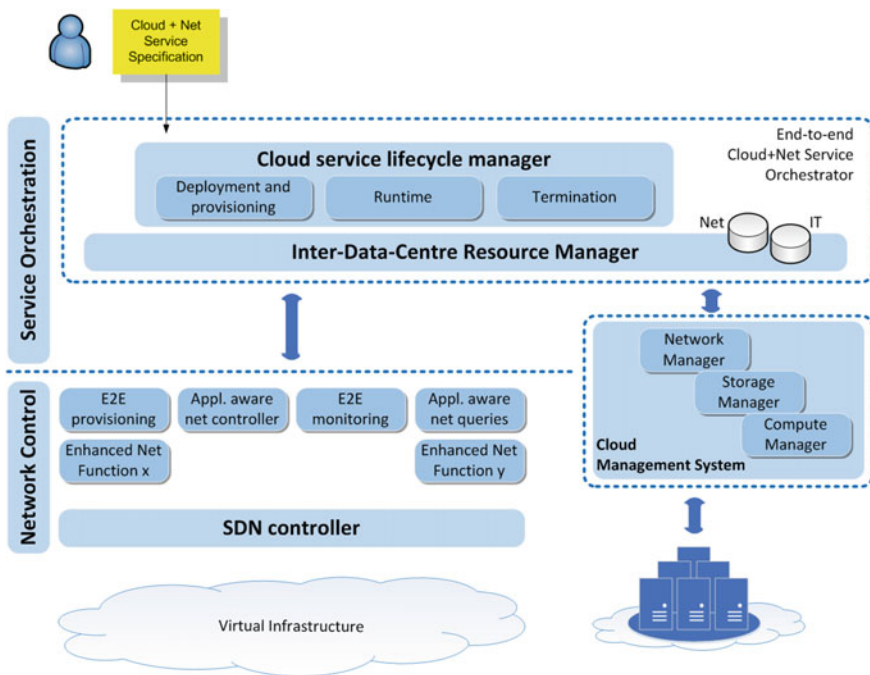


Fig. 14.15 Service orchestration layer high-level architecture

## 14.4 Architecture Evaluation

### 14.4.1 Network Scenario and Related Work

As already discussed in detail, one of the main innovations of the reference architecture proposed (Fig. 14.2) is that of cross-domain virtualization that allows the creation of infrastructure slices spanning the converged optical and wireless network domains as well as the IT resources in the DCs. Cross-domain virtualization is performed by the IML that is responsible for abstracting the physical infrastructure, composing the virtual resources created, and offering them as isolated MOVNOs exploiting the functionalities available through the adoption of the SDN principles. An important aspect of this process is that the formed MOVNOs are able to satisfy the virtual infrastructure operators’ requirements and the end users’ needs, while maintaining cost-effectiveness and other specific requirements such as energy efficiency. This involves the identification of the optimal virtual infrastructures that can support the required services in terms of both topology and resources and includes mapping of the virtual resources to the physical resources. To achieve this goal, the IML plays a key role as it allows taking a centralized approach with a complete view of the underlying infrastructure, thus allowing the identification of globally optimal MOVNOs.

In order to assess the performance of this type of infrastructures, we have developed a modeling framework based on integer linear programming (ILP) for the integrated wireless, optical, and DC infrastructure. In terms of wired technologies, computing resources are interconnected through the TSON WDM metro network with frame-based sub-wavelength switching granularity incorporating active nodes that will also interface the wireless microwave links supporting backhauling from the wireless access segment. This infrastructure is suitable to support traffic that is generated by both traditional cloud and mobile cloud applications. In this context, traffic demands corresponding to traditional cloud applications are generated at randomly selected nodes in the wired domain and need to be served by a set of IT servers. Mobile traffic on the other hand is generated at the wireless access domain and in some cases needs to traverse a hybrid multi-hop wireless access/backhaul solution before it reaches the IT resources through the optical metro network.

Using this modeling framework, an extended set of results is produced that are used to evaluate the performance of the proposed architecture in terms of metrics such resource and energy efficiency. Our study focuses on optimal planning of MOVNOs in terms of both topology and resources over the physical infrastructure. To identify the least energy-consuming dependable MOVNOs, detailed power consumption models taken from [36] for the optical metro, the wireless access networks and IT resources are considered. In the general case, the MOVNO planning problem is solved taking into account a set of constraints that guarantee the efficient and stable operation of the resulting infrastructures. The following constraints are considered:

- Every demand has to be processed at a single IT server. This allocation policy reduces the complexity of implementation.
- The planned MOVNO must have sufficient capacity for all demands to be transferred to their destinations.
- The capacity of each link in the MOVNO should be realized by specific PI resources.
- A critical function is the mapping and aggregation/de-aggregation of the traffic from one domain to the other. Given that the PI consists of a heterogeneous network integrating optical metro and wireless access domains, each physical link  $g$  is assumed to have a different modular capacity  $M_\kappa$ , ( $\kappa = \text{wireless, optical}$ ). For example, the wireless backhaul links are usually treated as a collection of wireless microwave links of 100 Mbps while the TSON solution may offer a minimum bandwidth and granularity of 100 Mbps. Therefore, during the MOVNO planning process the *conservation of flow* between the different technology domains is also considered.
- The planned MOVNO must have adequate IT server resources such as CPU, memory, and disk storage to support all requested services.
- As a final consideration, depending on the type of service that has to be provided, the end-to-end delay across all technology domains should be limited below a predefined threshold.

The objective of our formulation is to minimize the total cost during the planned time frame of the resulting network configuration that consists of the following components: (a)  $k_g$  the cost for operating capacity  $u_g$  of the PI link  $g$  in the optical domain, (b)  $w_l$  the cost for operating capacity  $u_l$  of the PI link  $l$  in the wireless domain, and (c)  $\sigma_{sr}$  the total cost of the capacity resource  $r$  of IT server  $s$  for processing the volume of demand  $h_d$ .

$$\text{Minimize } F = \sum_g k_g(u_g) + \sum_l w_l(u_l) + \sum_s \sum_r \sigma_{sr}(h_d)$$

The costs considered in our modeling are related to the energy consumption of the converged infrastructure comprising optical and wireless network domains interconnecting IT resources. This objective has been chosen as it addresses the energy efficiency target of the proposed solution, but also because it can be directly associated with the operational expenditure (OpEx) of the planned MOVNO. Apart from minimizing energy consumption, the planned MOVNOs can be also designed (based on the same formulation) taking into account other optimization objectives such as distance (or number of hops) between source and destination nodes, end-to-end service delay, load balancing, resource utilization, or number of active IT servers. More details on the modeling framework can be found in [6].

#### 14.4.1.1 Numerical Results

To investigate the performance of the proposed MOVNO design scheme across the multiple domains involved, the architecture illustrated in Fig. 14.16 is considered: The lower layer depicts the PI and the layer above depicts the VIs. For the PI, a macro-cellular network with regular hexagonal cell layout has been considered, similar to that presented in [36], consisting of 12 sites, each with 3 sectors and 10 MHz bandwidth, operating at 2.1 GHz. The inter-site distance (ISD) has been set to 500 m to capture the scenario of a dense urban network deployment. Furthermore, a  $2 \times 2$  MIMO transmission with adaptive rank adaption has been considered while the users are uniformly distributed over the serviced area.

As indicated in [36], each site can process up to 115 Mbps and its power consumption ranges from 885 to 1087 W, under idle and full load, respectively. For the computing resources, three Basic Sun Oracle Database Machine Systems have been considered where each server can process up to 28.8 Gbps of uncompressed flash data and its power consumption ranges from 600 to 1200 W, under idle and full load, respectively [37]. For the metro network, the TSON solution has been adopted assuming a single fiber per link, 4 wavelengths per fiber, wavelength channels of 10 Gb/s each, minimum bandwidth and granularity 100 Mbps, and maximum capacity of the link 40 Gbps. Finally, cloud and mobile cloud computing traffic is generated at randomly selected nodes in the optical metro network and LTE base stations and needs to be served to the three IT servers. Note that in order

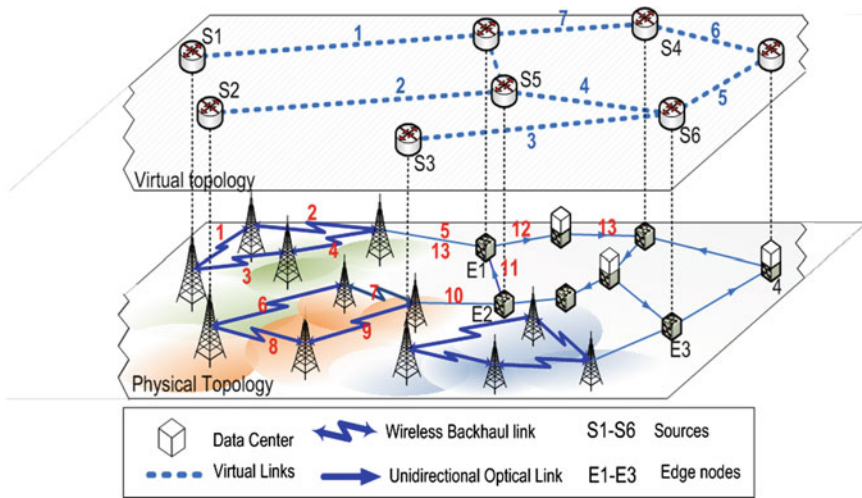


**Fig. 14.16** Virtualization over heterogeneous network infrastructures

to study how the end user mobility and the traffic parameters affect the utilization and power consumption of the planned VI the service-to-mobility factor [38] is introduced. The service-to-mobility factor is defined as the fraction of the service holding time over the cell residence time. It is assumed that the cell residence time is exponentially distributed with parameter  $\eta$  and the service holding time is Erlang distributed with parameters  $(m, n)$ .

Figure 14.17 illustrates the total power consumption of the converged infrastructure (wireless access, wireless backhaul, optical network, and IT resources) when applying the proposed approach optimizing for energy efficiency or network resources. Comparing these two schemes, it is observed that the energy-aware MOVNO (EA MOVNO) design consumes significantly lower energy (lower operational cost) to serve the same amount of demands compared to the closest IT scheme providing an overall saving of the order of 37 % for low traffic demands. This is due to the fact that in the former approach fewer IT servers are activated to serve the same amount of demands. Given that the power consumption required for the operation of the IT servers is dominant in this type of infrastructures, switching-off the unused IT resources achieves significant reduction of energy consumption. Furthermore, it is observed that for both schemes the average power consumption increases almost linearly with the number of demands. However, the relative benefit of the energy-aware design decreases slightly with the number of demands, when approaching full system load. It is also observed that the wireless access technology is responsible for 43 % of the overall power consumption, while the optical network consumes less than 7 % of the energy. Note that the results have been produced assuming that the traffic generated in the wireless access (mobile cloud) is 2 % of the traffic generated by fixed cloud services in the optical domain (cloud traffic).

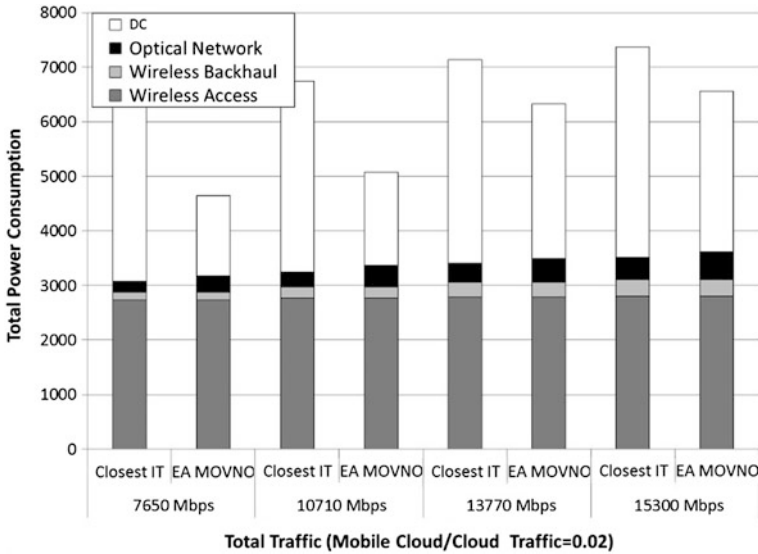


Fig. 14.17 Impact of traffic load on power consumption when the VI is planned for energy or distance

To further investigate how the service characteristics affect the optimum planned MOVNO, the impact of both traffic load and end user mobility on the total power consumption (operational cost) of the MOVNO is studied. Figure 14.18 shows that the total power consumption increases for higher end user mobility, as expected. More specifically, when mobility is higher (lower service-to-mobility factor) additional resources are required to support the MOVNO in the wireless access domain. However, it is interesting to observe that this additional resource requirement also propagates in the optical metro network and the IT domain. The additional resource requirements, across the various infrastructure domains, are imposed in order to ensure availability of resources in all domains involved (wireless access and backhauling, optical metro network, and DCs) to support the requested service and enable effectively seamless and transparent end-to-end connectivity between mobile users and the computing resources.

#### 14.4.1.2 Impact of the Virtualization Solution on the Proposed Architecture

Network and cloud convergence can bring significant benefits to both end users and physical infrastructure providers. In particular, end users can experience a better quality of service in terms of improved reliability, availability, and service ability, whereas physical infrastructure providers can gain significant benefits through improved resource utilization and energy efficiency, faster service provisioning

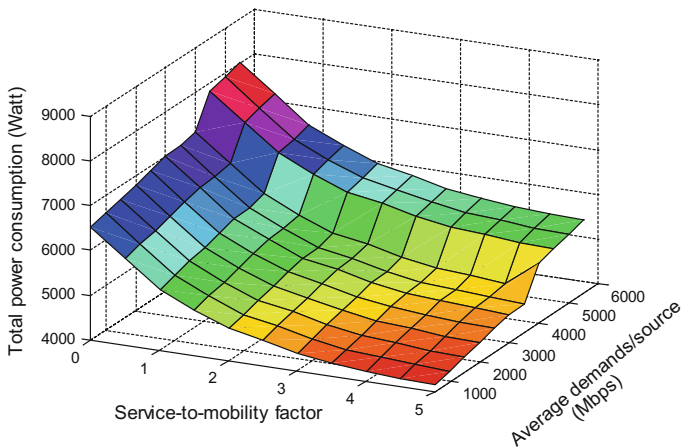


Fig. 14.18 Impact of mobility and traffic load on the total power consumption ( $m = 5$ )

times, greater elasticity, scalability, and reliability of the overall solution. In view of these, virtualization across multi-technology domains has recently gained significant attention and several solutions already exist (see [39]). Typical examples include the *pipe* and the *hose* virtual private network models [40]. Their main difference is that in the pipe model the bandwidth requirement between any two endpoints must be accurately known in advance, whereas the hose model requires only the knowledge of the ingress and egress traffics at each endpoint having the advantages of ease of specification, flexibility, and multiplexing gain [41] (Fig. 14.19).

Other similar research efforts have been focused on embedding virtual infrastructures (VI) over multi-domain networks [39]. A key assumption is that the details of each domain are not communicated to the other domains. Therefore, each infrastructure provider has to embed a particular segment of the VI without any knowledge of how the remaining VIs have already been mapped or will be mapped

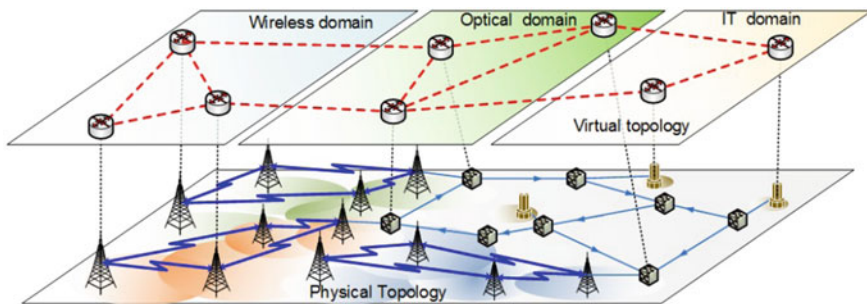
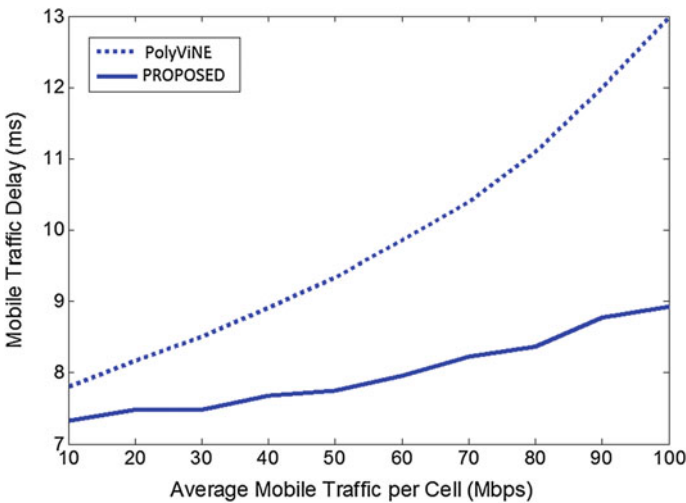


Fig. 14.19 Segmented multi-domain virtualization

(see [39] where this approach is referred to as the PolyViNE) with the objective to unilaterally maximize its payoff. A typical example includes the case where an infrastructure provider wishes to optimally allocate its resources without considering the impact of its decision on the other domains.

Although existing approaches (e.g., PolyViNE) target relatively straightforward solutions from an implementation perspective, they may lead to inability in meeting some cloud and mobile cloud service requirements (e.g., end-to-end latency) and inefficiencies in terms of resource requirements, energy consumption, etc. In the present study, it is argued that in order to optimally exploit the benefits of a converged cloud, some level of information exchange across the multi-technology domains must be provided. To facilitate this while offering a feasible solution, it is proposed to develop suitable abstraction models of the physical infrastructure that allow MOVNOs to maintain the information needed to be exchanged between technology domains, in order to overcome the issues described above. To give an example, the information required to be maintained may include the status of Rx/Tx queues of the TSON nodes, the physical layer impairments in the wireless and optical domains, the power consumption levels of the equipment, and the mobility profiles/characteristics of the end users. Preliminary modeling results (see Figs. 14.20 and 14.21) indicate that by means of maintaining and exchanging the required information across technology domains, significant performance improvements can be achieved. In more detail, our modeling results show that by maintaining this type of information through the relevant parameters the end-to-end delay for the mobile traffic has been reduced by up to 40 % (see Fig. 14.20) compared to [39]. In addition, approximately 20 % overall power savings



**Fig. 14.20** Comparison of the proposed converged approach with PolyViNE in terms of mobile cloud computing traffic delay (fixed traffic 800 Mbps/source, source nodes = 3)

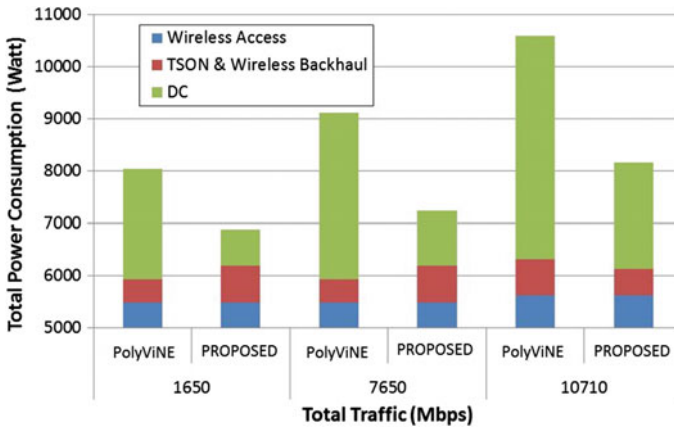


**Fig. 14.21** Impact of the proposed solution on the total power consumption

(see Fig. 14.21) for various loading conditions can be achieved, when compared to the existing approaches [39]. Details of the relevant models used are available in [6].

## 14.5 Conclusions

This chapter focused on a next-generation ubiquitous converged network infrastructure involving integration of wireless access and optical metro network domains to support a variety of cloud and mobile cloud services. The infrastructure model proposed is based on the IaaS paradigm and aims at providing a technology platform interconnecting geographically distributed computational resources that can support these services. The proposed architecture addresses the diverse bandwidth requirements of future cloud and mobile cloud services by integrating advanced optical metro network technologies offering fine granularity with state-of-the-art wireless access network technology (LTE/Wi-Fi), supporting end user mobility. The concept of virtualization across the technology domains is adopted as a key enabling technology to support our vision. This study also provided a description of the proposed architecture including the details of the individual architectural layers, i.e., physical infrastructure layer, infrastructure management layer, virtual infrastructure control layer, and orchestrated end-to-end service layer. In addition, a detailed description of the interaction between the different layers is provided. The proposed architecture is well aligned and fully compatible with the OGF SDN architecture and takes advantage of the associated functionalities and capabilities. A modeling/simulation framework was developed to evaluate the proposed architecture and identify planning and operational methodologies to allow global optimization of the integrated converged infrastructure. A description of the tool and some relevant modeling results were also presented.

**Acknowledgments** This work was carried out with the support of the CONTENT (FP7-ICT-318514) project funded by the EC through the 7th ICT Framework Program.

## References

1. Tzanakaki A et al (2014) Planning of dynamic virtual optical cloud infrastructures: the GEYSERS approach. *IEEE Commun Mag* 52(1):26–34
2. Satyanarayanan M, Bahl P, Caceres R, Davies N (2009) The case for VM-based cloudlets in mobile computing. *IEEE Pervasive Comput* 8(4):14–23
3. Mun K Mobile cloud computing challenges. *TechZine Mag*. <http://goo.gl/AuI5ZM>
4. <http://www.gogrid.com/>
5. <http://www.flexiscale.com/>
6. Tzanakaki A et al (2013) Virtualization of heterogeneous wireless-optical network and IT support of cloud and mobile services. *IEEE Commun Mag* 51(8):155–161
7. Yeganeh SH et al (2013) On scalability of software-defined networking. *IEEE Commun Mag* 51(2):136–141
8. Mateos G, Rajawat K (2013) Dynamic network cartography. *IEEE Signal Process Mag* 129–143
9. Rajawat K (2012) Dynamic optimization and monitoring in communication networks. University of Minnesota, Ph.D. dissertation
10. Channegowda M et al (2013) Software defined optical networks technology and infrastructure: enabling software-defined optical network operations (invited). *IEEE/OSA JOCN* 5(10): A274–A282
11. Zhang S, Tornatore M, Shen G, Zhang J, Mukherjee B (2014) Evolving traffic grooming in multi-layer flexible-grid optical networks with software-defined elasticity. *J Lightwave Technol* 32:2905–2914
12. France Telecom-Orange and Alcatel-Lucent deploy world's first live 400 Gbps per wavelength optical link, Alcatel Lucent press release Feb 2013. <http://goo.gl/xtvLBa>
13. Gerstel O, Jinno M, Lord A, Yoo SJB (2012) Elastic optical networking: a new dawn for the optical layer? *IEEE Commun Mag* 50(2):s12–s20
14. IEEE 802.3 Ethernet Working Group Communication (2012) IEEE 802.3™ industry connections ethernet bandwidth assessment. <http://goo.gl/Zp2Xym>
15. Jinno M et al (2009) Spectrum-efficient and scalable elastic optical path network: architecture, benefits, and enabling technologies. *IEEE Commun Mag* 47(11):66–73
16. Verisma ivx 8000, Optical Packet Switch and Transport. Intune Networks, 2011
17. Zervas GS, Triay J, Amaya N, Qin Y, Cervelló-Pastor C, Simeonidou D (2011) Time shared optical network (TSON): a novel metro architecture for flexible multi-granular services. *Opt Express* 19:B509–B514
18. Lehr W, Sirbu M, Gillett S (2004) Municipal wireless broadband policy and business implications of emerging technologies. In: *Competition in networking: wireless and wireline*. London Business School
19. [RFIC2013] Cellular versus Wi-Fi: future convergence or an utter divergence? In: *Radio frequency integrated circuits symposium (RFIC), 2013 IEEE*, pp I, II
20. Castelli MJ (2002) *Network sales and services handbook*. Cisco Press. ISBN 978-1-58705-090-9
21. Peng S, Nejabati R, Azodolmolky S, Escalona E, Simeonidou D (2011) An impairment-aware virtual optical network composition mechanism for future internet. *Opt Express* 19(26):B251–B259
22. Jinno M et al (2013) Virtualization in optical networks from network level to hardware level. *IEEE/OSA J Opt Commun Netw* 5(10):A46–A56

23. García-Espín JA, Ferrer Riera J, Figuerola S, Ghijsen M, Demchemko Y, Buysse J, De Leenheer M, Develder C, Anhalt F, Soudan S (2012) Logical infrastructure composition layer, the GEYSERS holistic approach for infrastructure virtualisation. In: Proceedings of TNC
24. Tzanakaki A, Anastasopoulos MP, Georgakilas K (2013) Dynamic virtual optical networks supporting uncertain traffic demands. *IEEE/OSA J Opt Commun Netw* 5(10) (Invited)
25. Li Y, Qiu L, Zhang Y, Mahajan R, Rozner E (2008) Predictable performance optimization for wireless networks. In: Proceedings of ACM SIGCOMM, Seattle, WA, USA
26. Bhanage G, Vete D, Seskar I, Raychaudhuri D (2010) SplitAP: leveraging wireless network virtualization for flexible sharing of WLANs. In: Proceedings of IEEE GLOBECOM 2010, pp 1–6
27. Aljabari G, Eren E (2010) Virtual WLAN: extension of wireless networking into virtualized environments. *Int J Comp Res Inst Intell Comput Syst* 10(4):1–9
28. Kokku R et al (2013) CellSlice: cellular wireless resource slicing for active RAN sharing. In: Proceedings of COMSNETS
29. <http://goo.gl/oT5E5t> <http://www.contextream.com/news/press-releases/2014/contextream-announces-first-commercially-available-opensdaylight-based-carrier-grade-sdn-fabric-for-nfv/>
30. Nyren R, Edmonds A, Papaspyrou A, Metsch T (2011) Open cloud computing interface—core. GFD-P-R.183, OCCI WG
31. Dhody D, Lee Y, Ciulli N, Contreras L, Gonzales de Dios O (2013) Cross stratum optimization enabled path computation. IETF Draft
32. Crabbe E, Medved J, Minei I, Varga R (2013) PCEP extensions for stateful PCE. IETF Draft
33. Tzanakaki A et al (2014) A converged network architecture for energy efficient mobile cloud computing. In: Proceedings of ONDM 2014, pp 120–125
34. MAINS Deliverable D2.3. OBST mesh metro network design and control plane requirements
35. Rofoee BR et al (2015) First demonstration of service-differentiated converged optical sub-wavelength and LTE/Wi-Fi networks over GEANT. In: Proceedings of OFC 2015, paper Th2A.35
36. Auer G, Giannini V (2011) Cellular energy efficiency evaluation framework. In: Proceedings of the vehicular technology conference
37. Valancius V, Laoutaris N, Massouli L, Diot C, Rodriguez P (2009) Greening the internet with nano data centers. In: Proceedings of the 5th international conference on emerging networking experiments and technologies (CoNEXT'09), ACM, New York, NY, USA, pp 37–48
38. Fang Y, Chlamtac I (2002) Analytical generalized results for handoff probability in wireless networks. *IEEE Trans Commun* 50(3):369–399
39. Chowdhury M, Samuel F, Boutaba R (2010) PolyViNE: policy-based virtual network embedding across multiple domains. In: Proceedings of ACM SIGCOMM workshop on VISA'10
40. Chu Jian, Lea Chin-Tau (2008) New architecture and algorithms for fast construction of hose-model VPNs. *IEEE/ACM Trans Netw* 16(3):670–679
41. Duffield NG, Goyal P, Greenberg A, Mishra P, Ramakrishnan KK, der Merwe JEV (1999) A flexible model for resource management in virtual private networks. In: Proceedings of ACM SIGCOMM, San Diego, California, USA

# Conclusion and Future Topics

This edited book has provided an overview of new enabling technologies for fiber-wireless (Fi-Wi) convergence in support of 5G mobile transport networks.

In the first part, to introduce the reader to the larger societal and economical ecosystem where transition to 5G is happening, Chap. 1 describes the current market and deployment status for broadband services. A similar, yet more technical, background on the current and evolutionary technical trends of LTE and LTE-A is provided in Chap. 2 that serves also as comprehensive technical introduction to relevant concepts for 5G wireless access. Chapter 3 elaborates on the main topic of the book, i.e., the role of fiber-wireless (Fi-Wi) convergence in support of 5G mobile transport networks, introducing the main technical issues motivating this book.

In Parts II, III, and IV, Fi-Wi technologies have been discussed at the three major network levels involved in the path toward convergence: system level, network architecture level, and network management level.

In Part II, devoted to system-level technologies, the basic principles and current standardization of the various analog-to-digital radio-over-fiber techniques currently available have been overviewed. These are instrumental to the understanding of the 5G transport network architectures described in Part III. As the backhaul/fronthaul of mobile traffic will not necessarily happen over optical fiber media, other competing wireless technologies in the field of millimeter wave have been also described.

In Part III, devoted to network architecture technologies, the concept of C-RAN is comprehensively overviewed under different viewpoints and by introducing a state-of-the-art picture of the level of advancement of important technologies at the network architecture level (NGPON, WDM-PON, BBU Hotelling, “No More Cell”). Chapter 8 shows how A-RoF, combined within an advanced PON architecture, can be used to build a scalable access network architecture. Chapter 9 overviews PON access architectures for building mobile backhuls, which will scale to the increased capacity requirements of future next-generation wireless broadband access network (NG-WBAN) technologies, and also includes the design of a fully distributed PON-based access architecture. Chapter 10 shows how the deployment of BBU hotels over a WDM access/aggregation network can be

optimized. Finally, Chap. 11 elaborates on the novel concept of “No More Cell” and how Fi-Wi convergence is a key enabler for it.

In Part IV, the next-generation point-of-presence architecture is initially described in Chap. 12, introducing the concept of a flexible platform that combines aggregation of fixed and mobile access traffic, IP edge routing, and the ability to host additional network functions and services, benefiting greatly from network functions virtualization (NFV) and software-defined networking (SDN) concepts. Subsequently, Chap. 13 describes the cooperative multipoint system that utilizes a base station (BS) cooperation technique to enhance the received signal quality, decrease the received interference, as well as improve the channel capacity of cell-edge users in the network.

The role of SDN is also extensively covered in two distinct Chaps. 7 and 14. While Chap. 7 focuses more on how SDN can cope with raising system-level challenges of convergence, Chap. 14 considers management aspects of SDN related to the support of cloud and mobile cloud computing services

#### *An overview of future topics in Fiber-Wireless (Fi-Wi) convergence*

In the quickly evolving landscape of 5G research, several projects worldwide are currently contributing to the 5G transition. As an example, in Europe, the EU 5G infrastructure public–private partnership (5G-PPP) has been established with the aim of fostering the European ICT industry [3].

Clearly, 5G research is quickly evolving, and it was not possible to cover in this book the latest trends that have emerged in the last months prior to publication. We provide in the following a quick overview of some emerging topics that we consider particularly relevant to our book.

**Impact of traffic dynamics and machine-to-machine (M2M) services.** The growth in mobile traffic will not be homogenous, with busy-hour Internet traffic expected to grow more rapidly than average Internet traffic. The uptake of M2M services will, in addition, result in locally and over time varying characteristics of the mobile traffic. Thus, not only the future 5G mobile transport infrastructure will have to support a fast-growing overall mobile data volume and a significantly increased number of connected mobile devices at significantly improved energy- and cost-efficiencies, but it also will have to provide the capability to flexibly adapt to dynamically fluctuating traffic demands (over time, location, and characteristics) and a broad range of potentially new service requirements of future service portfolios. The wider use of M2M communications requires wider geographic coverage, with implications for the network architecture.

**Mobile edge computing (MEC).** MEC is a new technology which is currently being standardized by ETSI. MEC promotes the insertion of cloud computing capabilities at the edge of the mobile network, within the radio access network (RAN), in close proximity to mobile subscribers. The aim is to reduce latency, ensure highly efficient network operation and service delivery, and offer an improved user experience. MEC represents a key technology and architectural concept to enable the evolution to 5G, as it helps advance the transformation of the mobile network toward a programmable platform, by contributing to satisfy the

demanding requirements of 5G in terms of expected throughput, latency, scalability, and reconfigurability.

**Midhaul/x-haul.** As seen in Chap. 10, in traditional CRAN implementations, the BBU-hoteling technique consists in geographically separating the BBU from its RRH, which remains located at the cell site, and consolidating BBUs into a common BBU hotel. In the first deployments of BBU-hoteling technique, the RRHs only perform basic layer 1 functions (i.e., digital-to-analog/analog-to-digital conversion (DAC/ADC) of the baseband signals, frequency up-/down-conversion, power amplification, and some signal measurements), but such configuration requires very high volumes of traffic, the so-called fronthaul traffic, to be exchanged between BBUs and RRHs through, e.g., the CPRI interface (see Chap. 5).

As of today, more efficient solutions are being investigated to reduce the amount of bandwidth to be exchanged between the RRH and the BBU. This is especially true if we consider future 5G deployment, where a large number of small cells are expected to be deployed, featuring high MIMO counts and large radio bandwidths. Therefore, different interface points (RAN splits), i.e., different functional separations between L1 and L2/L3 cell processing, are being investigated, in terms of potential cost/performance benefits and required capacity. These split points determine the separation of a cell site into two components, a central cell, where higher-layer cell functions are virtualized and consolidated for a set of cell sites, and remote cells, i.e., base stations. In contraposition to traditional fronthaul, the traffic transported between remote and centralized cell is also known as midhaul or x-haul. Some of these techniques are currently under standardization, e.g., in the IEEE 1914 workgroup, but research studies are needed to identify the most effective split point in the midhaul architecture. Even technical solutions enabling reconfigurability of the split point are currently being proposed, which could be used to select the split point according to the requested amount of traffic or to the specific coordination requirements of the cellular network.

**Energy efficiency.** 5G systems have to resolve the fundamental challenge of handling the anticipated dramatic growth in the number of terminal devices, the continuous growth of traffic (at a 50–60 % CAGR), and heterogeneous network layouts, without causing a dramatic increase in the power consumption and management complexity within the network. Specifically, 5G communication systems need to support unprecedented requirements for the wireless access connection, targeting cell throughput capacities of  $1000\times$  current 4G technology and round-trip latency of about 1 msec. Since the perlink data rates will be increased by about  $100\times$ , energy efficiency becomes a critical challenge of 5G systems, e.g., the joules per bit will need to fall by at least  $100\times$ . Thus, 5G will have to be designed to be a sustainable and scalable technology.

Potential solutions to the energy efficiency issue include recourse allocation, network planning, renewable energy, and hardware architectures. Thus, this energy chase will eventually cover terminal devices, network elements, and the network as a whole, including data centers. Specifically, sophisticated resource allocation policies that optimize system energy efficiency and can be implemented in a centralize/distributed fashion are of paramount importance. Energy-efficient

network planning refers to techniques that minimize the number of base stations (BSs) for a coverage target and intelligent BS sleep mode mechanisms for energy savings. On the other hand, the integration of renewable energy sources on 5G networks is a promising solution for network sustainability and energy efficiency. This technology enables the exploitation of natural energy resources such as solar power, wind, and mechanical vibration, as well as energy harvesting from ambient and/or controlled electromagnetic radiation. Finally, energy efficiency requires the design of low-power consumption circuits such as power amplifiers and analog front ends in microwave and millimeter frequency ranges, DSP-enabled optical transceivers for access and backhaul networks, and ultra-low-power wireless sensors harvesting ambient energy (e.g., solar, thermal, vibration, and electromagnetic energy). Further, hardware architectures incorporating wireless power transfer technologies and having sleep mode capabilities (i.e., specific hardware components can be switched off for energy savings) present another exciting alternative to battery-less sensor operation for machine-to-machine (M2M) and device-to-device (D2D) communications.

**Advanced modulation format in the wireless side.** 5G will support diverse use of various waveforms for enhanced mobile broadband connection, wide area Internet of Things and high-reliability services. Current OFDM modulation developed for the 4G system is not capable of serving the rapidly increasing demands for data volume and types of user equipment. In order to accommodate new applications carried by 5G, system operation issues of DSP complexity, system latency, and battery life are drawing more attention for researchers. The design and optimization of next-generation physical layer waveforms is a hot topic in both academia and industry.

Several waveforms are actively investigated and developed as the candidates for 5G system. OFDM-based multicarrier modulations are preferable for a balance between performance and complexity, including GFDM (Generalized FDM), FBMC (filter bank multicarrier), UFMC (universal and filtered multicarrier), and other minor modification versions of OFDM.

FBMC is a multicarrier modulation with filter-shaped subcarriers, which significantly suppress the out of band leakage and relax the carrier frequency offset (CFO) synchronization requirement in receiver. However, its high DSP complexity and PAPR issue limit it to downlink applications. UFMC, on the other hand, is beneficial in uplink due to its comparably lower DSP complexity in the transmitter and supports asynchronous transmission that omits the time-advance process in multiuser environment. The uplink transmission can benefit from reduced latency and increased compatibility with burst-mode packet uploading. The above modulations are widely investigated in traditional bands below 6 GHz and also millimeter-wave bands beyond 30 GHz.

Recently, more modulations closer to OFDM are being proposed and studied. One example is the CP-OFDM (CP stands for cyclic prefix) with weight overlap and add (WOLA), which does not change the FFT/IFFT-based OFDM core. By applying simple weight overlap and add, different OFDM symbols are combined within the time-domain windowing, which improves the performance with

out-of-band (OOB) leakage. Another candidate, flexible CP-OFDM (FCP-OFDM), is designed to provide a flexible trade-off between multipath handling and OOB leakage suppression by splitting the cyclic prefix (CP) to CP and zero prefix (ZP) portion before feeding into shaping filter. These modulations emphasize more on the DSP complexity and power efficiency aspect of the system, while maintaining an acceptable performance in terms of OOB leakage, spectral efficiency, and asynchronous transmission.

Currently, there is no clear winner on the next-generation 5G modulation. Hence, we believe traditional OFDM modulation will be around a little bit longer even beyond 3GPP release 14 for conventional carrier frequency up to 6 GHz and release 15 for higher frequency up to 110 GHz.

# Index

*Note:* Page numbers followed by *f* and *t* indicate figures and tables, respectively

## A

AAA (authentication, authorization, and accounting) mechanisms, 323, 329–330, 330*f*

Accelerator design, 307–308

- 8-antenna precoding, 307

Access gateway (AGW), 237, 239

- universal access gateway (UAG), 331–332

Adaptive photonics-aided CoMP, 348–349

Additive white Gaussian noise (AWGN), 354

All-band coverage, 89–91

Amplified spontaneous emission (ASE), 177

Analog and digitized radio-over-fiber, 99

- analog radio-over-fiber (A-RoF), 99–100, 109
  - by means of SCM, 112–114
  - by means of WDM, 114–117
  - for IF-over-fiber, 110–112
  - for RF-over-fiber, 109–110

A-RoF versus baseband-over-fiber, 102

- baseband-over-fiber, 104
- IF-modulated signals, 103–104
- RF-modulated signals, 103

digitized radio-over-fiber (D-RoF), 117

- band-pass sampling theory, 118–120
- for multiple-antenna site, 122–124
- for single-antenna site, 120–122

existing radio cellular networks, 100–102

transmission of microwave signals on optical fibers, 104

- external modulation and direct detection, 106–107
- intensity modulation and direct detection, 105–106
- photo-detector-based HE-DD, 107–109

Analog-to-digital conversion, 164, 167, 168*f*

Analog-to-digital converter (ADC), 120–121, 123, 352, 353

Antenna polarization multiplexing, 175–178

Application-Controller Plane Interface (A-CPI), 374

Application protocol convergence (APC) layer, 55

Application-specific integrated circuits (ASICs), 326

Arbitrary waveform generator (AWG), 166, 243

Architectures, convergence of, 80

- centralization, 80–83, 81*f*
- resource sharing, 83–84

Asymmetric Digital Subscriber Line (ADSL), 50–51

Automatic protection switching (APS) module, 258

## B

Backhaul network, 216*f*, 217, 218

Backhauling wireless traffic, 236–238

Band-pass sampling theory, 118–120

Bands, convergence of, 89

- all-band coverage, 89–91
- MMW links, 91–92

Bandwidth aggregation, 5

Baseband-over-fiber modulation, 104

BaseBand Unit (BBU) hotelling, 222, 265

- advantages of, 268
- cost reduction, 268–269
- energy savings, 269
- improved radio performance, 269–270

BPTR

- case study for, 286–289
- optimization problem, 283–284

challenges of, 270

- high, constant bitrate, 270–271
- maximum end-to-end latency, 271–272
- strict QoS requirements, 273

evolving the base station, 267–268

FMC network architecture for, 280

- BBU placement, 281–282
    - general network architecture, 280–281
    - traffic routing, 282–283
  - heuristic greedy algorithm for BPTR, 284
    - heuristic scheme, 286
    - heuristic subroutines, 285–286
    - notation and input data, 284–285
  - mobile network, 266–267
  - open issues, 289–290
  - pooling techniques, 278–279
  - RAN architectures based on, 273
    - classification on BBU implementation, 278
    - classification on BBU placement, 274–276
    - classification on fronthaul transport, 276–278
    - virtualization, 279–280
  - Baseband units (BBUs), 80, 84, 221, 227
    - centralization, 222
    - function, 320
    - pooling, 223
  - Base station controller (BSC), 309
  - Base station cooperation, 338*f*
  - Base stations (BS), 80, 226, 239, 266–267, 337
    - evolving, 267–268
  - BBU placement and traffic routing (BPTR)
    - case study for, 286–289
    - heuristic greedy algorithm for, 284
    - heuristic scheme, 286
    - heuristic subroutines, 285–286
    - notation and input data, 284–285
    - optimization problem, 283–284
  - Beamforming, 18
    - 3D, 24–25, 24*f*
  - Berkeley Wireless Research Center (BWRC), 67
  - Bit error rate (BER), 273
    - counting, 174, 181
  - Bit error rate tester (BERT), 231
  - Blind equal throughput, 17
  - Bring your own device (BYOD) networking environments, 200
  - Broadband access technologies, evolution and trends of, 43
    - broadband wireless access networks, 60
      - mobile network technology evolution and market status, 63–68
      - Wi-Fi technology evolution and market status, 60–63
    - broadband wireline access networks, 45
      - coaxial cable technology, 54–55
      - global roll-out strategies, 55–57
      - hybrid fiber–copper technology, 55
      - passive optical network (PON), 46–50
      - penetration of different broadband technologies, 57–60
      - twisted pair technology, 53
      - xDSL technology, 50–53
  - fiber-wireless convergence and technology evolution, 69
    - for backhaul and the fronthaul of HetNet, 71–74
  - distributed antenna systems (DASs), 69, 70*f*
    - ultra-high-speed fiber-wireless transmission, 70–71
  - traffic trend, 43–45
  - Broadband network gateway (BNG), 324, 324*f*, 331
    - in hardware on an existing network element, 325
    - with IT resources and dedicated hardware resources, 326
    - pure soft BNG, 325
  - Broadband passive optical network (BPON), 49, 241
  - Broadband remote access server (BRAS), 324, 331
  - Broadband residential gateway (BRG), 322
- ## C
- C&M data, 132
  - Cable TV (CATV), 54
    - 10BASE5, 54
  - Capital expenditures (CAPEX), 221, 223, 268, 283
  - Carrier aggregation (CA), 5*f*, 9, 28
    - definitions and terminologies, 9–10
    - of LTE-Licensed and LTE-U CCs, 28–30
    - radio resource management framework for CA, 15–17
    - types, 10–15
  - Carrier frequency offset (CFO) synchronization requirement, 392
  - Carrier-less amplitude and phase (CAP) modulation, 86
  - Cascaded multi-modulus algorithm (CMMA) equalization, 181
  - CDMA2000, 64–65
  - Cell selection bias (CSB), 34
  - Cell-specific Reference Signal (CRS), 35
  - Cellular networks, 215
  - Centimeter-wave (CMW) bands, 89–90
  - Centralization, 80–83, 81*f*
    - challenges on transport networks for, 299–300
  - Centralized CoMP, 22–23

- Centralized radio access network (C-RAN), 80
  - BBU hotelling in (*see* BaseBand Unit (BBU) hotelling)
- Centralized RANs, 81, 82*f*
- Central office (CO), 222
- Channel-aware CC assignment, 16
- Channel-blind CC assignment, 16
- Channel state information (CSI), 21, 338
- China mobile, recent progress on C-RAN from, 304
  - exploitation of C-RAN virtualization, 307
    - accelerator design, 307–308
    - prototype verification of soft C-RAN, 308–310
  - field trials on centralization with different FH solutions, 304–307
- Client jitter and wander accumulation over OTN, 151–153
- Client mapping over OTN, 149–151
- Cloud and mobile cloud services, existing technology solutions supporting, 362
  - infrastructure management, 363–365
  - physical infrastructure solutions supporting cloud services, 362
    - in metro optical network solutions, 362–363
    - in wireless technologies solutions, 363
  - service provisioning, 365–366
- Cloud management system (CMS), 365
- Cloud radio access network (C-RAN), 221–223, 222*f*, 293, 296*f*
  - 5G design of user-centric radio network, 294–296
  - advantages of, 299
  - architecture, 297*f*
  - challenges on
    - transport networks for centralization, 299–300
    - virtualization implementation to realize resource cloudification, 302–304
  - concept of, 296–298
  - evolving toward 5G, 310
    - CPRI redefinition, 311–312
    - C-RAN to enable key 5G technologies, 310–311
    - edge application on C-RAN, 313–314
  - features, 298
  - potential fronthaul solutions, 300–302
  - recent progress on C-RAN from China mobile, 304
    - accelerator design, 307–308
    - field trials on centralization with different FH solutions, 304–307
    - prototype verification of soft C-RAN, 308–310
- Cloudlet approach, 361*f*
- Coarse WDM (C-WDM), 277
- Coaxial cable technology, 54–55
- Commercial off-the-shelf (COTS) hardware, 223, 225
- Common Public Radio Interface (CPRI), 81, 100, 128, 221, 260–261, 268, 341, 357
  - compression, 137–138, 293
  - CPRI-based solutions, 192
    - frequency, time and latency requirements derivation with LTE fronthauling, 132*f*
  - interface description, 131
    - layer 1, 133–136
    - layer 2, 136–137
  - multiplexing, 148
  - over optical transport network, 149
    - client jitter and wander accumulation over OTN, 151–153
    - client mapping over OTN, 149–151
  - redefinition, 301, 311–312
  - requirements, 130–131
  - specification overview, 129
  - system description, 129–130
  - throughput examples, 137–138
  - transport budget dimensioning examples for front-hauling, 132*f*
    - versus OBSAI RP3-01, 145–146, 147*f*
  - viable network applications for, 153–154
- Communication over multi-antenna MIMO channel, 7*f*
- Composite PON (CPON) architecture, 243
- Compound annual growth rate (CAGR), 44
- Constant modulus algorithm (CMA), 92, 160, 180
  - equalization, 181
- Content delivery network (CDN), 320, 327, 328
- Continuous-wavelength (CW) lightwave, 158
- Converged fiber–wireless architecture, 349–350
- Converged service orchestration, 378, 379*f*
- Converged wireless access/optical metro networks, 359
  - architecture evaluation, 379
    - impact of virtualization solution on proposed architecture, 383–386
    - numerical results, 381–383
  - converged service orchestration, 378
  - infrastructure management, 363–365, 371–372
  - physical infrastructure layer, 369

- integrated infrastructure, 370–371
- optical physical infrastructure, 369
- wireless physical infrastructure, 370
- physical infrastructure solutions supporting
  - cloud services, 362
  - in metro optical network solutions, 362–363
  - in wireless technologies solutions, 363
- service provisioning, 365–366
- virtual infrastructure control layer (VICL), 373
  - provisioning of cross-domain connectivity, 376–377
- vision and architectural approach, 366–368
- Coordinated beamforming/scheduling, 21
- Coordinated multipoint (CoMP), 66, 191, 337
  - applicability of, 21
  - backhaul architecture, 341
    - adaptive photonics-aided CoMP, 348–349
    - converged fiber–wireless architecture, 349–350
      - FUTON prototype, 345–348, 346*f*, 347*f*
      - GROW-Net architecture, 342–345
  - backhaul network, requirements on, 339
  - capacity, 340–341
  - latency, 340
  - synchronization, 340
  - centralized, 22–23
  - distributed CoMP, 23–24
  - evolution of, 73*f*
  - fiber–wireless integration schemes enabling CoMP, 350
    - BS configuration, 350–352
    - experimental demonstration, 355–356
    - implementation of CoMP, 354–355
    - performance analysis, 352–354
  - processing (CoMP), 294
  - reception, 270
  - transmission, 19–22, 87, 214, 237, 270, 337
- Coordinated scheduling and coordinated beamforming (CS/CB), 338
- Core Network, 266
- CPE (customer-premises equipment), 322
- CRE (Cell-Range Expansion) region, defining, 35–37
- Cumulative distribution function (CDF), 348
- D**
- Data-Controller Plane Interface (D-CPI), 374
- Dense WDM (DWDM), 169, 175, 277
  - multiplexer/demultiplexer, 254–255
- Device-to-device (D2D) communications, 44, 203
- Digital Radio over Fiber (D-RoF),
  - standardization for, 127
- CPRI (Common Public Radio Interface), 128
  - compression and throughput examples, 137–138
  - interface description, 131–137
  - main requirements, 130–131
  - specification overview, 129
  - system description, 129–130
- D-RoF transport over optical networks, 146
  - CPRI over OTN, 149–153
  - viable network applications for CPRI over WDM/OTN, 153–154
- OBSAI (Open Base Station Architecture Initiative), 138
  - CPRI versus OBSAI RP3-01, 145–146
  - objectives, 139–140
  - RP3-01 insight, 142–145
  - specifications status, 139
  - system blocks and interfaces, 140–142
  - Open Radio Interface (ORI), 154–155
- Digital signal processing (DSP), 160, 167
  - advance algorithms based on, 184
- Digital Subscriber Line (DSL), 50
- Digital subscriber line access multiplexer (DSLAM), 50
- Digital-to-analog converter (DAC), 222
- Digitized baseband radio signals, 273
- Digitized radio-over-fiber (D-RoF), 117
  - band-pass sampling theory, 118–120
  - for multiple-antenna site, 122–124
  - for single-antenna site, 120–122
- Digitized Radio-over-Fiber (D-RoF), 100, 267
- Discrete Fast Fourier Transform (DFFT), 118
- Discrete Fourier transform (DFT), 184
- Discrete multi-tone (DMT), 50
- Distributed antenna system (DAS), 69, 70*f*, 84, 219–221, 227, 294, 345, 346
- Distributed CoMP, 23–24
- Distributed evolved packet core, 326–327
- Distributed feedback (DFB) lasers, 202
  - laser diode (LD), 243
- D-lightpaths, 282–283
- Downlink CA, 13
- Downlink CoMP transmission, 339*f*
- Downlink packet scheduling, 17
- Downstream traffic, wavelength assignment/sharing for, 257
- Dynamic bandwidth allocation (DBA), 82, 240, 252, 256
- Dynamic frequency reuse scheme, 33
- Dynamic host control protocol (DHCP), 330

- Dynamic Single-Frequency Networks (DSFN), 22
- E**
- Effective number of bits (ENOB), 353
- Electrical joint processing unit (JPUe), 347
- Electrical multi-carrier modulation, 173–174
- Electrical part of remote antenna unit (RAUe), 347
- Electrical-to-optical (E/O) conversion module, 224
- End-to-end (E2E) Multi-domain Connection Service, 377
- Energy efficiency, 391
- Enhanced Data Rates for GSM Evolution (EDGE), 64
- Enhanced Dedicated Channel (E-DCH), 65
- Enhanced inter-cell interference cancelation (eICIC), 31, 34, 65, 191, 270
- enhancement with CA, 38*f*
- with CA, 37
- Erbium-doped fiber amplifier (EDFA), 163, 167, 170, 176
- Error vector magnitude (EVM), 116
- Ethernet passive optical network (EPON), 46, 47–48, 241
- ETSI (European Telecommunications Standards Institute), 127
- Industry Specification Group (ISG), 154
- Evolved-Multicast Broadcast Multimedia Services (eMBMS), 6, 13, 25
- and MBSFN, 25
- Evolved node Bs (eNBs), 79, 237
- Evolved Packet Core (EPC), 304
- Existing fiber-wireless access architectures, 215
- cloud radio access network (C-RAN), 221–223, 222*f*
  - distributed antenna system (DAS) networks, 219–221
  - macrocell and small cell with fiber-optic backhaul, 215–219
- External cavity laser (ECL), 163
- External modulation and direct detection (EM-DD), 106–107, 107*f*
- F**
- Fast Fourier transformation (FFT), 165, 307
- Fault, Configuration, Accounting, Performance, Security (FCAPS) model, 364
- Fault detection, 259
- Fault recovery, 259–260
- Femtocell, 217
- Fiber cables, 158
- Fiber-to-the-building (FTTB), 55
- Fiber-to-the-curb (FTTC), 55
- Fiber-to-the-home (FTTH), 47, 48*f*, 55, 56, 58, 218, 236, 319
- Fiber-to-the-node (FTTN), 55
- Fiber-to-the-x (FTTx), 301
- Fiber-wireless access networks, 213
- existing fiber-wireless access architectures, 215
    - cloud radio access network (C-RAN), 221–223, 222*f*
    - distributed antenna system (DAS) networks, 219–221
    - macrocell and small cell with fiber-optic backhaul, 215–219
  - novel cloud radio-over-fiber access architecture, 224
    - generic cloud-RoF architecture and operational principle, 224–226
    - multi-service delivery including future-proof millimeter-wave services, 228–232
    - reconfigurable cloud-RoF architecture with WDM techniques, 226–228
- Fiber-wireless convergence and technology evolution, 69
- for backhaul and fronthaul of HetNet, 71–74
  - distributed antenna systems (DASs), 69, 70*f*
  - ultra-high-speed fiber-wireless transmission, 70–71
- Fiber-wireless integration schemes enabling CoMP, 350
- BS configuration, 350–352
  - experimental demonstration, 355–356
  - implementation of CoMP, 354–355
  - performance analysis, 352–354
- Fiber wireless integration system, 161*f*
- Fiber-wireless networks, convergence of, 71*f*
- Fifth-generation system (5G), 67–68
- design of user-centric radio network, 294–296
  - infrastructure public-private partnership (5G PPP), 261
  - key requirements of, 68*f*
  - network visions, 157
  - radio access networks, directions for, 214*f*
  - systems, 195, 314, 315, 391, 392
  - technologies, C-RAN to enable, 310–311
- Filter bank multi-carrier (FBMC), 86
- Finite impulse response (FIR) filter, 164
- Fi-Wi convergence, passive optical network (PON) and. *See* Passive optical network (PON) and Fi-Wi convergence

Fixed-Mobile Convergence (FMC), 276, 329  
*FlowMod* message, 205  
 4G telecommunication networks, 67, 87, 239  
 FP7 GEYSERS project, 366  
 Fractional frequency reuse (FFR), 31–33, 227  
   single macrocell interferer for, 35–36  
 France, national broadband strategy in, 57  
 Frequency division duplexing (FDD) systems, 22  
 Fronthaul traffic, 270  
 Fronthauling mobile traffic, 260–261  
 Full-duplex communication, 25–26, 51  
 Full Service Access Network (FSAN), 49, 241, 261, 301  
 Functional convergence, 321  
 FUTON prototype, 345–348, 346*f*, 347*f*  
 Future mobile communication system, 78*f*

## G

G.992.5, 51  
 Generalized frequency division multiplexing (GFDM), 86  
 General purpose platforms (GPPs), 223, 293, 298  
 Generic cloud-RoF architecture and operational principle, 224–226  
 Germany, national broadband plan, 57  
 Gigabit passive optical network (GPON), 46, 49–50, 241, 246, 320  
 Global IP traffic, 44*f*  
 Global roll-out strategies, 55–57  
 GROW-Net architecture, 342–345  
 GROW-Net backhaul using IF-ROF link, 345*f*  
 GROW-Net CoMP cluster, 344*f*  
 GROW-Net grid cell  
   downlink transmission, 343*f*  
   uplink transmission, 344*f*  
 GROW-Net optical subnetwork, 343*f*  
 GROW-Net topology and grid cell, 342*f*  
 GSM Packet Radio System (GPRS), 64  
 Guaranteed Bit Rate (GBR), 14

## H

HA system, 179, 183  
 Heterogeneous Networks (HetNets), 30, 223, 294  
   deployment, 294  
   self-organizing (*see* Self-organizing HetNets)  
 Heterodyning with direct detection (HE-DD), photo-detector-based, 107–109  
 Heterogeneous transmission devices, coexistence of, 7*f*  
 High-definition (HD) cameras, 158

High-definition multimedia interfaces (HDMIs), 158  
 Highly distributed content delivery networks, 327  
 High-Speed Downlink Packet Access (HSDPA), 65  
 High-speed DSL (HDSL), 50  
 High-Speed Packet Access (HSPA), 65  
 High-Speed Uplink Packet Access (HSUPA), 65  
 Horizontal-polarization (H-polarization) state, 175  
 Horn antennas (HAs), 161  
 Hybrid automatic repeat request (HARQ), 223  
 Hybrid Automatic ReQuest (HARQ), 271  
 Hybrid fiber-copper technology, 55  
 Hybrid PONs, 245–246

## I

IEEE 802.11ax, 62  
 IEEE 802.15, 60  
 IF-over-Fiber, 104  
 i-Japan strategy 2015, 57  
 Information-centric network (ICN), 320  
 Infrastructure as a Service (IaaS), 361  
 Infrastructure management, 363–365, 371–372  
 Infrastructure management layer (IML), 367, 372*f*  
 In-Phase and Quadrature (IQ) data, 129  
 Integrated infrastructure, 370–371  
 Intensity modulation and direct detection (IM-DD), 105–106, 105*f*  
 Inter-band non-contiguous CA, 11–12, 12*f*  
 Inter-cell D2D connectivity, 205  
 Inter-cell interference (ICI), 82, 337  
 Inter-cell Interference Coordination (ICIC), 31, 340  
   macrocell and small-cell ICIC, 33  
   macrocell ICIC, 31  
     fractional frequency reuse (FFR), 31–33  
     soft frequency reuse (SFR), 33  
 Intermediate frequency over fiber (IFoF) technology, 73  
 International Mobile Telecommunications (IMT), 4  
 Internet of Things (IoT), 77, 78  
   networking paradigm, 190  
 Internet service provider (ISP), 331  
   3rd party ISP, 218  
 Inter-site distance (ISD), 381  
 Inter-symbol interference (ISI), 106  
 Intra-band carrier aggregation, 11*f*  
 Intra-band contiguous CA, 10  
 Intra-band non-contiguous CA, 10–11

- Intra-symbol frequency-domain averaging (ISFA) algorithm, 174
- Inverse Fast Fourier Transformation (IFFT), 173, 307
- IP core, 79
- I/Q modulator, 163
- J**
- Joint processing (JP), 338, 340
- L**
- L2TP access concentrator (LAC), 331
- Large-scale antenna systems (LSASs), 298
- Light-emitting diode (LED), 243
- Line-of-sight (LOS) channel requirement, 229
- Links, convergence of, 84
  - mobile backhaul, 84–87, 85*f*
  - mobile midhaul and fronthaul, 87–89
- Local Access Router Network (LARNET) architecture, 243
- Local area networks (LANs), 236
- Logical Infrastructure Composition Layer (LICL), 364
- Long Term Evolution (LTE), 118, 360
  - Advanced (LTE-A), 4
  - Frequency Division Duplexing (FDD) radio interface, 271
  - network architecture, 238*f*
- Low-density parity-check (LDPC), 214
- LTE principles of operation and deployment, 4
  - bandwidth aggregation, 5
  - network heterogeneity, 6
  - spatial diversity and multiplexing, 6–9
  - transmission diversity, 6
- M**
- Machine-to-machine communications (M2M), 44, 390
- Machine-type communication (MTC), 78
- Mach-Zehnder modulator (MZM), 106, 163, 170
- MAC Layer, 8
- Macrocell and small cell with fiber-optic backhaul, 215–219
- Macrocells, 30, 33, 36, 216
  - backhaul networks, 216*f*
  - ICIC, 31
    - fractional frequency reuse (FFR), 31–33
    - soft frequency reuse (SFR), 33
- Maximum throughput scheduling, 17
- Medium access control (MAC) protocols, 203
- “Meta-MAC” concept, 203
- Metro optical network solutions, state of the art in, 362–363
- Metrocell, 218
- Microcell, 218
- Microwave photonics (MWP) techniques, 83
- Midhaul/x-haul, 391
- Millimeter microwave transmission, 301
- Millimeter-wave (MMW) bands, 89–90
- Millimeter-wave (MMW) links, 91–92
- Millimeter wave (MMW) small cells, 348
- mm-wave communication, 91, 158–159, 229
  - 16-ary quadrature amplitude modulation (16QAM), 159
- Mobile backhaul, 84–87, 85*f*
- Mobile broadband data, proliferation of, 3
- Mobile edge computing (MEC), 390
- Mobile fronthaul, 73, 87–89
- Mobile midhaul, 87–89
- Mobile network, 266–267
  - evolution and market status, 63–68
- Mobile optical virtual network operators (MOVNOs), 360, 379, 383
- Mobile subscribers (MS), 227
- Mobile telephone switching office (MTSO), 222
- Mobile terminal interface (MT IF), 347
- Mobility Management Entity (MME), 237
- Modulation and Coding Scheme (MCS) rate, 4, 5
- Multi-band multiplexing, 178–182
- Multicast Broadcast SFN (MBSFN), 25
- Multi-cell beamforming, 20*f*
- Multi-cell packet scheduling, 270
- Multi-layer Path Computation Service, 377
- Multi-level modulation, advanced, 166–169
- Multiple-input multiple-output (MIMO) systems, 7, 88, 90, 190, 214
  - OFDMA, 19
  - and spatial multiplexing, 18–19
  - three-dimensional MIMO (3D MIMO), 24
  - wireless links, 173, 183*f*
- Multi-point carrier aggregation (CA), 87
- Multi-point control protocol (MPCP), 240, 256
- Multi-radio access technology (multi-RAT) optimization, 295
- Multi-service delivery including future-proof millimeter-wave services, 228–232
- Multi-stream beamforming, 7–8
- Multi-user MIMO (MU-MIMO), 61
- N**
- Nanocell, 218
- Network address translation (NAT) functionality, 331
- Network as a Service (NaaS) paradigm, 366
- Network densification, 194–195, 195*f*

- Network functions virtualization (NFV), 68, 223, 302, 320, 325
  - Network heterogeneity, 6. *See also* Self-organizing HetNets
  - Network scenario and related work, 379
    - impact of virtualization solution on proposed architecture, 383–386
    - numerical results, 381–383
  - Network topology, 195–196
  - Network vG (N-vG), 323
  - Neutral-host DAS network architecture, 221*f*
  - Next-generation mobile network, KPIs for, 78*t*
  - Next-generation PON (NG-PON), 241, 246
    - NG-PON2, 248–249
  - Next-generation PoP (NG PoP), 319, 323*f*
    - broadband network gateway (BNG), 324
      - in hardware on an existing network element, 325
      - with IT resources and dedicated hardware resources, 326
      - pure soft BNG, 325
    - distributed evolved packet core, 326–327
    - highly distributed content delivery networks, 327
    - implementing, 333
      - design principles, 333–334
      - dimensioning NG PoP, 334–335
    - path toward fixed and mobile convergence, 329
      - converged subscriber data and session management, 329–330
      - universal access gateway, 331–332
    - virtual residential gateway, 322
      - implementing, with physical BNG, 323–324
  - “No More Cells” (NMC), 293, 294, 295
  - Novel cloud radio-over-fiber access architecture, 224
    - generic cloud-RoF architecture and operational principle, 224–226
    - multi-service delivery including future-proof millimeter-wave services, 228–232
    - reconfigurable cloud-RoF architecture with WDM techniques, 226–228
  - Nyquist region, 354
  - Nyquist sampling theorem, 117, 118
    - wavelength-division multiplexing (WDM), 159
- O**
- OBSAI (Open Base Station Architecture Initiative), 81, 138, 341, 357
    - CPRI versus OBSAI RP3-01, 145–146, 147*t*
    - objectives, 139–140
    - RP3-01 insight, 142–145
    - specifications status, 139
    - system blocks and interfaces, 140–142
      - Baseband Block, 142
      - Control and Clock Block (CCB), 141–142
      - RF Block, 142
      - Transport Block, 141
    - ODFM transmission, 116
    - OFDMA, 3, 19, 79
    - OOK signals, 202
    - OpenFlow 1.0 control, 201
      - based application programming interface (API), 202
    - Open Grid Forum (OGF) Open Cloud Computing Interface (OCCI), 365
    - Open Radio Interface (ORI), 154–155
      - and CPRI, 155*f*
    - OpenStack, 378
    - Open vSwitch (OVS), 376
    - Operating system (OS), 302
    - Operational expenditures (OPEX), 221, 223, 268–269, 381
    - Optical carrier suppression (OCS) modulation, 170
    - Optical code division multiplexing (OCDM), 248
    - Optical couplers (OCs), 161
    - Optical distribution network (ODN), 46, 239
    - Optical fiber-based backhaul, 218
    - Optical line terminal (OLT), 46, 47, 85, 158, 199, 350
    - Optical local oscillator (LO), 161
    - Optical mm-wave generation, 179*f*
    - Optical multi-carrier modulation, 169–172
    - Optical network unit/optical network terminal (ONU/ONT), 46, 47
    - Optical network units (ONUs), 85, 199, 239, 249, 350
    - Optical PDM combined with MIMO reception, 161–165
    - Optical physical infrastructure, 369
    - Optical splitters (OS), 227
    - Optical-to-electrical (O/E) conversion module, 224
    - Optical transport network (OTN)
      - CPRI and, 149–153
      - User-Network Interface (UNI) cards, 153
    - Orbital angular momentum (OAM), 185

- Orbit Management Framework
    - (OMF) Aggregate Manager service, 370
  - Organization for Economic Co-operation and Development (OECD), 57–58
  - Orthogonal frequency division multiplexing (OFDM), 86, 87, 159, 173, 362
    - PON, 239, 244–245
  - OTN (optical transport network) solutions, 301
  - Out-of-band (OOB) leakage, 393
  - Over-the-top (OTT) Internet companies, 313
  - Over-the-top (OTT) services, 44
- P**
- Packet Data Network gateway (P-GW), 237
  - Passive optical network (PON), 45, 46–50, 239
    - and Fi-Wi convergence (*see* Passive optical network (PON) and Fi-Wi convergence)
  - Passive optical network (PON) and Fi-Wi convergence, 235
    - 10G-Epon, 247
      - evolution scenarios, 249
      - NG-PON2, 248–249
    - 10G-PON, 247
    - allocation of network resources, 255
      - dynamic bandwidth allocation, 256
      - upstream traffic flows rerouting and sharing, 256
    - architecture design, 253–255
    - backhauling wireless traffic, 236–238
    - challenges in PON design, 251
    - distributed ring-based WDM-PON
      - architecture, 251–253
    - fault detection, 259
    - fault recovery, 259–260
    - fronthauling mobile traffic, 260–261
    - GPON/EPON, 246
    - technology options, 239
      - hybrid PONs, 245–246
      - OFDM-PON, 244–245
      - TDM-PON, 239–241
      - WDM-PON, 241–244
    - wavelength assignment/sharing for downstream traffic, 257
  - Passive WDM, 277
  - Path computation element (PCE) mechanisms, 366
  - Peak-to-average power ratio (PAPR), 12, 87
  - Photonic mm-wave generation, 158f
  - Photonics-aided coordination, 92
  - PHY layer, 8
  - Physical Downlink Control Channel (PDCCH), 307
  - Physical Downlink Shared Channel (PDSCH), 307
  - Physical infrastructure layer (PIL), 367
  - Physical Resource Block (PRB), 4–5
  - Picocells, 30–31, 217
  - Point-to-multi-point (P2MP) fiber optical networks, 236
  - Point-to-point (PtP) dedicated links, 276–277
  - Point-to-point (PtP) WDM, 249
  - Point-to-point protocol (PPP) tunnel, 331
    - over Ethernet (PPPoE), 330
  - Point-to-point wavelength division multiplexing (PtP-WDM) scheme, 247
  - Polarization beam combiner (PBC), 163
  - Polarization beam splitters (PBSs), 161, 162
  - Polarization division multiplexing (PDM), 91–92, 159
    - quadrature-phase-shift-keying (PDM-QPSK) signal, 163, 182
  - Potential fronthaul solutions, 300–302
  - Power spectral density (PSD), 354
  - Power-splitting PONs (PS-PONs). *See* TDM-PONs
  - Proof of Concept (PoC), 307
  - Proportional fair (PF) scheduling, 17
  - Protection switch (PS) capability, 306
  - Prototype verification of soft C-RAN, 308–310
  - Proximity-aware services, 44
  - Pulse pattern generator (PPG), 163
  - Pure soft BNG, 325
- Q**
- Quadrature amplitude modulation (QAM), 87
  - Quadrature-phase-shift-keying (QPSK), 170
  - Quality-of-experience (QoE), 4, 190, 200, 330
  - Quality-of-service (QoS), 4, 190, 251, 361, 364
    - requirements, 250
    - support, 200
- R**
- Radio access network (RAN), 78, 79f, 91, 216, 239, 266
    - architectures (*see* Radio access network (RAN) architecture)
    - radio performance of, 269
  - Radio access network (RAN) architectures, 146, 213, 253, 273
    - classification on BBU implementation, 278
      - BBU pooling, 278–279
      - BBU stacking, 278
      - BBU virtualization, 279–280
    - classification on BBU placement, 274
      - all-in-one BS (no hotelling), 274–275
      - BBU hotel at first CO, 175
      - BBU hotel at higher-level CO, 276
      - distributed BS (no hotelling), 275

- Radio access network (RAN) architectures (*cont.*)
    - classification on fronthaul transport, 276
      - dedicated point-to-point, 276–277
      - passive WDM, 277
      - TDM-over-WDM (OTN), 277–278
    - cloud/centralized, 148*f*
  - Radio access technologies (RAT), 68, 78, 266, 271, 296
  - Radio access units (RAUs), 81
  - Radio cellular networks, 100–102
  - Radio equipment (RE), 129
  - Radio equipment control (REC), 128, 129–130
  - Radio-over-fiber (RoF), 69, 81, 88, 158, 224, 341
  - Radio Resource Control (RRC) connection, 9–10
  - Radio Resource Head (RRH), 267
  - Radio resource management (RRM), 4, 82
    - framework for CA, 15–17, 15*f*
  - Raman amplification, 251
  - Rate Automatic adapt DSL (RADSL), 50
  - Reconfigurable cloud-RoF architecture with WDM techniques, 226–228
  - Reference points (RPs), 140
  - Reference signal generator, 347
  - Reference Signal Received Power (RSRP), 10, 34
  - Reflective modulation, 243
  - Reflective semiconductor optical amplifier (RSOA), 342
  - Remote access unit (RAU), 102, 103*f*, 123, 224–225, 341
  - Remote heterodyning detection (RHD), 107
  - Remote Interrogation of Terminal Network (RITENET) architecture, 243
  - Remote radio heads (RRHs), 81, 203
  - REPORT message, 256, 259
  - Representational State Transfer (REST), 376
  - Resource cloudification, challenges on
    - virtualization implementation, 302–304
  - Resource sharing, 83–84
  - RF-over-Fiber, 103
  - RP3-01 insight, 142–145
- S**
- Same frequency network (SFN) technology, 304
  - Scalable video coding, 14*f*
  - Second-generation (2G) systems, 63–64
  - Selected IP traffic offload (SIPTO), 327
  - Self-organized network (SoN), 31
  - Self-organizing HetNets, 6, 30
    - defining the CRE region, 35–37
    - definition and terminologies, 30–31
    - eICIC with CA, 37
    - Enhanced Inter-cell Interference Coordination (eICIC), 34
    - Inter-cell Interference Coordination (ICIC), 31–33
    - Service orchestration layer (SOL), 368
    - Service vG (S-vG), 323
    - Serving Gateway (S-GW), 237
    - Shannon theoretical limit, 214
    - Signaling formats, 193–194
    - Signal-to-Interference-plus-Noise Ratio (SINR), 18
    - Single-Carrier FDMA (SC-FDMA), 12–13
    - Single-Frequency Network (SFN), 18
      - multiple macrocell Interferers for, 36–37
    - Single-mode fiber-28 (SMF-28), 163
    - Small cell, 217
      - application scenarios, 217*f*
      - backhaul overview, 219*f*
      - eNBs, 6
      - ICIC, 33
    - Soft C-RAN, prototype verification of, 308–310
    - Soft frequency reuse (SFR), 33
    - Software-defined networking (SDN), 68, 189, 300, 320, 361, 368*f*
      - based control plane, 196–201, 199*f*
      - recent progress in, 201–206
      - system-level fiber wireless network challenges, 192, 193*f*
        - network densification, 194–195, 195*f*
        - network topology, 195–196
        - signaling formats, 193–194
    - Sorbas digital baseband unit, 347
    - Space division multiple access (SDMA), 19
    - Spatial diversity and multiplexing, 6–9
    - Spatially distributed CoMP Coordinated multipoint (CoMP), 191, 204. *See also* Coordinated multipoint (CoMP)
    - Spatial multiplexing, 18–19, 20*f*
    - Standards development organization (SDO), 64
    - Standard single-mode fiber (SSMF), 227
      - optical fronthaul network, 193
    - Static frequency reuse scheme, 33
    - Structural convergence, 321
    - Subcarrier multiplexing (SCM), 86, 112–114, 345
    - Super HD (SHD) video cameras, 158
    - Super-PON (SPON), 244
    - Synchronized eNBs, 6*f*
    - System-level fiber wireless network challenges, 192, 193*f*
      - network densification, 194–195, 195*f*

- network topology, 195–196
  - signaling formats, 193–194
- T**
- TDM-over-WDM, 277–278
  - TDM-PONs, 49–50, 239–241
  - 10G EPON, 48, 49, 241, 247–248
  - 10G-PON, 247
  - Thin-film filter (TFF)-based filters, 342
  - Third Generation Partnership Project (3GPP), 64–65
    - 3GPP LTE, 3
    - 3GPP LTE-Advanced (LTE-A), 9
  - Three-dimensional MIMO (3D MIMO), 24
  - Time division duplexing (TDD) systems, 22
  - Time Division Long-Term Evolution (TD-LTE) system, 299
  - Time-division multiple access (TDMA), 47
    - arbitration scheme, 256
  - Time-division-multiplexed passive optical network architectures, 240f, 245f
  - Time-division multiplexing (TDM) technique, 217, 277
  - Time Shared Optical Networks (TSON), 362
  - Time/wavelength division multiplexing (TWDM), 247
    - TWDM-PON, 249
  - Total cost of ownership (TCO) reduction, 299
  - Transmission diversity, 6
    - and spatial multiplexing, 18
      - applications, 25–26
      - coordinated multipoint (CoMP) transmission, 19–24
      - definition and terminologies, 18
      - MIMO and spatial multiplexing, 18–19
      - 3D beamforming, 24–25
  - Transmission of microwave signals on optical fibers, 104
    - external modulation and direct detection (EM-DD), 106–107
    - intensity modulation and direct detection (IM-DD), 105–106
    - photo-detector-based heterodyning (HE) with direct detection (HE-DD), 107–109
  - Transmission point (cell) selection (TPS), 338
  - Transport networks for centralization, challenges on, 299–300
  - Triple play, 45
  - Turbo encoding, 307
  - Twisted pair technology, 53
- U**
- Ultra dense network (UDN), 295
  - 8K ultra high definition (UHD), 43
    - evolution scenarios, 249
    - NG-PON2, 248–249
  - Ultra-high-speed fiber-wireless transmission, 70–71
  - Universal access gateway (UAG), 331–332
  - Universal filtered multi-carrier (UFMC), 86
  - Universal Mobile Telecommunication System (UMTS), 64, 236
  - Unlicensed LTE (LTE-U), 27
  - Uplink CA, 12
  - Upstream traffic flows rerouting and sharing, 256
  - User-centric radio network, 5G design of, 294–296
- V**
- Vectoring, 52
  - Vertical-polarization (V-polarization) state, 175
  - Very-high-bit-rate DSL (VDSL), 50, 51–53
  - Virtual infrastructure control layer (VICL), 367, 373
    - cross-domain connectivity, provisioning of, 376–377
  - Virtual infrastructures (VIs), 364
  - Virtualization implementation, challenges on, 302–304
  - Virtualization of optical networks, 364
  - Virtual machines (VMs), 296
  - Virtual optical networks (VONs), 364
  - Virtual PONs (VPONs), 203
  - Virtual residential gateway (vRGW) approach, 322, 322f
    - implementing virtual gateway with physical BNG, 323–324
  - Visual Networking Index (VNI), 44
  - Viterbi-Viterbi algorithm, 168
- W**
- Wavelength assignment/sharing for downstream traffic, 257
  - Wavelength division multiplexing (WDM), 49, 50, 114–117, 192, 196, 206, 248, 277, 293, 345
    - WDM PON, 85, 239, 241–244, 251–253, 301
  - Wavelength selective switch (WSS), 175
  - Wide area networks (WAN), 197
  - Wideband-CDMA (WCDMA), 64
  - Wi-Fi-LTE
    - interference management, 28
    - unlicensed LTE, 27
      - CA of LTE-Licensed and LTE-U CCs, 28–30

- definition and terminologies, [27–28](#)
  - Wi-Fi technologies
    - evolution of, [61f](#)
    - market status, [60–63](#)
  - WiMAX IEEE 803.16a WLANs,
    - characteristics of, [119f](#)
  - Wireless access network, [370f](#)
  - Wireless delivery of mm-wave signal in
    - W-band, [157](#)
    - advance algorithms based on DSP, [184](#)
    - approaches for realization of large capacity
      - fiber wireless integration system, [160](#)
      - advanced multi-level modulation, [166–169](#)
      - antenna polarization multiplexing, [175–178](#)
      - electrical multi-carrier modulation, [173–174](#)
      - multi-band multiplexing, [178–182](#)
      - optical multi-carrier modulation, [169–172](#)
      - optical PDM combined with MIMO reception, [161–165](#)
    - wireless multi-path effects due to different wireless transmission distances, [182–184](#)
  - Wireless local area network (WLAN), [229](#)
  - Wireless Metropolitan Area Networks (WMANs), [60](#)
  - Wireless Personal Area Networks (WPANs), [60](#), [229](#)
  - Wireless physical infrastructure, [370](#)
  - Wireless side, advanced modulation format in, [392](#)
  - Wireless technologies solutions, state of the art in, [363](#)
- X**
- xDSL Technology, [45](#), [50–53](#), [55](#)